



Offshore Wind Power Limited

# West of Orkney Windfarm Offshore EIA Report

## Volume 2, Supporting Study 3: Marine Physical and Coastal Processes Supporting Study

WO1-WOW-CON-EV-RP-0042: Approved by S.Kerr  
Document Control 13/09/2023

ASSIGNMENT L100632-S05  
DOCUMENT L-100632-S05-A-REPT-007





## REVISIONS & APPROVALS

This report has been prepared by Xodus Group exclusively for the benefit and use of Offshore Wind Power Limited. Xodus Group expressly disclaims any and all liability to third parties (parties or persons other than Offshore Wind Power Limited ) which may be based on this report.

The information contained in this report is strictly confidential and intended only for the use of Offshore Wind Power Limited. This report shall not be reproduced, distributed, quoted or made available – in whole or in part – to any third party other than for the purpose for which it was originally produced without the prior written consent of Xodus Group and Offshore Wind Power Limited.

The authenticity, completeness and accuracy of any information provided to Xodus Group in relation to this report has not been independently verified. No representation or warranty express or implied, is or will be made in relation to, and no responsibility or liability will be accepted by Xodus Group as to or in relation to, the accuracy or completeness of this report. Xodus Group expressly disclaims any and all liability which may be based on such information, errors therein or omissions therefrom.

---

A01	08/09/2023	Issued for Use	CM	AC	DB	OWPL
R02	31/05/2023	Re-issued for review	CM	AC	DB	OWPL
R01	24/04/2023	Issued for review	CM	AC	DB	OWPL

---

REV	DATE	DESCRIPTION	ISSUED	CHECKED	APPROVED	CLIENT
-----	------	-------------	--------	---------	----------	--------

---



## CONTENTS

<b>1</b>	<b>INTRODUCTION</b>	<b>7</b>
<b>1.1</b>	<b>Report overview</b>	<b>7</b>
<b>1.2</b>	<b>Offshore Project Overview</b>	<b>7</b>
<b>1.3</b>	<b>Marine Physical and Coastal Processes Study Area</b>	<b>8</b>
<b>1.4</b>	<b>Marine Physical and Coastal Processes Model Domain</b>	<b>10</b>
<b>2</b>	<b>DATA SOURCES</b>	<b>12</b>
<b>2.1</b>	<b>Site-Specific Surveys, Studies and Data</b>	<b>12</b>
2.1.1	Geophysical and Shallow Geology Survey	12
2.1.2	Reconnaissance geotechnical investigation	14
2.1.3	Environmental survey	14
2.1.4	Intertidal survey	18
2.1.5	Metocean hindcast datasets	18
2.1.6	Numerical Modelling Study	19
<b>2.2</b>	<b>Secondary Data Sources</b>	<b>22</b>
<b>3</b>	<b>BASELINE CHARACTERISATION</b>	<b>25</b>
<b>3.1</b>	<b>Designated sites</b>	<b>25</b>
<b>3.2</b>	<b>Bedrock Geology</b>	<b>31</b>
3.2.1	Overview	31
3.2.2	Offshore Project Area	31
<b>3.3</b>	<b>Quaternary Geology and Seabed Sediment</b>	<b>35</b>
3.3.1	Overview	35
3.3.2	Offshore Project Area	35
<b>3.4</b>	<b>Seabed Bathymetry</b>	<b>45</b>
3.4.1	Overview	45
3.4.2	Offshore Project Area	47
<b>3.5</b>	<b>Seabed Morphology</b>	<b>50</b>
3.5.1	Overview	50
3.5.2	Offshore Project Area	50
<b>3.6</b>	<b>Water Levels</b>	<b>58</b>
3.6.1	Overview	58
3.6.2	Offshore Project Area	62
3.6.3	Storm Surge, Extremes and Sea Level Rise	63
<b>3.7</b>	<b>Tidal and Residual Flows/Currents</b>	<b>64</b>
3.7.1	Overview	64
3.7.2	Offshore Project Area	66
3.7.3	Extreme Tidal and Residual Flows/Currents	71
<b>3.8</b>	<b>Waves</b>	<b>71</b>
3.8.1	Overview	72
3.8.2	Offshore Project Area	72



3.8.3	Extreme Waves	78
<b>3.9</b>	<b>Sediment Transport</b>	<b>79</b>
3.9.1	Overview	79
3.9.2	Project Area	80
<b>3.10</b>	<b>Stratification and Fronts</b>	<b>94</b>
3.10.1	Overview	94
3.10.2	Offshore Project Area	94
<b>3.11</b>	<b>Coastline Morphology</b>	<b>104</b>
<b>4</b>	<b>ASSESSMENT APPROACH</b>	<b>107</b>
<b>4.1</b>	<b>Sources of Effects on Marine Physical and Coastal Processes</b>	<b>107</b>
<b>4.2</b>	<b>Impacts Requiring Assessment</b>	<b>107</b>
<b>4.3</b>	<b>Project Description</b>	<b>108</b>
<b>4.4</b>	<b>Approach to Assessment</b>	<b>115</b>
4.4.1	Modelling Approach	115
4.4.2	Analytical Methods	121
4.4.3	Assessment for Potential Changes to Water Column Stratification	124
4.4.4	Assessment of Scour	124
<b>5</b>	<b>ASSESSMENT OF CONSTRUCTION ACTIVITIES</b>	<b>125</b>
<b>5.1</b>	<b>Seabed Disturbance Sediment Plume and Concentrations</b>	<b>125</b>
5.1.1	Overview	125
5.1.2	Seabed Preparation	126
5.1.3	WTG and OSP Foundation Installation	140
5.1.4	Cable Installation	146
5.1.5	Project in-combination Construction Activities	150
5.1.6	HDD Installation	152
<b>5.2</b>	<b>Loss or Alteration of Seabed Type</b>	<b>152</b>
5.2.1	Seabed Preparation	153
5.2.2	WTG and OSP Foundation Installation	159
5.2.3	Cable Installation	162
<b>5.3</b>	<b>Potential Landfall Changes</b>	<b>165</b>
<b>6</b>	<b>ASSESSMENT OF OPERATION STAGE</b>	<b>169</b>
<b>6.1</b>	<b>Potential Changes to Tides</b>	<b>169</b>
6.1.1	Overview	169
6.1.2	Assessment	169
<b>6.2</b>	<b>Potential Changes to Waves</b>	<b>175</b>
6.2.1	Overview	175
6.2.2	Assessment	176
<b>6.3</b>	<b>Potential Changes to Sediment Transport</b>	<b>189</b>
6.3.1	Overview	189
6.3.2	Assessment	189
<b>6.4</b>	<b>Potential Changes to Water Column Stratification</b>	<b>200</b>



6.4.1	Overview	200
6.4.2	Assessment	200
<b>6.5</b>	<b>Potential Seabed Scour</b>	<b>203</b>
6.5.1	Overview	203
6.5.2	Scour formation	204
6.5.3	OAA Scour Assessment	205
<b>6.6</b>	<b>Potential Changes to Landfall</b>	<b>208</b>
6.6.1	Overview	208
6.6.2	Assessment	209
<b>7</b>	<b>REFERENCES</b>	<b>211</b>
<b>8</b>	<b>ABBREVIATIONS</b>	<b>218</b>
<b>9</b>	<b>GLOSSARY</b>	<b>222</b>

## APPENDIX A MARINE PHYSICAL PROCESSES MODELLING CALIBRATION AND VALIDATION REPORT

<b>A.1</b>	<b>Introduction</b>
A.1.1	Project Overview
A.1.2	Report structure
<b>A.2</b>	<b>Modelling approach</b>
A.2.1	Software
A.2.2	Model Setup
<b>A.3</b>	<b>Model Calibration</b>
A.3.1	Calibration and Validation Metrics
A.3.2	Calibration and Validation data
A.3.3	Hydrodynamic Model Calibration
A.3.4	Hydrodynamic Model Validation
A.3.5	Wave Model Calibration
<b>A.4</b>	<b>Summary</b>
<b>A.5</b>	<b>References</b>
<b>A.6</b>	<b>Abbreviations</b>

## APPENDIX B MARINE PHYSICAL PROCESSES MODELLING RESULTS REPORT

<b>B.1</b>	<b>Introduction</b>
<b>B.2</b>	<b>The offshore Project</b>
B.2.1	Construction
B.2.2	Operation
<b>B.3</b>	<b>Baseline Characterisation</b>
B.3.1	Hydrodynamic Conditions
B.3.2	Wave Conditions



**B.4 Construction Impacts**

- B.4.1 Seabed Preparation
- B.4.2 Cable Burial
- B.4.3 Pile Drilling
- B.4.4 In-combination

**B.5 Operational Impacts**

- B.5.1 Hydrodynamic Impacts
- B.5.2 Wave Impacts

**B.6 Summary**

**B.7 References**

**B.8 Acronyms**

**B.9 Additional Figures**

- B.9.1 Baseline H<sub>s</sub> Map Plots
- B.9.2 Layout 1 Post-Construction Scheme Impacts on Waves
- B.9.3 Layout 2 Post-Construction Scheme Impacts on Waves



# 1 INTRODUCTION

## 1.1 Report overview

The applicant, Offshore Wind Power Limited (OWPL) is proposing the development of the West of Orkney Windfarm ('the Project'), an Offshore Wind Farm (OWF), located approximately 23 kilometres (km) from the north coast of Scotland and 28 km from the west coast of Hoy, Orkney, with landfall options at Crosskirk and Greeny Geo. The offshore Project comprises the offshore components of the Project (seaward of Mean High Water Springs (MHWS)), which includes the offshore wind farm array area (i.e. the OAA), the offshore Export Cable Corridor (ECC) and landfall options. OWPL are seeking statutory consent for the development of the Project.

This marine physical and coastal processes assessment supports the Offshore Environmental Impact Assessment (EIA) Report, with respect to the statutory application. This marine physical and coastal processes supporting study is structured as follows:

- An introduction to the offshore Project properties and the study area applied in the completed studies are set out in this section;
- Data sources, from both site-specific surveys and secondary information, are presented in section 2;
- The baseline environment that underpins the completed assessments is described in section 3;
- The analyses and assessment methodology including the applied realistic worst case Project design used to inform the assessments are presented in section 4;
- Assessment of construction effects (including pre-construction) is set out in section 5;
- Assessment of operational stage effects is set out in section 6; and
- Concluding statements are provided in section 7.

## 1.2 Offshore Project Overview

The OAA is located approximately 23 km from the north coast of Scotland and covers an area of approximately 657 km<sup>2</sup>. The offshore ECC which extends from the OAA to the landfall options at Caithness with a total area of 125 km<sup>2</sup>. Together the OAA and offshore ECC comprise the offshore Project area, for which the key components will include:

- Up to 125 Wind Turbine Generators (WTGs) with fixed foundations;
- Up to five Offshore Substation Platforms (OSPs);
- Up to 500 km of inter-array cables;



- Up to 150 km of inter-connector cables;
- Up to five offshore export cables to landfall options at Caithness, with a total distance of up to 320 km; and
- Horizontal Direction Drilling (HDD) subtidal exits, associated with the landfall methodology.

Since submission of the Scoping Report (OWPL, 2022a) the Project design has been refined to exclude floating foundations. Therefore, the Project design discussed and presented within this report (section 4.3) represents the worst case that could be implemented.

### 1.3 Marine Physical and Coastal Processes Study Area

The marine physical and coastal processes study area ("the study area") has been established using a 10 km buffer around the OAA and a 15 km buffer around the offshore ECC (Figure 1-1). This is based on the mean spring tidal excursion distance from the UK Atlas of Marine Renewable Energy Resources meso-scale model (ABPmer, 2008). Different buffer distances are applied between the OAA and offshore ECC to account for the variation in excursion distance between the two offshore Project elements. The proximity of the offshore export cable to faster and stronger flows through the Pentland Firth between the Scottish mainland and Orkney Islands accounts for the larger excursion distance for the offshore ECC.

The applied buffer (10 km and 15 km for the OAA and offshore ECC, respectively) is considered to be appropriate on the basis of the flow characteristics from regional model data, to capture effects that extend beyond the offshore Project. This includes effects associated with pathways for tidal advection, net drift and dispersion of sediment plumes from seabed disturbance activities and the extent of wakes and water column mixing due to flows and waves passing individual foundations and the wider array. Note that while the marine physical and coastal processes study area has been used to inform the impact assessment, a wider region has been used for the numerical modelling as discussed in Section 4.4.1.

Seabed depths across the offshore Project area range between 41 mLAT and 90 mLAT within the OAA, with shallower depths occurring over Whiten Head Bank and Stormy Bank. Depths along the offshore ECC range between from 43 mLAT and 110 m LAT. Depths across the study area range between that described for the offshore Project. Further description of the seabed depths across the offshore Project is shown in Figure 1-2 and presented in section 2.1.1.

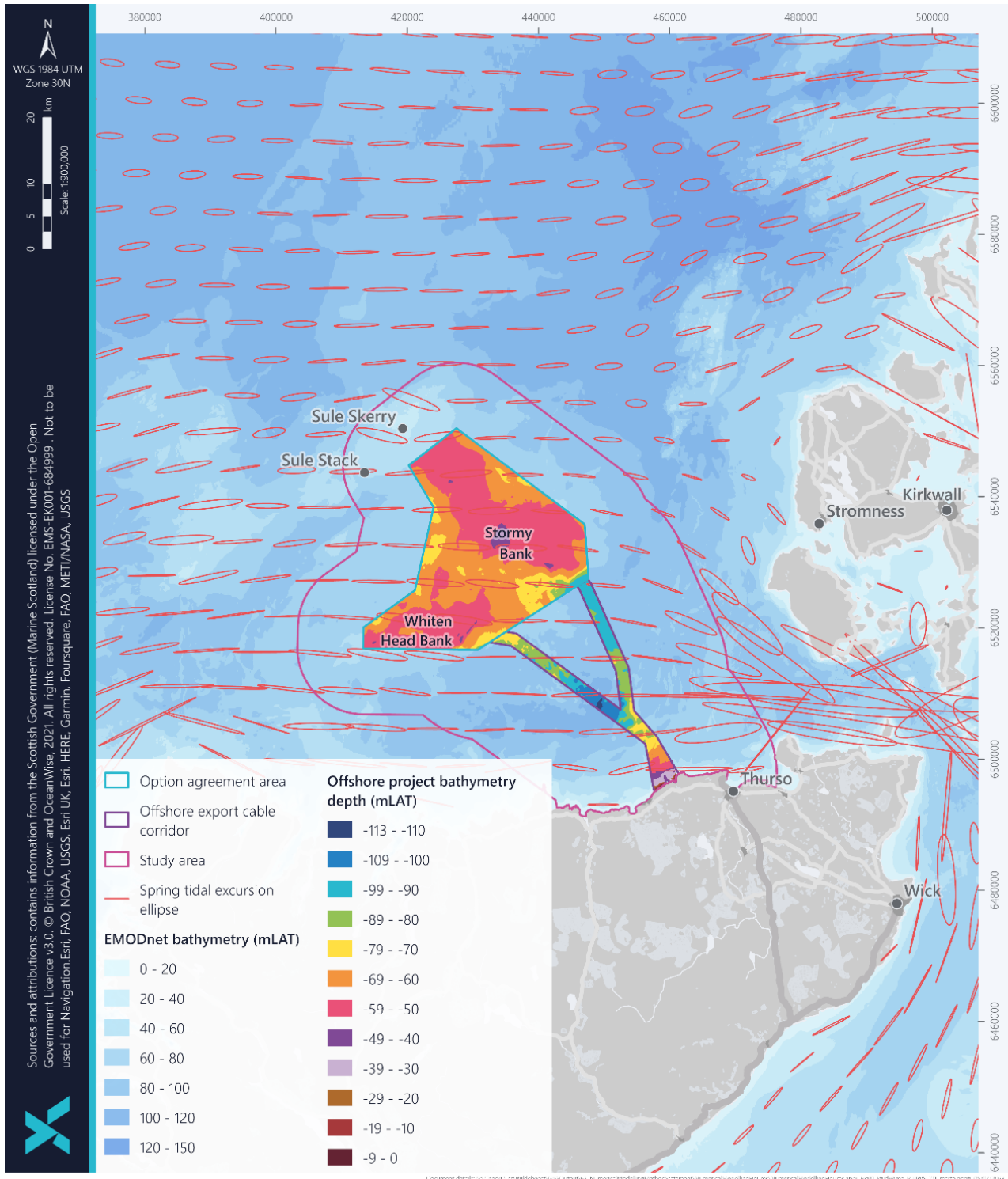


Figure 1-1. Marine physical and coastal processes study area



## 1.4 Marine Physical and Coastal Processes Model Domain

The marine physical and coastal processes model domain (“model domain”) agreed during consultation and applied in the numerical modelling is illustrated in Figure 1-2. The applied model domain extends across an area of approximately 85 km east-west and 30 km north-south centred on the OAA and Orkney Islands, capturing the north coast of mainland Scotland. A wider model is applied to enable the marine physical processes through the study area to be more accurately represented and modelled. The model developed to inform the Project impact assessment is known as the West of Orkney model.

For information, two key models are referenced within this technical report, which were integral to supplementing the baseline environmental characterisation for a range of environmental properties (as discussed in sections 3.6, 3.7, 3.9 and 3.10). The models include:

- The West of Orkney model, which was developed in support of the offshore Project and described in more detail in section 2.1.6 and Appendix A. In addition to informing the baseline (section 3) , the West of Orkney model generated results of potential Project impacts at construction (section 5) and operational stages (section 6.2); and
- The Pentland Firth Orkney Waters (PFOW) model was created by Marine Scotland in recognition of the region’s importance for marine renewable energy (the model boundary is shown opposite). A number of model runs, variations, and outputs have been produced. The main model output is the PFOW climatology, which is used to inform the baseline conditions for a range of environmental properties in section 3, as well as calibrate and validate the West of Orkney model.

In addition to the above, a number of publicly available hindcast models also provided source data for the West of Orkney model, which are fully detailed above in section 2.1.5.

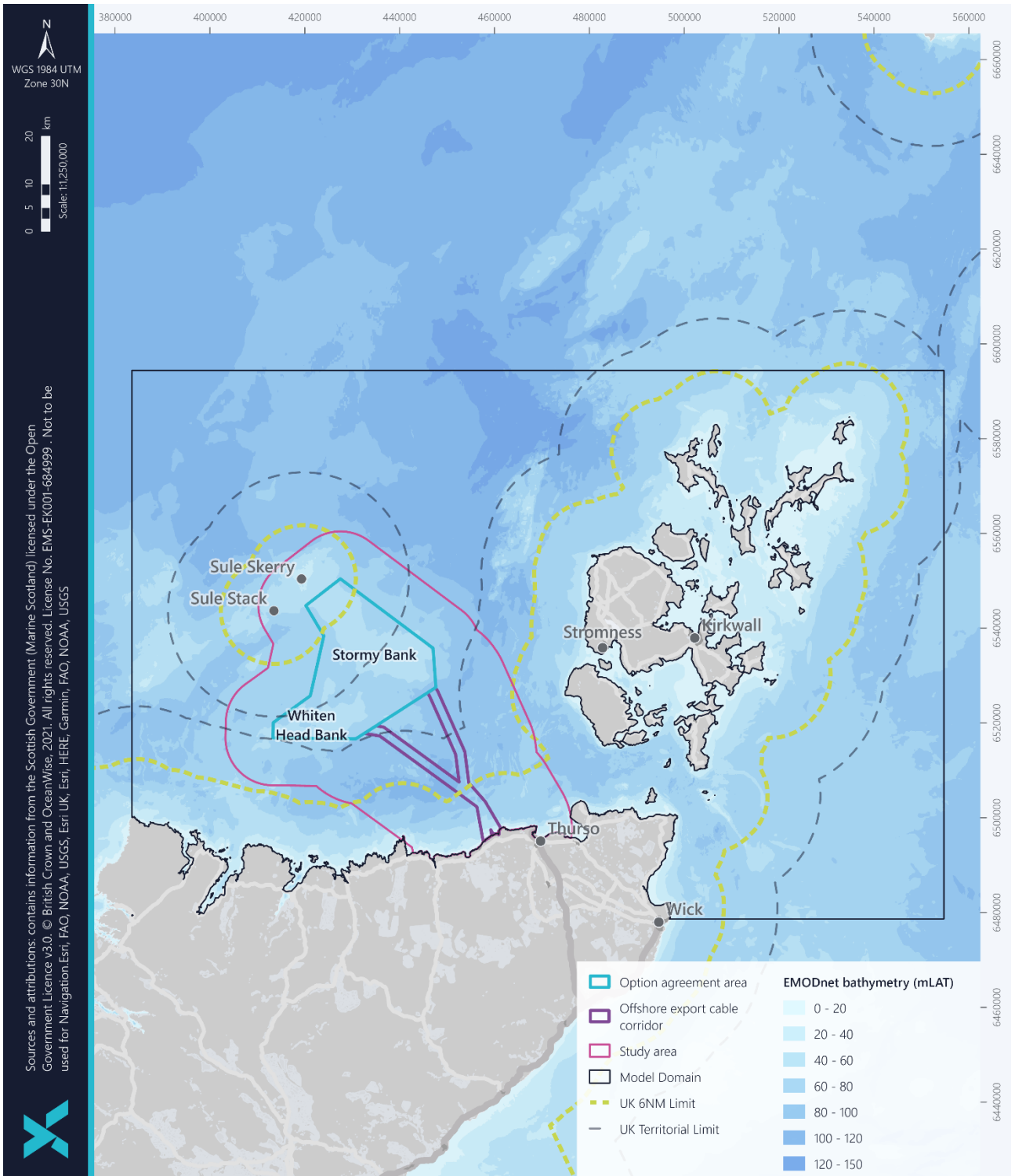


Figure 1-2. Marine physical and coastal processes applied model domain



## 2 DATA SOURCES

### 2.1 Site-Specific Surveys, Studies and Data

A number of site-specific surveys have been completed that directly inform the baseline characterisation across the offshore Project area, with respect to marine physical and coastal processes. Where information is available this has been used to inform the baseline and numerical modelling of impact scenarios. Site-specific surveys which have been utilised to inform this technical report are summarised in Table 2-1 and detailed further in the sections following the table.

Table 2-1 Site specific data used to inform the Marine Physical and Coastal Processes Technical Report

SURVEY TYPE	DESCRIPTION	SURVEY DATE
<b>Geophysical (Nearshore)</b>	Geophysical survey covering the Caithness landfall options	August – October 2021
<b>Geophysical (Offshore)</b>	Geophysical survey covering OAA and offshore ECC	April – September 2022
<b>Environmental</b>	Environmental seabed sediment and water column sampling covering the OAA and offshore ECC. Sediment sampling completed for particle size analysis and water column sampling completed for conductivity, temperature and depth (CTD), turbidity (with salinity being calculated from the conductivity and density values).	August – October 2022
<b>Geotechnical</b>	Reconnaissance geotechnical investigation covering the OAA and offshore ECC	October 2022
<b>Geophysical (Nearshore) and Environmental</b>	Nearshore geophysical and environmental (seabed sediment and water column sampling) surveys covering Caithness landfall options – Crosskirk and Greeny Geo	August – October 2022
<b>Intertidal survey</b>	Unmanned aerial vehicle (UAV) survey at low water to obtain high-resolution imagery of the coastal landfall area	August 2022

#### 2.1.1 Geophysical and Shallow Geology Survey

##### 2.1.1.1 Offshore

Ocean Infinity were contracted by OWPL to conduct an offshore geophysical survey across the offshore Project area between April and September 2022. The geophysical survey campaign was conducted in phases, in order to characterise the seabed and sub-seabed conditions:



- Phase I: Survey of the OAA through loose grid (2 km x 2 km) mapping over 657 km<sup>2</sup> and the centre line of the offshore ECC – This survey was completed utilising Ultra High Resolution Seismic (UHRS), multibeam echosounders (MBES) and sub-bottom profiler (SBP) equipment;
- Phase II: Survey of the OAA utilising MBES, side-scan sonar (SSS), single magnetometer and SBP tight grid mapping (62.5 m x 1000 m) over 657 km<sup>2</sup>; and
- Phase III: Survey of the offshore ECC utilising MBES, SSS, single magnetometer and SBP tight grid mapping (62.5 m x 1000 m) over the 2 km width of the offshore ECC.

The geophysical data acquired during the survey consisted of:

- Multibeam echo sounder (MBES) bathymetry and backscatter (0.5 x 0.5 m bin size);
- Side-scan sonar (SSS) both low frequency (LF) 300 kilohertz (kHz) and high frequency (HF) 600 kHz at 75 m range (0.15 m pixel size mosaic);
- Magnetometer;
- Sub-bottom profiler (SBP) to approximately 10 m below seabed; and
- Ultra-High Resonance Spectrometry (UHRS) to approximately 100 m below seabed.

Both the SBP and UHRS data were acquired to inform the shallow geological properties, with more detailed geotechnical investigations planned at a future stage which will inform the final design of the offshore Project. The SBP and UHRS data were acquired during Phase I and was restricted to a 2 km x 2 km survey grid over the OAA and along the offshore ECC centre lines. Data from the other geophysical sensors was acquired during Phase II, along a much tighter survey grid with main line separation of 62.5 m and cross line separation of 1,000 m.

Three reports detail the findings of the surveys and have been used to establish the detailed baseline conditions and inputs for modelling parameters. The interpretation is solely based upon geophysical data acquired during Phases I, II and III.

- Volume 1 – OAA Results Report (Ocean Infinity, 2023a): This report presents the interpretation and results from the geophysical survey conducted in the OAA of the offshore Project area;
- Volume 2a – Export Cable Corridor (ECC) Results Report (Whiten Head Bank to Crosskirk) (Ocean Infinity, 2023b): This report presents the interpretation and results from the geophysical survey conducted in the offshore export cable corridor Option 1 (Whiten Head Bank to Crosskirk) of the offshore Project area and termed the western ECC in this report; and
- Volume 2b – ECC Results Report (Stormy Bank to Crosskirk) (Ocean Infinity, 2023c): This report presents the interpretation and results from the geophysical survey conducted in the offshore export cable corridor Option 2 (Stormy Bank to Crosskirk) of the offshore Project area and termed the eastern ECC in this report.



### 2.1.1.2 Nearshore

In addition to the offshore geophysical survey, OWPL contracted Spectrum Geosurvey Limited ("Spectrum") between August and October 2022 to complete a marine geophysical survey across the nearshore area of the offshore ECC and proposed landfalls. The survey was completed to a similar specification as that described for offshore (section 2.1.1.1) and included the acquisition of MBES, SSS, magnetometer and SBP data. Also associated with this survey is the completion of an intertidal survey described further in section 2.1.4. The results of nearshore marine geophysical survey are detailed in the Volume 1 – West of Orkney Windfarm Nearshore Geophysical Survey Results and Charts Report (Spectrum, 2023).

## 2.1.2 Reconnaissance geotechnical investigation

An initial reconnaissance geotechnical investigation comprised seabed sampling using a high power vibrocorer (VC) and in-situ seabed testing using cone penetration tests (CPT). A total of 50 locations were sampled through VC or CPT across the OAA, and offshore ECC. Results of the reconnaissance geotechnical testing are reported in Offshore Geotechnical Site Investigation, Volume I – Shallow Geotechnical Report (Ocean Infinity, 2023d).

## 2.1.3 Environmental survey

An environmental baseline survey was completed by Ocean Infinity between August and September of 2022. This survey was undertaken within the OAA and along the offshore ECC. Additionally, a nearshore environmental survey was carried out in October 2022 by Spectrum Geosurvey Limited and Ocean Ecology Limited.

The offshore benthic and environmental survey data acquisition included sediment sampling and imagery, with continuous video, water sampling and conductivity, temperature and depth (CTD) profiling to establish a baseline for the habitats and faunal communities within the survey area. The findings from both environmental surveys are fully detailed within Supporting Study 5 (SS5): Benthic environmental baseline report and Supporting Study 6 (SS6): Intertidal survey habitat assessment. The relevant information gathered through these environmental surveys pertaining to the marine physical and coastal processes baseline is summarised below.

### 2.1.3.1 Seabed Sediments

Environmental sampling was completed for seabed sediments as detailed below. The sampled locations used to inform the environmental baseline characterisation and analyses for marine physical and coastal processes are illustrated in Figure 2-1.

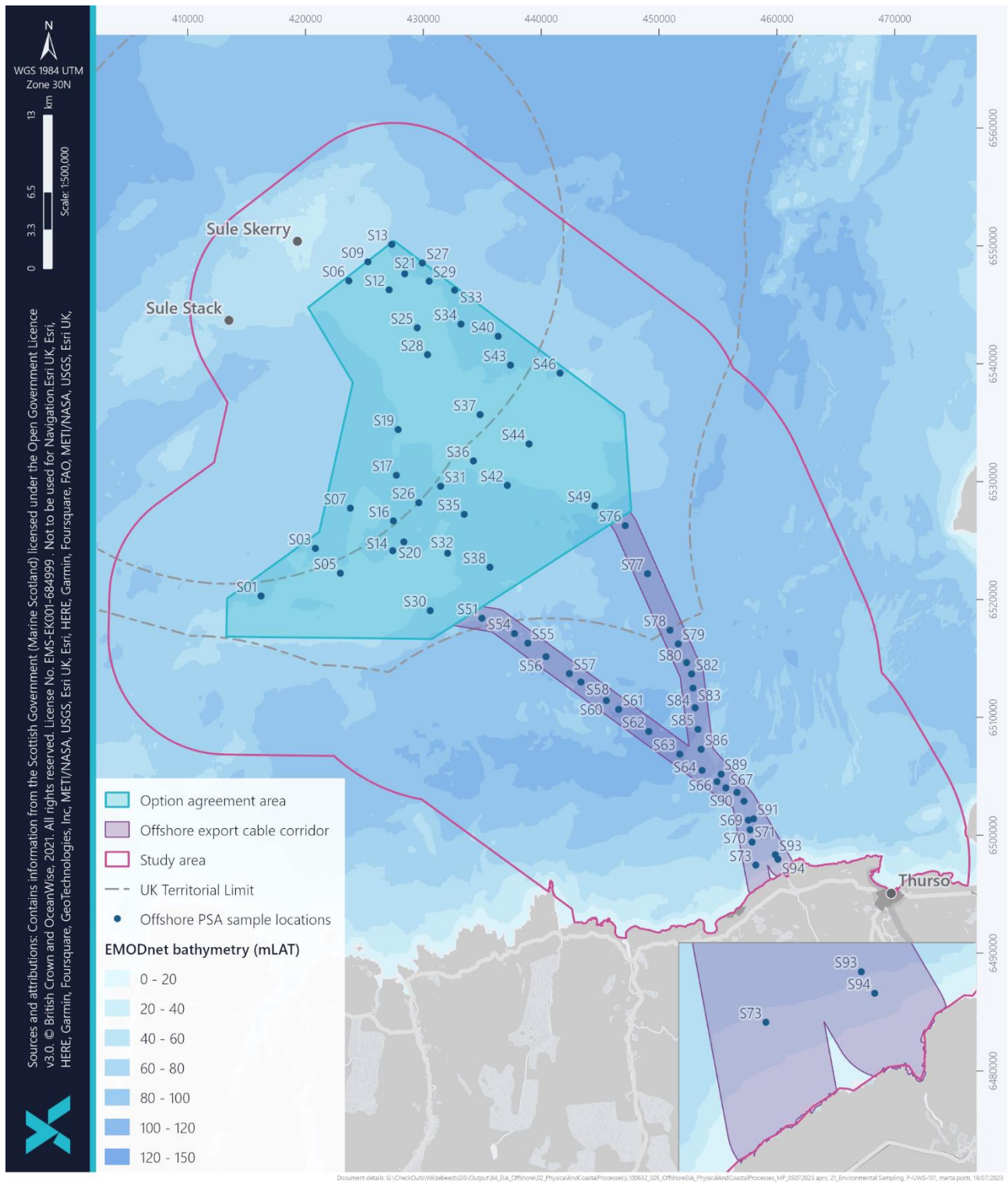


Figure 2-1 Environmental sampling locations (PSA) used to inform the marine physical and coastal processes technical report



#### **2.1.3.1.1 Offshore**

For the environmental baseline survey conducted in the OAA and ECC, grab sampling was planned at a total of 82 sample stations with 73 successfully sampled, due to seabed conditions. At each sample station, one sample was acquired for taxonomic and biomass analyses, one sample for Particle Size Analysis (PSA), and one sample for sediment chemistry and contaminants analysis. Replicate grab samples for fauna, PSA and contaminants analyses were planned at a total of 16 sites (as a backup and not for analyses).

Of relevance to this technical report are the results of the PSA sampling, for which a total of 67 samples were achieved and analysed, 34 across the OAA, 18 from the western ECC and 15 from the eastern ECC, the sampled locations are illustrated in Figure 2-1. For PSA sampling, the primary grab sampler utilised in the majority of the survey area was the dual van Veen (DVV;  $2 \times 0.1 \text{ m}^2$ ) and the secondary grab sampler, e.g. in areas of coarse sediment, was the Hamon grab (HG;  $0.1 \text{ m}^2$ ). In the nearshore area, PSA samples were obtained using a HG or a Shipek grab ( $0.05 \text{ m}^2$ ). Upon retrieval, PSA samples were checked for adequate sample volume and samples covering less than  $0.1 \text{ m}^2$  of bottom surface sediment were deemed unacceptable. No samples of less than 5 cm (7 cm in fine sediments) of penetration depth for the DVV or 2.7 litres for HG were considered acceptable samples (Worsfold & Hall, 2010; Davies, et al., 2001).

#### **2.1.3.1.2 Nearshore**

During the environmental nearshore survey, grab sampling was planned at four sites for taxonomic and biomass analyses, PSA, and contaminant analyses. Three out of the four sites were successfully sampled. The primary grab sampler utilised for PSA and contaminants grab sampling during the nearshore survey was a Shipek grab sampler ( $0.05 \text{ m}^2$ ). Upon retrieval, samples were checked for adequate sample volume. Should a sufficient sample not be acquired after three attempts with the Shipek grab, the sample station was abandoned.

### **2.1.3.2 Water Column Properties**

Sampling for water column properties was completed at 25 sample stations with a total of 29 samples being acquired across the offshore Project area, comprising 13 in the OAA, seven in the offshore ECC, five in the nearshore area and four replicate samples within the OAA. The sampled locations used to inform the environmental baseline characterisation and analyses for marine physical and coastal processes are illustrated in Figure 2-2, with further detail on the sampling approach described in the following sections.

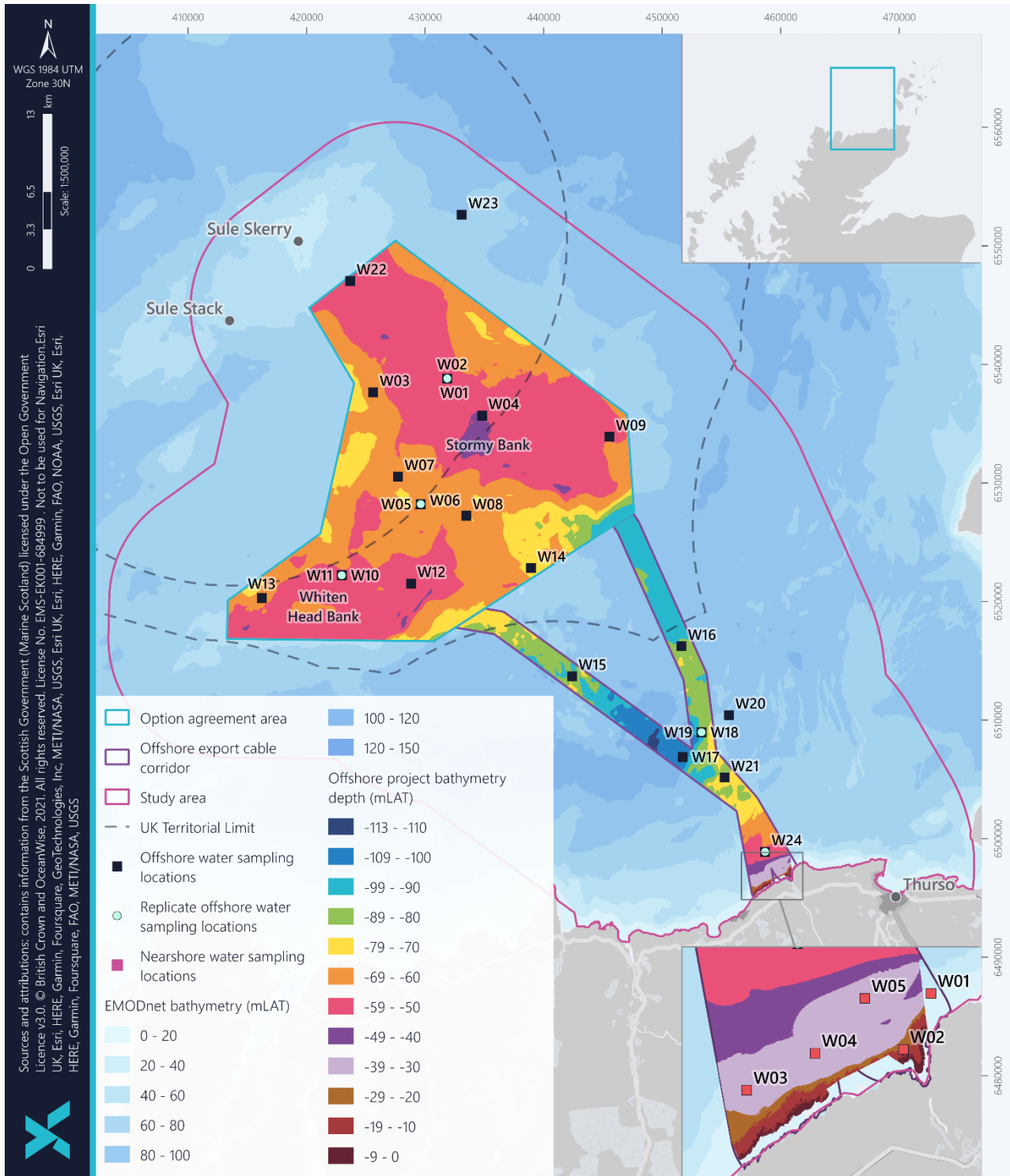


Figure 2-2 Water sampling locations used to inform the marine physical and coastal processes technical report



#### 2.1.3.2.1 Offshore

Water sampling for total suspended solids (TSS) as an indication of suspended sediment concentration (SSC), together with CTD profiling was completed at a total of 20 sampling stations across the OAA and offshore ECC. At four of these stations, replicate samples were acquired, with sampling occurring at spring and neap conditions, as indicated in Figure 2-2. Water samples were collected at three depths (bottom, middle and top). All of the 20 planned water sample locations, including the four replicated sampled at two different tidal states, were successfully completed.

Water sampling for TSS was performed using 5 L Niskin bottles attached to a Rosette sampler. The open bottles were lowered into the water and closed at pre-assigned depths. A CTD and external turbidity sensor was fitted to the Rosette sampler, acquiring depth, conductivity, dissolved oxygen, turbidity, pH, and temperature profile through the water column. The water sampling was acquired prior to the deployment of the DVV or grab sampler. Full details of the water sampling methodology are provided in the SS5: Benthic environmental baseline report.

#### 2.1.3.2.2 Nearshore

For the nearshore surveys, water sampling and profiling was planned at five sites. Water samples were collected at three depths (bottom, middle and top). All five planned water sampling sites were successfully sampled. Similar to the offshore surveys, water sampling was performed using a 5 L Niskin bottle, with deployment of CTD and turbidity sensors to collect water column profile data. Full details of the water sampling methodology are provided in the SS5: Benthic environmental baseline report.

### 2.1.4 Intertidal survey

An intertidal survey, extending between the Mean Low Water Springs (MLWS) and Mean High Water Springs (MHWS), was completed by Ocean Ecology Limited (OEL) at the Dounreay and Crosskirk landfall locations between 24<sup>th</sup> and 26<sup>th</sup> October 2022 (SS6: Intertidal survey habitat assessment). The survey comprised collecting high resolution Unmanned Aerial Vehicle (UAV) imagery at low water across the landfalls as well as a Phase I walk over survey to characterise the intertidal habitats and substrates. The acquired UAV imagery, were stitched together to generate ortho-mosaic and Digital Terrain Model (DTM) outputs for the intertidal survey areas (SS6: Intertidal survey habitat assessment). For the purpose of marine physical and coastal processes, the UAV imagery was used inform shoreline extents, while outputs of the Phase I walkover survey were used to inform the characteristics of the intertidal substrate.

### 2.1.5 Metocean hindcast datasets

OWPL commissioned metocean operational and extreme statistics analyses based on hindcast timeseries from three locations within the OAA. The hindcast datasets included the following:

- Hydrodynamic hindcast dataset was obtained from the MetOceanWorks European model. This data comprised 39-year (1979 – 2018) water levels, depth averaged current speed and direction hindcast data at 20-minute intervals and illustrated as Current Point 1 in Figure 2-3;
- Hydrodynamics climatology: 1-year (2010) 15-minute interval hindcast timeseries, comprising water level relative to Mean Sea Level (MSL), current speed and direction, from one location derived from the TPXO global model and illustrated as Current Point 2 in Figure 2-3;



- Hydrodynamics residuals: 10-year (2008 – 2018) daily residuals of current speed and direction from four depth layers through the water column, from two locations (separate to the hydrodynamics climatology data), derived from the HYCOM model and illustrated as Hycom 28W and Hycom 32W in Figure 2-3; and
- Waves: 37-year wave hindcast timeseries (1979 – 2015), comprising hourly waves height, period and direction from the MetOceanWorks European model and illustrated as Wave Hindcast in Figure 2-3.

All the above metocean hindcast datasets were used to inform assessments completed and presented within this technical report, from helping to characterise the environmental baseline and providing validation for the developed numerical model to enabling interpretation of the completed modelling and analyses results. The locations of the applied metocean hindcast datasets and additional data acquired from secondary sources are illustrated in Figure 2-3.

In addition to the metocean hindcast datasets introduced above, hydrodynamic climatology dataset was also acquired from Marine Scotland's Pentland Firth and Orkney Waters (PFOW) model as introduced in section 2.2. The PFOW model was created by Marine Scotland in recognition of the region's importance for marine renewable energy. The PFOW model is an implementation of the Finite Volume Community Ocean Model (FVCOM) and has a domain covering the northern Isles of Orkney and Shetland and Moray Firth. The main output from the model to date is a one year long climatology representing typical present day conditions (1990-2014). Hindcast climatology data of water levels and depth averaged current speeds were extracted from the PFOW model for 10 locations across the offshore Project area, as illustrated in Figure 2-3. Although current speeds were also available at depth layers through the water column, only the depth averaged values were used in this study.

## 2.1.6 Numerical Modelling Study

As introduced in section 1, a numerical modelling study has been completed to inform the potential for Project impacts at varying Project stages. Detailed reporting of the completed modelling is presented as Appendix A and Appendix B of this technical report. Outputs from the developed West of Orkney model were used to inform the baseline characterisation of water levels, tidal and residual flows, waves and sediment transport discussed in section 3, in addition to potential impacts from the offshore Project under the construction (section 5) and operational (section 6) stages.

To enable the analyses and assessment, 28 model extraction locations across the offshore Project area, comprising 18 and 10 within the OAA and offshore ECC respectively, were selected, as illustrated in Figure 2-4. Results and outputs were acquired from the model extraction locations at varying stages throughout the modelling process to support this marine physical and coastal processes technical report.

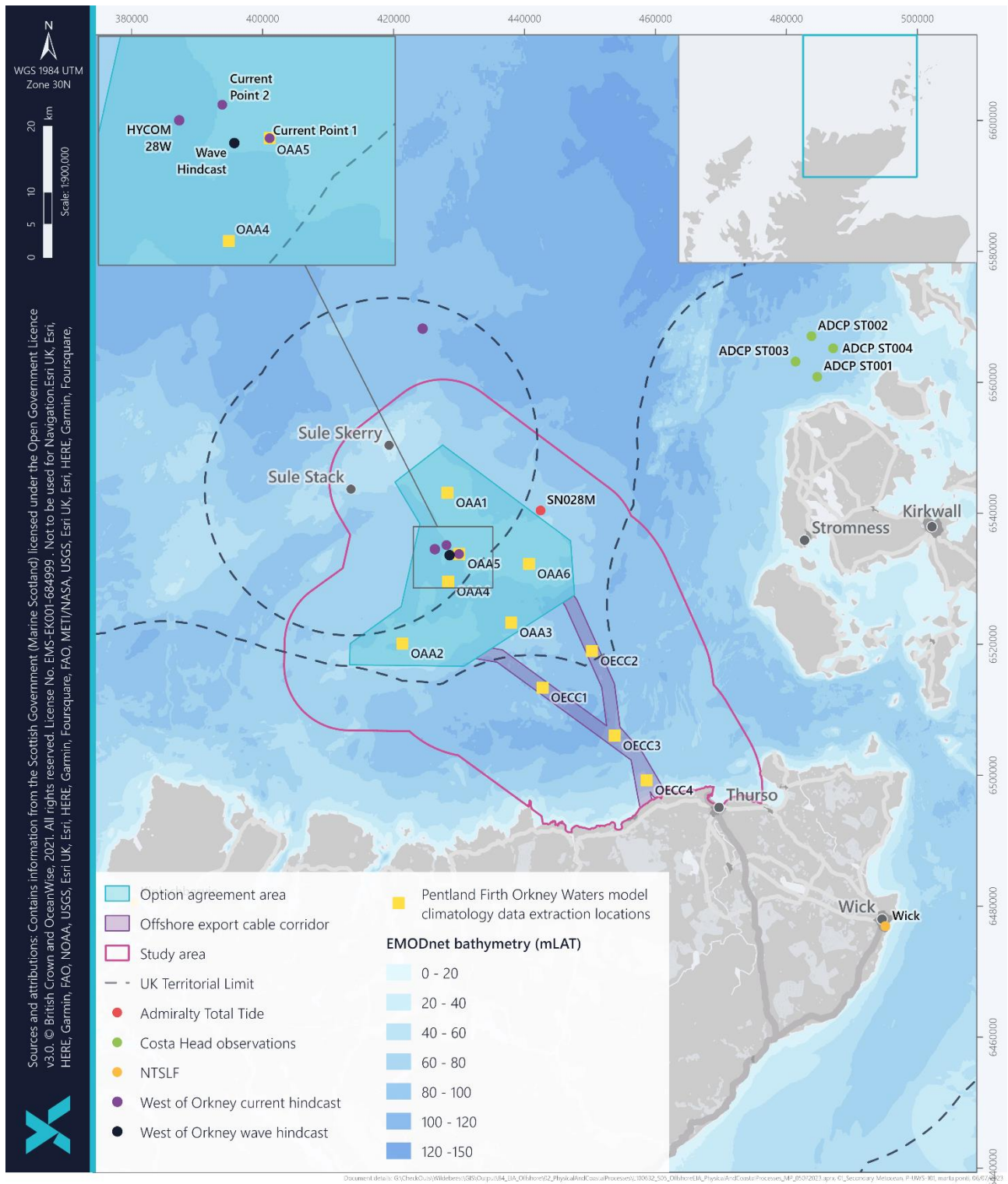


Figure 2-3 Metocean data locations used to inform the marine physical and coastal processes technical report

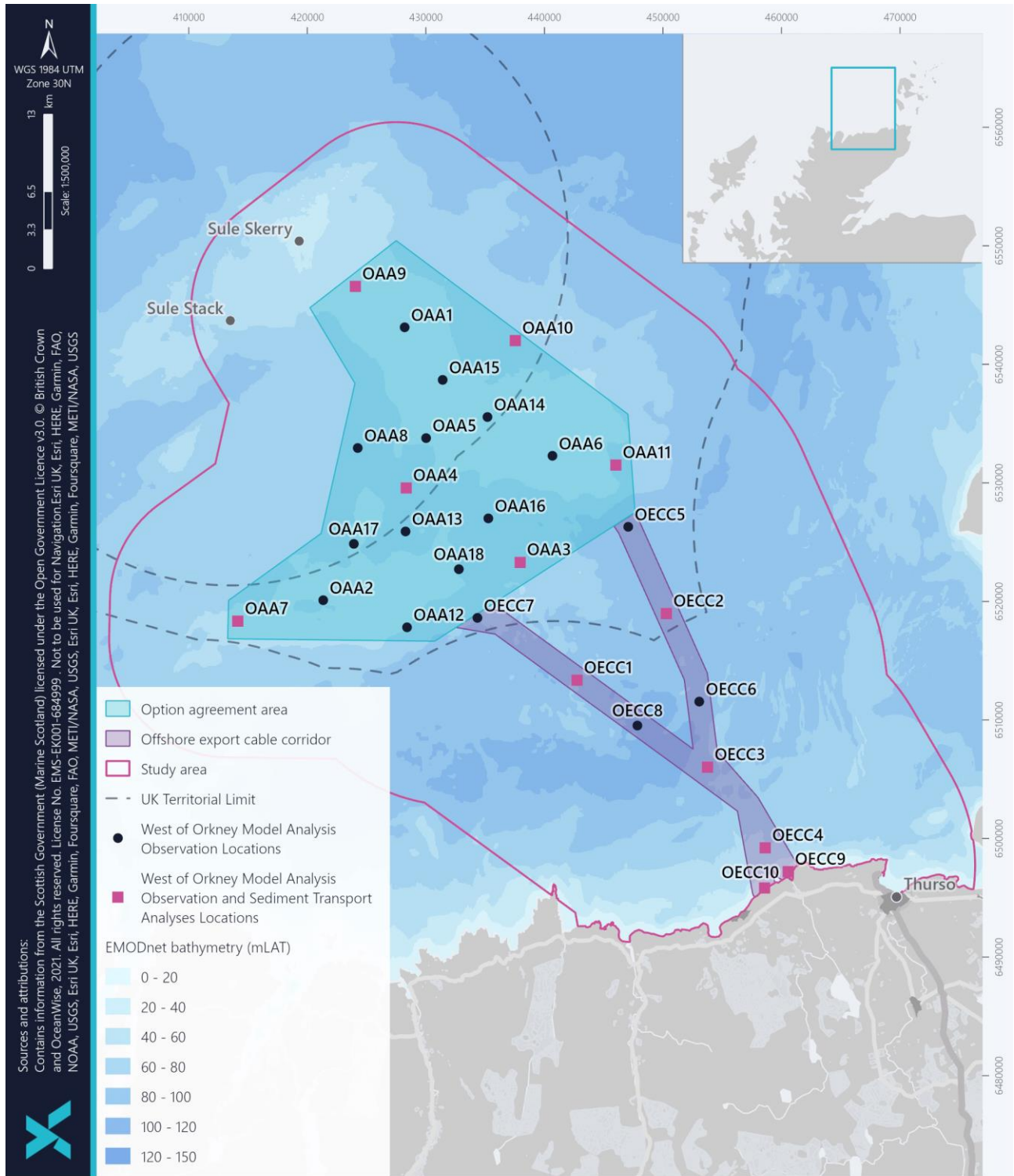


Figure 2-4 Locations across the project area, for which modelled parameters were extracted from the West of Orkney model



## 2.2 Secondary Data Sources

In addition to the site specific surveys and hindcast data acquired for the offshore Project, a number of additional secondary data sources have been used to inform this technical report as summarised in Table 2-2.

Table 2-2 Data sources used to inform the marine physical and coastal processes technical report

	Data	Source	Year
<b>General</b>	Marine Scotland Data Portal	<a href="https://marine.gov.scot/data/marine-scotland-data-portal">https://marine.gov.scot/data/marine-scotland-data-portal</a>	2023
	Marine Scotland NMPI maps	<a href="https://marinescotland.atkinsgeospatial.com/nmpi/">https://marinescotland.atkinsgeospatial.com/nmpi/</a>	2023
	Offshore Wind Energy in Scottish Waters Regional Locational Guidance	<a href="https://www.gov.scot/publications/sectoral-marine-plan-regional-locational-guidance/documents/">https://www.gov.scot/publications/sectoral-marine-plan-regional-locational-guidance/documents/</a>	2020
	Coasts and seas of the United Kingdom, Region 3 North-east Scotland: Cape Wrath to St. Cyrus	<a href="https://data.jncc.gov.uk/data/6473ed35-d1cb-428e-ad69-eb81d6c52045/pubs-csuk-region-03.pdf">https://data.jncc.gov.uk/data/6473ed35-d1cb-428e-ad69-eb81d6c52045/pubs-csuk-region-03.pdf</a>	1996
	Coastal Cells in Scotland: Cell 4 - Duncansby Head to Cape Wrath	<a href="https://www.dynamiccoast.com/files/Ramsay_Brampton_Cell_04.pdf">https://www.dynamiccoast.com/files/Ramsay_Brampton_Cell_04.pdf</a>	2000
	Dynamic Coast 2 Outputs	<a href="https://www.dynamiccoast.com/reports">https://www.dynamiccoast.com/reports</a>	2021
	Dynamic Coast 1 – Dynamic Coast - National Coastal Change Assessment: Cell 4 - Duncansby Head to Cape Wrath	<a href="https://www.dynamiccoast.com/files/reports/NCCA%20-%20Cell%204%20-%20Duncansby%20Head%20to%20Cape%20Wrath.pdf">https://www.dynamiccoast.com/files/reports/NCCA%20-%20Cell%204%20-%20Duncansby%20Head%20to%20Cape%20Wrath.pdf</a>	2017
<b>Sediments, Geology and Geomorphology</b>	British Geological Survey (BGS) Offshore GeoIndex Map	<a href="http://mapapps2.bgs.ac.uk/geoindex_offshore/home.html">http://mapapps2.bgs.ac.uk/geoindex_offshore/home.html</a>	2020
<b>Bathymetry</b>	United Kingdom Hydrographic Office (UKHO) bathymetry from the INSPIRE data portal	<a href="https://www.gov.uk/guidance/inspire-portal-and-medin-bathymetry-data-archive-centre">https://www.gov.uk/guidance/inspire-portal-and-medin-bathymetry-data-archive-centre</a>	Variable
	EMODnet Bathymetry	<a href="https://www.emodnet-bathymetry.eu/">https://www.emodnet-bathymetry.eu/</a>	2022
	Marine Scotland bathymetry: Farr Point, West and North Orkney and Pentland Firth	<a href="http://marine.gov.scot/information">http://marine.gov.scot/information</a>	Variable
<b>Waves, Flows and Water Levels</b>	Costa Head metocean, ADCP data and report	The Crown Estate Marine Data Exchange	2013
	British Oceanographic Data Centre (BODC) current metre series for a number of sites between 1971 and 2021	<a href="https://www.bodc.ac.uk/data/bodc_database/currents/search/">https://www.bodc.ac.uk/data/bodc_database/currents/search/</a>	2021



	Data	Source	Year
	National Tidal and Sea Level Facility- Observational Water Level Records	<a href="https://www.ntsfl.org/">https://www.ntsfl.org/</a>	2022
	WaveNet wave buoy data	<a href="https://wavenet.cefas.co.uk/map">https://wavenet.cefas.co.uk/map</a>	2022
	The Scottish Shelf Model. Part 2: Pentland Firth and Orkney Waters Sub-Domain	<a href="https://marine.gov.scot/information/pentland-firth-and-orkney-waters-model#:~:text=The%20Pentland%20Firth%20and%20Orkney%20Waters%20(PFOW)%20is%20an%20important,total%20Scottish%20tidal%20stream%20resource">https://marine.gov.scot/information/pentland-firth-and-orkney-waters-model#:~:text=The%20Pentland%20Firth%20and%20Orkney%20Waters%20(PFOW)%20is%20an%20important,total%20Scottish%20tidal%20stream%20resource</a>	2016
	Scottish Shelf Waters Reanalysis Service	<a href="https://tinyurl.com/SSW-Reanalysis">https://tinyurl.com/SSW-Reanalysis</a>	2020
	Pentland Firth and Orkney Waters Climatology 1.02	<a href="https://data.marine.gov.scot/dataset/pentland-firth-and-orkney-waters-climatology-102">https://data.marine.gov.scot/dataset/pentland-firth-and-orkney-waters-climatology-102</a> O'Hara and Campbell	2021
	United Kingdom Hydrographic Office (UKHO) Admiralty TotalTide	Software	2022
	SEASTATES Metocean Data and Statistics Interactive Map	<a href="https://www.seastates.net/explore-data/">https://www.seastates.net/explore-data/</a>	1979 - 2022
	UK Climate Projections (UKCP) 18	<a href="https://www.metoffice.gov.uk/research/approach/collaboration/ukcp">https://www.metoffice.gov.uk/research/approach/collaboration/ukcp</a>	2022
<b>Stratification and Frontal Systems</b>	Atlantic - European North West Shelf - Ocean Physics Analysis and Forecast	<a href="https://resources.marine.copernicus.eu/products/detail/NORTHWESTSHELF_ANALYSIS_FORECAST_PHY_004_013/INFORMATION">https://resources.marine.copernicus.eu/products/detail/NORTHWESTSHELF_ANALYSIS_FORECAST_PHY_004_013/INFORMATION</a> ( <a href="https://doi.org/10.48670/moi-00054">https://doi.org/10.48670/moi-00054</a> )	2021
	Atlantic - European North West Shelf - Ocean Physics Reanalysis	<a href="https://resources.marine.copernicus.eu/products/detail/NWSHELF_MULTIYEAR_PHY_004_009/INFORMATION">https://resources.marine.copernicus.eu/products/detail/NWSHELF_MULTIYEAR_PHY_004_009/INFORMATION</a> ( <a href="https://doi.org/10.48670/moi-00059">https://doi.org/10.48670/moi-00059</a> )	2019
	Pentland Firth and Orkney Waters Climatology 1.02	<a href="https://data.marine.gov.scot/dataset/pentland-firth-and-orkney-waters-climatology-102">https://data.marine.gov.scot/dataset/pentland-firth-and-orkney-waters-climatology-102</a> O'Hara and Campbell	2021
	BODC Conductivity Temperature Depth (CTD) Records for a number of sites between 1971 and 2021	<a href="https://www.bodc.ac.uk/data/bodc_database/ctd/search/">https://www.bodc.ac.uk/data/bodc_database/ctd/search/</a>	2019
	Frequent locations of oceanic fronts as an indicator of pelagic diversity: Application to marine protected areas and renewables.	Miller and Christodoulou	2014



	Data	Source	Year
	Emergence of Large-Scale Hydrodynamic Structures Due to Atmospheric Offshore Wind Farm Wakes	Christiansen <i>et al.</i>	2022
	Increased mixing and turbulence in the wake of offshore wind farm foundations	Schultze <i>et al.</i>	2020
	Anthropogenic Mixing in Seasonally Stratified Shelf Seas by Offshore Wind Farm Infrastructure	Dorrell <i>et al.</i>	2022
	Potential Impacts of Offshore Wind Farms on North Sea Stratification	Carpenter <i>et al.</i>	2016
	Unstructured grid modelling of offshore wind farm impacts on seasonally stratified shelf seas	Cazenave <i>et al.</i>	2016
<b>Coastal Morphology</b>	Scottish Government Dynamic Coast: Scotland's National Coastal Change Assessment Map	<a href="https://www.dynamiccoast.com/webmaps">https://www.dynamiccoast.com/webmaps</a>	2017
	Dynamic Coast 2	<a href="https://snh.maps.arcgis.com/apps/webappviewer/index.html">https://snh.maps.arcgis.com/apps/webappviewer/index.html</a>	2020



## 3 BASELINE CHARACTERISATION

### 3.1 Designated sites

There are a number of designated sites in the wider marine environment of Orkney and the Pentland Firth with designated features which are of interest to marine physical and coastal processes. The designated sites and associated features of interest that intersect the study area (with respect to the OAA and offshore ECC) and those raised through consultation are summarised in Table 3-1 and illustrated in Figure 3-1. The identified sites include Special Areas of Conservation (SAC), Sites of Special Scientific Interest (SSSI) and Geological Conservation Review (GCR) sites (JNCC, 2019). Special Protected Areas (SPA) are also included in the list, although marine seabirds are not direct features of interest to the marine physical and coastal processes receptors.

As agreed through a consultation meeting held 29<sup>th</sup> June 2022 and subsequent meeting minutes comments (received 22<sup>nd</sup> September 2022) (OWPL, 2022b), the North-West Orkney Nature Conservation Marine Protected Area (NCMPA) is excluded from further assessment as it does not overlap with the study area and designated features are over 20 km away from the offshore Project area.

Table 3-1 Designated sites and associated interest features that intersect the study area

SITE NAME	DESCRIPTION OF SITE	INTEREST FEATURE	DISTANCE TO OFFSHORE PROJECT AREA
<b>Red Point Coast SSSI</b>	Red Point Coast SSSI is a 6 km stretch of coast between Sandside Bay in Caithness and Melvich Bay in Sutherland. The site is located to the west of Sandside Bay and is nationally important for geology, coastal vegetation and colonies of breeding seabirds. (NatureScot, 2009a; 2009b; 2009c). The coastline along this site is not considered to be erodible (Dynamic Coast, 2021), with the maritime cliff interest feature mostly affected by terrestrial factors.	Quaternary of Scotland (Non-marine Devonian) Maritime cliff	4.6 km
<b>Sandside Bay SSSI</b>	Sandside Bay SSSI lies just north of Reay, on the north coast of Caithness. The site is located to the west of the offshore ECC and covers the entire area of Sandside Bay. The site is comprised of two parts; the main part of the site includes the foreshore, dunes, dune slacks and the banks of the Burn of Isauld (NatureScot, 2008d; 2008e). The second part of the site, known locally as the Sahara, is an area of herb-rich grassland within Reay Golf Course.	Sand dunes	3.7 km



SITE NAME	DESCRIPTION OF SITE	INTEREST FEATURE	DISTANCE TO OFFSHORE PROJECT AREA
<b>Ushat Head SSSI</b>	Ushat Head SSSI is a low exposed headland, on the north coast of Caithness, adjacent to the Crosskirk landfall. It is of particular botanical importance for its maritime heath, which is a northern, species rich type of heathland that is found only in Caithness, Sutherland and Orkney. There is a good representation of species-rich maritime heath communities in a mosaic with maritime grassland (NatureScot, 2008c). The vegetation within this site is known to have developed in relation to sea spray occurring.	Maritime cliff	Adjacent to the offshore ECC (at the landfall)
<b>Dunnet Head SSSI</b>	Located on the north coast of Caithness east of the offshore ECC landfall, the site is designated for the nationally important coastal vegetation and breeding seabirds (NatureScot, 2010b). Maritime cliff vegetation grows in a narrow strip along the cliff tops and on some of the cliff ledges. Species-rich maritime heath grows in a mosaic with maritime grassland on the cliff tops. The cliff ledges support a range of plant species which thrive close to the sea. Negative pressures on this site are in relation to livestock grazing activities.	Maritime cliff	10.5 km
<b>Pennylands SSSI</b>	Pennylands SSSI is located on the foreshore between Thurso and Scrabster on the north coast of Caithness. The site has been notified due to the exposure of a sequence of layers of sedimentary rocks which contain both fossil fish and evidence of the geography and environment in which the fish lived. These rocks were deposited around 380 million years ago during the Middle Devonian geological era (NatureScot, 2008a). The site and interest feature are considered to be in a favourable maintained condition and are not believed to be exposed to any negative pressures..	Non-marine Devonian	7 km
<b>Holborn Head SSSI</b>	Holborn Head SSSI lies east of the offshore ECC. The site covers 4.5 km of coast west of the lighthouse at Scrabster. The site is designated for its nationally important Middle Devonian fossil fish and coastal vegetation, with terrestrial factors influencing its condition (NatureScot, 2009d).	Maritime cliff	4 km



SITE NAME	DESCRIPTION OF SITE	INTEREST FEATURE	DISTANCE TO OFFSHORE PROJECT AREA
<b>Strathy Coast SSSI</b>	Strathy Coast SSSI covers a section of the north Sutherland coast centred around Strathy Point, west of the offshore ECC landfall. It comprises north, east and west facing cliffs, interrupted by beach systems at Armadale, Strathy and Melvich. The site is notified for the nationally important maritime cliff, sand dune, machair and salt marsh habitats found along the coast and for the assemblage of rare plants. It is also notified for the Moine rocks around Portskerra (NatureScot, 2010a). Pressures on the sites and some interest features are noted as being terrestrial.	Maritime cliff Saltmarsh Sand dunes Moine Machair	11.8 km
<b>Strathy Point SAC</b>	Strathy Point SAC is a terrestrial designated site along the headland of Strath Point. The SAC is an important example of northern, hard acidic rock cliffs, subject to extreme wind and wave exposure, which contribute the diverse vegetation communities. As a result, the vegetated sea cliffs are considered to be one of the best representative areas of vegetated sea cliffs of the Atlantic and Baltic coasts in the UK. . The vegetated sea cliff interest feature is considered to be in favourable maintained condition, with the primary negative pressures being from over grazing and a lack of proactive management (NatureScot, 2019).	Vegetated sea cliffs	16.4 km
<b>Red Point GCR</b>	The site provides the best example of Middle Devonian lake-margin deposits associated with an unconformity in Scotland (JNCC, 2019). In this area, the Orcadian Basin lake lapped against the metamorphic basement. Features formed at this lake-margin include unusual (possibly algal) limestones draping the sides of the exhumed hill of metamorphic rock, and small beach-ridges of angular gravel derived from the basement. The vertical extent of the limestones indicates the large fluctuations there must have been in lake-level within short periods of time. The rapid transition from the basement hill to the flat-bedded flagstones, typical of the main lake, is of importance and this is a facies unique to the Orcadian Basin (JNCC, 2019).	Non-marine Devonian	6.8 km



SITE NAME	DESCRIPTION OF SITE	INTEREST FEATURE	DISTANCE TO OFFSHORE PROJECT AREA
<b>Drumhollistan GCR</b>	Geological sedimentary units demonstrating key Quaternary of Scotland deposits, particularly the Quaternary stratigraphy of Caithness and comprising two till units (of varying origin) separated by a layer of sand and gravel. The sediment provide evidence for the pattern of ice movements in Caithness and the interaction between two separate ice masses of local and external origin. The age(s) of the tills is uncertain, and the site has important research potential.	Quaternary of Scotland	8.2 km
<b>Sgeir Ruadh Portskerra GCR</b>	Exposures of the quartzose Moine gneisses, amphibolite and several generations of granite. It is the northernmost part of the Strath Halladale migmatite-granite complex, with examples of unconformable contact with the overlying Old Red Sandstone breccias and sandstones. At least three different ages of granites can be recognised within this site with a clear exposition of relationships within the Strath Halladale migmatite-granite complex. The fine development of the Old Red Sandstone overlying the unconformity is itself of first rate importance. The deposits demonstrated in this GCR are rarely seen inland due to very poor exposure in critical areas. The greatest significance attaches to the red granitic sheets, which are believed to be part of the Strath Halladale granite dated at 649±30 Ma. This is crucially important as it represents the proof of the late Precambrian and Caledonian (sl) granites cutting the earlier (mid-Proterozoic) migmatite complex which is developed throughout east Sutherland (JNCC, 2019).	Moine	11.6 km
<b>Holborn Head Quarry GCR</b>	Large quarry with evidence of middle Devonian, Givetian, lacustrine sediments from the Ham-Scarfskerry Subgroup of the Upper Caithness Flagstone Group. The deposit contains large evidence of fossil fish and is the best site to collect <i>Osteolepis panderi</i> which makes up the largest percentage of the fauna here. The deposit is largely unexposed just beneath the quarry floor (JNCC, 2019).	Silurian - Devonian Chordata	4.4 km



SITE NAME	DESCRIPTION OF SITE	INTEREST FEATURE	DISTANCE TO OFFSHORE PROJECT AREA
<b>Pennyland GCR</b>	Occurs along the coast as a section of Old Red Sandstone (Upper Givetian) sediments and contains several fish beds. The sequence of sediment in this GCR demonstrates the transition from the mainly lacustrine Mey Subgroup of the Upper Caithness Flagstone Group to the predominantly fluvial John o'Groats Sandstones, which is usually faulted out in Caithness. It is also the richest remaining occurrence and well preserved of the <i>Millerosteus</i> minor geological sub-group (JNCC, 2019). Fossil fauna assemblages that occur here can be compared with species from the Baltic.	Silurian - Devonian Chordata	7.1 km
<b>Pennyland to Castlehill (Thurso-Scrabster) GCR</b>	A well-exposed section through the topmost part of the Middle Devonian Caithness Flagstones and the transition to the predominantly fluvial John o'Groats Sandstone. The section shows a variety of interbedded, mainly shallow-lake sediments with a few fish beds, and several sand bodies (possibly of both fluvial and aeolian origin). This example of a sand-rich flagstone sequence from a more marginal part of the basin contrasts with sections at Wick and Stromness. It occurs in a critical, often poorly-exposed, part of the Middle Old Red Sandstone succession, with the potential to extend knowledge of the Orcadian Basin environments and palaeogeography (JNCC, 2019).	Non-marine Devonian	7.1 km

Of the range of designated sites with maritime or vegetated sea cliffs interest features that intersect the applied marine physical and coastal processes study area as detailed in Table 3-1, only the Ushat Head SSSI directly borders the offshore Project area. For the other designated sites comprising the Red Point Coast SSSI (NatureScot, 2009a), Dunnet Head SSSI (NatureScot, 2010b), Holborn Head SSSI (NatureScot, 2009d), Strathy Coast SSSI (NatureScot, 2010a) and Strathy Point SAC (NatureScot, 2019), the sites are either considered to be in a favourable condition or the pressures are from terrestrial factors such as grazing. For these designated sites that do not directly overlap the offshore Project area, but intersect the applied study area, there is not considered to be a pathway for impacts to the interest features within the designated sites, due to their terrestrial control. Therefore, the SSSIs' and one SAC are not considered further in this study. The only designated site with the maritime or vegetated sea cliffs interest feature that is considered to be relevant is the Ushat Head SSSI, due to its proximity with the offshore Project area.

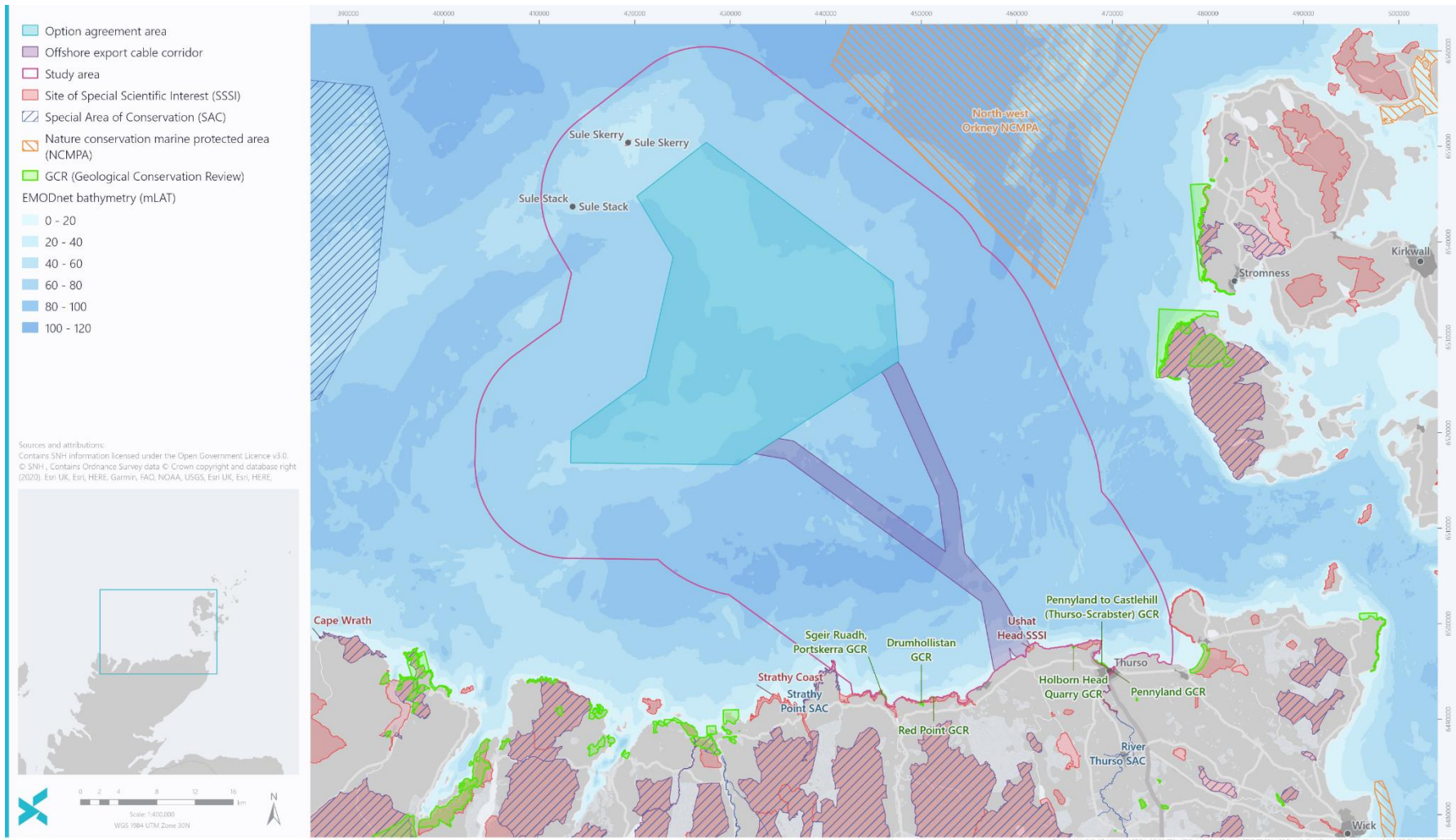


Figure 3-1 Designated sites and associated features of interest that intersect the study area



## 3.2 Bedrock Geology

### 3.2.1 Overview

The wider Pentland Firth and Orkney waters area is recognised as being rich in geodiversity, containing a variety of seabed features which contribute to both natural resources and heritage (Scottish Government, 2016). The bedrock geology of the north and northwest Scottish continental shelf (Figure 3-2) predominantly comprises Mesozoic interbedded Permian-Triassic sedimentary rocks, interspersed with Pre-Cambrian metamorphic rocks (such as the Nun Rock – Sule Skerry High) and Palaeozoic sedimentary Devonian undifferentiated siltstone and mudstone, which occurs near the Scottish coast and across the Orkney Islands (BGS 1981; 1989). The Permian-Triassic bedrock within the region is described as a conglomerate of undifferentiated sandstone, siltstone and mudstone with evaporites. Across the region, bedrock depth varies between outcropping rock to depths of tens of metres. Bedrock depths relevant to the study area are described further in Section 3.2.2.

### 3.2.2 Offshore Project Area

The offshore Project area is largely located within the Stormy Bank Basin. As introduced for the northwest continental shelf (Section 3.2.1), the bedrock across the offshore Project area and study area primarily comprises Permian-Triassic undifferentiated sandstone, siltstone and mudstone with evaporites occurring over most of the OAA and offshore ECC, with Devonian mudstone and siltstone occurring closer to the coast, on approach to landfall (Figure 3-2) (BGS, 1981; 1989).

Bedrock depths are informed by BGS borehole records. Two historical BGS borehole cores records are located west of the OAA (BH72/28 and BH73/31), within approximately 3 km of the OAA boundary. Borehole BH73/31 recorded between 28 m and 36 m of Quaternary sediments before transitioning to bedrock which consists of soft, friable, well sorted dark red sandstone, while the other was unsuccessful as the material disintegrated on retrieval (Institute of Geological Sciences, 1972a). At greater depths, the sandstone was interbedded with occasional mudstone films. The consistency of the sand making up the red sandstone was described as subangular rounded with occasional coarser grains (Institute of Geological Sciences, 1972b). Closer to the offshore ECC, a further BGS borehole (BH72/27), in a water depth of 84 m and approximately 7 km from the coast, noted that the depth of overlying sediment was to a depth of approximately 18 m before bedrock was recorded. BGS information describe the bedrock was described as red, soft, friable sandstone with occasional hard bands. The material was so soft that it was difficult to recover and collapsed to fine sand upon retrieval (Institute of Geological Sciences, 1972c). Other BGS and borehole and core evidence (Institute of Geological Sciences, 1972d) indicate the prevalence of sandstone bedrock as indicated in solid geology charts (BGS, 1981; 1989).

Quaternary sediment characteristics are described further in Section 3.3. However, BGS data indicate that bedrock occurs between 5 m and over 50 m below the surficial Quaternary and seabed sediments across the majority of the offshore Project area. BGS data indicates that within the OAA, although bedrock can occur at depths of 5 m below the seabed, bedrock depths mainly range between 20 m and 50 m, while along the offshore ECC, bedrock depths are typically between 5 m and 20 m (Figure 3-5).

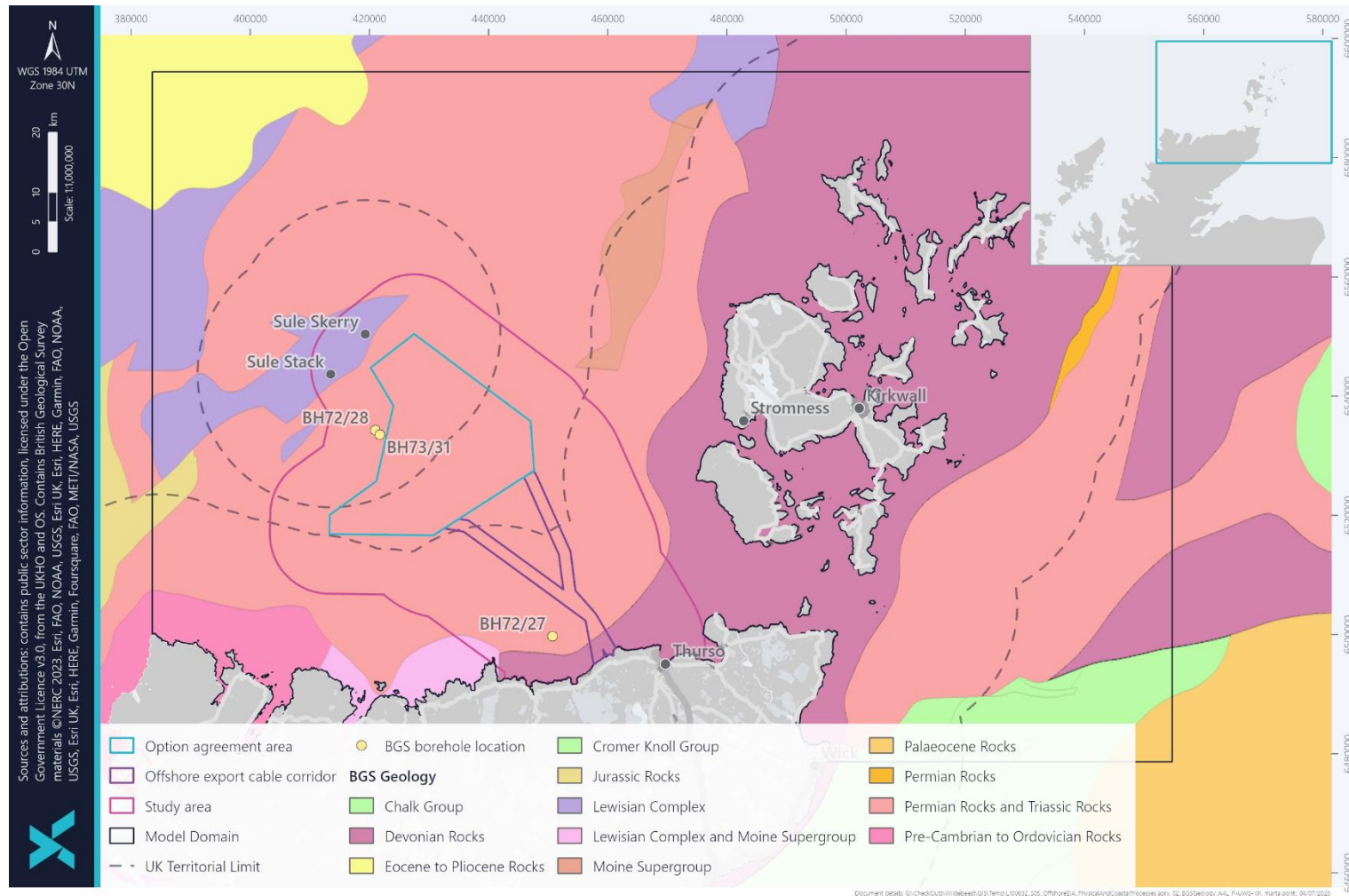


Figure 3-2 BGS bedrock geology (BGS 2022)



Shallow geology geophysical survey results (through SBP and UHRS) indicate the presence of bedrock (identified as Unit U50 in Ocean Infinity (2023a; 2023b; 2023c)) at depths of less than 10 m below the seabed across a large proportion of the OAA and offshore ECC. In isolated locations across the OAA and offshore ECC, the bedrock is noted as outcropping and exposed at the seabed surface. The geophysical survey of the OAA defined the top of the bedrock geology as the bottom of all surficial sediment deposits. The top of the bedrock varied from 0 m (where overlying sediments were absent and the bedrock was exposed) to 133.7 m below the seabed. The depth of sediment cover in relation to the underlying bedrock is shown in Figure 3-3. Vibrocore and CPT samples from across the offshore Project area, acquired during site-specific geotechnical surveys, further indicate bedrock occurring at varying depths, from surface exposures to depths well below the potential cable burial depth within the offshore ECC (Ocean Infinity, 2023d) and in some instances, over 100 m below the seabed (Ocean Infinity, 2023a; 2023b; 2023c), as illustrated in Figure 3-3.

Overall, the depth below seabed of the top of the bedrock in the main area is greater in the east of Stormy Bank shallowing towards the north of Whiten Head Bank. The top of bedrock surface is an angular conformity in most instances. In particular, in the north of Whiten Head Bank, the bedrock appears to be outcropping at or close to the seabed (Ocean Infinity, 2023a). The bedrock depth data in Figure 3-3 corresponds well with the BGS data in Figure 3-5 which shows shallower bedrock occurring along the westernmost edge of the OAA and at much deeper depths along the eastern margin of the OAA (Ocean Infinity, 2023a). From site-specific surveys across the offshore ECC, bedrock was determined to be at depths of less than 10 m below the seabed for large proportions of the offshore ECC, with frequent outcropping on approach to the landfalls (Ocean Infinity, 2023b; 2023c), as illustrated in Figure 3-3. Nearshore site-specific geophysical investigations across the landfall locations, identified that bedrock consists of Devonian sandstones comprising the Crosskirk Bay formation, which dips to the northwest. The nearshore surveys indicate the presence of outcropping bedrock at the landfalls (Spectrum, 2023) and this is likely to continue through the intertidal, where the intertidal surveys completed by Ocean Ecology (SS6: Intertidal survey habitat assessment) identified rocky substrates and associated habitats.

Overlying the bedrock across the offshore Project area are intermittent and varied deposits all comprising Quaternary glacial till, which is described further in section 3.3.





## 3.3 Quaternary Geology and Seabed Sediment

### 3.3.1 Overview

The Quaternary deposits across the northwest Scottish continental shelf, illustrated in Figure 3-4, are varied and considered to be predominantly undifferentiated, with diamict occurring further offshore (BGS, 2022). There is little recent sediment input to the continental shelf in this area – the modern seabed environment represents the rework by currents of the topography and sediments which originated during former glacial periods (DECC, 2016a). The seabed across the study area is dominated by a succession of Quaternary sandy deposits overlying glacial till. The glacial till overlays the top of sandstone and mudstone bedrock geology (BGS, 2022). The thickness of Quaternary deposit range between no deposit (i.e. in locations of outcropping bedrock), to up to 100 m thick (BGS, 1989b).

Seabed sediment across the northwest continental shelf is dominated by coarse sediment varying between sand and gravel sediment, with large regions of gravelly sand (and variations of this) and sandy gravel illustrated in Figure 3-6 (BGS, 2022).

### 3.3.2 Offshore Project Area

#### 3.3.2.1 Quaternary Sediment

The Quaternary deposits present within the offshore Project area and study area are predominantly undifferentiated, with a small area of diamict in the north of the OAA (Figure 3-4). As described for the northwest Scottish continental shelf, the Quaternary deposits mainly comprise Holocene sandy units overlying and lower Quaternary glacial till, which is also true for the offshore Project area. Based on site-specific geophysical surveys across the OAA and offshore ECC, Quaternary deposit thickness is predicted to be highly variable, and up to 133.7 m thick in places associated with bank features (Ocean Infinity, 2023a; 2023b; 2023c; 2023d). Thickness of Quaternary deposits across the study area, with additional information on thickness of varying Quaternary sediment units identified across the offshore Project from the site-specific geophysical and geotechnical surveys (Ocean Infinity, 2023a; 2023b; 2023c; 2023d) are illustrated in Figure 3-5.

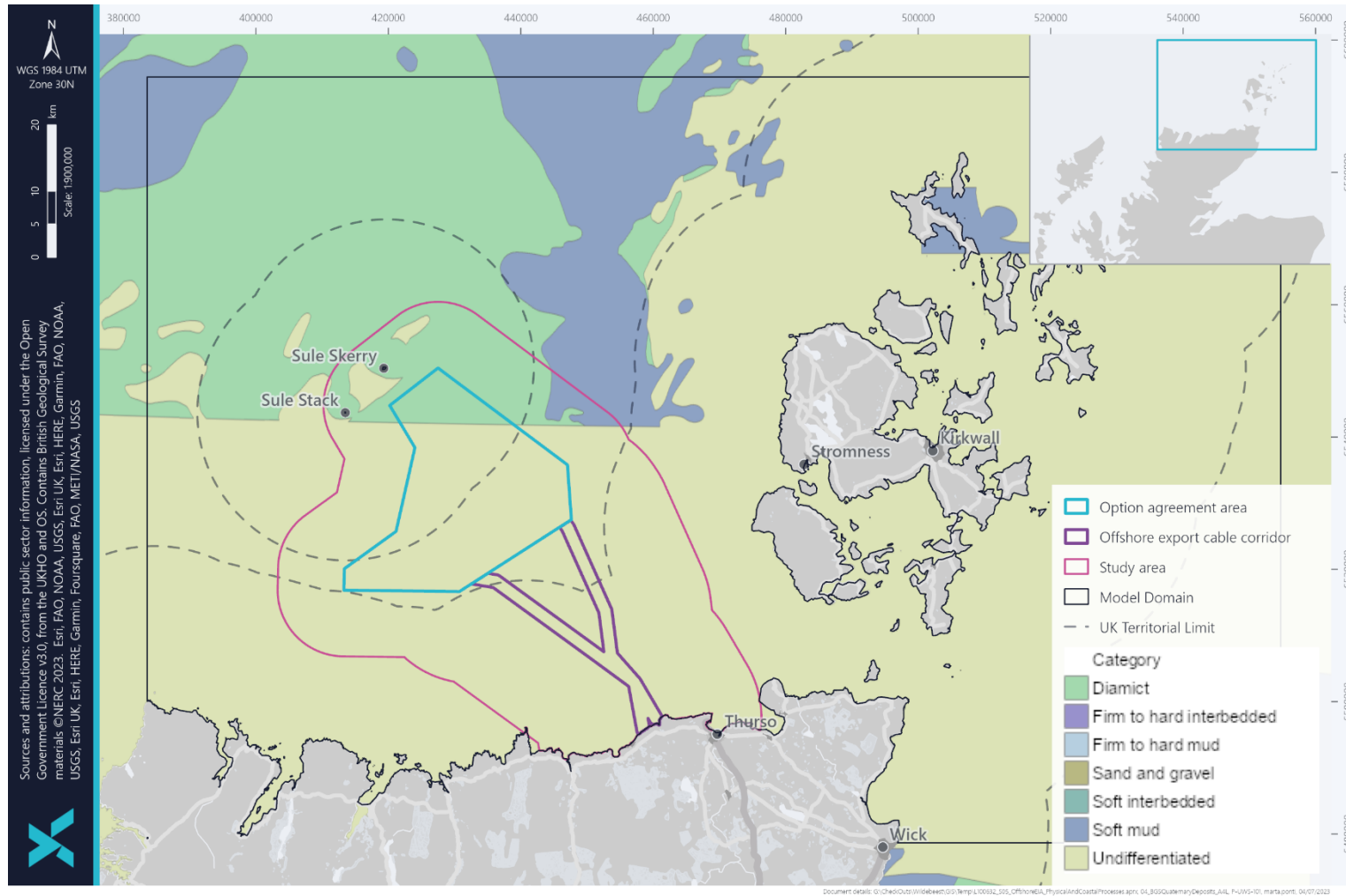


Figure 3-4 Quaternary deposits in the offshore Project and study area (BGS, 2022)



Site specific geophysical data determined that there were a number of Holocene (Quaternary) deposit units within the OAA, which varied in thickness across the site. The uppermost deposit later ranged from 0 m (where absent) to a maximum thickness of 11.4 m (associated with the Stormy Bank). Geomorphological features, such as megaripples (see section 3.5), are associated with this uppermost layer of sediments, as this top unit was comprised of sand and gravel-rich sediments, identified as Unit U01A in geophysical surveys and Figure 3-5 (Ocean Infinity, 2023a). The secondary unit below, was also a Holocene deposit which reached thicknesses of up to 10 m, this is identified and illustrated as Unit U01B in Figure 3-5. This unit represented unconsolidated sediments recently deposited after the Last Glacial Maximum, predominantly composed of muddy and silty sands and restricted to small, isolated areas on Stormy Bank and Whiten Head Bank. A third, and final, Holocene unit had thicknesses of up to 17.3 m. This unit is the final unit above the lower glacial till deposits. This Holocene layer is found relatively extensively in areas associated with the bank features within the OAA (Ocean Infinity, 2023a) and is illustrated as Unit U01C in Figure 3-5. Below the Holocene sediments is a layer of irregular glacial till which often outcrops within the OAA (i.e. Unit U02 in Ocean Infinity (2023a)). These outcrop ridges often exhibit a rounded, mound-like morphology and are associated with cobbles and boulders on the ridge crests. This geological layer is associated with the boulder fields described throughout the site. Often, the depressions in this irregular geological lower Quaternary glacial till unit are filled with pockets of Holocene sediments (Ocean Infinity, 2023a). Distribution of seabed sediment from BGS information and site-specific surveys are represented in Figure 3-6, while backscatter data, indicating the extent of coarse seabed deposits is shown in Figure 3-7.

Quaternary deposits overlying the bedrock around through the offshore ECC and Crosskirk Bay (comprising the Crosskirk and Greeny Geo landfalls) are dominated by Devensian glacial till. The till is made up of a number of lesser formations which are described as largely clayey with clasts of siltstone, sandstone and some mudstone (Spectrum, 2023). This is reflected in the composition of the seabed substrate which indicates that rocks and boulders are found along the nearshore area before slowly transitioning to coarse sediment as the water deepens. While these coarse deposits are the only superficial deposits expected in the area, fluvial deposits originating from local water courses may also be present (Spectrum, 2023). The thickness of Quaternary deposit based on BGS information, along with interpreted unit thickness from the site specific surveys also illustrated Figure 3-5 for the offshore ECC. At the coast and directly offshore of the Crosskirk landfall, the site-specific survey data identified an area of thick sediment deposits located approximately 1 km offshore from the Crosskirk landfall location. This deposit is up to 13 m thick at the most (Spectrum, 2023) and may be indicative of a morphological bedform. This, and other morphological features are described in Section 3.5. Unlike the Crosskirk landfall, no thick sedimentary units are noted towards the Greeny Geo landfall. Instead the Quaternary units at this landfall are characterised by much of what has previously been described across most of the OAA and offshore ECC but occurring at smaller thicknesses below the seabed.

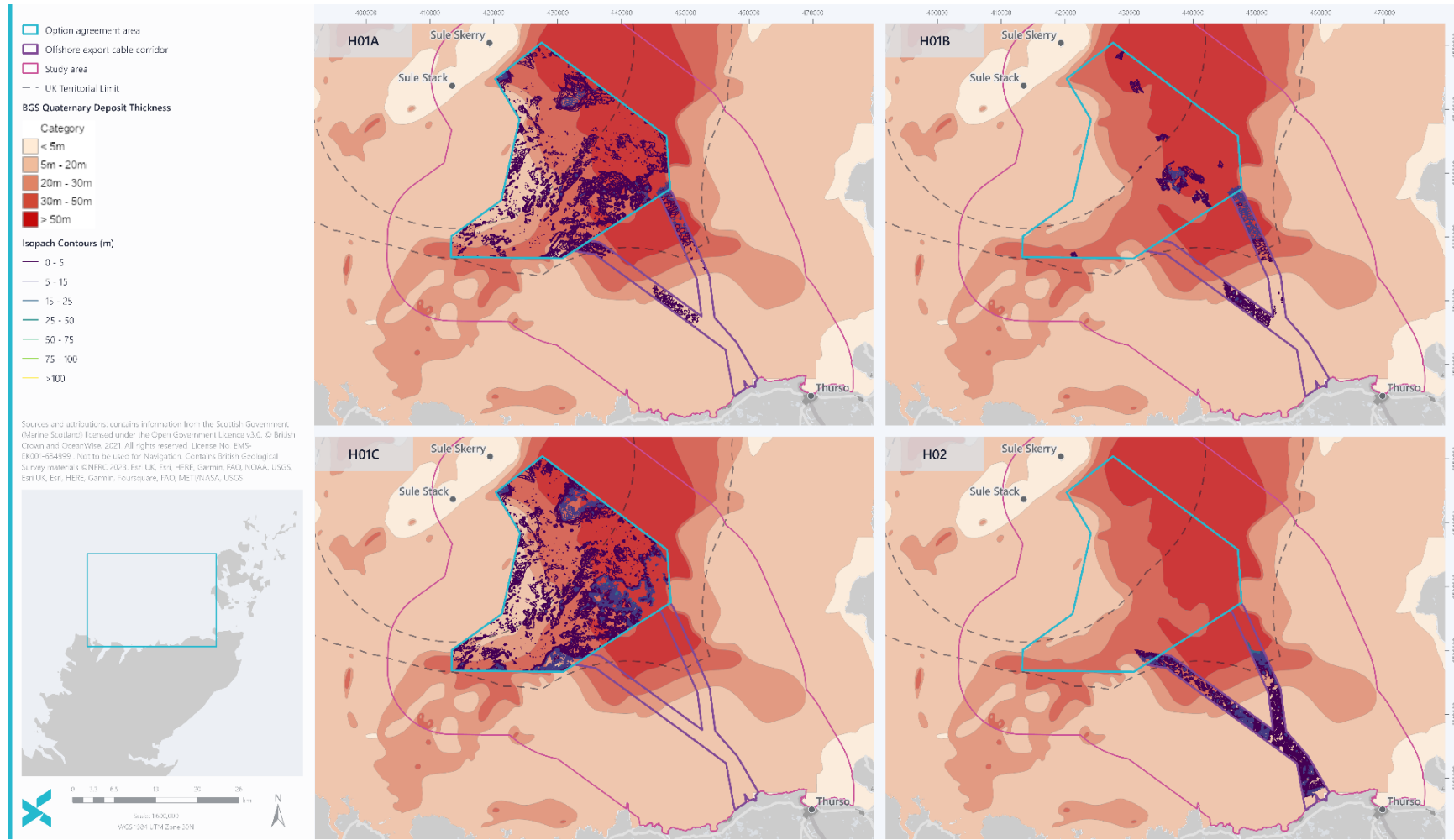


Figure 3-5 Thickness of Quaternary deposits in offshore Project and study area (BGS, 2022)



### 3.3.2.2 Surficial Seabed Sediment

Surficial sediment, which comprises Holocene units of loose non-cohesive sediment, overlying Quaternary glacial till, is widely distributed across the offshore Project area. Within the offshore Project area and study area, surficial seabed sediment is mostly of sandy nature with the following typologies being present, as indicated by BGS seabed sediment (BGS, 2022) and site-specific environmental surveys (Ocean Infinity, 2023b; 2023c; and SS5: Benthic environmental baseline report):

- Gravelly sand;
- Slightly gravelly sand;
- Sand; and
- Sandy gravel.

BGS (2022), however, indicates a dominance of gravelly sand across the OAA and slightly gravelly sand across the offshore ECC (Figure 3-6). Particle size analysis (PSA) conducted for the seabed samples taken across the offshore Project area and superimposed on the BGS data is also illustrated in Figure 3-6. Information from the site-specific environmental survey confirmed that the seabed sediment across the offshore Project area mainly comprises a coarse sediment fraction, with marginally more fine sediment occurring within the offshore ECC, although mean grain sizes were highly variable (see SS5: Benthic environmental baseline report). Also present, as interpreted from site-specific information from geophysical surveys and confirmed through environmental sampling, is the frequent occurrence and wide distribution of cobbles (i.e. 64-75 mm) and boulders (measuring >75 mm). These cobbles and boulders commonly occur as “fields” across the offshore Project area, but also as isolated targets identified in geophysical surveys. The properties of the potential mobile sediment fraction and larger cobble and boulder deposits are each considered further in the following sections.

#### 3.3.2.2.1 Mobile sediment fraction particle size distribution

Over the years, the BGS database has accumulated sediment sample information taken during multiple surveys. PSA has been conducted on sediment grab samples, many of which have been taken within the study area. The findings of the PSA show that throughout the OAA, sediments are mostly gravelly sand, slightly gravelly sand and gravelly muddy sand (Figure 3-6). Along the offshore ECC, the number of samples which were classed as sand increases, compared to the OAA as illustrated in Figure 3-6. This is consistent with the findings of the site-specific environmental survey PSA (less than cobble and boulder size) undertaken within the OAA and along the offshore ECC (see SS5: Benthic environmental baseline report), illustrated in Figure 3-6 and Table 3-2. An overview of the PSA results from the offshore Project area is shown in Figure 3-7 over the backscatter information, which indicates the areas of coarser sediment on the seabed surface.

Across the 70 samples obtained from the offshore Project area (34 from the OAA, 18 and 13 from the western and eastern offshore ECC respectively and three in the nearshore area), sediments were recorded as ranging from fine sand with a mean size of 0.12 mm (at sample S62 midway along the offshore ECC), to medium gravel with a mean size of 11.12 mm (at sample S36 in the middle of the OAA). The overall mean sediment size within the offshore Project area was 1.50 mm, which is classed as very coarse sand (SS5: Benthic environmental baseline report). Within the OAA specifically, the mean sediment size was 2.21 mm. Most samples were described as being medium or coarse sand or



very fine/fine gravels. Only one sample was classed as medium gravel (sample S36). Along the offshore ECC, generally sediment sizes were smaller, with an average size of 0.80 mm. Sediments along the offshore ECC ranged from fine sand to fine gravel, which occurred at one sample station (sample S54) close to the OAA. In the nearshore area, average sediment size was around 0.5 mm, i.e. medium to coarse sand. Within individual samples, the sediment composition and proportion of sediments of different sizes varied (i.e. sediment fractions) varied considerably. Sand of varying sizes is present in all samples from across the offshore Project area at varying proportions, with gravel, silt and finer sediment also occurring at lower proportions and less frequently (Table 3-2). As a result, sediments across the whole offshore Project area were generally classed as poorly to moderately sorted, with only a few stations being moderately well sorted (SS5: Benthic environmental baseline report).

Table 3-2 Summary of particle size distribution based on site-specific environmental survey (SS5: Benthic environmental baseline report)

Sediment fraction	Grain Size Range (mm)	Median Grain Size (mm)	OAA		Offshore ECC (including nearshore)	
			Percentage Occurrence Across Samples (%)	Maximum Content Within Samples (%)	Percentage Occurrence Across Samples (%)	Maximum Content Within Samples (%)
Very Coarse Gravel	32 - 64	48	15%	43.1%	8%	27.2%
Coarse Gravel	16 - 32	24	47%	40.5%	31%	23.9%
Medium Gravel	8 - 16	12	68%	23.7%	50%	12.2%
Fine Gravel	4 - 8	6	79%	39.5%	81%	22.0%
Very Fine Gravel	2 - 4	3	100%	33.3%	92%	39.8%



			OAA		Offshore (including nearshore)	ECC (including nearshore)
<b>Very Coarse Sand</b>	1 - 2	1.5	100%	47.5%	97%	69.2%
<b>Coarse Sand</b>	0.50 - 1	0.75	100%	43.6%	100%	54.9%
<b>Medium Sand</b>	0.25 - 0.50	0.35	100%	69.0%	100%	57.7%
<b>Fine Sand</b>	0.063 - 0.250	0.157	99%	23.3%	100%	60.5%
<b>Coarse Silt</b>	0.016 - 0.063	0.039	88%	0.4%	89%	1.8%
<b>Medium Silt</b>	0.008 - 0.016	0.012	88%	0.5%	86%	2.0%
<b>Fine Silt</b>	0.002 - 0.008	0.004	88%	0.4%	86%	1.3%

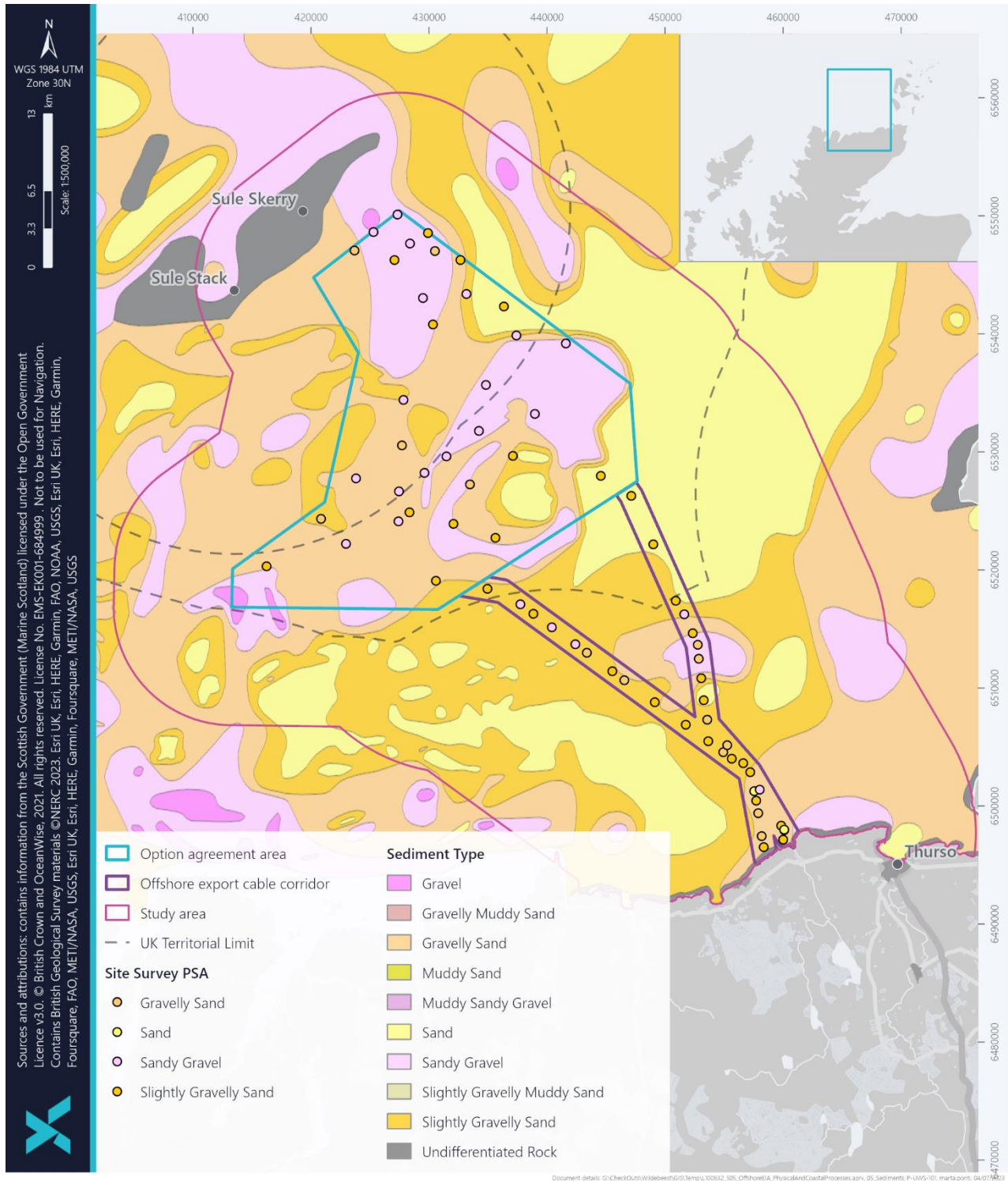


Figure 3-6 Seabed sediments in the offshore Project and offshore study area (BGS, 2022)

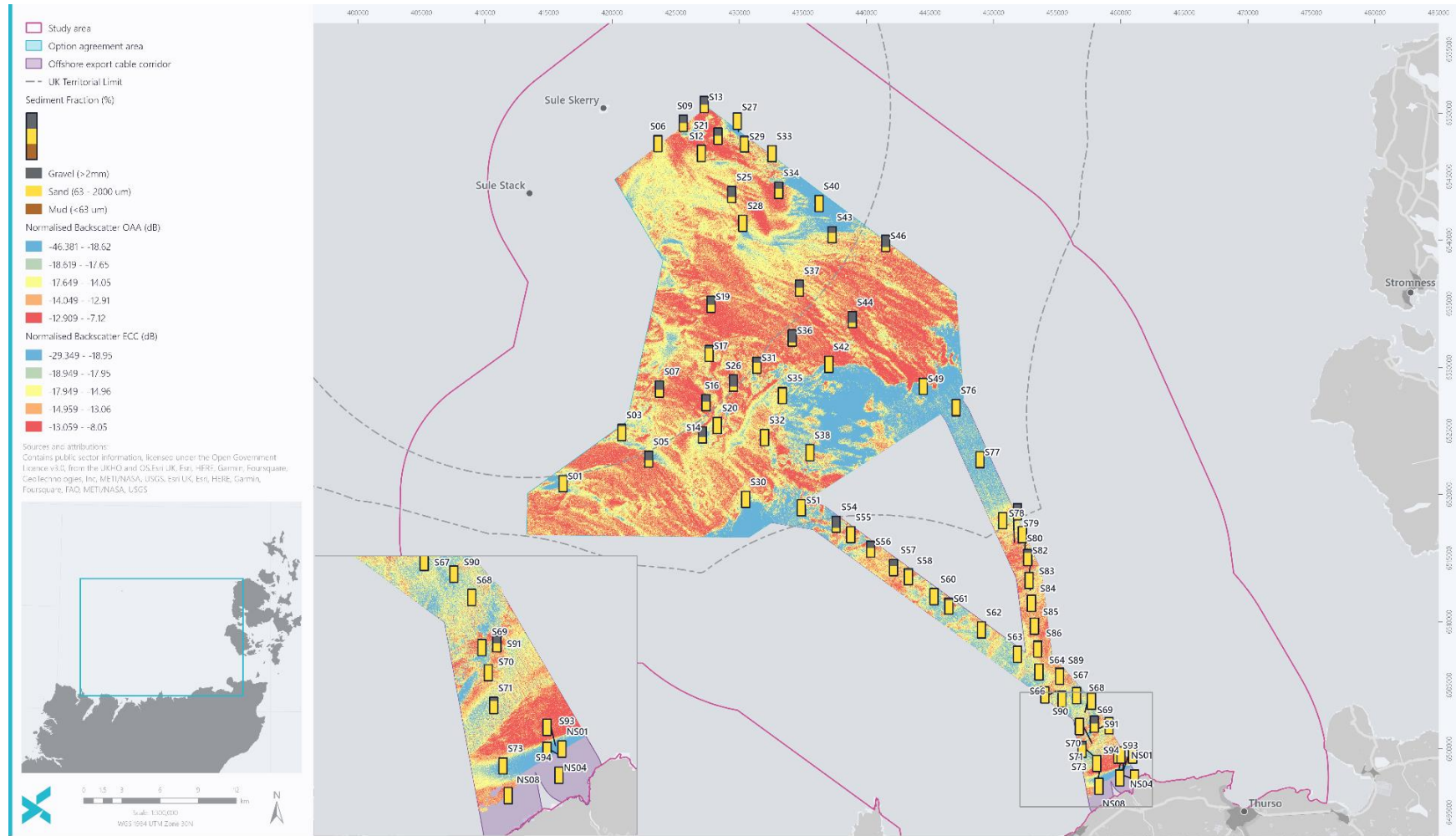


Figure 3-7 Overview of PSA results superimposed on the backscatter data (Ocean Infinity, 2023a)



### 3.3.2.2 Cobble and boulder clasts

While BGS (2022) records would suggest that there is no exposed bedrock within the offshore Project and study area (section 3.2), Project-specific survey findings within the OAA did note areas of high acoustic reflectivity – indicating the presence of hard substrate without any sediment cover (Ocean Infinity, 2023a; 2023b; 2023c). Boulders occur throughout the OAA. Areas where there is a significant concentration of boulders have been termed boulder fields. Boulder fields of medium boulder density (10-20 boulders per 50 x 50 m area) and high boulder density (>20 boulders per 50 x 50 m area), covered extensive areas of the OAA. These cobbles and boulders occur at a high density throughout most of the site with areas of medium density boulder fields along the northeast boundary of the OAA, in association with Stormy Bank (shown in Figure 3-8). Boulder fields are often found adjacent to till outcrops surrounded by mobile sediments likely composed of sand (Ocean Infinity, 2023a). The extent and coverage of the boulder fields are largely represented by high acoustic reflectivity as illustrated in Figure 3-7.

Site-specific surveys identified the presence of boulder fields along a large proportion of the offshore ECC and towards the coast, close to the landfalls as illustrated in Figure 3-9 (Ocean Infinity, 2023b; 2023c; Spectrum, 2023). Within the nearshore survey, in close proximity to the landfalls, a total of 414 boulders were identified across the surveyed area (Spectrum, 2023). Most boulders were less than 1 m in size but some were as large as 3.5 m. The boulder fields within the offshore ECC were generally associated with areas of till, areas of sandy substrate or areas adjacent to rock shelf (along the coast) (Ocean Infinity, 2023b; 2023c; Spectrum, 2023).

In addition to the presence of boulder fields there are individual boulders in lower densities across the OAA and offshore ECC.

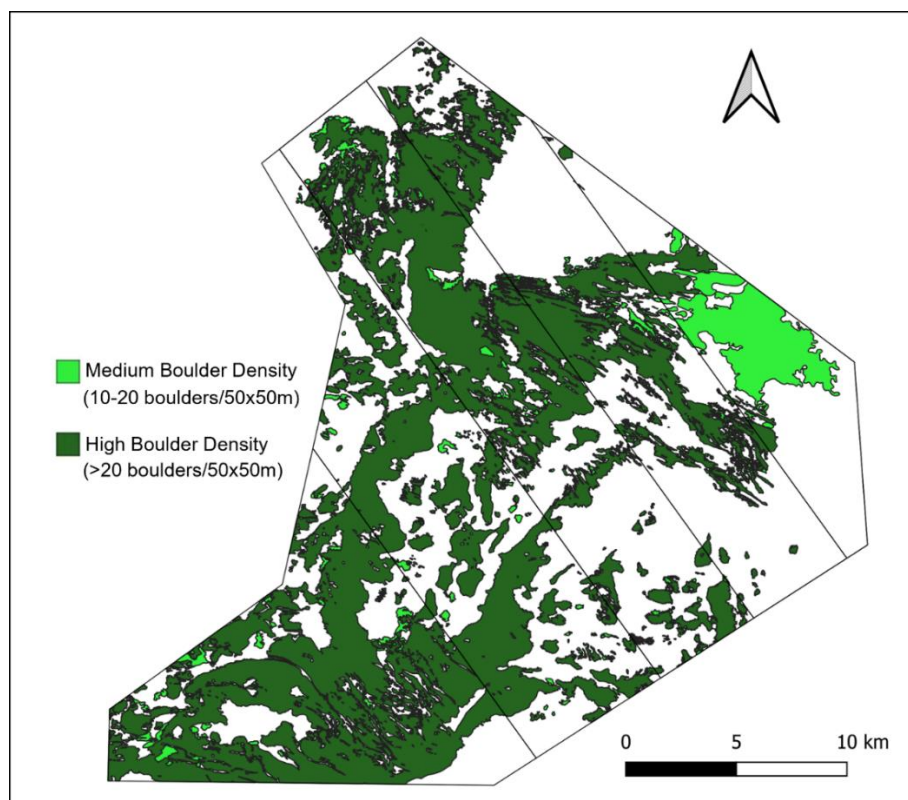


Figure 3-8 Boulder field coverage within the OAA (from Ocean Infinity, 2023a)

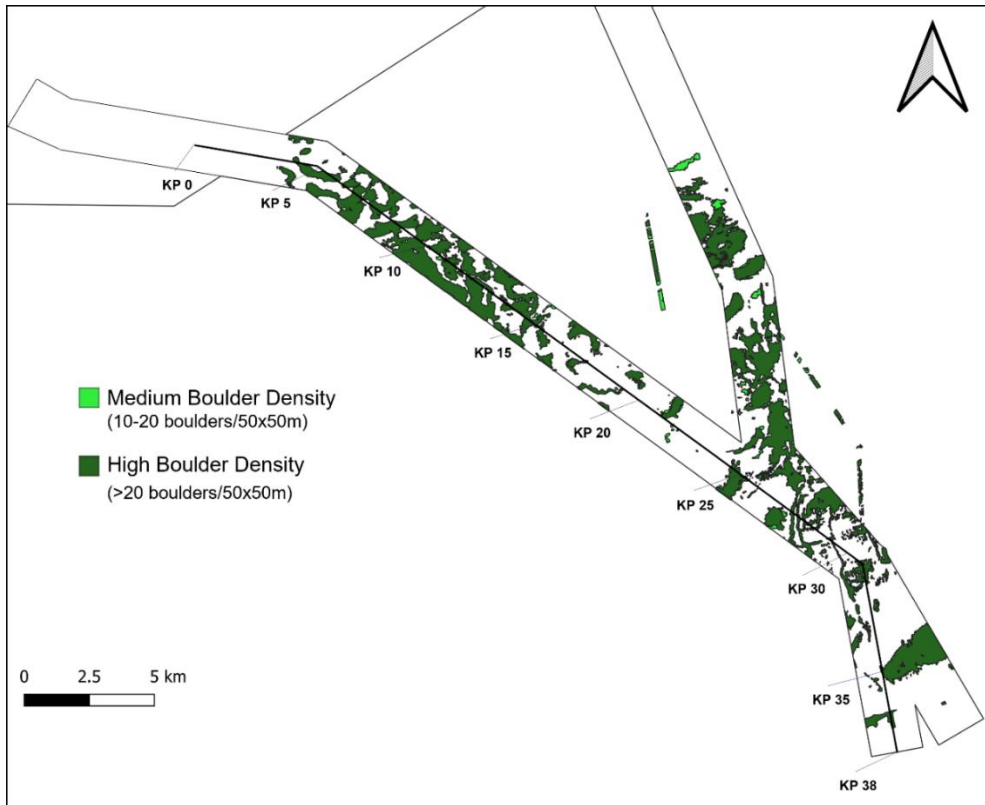


Figure 3-9 Boulder field coverage within the offshore ECC (from Ocean Infinity, 2023b; 2023c)

## 3.4 Seabed Bathymetry

### 3.4.1 Overview

Seabed depths across the northwest Scottish continental shelf are highly variable, with the presence of deeps and morphological bedforms. Slopes across the shelf do not frequently exceed 3°, with the majority of the area having a slope of less than 2° (Figure 3-10). Exceptions to this are seen in the Pentland Firth and in the offshore area northwest of the Orkney mainland where areas of slope of up to 5° can be seen.

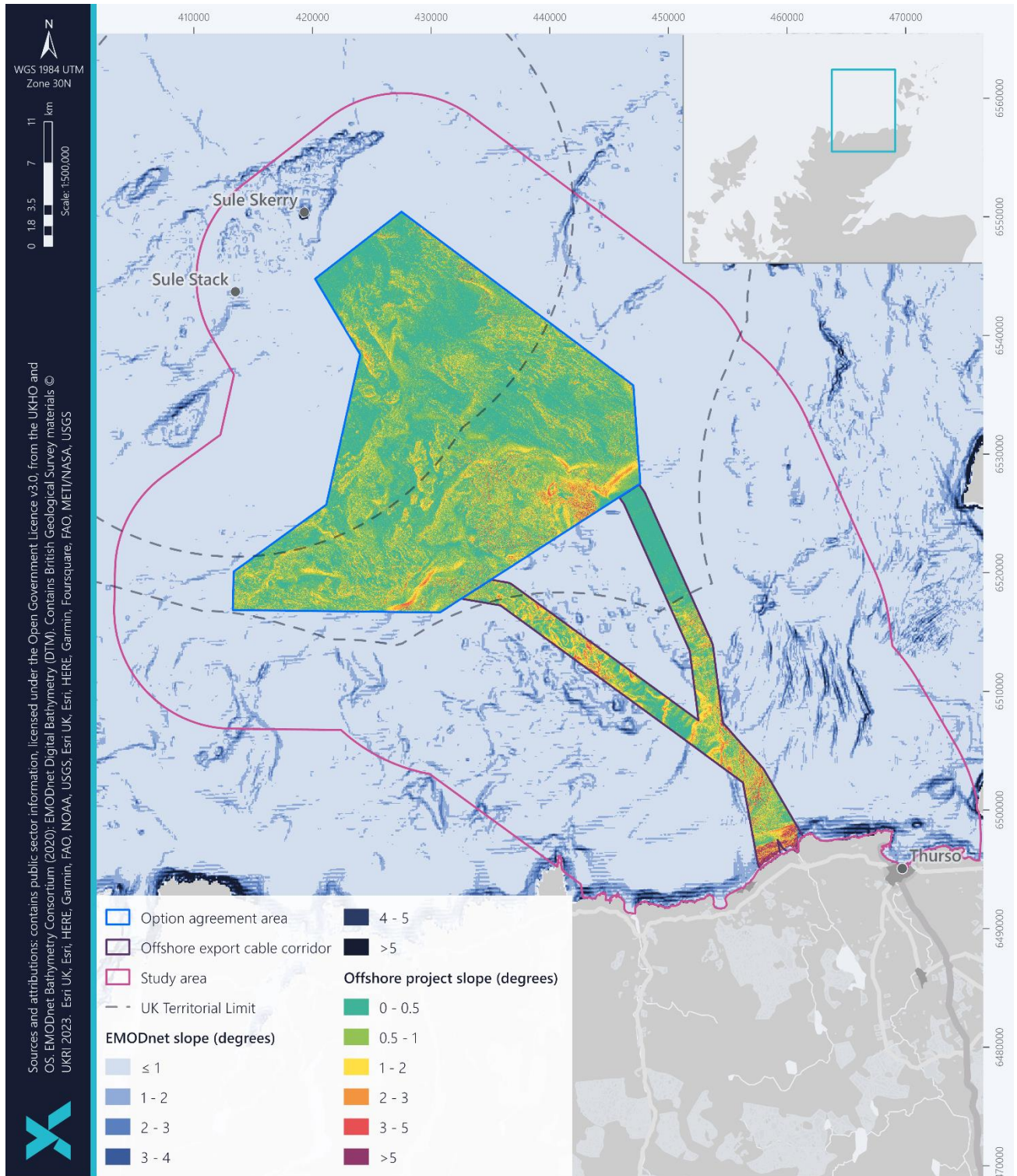


Figure 3-10 Slope in the offshore Project and offshore study area



## 3.4.2 Offshore Project Area

### 3.4.2.1 OAA

The bathymetry of the OAA, as illustrated in Figure 3-11, has a water depth range between 45 mLAT and 99 mLAT with shallower depths recorded over the Whiten Head and Stormy Banks that occur within the OAA, as observed in site-specific geophysical surveys (Ocean Infinity, 2023a). Whiten Head Bank is located in the south of the OAA, close to the southeastern boundary where the offshore ECC begins. Stormy Bank is located north of centre in the OAA. According to the site-specific survey, Stormy Bank is aligned northwest to southeast roughly parallel with the northern border of the OAA. Whiten Head Bank is oriented southwest to northeast and is comparatively narrower in shape and features a relatively sharp crest along the leading eastern edge of the bank, with marginally steeper slopes than the surrounding seabed, of up to 3°.

The depth variation in relation to Stormy Bank ranges between 45 to 100 mLAT. Stormy Bank has a relatively uniform bathymetric profile which falls sharply at the southeastern-most extent (to a maximum depth of approximately 100 mLAT at the start of the offshore ECC), marking the edge of the bank. Water depths over Whiten Head Bank vary from 47 mLAT at the top of the bank to 82 mLAT to the southeast (Ocean Infinity, 2023a). The banks, and other bedform features within the offshore Project area are discussed in section 3.5. The bank features are separated from one another by a deeper area in the centre of the OAA (which reaches varying depths of 60-70 mLAT).

Across the offshore project and study area, slope gradient generally represents that found in the wider environment. Generally, slope within the OAA is considered to be very gentle (<1°) to gentle (<5°). Localised areas of higher slope angles are associated with seabed features such as ridges, rippled scour depressions and megaripples (Ocean Infinity, 2023a; SS5: Benthic environmental baseline report).

### 3.4.2.2 Offshore ECC

Within the offshore ECC, the offshore site-specific geophysical survey recorded a range from 34 mLAT to approximately 110 m LAT (Ocean Infinity, 2023b, 2023c), as illustrated in Figure 3-11. The bathymetry along the offshore ECC is much more variable compared to the OAA but, on the whole, water depths are greater within the corridor. The eastern ECC starts at a depth of approximately 60 m LAT. This drops off quickly to a depth of approximately 90 mLAT which remains relatively consistent until it turns merges with the western ECC. The western corridor is initially slightly shallower and has a more gradual increase in depth as it travels southeast, shown in Figure 3-11. The western ECC starts at a depth of approximately 71 mLAT and reaches a maximum depth of approximately 110 mLAT prior to where the eastern and western ECC merge, which is the deepest point along the offshore ECC.

Where the two eastern and western ECC merge and continue to the coast, the topography of the seabed slopes towards the south, with water depths reaching approximately 90 mLAT within this section of the offshore ECC. Along the final approach to the coast, the water depth within the offshore ECC gradually shallows before reaching a depth of approximately 60 mLAT approximately 2 km from the coastline. Beyond this point, the ascent to shore is relatively rapid, as indicated by the seabed slope in Figure 3-10. Across the offshore ECC slope varies from 0 to 2° with sporadic areas recorded as 3 and 4°. Isolated sections of the ECC contain steeper slope sections of up to 11° (Ocean infinity, 2023b, 2023c). The slope of the seabed within the eastern and western corridors of the offshore ECC is shown in



Figure 3-12 and Figure 3-13 respectively; presented against kilometre points (KPs) along the corridor. This shows the steep incline within the final few kilometres as the offshore ECC nears the coast.

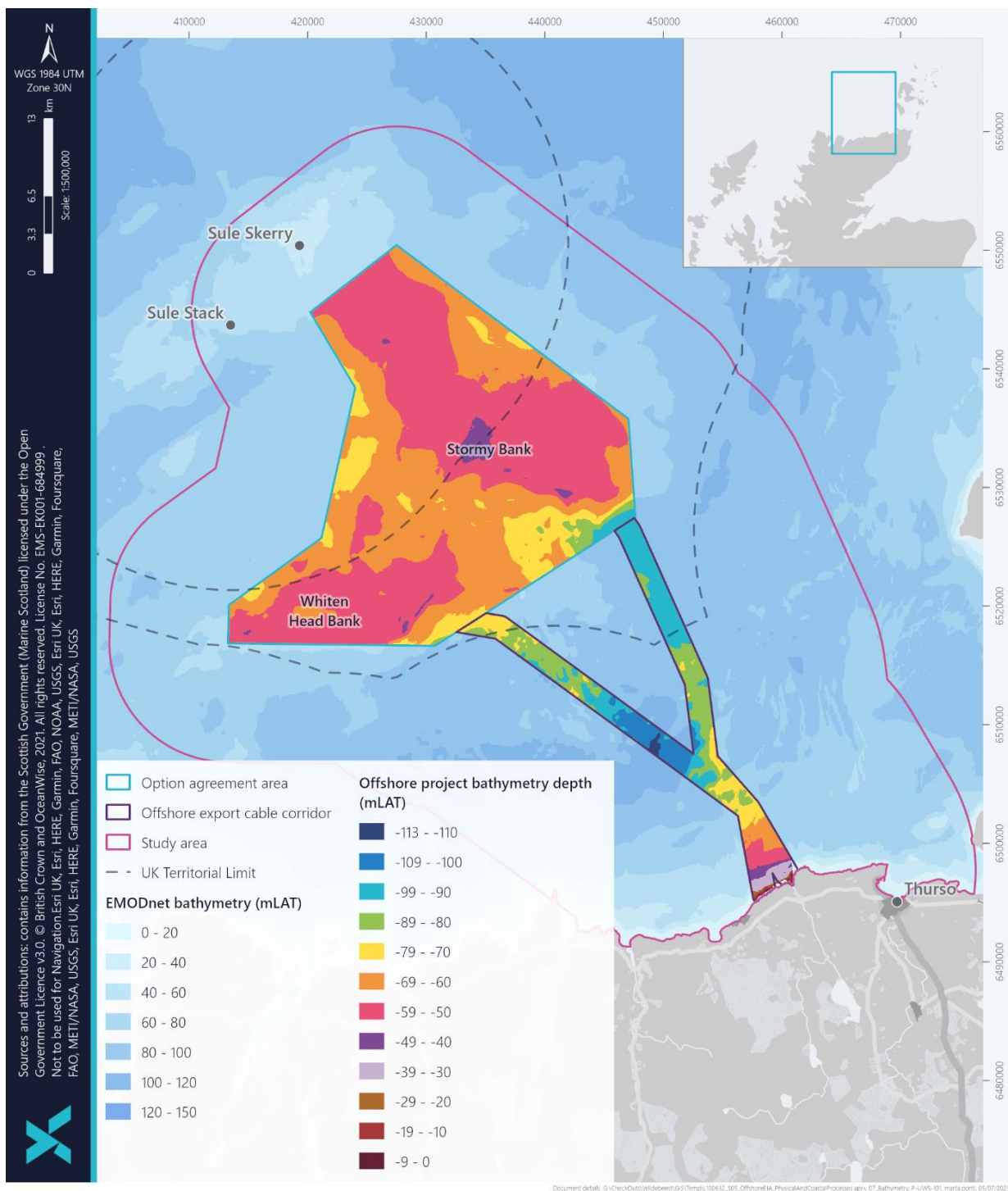


Figure 3-11 Bathymetry in the offshore Project area

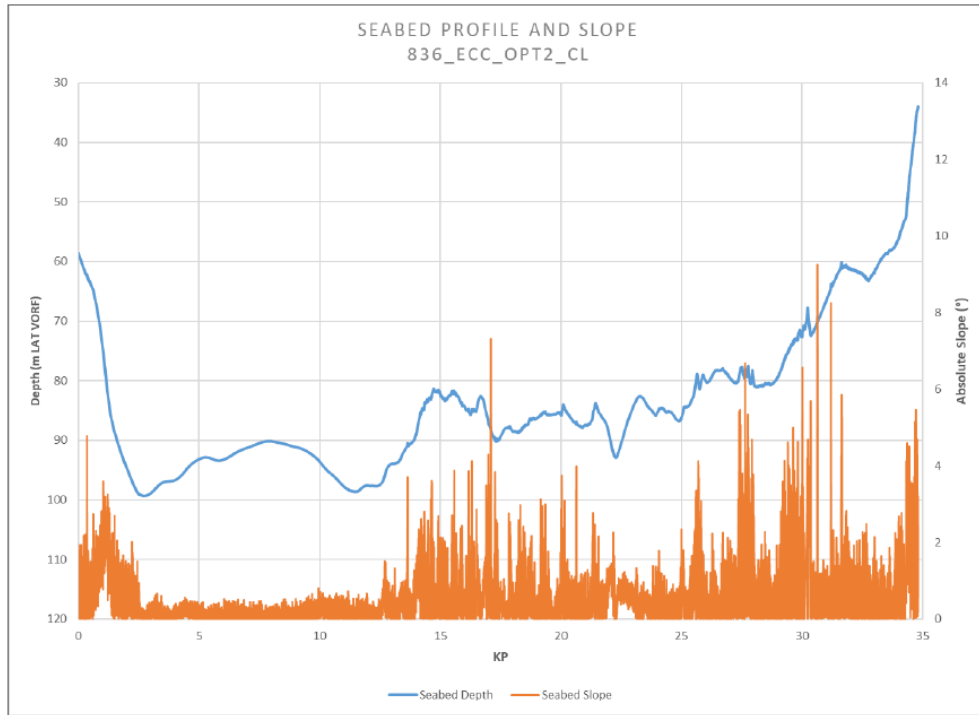


Figure 3-12 Seabed and slope profile along the eastern ECC (Ocean Infinity, 2023c)

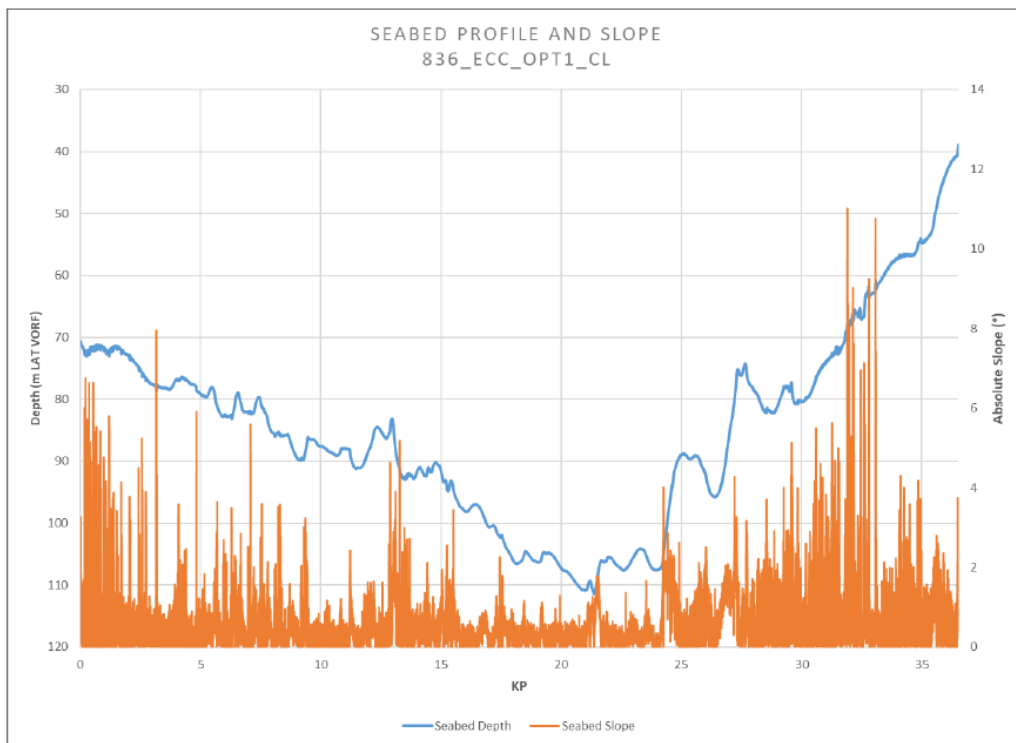


Figure 3-13 Seabed and slope profile along the western ECC (Ocean Infinity, 2023b)



## 3.5 Seabed Morphology

### 3.5.1 Overview

The seabed across the northwest Scotland continental shelf is variable. In addition to the Whiten Head Bank and Stormy Bank within the OAA, smaller bedform features such as sandwaves and megaripples are found throughout. These bedforms are found in association with seabed depressions and areas of increased water depth within the OAA and offshore ECC (BGS, 2022).

### 3.5.2 Offshore Project Area

#### 3.5.2.1 OAA

Depths across the OAA ranging between 41 mLAT and 90 mLAT, with a greater range occurring along offshore ECC, with depths up to 110 mLAT (Figure 3-11, Section 3.4.2). There are two shelf banks within the OAA, Whiten Head Bank and Stormy Bank. Both of these bedform features appear on Admiralty Charts and show the shallowest point on each bank to be 48 m and 44 m below Chart Datum (CD) respectively (UKHO, 1954). However, site-specific geophysical surveys indicate depths of 47 mLAT and 48 mLAT respectively (Ocean Infinity, 2023a). Whiten Head Bank is located in the south of the OAA, close to the southeastern boundary where the offshore ECC begins. Stormy Bank is located north of centre in the OAA. According to the site-specific survey, Stormy Bank is aligned northwest to southeast roughly parallel with the northern border of the OAA. Whiten Head Bank is oriented southwest to northeast and is comparatively narrower in shape and features a relatively sharp crest along the leading eastern edge of the bank, with marginally steeper slopes than the surrounding seabed, of up to 3°.

Anecdotal information from local fishermen (obtained during discussions in the Project's Fisheries working group) suggests that sediment overlying shelf bank features in the north of Scotland can be highly variable and dynamic, which may apply to the seabed across Stormy Bank and Whiten Head Bank. This variability is commonplace offshore in the north of Scotland and, as noted during the sampling undertaken in the offshore Project area, there were a number of locations within the OAA from which samples could not be obtained due to the overall lack of sediment cover (Ocean Infinity, 2023d). Consequently, it is possible that the sediment overlying Whiten Head and Stormy Bank features within the OAA are highly mobile, with the thickness and composition of overburden varying over time or in relation to storm events).

The site-specific geophysical surveys shows a uniformity in bathymetry on Stormy Bank. Sandwaves are more apparent along the edges of the bank, as the water depth increases. Sandwave fields are found in the slightly deeper water which separates the two named bank features. The sandwaves occur on a scale of up to approximately 1 km in length. The sandwaves are orientated almost due north-south. The shape of these features suggests they are moving from west to east. Sandwaves are also present along the leading edge of the Whiten Head Bank, to the east of the steep crest described above.

Rippled scour depressions are characteristic of the whole OAA, including both Whiten Head Bank and Stormy Bank (Ocean Infinity, 2023a). Geophysical survey findings suggest the presence of megaripples, rippled scour depressions and surficial gravel deposits at seabed is probably a result of strong currents (Ocean Infinity, 2023a). These features



appear as elongated areas of coarser-grained sediments with ripples depressed by up to 1 m below the surrounding seabed. They are probably formed and maintained by currents and wave interaction with the seafloor sediments (Ocean Infinity, 2023a).

The top of the banks are defined by rougher sediments with a scattering of boulders with associated scouring. An area of deeper water (81-90 mLAT), east of centre in the OAA and south of the Stormy Bank, is densely filled with megaripple features (shown in purple in Figure 3-14). The megaripples cover an area of approximately 7 km<sup>2</sup> within the boundary of the OAA. In areas where the sand associated features are not found, boulders are found across the OAA (see section 3.3).

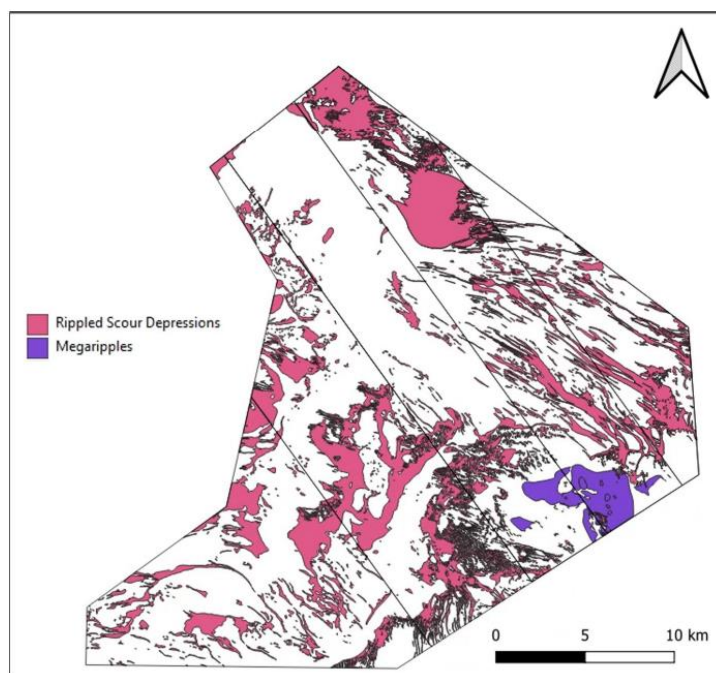


Figure 3-14 Seabed features within the OAA (from Ocean Infinity, 2023a)

Potential bedform mobility and migration of larger bedform features within the OAA over time were assessed, including any movement of Stormy Bank and Whiten Head Bank, given the anecdotal information described above. This was achieved through a comparison between available broadscale EMODnet bathymetry (EMODnet, 2020) and the recently completed site-specific geophysical surveys. There is the potential for the morphological features present across the offshore Project area to evolve over relatively long timescales. For this reason, investigating changes on bank features is best undertaken by analysing the position and extent of the depth contours associated with these large bedforms. The contour analysis was completed using functionality in the Spatial Analyst tool in ArcGIS ArcMap software, where contours were extracted at regular intervals across the available bathymetry datasets. The lateral translation and difference in the position of the depth contours was visually and analytically assessed to determine any changes that occurred over time. In addition, analysis transects were extracted across the available bathymetry data sets to inform on potential bedform migration. Longitudinal and transverse analysis transects were applied across the OAA area as illustrated in Figure 3-15. Longitudinal transects were oriented perpendicular to the bank crest alignment, along the length of the bedform feature. Transverse transects ran over the crest of the bank. The



rate of migration was calculated by extracting the bedform crest/trough depths and position from the from the available bathymetry data along these analyses transects. The movement of the crests along a transect chainage between the surveys was used to indicate the direction and rate of bedform migration.

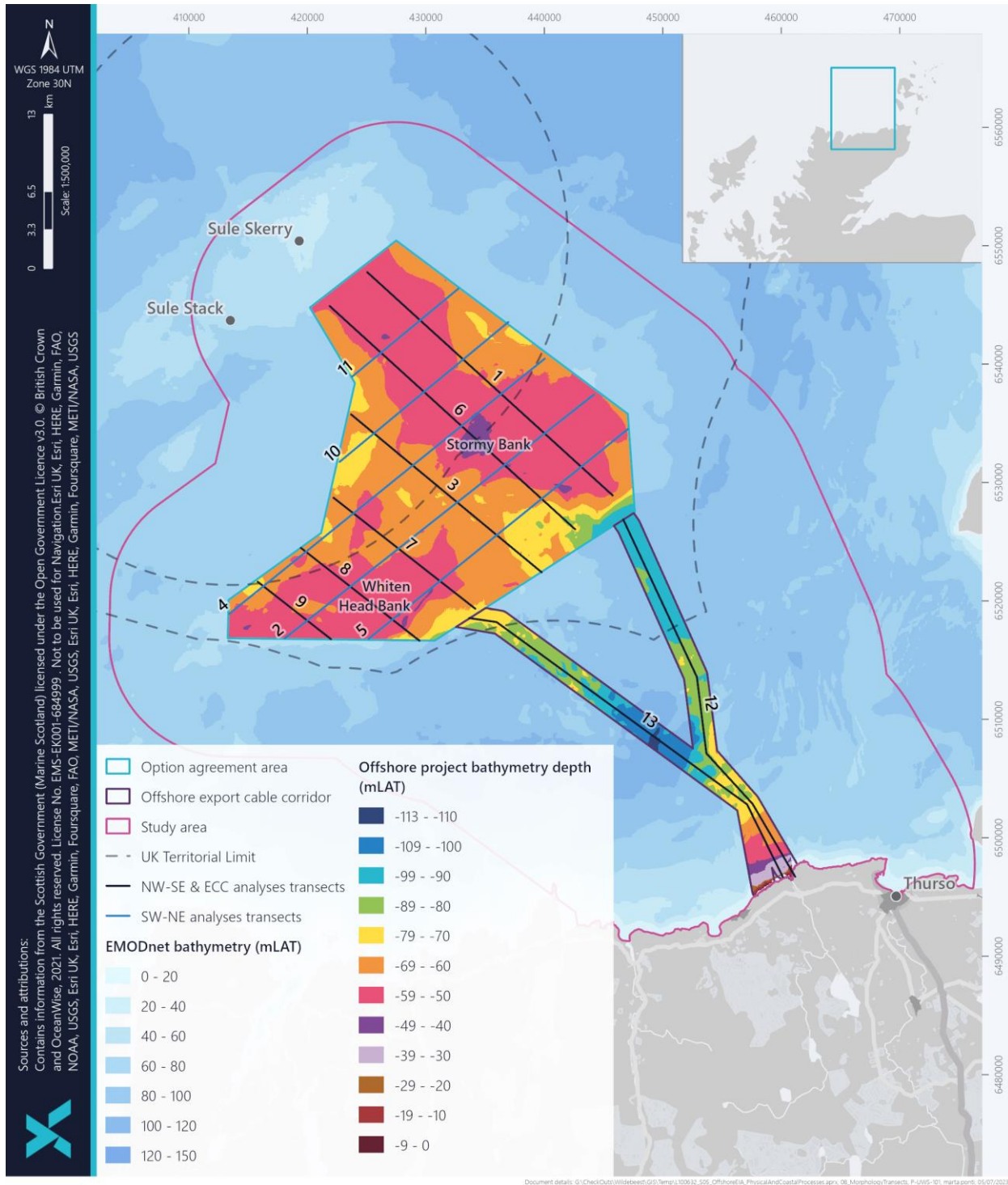


Figure 3-15 Analyses transects used to investigate the potential for bedform migration across the offshore Project area



Overall, the results of the analyses demonstrate that over time (between the timescales represented by the EMODnet and site survey bathymetries), there has been relatively little change in the bedforms. Within the centre of the OAA, between Stormy Bank and Whiten Head Bank, is a deeper area. Transects within this central area are shown in Figure 3-16. While the EMODnet data against which the site-specific information was compared is much more granular, overall, there is no evidence of change between the two data sets. The site-specific data follows the EMODnet data closely. This suggests that the features within this area are relatively stable.

This is similar to the transects corresponding to the location of Stormy Bank (Figure 3-17). The transects show that the bathymetry along the length of this bank is less variable than in other places within the OAA. Both transects here capture the end of Stormy Bank and show that the EMODnet and site-specific bathymetry are well aligned. This would suggest that there is no movement along that margin of Stormy bank.

Figure 3-18 shows the bathymetric profile of Whiten Head Bank. Both transect 7 and 8 show the sharp crest on the bank, as described above. Whereas a sharp feature like that might suggest mobility in the direction parallel to the crest, the alignment between the EMODnet and site-specific data instead suggests that the feature is relatively stable as there is no variation between the data sets. Consequently, the anecdotal evidence described above is unlikely to apply to the larger equivalent bedforms within the OAA.

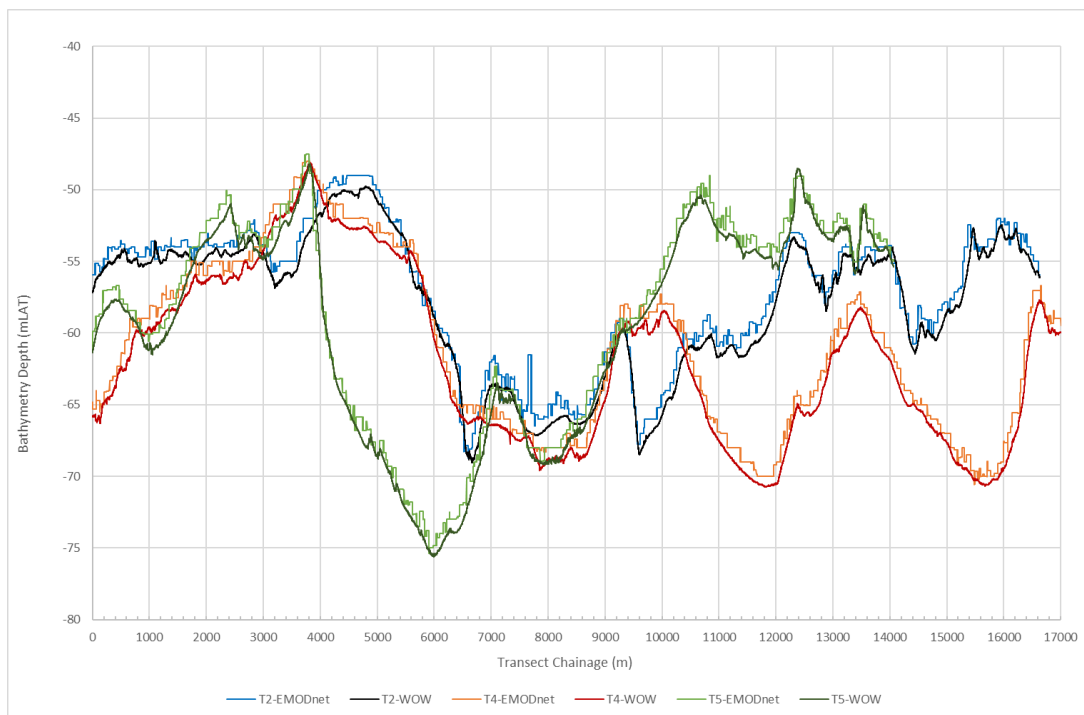


Figure 3-16 Southwest – northeast analyses transects 2, 4 and 5 as per Figure 3-15, which illustrate the seabed profiles across the OAA. Cross section profiles cross Whiten Head Bank, approximately between chainage 100 m and 7000 m and Stormy Bank, approximately between chainage<sup>1</sup> 1100 m and 16000 m)

<sup>1</sup> Chainage is the distance in metres along the profile transect used for analysis.

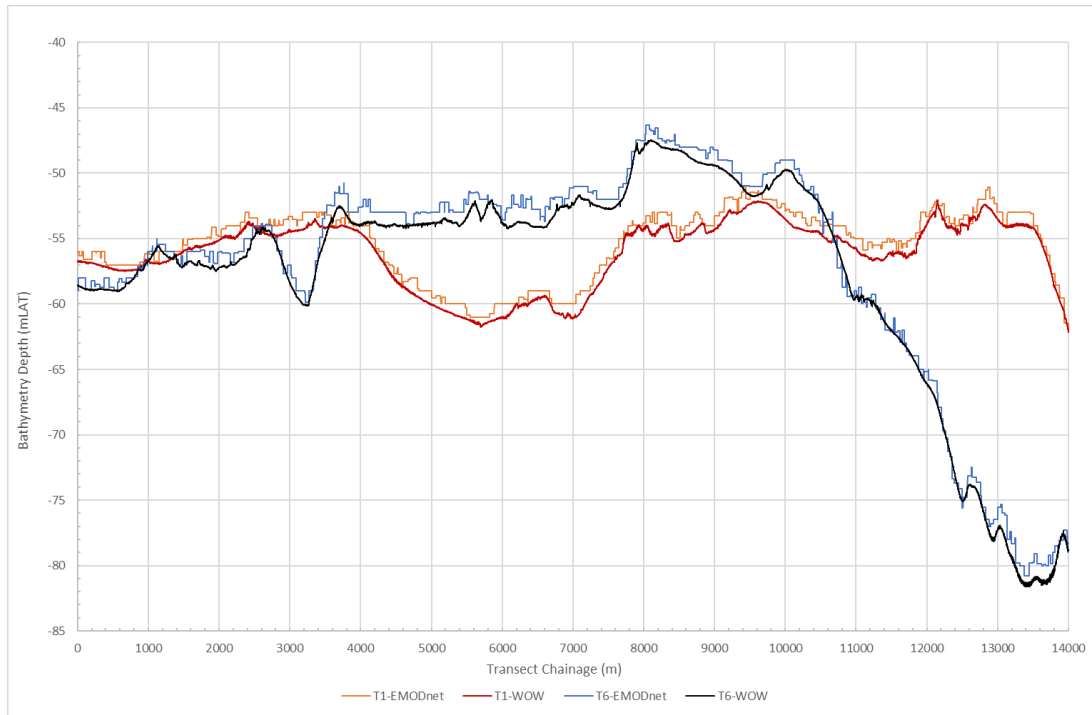


Figure 3-17 Analyses transects 1 and 6 as per Figure 3-15, which illustrate the seabed profiles approximately along the northwest – southeast axis of Stormy Bank

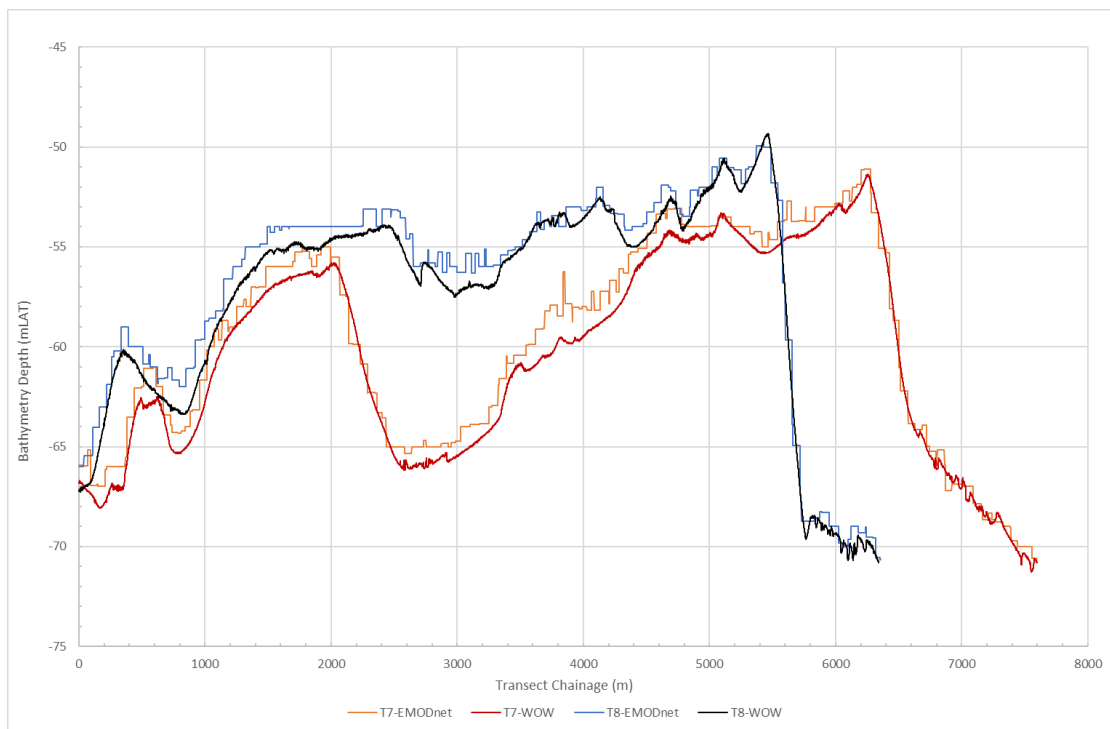


Figure 3-18 Analyses transects 7 and 8 as per Figure 3-15, which illustrate the seabed profiles approximately across the northwest – southeast axis of Whiten Head Bank



### 3.5.2.2 Offshore ECC

Where the eastern ECC begins at the boundary of the OAA, the water is relatively deep and the seabed is featureless, based on information interpreted from site specific geophysical survey (Ocean Infinity, 2023b; 2023c). However, approximately 11.6 km along the offshore ECC from the OAA boundary, there is evidence of sandwave features. These larger features are oriented southwest to northeast. The features extend beyond the width of the offshore ECC; therefore the length of the features is not known. However, they appear to be at least >1 km long. The spacing between the crests is relatively uniform, with the troughs occasionally filled with smaller sandwaves. Megaripples appear to be superimposed on the sandwaves oriented perpendicular to the larger sandwaves. The sandwaves become increasingly sparse until the offshore ECC turns south towards the coast. From this point until the junction between the eastern and western, ECCs the seabed becomes relatively featureless again with occasional sandwaves and areas of megaripples, notably, the identified sandwave fields is in line with that described in the BGS dataset (BGS, 2022).

At the start of the western ECC, and within the boundary of the OAA, there is evidence of long sandwaves on the seabed, up to approximately 2.5 km. The bathymetry within a few km of the OAA boundary is more variable, with some evidence of megaripples and movement of seabed sediments within shallower pockets of the offshore ECC. As described in section 3.4.2, the southern offshore ECC passes through areas which have the greatest water depth throughout the whole offshore Project area. As the water depth begins to increase towards the deepest point, megaripples become common, oriented due north-south. Where the bathymetry is at its deepest, the seabed is featureless and flat. Megaripples are present as the water depth becomes gradually shallower again at the junction between the two offshore ECCs.

Along the final section of the offshore ECC where the eastern and western corridors meet, sandwaves are common. Megaripples are superimposed on these features and are parallel to the sandwaves. All features are oriented north-south, which continues towards the coast. As introduced in section 3.3, there is a feature close to the Crosskirk landfall defined by deeper superficial sediments. The feature appears to be a bank formation, or similar, approximately 3.5 km in length and is illustrated in Figure 3-19. The crest of the feature (i.e. the greatest sediment depth) is oriented southwest to northeast, parallel with the coast (Spectrum, 2023).

Analysis of the seabed morphology within the offshore ECC, as for the OAA, compares the bathymetry from EMODnet against the site-specific data. The two data sets follow one another closely (Figure 3-20) indicating that there is little change in the morphology along the offshore ECC. At the landfall, a strip of exposed bedrock is apparent which is bordered by loose rock (as described in section 3.3). Steep escarpments and areas of tessellated pavement are visible along the coastal bedrock. In the west of the landfall location, there is an area of rough ground, which has been interpreted as till (Spectrum, 2023). In addition, a number of boulder fields were identified across much of the landfall site (as discussed in section 3.3). The difference represented in the bathymetry between the EMODnet and site-specific bathymetries is more likely to relate to data quality from the EMODnet, which is not identifying the escarpment indicated in the site-specific surveys (Ocean Infinity, 2023b; 2023c).

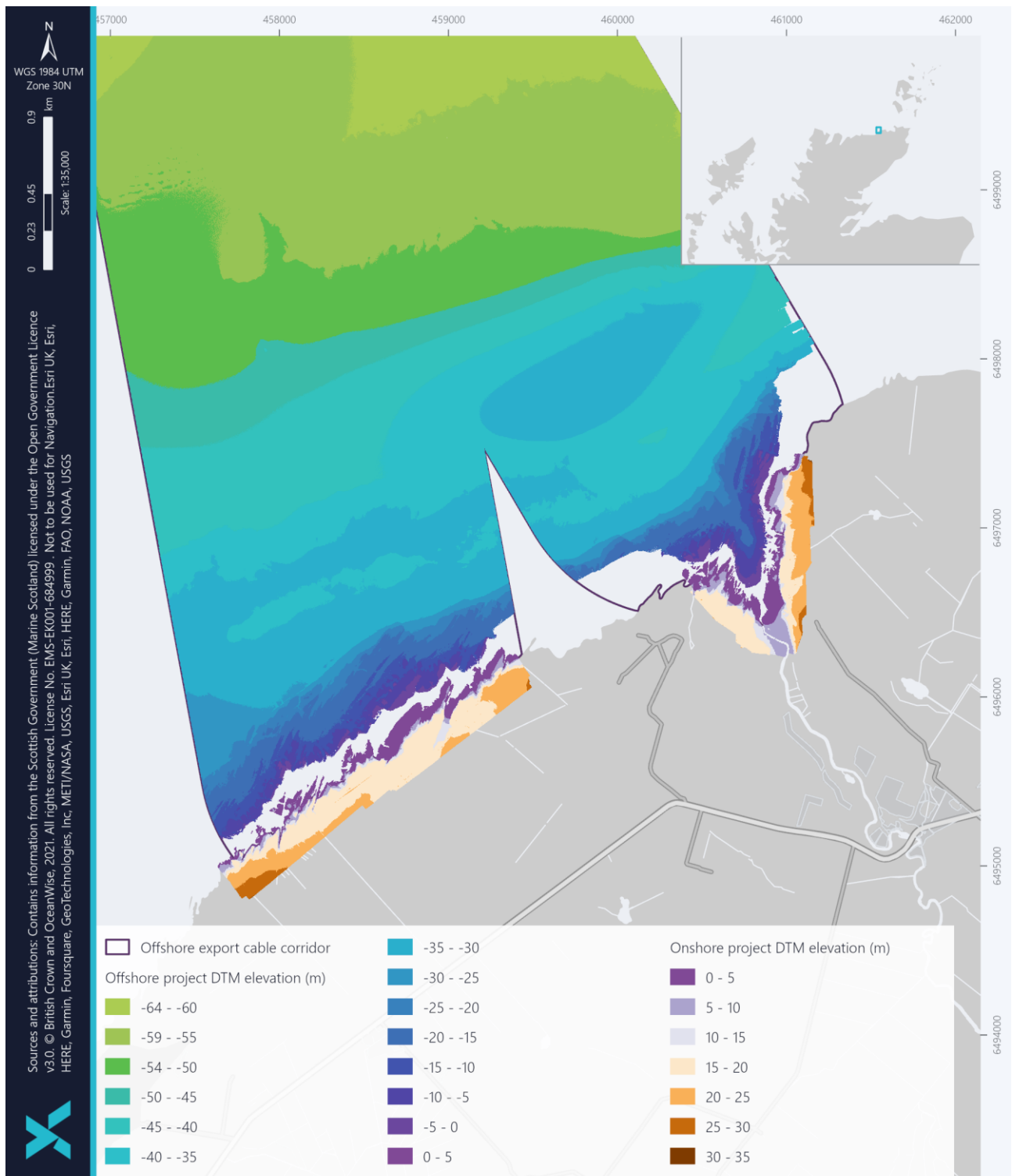


Figure 3-19 Nearshore morphological feature near the Crosskirk landfall represented in the seabed bathymetry

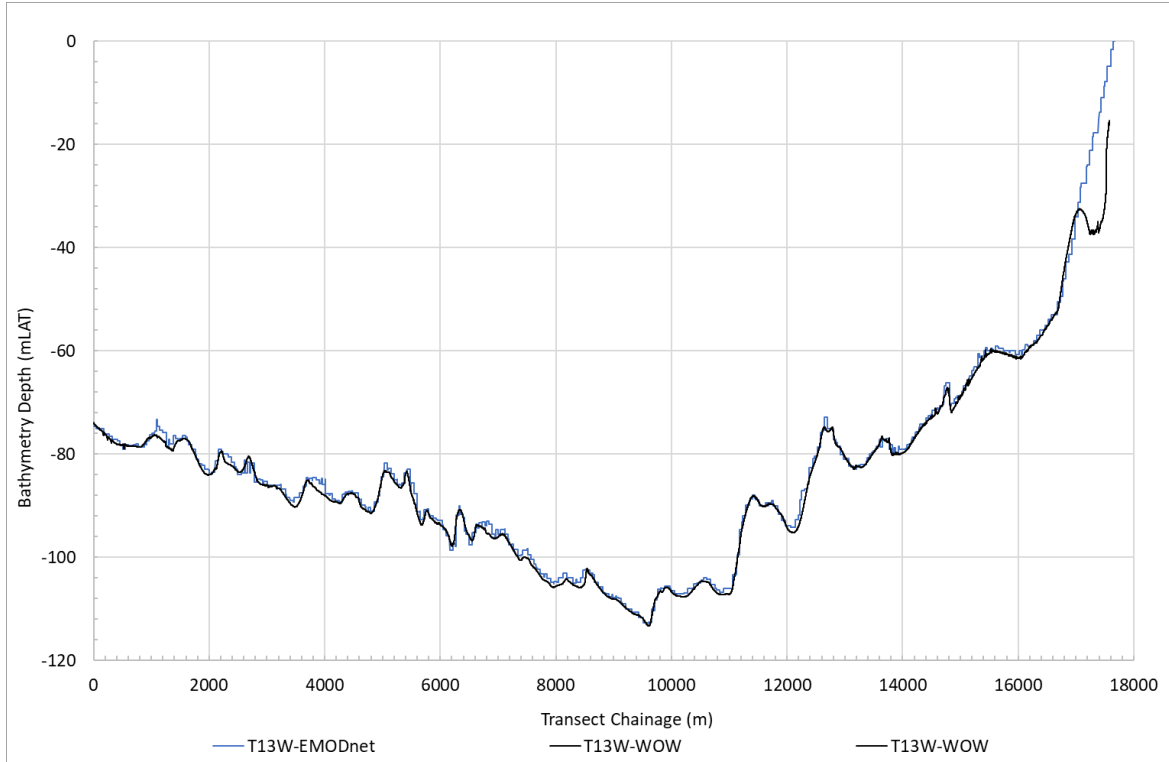
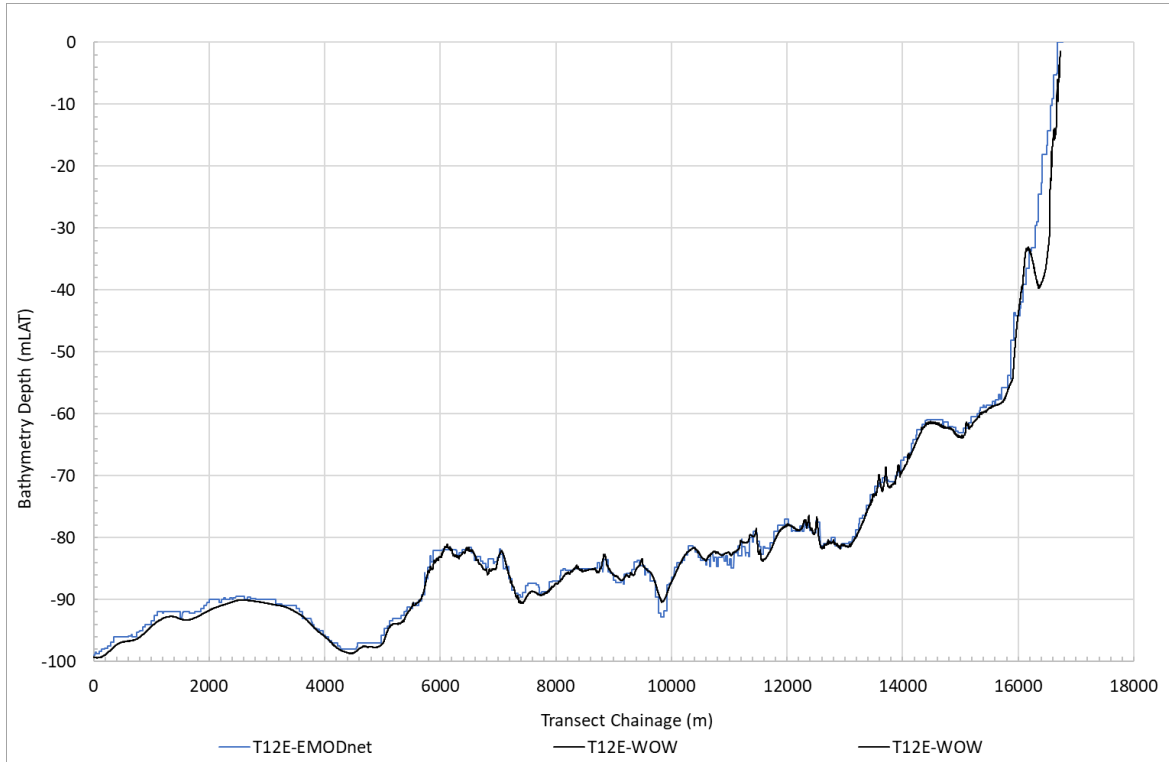


Figure 3-20 Cross sectional bedform profiles within the offshore ECC (corresponding to transects in Figure 3-15)



## 3.6 Water Levels

Sea level variation generally occurs as a result of periodic tides, with the infrequent contribution from storm surge events. At much longer timescales, on the order of decades to centuries, isostatic recovery and global climate changes contribute to the long-term changes to sea level. As a result of the global change in climate, mean sea levels around the coast of Scotland are increasing and are expected to continue to do so (Marine Scotland, 2020).

### 3.6.1 Overview

Available modelled spatial information on water levels across the northwest Scottish continental shelf and the Pentland Firth suggests a north to south variation in tidal range, with a larger range in water level occurring to the south, as illustrated in Figure 3-21. There are also variations according to proximity to the Orkney coastline; mean spring ranges north of the Orkney Islands are between 2.01 m to 2.50 m, compared with 3.51 m to 4.0 m along the coast (O’Hara and Gallego, 2017). In the State of the Environment Assessment – A Baseline Assessment of the Orkney Islands Marine Region, the difference in tidal range is reported as being 30% greater to the west of the Orkney Islands compared to the east and amongst the Orkney Islands (Orkney Islands Council, 2020), which is also visible in Figure 3-21. Generally, the tidal range in Orkney is relatively small with a mean range of 2.6 m on a spring tide and 1.22 m on a neap tides. The mean spring range and spatial variability demonstrated in O’Hara and Gallego (2017), is also represented in the model developed for the West of Orkney Project, where spring tide water levels at high and low water are +2 mMSL and -2 mMSL respectively at the coast (equating to a range of up to 4 m, Figure 3-22).

Water level observations from the National Tidal and Sea Level Facility (NTSLF) are available for two long-term tidal gauge sites at Wick and Kinlochbervie along the mainland Scottish coast. The tidal levels from these locations indicate a west to east variation, with marginally higher water levels and ranges at Kinlochbervie, which is located along the northwest coast of the mainland compared to levels at Wick, in the northeast. These water levels are predicted based on years of observational data. Predicted tidal levels at Sule Skerry, an isolated stack offshore to the west of the OAA fall between those at Kinlochbervie and Wick (Ramsay and Brampton, 2000). The water levels for Kinlochbervie, Sule Skerry and Wick are shown in Table 3-3. The tidal wave progresses from west to east with high tide taking approximately 1 hour to travel the length of the northern coastline of Scotland (Ramsay and Brampton, 2000).

*Table 3-3 Tidal levels from the Wick and Kinlochbervie tidal gauge sites (NTSLF, 2022), and the predicted tidal levels at Sule Skerry (Ramsay and Brampton, 2000); all in relation to Chart Datum (CD)*

TIDAL LEVEL	KINLOCHBERVIE	WICK	SULE SKERRY
Highest Astronomical Tide	5.52 m	3.97 m	-
Lowest Astronomical Tide	-0.03 m	0.06 m	-
Mean High Water Springs	4.89 m	3.51 m	3.9 m
Mean High Water Neaps	3.75 m	2.78 m	3.1 m
Mean Low Water Neaps	2.01 m	1.43 m	1.6 m
Mean Low Water Springs	0.72 m	0.63 m	0.8 m



TIDAL LEVEL	KINLOCHBERVIE	WICK	SULE SKERRY
Mean Spring Range	4.17 m	2.88 m	3.1 m
Mean Neap Range	1.74 m	1.35 m	1.5 m

Predicted tidal information for Wick from 2008 to 2026, as provided by the NTSLF, shows that all of the 40 lowest equinoctial spring tides<sup>2</sup> are in the range of 0.07 m and 0.32 m, and all of the 40 highest equinoctial spring tides are in the range of 3.70 m to 3.96 m. The predicted range is within the LAT and HAT for this tidal station as presented in Table 3-3. However, NTSLF (2022) goes on to suggest that even higher water levels occur, which are higher than HAT and therefore likely to have a surge component, the levels of which are described further in section 3.6.3. The highest recorded tidal levels at Wick (based on observations up to 2012) range between 4.2 m and 4.5 m (NTSLF, 2022).

Similar predicted tidal information for Kinlochbervie shows that the 40 lowest equinoctial spring tides range from -0.03 m to 0.31 m, while the highest equinoctial tides range from 5.19 m to 5.5 m. Data from NTSLF (2022) for the Kinlochbervie tide gauge report the highest tidal levels (based on observations up to 2012) to range between 5.8 m and 6.28 m, which is also considered to have a surge component. At both Wick and Kinlochbervie these maximum water levels occurred in the winter months and are most likely associated with the occurrence of surge, considered further in section 3.6.3.

<sup>2</sup> Happening at or near the time of an equinox.

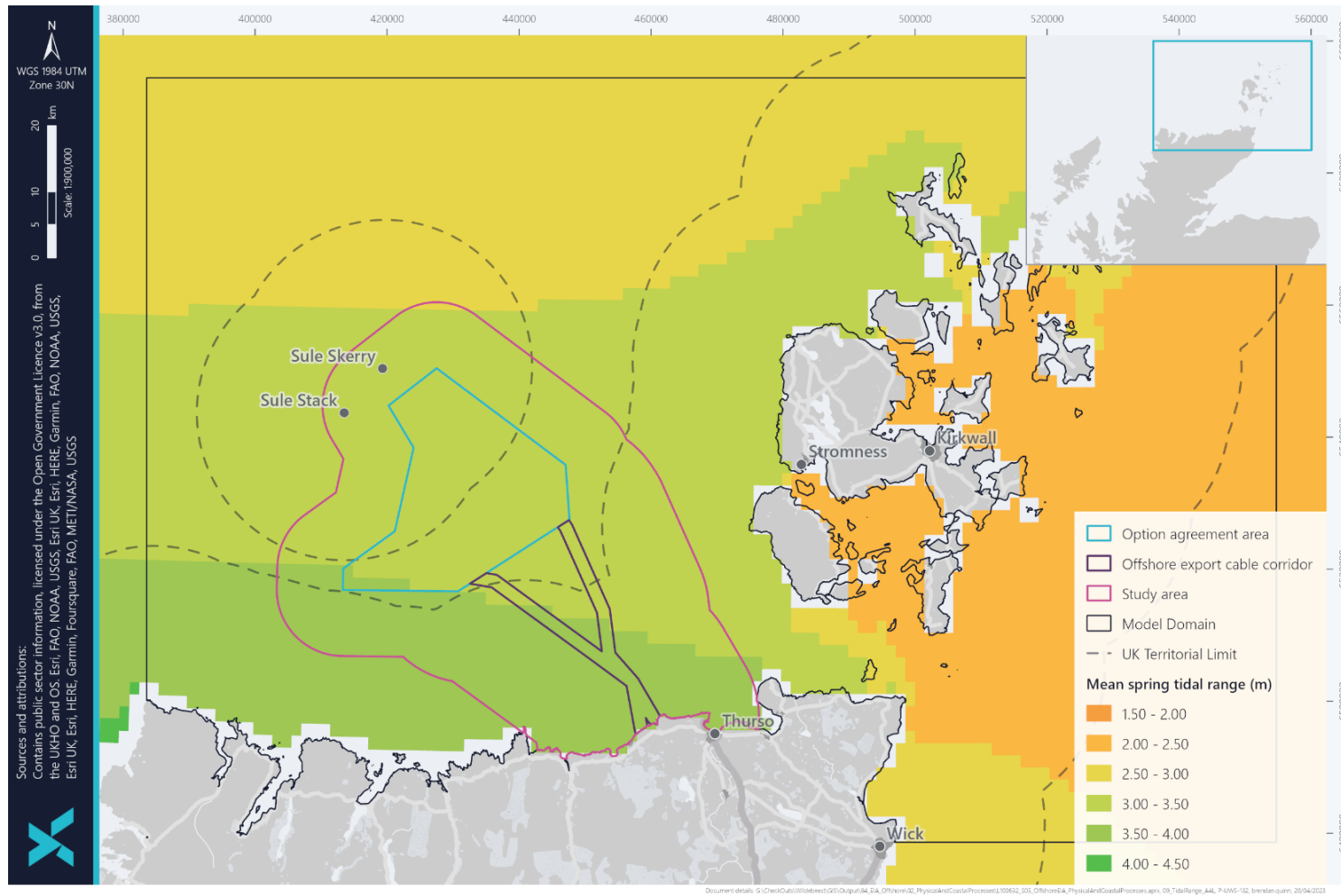


Figure 3-21 Mean spring tidal range in the model domain, offshore Project area and study area (O'Hara and Gallego, 2017)

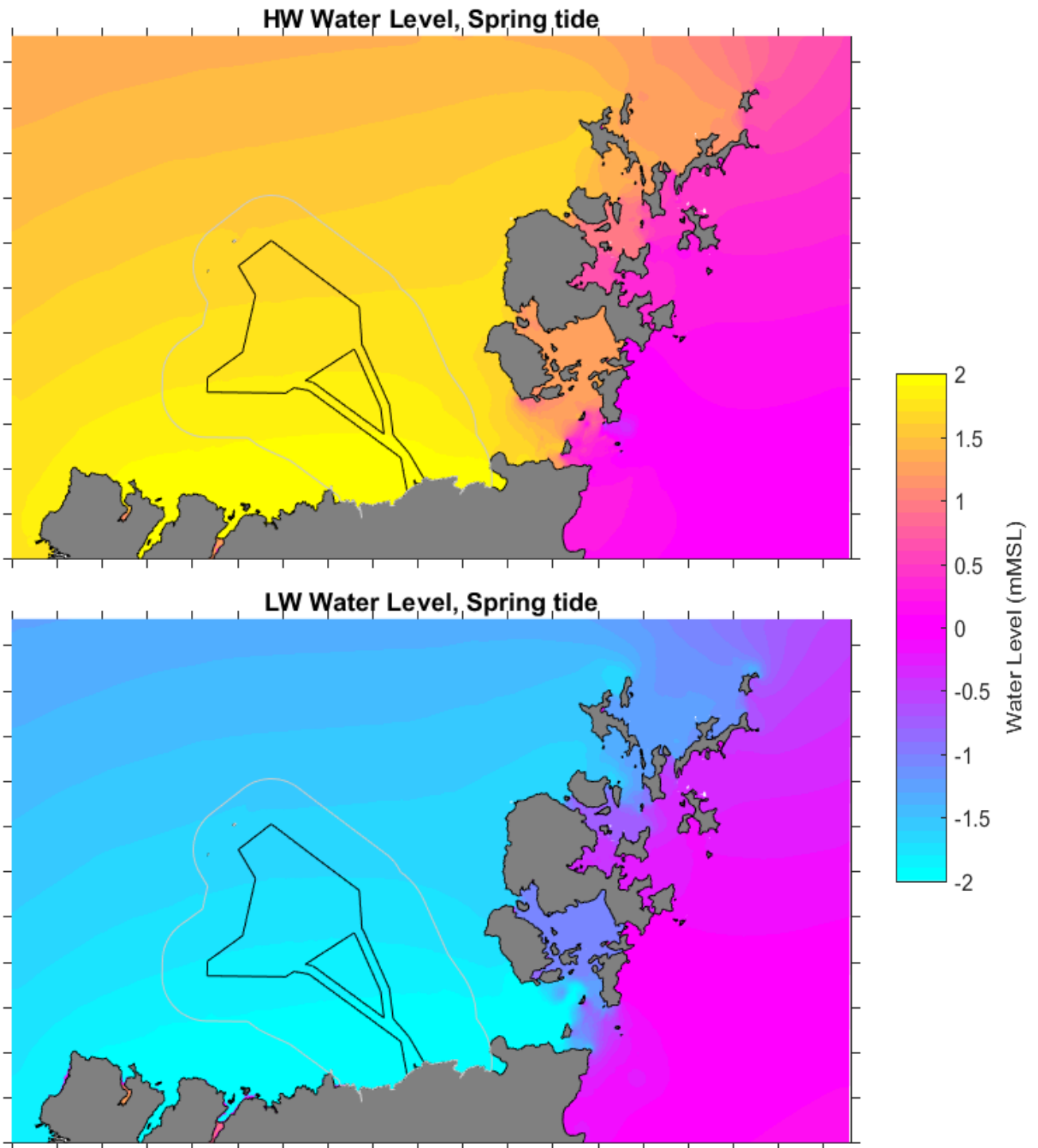


Figure 3-22 Spring tide water levels at high and low water output from the West of Orkney model



### 3.6.2 Offshore Project Area

The offshore Project area is located in a meso-tidal setting, with a mean spring tidal range of 3.01 m to 3.50 m, increasing to between 3.51 m to 4.00 m on the approach to the coast (Figure 3-21 and Figure 3-22). A wider range then occurs between the north and south of the study area, in line with the wider marine area discussed in Section 3.6.1. Water levels derived from current hindcast 1 within the OAA (Figure 2-3) and presented in Table 3-4 indicate a mean spring and neap tidal range of 3.36 m and 1.52 m respectively (OWPL, 2023), which fits with the wider understanding of the area, as described above.

Observational data showing MSL (m) was collected by Cefas at a nearshore location just offshore of Dounreay in 2001. The highest water levels recorded by Cefas were in the region of 2 m, with the lowest being approximately - 3 m. Hindcast data collected for the Pentland Firth Offshore Windfarm (PFOWF) array area (which is equitable to the offshore ECC) was plotted along with the Cefas data. The two datasets were highly comparable, with the observational data collected at Dounreay (shore location) demonstrating a slightly greater amplitude than the hindcast data for the array area (Highland Wind Limited, 2022). This suggests that the variation in water levels recorded at Dounreay is likely to be representative of conditions along the offshore ECC closer to shore.

Further information on water level from the Billia Croo Metocean Characterisation Report (EMEC, 2020), off the west coast of mainland Orkney (Figure 2-3), indicates a HAT of 2.19 m, based on 19 years of predicted tide levels (EMEC, 2020). This is comparable to the highest water levels recorded by Cefas at Dounreay and in the region of the offshore ECC and is also in line with expectations for the offshore Project area, per the HAT indicated in Table 3-4.

Table 3-4 Tidal levels for the Project calculated from a hindcast timeseries (OWPL, 2023)

TIDAL LEVEL		CURRENT HINDCAST 1 (m) MIKE21
Highest Astronomical Tide	HAT	4.82
Mean High Water Springs	MHWS	4.15
Mean High Water	MHW	3.69
Mean High Water Neaps	MHWN	3.23
Mean Sea Level	MSL	2.47
Mean Low Water Neaps	MLWN	1.71
Mean Low Water	MLW	1.25
Mean Low Water Springs	MLWS	0.79
Lowest Astronomical Tide	LAT	0



### 3.6.3 Storm Surge, Extremes and Sea Level Rise

Across the offshore Project area and wider northwest Scottish continental shelf, non-tidal influences on water levels (i.e. surges) are typically on the order of  $\pm 0.5$  m on the tidal level, but can occasionally increase during storm events to around  $\pm 1.6$  m.

Surges occur as positive or negative resulting in an increase or decrease in water levels respectively above the expected tide. Data on surges at Kinlochbervie has been recorded since 1991, and at Wick since 1990, up to the 2021 for both sites. Table 3-5 lists the five largest surges for Kinlochbervie and Wick since records began at both locations. Notably at both locations the surges, the largest surges are associated with a positive surge that occurred in the winter months. Typically, surges at both locations do not exceed 1 m, with lower surge levels occurring at Wick compared with Kinlochbervie. Monthly extreme surges are up to  $\pm 1.1$  m and  $\pm 1.7$  m at Wick and Kinlochbervie respectively, with both having larger positive surges (British Oceanographic Data Centre, 2022). Surges at Kinlochbervie are considerably higher than those at Wick, due to the influence of waves from the North Atlantic reaching Kinlochbervie. Surges in January 2020 and November 1998 were notable at both locations suggesting those were particularly severe storm events.

Table 3-5 Largest recorded surges (positive / negative) recorded at Kinlochbervie and Wick (1990-2021)

KINLOCHBERVIE		WICK	
Surge height (m) (positive / negative)	Date	Surge height (m) (positive / negative)	Date
1.68	Jan 2005	1.126	Jan 2016
1.31	Jan 1993	1.114	Nov 1998
1.31	Jan 2020	1.096	Feb 1990
1.20	Nov 1998	1.05	Jan 2020
1.20	Jan 2013	1.01	Nov 2015

At present, climate change is expected to attribute to 1–2 mm increase in the sea level rise per year in the UK. Horsburgh *et al.* (2020) estimated predicted sea-level rise under the high-emissions scenario (RCP8.5<sup>3</sup>) at all four capitals of the UK. In Edinburgh, sea levels are expected to rise by 0.23–0.54 m by 2100. Time series estimates in changes in sea level are available from the UK Met Office. Under the high-emissions scenario by 2100, the sea level at the offshore ECC landfall location will have risen by approximately 1 m, based on the 95<sup>th</sup> percentile estimate.

Over the last approximately thousand years, the average relative sea-level rise around the Orkney Islands, has been around 0.2 mm per annum. This is attributable to the ongoing isostatic emergence of the Scottish land mass after

<sup>3</sup> The UK Climate Projections 2018 (UKCP18) are based on the latest findings in climate science and, as per Institute of Environmental Management and Assessment (IEMA) guidance, predictions associated with the highest emissions scenario (Representative Concentration Pathway (RCP) 8.5) are referred to in this report. The projections are most applicable to onshore and coastal areas (mean sea level and storm surge trends) (Met Office, 2021).



the effects of glaciation due to the thawing of the Scottish Ice Sheet (Dawson *et al.*, 2013). This isostatic adjustment will continue in tandem with the predicted rise in sea level attributed to changes in the climate described above.

## 3.7 Tidal and Residual Flows/Currents

Tides are the dominant influence on local flows, although non-tidal influences (i.e. winds and surges) can also make a contribution, albeit on an episodic basis. The description of flow speeds within this technical report primarily refers to depth-averaged flow speeds, except where explicitly stated otherwise.

### 3.7.1 Overview

Waters in the north of Scotland are influenced by oceanic conditions from beyond the continental shelf. The residual flow is to the northeast and includes intrusions of warm Atlantic Water onto the shelf (Marine Scotland, 2020). Along the coast of mainland Scotland, local patterns are influenced by coastal topography, fluvial flow and wind-induced currents. These influences result in flood streams moving generally from west to east and ebb tides run east to west in the offshore areas, through the Pentland Firth and between the Orkney Islands (BEIS, 2009; Orkney Islands Council 2020). Strong tidal flows are associated with tidal flows that travel around the top of mainland Scotland, and most of the channels and headlands within the Orkney Islands and create oscillating falls in water level across the Orkney Islands (Orkney Islands Council, 2020). Within many of these channels a large range of tidal asymmetry can be observed with flood tides largely showing dominance (Orkney Islands Council, 2020).

The Pentland Firth channel separates the Orkney Islands from the Scottish mainland and connects the Atlantic Ocean with the North Sea. The Pentland Firth is characterised by strong tidal currents with widespread and highly energetic tidal races, eddies, overfalls and areas of general turbulence. Here, orbital currents (generated from wind and internal waves) are important energy sources for mobilising sediments into tidal streams.

Tidal flows were modelled across the West of Orkney model domain in order to inform potential impacts from development (sections 1.4 and 4.4.1.1). The modelled flow speed output from the West of Orkney model were largely in agreement with that from the Marine Scotland's Pentland Firth and Orkney Waters model (PFOW) (Marine Scotland, 2016) (Figure 3-23), with the exception of peak flows within the middle of the Pentland Firth, where slightly lower speeds were calculated in the West of Orkney model. Peak spring tidal currents in the middle of the Pentland Firth are about 4.5 m/s on both the flood and ebb tides (Marine Scotland, 2016), compared with just over 3 m/s in the West of Orkney model. Elsewhere, strong flows occur between the northern isles of Orkney Islands, with peak flow speeds of up to 3.01 m/s. Within most of the OAA, and across much of the wider offshore region in shallower water depths, current speeds are less than 1 m/s on a spring tide, and reducing further offshore, which is also the case for the PFOW model (Marine Scotland, 2016).

Modelled current speeds from ATT for tidal diamond SN028M, located to the northwest of the OAA, varied from 0.05 m/s to 0.41 m/s on a spring tide. Faster current speeds occurred on an ebb tide. Current speeds on a neap tide were reduced and ranged between 0.05 m/s and 0.21 m/s. Tidal diamond SN028F is located closer to the mainland Scottish coast, approximately mid-way between the OAA and the coast and 30 km west of the landfall location of the offshore ECC. Here, peak spring currents have a larger range from 0.21 m/s to 0.72 m/s. On a neap tide, currents range from 0.05 m/s to 0.26 m/s (UKHO, 2022).

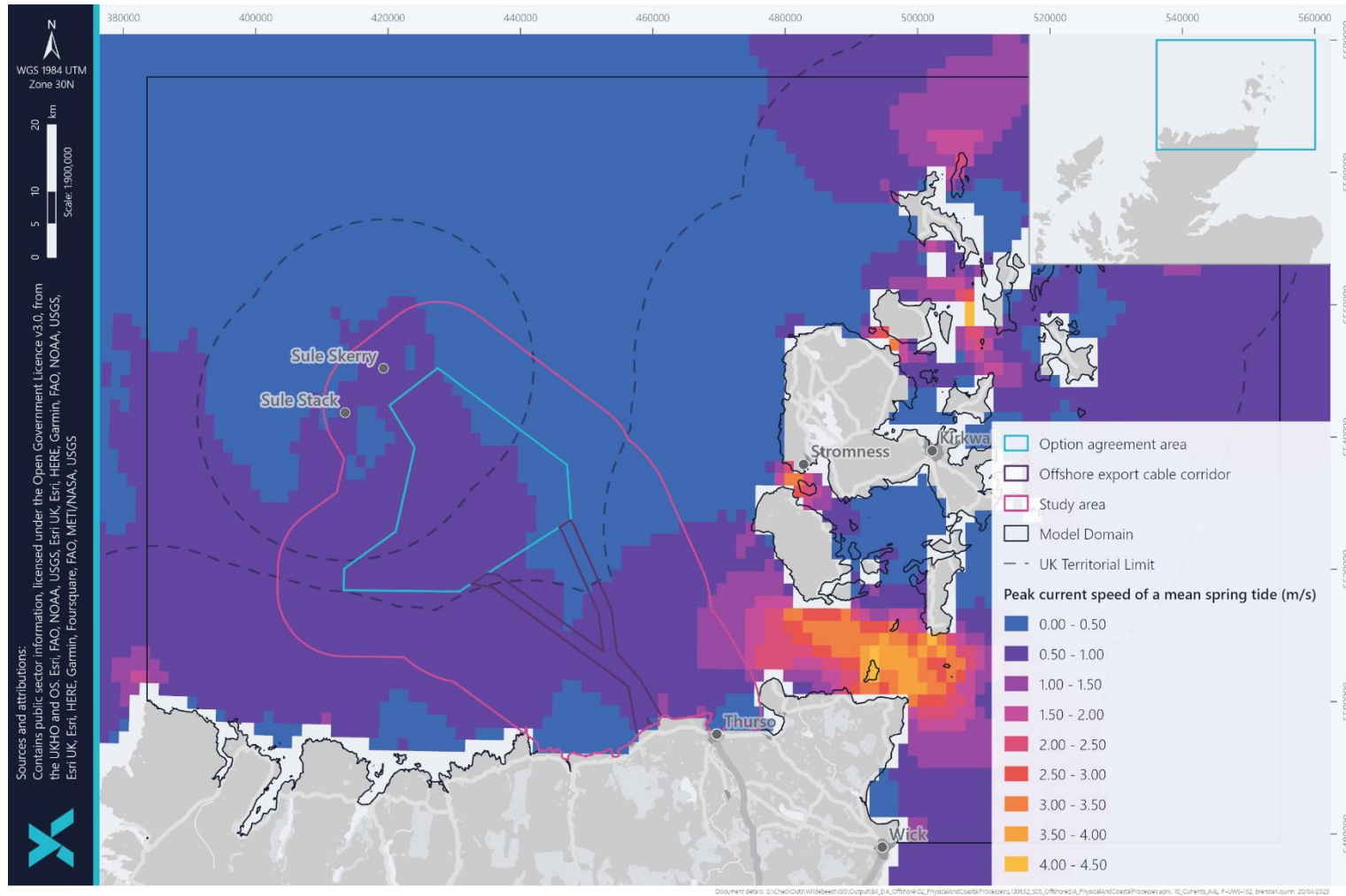


Figure 3-23 PFOV model peak (depth-average) flows on a mean spring tide (Marine Scotland, 2016)



### 3.7.2 Offshore Project Area

Modelled flow speeds and directions across the offshore Project area for varying tidal states were produced from the West of Orkney model and are primarily used to characterise the baseline tidal flows in association with available measured and hindcast within and in proximity to the offshore Project area. Modelled flow speeds at varying tidal states are summarised for spring and neap tides in Figure 3-24 and Figure 3-25 respectively and discussed further in the following sections.

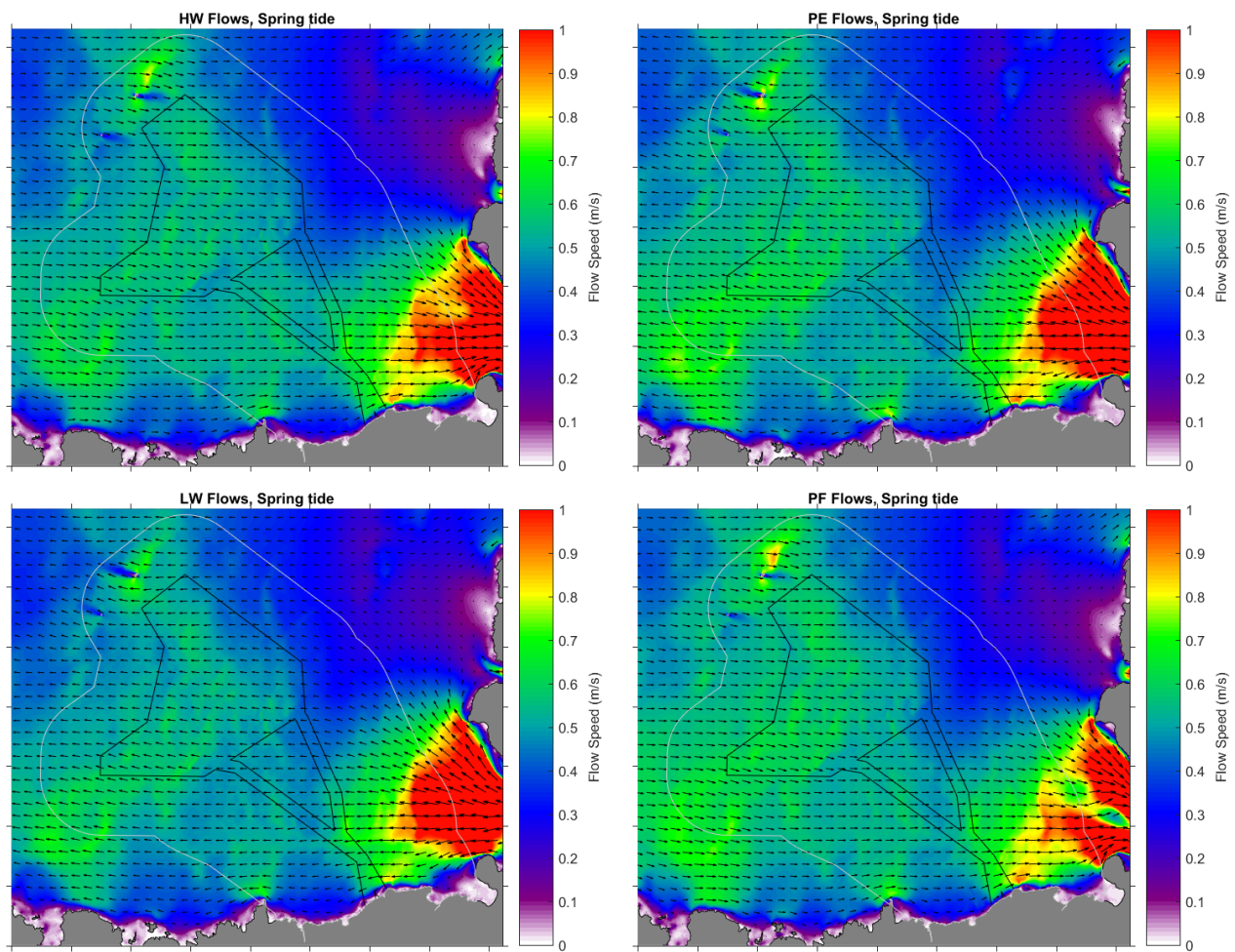


Figure 3-24 Mean spring flow speeds at varying tidal states output from the West of Orkney model (HW = High water, PE = Peak ebb, LW = Low water and PF = Peak flood)

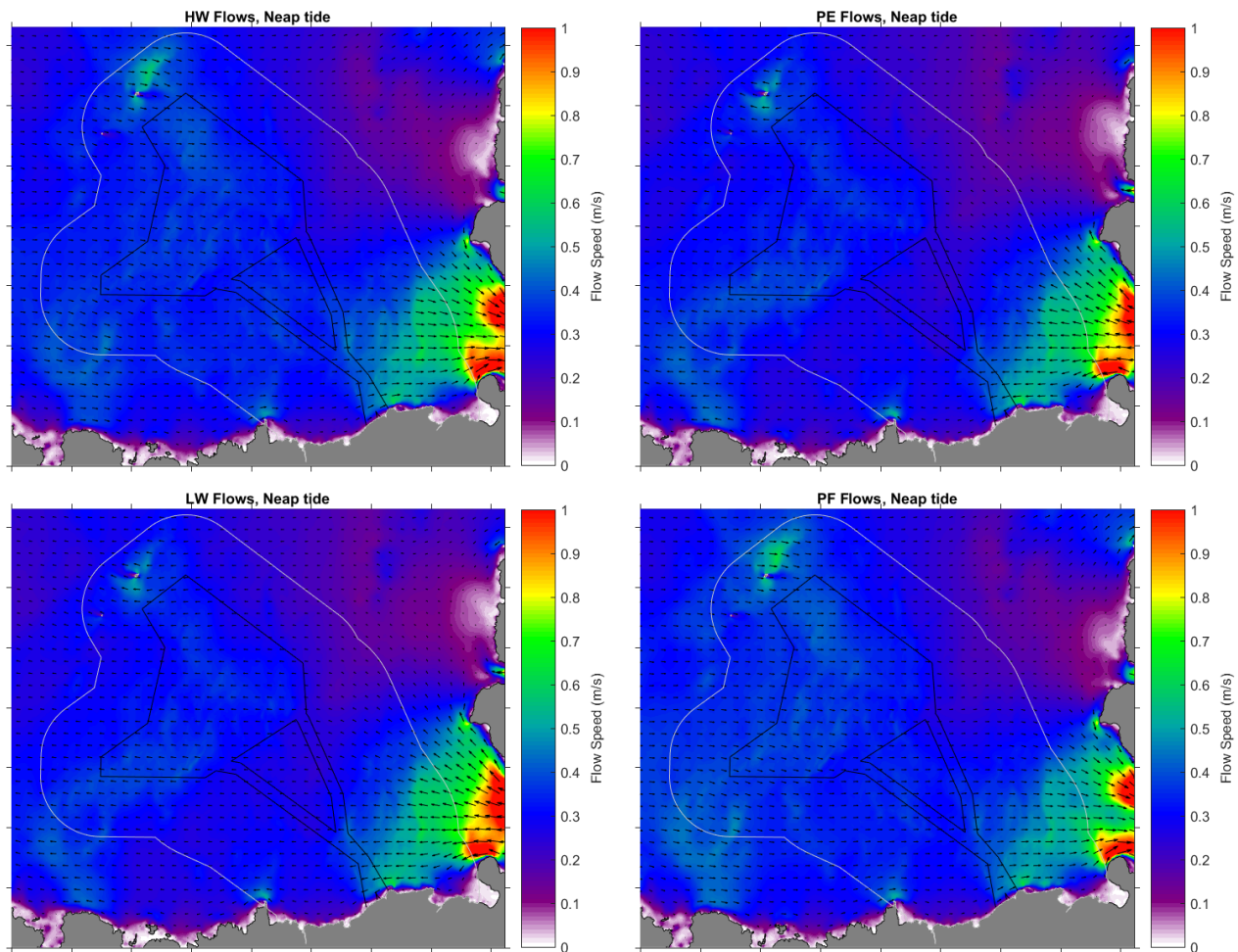


Figure 3-25 Mean neap flow speeds at varying tidal states output from the West of Orkney model (HW = High water, PE = Peak ebb, LW = Low water and PF = Peak flood)

### 3.7.2.1 Tidal current / flow speeds

For the majority of the OAA and the offshore ECC, mean peak flow for a spring tide is recorded as being between 0.5 m/s and 1.0 m/s (Figure 3-24). Equivalent peak neap flows are typically expected to be around 50% less than those on springs, with Figure 3-25 demonstrating flow speeds of less than 0.5 m/s.

As introduced in section 2.1.5, hindcast current data was sourced from MetOceanWorks European model for a 39-year period between 1979 and 2018, for a location within the OAA at approximately 58 m water depth (i.e. Current Point 1 in Figure 2-3). The flow properties from the current hindcast timeseries, indicate maximum spring and neap peak flows of 0.74 m/s and 0.56 m/s respectively (Table 3-6), with similar flow speeds occurring on the flood and ebb at this location. However, information from the PFOV model indicates a marginal flood dominance, with slightly more energetic tidal flood flows (Marine Scotland, 2016). Just to the west of the offshore ECC tidal stream data is available at the ATT tidal diamond SN028E (located in a water depth of approximately 45 m LAT). Peak flows on a spring tide are estimated to be 0.72 m/s and peak flow on a neap tide is estimated to be 0.26 m/s.



Table 3-6 Hindcast flow properties for a location (Current Hindcast 1, Figure 2-3) within the OAA

PARAMETER	VALUE
Peak ebb tidal speed (m/s)	0.74
Peak ebb tidal direction (°N)	92
Peak flood tidal speed (m/s)	0.74
Peak flood tidal direction (°N)	265
Main current direction (°N)	152
Average surface current (m/s)	0.34
Max spring peak tidal flow (m/s)	0.74
Max neap peak tidal flow (m/s)	0.56
Max non-tidal flow (m/s)	0.90

EMEC were contracted by OWPL to conduct a review of metocean characteristics across offshore Project area, based on a combination of hindcast records within the offshore Project area coincident with long-term observational records from the Billia Croo wave test site (EMEC, 2020). Calculated flow speeds across the OAA are noted to be similar to that described from the West of Orkney model, although results suggest a potential east-west divide, with very marginal (around 0.1 m/s) faster flow speeds in the west compared to the east.

Floating light detection and radar (FLiDAR) buoys were deployed within the PFOWF project area (comparable with the expected conditions in the offshore ECC). Near-bed current speed observations indicated flows close to the seabed are much reduced compared to depth average values, since they are slowed by the influence of seabed drag forming a boundary layer (Highland Wind Limited,, 2022).

### 3.7.2.2 Tidal direction

Figure 3-26 provides an indication of the orientation of tidal flows across the model domain, study area and offshore Project area based on the mean spring tidal ellipses (ABPmer, 2008). For the offshore Project area, the general orientation of the tidal ellipse is east to west. Modelled tidal flow direction from the West of Orkney model on spring and neap tides at various tidal states are illustrated Figure 3-24 and Figure 3-25 respectively. The figures demonstrate that the flood tide is largely towards the east, turning towards the south-east and approaching the Pentland Firth. Ebb tides are largely towards the west on exiting the Pentland Firth.

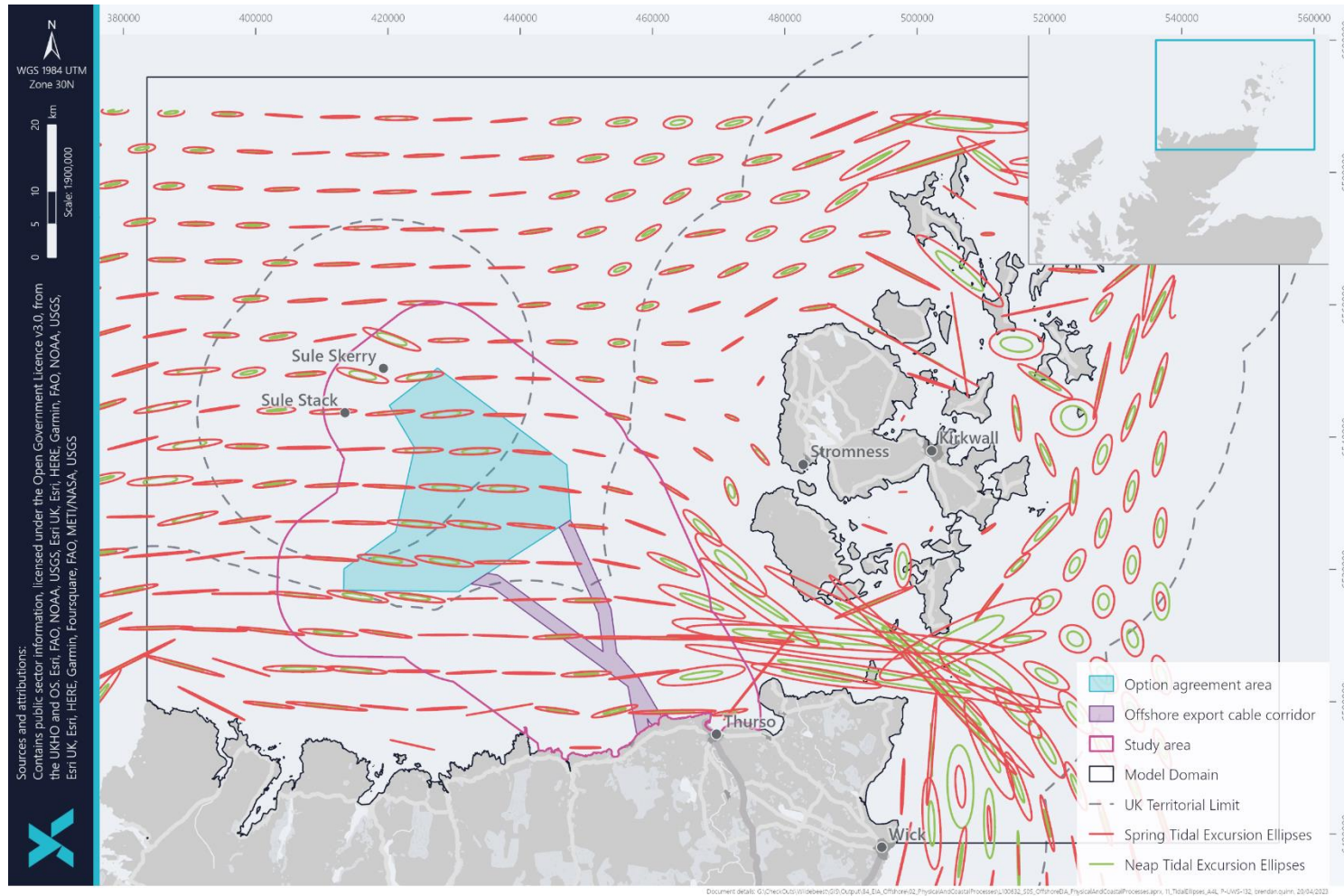


Figure 3-26 Tidal excursion ellipses from ABPmer (2008) across the offshore Project area and study area



### 3.7.2.3 Tidal residual

Tides across the offshore Project area are also asymmetric, with slightly more energetic tidal flows associated with the flood, and marginally less energetic tidal flows associated with the ebb (Marine Scotland, 2016). This results in a flood residual, which may occur in relation to speeds and (or) duration. Although peak flow speeds for the flood and ebb were of the same magnitude, demonstrated for Current Point 1 (Table 3-6), the hindcast timeseries for Current Point 2 demonstrate a flood residual, although the magnitude was low very low.

Tidal residual for a spring-neap tidal cycle was modelled for the offshore Project and study area using the West of Orkney model, with the result presented in Figure 3-27. Although the wider region encompassing the northwest Scottish continental shelf is considered to be flood dominant, with flow towards the east, the dominance is not reflected in the spring-neap cycle tidal residual. The figure demonstrates that the spring-neap residual flow speeds are very low, at less than 0.05 m/s across the majority of the offshore Project area, with no dominant residual flow direction. Across the study area, tidal residual flow speeds are again at or below 0.05 m/s, with only a small region reaching up to 0.1 m/s along the eastern margin of the study area adjacent to the Pentland Firth. The low tidal residual across the majority of the offshore Project area strongly indicates a low sediment transport potential, considered further in Section 3.9.

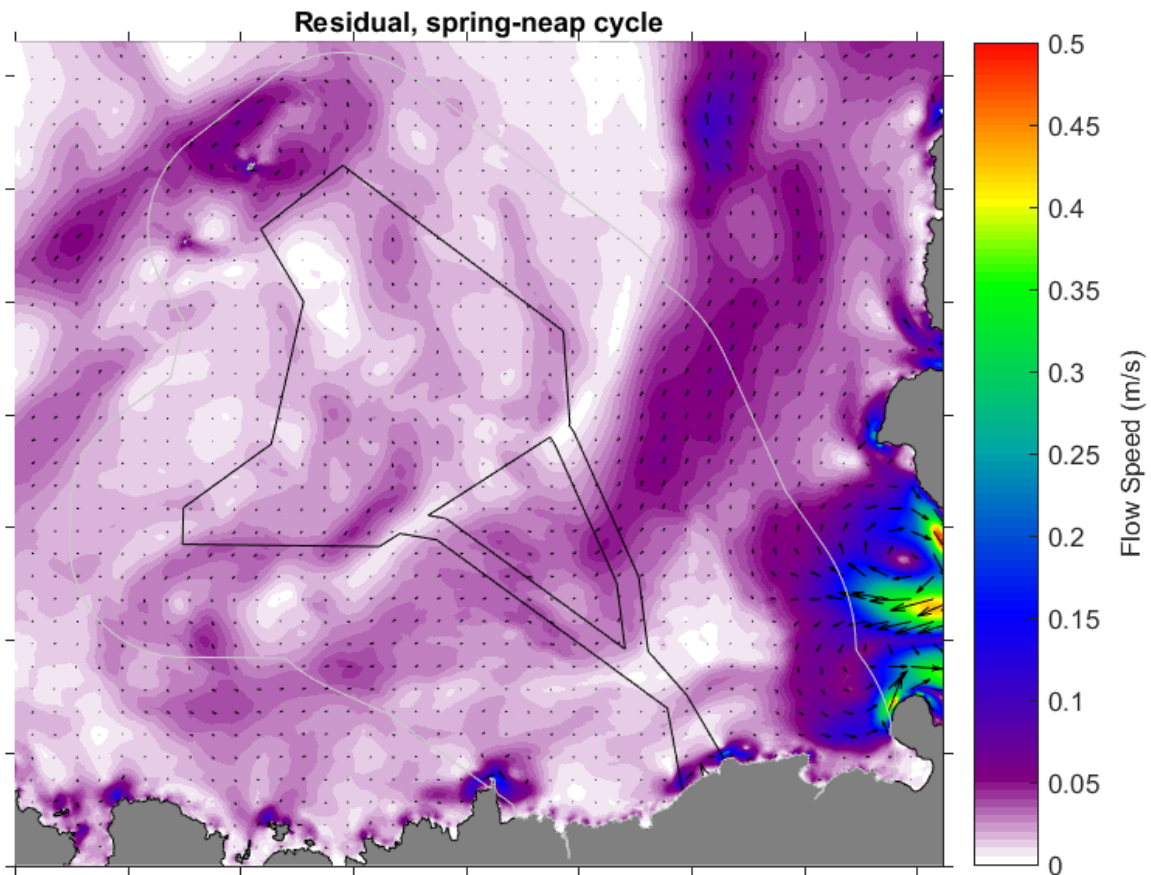


Figure 3-27 Modelled spring-neap tidal residual across the offshore Project and study areas, output from the West of Orkney model. Colours illustrate the residual flow speed and the vectors illustrate the flow speed and direction

### 3.7.3 Extreme Tidal and Residual Flows/Currents

Data from the Marine Renewables Atlas (ABPmer, 2008) indicates that tidal stream speeds of over 2 m/s do not occur anywhere across the offshore Project area, although exceedance of 1 m/s occurs at less than 11% of the time in proximity to Sule Skerry, within the study area. Speed exceedance increases towards the Pentland Firth, with over 50% annual exceedance of 2 m/s. Across the Project area, extreme non-tidal current speeds with respect to surge events are around 1.5 m/s at the surface and 0.8 m/s at the seabed based on a 5-year return period event. For a 100-year return period event, speeds of up to 2.2 m/s occur at the surface and 1.2 m/s near the seabed (OPWL, 2023).

## 3.8 Waves

The characterisation of wave properties within this technical report, relates to the description of significant wave height ( $H_s$ ), peak period (seconds) and mean direction (degrees), except where explicitly stated otherwise.



### 3.8.1 Overview

There is large natural variability to Scotland's wave climate with seasonal variation as a result of large scale weather conditions such as autumnal and winter storms (DECC, 2016b). Wave type varies from short steep waves which are created locally to waves with longer swell which originate from further afield in the Atlantic Ocean. Comparatively, the east coast of Shetland, Orkney Islands and the Scottish mainland are relatively more sheltered and less frequently exposed to large, powerful waves originating in the Atlantic. However relatively large wave heights can still occur as a result of North Sea storms and swells (DECC, 2016b). Annual mean significant wave heights across the study area range from <0.76 m amidst the Orkney Islands to approximately 3 m offshore northwest of the Orkney Islands and within the study area (ABPmer, 2008). The increase in wave heights occurs relatively rapidly with distance offshore from the west coast of the Orkney Islands. Immediately along the west coast of the Orkney Islands and the north coast of mainland Scotland wave heights are between 1.51 m and 2.25 m (ABPmer, 2008).

Throughout the study area, waves come predominantly from the west with the exception of the northern coastline of mainland Scotland where waves are mostly from the north and northwest (ABPmer, 2018). This trend of waves from the west continues into the Pentland Firth. Only to the east of the Orkney Islands does the directionality change as the influence of waves generated in the North Sea increases; the wave regime to the east of the Orkney Islands is mainly influenced by waves from the northeast and southeast (ABPmer, 2018).

Tidal influence on the wave regime in the Pentland Firth and Orkney Islands is more pronounced in the summer months when shorter period waves are more common. When considering annual timescales, the tidal influence on the wave resource is considered relatively modest as this takes into account the longer period waves associated with the more energetic autumn and winter months (Neil *et al.*, 2014). Within the Pentland Firth itself, a combination of deep open water and exposure to prevailing winds produces a high-energy wave climate, especially during north and northwest incident storms. Within the Pentland Firth, the sea floor falls steeply away from the west to 60 m, and so the coast of the island of Hoy, which borders the Firth to the north, is exposed to relatively high wave energies (OpenHydro and SSE, 2015).

### 3.8.2 Offshore Project Area

Data on mean significant wave height from the northwest European shelf seas model (Hashemi, Neill and Davies, 2014), indicates that in the north of the OAA and study area, mean significant wave height is  $\geq 2.5$  m, reducing to  $\geq 2$  m for the remainder of the OAA and the majority of the offshore ECC. This is consistent with the wave properties shown in Table 3-7. Closer to the coast, the mean significant wave height is  $\geq 1.0$  m (Hashemi, Neill and Davies, 2014). Data from the PFOW model (Marine Scotland, 2016) also indicates a gradual decrease in mean significant wave height from the north of the study area and OAA, reducing along the offshore ECC on the approach to the coast (Marine Scotland, 2016).

Wave conditions within the offshore Project area are informed by hindcast dataset spanning 1979 to 2015 extracted from the SWAN wave model developed by TU-Delft in Holland (OWPL, 2023). The wave hindcast timeseries was extracted at the Wave Hindcast 1 location within the OAA, as illustrated in Figure 2-3. Results of the extracted data is shown in Figure 3-28, which indicate that the significant waves are from westerly and northwesterly directions, which is expected given the dominant wind direction increased length of fetch in this area.

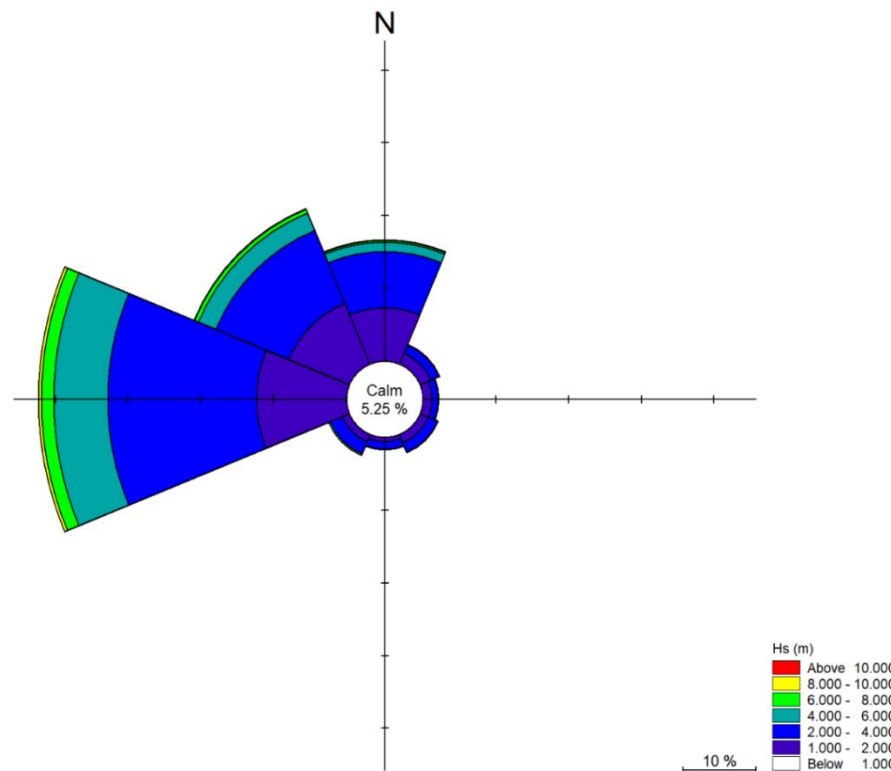


Figure 3-28 Wave rose for the offshore Project area using data from Wave Hindcast 1

Table 3-7 shows the frequency of occurrence of waves of a certain size as a percentage of all waves, based on the hindcast wave timeseries from Wave Hindcast 1. Waves with a significant height of 1-1.5 m and corresponding periods of 9-10 s are most frequent in the Project area; these waves occur 4.43% of the time (Table 3-7). The distribution of frequencies of wave occurrences in Table 3-7 shows that waves with periods longer than 10 s are also likely to occur regularly in the OAA. Waves with long periods (typically >10 s) tend to be indicative of swell-dominated climatologies. Overall, according to the data extracted from Wave Hindcast 1, both locally generated waves and swell waves originating further afield are influential over the wave climate within the offshore Project area. Considering the directionality of most waves in the offshore Project area (Figure 3-28), these swell waves originate in the Atlantic, or beyond.

The wave parameters outlined in Table 3-8 represent directional non-exceedance percentiles<sup>4</sup> calculated based on the Wave Hindcast 1 hindcast timeseries (OWPL, 2022). The omni-directional mean significant wave height (with the omni-directional statistic considered to be an average across all directional sectors) is 2.63 m with a corresponding period of 11 s. Per the data shown in Table 3-8, the average omni-directional wave has a greater height and period than the most frequently occurring waves, shown in Table 3-7. This further supports the narrative that swell waves are important to the wave climate within the offshore Project area. The non-exceedance percentiles relating to the 50<sup>th</sup> and 90<sup>th</sup> non-exceedance percentiles have been used to inform the modelling approach. In particular, waves from the prevailing directions (north, northwest and west, per Figure 3-28) are considered within the West of Orkney model.

<sup>4</sup> The non-exceedance percentiles indicate the point beyond which a wave of a certain size will not occur; for instance, the 50th percentile statistics represent the parameters which 50% of waves will not exceed.



Table 3-7 Wave properties and percentage occurrence (as a percentage of all waves), Wave Hindcast 1 (1979 – 2015)

Significant wave height (m)	Peak wave period (s)																	
	2-3	3-4	4-5	5-6	6-7	7-8	8-9	9-10	10-11	11-12	12-13	13-14	14-15	15-16	16-17	17-18	18-19	19-20
0-0.5	0.00%	0.00%	0.00%	0.00%	0.01%	0.04%	0.02%	0.01%	0.01%	0.00%								
0.5-1	0.00%	0.09%	0.18%	0.15%	0.41%	1.00%	1.59%	1.15%	0.43%	0.15%	0.05%	0.06%	0.02%	0.00%	0.01%	0.00%	0.00%	
1-1.5		0.01%	0.76%	0.51%	0.73%	2.03%	4.17%	4.43%	2.40%	1.02%	0.50%	0.24%	0.09%	0.03%	0.02%	0.01%	0.00%	0.00%
1.5-2			0.07%	1.26%	0.50%	1.04%	2.46%	4.36%	3.89%	2.16%	0.96%	0.57%	0.26%	0.08%	0.03%	0.01%	0.00%	0.00%
2-2.5			0.00%	0.53%	0.65%	0.66%	1.29%	2.57%	3.74%	3.00%	1.74%	0.90%	0.49%	0.16%	0.07%	0.03%	0.00%	0.00%
2.5-3				0.02%	0.72%	0.36%	0.68%	1.38%	2.46%	2.89%	1.96%	1.25%	0.54%	0.23%	0.10%	0.03%	0.01%	0.00%
3-3.5					0.30%	0.30%	0.42%	0.84%	1.38%	1.92%	1.92%	1.45%	0.72%	0.30%	0.12%	0.03%	0.02%	0.01%
3.5-4					0.03%	0.21%	0.17%	0.54%	0.81%	1.25%	1.36%	1.30%	0.76%	0.29%	0.12%	0.04%	0.01%	0.00%
4-4.5					0.00%	0.08%	0.05%	0.26%	0.51%	0.76%	0.97%	1.03%	0.72%	0.27%	0.15%	0.05%	0.01%	0.00%
4.5-5						0.01%	0.02%	0.07%	0.29%	0.48%	0.62%	0.73%	0.54%	0.25%	0.14%	0.03%	0.00%	
5-5.5						0.00%	0.01%	0.01%	0.14%	0.33%	0.40%	0.49%	0.44%	0.25%	0.13%	0.02%	0.01%	
5.5-6							0.00%	0.00%	0.04%	0.20%	0.28%	0.33%	0.34%	0.22%	0.13%	0.02%	0.00%	
6-6.5							0.00%	0.00%	0.01%	0.09%	0.21%	0.23%	0.23%	0.16%	0.09%	0.02%	0.00%	
6.5-7									0.00%	0.03%	0.13%	0.16%	0.15%	0.11%	0.06%	0.02%	0.00%	
7-7.5									0.00%	0.01%	0.06%	0.13%	0.10%	0.08%	0.04%	0.02%	0.01%	
7.5-8										0.00%	0.02%	0.08%	0.09%	0.04%	0.05%	0.01%	0.00%	
8-8.5										0.00%	0.01%	0.05%	0.07%	0.04%	0.03%	0.01%	0.00%	
8.5-9											0.00%	0.03%	0.05%	0.03%	0.02%	0.01%	0.00%	
9-9.5											0.00%	0.02%	0.03%	0.02%	0.01%	0.01%		
9.5-10												0.01%	0.02%	0.02%	0.01%	0.01%		
10-10.5												0.00%	0.01%	0.02%	0.01%	0.01%		
10.5-11												0.00%	0.00%	0.01%	0.00%	0.00%	0.00%	
11-11.5													0.00%	0.01%	0.00%	0.00%	0.00%	
11.5-12													0.00%	0.01%	0.00%	0.00%	0.00%	
12-12.5														0.00%	0.00%	0.00%	0.00%	
12.5-13														0.00%	0.00%			
13-13.5														0.00%				



Table 3-8 Calculated non-exceedance statistics based on the Wave Hindcast 1 hindcast timeseries (OWPL, 2023)

DIR (°N)	MIN HS (M)	MEAN HS (M)	MAX HS (M)	NON-EXCEEDANCE PERCENTILES						
				1%	5%	10%	50%	90%	95%	99%
0	0.37	2.32	11.08	0.71	0.94	1.10	2.06	3.88	4.65	6.40
45	0.38	1.96	8.52	0.66	0.88	1.02	1.76	3.15	3.59	4.77
90	0.40	1.94	6.24	0.74	0.92	1.05	1.77	3.10	3.47	4.33
135	0.47	2.14	6.12	0.82	1.00	1.16	2.00	3.29	3.60	4.28
180	0.38	2.32	6.33	0.74	1.05	1.23	2.24	3.45	3.83	4.64
225	0.40	2.50	8.90	0.79	1.08	1.26	2.35	3.89	4.43	5.75
270	0.28	2.95	13.17	0.77	1.05	1.26	2.62	5.06	5.95	8.00
315	0.25	2.52	12.93	0.72	0.94	1.11	2.22	4.34	5.26	7.21
OMNI	0.25	2.63	13.17	0.74	0.98	1.16	2.31	4.51	5.41	7.38
<b>Tp (s) associated with the above Hs statistics</b>										
0	6.8	10.7	15.9	8.0	8.5	8.9	10.4	12.1	12.7	13.7
45	6.9	10.2	14.8	7.8	8.4	8.7	10.0	11.5	11.9	12.8
90	7.0	10.2	13.7	8.1	8.5	8.8	10.0	11.5	11.8	12.5
135	7.2	10.5	13.6	8.3	8.7	9.0	10.3	11.7	11.9	12.4
180	6.9	10.7	13.7	8.0	8.8	9.1	10.6	11.8	12.1	12.7
225	7.0	10.9	15.0	8.2	8.8	9.2	10.7	12.1	12.5	13.4
270	6.4	11.3	16.7	8.1	8.8	9.2	11.0	13.0	13.5	14.6
315	6.3	10.9	16.6	8.0	8.5	8.9	10.6	12.5	13.1	14.2
OMNI	6.3	11.0	16.7	8.0	8.6	9.0	10.7	12.6	13.2	14.3

EMEC were contracted to undertake a review of available data for the OAA in 2020. As part of this, OWPL were provided with a suite of data for the OAA area (EMEC, 2020). This included information on the mean significant wave height within the OAA which was extracted using an in-house hindcast dataset. Mean significant wave height was shown to vary from the north to the south of the OAA, with the highest mean Hs recorded as 2.7 m to 2.8 m in the



north of the site. Wave heights gradually reduce in a southerly direction through the OAA, to a minimum of 2.4 m to 2.5 m in the very south of the OAA. This correlates with the data described above which suggests that wave heights become reduced towards the coast.

Annual occurrence of significant wave heights throughout the year at the OAA and at the EMEC Billia Croo test site (off the west coast of Orkney mainland) are presented in Table 3-9 for comparison. OWPL (2023) reported that the modelled mean annual significant wave height in the OAA was 2.6 m. At Billia Croo the mean annual significant wave height was 2.0 m (EMEC, 2020). This is likely given the proximity of the Billia Croo site closer to shore. At the OAA the annual average wave heights exceeding 1.0 m 95% of the time (OWPL, 2023). At Billia Croo this is significantly lower with a wave height of 0.6 m being exceeded 95% of the time (EMEC, 2020). This can likely be attributed to the offshore wind conditions at the OAA. In the autumn and early winter months (October to January) waves exceed 5 m 5% of the time within the OAA (OWPL, 2023), with similar wave heights occurring at Billia Croo. Extreme wave conditions are discussed in Section 3.8.3.

Table 3-9 Monthly exceedance statistics for significant wave height at the OAA (OWPL, 2023) and Billia Croo (EMEC, 2020)

MONTH	SIGNIFICANT WAVE HEIGHT (M)									
	OAA					Billia Croo				
	min	mean	max	5%	95%	min	mean	max	5%	95%
Jan	0.7	3.7	13.2	7.1	1.8	0.5	2.8	10.7	5.6	1.0
Feb	0.8	3.5	12.3	6.5	1.6	0.4	2.6	10.5	5.0	1.0
Mar	0.6	3.3	12.0	6.0	1.5	0.0	2.4	8.0	4.7	0.8
Apr	0.6	2.5	9.7	4.5	1.2	0.0	1.9	7.6	3.9	0.7
May	0.3	1.9	8.7	3.6	0.9	0.0	1.5	7.4	3.6	0.5
Jun	0.5	1.6	8.7	2.9	0.9	0.1	1.2	6.0	2.6	0.4
Jul	0.4	1.5	4.9	2.7	0.8	0.2	1.2	4.9	2.5	0.4
Aug	0.4	1.7	7.0	3.1	0.8	0.2	1.3	6.3	2.9	0.4
Sep	0.5	2.3	12.4	4.4	1.1	0.3	1.9	8.3	4.0	0.6
Oct	0.5	2.8	10.9	5.3	1.3	0.3	2.2	9.9	4.9	0.6
Nov	0.7	3.2	12.3	5.8	1.5	0.4	2.6	8.2	5.4	0.8
Dec	0.7	3.5	11.8	6.3	1.5	0.3	3.0	11.2	6.0	1.0
All-year	0.3	2.6	13.2	5.4	1.0	0.0	2.0	11.2	4.7	0.6

The small rocky islands of Sule Skerry and Sule Stack are located less than 5 km north of the OAA. Sule Skerry is approximately 16 hectares (160,000 m<sup>2</sup>) in area and 800 m long and reaches a height of 12 m. Sule Stack is smaller in size. Despite the small size of the island and stack, given their close proximity to the OAA they may have an impact



on the wave regime through the OAA, particularly for long period swell waves. The movement of waves may be interrupted by the land masses to produce a wave shadow in the wave lee of the island (Arthur, 1951). There is currently no site-specific evidence to describe the impact that Sule Skerry and Sule Stack have on the surrounding wave environment.

At the landfall locations, information on the nearshore wave properties are illustrated from the wave rose for the grid cell that overlaps the landfalls, obtained from the Seastates data explorer (ABPmer, 2018b) and illustrated in Figure 3-29. Nearshore significant wave heights are typically around 1.6 m, with waves largely approach from the north, but also the northwest and west approach sectors (Figure 3-29). Based on the modelled data the mean wave height at the landfalls is still similar to the most frequent wave height observed offshore (i.e. taken to be around 1.5 m, with an associated period of 9.5 seconds). However, further west and slightly offshore of the landfalls, located in a water depth of 24 mLAT is the Dounreay WaveNet buoy, which provided, observations between October 1997 and May 2001 and indicates a reduction in significant wave height, but a consistent period as illustrated in Table 3-10 (Cefas, 2022). Based on the observation data, the most frequent waves are associated with a significant height ranging between 0.5 and 1 m and period between 9 and 10 seconds (Table 3-10). At a finer resolution, the most frequent waves are associated with a wave height of 0.8 m or 0.9 m, between 9 and 10 seconds. No direction information is provided to confirm the approach.

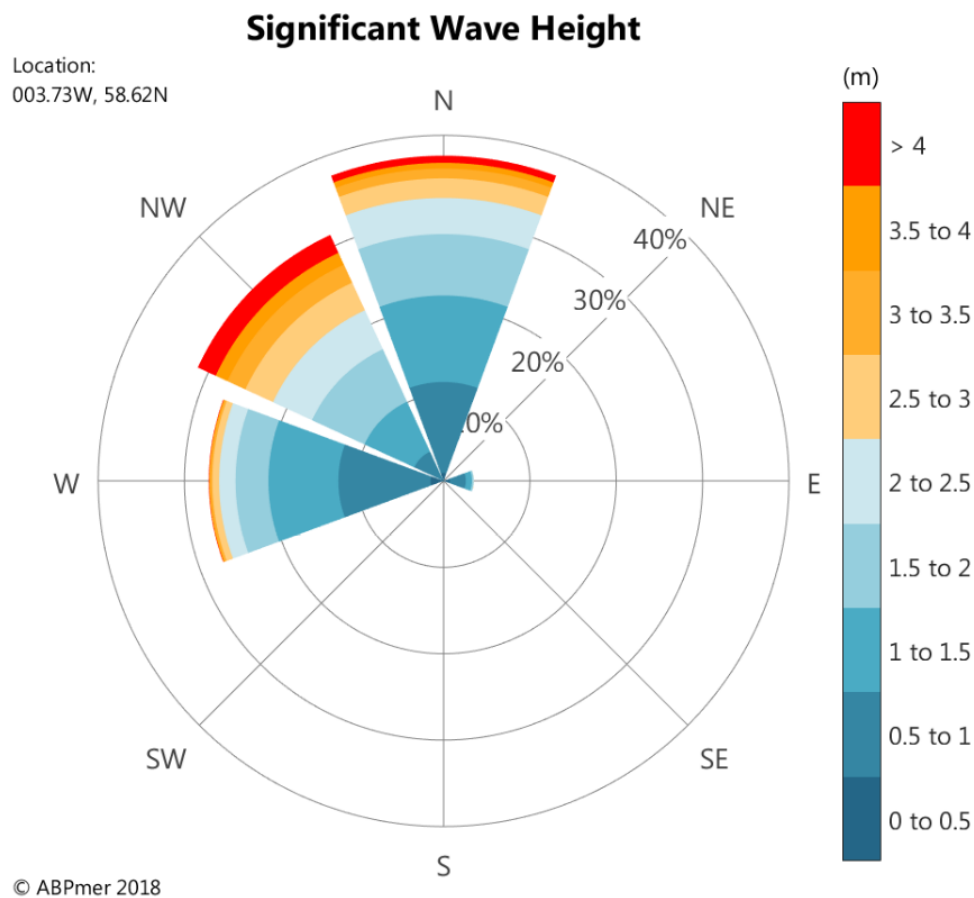


Figure 3-29 Wave rose for the landfall area from ABPmer (2018b)



Table 3-10 Wave properties from Dounreay WaveNet site for observations between October 1997 and May 2001

Significant wave height (m)	Average zero wave crossing period (s)													
	5-6	6-7	7-8	8-9	9-10	10-11	11-12	12-13	13-14	14-15	15-16	16-17	17-18	18-19
0 -0.5		0.07%	1.53%	3.90%	2.44%	2.58%	3.48%	2.44%	1.18%	0.35%	0.14%	0.14%	0.14%	0.07%
0.5-1	0.07%	0.14%	2.93%	7.74%	10.52%	9.69%	4.67%	4.25%	0.91%	0.77%	0.63%	0.21%	0.42%	0.07%
1-1.5		0.14%	1.32%	3.90%	7.46%	5.78%	3.00%	0.91%	0.56%	0.35%	0.14%			
1.5-2		0.21%	0.56%	1.46%	2.16%	1.32%	1.32%	0.42%	0.28%	0.07%	0.07%			
2-2.5			0.35%	0.42%	1.05%	0.91%	0.35%	0.14%	0.14%	0.07%	0.07%			
2.5-3			0.07%	0.42%	0.49%	0.56%	0.35%							
3-3.5			0.07%		0.42%	0.21%	0.14%			0.14%				
3.5-4				0.07%	0.21%			0.07%						

The relevance of waves to marine processes is their capacity to stir local seabed sediments and contribute to sediment transport, as well as the influence of wave energy dissipation at the coast. The projected change in significant wave height over the next 110 years is between 0.18 m lower to the west of the Orkney Mainland to 0.35 m lower to the north and east of the Orkney (Orkney Islands Council, 2020).

### 3.8.3 Extreme Waves

The west coast of the Orkney Islands is exposed to a fetch of over 3,000 km across the Atlantic Ocean, resulting in wave heights of over 18 m during storm events. Scapa Flow and areas between the North Isles of Orkney have a more limited fetch and in turn reduced wave heights are experienced (Orkney Islands Council, 2020). The longest uninterrupted fetches for wave exposure around the offshore Project area are from the west to northerly sectors, with reduced fetches to the east due to the Orkney Islands.

Extreme wave conditions for the OAA show that largest waves come from the west, from the Atlantic. Based on the wave hindcast timeseries from Wave Hindcast 1, wave properties were calculated for a number of extreme statistics and summarised in Table 3-11 (OWPL, 2023). Wave properties associated with the 1 in 1-year storm event from the dominant westerly approach sector (i.e. 270 °) indicates a significant wave height of 10.2 m with a corresponding wave period of 15.7 s. During a 1 in 100-year storm event, the mean significant wave height reaches 14.0 m with a corresponding period of 17.2 s.

Within the PFOWF array area, extreme wave heights for 50 and 100-year return periods were 13.6 m and 14.2 m respectively; the direction of these waves is consistent with other findings for the area (Highland Wind Limited, 2022). At the OAA and based on data from Wave Hindcast 1, the maximum wave height was noted as 13.2 m in January (OWPL, 2023). At Billia Croo, the maximum wave height occurred in December as 13.2 m (EMEC, 2020). The maximum wave heights at two ADCPs (ST003 and ST004) deployed within the Costa Head tidal site, off the north coast of the Orkney mainland, were 13.99 m and 12.23 m respectively (Partrac, 2013); these observed statistics are in keeping with the modelled information described for the OAA and Billia Croo sites. Extreme wave results for different return periods from Billia Croo, based on ten years of in-situ observations, again confirm the largest waves under extreme conditions



approach from west to northerly sectors. Therefore, as the largest and longest waves approach from the west, northwest and north (i.e. 270, 315 and 0 °N respectively), these are the directions used to inform the modelling of wave effects within the West of Orkney model.

Table 3-11 Extreme wave conditions for different return periods in the OAA (OWPL, 2023)

DIRECTIONAL SECTOR (°N)	1		5		10		50		100	
	Hs (m)	Tp (s)								
0	8.2	14.8	9.6	15.4	10.1	15.7	10.9	16.0	11.2	16.2
45	6.1	13.7	7.2	14.2	7.5	14.5	8.1	14.7	8.3	14.9
90	5.5	13.4	6.5	13.9	6.8	14.1	7.4	14.4	7.6	14.5
135	5.5	13.3	6.4	13.9	6.7	14.1	7.3	14.3	7.5	14.5
180	5.9	13.6	7.0	14.1	7.3	14.4	7.9	14.6	8.1	14.8
225	7.3	14.4	8.6	15.0	9.0	15.2	9.8	15.5	10.1	15.7
270	10.2	15.7	12.0	16.4	12.6	16.7	13.6	17.0	14.0	17.2
315	9.2	15.3	10.8	15.9	11.4	16.2	12.3	16.5	12.6	16.7
Omni	10.2	15.7	12.0	16.4	12.6	16.7	13.6	17.0	14.0	17.2

## 3.9 Sediment Transport

The interaction of the seabed with wave and tidal processes determines how often unconsolidated surficial sediments become mobilised and the way they are transported (i.e. bed load transport and/or suspended load transport). Section 3.3 provides an overview of the seabed sediment distribution across the study area, which is used in association with tidal and wave properties considered in Section 3.7 and Section 3.8 respectively, to inform the sediment transport potential. The frequent presence and wide distribution of cobbles and boulders across the offshore Project is recognised; however, the assessment of sediment transport potential is completed for up to the gravel fraction.

### 3.9.1 Overview

The Pentland Firth has been identified as a bedload parting zone with transport directed into the North Sea in the eastern section and into the north Atlantic in the western section. While the current speeds within the Pentland Firth are particularly high, there are areas of mobile sediment associated with headlands, islands and areas of weaker current in and amongst the Orkney Islands, which also show areas of highly mobile sediments. Within the Pentland Firth, Fairley *et al.*, (2015) found that the rate of bed level change on a spring tide was almost 1 m/day. On a neap tide, this was considerably lower at <0.1 m/day. Sediment transport corresponds to the direction of flow, with transport to the east on a flood and west on an ebb.



## 3.9.2 Project Area

Seabed sediment across the Project area are generally coarse comprising sands and gravels, with percentages of the coarse fraction being over 95% and the finer silt fraction being only up to 2% (Table 3-2). Based on the sampled sediment across the Project area, as described in Section 3.3, the mean sediment size within the OAA is around 2.21 mm (i.e. very fine gravel) and around 0.80 mm (i.e. coarse sand) within the offshore ECC.

### 3.9.2.1 Coarse sediments

Coarser sediments (i.e. sands and gravels) typically move as bedload transport in response to waves and tides. Using the time series data of current speeds at two hindcast locations (Current Point 1 and Current Point 2, as shown in Figure 2-3) within the OAA, along with 28 locations across the OAA and offshore ECC extracted from the West of Orkney Model (Figure 2-4), the mobility potential was calculated.

Current Point 1 and 2, located within the OAA are in water depths of 66 m and 65 m respectively. The timeseries of flows for a representative spring-neap period were extracted from both datasets to calculate the sediment transport potential and percentage mobility for the range of sediments that occur across the offshore Project (Section 3.3.2).

Table 3-12 shows the mobility, as a percentage of time for the different sediment sizes. While currents are the main driving force behind generating sediment mobility, waves also can influence this transport to a lesser extent, but also act with currents in the resulting mobility. The results of the sediment mobility analysis varied slightly between the two current data points, which can be attributed the differences in the hindcast timeseries (Section 3.6).

Smaller sediment sizes, encompassing fine sand, medium sand and coarse sand, were all mobile at some point during a tidal cycle at Current Point 1. These sediments were mobile on both spring and neap tides however, on the lowest neaps during the tidal cycle these sediments were not mobile (Table 3-12). The influence of currents was also combined with wave properties, using a single representative wave of a significant wave height of 1.5 m, with a corresponding period of 9.5 s (per the wave conditions described in Section 3.8.2). Under the combined current and wave scenario, sediment mobility remained the same. Only for the coarse sediment did the additional influence of waves generate a slight increase in mobility (20%, up from 19% under a current only scenario). At Current Point 2, results overall indicated a lower sediment mobility across all sediment sizes (Table 3-12). The addition of wave influences to the analysis showed a similarly minor response – there was a 1% increase in sediment mobility for fine and coarse sands when currents and waves were combined.

Common to both sets of current data (Current Point 1 and 2, Figure 2-3), was the result that under all scenarios larger sediment sizes (i.e. gravels) were never mobilised (Table 3-12).



Table 3-12 Sediment mobility potential as a percentage of time for varying sediment sizes that occur across the offshore Project area

SEABED SEDIMENT	FINE SAND	MEDIUM SAND	COARSE SAND	VERY FINE GRAVEL	FINE GRAVEL	MEDIUM GRAVEL
SEDIMENT SIZE (MM)	0.175	0.35	0.63	3	6	11
Current Point 1	40%	32%	19%	0%	0%	0%
	Mobile spring and peak neap tides, not mobile at lowest neaps		Mobile spring tides only		Not mobile	
Current Point 1	40%	32%	20%	0%	0%	0%
	Mobile spring and peak neap tides, not mobile at lowest neaps		Mobile spring tides only		Not mobile	
Current Point 2	26%	18%	7%	0%	0%	0%
	Mobile spring tides only		Mobile peak spring tides only		Not mobile	
Current Point 2	27%	18%	8%	0%	0%	0%
	Mobile spring tides only		Mobile peak spring tides only		Not mobile	

A timeseries of water levels and flows (speed and direction) for a 15-day period between 16<sup>th</sup> January 2013 and 31<sup>st</sup> January 2013, across a spring neap tidal cycle, was extracted for the 28 model extraction locations across the offshore Project area (Figure 2-4). Of the model time series extraction locations across the Project area, results for six across the OAA and four across the offshore ECC are presented for their sediment transport potential. The illustrated and discussed locations were selected on the basis of the varying water depths, seabed sediment and flow residual properties, to therefore assess for the possibility of spatial variability in the sediment transport potential across the offshore Project area. The timeseries data extraction locations, as well as those analysed for the sediment transport potential, are illustrated in Figure 2-4. The calculated percentage of time sediment would be mobile at these locations during the analysed spring neap tidal cycle is presented Table 3-13 and Table 3-14, in accordance with the wave parameters which were used in the analysis. Per the wave statistics outlined in section 3.8.2, the most frequent wave to occur in the offshore Project area has a significant height of 1.5 m and a corresponding period of 9.5 s, for which results are set out in Table 3-13. In addition to the most frequent type of wave, the average omni-directional wave has a height of 2.6 m and a period of 11 s; these results are shown in Table 3-14. Along with the model-extracted flows, these two wave parameters were used to determine sediment transport.

Sediment transport mobility appears to be relatively consistent across the offshore Project area. As stated previously, currents are the principal driving force behind sediment transport. The sediment transport results reflect this; currents acting in isolation were able to generate sediment mobility of fine, medium and coarse sand at most locations within the OAA. However, at some locations the influence of waves is evident. In particular, this is clear under the larger wave parameters in Table 3-14. At some locations within the OAA and offshore ECC there is evidence of smaller



sediments being disturbed under the influence of waves alone. In combination with the effect of currents, the percentage of mobile sediments decreases. The reason for 100% sediment mobility under waves alone is due to the ability of large waves to pick up sediments. However, sediments which are suspended by swell are only moved in an orbit associated with each swell wave. Ultimately, sediments are picked up by the oscillation of the wave and deposited in the same location. Therefore, the high percentages of mobility associated with waves are not necessarily representative of transport over a distance, but a localised disturbance event. While waves act to lift material off the seabed, flows are responsible for transporting that material over any kind of distance. Therefore, flows remain to be the most important factor in sediment transport.

Under the smaller wave parameters, fine sands (0.175 mm) are mobile at most of the sample locations between 20-40% of the time (Table 3-13). This mobility generally corresponds to spring tides, with peak neap tides in certain locations also having conditions conducive to generating mobility. The sediment transport mobility described as a result of the combined influence of currents and wave action, is marginally higher than reported for currents alone. Exceptions to this are in locations which show significant mobility due to waves alone (i.e. OAA7). As explained above, this mobility is not necessarily reflective of transport over longer distances. Under the larger wave scenario, sediments are generally mobile more of the time; on average, sediments across the offshore Project area as a whole are mobile 48% of the time (Table 3-14). The influence of the larger wave is evident through the elevated sediment mobility. However, at no location are conditions able to mobilise gravel sized sediments ( $\geq 3$  mm) at any point under either wave parameter.

OAA10 and OAA11 (see Figure 2-4), which are located on the flanks of the Stormy Bank, exhibit mobility of fine and medium grained sand under the smaller wave conditions, albeit at lower levels than elsewhere within the OAA. However, coarse sand (0.63 mm) is mobile approximately 1% of the time, or not at all at OAA11. With regards to depth, these points are located in 69 mLAT and 63 mLAT respectively. These depths are relatively consistent with other points within the OAA which implies that the water depth is not necessarily responsible for the difference in sediment mobility at these two locations compared to others. Under the larger wave parameters, these locations are more in-keeping with general trends across the whole offshore Project area. Another factor which influences sediment mobility is bed roughness, which accounts for the sediment type at each location and its influence on the movement of the flow locally (i.e. turbulent versus laminar). This explains the difference in results at OAA3 and OAA4 when compared against OAA11. Despite all three locations having the same water depth, the assumed presence of a coarser seabed applied at OAA3 and OAA4 results in more turbulent flows, sediment disturbance and transport potential.

Sediment transport within the offshore ECC differs from what is seen within the OAA. The range in sediment mobility also varies considerably throughout the offshore ECC, increasing towards the coast. Under the smaller wave conditions, fine sands within the offshore ECC are mobile upwards of 30% of the time, with the exception of ECC2 which shows mobility of fine sediments occurs 20% of the time (under a combined currents and wave scenario). Under larger wave conditions, mobility is upwards of 41%, again with the exception of ECC2. At ECC4, located closest to the coast in 56 mLAT, fine sand is mobile 61% of the time, with medium and coarse sand also mobile >40% of the time under the smaller wave scenario (Table 3-13). When the wave parameters are increased, mobility of fine sediments occurs 71% of the time. Medium and coarse sands are mobile >55% of the time (Table 3-14).



Table 3-13 Sediment mobility potential at analysed locations across the Offshore project area (OAA and ECC respectively) using extracted time series flows from the West of Orkney model and a wave with a height of 1.5 m and a period of 9.5 s; mobility potential is given as a percentage of time for varying sediment sizes

SEABED SEDIMENT		FINE SAND	MEDIUM SAND	COARSE SAND	VERY FINE GRAVEL	FINE GRAVEL	MEDIUM GRAVEL
SEDIMENT SIZE (MM)		0.175	0.35	0.63	3	6	11
OAA3 (69 mLAT)	Currents only	27%	19%	8%	0%	0%	0%
		Mobile spring and peak neap tides, not mobile at lowest neaps	Mobile spring tides only	Mobile spring tides only	Not mobile	Not mobile	Not mobile
	Waves only	0%	0%	0%	0%	0%	0%
Not mobile		Not mobile	Not mobile	Not mobile	Not mobile	Not mobile	
Currents and waves	33%	25%	12%	0%	0%	0%	
	Mobile spring and peak neap tides, not mobile at lowest neaps	Mobile spring and peak neap tides, not mobile at lowest neaps	Mobile spring tides only	Not mobile	Not mobile	Not mobile	
OAA4 (69 mLAT)	Currents only	31%	23%	12%	0%	0%	0%
		Mobile spring and peak neap tides, not mobile at lowest neaps	Mobile spring tides, not mobile at lowest neaps	Mobile peak spring tides	Not mobile	Not mobile	Not mobile
	Waves only	0%	0%	0%	0%	0%	0%
Not mobile		Not mobile	Not mobile	Not mobile	Not mobile	Not mobile	
Currents and waves	37%	29%	16%	0%	0%	0%	
	Mobile spring and peak neap tides, not mobile at lowest neaps	Mobile spring tides, not mobile at lowest neaps	Mobile peak spring tides	Not mobile	Not mobile	Not mobile	
OAA7 (54 mLAT)	Currents only	39%	32%	20%	0%	0%	0%
		Mobile spring and peak neap tides, not mobile at lowest neaps	Mobile spring and peak neap tides, not mobile at lowest neaps	Mobile spring tides, not mobile at lowest neaps	Not mobile	Not mobile	Not mobile
	Waves only	100%	100%	9%	0%	0%	0%
Always mobile		Always mobile	Always mobile	Not mobile	Not mobile	Not mobile	
Currents and waves	50%	41%	29%	0%	0%	0%	
	Mobile spring and peak neap tides, not mobile at lowest neaps	Mobile spring and peak neap tides, not mobile at lowest neaps	Mobile spring tides, not mobile at lowest neaps	Not mobile	Not mobile	Not mobile	
OAA9 (54 mLAT)	Currents only	36%	28%	16%	0%	0%	0%
		Mobile spring and peak neap tides, not mobile at lowest neaps	Mobile spring and peak neap tides, not mobile at lowest neaps	Mobile spring tides only	Not mobile	Not mobile	Not mobile
	Waves only	0%	0%	0%	0%	0%	0%
Not mobile		Not mobile	Not mobile	Not mobile	Not mobile	Not mobile	
Currents and waves	51%	40%	26%	0%	0%	0%	
	Mobile spring and peak neap tides, not mobile at lowest neaps	Mobile spring and peak neap tides, not mobile at lowest neaps	Mobile spring tides only	Not mobile	Not mobile	Not mobile	
OAA10 (69 mLAT)	Currents only	20%	11%	1%	0%	0%	0%
		Mobile only peak spring tides	Mobile only peak spring tides	Mobile only peak spring tides	Not mobile	Not mobile	Not mobile
	Waves only	0%	0%	0%	0%	0%	0%
Not mobile		Not mobile	Not mobile	Not mobile	Not mobile	Not mobile	
Currents and waves	27%	17%	4%	0%	0%	0%	
	Mobile spring and peak neap tides, not mobile at lowest neaps	Mobile only peak spring tides	Mobile only peak spring tides	Not mobile	Not mobile	Not mobile	
OAA11 (63 mLAT)	Currents only	20%	12%	0%	0%	0%	0%
		Mobile only peak spring tides	Mobile only peak spring tides	Not mobile	Not mobile	Not mobile	Not mobile
	Waves only	0%	0%	0%	0%	0%	0%
Not mobile		Not mobile	Not mobile	Not mobile	Not mobile	Not mobile	
		29%	19%	5%	0%	0%	



SEABED SEDIMENT		FINE SAND	MEDIUM SAND	COARSE SAND	VERY FINE GRAVEL	FINE GRAVEL	MEDIUM GRAVEL
	Currents and waves	Mobile only peak spring tides	Mobile only peak spring tides	Mobile only peak spring tides	Not mobile	Not mobile	Not mobile
ECC1 (83 mLAT)	Currents only	31%	23%	12%	0%	0%	0%
		Mobile spring and peak neap tides, not mobile at lowest neaps	Mobile spring and peak neap tides, not mobile at lowest neaps	Mobile peak spring tides only	Not mobile	Not mobile	Not mobile
	Waves only	0%	0%	0%	0%	0%	0%
		Not mobile	Not mobile	Not mobile	Not mobile	Not mobile	Not mobile
Currents and waves	34%	26%	14%	0%	0%	0%	
	Mobile spring and peak neap tides, not mobile at lowest neaps	Mobile spring and peak neap tides, not mobile at lowest neaps	Mobile peak spring tides only	Not mobile	Not mobile	Not mobile	
ECC2 (98 mLAT)	Currents only	19%	10%	0%	0%	0%	0%
		Mobile peak spring tides only	Mobile peak spring tides only	Not mobile	Not mobile	Not mobile	Not mobile
	Waves only	0%	0%	0%	0%	0%	0%
		Not mobile	Not mobile	Not mobile	Not mobile	Not mobile	Not mobile
Currents and waves	20%	11%	1%	0%	0%	0%	
	Mobile peak spring tides only	Mobile peak spring tides only	Not mobile	Not mobile	Not mobile	Not mobile	
ECC3 (95 mLAT)	Currents only	37%	29%	17%	0%	0%	0%
		Mobile spring and peak neap tides, not mobile at lowest neaps	Mobile spring tide only	Mobile peak spring tides only	Not mobile	Not mobile	Not mobile
	Waves only	0%	0%	0%	0%	0%	0%
		Not mobile	Not mobile	Not mobile	Not mobile	Not mobile	Not mobile
Currents and waves	38%	30%	18%	0%	0%	0%	
	Mobile spring and peak neap tides, not mobile at lowest neaps	Mobile spring tide only	Mobile peak spring tides only	Not mobile	Not mobile	Not mobile	
ECC4 (56 mLAT)	Currents only	54%	46%	33%	0%	0%	0%
		Mobile spring and peak neap tides, not mobile at lowest neaps	Mobile spring and peak neap tides, not mobile at lowest neaps	Mobile spring and peak neap tides, not mobile at lowest neaps	Not mobile	Not mobile	Not mobile
	Waves only	0%	0%	0%	0%	0%	0%
		Not mobile	Not mobile	Not mobile	Not mobile	Not mobile	Not mobile
Currents and waves	63%	56%	42%	0%	0%	0%	
	Mobile spring and peak neap tides, not mobile at lowest neaps	Mobile spring and peak neap tides, not mobile at lowest neaps	Mobile spring and peak neap tides, not mobile at lowest neaps	Not mobile	Not mobile	Not mobile	
ECC9 (-9 mLAT)	Currents only	0%	0%	0%	0%	0%	0%
		Not mobile	Not mobile	Not mobile	Not mobile	Not mobile	Not mobile
	Waves only	100%	100%	100%	34%	0%	0%
		Always mobile	Always mobile	Always mobile	Mobile spring and peak neap tides, not mobile at lowest neaps	Not mobile	Not mobile
Currents and waves	62%	49%	19%	0%	0%	0%	
	Mobile during faster flows	Mobile only during periods of fastest tidal (spring and neap) flows	Mobile only during periods of fastest spring tidal flows	Not mobile	Not mobile	Not mobile	
ECC10 (-1 mLAT)	Currents only	0%	0%	0%	0%	0%	0%
		Not mobile	Not mobile	Not mobile	Not mobile	Not mobile	Not mobile
	Waves only	100%	100%	100%	34%	0%	0%
		Always mobile	Always mobile	Always mobile	Mobile spring and peak neap tides, not mobile at lowest neaps	Not mobile	Not mobile
Currents and waves	46%	29%	11%	0%	0%	0%	
	Mobile during faster flows	Mobile only during periods of fastest tidal (spring and neap) flows	Mobile only during periods of fastest spring tidal flows	Not mobile	Not mobile	Not mobile	



Table 3-14 Sediment mobility potential at analysed locations across the Offshore project area (OAA and ECC respectively) using model-extracted time series flows and a wave with a height of 2.6 m and a period of 11 s; mobility potential is given as a percentage of time for varying sediment

SEABED SEDIMENT		FINE SAND	MEDIUM SAND	COARSE SAND	VERY FINE GRAVEL	FINE GRAVEL	MEDIUM GRAVEL
SEDIMENT SIZE (MM)		0.175	0.35	0.63	3	6	11
OAA3 (69 mLAT)	Currents only	27%	19%	8%	0%	0%	0%
		Mobile spring and peak neap tides, not mobile at lowest neaps	Mobile spring tides only	Mobile spring tides only	Not mobile	Not mobile	Not mobile
	Waves only	100%	22%	0%	0%	0%	0%
		Always mobile	Not mobile	Not mobile	Not mobile	Not mobile	Not mobile
	Currents and waves	46%	35%	22%	0%	0%	0%
		Mobile spring and peak neap tides, not mobile at lowest neaps	Mobile spring and peak neap tides, not mobile at lowest neaps	Mobile spring tides only	Not mobile	Not mobile	Not mobile
OAA4 (69 mLAT)	Currents only	31%	23%	12%	0%	0%	0%
		Mobile spring and peak neap tides, not mobile at lowest neaps	Mobile spring tides only	Mobile spring tides only	Not mobile	Not mobile	Not mobile
	Waves only	100%	21%	0%	0%	0%	0%
		Always mobile	Not mobile	Not mobile	Not mobile	Not mobile	Not mobile
	Currents and waves	50%	40%	26%	0%	0%	0%
		Mobile spring and peak neap tides, not mobile at lowest neaps	Mobile spring and peak neap tides, not mobile at lowest neaps	Mobile spring tides only	Not mobile	Not mobile	Not mobile
OAA7 (54 mLAT)	Currents only	39%	32%	20%	0%	0%	0%
		Mobile spring and peak neap tides, not mobile at lowest neaps	Mobile spring and peak neap tides, not mobile at lowest neaps	Mobile spring tides only	Not mobile	Not mobile	Not mobile
	Waves only	100%	100%	100%	0%	0%	0%
		Always mobile	Always mobile	Always mobile	Not mobile	Not mobile	Not mobile
	Currents and waves	62%	54%	40%	0%	0%	0%
		Mobile spring and peak neap tides, not mobile at lowest neaps	Mobile spring and peak neap tides, not mobile at lowest neaps	Mobile spring and peak neap tides, not mobile at lowest neaps	Not mobile	Not mobile	Not mobile
OAA9 (54 mLAT)	Currents only	36%	28%	16%	0%	0%	0%
		Mobile spring and peak neap tides, not mobile at lowest neaps	Mobile spring and peak neap tides, not mobile at lowest neaps	Mobile spring tides only	Not mobile	Not mobile	Not mobile
	Waves only	100%	100%	100%	0%	0%	0%
		Always mobile	Always mobile	Always mobile	Not mobile	Not mobile	Not mobile
	Currents and waves	65%	56%	39%	0%	0%	0%
		Mobile spring and peak neap tides, not mobile at lowest neaps	Mobile spring and peak neap tides, not mobile at lowest neaps	Mobile spring and peak neap tides, not mobile at lowest neaps	Not mobile	Not mobile	Not mobile
OAA10 (69 mLAT)	Currents only	20%	11%	1%	0%	0%	0%
		Mobile spring tides only	Mobile spring tides only	Mobile peak spring tides only	Not mobile	Not mobile	Not mobile
	Waves only	0%	0%	0%	0%	0%	0%
		Not mobile	Not mobile	Not mobile	Not mobile	Not mobile	Not mobile
	Currents and waves	39%	29%	14%	0%	0%	0%
		Mobile spring and peak neap tides, not mobile at lowest neaps	Mobile spring and peak neap tides, not mobile at lowest neaps	Mobile spring tides only	Not mobile	Not mobile	Not mobile
OAA11 (63 mLAT)	Currents only	20%	12%	0%	0%	0%	0%
		Mobile on spring tides only	Mobile on spring tides only	Not mobile	Not mobile	Not mobile	Not mobile
	Waves only	94%	0%	0%	0%	0%	0%
		Mobile spring and peak neap tides, not mobile at lowest neaps	Not mobile	Not mobile	Not mobile	Not mobile	Not mobile
	Currents and waves	42%	32%	17%	0%	0%	0%
		Mobile spring and peak neap tides, not mobile at lowest neaps	Mobile spring and peak neap tides, not mobile at lowest neaps	Mobile on spring tides only	Not mobile	Not mobile	Not mobile
ECC1 (83 mLAT)	Currents only	31%	23%	12%	0%	0%	0%
		Mobile spring and peak neap tides, not mobile at lowest neaps	Mobile spring tides only	Mobile spring tides only	Not mobile	Not mobile	Not mobile



SEABED SEDIMENT		FINE SAND	MEDIUM SAND	COARSE SAND	VERY FINE GRAVEL	FINE GRAVEL	MEDIUM GRAVEL
	Waves only	0%	0%	0%	0%	0%	0%
		Not mobile	Not mobile	Not mobile	Not mobile	Not mobile	Not mobile
	Currents and waves	43%	34%	21%	0%	0%	0%
		Mobile spring and peak neap tides, not mobile at lowest neaps	Mobile spring and peak neap tides, not mobile at lowest neaps	Mobile spring tides only	Not mobile	Not mobile	Not mobile
ECC2 (98 mLAT)	Currents only	19%	10%	0%	0%	0%	0%
		Mobile spring tides only	Mobile peak spring tides only	Not mobile	Not mobile	Not mobile	Not mobile
	Waves only	0%	0%	0%	0%	0%	0%
		Not mobile	Not mobile	Not mobile	Not mobile	Not mobile	Not mobile
Currents and waves	27%	18%	4%	0%	0%	0%	
	Mobile spring tides only	Mobile peak spring tides only	Mobile peak spring tides only	Not mobile	Not mobile	Not mobile	
ECC3 (95 mLAT)	Currents only	37%	29%	17%	0%	0%	0%
		Mobile spring and peak neap tides, not mobile at lowest neaps	Mobile spring and peak neap tides, not mobile at lowest neaps	Mobile spring tides only	Not mobile	Not mobile	Not mobile
	Waves only	0%	0%	0%	0%	0%	0%
		Not mobile	Not mobile	Not mobile	Not mobile	Not mobile	Not mobile
Currents and waves	45%	36%	24%	0%	0%	0%	
	Mobile spring and peak neap tides, not mobile at lowest neaps	Mobile spring and peak neap tides, not mobile at lowest neaps	Mobile spring tides only	Not mobile	Not mobile	Not mobile	
ECC4 (56 mLAT)	Currents only	54%	46%	33%	0%	0%	0%
		Mobile spring and peak neap tides, not mobile at lowest neaps	Mobile spring and peak neap tides, not mobile at lowest neaps	Mobile spring and peak neap tides, not mobile at lowest neaps	Not mobile	Not mobile	Not mobile
	Waves only	100%	100%	100%	0%	0%	0%
		Always mobile	Always mobile	Always mobile	Not mobile	Not mobile	Not mobile
Currents and waves	71%	66%	55%	0%	0%	0%	
	Mobile spring and peak neap tides, not mobile at lowest neaps	Mobile spring and peak neap tides, not mobile at lowest neaps	Mobile spring and peak neap tides, not mobile at lowest neaps	Not mobile	Not mobile	Not mobile	
ECC9 (-9 mLAT)	Currents only	0%	0%	0%	0%	0%	0%
		Not mobile	Not mobile	Not mobile	Not mobile	Not mobile	Not mobile
	Waves only	100%	100%	100%	100%	8%	0%
		Always mobile	Always mobile	Always mobile	Always mobile	Mobile peak spring tides only	Not mobile
Currents and waves	79%	71%	58%	0%	0%	0%	
	Mobile under most tidal conditions, except for a duration either side of high water	Mobile under most tidal conditions, except for a duration either side of low water	Mobile only during periods of fastest tidal flows	Not mobile	Not mobile	Not mobile	
ECC10 (-1 mLAT)	Currents only	0%	0%	0%	0%	0%	0%
		Not mobile	Not mobile	Not mobile	Not mobile	Not mobile	Not mobile
	Waves only	100%	100%	100%	100%	8%	0%
		Always mobile	Always mobile	Always mobile	Always mobile	Mobile peak spring tides only	Not mobile
Currents and waves	79%	68%	40%	0%	0%	0%	
	Mobile under most tidal conditions, except for a duration either side of high water	Mobile under most tidal conditions, except for a duration either side of low water	Mobile only during periods of fastest tidal flows	Not mobile	Not mobile	Not mobile	



### 3.9.2.2 Fine sediments

When finer sediments (i.e. silts and muds) are mobilised they are typically carried in suspension, contributing to higher concentrations of Suspended Particulate Matter (SPM) and increasing the turbidity of the water column until they are able to settle out and deposit. Rivers, estuaries and coastal erosion can also provide local sources of increased turbidity.

Long-term (1998 to 2015) monthly average concentration of sea surface SPM have been deduced from satellite data (Cefas, 2016). The highest values are seen to the east of the model domain which can be attributed to the proximity to the rocky coastline of Orkney and thus coastal erosion releasing sediment into the sea. Within the OAA, concentrations can be considered relatively low, in the region of 0.5 to 1.0 mg/l (Figure 3-30). Along the offshore ECC, the concentration of suspended sediment generally reduces to 0.08 to 0.6 mg/l (Cefas, 2016). There are occasionally areas of higher suspended sediments along the coastline itself, suggesting these areas are exposed to more active metocean conditions.

To characterise the suspended sediment concentration (SSC) across the offshore Project area, water sampling was completed as part of the site-specific environmental sampling (SS5: Benthic environmental baseline report). Total suspended sediment (TSS) water samples were taken from a total of 29 locations across the offshore Project area (Figure 2-2). Seven were taken within the offshore ECC, 17 within the OAA and five in the nearshore area. Eight samples across the OAA and offshore ECC (W01/W02, W05/W06, W10/W11, W18/W19) are replicates of the same location in order to capture different tidal conditions (spring/neap respectively) as illustrated in Figure 2-2.

Offshore samples were taken on different days between 23<sup>rd</sup> August 2022 and 11<sup>th</sup> September 2022, with the nearshore samples acquired between 22<sup>nd</sup> and 25<sup>th</sup> October 2022. The offshore samples are shown in accordance with the tidal cycle reported at Kinlochbervie in Figure 3-31. The cluster of sample points on the left of the graph correspond to tides in the lead up to a spring tide at the end of August. The cluster of sample points on the right of the graph were taken during a neap period in the cycle.

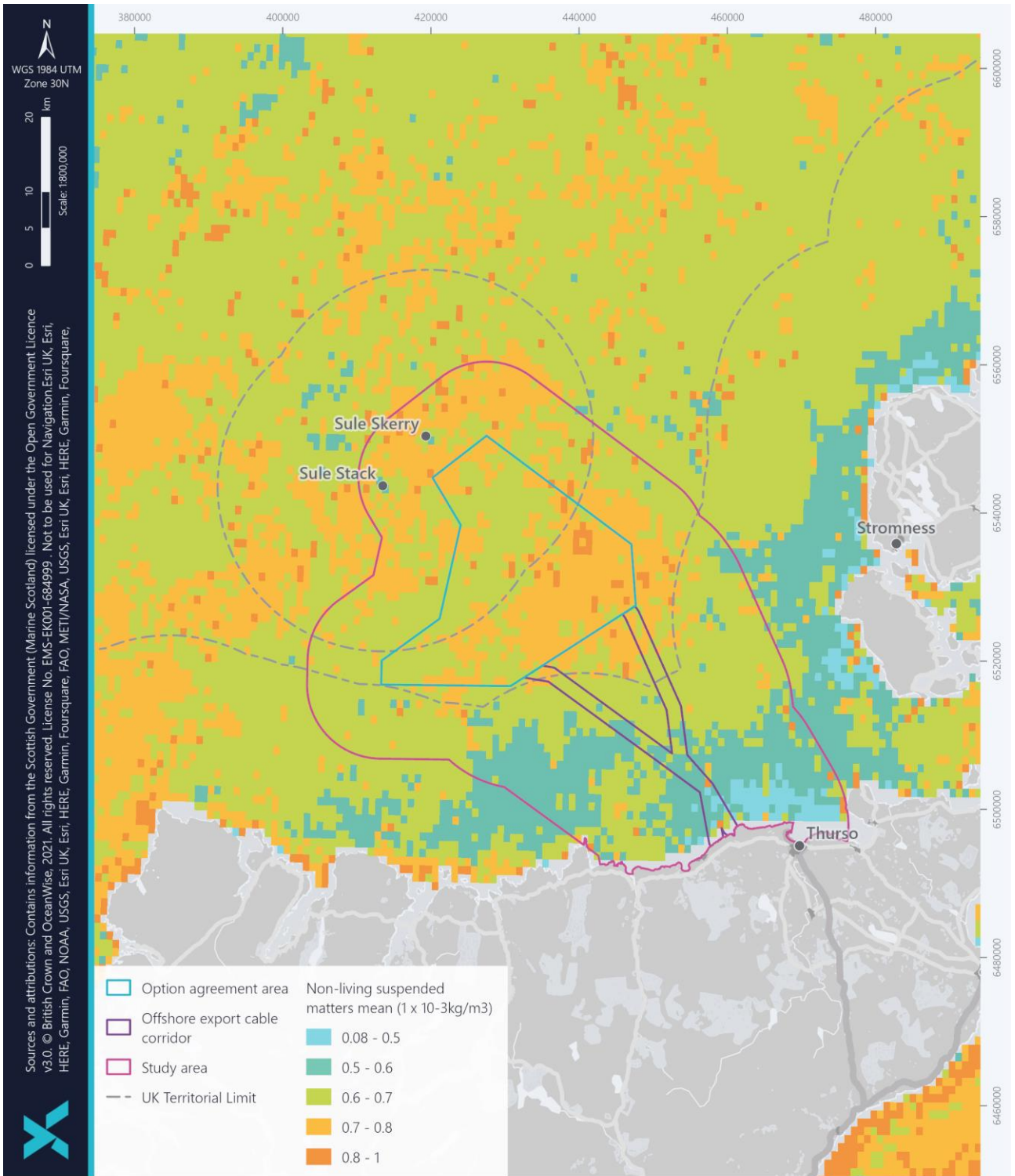


Figure 3-30 Monthly average sea surface SPM concentrations (after Cefas, 2016)

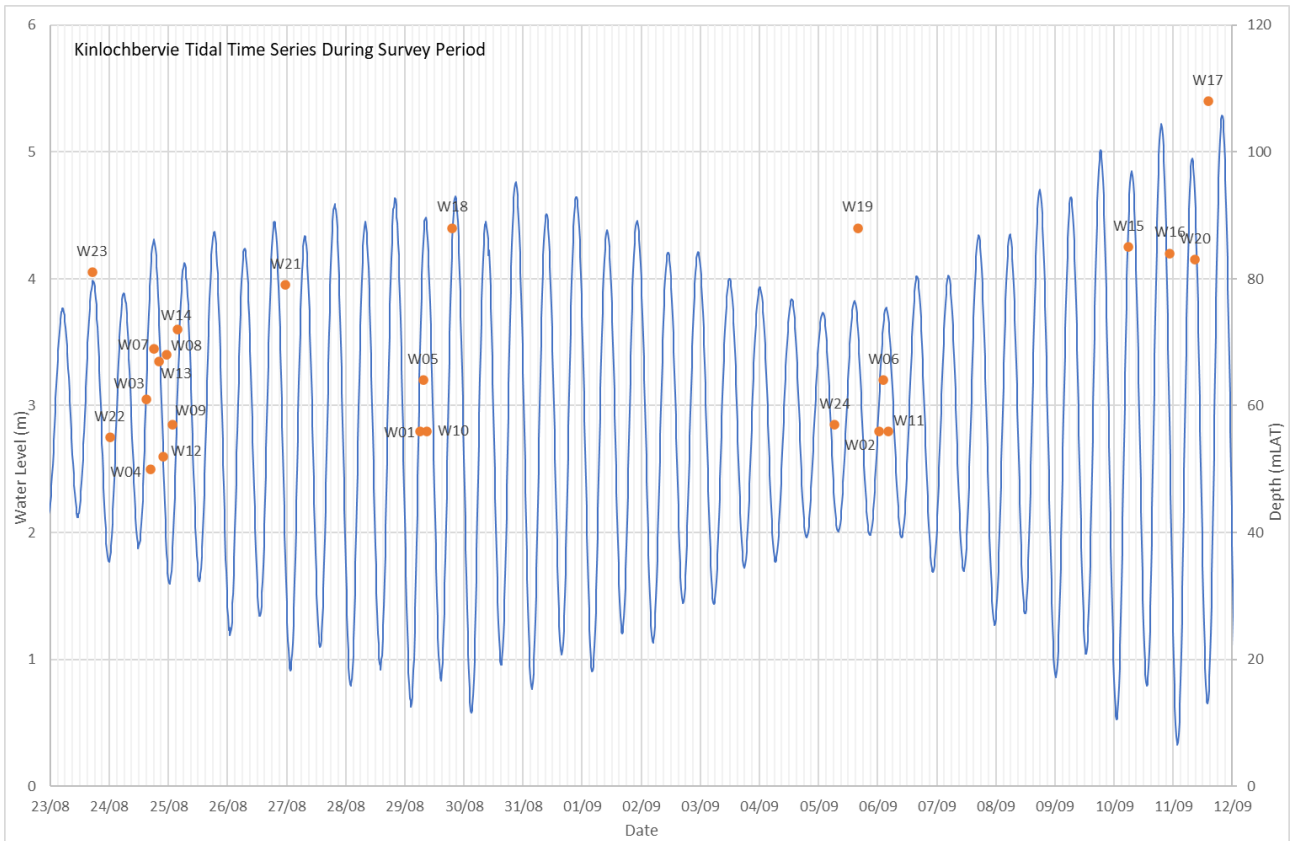


Figure 3-31 TSS survey points (including water depth) in relation to the tidal levels from Kinlochberrie

As described in Section 2.1.3.2, three samples were taken throughout the water column at each location, one at the surface, one mid-way through the water column and one at the bottom, close to the seabed. The concentration of TSS, as recorded by the samples, are presented in Table 3-15. The water depth at each location is given, in addition to the depth through the water column at which the samples were taken (surface, mid or bottom). Overall, most samples showed a TSS of <5 mg/l, which is in line with the general understanding of the region (Figure 3-30). TSS in Table 3-15 are colour coded in accordance with the concentration; from <5 mg/l (darkest green) to 35 mg/l (darkest red).



Table 3-15 TSS concentrations throughout the water column (surface, mid, bottom) within the offshore Project area (corresponding to locations in Figure 2-2). TSS concentrations are colour coded in accordance with the concentration, from <5 mg/l (darkest green) to 35 mg/l (darkest red).

SAMPLE POINT	WATER DEPTH (MLAT)	SURFACE WATER DEPTH (MLAT)	MID WATER DEPTH (MLAT)	BOTTOM WATER DEPTH (MLAT)	SURFACE TOTAL SUSPENDED SOLIDS (MG/L)	MID TOTAL SUSPENDED SOLIDS (MG/L)	BOTTOM TOTAL SUSPENDED SOLIDS (MG/L)
W01*	56	2	29	52	<5	<5	<5
W02*	56	2	28	55	<5	<5	<5
W03	61	<2	31	56	<5	<5	<5
W04	50	<2	25	45	<5	<5	<5
W05*	64	<2	30	54	<5	<5	<5
W06*	64	<2	33	63	<5	<5	<5
W07	69	<2	35	66	<5	<5	<5
W08	68	<2	35	66	<5	<5	<5
W09	57	<2	30	54	24	<5	<5
W10*	56	<2	37	55	<5	<5	<5
W11*	56	<2	30	54	<5	19	<5
W12	52	<2	25	50	<5	6	<5
W13	67	<2	33	65	<5	<5	<5
W14	72	<2	37	69	<5	<5	<5
OAA W22	55	5	25	49	<5	<5	<5
W23	81	5	40	76	<5	<5	<5
W15	85	<2	40.5	82	35	11	23
W16	84	2	44	83	<5	26	9
W17	108	<2	55	105	8	10	13
W18*	88	<2	44	83	<5	10	8
W19*	88	<2	46	87	7	23	10
W20	83	<2	40	81	7	31	<5
W21	79	<2	42	78	<5	<5	<5
W24	57	<2	30	56	<5	10	18
Nea NSW01		<2	19	36	<5	<5	<5
NSW02		<2	10	19	<5	<5	<5



SAMPLE POINT	WATER DEPTH (MLAT)	SURFACE WATER DEPTH (MLAT)	MID WATER DEPTH (MLAT)	BOTTOM WATER DEPTH (MLAT)	SURFACE TOTAL SUSPENDED SOLIDS (MG/L)	MID TOTAL SUSPENDED SOLIDS (MG/L)	BOTTOM TOTAL SUSPENDED SOLIDS (MG/L)
NSW03	-	-	-	-	No Data		
NSW04	<2	16	34		<5	<5	<5
NSW05	<2	17	34		<5	<5	<5

\* Samples W01/W02, W05/W06, W10/W11, W18/W19 are replicates of one another, taken during spring/neap tides

There are no obvious differences in the TSS between spring and neap or flood an ebb conditions and at the varying depths across the OAA and can be considered to generally have low background levels of SSC at typically <5 mg/l. The TSS data shows that, generally, higher concentrations are more common along the offshore ECC, although not in the nearshore area (even though was sampled over a different period from offshore locations). Overall, as the majority of samples were taken on a spring tide, slightly higher TSS levels appear to be associated with spring tides (Table 3-15 and Figure 3-31). Points W21 in a water depth of 79 mLAT is the only exception to this. The highest concentration occurred within the surface sample at W15 (35 mg/l), taken from the offshore ECC and associated with a spring flood tide. The increased levels of offshore ECC are more likely in relation to the larger degree of finer sediment as described in Section 3.3.2 (Table 3-2).

For two pairs of the replicate sample locations (i.e. W01/W02 and W04/W05), TSS concentrations were <5 mg/l. From the remaining two pairs of replicates (W10/W11 within the OAA and W18/W19 within the offshore ECC), the measured TSS would seem to suggest concentrations are higher on a neap tide, i.e. W11 and W19. However, as the number of replicates is limited, it is not possible to conclude this with certainty, because based on the results from across the offshore ECC in general (irrespective) of replicates, higher concentrations occur, which may be a result of both the tidal flow and seabed sediment. A comparison of the TSS concentration with regards to the changes in TSS throughout the water column, of the samples taken, concentrations appear to be highest at the mid-point in the water column.

In addition to the TSS samples, turbidity measurements were also taken during the water sampling at the 24 sampled locations (Figure 2-2), with measurements taken through the water column. Measures of turbidity are only available with respect to the instrument readings of Nephelometric Turbidity Units (NTU) and illustrated for observations across the OAA (Figure 3-32), the offshore ECC (Figure 3-33) and nearshore area (Figure 3-34).

The turbidity NTU measurements indicate a negative to positive 4 range (Figure 3-32 and Figure 3-33). The negative values occur mainly due to the low SSC that occurs across the offshore Project area, so the actual SSC is less than the instrumentation thresholds. Within the OAA, for the water sample at W09, which demonstrated TSS measurements of up to 24 mg/l in the surface sample (Table 3-15), the equivalent NTU is only in the order of 0.5 NTU (Figure 3-32). Similarly at sample W11, mid-water depth of 30 m LAT, a TSS of 19 mg/l (Table 3-15) equated to negative NTU, although a NTU of 4.4 was measured at a depths of less than 1 m (Figure 3-32), for which the equivalent water sample (i.e. surface sample at 2 m LAT) had a TSS of <5 mg/l (Table 3-15). Overall, the low SSC across the OAA is considered to again be reflected in the measured NTUs through the water column, with low readings occurring. This suggests that the water within the offshore Project area is relatively clear.

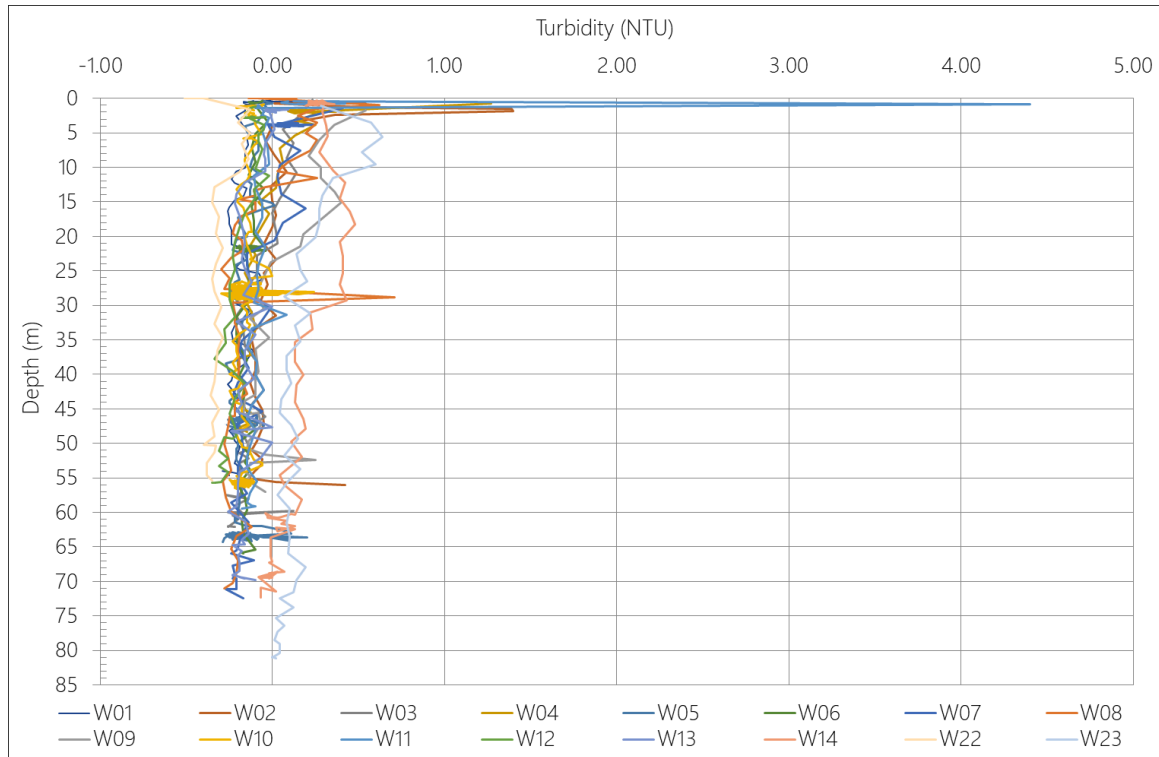


Figure 3-32 NTU turbidity measurements for OAA sampled locations, as per locations in Figure 2-2

Negative NTUs are again observed across the offshore ECC, with the largest NTU reading associated with samples W21 at 2.17 NTU at a depth of around 1 m and W15 at 2.09 NTU at a depth of around 1.5 m (Figure 3-33). As illustrated in Table 3-15, sample W15 surface sample demonstrated the largest TSS with 35 mg/l, with above background levels of 11 mg/l and 23 mg/l for the mid-water and seabed water samples respectively. The NTU readings for W15 similarly reflect a reduction in NTU, although not at the same magnitude. Across the nearshore area, turbidity sampling ranges from about 1.6 NTU, down to -0.4 NTU (Figure 3-34). Overall, the degree of noise associated with the NTU readings as the turbidity was largely below instrument thresholds, support the water sampling observations of low TSS and SSC across the offshore Project area.

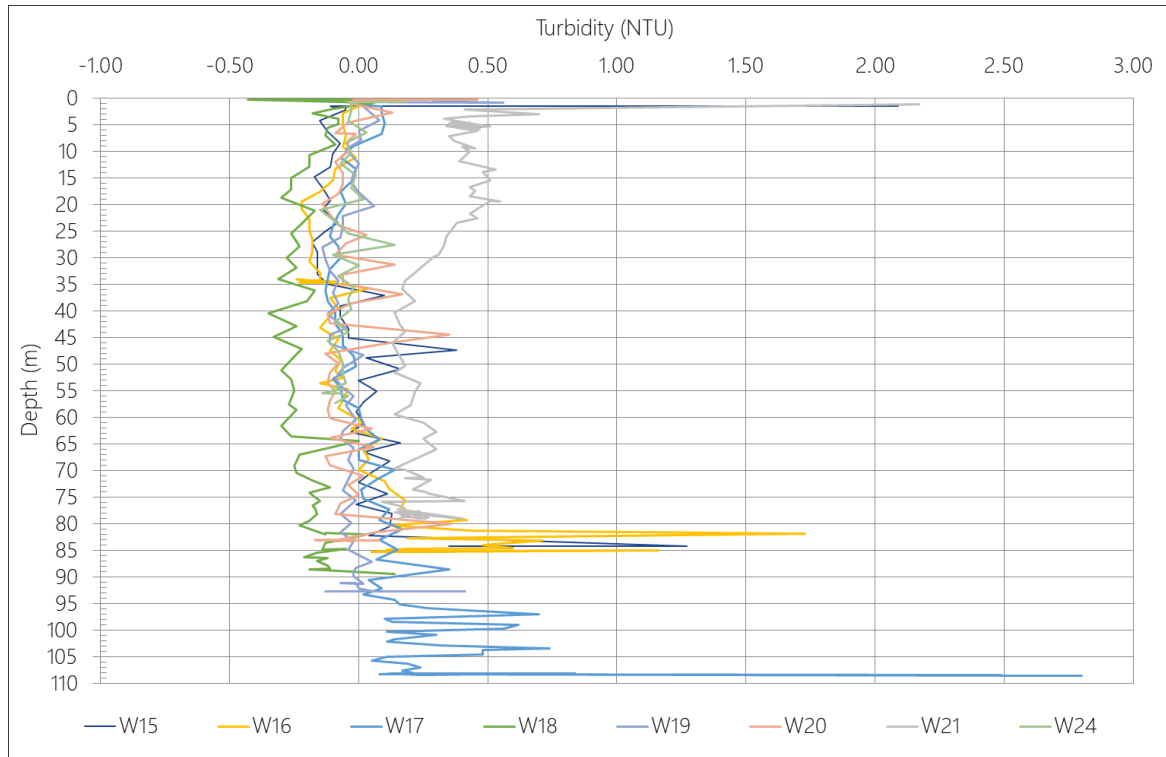


Figure 3-33 NTU turbidity measurements for offshore ECC sampled locations, as per locations in Figure 2-2

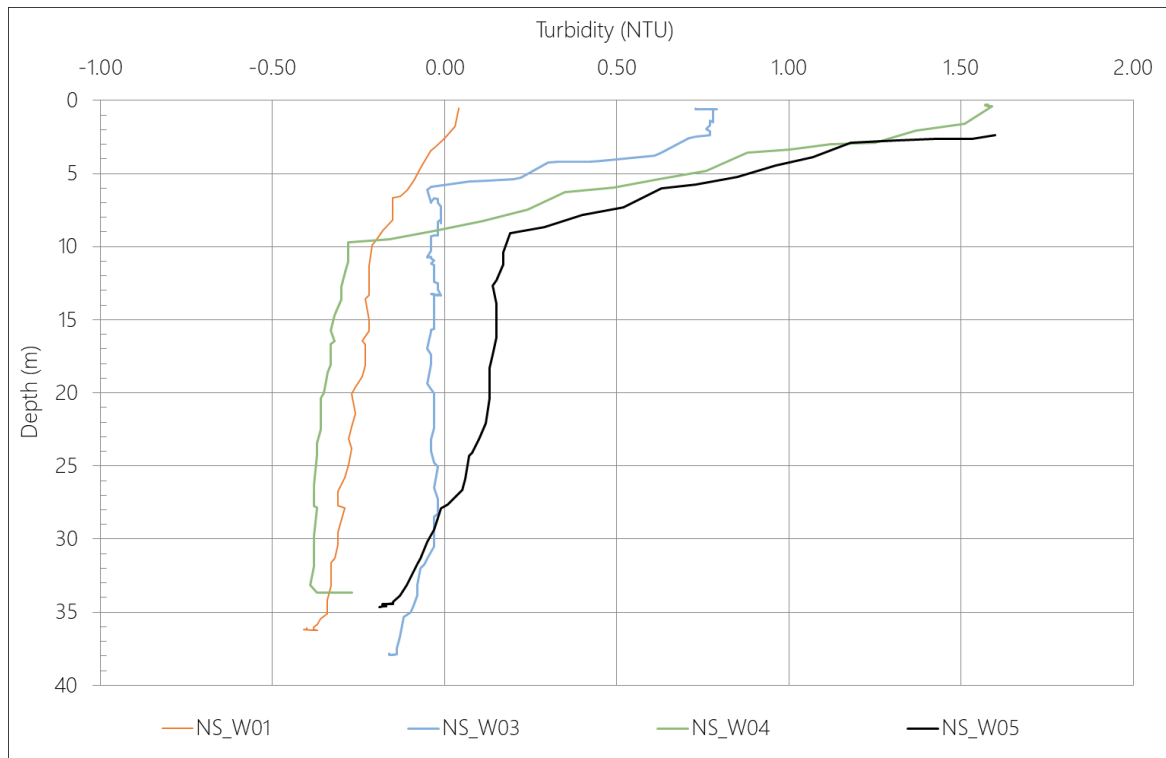


Figure 3-34 NTU turbidity measurements for nearshore sampled locations, as per locations in Figure 2-2



## 3.10 Stratification and Fronts

### 3.10.1 Overview

Fronts are one of five large-scale features included on the list of Marine Protected Area (MPA) search features. SNH (2014) (now NatureScot) utilised front detection and aggregation techniques to high resolution satellite ocean colour data to describe frequently occurring fronts near to the Scottish coast. The key frontal zones were selected through detailed analysis of the seasonal chlorophyll and thermal front distributions. The offshore Project area does not coincide with any area of strong frontal activity, such as those identified in SNH (2014).

Figure 3-35 provides a seasonally averaged front frequency map for summer based on an interpretation of ten years of satellite data (1998 to 2008), based on Miller and Christodoulou (2014). Along the north coast of Scotland, seasonal water mass and water column structure are characterised as well-mixed shelf waters through all seasons except summer, where weakly stratified shelf waters are recorded, with the dominant stratification category defined as intermittently stratified (DECC, 2016b). Although freshwater inputs can influence the development or timing of stratification (Sharples, et al., 2022), there is no evidence presently to suggest this is the case across the northwest Scottish continental shelf. The understanding of stratification across the offshore Project area is reviewed in terms of the information available from secondary sources and that acquired from site-specific surveys, as presented in the respective sections below.

### 3.10.2 Offshore Project Area

#### 3.10.2.1 Understanding of stratification from modelled sources

Data extracted from the PFOW climatology model (O'Hara and Campbell, 2021) for points within the OAA and offshore ECC (Figure 2-3), provided information on the seasonal temperature stratification through the water column within the offshore Project area. According to data from the PFOW climatology, over the course of the year the range in temperatures within the offshore Project area remains relatively consistent, with a low of approximately 7°C and high of 15°C. Thermal stratification is most notable in waters in the northwest and centre of the OAA. Figure 3-36 shows the difference in stratification over a one-year period at various points within the OAA (Marine Scotland, 2016). Figure 3-36 also shows the same information for a point within the offshore ECC (ECC4). Of the points shown in Figure 3-36, OAA1 is located the furthest offshore, while OAA4 is located centrally within the OAA in an area which corresponds to a slightly greater water depth (Figure 2-3). OAA3 is located along the southeastern border of the OAA and OAA2 is located closest to the coast, along the southern-most border of the OAA (Figure 2-3). Between mid-May and mid-August, stratification is apparent at the locations further offshore (OAA1 and OAA4), as near surface waters are up to 2°C higher than waters mid way through the water column (Figure 3-36; Marine Scotland, 2016). Within the OAA there does not appear to be a correlation between water depth and the extent of stratification.





Results from the PFOW climatology for locations across the offshore ECC, indicate stratification is less apparent within the offshore ECC, with water column properties largely being the same at all depths throughout the year (Figure 3-36). For example, at ECC3 and ECC4 (Figure 2-3) and based on outputs from the PFOW climatology, the temperature ranges approximately between 7°C and 15°C, at its lowest in March and at its highest in August, with no evidence of stratification in the summer months (Figure 3-36). In May, June and July there are three small fluctuations in temperature in the water column. While the mid-depth and near-bottom temperatures remain consistent, at these three points the surface temperature is marginally higher compared to the rest of the water column. However, these fluctuations only represent a difference of <1°C (Figure 3-36).

Based on information from the PFOW climatology at the analysed data locations (Figure 2-3), temperature stratification coincides with a seasonal increase in salinity within the OAA (Figure 3-37). While salinity is marginally higher in the spring months, stratification occurs between May and August. Salinity stratification is most pronounced at OAA1, which aligns with the greatest extent of thermal stratification (Marine Scotland, 2016). Data from the PFOW climatology was provided in parts per thousand (ppt), which is exactly the same as practical salinity units (psu) used in the rest of this report. Information from the PFOW climatology indicates a salinity level of between 34.6 and 35.4 psu for the OAA (Figure 3-37). This correlates with data from the World Ocean Data Centre (WODC) for the offshore Project area, where an annual average surface and seabed salinity of between 34.75 to 35 psu is recorded (NMPi, 2022). Offshore, at OAA1, salinity at the surface during the summer months can be up to 0.4 psu higher than lower in the water column.

In the offshore ECC, fluctuations in salinity throughout the year are less prominent compared with that observed for that OAA and salinity is relatively consistent throughout the water column despite small variations over the course of the year (Figure 3-37). The range in salinity within the offshore ECC is between approximately 33.7 to 34.5 psu, which is slightly lower on the whole than within the OAA. In the winter months there is marginally more variation throughout the water column. In the summer months this is less obvious with the exception of two points at which there is very slight indication of stratification. These points occur in May and June and correspond well to the corresponding changes in water column stratification at those times, as described above. However, these peaks are very temporary in duration and the extent of this stratification is equivalent to a change of <0.1 psu (Figure 3-37).

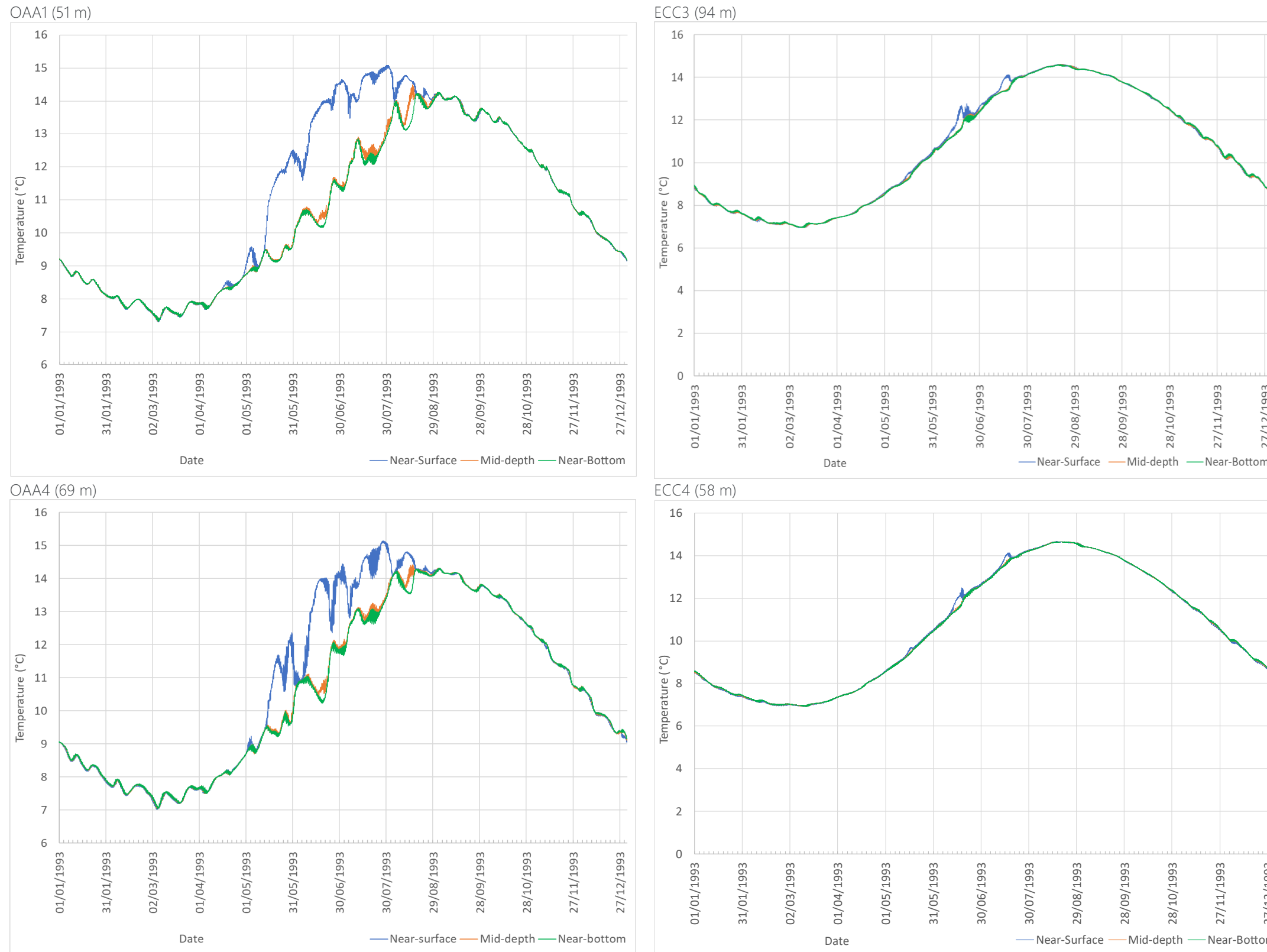


Figure 3-36 Thermal stratification across the year within the offshore Project area, at points OAA1, OAA4, ECC3 and ECC4 as illustrated in Figure 2-3. PFOV climatology data from O'Hara and Campbell (2021)

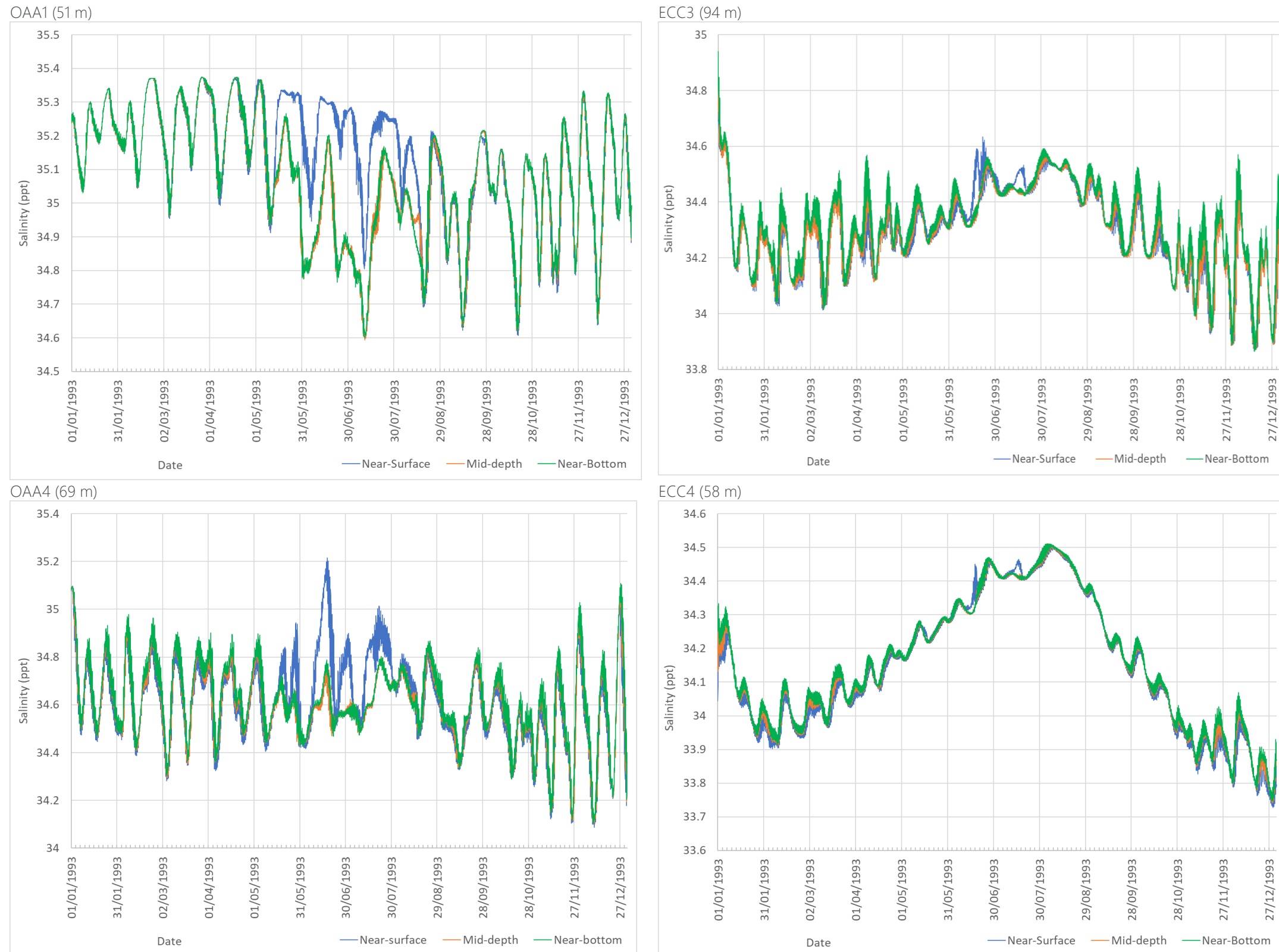


Figure 3-37 Salinity stratification across the year within the OAA, at points OAA1, OAA4, ECC3 and ECC4 as illustrated in Figure 2-3. PFOV climatology data from O'Hara and Campbell (2021)



### 3.10.2.2 Understanding of stratification from site-specific measurements

Measured CTD from 29 water samples collected from 25 locations across the offshore Project area (Figure 2-2) during the site-specific environmental survey provided vertical temperature profiles for the water column at points within the offshore Project area. The thermal and salinity vertical profiles are summarised in Figure 3-38. At nearly all locations within the OAA and offshore ECC there is some evidence of thermal or salinity stratification (Figure 3-37). However, the results from the nearshore sampling stations indicate that stratification of temperature and salinity is no longer apparent in the nearshore locations (Figure 3-39).

Across the OAA and offshore ECC, the present stratification is associated with a maximum range in temperature of 1.2 °C, with temperature ranging between 13.3 °C and 14.5 °C and for salinity being approximately 0.5 psu, with salinity ranging between 34.55 psu and 35.00 psu (Figure 3-37). The only exception to the above is at sample W20 (within the offshore ECC), where neither salinity nor temperature appears to vary through the water column (Figure 3-38), which seems unlikely given the results obtained everywhere else, across a range of tidal states and water depths (as described in relation to the TSS water samples in Section 3.9.2). The measured and observed stratification within the offshore ECC is also contrary to the information suggested by the PFOW climatology discussed in section 3.10.2. The PFOW climatology indicates there is little to no stratification within the offshore ECC, although the results from the site-specific environmental demonstrate the presence of stratification (Figure 3-37). The difference with the PFOW climatology may be due to model parameter and applied assumptions.

In terms of measured temperature and salinity stratification within the OAA and offshore ECC, the stratification occurs within the upper 30 m of water and shows that surface waters are warmer and less saline (Figure 3-38). From Figure 3-38, it is also clear that there is a difference between stratification in the OAA and the offshore ECC. Generally, stratification (mainly salinity but also observed for temperature) appears to be more pronounced in the offshore ECC (Figure 3-38), although W02, W06 and W14 within the OAA also appear to show a significant level of stratification. These three points are variably located throughout the OAA and do not have a consistent depth so show no commonality with one another, or to the points within the offshore ECC. Within the offshore ECC, the sample locations are generally in greater water depths and these points appear to correspond to areas with stronger stratification, whereas the rate of change in salinity within the OAA appears to be more gradual. The freshwater inflow from the coast could be contributing to the higher degree of stratification observed across the offshore ECC, with the OAA being a more mixed environment, with less pronounced stratification. However, the measured observation of a more prominent stratification in the offshore ECC was not identified in the PFOW climatology (O'Hara and Campbell, 2021), where no thermal or salinity stratification was observed in the nearshore model point at ECC4 (Figure 3-37), the reason for this could be due to the model resolution and the assumptions made.

With respect to the nearshore area and absence of any stratification, sampling in the nearshore area was completed in October, where available information for the wider PFOW climatology (O'Hara and Campbell, 2021) indicates the absence of stratification in offshore waters (section 3.10.2). The season is therefore likely to be the main reason why no stratification is apparent given the water depths present within the nearshore locations. Although, there is also the possibility that the shallower water depths and also the proximity to the coast, with the potential influence of freshwater inflows from fluvial sources with increased wave activity resulting in increased mixing and the occurrence of any stratification in nearshore locations.



To explore the potential variation in stratification between tidal conditions, Figure 3-40 compares the temperature and salinity stratification between the four replicate pairs. As explained previously, each replicate profiles the change in temperature and salinity on a spring versus neap tides. Overall, for both salinity and temperature, stratification is more apparent on a neap tide; samples W02, W06, W11, W19 show greater variation in salinity and temperature than their respective spring tide samples. This suggests that stratification is not a permanent feature and changes on a scale in line with the change from a spring to neap tide.

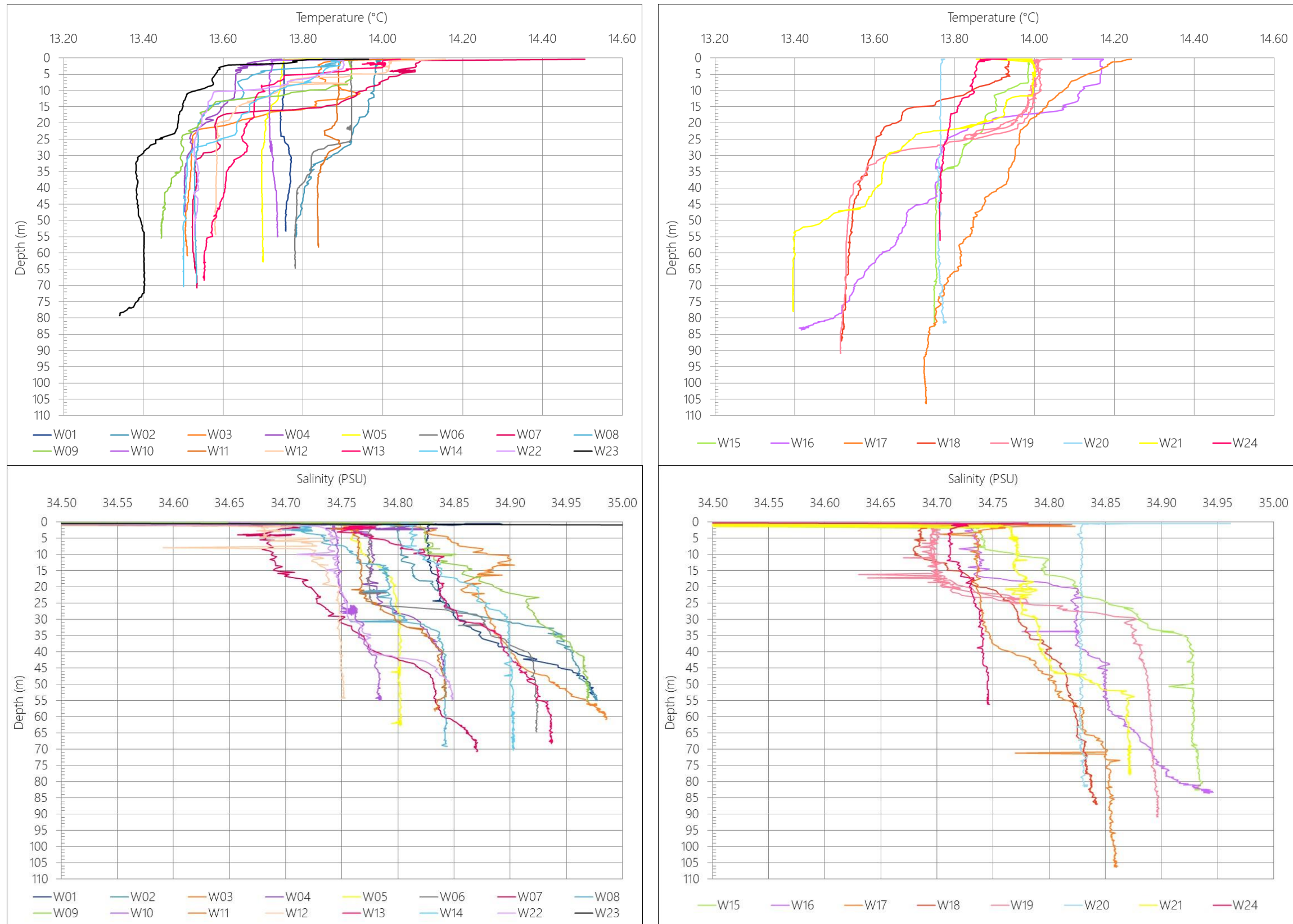


Figure 3-38 Temperature (top) and salinity (bottom) throughout the water column within the OAA (left) and offshore ECC (right) (corresponding to locations in Figure 2-2)

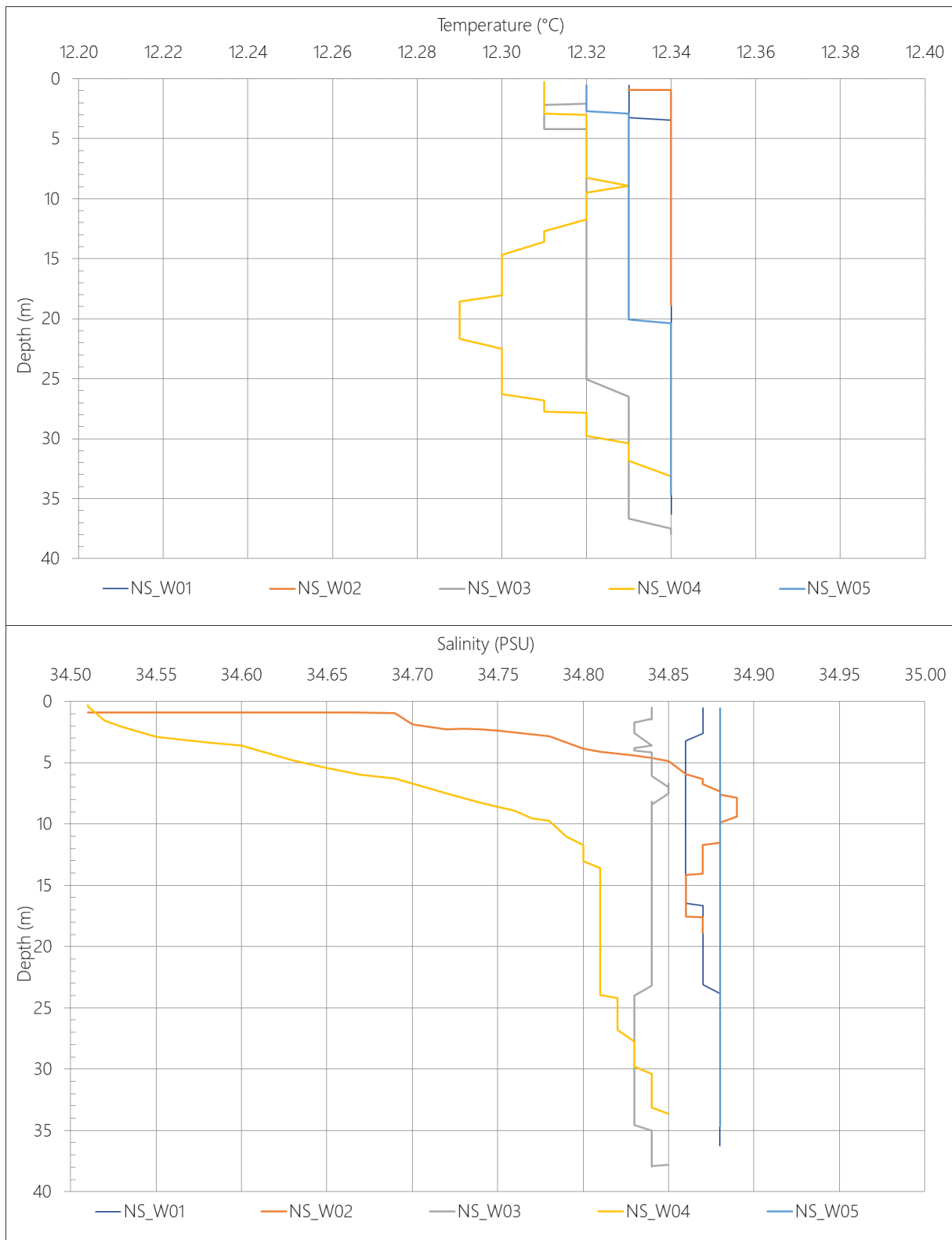


Figure 3-39 Temperature (top) and salinity (bottom) throughout the water column within the nearshore area (corresponding to locations in Figure 2-2)

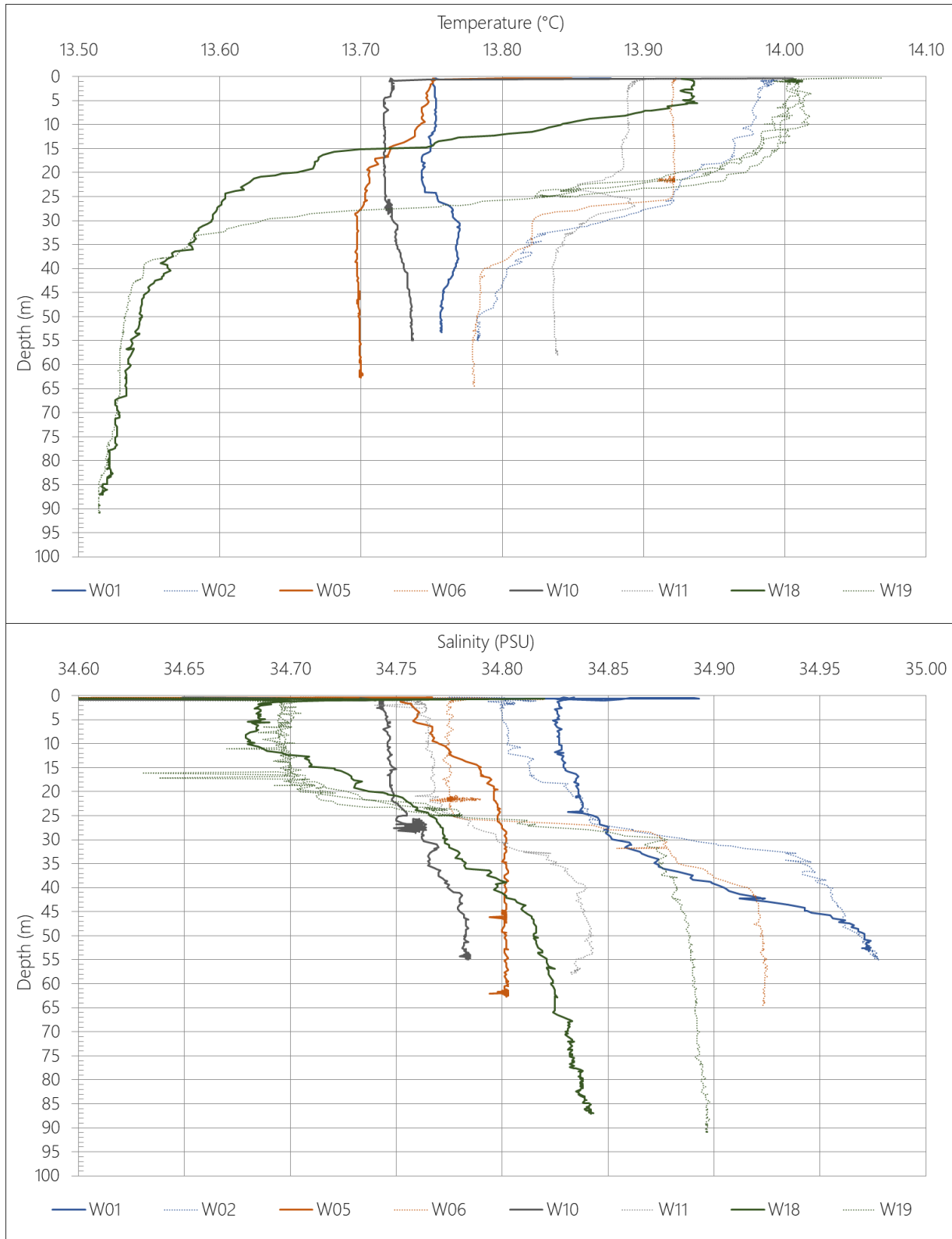


Figure 3-40 Variation in temperature and salinity on a spring/neap tide (corresponding to locations in Figure 2-1). Colours apply to the same locations, with solid lines for spring observations and dashed lines for neap observations



### 3.11 Coastline Morphology

According to the results of the Dynamic Coast project, which provides an evidence base for the extent of coastal erosion in Scotland, 24% of the area between Duncansby Head and Cape Wrath has experienced accretion and 22% has experienced erosion between the 1970's and 2017 (Fitton *et al.*, 2017). Historically, the rate of erosion pre-1970 along the coastline was approximately 0.4 m/year. This has increased to 6 m/year from 1970 to present. The rate of accretion has also increased to 1.7 m/year. These trends are consistent with among rock-dominated coastlines which offer the surrounding soft coast (i.e. sandy bays) greater protection (Fitton *et al.*, 2017). At present, there is likely to be little fresh material to these beach systems from offshore or from erosion of cliffs due to the nature of the cliffs along the coastline as described below. Instead, fluvial erosion is more likely to supply material for accretion along the coast.

However, the area of shoreline where the offshore ECC achieves landfall is characterised by hard and mixed substrate, with cliffs along much of the coast (Hurst *et al.*, 2021) based on the updated Dynamic Coast project (Dynamic Coast, 2021). This is consistent along the length of the north coast of the Scottish mainland; 74% of this coastline is categorised as hard and mixed (Fitton *et al.*, 2017). The coastline at the offshore ECC landfall is considered not erodible according to NatureScot's Dynamic Coast mapping tool (Dynamic Coast, 2021). The EMODnet CoastalType is classed as "Erosion-resistant rock and/or cliff, without loose eroded material in the fronting sea" (EMODnet, 2021). The rocky coastline at the landfall location is shown in Figure 3-42 in 2004, 2019 and 2021. As evidenced by Figure 3-42, there has been little change along the coastline over that time. The difference in the coastline between years largely corresponds to changes in the tidal cycle and the points at which the aerial images were taken. This supports the understanding of the coast here as being not erodible.

Figure 3-41 shows the substrate type in the intertidal area of the offshore ECC and study area. The majority of the coastline within the offshore ECC is classed as rock platform with boulders/loose rock. The completed nearshore geophysical and intertidal survey identified the presence of exposed resistant bedrock, with acquired ortho-imagery also demonstrating the presence of rock platform (Spectrum, 2023). The site-specific observations at the landfalls are in agreement with the wider understanding of this coastline (Dynamic Coast, 2021). The wider study area is predominantly the same intertidal substrate type interspersed with areas of sand and sandy gravel.

The predicted relative sea level rise (discussed in section 3.6.3), and the associated landward movement of the high water level, provides a potential for coastal erosion to occur in locations along the sections of the study area coastline that are characterised as having a more erodible frontage (Horsburgh *et al.*, 2020). However, this is considered to be less likely along the shoreline where offshore ECC landfall occurs, primarily due to the presence of erosion resistant rock.

An increase in sea level is anticipated when accounting for emissions under the high-emissions (RCP8.5) and low-emissions scenarios (RCP2.6). Under the low-emissions scenario, a sea level rise of 0.35 m can be expected at the offshore ECC landfall by 2100. Under the high-emissions scenario, this increase is expected to be significantly higher; an increase of 1 m in sea level at the landfall location by 2100 (Dynamic Coast, 2022).

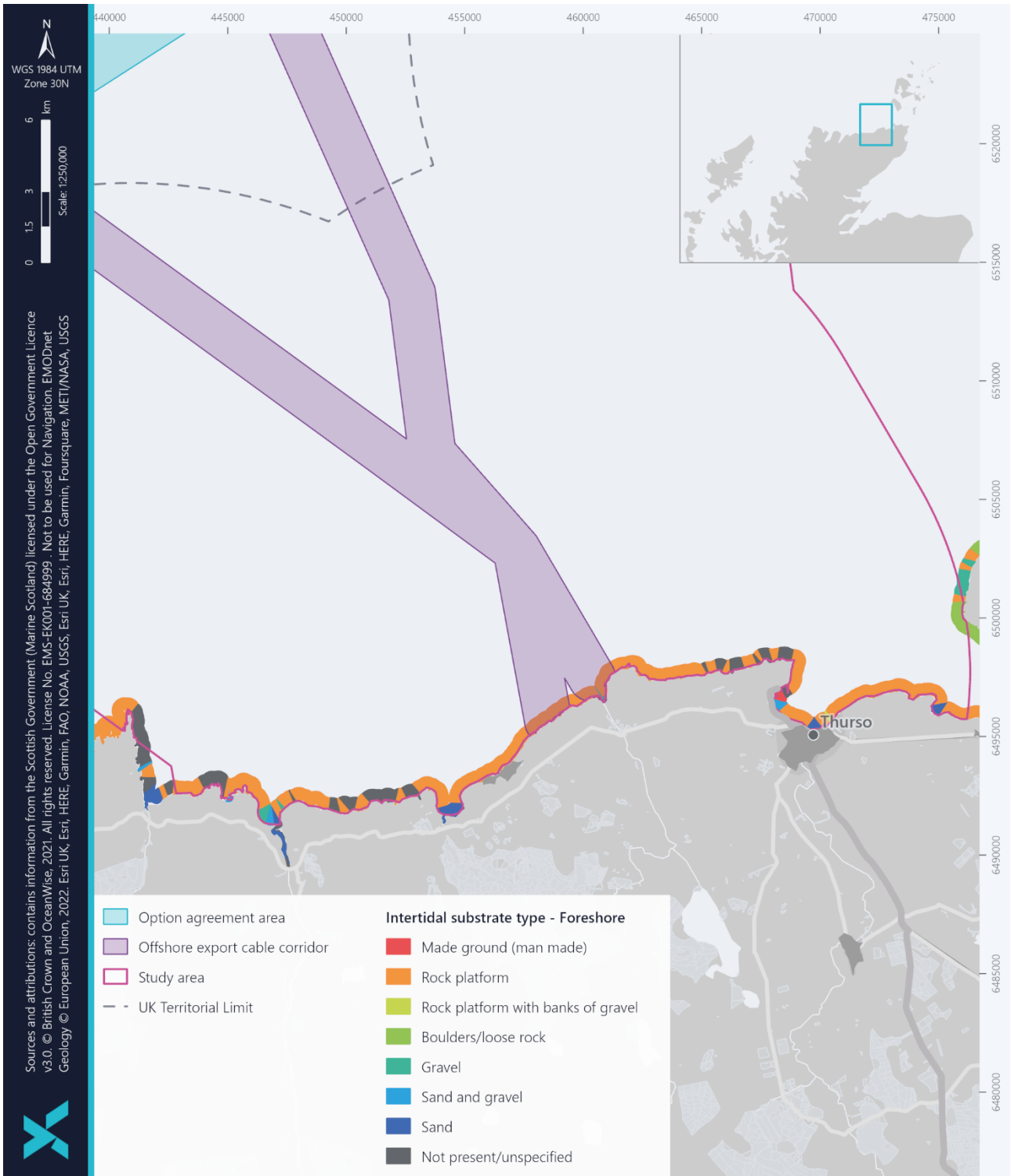


Figure 3-41 Intertidal substrate in the foreshore of the offshore Project area

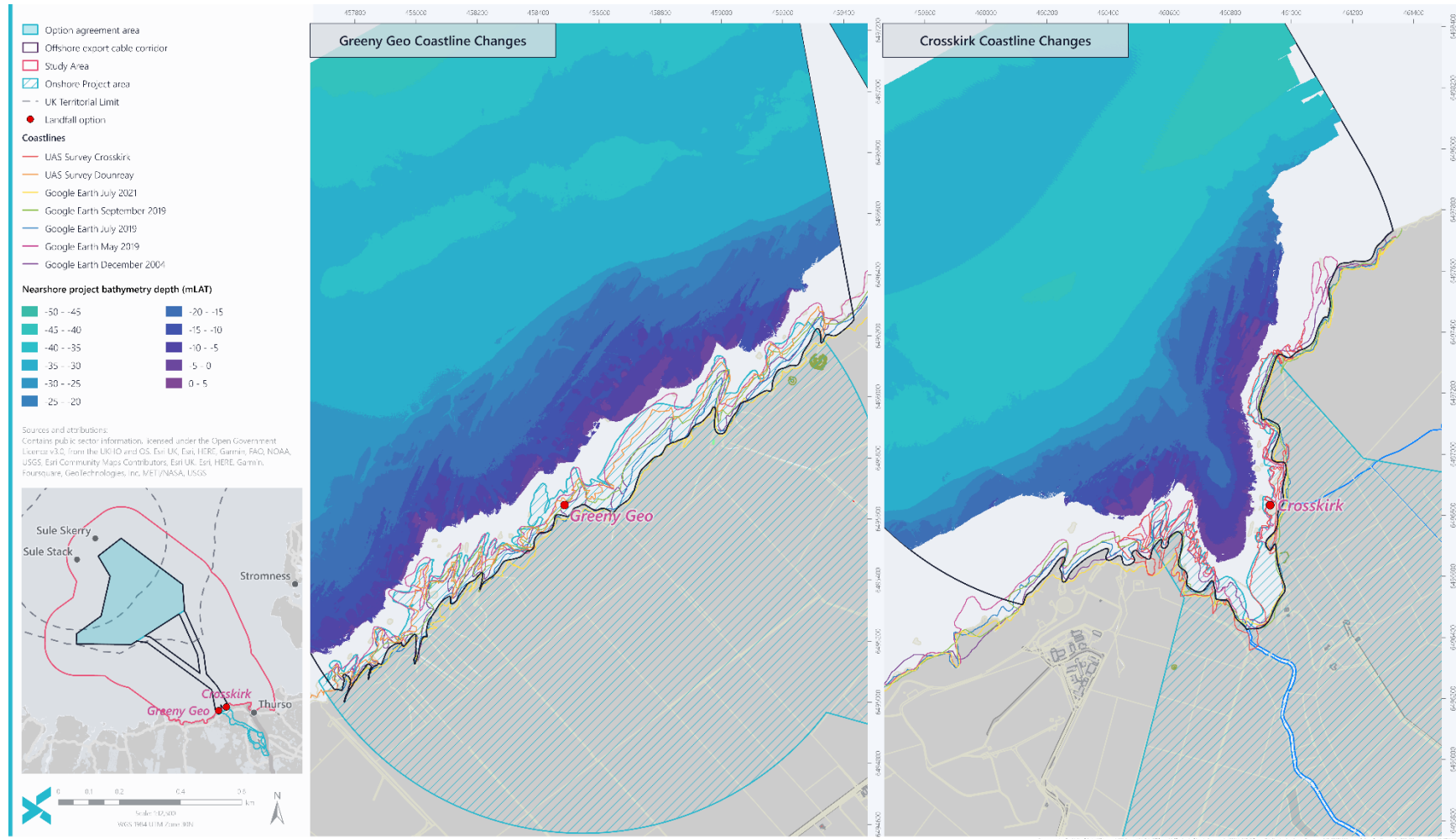


Figure 3-42 Shoreline change at offshore ECC landfalls



## 4 ASSESSMENT APPROACH

### 4.1 Sources of Effects on Marine Physical and Coastal Processes

Sources of effects on Marine Physical and Coastal Processes from the offshore Project are primarily through:

- Seabed disturbance – these include short-term effects during construction (including pre-construction) and decommissioning stages of the development, which can lead to increased suspended sediment concentration and seabed deposition;
- Loss of or alteration of seabed type – includes the medium to long-term loss of seabed or change in seabed sediment type, as a result of the development, as well as the potential development of seabed scour around infrastructure due to the local modified flows; and
- Blockage – medium to long-term effects from the layout of offshore infrastructure and remedial protection, during the operational stage which can locally modify flows and waves energy transmission that affect mixing and potentially introduce barriers to sediment transport pathways, with onward effects on the coast.

The assessment completed for the Marine Physical and Coastal Processes considers the above effects as pathways, resulting on impacts on receptors and it is on this basis that potential impacts have been identified, as presented in Section 4.2 below.

### 4.2 Impacts Requiring Assessment

Based on the information presented in the Scoping Report (OWPL, 2022a) and consultee responses provided in the Scoping Opinion, the impacts requiring assessment are summarised in Table 4-1. The analyses and assessment of potential environmental impacts associated with construction and decommissioning activities are presented in Section 5, and impacts associated with the operational stage of the offshore Project are presented in Section 6.

*Table 4-1 Impacts assessed within the Marine Physical and Coastal Processes EIA*

PROJECT STAGE	IMPACT
<b>Construction (including pre-construction) and Decommissioning</b>	Change to seabed levels, sediment properties and suspended sediment concentrations
	Impact on designated features within the designated sites due to export cable construction
	Change to coastal landfall morphology
<b>Operations and Maintenance</b>	Change to the tidal, wave and sediment transport regimes resulting in impacts on morphology and coast receptors
	Introduction of scour
	Changes to water column structure with impact to stratification



PROJECT STAGE	IMPACT
	Re-exposure of buried cables at landfall and changes to coastal processes and landfall morphology from remedial protection measures

### 4.3 Project Description

This section provides a high level overview of the Project design which, at present, covers a range of possible installation and construction activities and methods. Where additional detail is required within the context of the analysis undertaken for the construction and operational stages of the offshore Project, this has been provided in section 5 and 5 as appropriate.

Prior to construction within the OAA and offshore ECC, the seabed will require preparation. In particular, boulder clearance will be completed along all cable routes (inter-array, interconnector and export cables), using a boulder clearance plough and/or grabs. Boulders will be moved to the side and not removed from the site. A corridor of up to 30 m per export cable circuit could be cleared (15 m each side of the proposed cables). A Pre-Lay Grapple Run (PLGR) of the final cable routes will take place following any boulder clearance works and prior to the cable laying campaign. The PLGR is assumed to take place along the entire length of all cables, and the disturbance footprint would be within the clearance corridor, with the effects being less than assessed for other seabed preparation.

Further seabed preparation may also include sandwave / bedform clearance which can be performed using dredging techniques, jetting tools or Controlled Flow Excavators (CFEs). Of the range of methods available, CFE and dredging by Trailing Suction Hopper Dredger (TSHD) are used for seabed levelling and sandwave clearance when more conventional equipment like ploughing may not be applicable and constitute the clearance methods with the wider seabed footprint. Based on the seabed characteristics across the offshore Project area, a TSHD dredge and disposal approach may be more applicable for clearance operations, with the use of CFE only in isolated discrete areas. However for completeness, the potential for impacts based on the entire Project clearance volumes are applied to each clearance method to understand the potential impacts from each method. It is not the case that the assessed impacts from each method are cumulative. Should TSHD be used, excavated material may be disposed of in designated/licensed disposal sites or within the offshore Project, to be determined post-consent. The range of potential seabed preparation methods generate different pathways for disturbance. For instance, material can be excavated and disposed through a surface discharge in the case of a TSHD. In the case of CFE, while it does not involve direct contact with the seabed, it generates near-bed sediment disturbance with a relatively large footprint. Therefore, disturbance by TSHD and CFE are considered as the worst case scenario in the analysis undertaken in sections 5.1 and 5.2. The anticipated seabed preparation (boulder and bedform clearance) for all offshore infrastructure is summarised in Table 4-2.



Table 4-2 Worst case seabed clearance construction parameters

	WTG & OSP	EXPORT CABLE	INTER-ARRAY	INTERCONNECTOR CABLES
Boulder clearance footprint (m <sup>2</sup> )			30,442,900	
Bedform clearance and levelling width (m)	N/A	1,000	150	150
Bedform clearance and levelling length (km)	N/A	19.2	33.8	19.5
Bedform clearance and levelling footprint (m <sup>2</sup> )	39	19,200,000	3,375,000	2,925,000
Bedform clearance and levelling volume (m <sup>3</sup> )	250,000	495,000	382,360	382,360

Once seabed preparation has concluded, installation of the offshore Project structures can commence, including installation of the WTGs and (offshore substation platform) OSP foundations, cable lay, and any associated protection. There are three proposed foundation types for the 125 WTGs: monopile, piled jacket and suction bucket jacket, with numerous sub-options. For each proposed foundation type there is a worst case sub-option associated with the varying impact pathways, however, the worst case largely equates to the largest structure represented by the sub-options. Some key parameters for each of these foundation options are shown in Table 4-3. The method of WTG foundation installation is dependent on the chosen foundation type and ground conditions. The monopile and piled jacket WTG foundations may be installed through piling or drilling (partial or fully). With respect to impacts on the marine physical processes, in particular seabed disturbance, the worst case may be considered to apply to the fully drilled and specifications relating to each of these installation methods are shown in Table 4-3.

Table 4-3 Worst case WTG foundation construction specifications

	MONOPILE	PILED JACKET	SUCTION BUCKET JACKET
Minimum WTG spacing (m) <sup>5</sup>	1,320	1,200	1,200
Foundation length (m)	18	20	20
Foundation breadth (m)	18	20	20
Seabed footprint per WTG foundation (m <sup>2</sup> ) excluding scour protection	255	170	2,100
Number of piles per WTG	1	4	N/A

<sup>5</sup> A smaller WTG spacing of 944 m is relevant to the smallest foundation size, however it is noted that with this smaller spacing the ratio between the spacing and foundation diameter is larger than that for the larger diameter, so the spacing for the largest foundation size is still considered to be the worst case.



	MONOPILE	PILED JACKET	SUCTION BUCKET JACKET
Pile/suction bucket diameter (m)	18 <sup>6</sup>	4	13
Pile penetration depth (m)	40	53	N/A
Drilling depth (m)	40	53	N/A
Maximum suction bucket penetration depth (m)	N/A	N/A	30
Drill volume per WTG (m <sup>3</sup> )	11,000	2,660	N/A
Drill volume OWF (m <sup>3</sup> )	1,375,000	332,500	N/A
Scour protection height (m)	up to ~2.5	up to ~2.5	up to ~2.5
Scour protection area per WTG (excluding pile area) (m <sup>2</sup> )	~8,000	~9,500	~9,500
Total footprint per WTG (including scour protection) (m <sup>2</sup> )	~8,255	~11,200	~11,600
Total footprint OWF (including scour protection) (m <sup>2</sup> )	1,031,900	1,197,400	1,253,900
Extent of scour protection from edge of pile (m)	~41	~20	~20
Scour protection material per foundation (m <sup>3</sup> )	~19,000	~23,500	~23,000
Scour protection volume for OWF (m <sup>3</sup> )	~2,380,000	~2,900,000	~2,860,000

There are two proposed foundation types for the five OSPs, with two sub-options for each. The larger sub-option structures constitute the worst case scenario with regards to the varying impact pathways and the influence these may have on the surrounding physical environment, the parameters for which are summarised in Table 4-4 and discussed in section 5 as appropriate.

Table 4-4 Worst case OSP foundation construction specifications

	PILED JACKET	SUCTION BUCKET JACKET
Number of legs per foundation	8	8
Number of piles per leg	2	N/A
Seabed footprint per foundation (m <sup>2</sup> )	3,700	4,120
Jacket leg diameter (m)	4	4
Pile diameter (m)	4	N/A

<sup>6</sup> Following development of the numerical model, during and informed by the Offshore EIA certain design parameters in the PDE were amended, including reduction of monopile diameter from 18 m to 14 m. As 18 m was larger than the revised parameter (and therefore represented a worst case assessment), it was not necessary to update the numerical model for a smaller monopile diameter.



	PILED JACKET	SUCTION BUCKET JACKET
Pile penetration depth (m)	40	N/A
Suction bucket diameter (m)	N/A	8
Suction bucket penetration depth (m)	N/A	14
Drilling depth (m)	40	N/A
Scour protection material per foundation (m <sup>3</sup> )	37,200	39,200
Scour protection height (m)	2.5	2.5
Scour protection area per foundation (excluding pile area) (m <sup>2</sup> )	16,500	17,300
Total footprint per foundation (including scour protection) (m <sup>2</sup> )	20,200	21,420
Extent of scour protection from edge of pile (m)	22	26
Scour protection volume per OSP foundation (m <sup>3</sup> )	41,100	43,200
Scour protection volume for OWF (m <sup>3</sup> )	205,500	216,000

During the construction stage, protection materials will also be installed in association with the WTG and OSP foundations to mitigate against the potential formation of scour, which could take the form of rock placement, with a maximum height of 2.5 m. The area and volume of scour protection (assumed to be rock) associated with the WTG and OSP foundations are shown in Table 4-3 and Table 4-4 respectively.

The offshore Project will include a number of inter-array and export cables and interconnector cables. A summary of the cable parameters for the offshore Project is included in Table 4-5. For the export cable five cables of up to 64 km each in length, with a total of up to 320 km within a 1 km corridor is assumed, while for the inter-array cables and interconnector cables, a total length of up to 500 km and up to 150 km respectively are anticipated. External cable protection materials could be required as protection or at a crossing. Such materials could include concrete mattresses, rock placement, grout bags, cement bags, sandbags, articulated pipes, cast iron shells, bend restrictors, suppression strakes, filter units, and gabion bags (i.e., rock bags). Should rock placement be required along a cable, it is estimated that the berm will have a trapezoidal profile, with approximate dimensions of 3 m height and 1:3 side slope, resulting in a berm base width of 20 m.

At landfall, Horizontal Directional Drilling (HDD) is proposed. The HDD will be drilled from land out to sea and the location of the offshore exit point is expected to occur between 10 mLAT and 40 mLAT. The minimum HDD exit depth of 10 mLAT is approximately 188 m offshore (from 0 mLAT) at the Greeny Geo landfall and 100 m offshore at the Crosskirk landfall, while a more realistic HDD exit depth is from 20 mLAT at a distance of approximately 340 m and 230 m offshore at the Greeny Geo and Crosskirk landfalls respectively. Approximately 1,360 m<sup>3</sup> of cuttings will be removed from each of the six HDD bores. Overall, material excavated during HDD will be extracted back on land with little to no release at sea. The exception is only at punch-out at the HDD exit, where small volumes of drilling fluid may be discharged. The drilling fluid will comprise bentonite, which is an inert substance and recognised by the Centre for Environment, Fisheries and Aquaculture Science (Cefas) as being fully biodegradable. It is also on the Oslo/Paris convention (OSPAR) List of Substances Used and Discharged Offshore which are considered to Pose Little



or No Risk to the Environment (PLONOR). Some dredging, including the excavation of exit pits may be required at the exit point to ensure the duct ends, and subsea cables end up buried below the seabed. Typical exit pits would be 10 m wide x 30 m long x up to 5 m deep and a volume of 1,500 m<sup>3</sup> per pit. Up to six pits may be excavated, including five for the proposed HDD and one spare. These pits may additionally be used as plough starter pits allowing access for cable installation. Excavation may be done by use of backhoe dredgers or suction dredgers depending on ground type and water depths. Using the above pit dimension assumptions, for six pits, the anticipated volume of material moved will be 9,000 m<sup>3</sup> in total. The dredged material would be disposed of or stored beside the exit pits as sediment berms (assumed to have up to the same height of nearshore cable protection at up to 3 m and minimum berm width of around 17 m). The sediment berms could be left as is or backfilled after the operation. The requirement for backfilling the exit pits will be determined post-consent following further engineering investigations. Depending on ground conditions, it is possible that a single pit for all five cables may be considered. Consideration of the impacts associated with the cable installation and the landfall methodology are considered in section 5.

Table 4-5 Worst case cable installation specifications

	EXPORT CABLE	INTER- ARRAY	INTERCONNECTOR
Number of cables	5	140	6
Maximum total length of cables (km)	320	500	150
Corridor width (m)	1,000	150	150
Target burial depth (m)	3	3	3
Maximum trench width (m)	5	5	5
Total area of seabed disturbance (km <sup>2</sup> )	16	25	8
Total length of expected cable burial (km)	224	400	51
Total length of expected cable protection (km)	93.5	100	99
Cable protection berm height (m)	3	3	3
Cable protection berm width (m)	20	20	20
Cable protection berm footprint (m <sup>2</sup> )	1,870,000	2,000,000	1,980,000
Number of crossings	5		10
Crossing berm height (m)	4		4
Crossing berm width (m)	25		25
Crossing berm length (m)	500		500
Crossing berm footprint (m <sup>2</sup> )	62,500		62,500

Two layouts, illustrated in Figure 4-1, were considered to provide the worst case for marine physical and coastal processes, specifically through blockage to flows and waves. The West of Orkney model developed for the Project,



only focussed on the proposed installation activities and presence of the infrastructure within the OAA, the offshore ECC was not included in the model.

Layout 1 (Figure 4-1) was orientated in relation to the dominant wave and flow direction, with the minimum spacing applied and the potential for coalescence of effects within the OAA. Layout 1 assumes all the WTGs will be arranged in a single block across the centre of the OAA from west to east. The WTGs will be seven deep and spaced in a linear fashion. Layout 1 assumes three of the OSPs will be along the western boundary of the OAA in line with the WTGs, the remaining two OSPs will be along the eastern boundary.

Layout 2 (Figure 4-1) was set out to represent an orientation in relation to the northwest wave approach direction, with foundations installed across the OAA, and limited to the shallower areas within the OAA. Layout 2 assumes the larger grouping of WTGs will be in the north of the OAA on Stormy Bank. The smaller grouping will be located in the south of the OAA, in areas of shallower water depth associated with Whiten Head Bank and the surrounding areas. Three OSPs will be located in the north of the OAA (two in the northwest corner and one to the east). The remaining two OSPs will be in the south of the OAA, on either side of the southern grouping of WTGs.

For both modelled layouts, both the WTGs and OSPs were included in the modelling process. However, the West of Orkney model does not account for installation of scour protection at WTGs or OSPs.

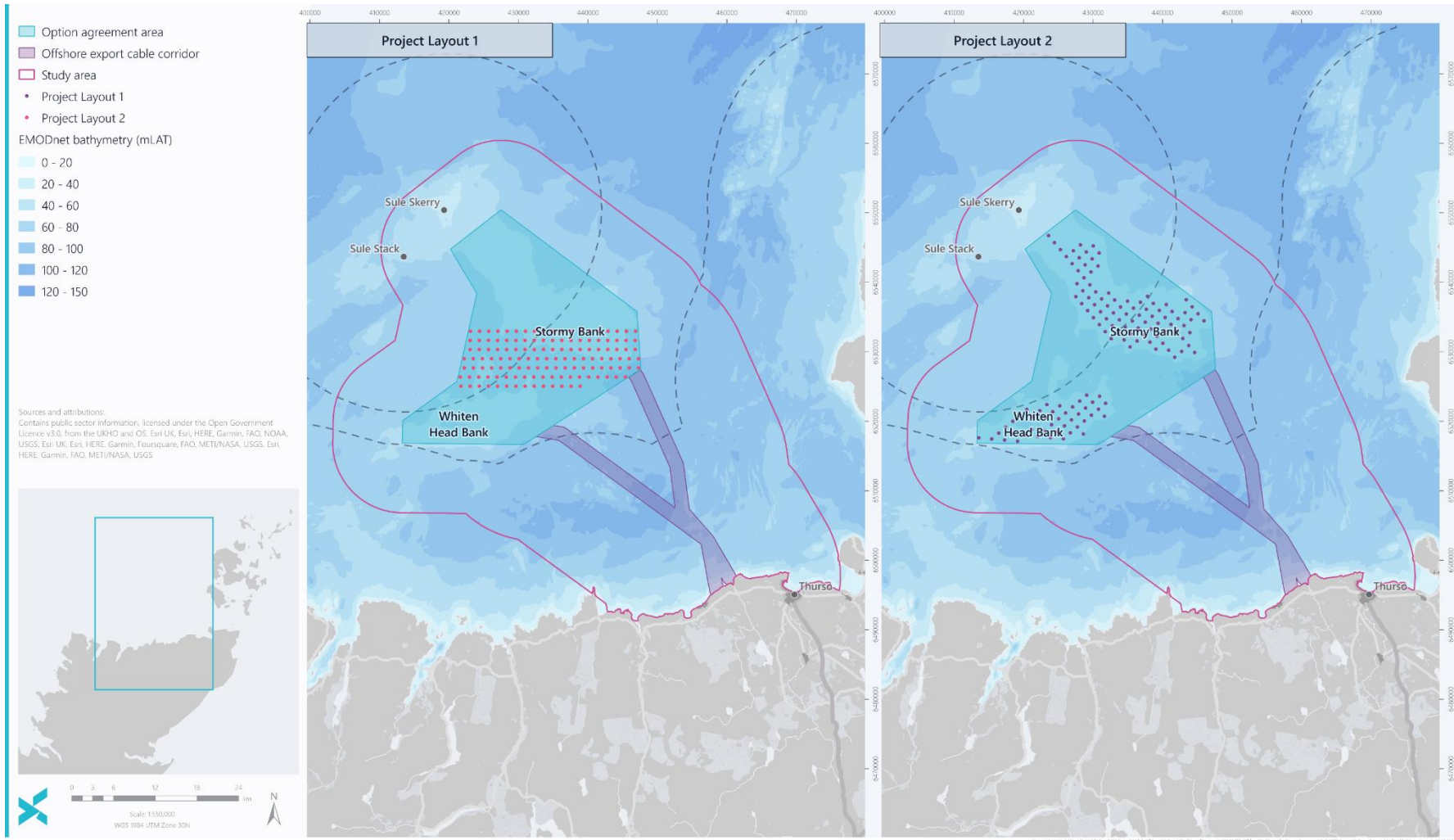


Figure 4-1 Worst case foundation layouts for marine physical and coastal processes



## 4.4 Approach to Assessment

The assessment approach detailed in the following sections have been identified and implemented in relation to the impacts requiring assessment, environmental sensitivities across the study and responses provided within the Scoping Opinion (MS-LOT, 2022). An important element of the assessment approach and as necessitated by consultees is the use of numerical modelling to inform the potential extent and magnitude of impacts associated with the construction and operation of the offshore Project. The West of Orkney model has been developed as part of this study to investigate and assess for potential offshore Project impacts at various Projects stages and associated offshore Project activities. Section 4.4.1 below summaries the applied modelling approach (including setup, assumptions, parameters and scenarios), with a detailed report on the model set-up, calibration and validation provided in 8. Modelling results presented and discussed as relevant within section 5 (for Construction impacts) and section 5 (for operational impacts), with a technical modelling report included in Appendix B. In addition to the numerical modelling of potential environmental impacts, a number of analytical methods have been applied to assess and inform potential impacts and are described in section 4.4.2.

### 4.4.1 Modelling Approach

The modelling that has been used to inform this technical report, has been completed by Port and Coastal Solutions Ltd, for which more detailed outputs are presented in 8 and Appendix B for the setup and results respectively.

#### 4.4.1.1 Modelling Method

Full detail on the applied numerical modelling method, including set-up, calibration and validation is presented in 8, with only a summary of key information presented here as applicable. The numerical modelling completed for the offshore Project, has been configured in the MIKE software, using the hydrodynamic, spectral wave and particle tracking modules. For the offshore Project, a flexible mesh has been applied, which allows the spatial resolution of the model mesh to be varied across the model domain. The model domain extends across an area of approximately 85 km east-west and 30 km north-south centred on the OAA and Orkney Islands, capturing the north coast of mainland Scotland (section 1.4). The east, north and west model boundaries, were represented as open boundaries and used to define the water level, flow and wave properties to propagate through the model domain. The model was implemented in two dimension (2D), enabling the derivation of depth-averaged flows and suspended sediment concentrations.

Bathymetry data incorporated in the model originated from multiple sources as outline in 8. No site bathymetry data was available to use in the model at the time of its development and implementation. However, on completion of the modelling, the EMODnet (2020) bathymetry used to develop the West of Orkney model, was compared with the site-specific bathymetry data when it became available. It should be noted that the model bathymetry itself was at a resolution of around 100 m across the offshore Project area and along coastlines, with coarser resolution towards the West of Orkney model boundaries. The site-specific bathymetry was identified to be generally about 1 m deeper than the EMODnet bathymetry, and due to the survey resolution (at up to 0.5 m), a lot more resolved in identifying more morphological features on the seabed. It was noted that the captured morphological features were often at a scale (i.e. less than 1 km in length) and so are unlikely to be greatly resolved or represented in the interpolated West of Orkney model bathymetry (at a resolution of 100 m). Also as represented in the modelled baseline tidal conditions



discussed in section 3.7.2, no localised flow circulations or large variations in flow speed are observed across the OAA and offshore ECC, to be greatly influenced by the more resolved seabed and morphological features represented in the site-specific bathymetry. Overall, due to the shallower depths as represented in the EMODnet (2020) bathymetry and applied in the West of Orkney model, the model can be considered to be more conservative in terms of the modelled flows, as shallower depths are applied. Furthermore, the implemented model and achieved results did not demonstrate large variances in flow properties across the offshore Project area, with the more conservative EMODnet (2020) bathymetry. Therefore, the EMODnet (2020) bathymetry as applied in the West of Orkney model and the achieved results are all considered valid to inform the potential impacts of the offshore Project on the physical environment as discussed in sections 5 and 6 for the construction and operation stages respectively.

Tidal boundaries from the DTU10 tidal model (Cheng and Andersen, 2011) were used to derive water level timeseries across the model area. The influence of freshwater flows on modelled flows and water levels were also investigated but were found to be insensitive and therefore were not included. Due to the offshore location of the Project and relative depth, waves were not considered to be a dominant forcing mechanism, even though the Project is located within a swell dominated wave environment. The minimal contribution of waves to the sediment transport regime is described in the baseline characterisation in section 3.9.2. Therefore, the decision was made not to model for time-varying waves, but instead model for impacts associated episodic statistical wave conditions described further in section 4.4.1.3 below. With this approach, a consistent wave statistic was applied at the model boundaries to propagate the model domain in association with time-varying flows.

Model calibration and validation was completed for the developed West of Orkney model and described in detail in Appendix A. The completed calibration and validation involved the model being tested against a number of water level, tidal flow and wave metrics to ensure that the model represented the area to a degree of accuracy. Iterative changes were applied to the model setup to improve the model calibration as it was undertaken. The data against which the model was calibrated and validated was obtained from publicly available sources. Due to the approach applied for including waves in the model, the wave calibration focussed on replicating a range of statistical wave conditions rather than a time series of wave conditions.

Overall, the West of Orkney hydrodynamic model was considered to accurately simulate water levels throughout the model domain and the flows through the Pentland Firth where high quality calibration data exists. However, in areas of the model where non-tidal influences can dominate (due to a combination of weak tidal flows and the strong influence of meteorological forcing at times) the modelled flows (which only include for the effect of tidal forcing) did not fully replicate the measured flows. However, given the West of Orkney model's ability to accurately simulate flows from high quality observations it was considered to provide the appropriate accuracy to investigate and assess Project impacts. For waves, the model was considered to provide a conservative assessment of wave conditions in the nearshore area.

#### 4.4.1.2 Construction Modelling Scenarios

A number of scenarios were run in the West of Orkney model covering the worst case activities and parameters during the construction and operational stages of the Project. Instead of modelling project activities as specific tidal states, modelling was continued over a continuous 16-day period during which the construction activities would occur. For example, as drilling a monopile foundation is to occur over 135-hours, the installation of one monopile was modelled with a short (9-hour) break to allow installation vessel relocation, after which the drilling for the next



foundation would commence. With this approach, the resulting sediment plume is considered to more realistically represent the associated disturbance as typically construction would occur continuously for a period of time.

The modelling scenarios were determined on the basis of the worst case as informed by the Project design, introduced in section 4.3. At present there are a wide range of construction methods being considered for site preparation and cable, WTG and OSP foundation installation, as introduced in section 4.3. However, It should be noted that more conservative parameters relating to the Project’s design were applied in the modelling. Since completion of the modelling, the Project design has been revised, however, the previous modelling for larger parameters covered the worst case scenario. Therefore, the underlying assumptions used to inform the modelling for clearance and installation of cables are larger than that represented in the Project design in section 4.3. Where there are differences, these will be presented in the relevant text.

With construction activities, the main impact pathway for marine and physical processes is through seabed disturbance, potentially resulting in the development of a plume; and loss / change of seabed type as a result of the deposition of disturbed sediment. In light of the range of proposed methods associated with construction, Table 4-6 summarises the scenarios modelled to assess construction impact, with further detailed provided in the following sub-sections. The modelling was also only completed based on the fine sediment fraction that can be expected to develop into a plume, associated with the passive deposition phase. This therefore equates to only a small proportion of the sediment bulk as presented in the following sub-sections. The larger proportion of sediment would fall directly to the seabed associated with the active deposition phase. The relevance of the varying sediment volumes associated with the different deposition phases is described in further detail as applicable throughout this technical report.

Table 4-6 Summary of modelling scenarios

ACTIVITY	SCENARIO	JUSTIFICATION
Seabed preparation	Seabed preparation by dredge and disposal (TSHD)	Sediment removal by a TSHD involves disturbance at the seabed as result of the draghead and as overspill on the sea surface as the vessel moves. There is also the water surface discharge from the hopper at periodic intervals associated with disposal, during the seabed preparation. This disturbance pathway results in both sea surface and seabed disturbance.
	Seabed Preparation by CFE	Disturbance pathway associated with CFE remains close to the seabed.
Cable installation (export and inter-array)	Cable burial by CFE	Although various methods are being considered for cable installation, jetting and CFE methods have a similar disturbance effect on the seabed and also remain near-bed. However, due to the fact that CFE is likely to cause more disturbance, it is considered to provide the worst case and is therefore modelled.
	Monopile drilling from one WTG foundation at a time	Drilling of the bedrock disintegrates the rock, which is discharged at the sea surface.



ACTIVITY	SCENARIO	JUSTIFICATION
WTG and OSP foundation installation	Monopile drilling from two TWG foundations at a time	Applying the same approach for monopile drilling, with two foundations being drilled concurrently.
In-combination impact from construction activities	In-combination impact due to pile drilling and cable installation occurring in tandem	Accounting for the fact that multiple construction activities could be ongoing concurrently within one WTG spacing.

Full details on the assumptions that underpin the completed modelling of construction activities is set out in Appendix B.2.1, with key and relevant information used to inform the assessments in section 5, provided in the sections below.

#### 4.4.1.2.1 Seabed preparation by dredge and disposal (TSHD)

The inter-array and interconnector cables within the OAA and the export cables connecting the windfarm to the mainland in the offshore ECC will require burying in areas where bedforms such as sandwaves are present. To inform the modelling, the *in situ* volume of sediment estimated to require removal as part of seabed preparation is as set out in Table 4-2, equating to a total of 1,014,720 m<sup>3</sup> of material being dredged in the OAA and a further 495,000 m<sup>3</sup> within the offshore ECC. This results in a total dredged volume of 1,509,720 m<sup>3</sup>. Based on an *in situ* density of 1,900 kg/m<sup>3</sup> and dry density of 1,500 kg/m<sup>3</sup> informed from site-specific geotechnical investigations (OWPL, 2023), and a water density of 1025 kg/m<sup>3</sup>, the equivalent dry sediment mass to be dredged for the total offshore Project is 2,264,580 tonnes.

A large TSHD with a hopper volume of 35,000 m<sup>3</sup> is applied for the modelling and assumes that the hopper would on average take two hours to fill and that overflow would occur after the initial 30 minutes of dredging. In addition, the placement of dredge sediment through the hydraulic hopper doors is assumed to occur over a 10 minute duration. Each hopper load is assumed to hold 15,050 tonnes of dry sediment (equivalent to approximately 16,050 m<sup>3</sup> *in situ*), therefore based on the dredge volumes quoted above it will take up to 101 dredger loads to prepare the seabed in the OAA and 49 dredger loads to prepare the seabed in the offshore ECC, with a total of 150 loads for the offshore Project. Based on an assumed vessel speed of 4 knots for seabed preparation, dredging within the OAA is estimated to occur for 202-hours, while for the offshore ECC, dredging is estimated to occur for 98-hours. The applied timeframes and dredger loads are indicative for the purposes of informing the numerical modelling and should be noted that clearance could actually be on the order of weeks to months within the 18-month offshore Project seabed preparation programme.

The dredged sediment will be placed within the offshore project area boundaries. For the purposes of modelling, an indicative central Dredge Material Placement Area (DMPA) within the offshore project area has been assumed along the southeast boundary of the OAA, as illustrated in Figure 5-1. It should be noted that the indicative DMPA has been selected so as not to intersect the modelled layouts and is only to inform modelling. Each of the 150 dredger loads will be placed in a different cell within the DMPA, with the cells spread across the full extent of the area, with an estimated dredge cycle time of three hours and ten minutes between disposal events.



Based on the proposed clearance volumes, percentage sediment suspended from TSHD operations and the varying sediment properties and percentage of fine sediment between OAA and offshore ECC, varying release rates were calculated across the offshore Project area as presented in Table B-2 (Appendix B.4.1). Further detail on the applied modelling assumptions are also included in Appendix B.2.1.1.

#### 4.4.1.2.2 Seabed preparation by CFE

Bedform clearance by CFE will result in different sediment disturbance pathways than dredging with TSHD, as all of the sediment disturbance will occur close to the seabed and at the location where clearance is required. The expected rate of sand wave clearance using an CFE is 25 m/hr with a head disturbance footprint width of 50 m. It is expected that the clearance to the required depth could be achieved in one pass across the footprint width, where the average height of bedform requiring clearance is 3.5 m. Based on the above, the CFE clearance cross-section *in situ* volume of 262,500 kg/m disturbed on one pass. Based on the bedform clearance rate, CFE footprint, 1 km wide corridor and 19.2 km to be cleared, it is estimated that each clearance episode could occur over a period of weeks to months, with one or more clearance episodes within the 18-month offshore Project seabed preparation programme. Given the Project parameters as described in section 4.3, an indicative rate of sediment disturbance of 1,823 kg/s, associated with the CFE passing is applied. It is assumed the sediment disturbance rate would be the same for the clearance of bedforms along all cables (inter-array, export and interconnector) and any clearance from the WTG foundation locations. The high concentration of sediment suspended will result in the formation of a dynamic plume which will descend rapidly back to the bed. Further detail on the applied modelling assumptions is included in Appendix B.2.1.2.

#### 4.4.1.2.3 Cable burial by CFE

CFE will be used for cable installation for both the export cable and the inter array/ inter connector cables. The expected rate of cable burial using an CFE is 150 m/hr. Assuming a trench width of 5 m and a depth of 3 m the *in situ* volume of sediment disturbed by CFE along the entire 320 km export cable route is 4,800,000 m<sup>3</sup>. This is equivalent to a dry sediment mass of 7,200,000 tonnes. Based on the cable burial rate it will take an approximate total of 2,133 hours (89 days) to install the export cable within an anticipated 6-month cable installation programme. However, it should again be noted that the installation period is indicative, as actual installation may not be continuous, but staged, whereby installation occurs over a period of days to weeks for each installation episode, within the overall installation programme. Therefore, an indicative rate of sediment disturbance of 938 kg/s is applied for cable installation activities. The sediment disturbance rate would be the same for the installation of the inter array and inter connector cables. Further detail on the applied modelling assumptions is included in Appendix B.2.1.3.

#### 4.4.1.2.4 Foundation installation: monopile drilling one WTG foundation at a time

Installation of the WTG and OSP foundations will generate disturbance to the seabed within the OAA. As stated in section 4.3, the method of installation could be drilling or piling (or a combination of the two), with drilling considered to generate the largest impact to the seabed.

Based on the available geological information for the OAA (see sections 3.2.2 and 3.3.2, the depth of the surface sediment layer varies significantly across the site. The Holocene sediment, which is expected to be similar to the surface sediment samples detailed in section 3.2.2, occurs at depths of 0 to 50 m below the seabed, with bedrock also occurring at depths of 5 m below the seabed. To provide a conservative assessment for the model with respect to sediment dispersion during construction, a depth of 5 m for surface sediment is assumed across the OAA. The bedrock is considered to comprise friable sandstone, and for the modelling, it is assumed that 30% of the sediment



making up the sandstone is silt and clay and that the drilling will fully breakdown all of the sediment in the sandstone to its individual particles, which is considered to represent a conservative assumption.

The highest drilling rate and sediment disturbance rate is expected for the installation of the largest monopile, which has an 18 m diameter on the seabed and associated drill volume of 11,000 m<sup>3</sup> per foundation (Table 4-3). The foundations will be drilled to a depth of 40 m below the seabed at a rate of 0.3 m per hour, with drilling expected to take approximately 135 hours per foundation. Although OSPs are also to be installed across the OAA, the drillings volumes involved per drill event are less than that for the largest 14 m diameter monopile (Table 4-3 and Table 4-4). It is assumed that up to two foundations can be installed concurrently, with the worst case surface discharge of drill spoil applied in the modelling.

Based on the drilling approach detailed above, and assuming a density of 2,600 kg/m<sup>3</sup> for sandstone, the sediment release rate during drilling is approximately 60 kg/s. Similar to sediment released during overflow, the high sediment concentration will affect the way the particles disperse in the water column – a dynamic plume will form which will descend to the bed at a much faster rate than the individual particles would settle, reducing the potential for fine-grained sediment to remain in suspension. For the purposes of modelling, it is assumed that drilling will be continuous during the installation of each WTG foundation and that there will be a nine hour gap between drilling subsequent foundations. The model simulation is 16-days in duration allowing the simulation of the drilling of two complete foundations and half of the drilling of one additional. Three WTGs to the east of the OAA were selected for consideration in the modelling. Further detail on the applied modelling assumptions is included in Appendix B.2.1.4.

#### **4.4.1.2.5 Foundation installation: monopile drilling two WTG foundations concurrently**

This scenario models for two 18 m diameter monopile foundations adjacent to each other being drilled concurrently. This scenario aims to investigate the potential for coalescing sediment plumes and therefore applies the parameters as described for the drilling of one monopile. The 16-days model simulation period enabled the four complete foundations and half of two additional foundation based on six WTGs to the east of the OAA. Further detail on the applied modelling assumptions is included in Appendix B.2.1.4.

#### **4.4.1.2.6 Multiple and concurrent construction activities (including seabed preparation, pile drilling and cable installation)**

There is a possibility that some of the construction activities will overlap. The activities which have the greatest potential to result in effects are those which occur within the OAA, which are pile drilling, bedform clearance by CFE and cable burial by CFE. The parameters of each of these construction activities described in the preceding sections are applied in this scenario within the 16-day modelling period. Further detail on the applied modelling assumptions is included in Appendix B.2.1.5.

### **4.4.1.3 Operation Modelling Scenarios**

Forty two scenarios associated with the operational stage of the offshore Project were run in the West of Orkney model. These models were based on each of potential OAA WTG and OSP layouts of 125 foundations and five OSPs. In addition to the layouts being varied, wave approach directions were varied based on the prevailing wave conditions in the area (westerly and northwesterly, as described in section 3.8). The foundation size and spacing applied in the modelling of operational impacts, was based on the structures that provided the largest length scale and the smallest ratio between the size and spacing, thereby indicating a smaller potential for recovery. Based on this high-level initial



assessment, it was determined that the largest monopile foundation of 18 m, associated with a spacing of 1,320 m, i.e. approximately 73 times the foundation diameter was the worst case and therefore informed the modelled layouts. The final factor contributing to the operational stage model runs was the wave conditions which were varied according to differing return periods (RP), as follows:

- 50<sup>th</sup> percentile;
- 90<sup>th</sup> percentile;
- 1 in 1 year RP;
- 1 in 5 year RP;
- 1 in 10 year RP;
- 1 in 50 year RP; and
- 1 in 100 year RP.

Full details on the assumptions that underpin the completed modelling of the operational stage are set out in Appendix B.2.2.

## 4.4.2 Analytical Methods

### 4.4.2.1 Seabed Disturbance and Deposition Thickness

#### 4.4.2.1.1 Seabed loss / change of type and disturbance footprint

The installation of the WTG and OSP foundations, and their presence for the lifespan of the offshore Project, will result in a footprint of direct impact on the seabed. This may be in the form of loss or change of the seabed type, with the installation of infrastructure and any required protection or temporary changes associated with clearance activities or the deposition of disturbed sediment. The infrastructure (and associated protection) footprints, which will result in a direct loss, along with the disturbance areas associated with construction activities are set out in Table 4-2 for clearance, Table 4-3 for WTGs, Table 4-4 for OSPs and Table 4-5 for cables.

#### 4.4.2.1.2 Deposition thickness

The thickness and extent of seabed deposition will depend on the volume of sediment locally displaced, the CFE height of above the seabed, the current speed at the time of the release, and the nature of the sediment. Seabed preparation, drilling, CFE and jetting will all result in the deposition of sediments on the seabed. However, these activities have differing properties which will generate variable levels of deposition. The exact pattern of re-deposition of sediment to the seabed will depend on the actual combination of operational methods and environmental conditions at the time of the event which will be variable. The total volume of sediment disturbed is known and, in combination with other set variables, a range of potential combinations of deposit shape, thickness and area (corresponding to the same total volume) can be calculated.



In determining the deposition footprint and thickness of disturbed sediment as a result of construction activities, in line with the assumed percentages applied for the modelling, it is estimated that the main mass (at 80% and above, as part of the active phase of deposition) of disturbed material will descend directly to the seabed and result in a sizable deposit of variable (not predictable) shape, extent and thickness. The sediment in suspension that develops into a plume may settle out over a wider area with greater extent but proportionally smaller thickness<sup>7</sup>. In practice, the thickness and extent will depend on the volume actually released / disturbed, the spread of the material on impact with the seabed, the current speed at the time of the release, and the nature of the sediment put into suspension. However, the maximum deposition extent or area of effect is inherently limited by the finite volume of sediment released / disturbed as detailed in the Project design (section 4.3). Based on the above, the proposed construction activities and the sediment characteristics (including the proportion of fine sediment fraction across the offshore Project), approximately 99.75% or greater of the disturbed sediment volume would fall directly back to the seabed on disturbance / release as part of the main mass, with only a small percentage developing into a plume, as investigated through numerical modelling (section 4.4.1.1).

Estimation of the impact of varying deposition thickness relative to different deposition extents, was determined for each construction activity independently and cumulatively for the OAA, offshore ECC and the entire offshore Project, based on the volumes that would fall directly to the seabed. The area associated with the different deposition extent (associated with varying deposition thickness), was then compared against the offshore Projects areas (i.e. DMPA, OAA, offshore ECC and total offshore Project area), by which an understanding of the potential scale of impact could be adequately assessed. Estimation of the deposition extent was based on the larger mass of material that would directly descend to the seabed on release (i.e. during the active phase).

## 4.4.2.2 Analytical Assessment of Blockage Effects

### 4.4.2.2.1 Blockage density

The blockage density effects associated with the presence of the WTGs in the water column were assessed. The assumption was applied that the worst case blockage would be from solid structures through the water column, which in this case relates to monopile foundations. For jacket foundations, although these have larger overall diameters (Table 4-3), these are not solid structures, but instead include smaller diameter legs with braces in between, which do not ultimately obstruct the flow over a large area. Therefore, the assessment was completed for the range of monopile foundation sizes, based on the diameter dimensions at the base (seabed) and sea surface, which were used to calculate the representative blockage width per foundation. Smaller monopile foundation sizes were also evaluated for the potential blockage density based on parameters provided in the Project description, chapter 5: Project Description of the Offshore EIA Report. In all cases, the number of WTGs is consistently assumed to be 125. Please note, OSP foundations are not considered as only five will be installed.

The blockage density calculations presented two alternative statistics. The mean blockage density assumes the WTGs are equally distributed spatially within the OAA and the maximum blockage density is based on the minimum WTG spacing for the various foundation types and sizes considered within the Project design (section 4.3 and chapter 5:

---

<sup>7</sup> It should be noted that estimation of the deposition extent is independent of the plume extent, modelled and introduced in Section 4.4.1.1, sedimentation from the modelled plume would significantly smaller compared to that from the main mass.



Project description of the Offshore EIA Report). These blockage density statistics offer a range within which the actual blockage density achieved by the presence of the WTGs will occur.

Also calculated was the ratio between the foundation size and spacing as an indication of the length scale of the foundation structure. The aim of this property was to determine the potential extent for recovery of localised flow disturbance around the structure in association with the modelled outputs.

#### 4.4.2.2.2 Sediment transport potential

The sediment transport potential was analysed to assess for the potential for blockage effects on sediment transport as a result of the offshore Project. To inform the sediment transport characteristics and potential changes to these processes following completion of the offshore Project, the sediment transport potential was determined at locations across the OAA and offshore ECC. As introduced in the baseline characterisation for sediment transport (section 3.9), 28 locations were analysed for the transport potential based on extracted timeseries of modelled flow conditions from the West of Orkney model (locations shown in Figure 2-4). Critical shear stress thresholds for mobility of representative sediments in the offshore Project area were established using equations from Soulsby (1997). Of the 28 locations, the transport potential results associated with 10 locations were presented in section 3.9, as a subset of conditions across the offshore Project area.

As described in section 4.4.1, a number of model scenarios focussing on the operational stage of the offshore Project have been run. These scenarios captured any changes in the local metocean conditions, the effect of which was reciprocated in the sediment mobility. Following, the implementation of the WTG layouts (section 4.3) within the model domain, the timeseries of flows and waves were obtained for all 28 analyses locations for each layout, to inform the potential changes to flows, waves and sediment transport. Based on the same seabed properties as applied within the baseline, the sediment transport was calculated for the operation stage timeseries of flows and waves. The changes to seabed transport in the wake of the construction of the OWF are discussed in with results discussed in section 5.

#### 4.4.2.2.3 Blockage due to cable protection

The influence of blockages in the water column is also relevant to the sediment transport regime through the influence of the blockage on flows. This relates specifically to changes in the vertical plane, as the presence of rock placement (or other protection) associated with cables within the offshore Project will locally reduce the water depth at a given location. As described in section 4.3, any rock berms installed along the offshore ECC will have a maximum height of 3 m and base width of 20 m (Table 4-5). In deeper water, as present within the OAA, and along parts of the offshore ECC, the presence of the protection would be indiscernible. Consequently, the area most likely to be affected by blockage due to rock placement is close to the landfall of the export cable, where water depths are shallower.

Empirical formulae on determining the depth-averaged flow speed above a submerged near-bed structure from the Construction Industry Research and Information Association (CIRIA) rock manual (CIRIA, 2007) were applied to investigate if the presence of cable protection could influence flows at shallower depths that occur within the offshore ECC. The data used in these calculations included:

- Water depths at a mid-tide state (in line with when peak current speeds occur), upstream, downstream and above the proposed remedial protection at the shallowest depth within the offshore ECC (10 m below LAT – this is the



shallowest point at which the HDD exit point could be). For context, varying water depths along the offshore ECC and within the OAA (ranging from 41 mLAT up to 120 mLAT), were also analysed;

- Peak spring and neap near-bed flow speeds as presented in section 3.7.2;
- Water levels across the offshore ECC as presented in section 3.6.2; and
- A discharge coefficient of one, which is relevant for a vertical closure, subcritical flow (CIRIA, 2007), which is characteristic of the site conditions with a cable protection in place.

### **4.4.3 Assessment for Potential Changes to Water Column Stratification**

Outputs of the operational stage numerical modelling of flows and waves and any changes to these are used to evaluate and assess for the potential changes to water column stratification, in association with the occurrence and prevalence of the stratification as represented through site-specific environmental surveys (section 2.1.3.2) as introduced and described in section 3.10.2.

### **4.4.4 Assessment of Scour**

The Project design as introduced in sections 4.3, provides the underlying scour assumption and parameters against which the protection requirements have been determined and is the basis on which the assessment of scour is completed.



## 5 ASSESSMENT OF CONSTRUCTION ACTIVITIES

Section 4.1 introduced the pathways for impacts on marine physical and coastal processes and the particular pathways for impacts as a result of construction activities (including pre-construction) are as follows:

- Seabed disturbance; and
- Loss of or alteration of seabed type.

An assessment of the potential extent, magnitude and duration of impacts based on the above pathways as a result of construction activities are presented in the following sections. Further modelling results are included in the completed modelling report Appendix B, with direct reference made as relevant.

### 5.1 Seabed Disturbance Sediment Plume and Concentrations

Construction activities resulting in seabed disturbance include:

- Seabed preparation;
- WTG and OSP and associated protection installation;
- Cable trenching and protection installation; and
- HDD installation.

The above construction activities, with the exception of HDD installation, were modelled to investigate for seabed disturbance and as described in section 4.4.1.2.

This section will consider the modelling results with respect to generation of sediment plumes. In particular, focus will be on the spatial extent (direction and distance), magnitude and duration of the presence of sediment plumes generated during Project activities. The results are grouped according to the construction activities listed above, with further modelled results presented in Appendix B and referenced as relevant.

#### 5.1.1 Overview

The modelling, as per the approach described in section 4.4.1.2, was completed to inform the potential for plume generation. Having accounted for scaling down of the fine sediment component across the offshore Project area, this assessment assumes approximately 0.25% of sediments disturbed during construction activities will form a plume, the remaining 99.75% falling to the seabed in active phase transport, the assessment of which is completed in section 5.2. This 0.25% is representative of the offshore Project area as a whole and takes into consideration the difference in sediment composition within the OAA and offshore ECC – with sediments likely to enter into a plume comprising approximately 0.12% and 0.52% respectively. This difference is due to the higher percentage fines content within the



offshore ECC. The variations in water depth and seabed properties across the offshore Project area (section 3.4.2) were also taken into account throughout the modelling process.

It should therefore be noted that the plume extent and magnitude discussed within this section, with respect to the varying construction activities, relates only to the material that forms the finer sediment fraction associated with the passive phase of deposition. As above, the sediment volumes associated with this deposition phase equate to only a small percentage of the sediment bulk (i.e. approximately 0.25%) due to the coarse nature of the seabed sediment across the offshore Project area. The majority of the sediment bulk (i.e. 99.75%) would fall directly to the seabed within a relatively short distance from the disturbance site as part of the active deposition phase. SSC associated with this active deposition phase are not modelled but are considered to be several orders of magnitude greater (i.e. over thousands of mg/l), than the background levels of <5 mg/l characteristic to the study area. However these high concentrations, would only be within tens of metres of the disturbance. The high SSC would also only be short-lived, on the order of minutes and reduce very quickly with increasing distance from the disturbance site as the sediment quickly settles to the seabed. It is only a much smaller proportion of sediment that would develop into a plume over a greater extent, which is modelled and discussed within this section for each respective construction activity.

The modelling approach focussed on construction activities and Project design parameters within the OAA and offshore ECC that were considered to provide the worst case for marine physical and coastal process impact pathways, as described in section 4.4.1.2. A number of methods were associated with these activities which had the potential to generate a sediment plume, including dredging and disposal, CFE, and drilling.

Section 5.1 addresses the plume extent, duration and concentration, while section 5.2 focusses on the larger sediment component which does not enter into suspension, but instead falls directly to the seabed during the active phase of sediment deposition, where the primary impact pathway is the loss or alteration of seabed type.

## 5.1.2 Seabed Preparation

Seabed preparation across the offshore Project, as introduced in section 4.3, is to include boulder clearance and bedform clearance by a range of methods. Dredge and disposal using a TSHD and CFE are considered to provide the worst case for sediment disturbance impact pathways and are therefore assessed.

### 5.1.2.1 Boulder Clearance

The offshore geophysical report detailed a number of boulder fields within the OAA and offshore ECC (section 3.3.2.2.2). In this context, boulders are defined as being >0.5 m. A large part of the OAA is considered to be high boulder density (>20 boulders per 50 x 50 m area) with some medium boulder density areas associated with Stormy Bank (10-20 boulders per 50 x 50 m area). High and medium density boulder fields were also identified throughout the offshore ECC and also across a significant portion of the nearshore area of the offshore ECC (Ocean Infinity, 2023a, 2023b, 2023c). Individual boulders are also present across the OAA and offshore ECC in lower densities.

While the intention is to avoid boulders wherever possible through micro-siting, this may not be feasible in areas where a large number of boulders are present (i.e. in the higher density boulder field areas), therefore boulder clearance in discrete areas will take place across the OAA and offshore ECC. The estimated area requiring boulder



clearance is summarised in the Project design Table 4-2. For all cables, a corridor of up to 30 m per cable circuit could be cleared (15 m each side of the proposed cable route). Boulder clearance will be achieved through use of a boulder clearance (SCAR) plough and/or grabs. Boulders will be picked up and will be moved to a suitable distance from the required location to enable a safe and efficient installation which eliminates any risk to the cables or installation equipment, although boulders will not be removed from the offshore Project area.

A predicted total area of 30.4 km<sup>2</sup> will be cleared along all the cable routes across the offshore Project area and is expected to take up to a total of 42 weeks, within the 18-month seabed preparation programme. However this will not be a continuous effort and disturbance will not be constant for that entire time, as clearance will occur intermittently within the site-preparation program of approximately 21-months. In terms of the seabed disturbance associated with the boulder clearance, the removal by plough/grab constitutes low degree mechanical disturbance very short-term in duration. Overall, it is expected that the removal and relocation of boulders will result in a highly localised disturbance of sediment i.e. on a scale of metres. This disturbance will only last for the immediate duration of the boulder movement i.e. for a matter of seconds. Once the boulder clearance has been completed, a pre-lay grapnel run (PLGR) on the final cable routes will take place prior to cable lay. The PLGR will have a maximum width of 2 m. The footprint of the PLGR will be included within the footprint of the cable installation works. Overall, with the prevalence of coarse sediment across the offshore Project (section 3.3.2) and the mechanical process of picking and relocating boulders or use of a pre-grapnel, the level of disturbance is not sufficient to generate a sediment plume.

### 5.1.2.2 Bedform Clearance By Dredge And Disposal

Seabed bedform clearance is to be completed across the OAA and offshore ECC to enable the installation of offshore infrastructure. The expected clearance extents and volumes used to inform the modelling and assessment are summarised in Table 4-2, while the modelling process and parameters are detailed in section 4.4.1.2.1. Modelling results of the potential seabed disturbance and sediment plume associated with the dredge and disposal activity are presented in the following sections, with consideration of the deposition impact (extent and thickness) assessed in section 5.2.1.2.

Modelling results for the clearance activity by dredge and disposal are considered in terms of the potential disturbance pathways, this includes near-bed disturbance at and around the drag head, at the surface associated with overflow during active dredging and at the disposal site during discharge from the hopper. An indicative central DMPA within the offshore Project area has been assumed along the southeast boundary of the OAA, illustrated in Figure 5-1. Also included in Figure 5-1 is representation of the modelled TSHD clearance track and disposal locations within the DMPA, alongside the model extraction locations, where a timeseries of flows, suspended sediment concentrations were extracted to evaluate the potential disturbance effects associated with the construction activity. As introduced in 5.1.1, SSC concentrations associated with the active deposition phase (i.e. not the plume) would be several orders of magnitudes greater than background levels but would be short-lived and localised to the disturbance site. The SSC would reduce within minutes and tens of metres from the disturbance as the sediment quickly settles to the seabed during the active deposition phase. The effect associated with the active deposition phase is short-lived and therefore not assessed further here. Instead, the following assessment focusses on the potential plume that could develop and extend over a larger distance and occur for a longer period of time.

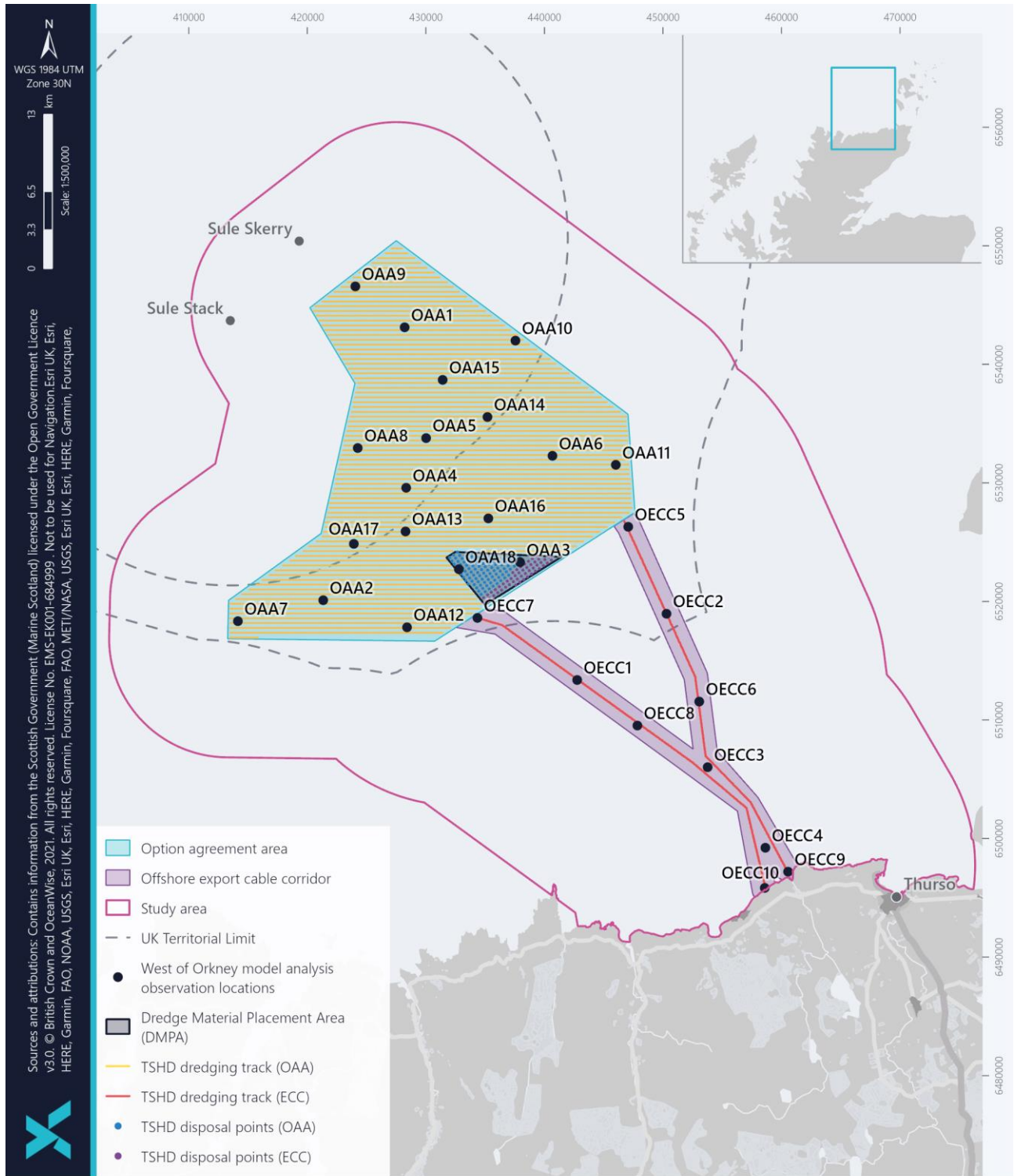


Figure 5-1 Modelled TSHD clearance track and disposal locations within the DMPA, in association with the model extraction locations, as illustrated in Figure 2-4



#### 5.1.2.2.1 OAA

Modelling results for the dredge and disposal activity within the OAA are illustrated in Figure 5-2, with further modelled outputs included in the modelling report in Appendix B.4.1.1. With respect to the potential disturbance associated with the clearance activity, Figure 5-2 illustrates the modelled maximum SSC and extent that could occur over the course of the 16-day period, associated with bedform clearance by TSHD (with disturbance pathways near-bed and from the sea surface) and disposal within the DMPA (where disposal and dispersion of dredged material will occur at the sea surface). Based on the completed modelling and clearance volumes as set out in the Project design, the whole OAA could be dredged within the applied 16-day model period, (the clearance rates applied are for modelling purposes only and is not a direct representation of the construction programme to be completed by the Project). Therefore, the TSHD process is relatively rapid compared to other activities (such as CFE, discussed in section 5.1.2.3). Due to the coarse nature of the seabed, with low fine sediment fraction, increases in SSC from the dredge and disposal activity are short-lived, with the SSC levels generally remaining below 1 mg/l for large parts of the OAA for the majority of the model period. This is demonstrated by the fact that the 99<sup>th</sup> percentile result<sup>8</sup>, which is indicative of locations that have experienced SSC levels for over 3.2 hours across the model period (Figure 5-2), only occurs over a small area within the DMPA.

In terms of the potential plume, the modelled increases in SSC associated with the dredger itself occurs within the immediate trail of the activity within the OAA, in relation to the east-west flow axis. SSC levels within the dredged area reach maxima of approximately 8 mg/l in the wake of the activity. The smallest plumes occur in the southern part of the OAA, reflecting the difference in tidal conditions during the time the dredger was operating in this area (i.e. associated with small neap tides when slow flows reduced plume dispersion). While similar tidal conditions also occurred during dredging of the northern section of the OAA, the assumed dredger track was such that plumes from subsequent tracks resulted in some additive plume effects due to the short east-west extent in the northern part of the OAA. As dredging is so widespread within the OAA, there are a number of model extraction locations which coincide with the dredger trail of activity (Figure 5-1). As the dredger moves over these points, spikes in the SSC occur, which area associated with that activity. However, these spikes in SSC are below 4 mg/l across all points. The modelled maximum SSC from the dredger overflow and drag head and disposal events are represented in the timeseries from model observation point OAA14 (Figure 5-2). SSC increases at OAA14, which coincided with the dredging track (Figure 5-1), is around 4 mg/l (based on a model background of 0 mg/l). However, the modelled timeseries indicates that after the immediate peak in SSC in the wake of a dredger, the SSC levels quickly return to below background levels of <5 mg/l, which occur at the site, as informed by site-specific surveys.

In terms of the disposal within the indicative DMPA applied within the modelling, based on dredging of sediment from the OAA (with modelled fine fraction of around 0.6%, section 3.3.2.2.1), the largest increases in SSC are modelled to occur during disposal events. The maximum SSC modelled associated with the dredge and disposal clearance at any given moment during the activity is 190 mg/l, which primarily relates to disposal events. The timeseries of modelled SSC for model observation points at OAA3 and OAA18, both located within the DMPA area (Figure 5-1)

---

<sup>8</sup> Due to the shorter duration of sandwave clearance by TSHD, the percentile plots are calculated based on the time involved with the active dredge, so excludes the transit time to and from the DMPA. Therefore, across the 16-day modelling period, active dredging and placement / disposal within the DMPA, only occurs for approximately 13.3-days of active dredging within the OAA. Therefore, the 99<sup>th</sup> percentile result is taken to represent a total time of 3.2 hours above which a certain condition occurs. It is important to note that the 3.2 hours are not necessarily representative of a single continuous period, instead the figure is a cumulative additive total time i.e. over the 13.3-days of active dredging and disposal within the OAA (within the 16-day model period). Therefore, the results indicate the locations that experienced concentrations at the given levels for over 3.6 hours (not necessarily continuous) across the model period.



are also illustrated in Figure 5-2. Modelled SSC from OAA3, demonstrates maximum concentrations of around 13 mg/l, where the model point is located approximately 200 m upstream and downstream (with respect to the flow axis) of two separate disposal events (Figure 5-1). Figure 5-2 demonstrates the initial increase in SSC associated with a disposal in the same flow direction flood / ebb, however by the next tidal, concentrations return back to below background levels of <5 mg/l. For model observation locations not directly inline with the flow axis, the increases in SSC are even lower (Figure 5-1). By way of example, location OAA18 within the DMPA, which is approximately 130 m north of a disposal event, records SSC increases of less than 4 mg/l within a short distance from the point of discharge (Figure 5-2).

Figure 5-2 shows that the resulting plume associated with this construction activity is strongly aligned with the flow axis. The extent of the plume associated with disposal does extend beyond the OAA by approximately 3 km, in line with the flow axis, but it still remains well within the study area boundary. Comparatively, plumes attributed to the dredging itself are much smaller and highly localised to the immediate area; there is no evidence of the dredging activity resulting in distribution of sediments beyond the applied study area, with the majority staying within the plume extent.

#### 5.1.2.2.2 Offshore ECC

Modelling results for the dredge and disposal activity within the offshore ECC are illustrated in Figure 5-3, with further modelled outputs included in the modelling report in Appendix B.4.1, where in this model scenario dredging was completed within the offshore ECC, with disposal still occurring within the DMPA. Plume extents for the dredging within the offshore ECC differ from those observed further offshore. This is largely due to the differing environmental conditions in the offshore ECC. As described in section 3.3.2.2.1, there is a larger proportion of fine sediment fraction within the offshore ECC (modelled at 2.6% fine material, compared with 0.6% fines within the OAA). This results in the potential for a greater proportion of sediments to enter into suspension and contribute to the presence of a plume. In addition, as stated in section 3.7.2, flow speeds are higher within the offshore ECC, which is key to determining the extent of the plume. The DMPA is common to dredging activity occurring in both the OAA and offshore ECC. However, the model separated deposition activity according to sediment dredging in the OAA versus the offshore ECC (Figure 5-1). Thus, the area of the plume associated within the DMPA in Figure 5-3 is attributed to sediments from offshore ECC only.

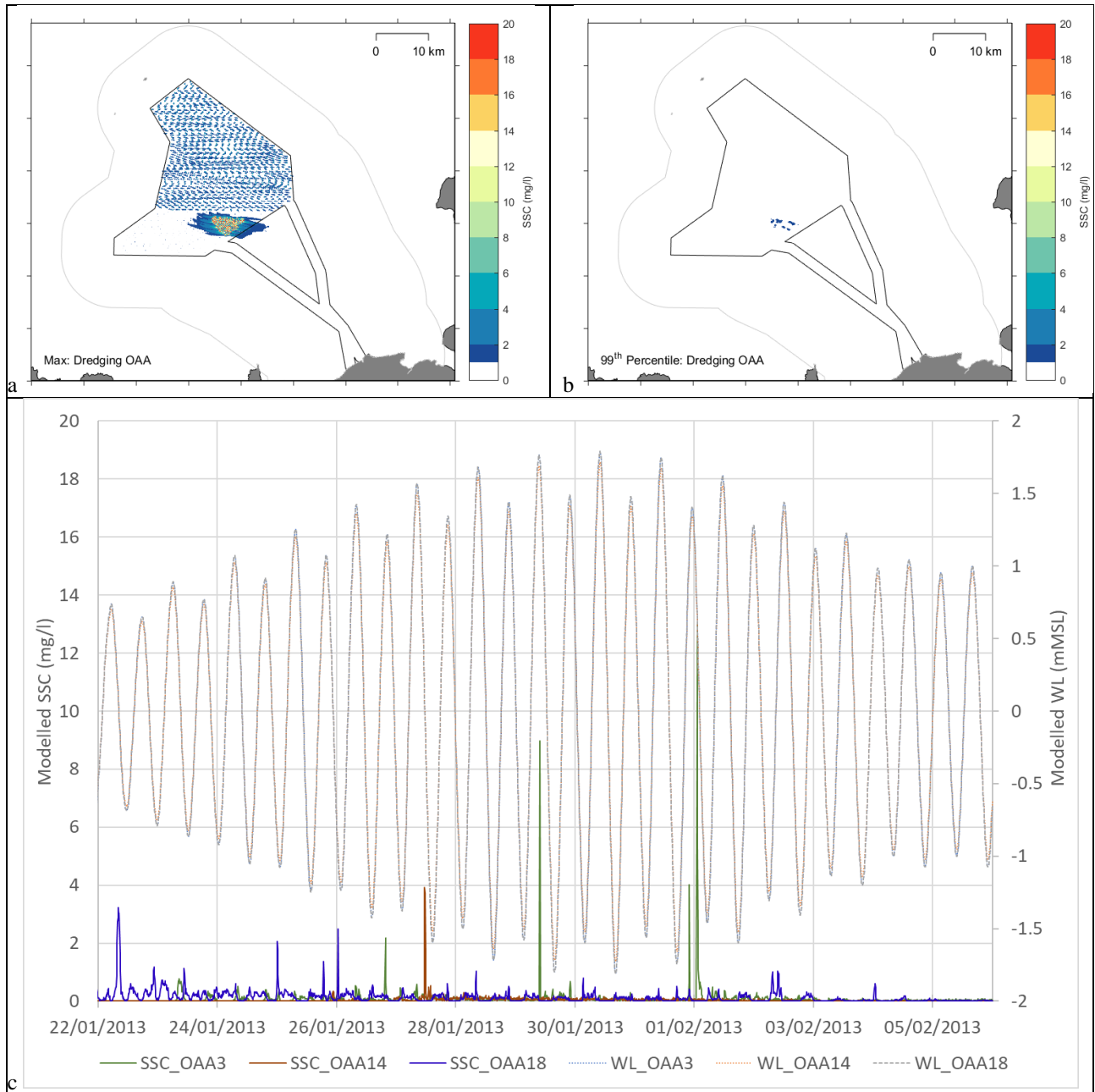


Figure 5-2 Model results for dredge and disposal for the OAA, (a) maximum plume SSC and extent modelled across the 16-day model period; (b) 99<sup>th</sup> percentile SSC and extent and (c) SSC timeseries from model observation locations OAA3, OAA14 and OAA18, as illustrated in Figure 2-4

Figure 5-3 demonstrates that maximum SSC occurs in relation to the disposal events within the DMPA and dredging towards the landfall and coast. The modelled maximum SSC across the model domain at any given time was up to 800 mg/l. However, the 99<sup>th</sup> percentile results for this activity indicate only locations within the DMPA with

<sup>9</sup> As for dredging within the OAA, the shorter duration of sandwave clearance by TSHD means the percentile plots are calculated based on the time involved with the active dredge, so excludes the transit time to and from the DMPA. For the ECC, active dredging and placement / disposal within the DMPA, only occurs for approximately 6.5-days within the 16-day modelling period. Therefore, the 99<sup>th</sup> percentile result is taken to



concentration of less than 4 mg/l for over 1.6 hours, everywhere else SSC has returned to below background levels. With regards to the extent of the plume, Figure 5-3 also shows that the plume travels further on a flood tide (to the east) to a maximum distance of approximately 8 km. On an ebb tide the extent is approximately halved. While there is a difference in plume extent over the course of an individual tidal cycle, there is little difference in the plume extent between spring and neap tides. The maximum extent is observed closer to the coast, where flow speeds are marginally faster compared with more offshore locations along the offshore ECC. The largest SSC magnitude is also modelled to occur closer to the coast due to the shallower water depths compared to the remainder of the offshore ECC (depths of 65 to 2 m mLAT compared to depths of 80 to 115 m mLAT in the remainder of the offshore ECC) combined with the higher resolution model mesh (100 m, compared to 500 m), meaning that the initial dilution of the suspended sediment is less compared to the remainder of the offshore ECC.

Closer evaluation of the plume extent, magnitude and duration was assessed based on the modelled SSC timeseries from ECC4, ECC9 and ECC10 within the offshore ECC and OAA3 within the DMPA in Figure 5-3. ECC9 is located within 50 m of the dredger trail to the east (Figure 5-1). At this distance, the peak in SSC is evident, particularly on a flood tide (which would disperse the plume in the direction of ECC9). The peaks in SSC are sharp in relation to the tidal regime. Figure 5-3 shows that SSC is just under 8 mg/l as the dredger passes close to point ECC9 (Figure 5-1). On the ebb tide the plume is directed to the west and away from ECC9, hence SSC falls. On the next flood tide, SSC increases again as the plume changes direction with the tide. However, by this time, SSC has fallen to less than 4 mg/l. Therefore, within one tidal cycle (approximately six hours), SSC has returned to levels consistent with background concentrations. ECC4 is located slightly further offshore from ECC9. During the model run, the dredger passed the location twice (Figure 5-1), hence the multiple peaks in SSC in Figure 5-3, where ECC4 is located approximately 600-700 m between the two dredger tracks. When compared against ECC9, this shows that over the course of a few hundred metres, SSC drops from a peak of about 8 mg/l to background levels with durations again showing that returns to background should occur within a tidal cycle. Additionally, at point ECC10 which is located immediately off the coast at the landfall (Figure 5-1), and closer to shore than any dredging would occur, no spikes in SSC were observed. Suggesting that the physical processes in the area do not bring the suspended sediment towards the coast from the location of dredging. Closer to the coast and landfall, the orientation of the plume is strongly aligned with the flow axis in proximity to the coast, so disturbed material would move parallel to the coastline and changes on an east-west axis according to the tide, without necessarily moving sediment north or south.

In terms of disposal within the DMPA, the increases in SSC modelled at OAA3, are illustrated in Figure 5-3, where OAA3 is located approximately 400 m northeast and northwest of two disposal events (Figure 5-1), with increasing distance from other offshore ECC disposal events within the DMPA. The two highest peaks (at around 5 mg/l at approximately 26<sup>th</sup> January and 4 mg/l at approximately 31<sup>st</sup> January) in Figure 5-3 relate to the two closes disposal events (occurring approximately 400 m southeast and southwest), and these demonstrate only small increases in SSC, to less than 6 mg/l, with SSC reducing to below site-observed background levels (i.e. <5 mg/l) with successive ebb and flood tides.

---

*represent a total time of 1.6 hours above which a certain condition occurs. Again, it should be noted that the 1.6 hours are not necessarily representative of a single continuous period, instead the figure is a cumulative additive total time i.e. over the 6.5-days of active dredging and disposal within the ECC (within the 16-day model period). Therefore, the results indicate the locations that experienced concentrations at the given levels for over 1.6 hours (not necessarily continuous) across the model period.*

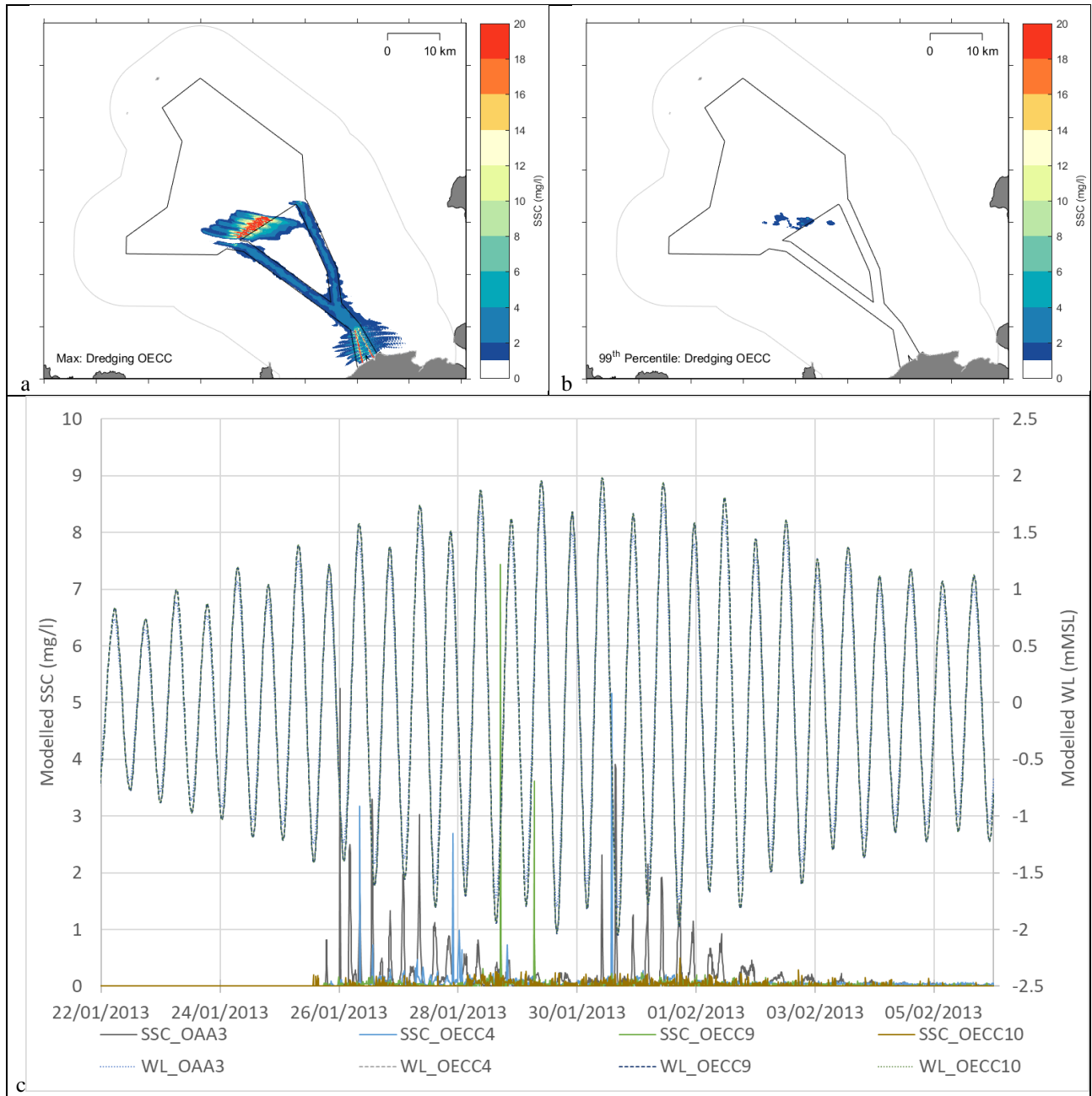


Figure 5-3 Model results for dredge and disposal, with dredging of the offshore ECC and disposal within the DMPA, (a) maximum plume SSC and extent modelled across the 16-day model period; (b) 99<sup>th</sup> percentile SSC and extent and (c) SSC timeseries from model observation locations ECC4, ECC9, ECC10 and OAA3, as illustrated in Figure 2-4



### 5.1.2.3 Bedform Clearance By Controlled Flow Excavator

CFE could be used for bedform clearance within the OAA and offshore ECC in order to prepare the seabed prior to installation of infrastructure. The expected clearance extents and volumes used to inform the modelling and assessment are as summarised in Table 4-2, while the modelling process and parameters are detailed in section 4.4.1.2.2. Despite the bedform clearance process being a continuous one as the CFE moves, the rate of transit is quite slow (section 4.3). Therefore, using the same 16-day modelled period, the CFE will only cover a small extent of the OAA and offshore ECC. Figure 5-4 illustrates the modelled CFE clearance track alongside the model extraction locations, where a timeseries of flows, suspended sediment concentrations were extracted to evaluate the potential disturbance effects associated with the construction activity. Modelling results of the potential seabed disturbance and sediment plume associated with the CFE clearance are presented in the following sections, with consideration of the deposition impact (extent and thickness) assessed in section 5.2.1.3. Modelling results for the CFE clearance activity are considered in terms of the potential disturbance pathways, which is only near-bed. As introduced in 5.1.1 and described for bedform clearance by dredge and disposal in section 5.1.2.2, the same approach is applied in terms of only assessing for the SSC magnitude and extent associated with the sediment plume as a result of the passive deposition phase.

#### 5.1.2.3.1 OAA

Model results for bedform clearance by CFE are illustrated in Figure 5-5. The southern part of the OAA was adopted as an area of potentially higher spreading due to the slightly faster flow residuals (although everywhere across the offshore Project area generally had very slow residual flow speeds at less than 0.05 m/s) modelled during the baseline (section 3.7.2), hence the model focussed on CFE occurring in this area (Figure 5-4). Modelled results for this construction activity within the OAA is illustrated in Figure 5-5 for the maximum along with the 99<sup>th</sup> percentile result. In terms of the maximum results, the maximum plume extents are approximately 5 km to the east and 4 km to the west, associated with the flood and ebb respectively (Figure 5-5), while the maximum SSC during the clearance process is around 48 mg/l. Concentrations within the rest of the plume are shown in Figure 5-5. The slow clearance rate associated with CFE transit during clearance (i.e. at 25 m/hr) means concentrations may be elevated above background levels for longer periods. This is demonstrated by the 99<sup>th</sup> percentile where larger areas are at concentrations of 4 mg/l and above for over to 3.6 hours, which is largely due to the fact that CFE is a slow moving process. By the 95<sup>th</sup> percentile (representative of approximately 18 hours), concentrations are already generally less than 2 mg/l, with the exception of a small area being between 2 and 6 mg/l.

A model extraction data point (OAA12) is located approximately 2 km due east of the modelled CFE activity (Figure 5-4), with the modelled timeseries of SSC illustrated in Figure 5-5. While instantaneous maximum SSC concentration at the CFE disturbance site are around 48 mg/l, this reduces to less than 4 mg/l by the time the plume reaches OAA12, 2 km away (Figure 5-4). The peaks in SSC correspond to the change in tides – as OAA12 is located east of the activity (Figure 5-4), the sediment plume reaches the location on a flood tide, reducing on the ebb and increasing on the proceeding flood. It is evident that 2 km from the CFE disturbance site, SSC has almost returned to background levels. The return to background levels also occurs rapidly with the cessation of activity as indicated by the decrease in SSC levels associated with the ebb flow and the 95<sup>th</sup> percentile result only showing concentrations of around 2 mg/l occurring over longer durations.

---

<sup>10</sup> For sandwave clearance by CFE across the OAA and ECC, the 99<sup>th</sup> percentile result is taken to represent a total time of 3.6 hours above which a certain condition occurs. As described for TSHD activities, the 3.6 hours are not necessarily representative of a single continuous period, instead the figure is a cumulative additive total time i.e. over the 16-day model period. Therefore, the results indicate the locations that experienced concentrations at the given levels for over 3.6 hours (not necessarily continuous) across the model period.

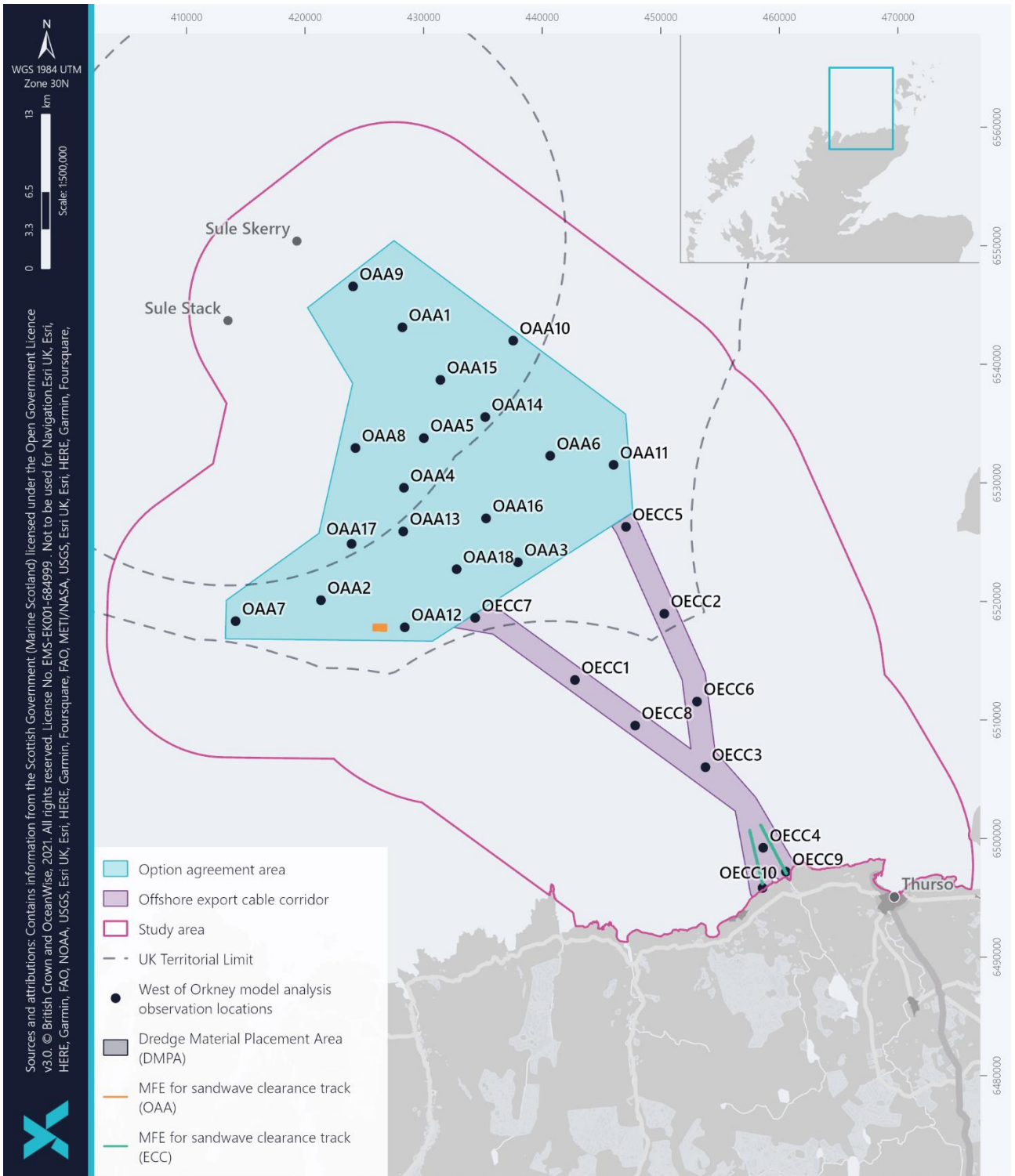


Figure 5-4 Modelled CFE clearance track, in association with the model extraction locations, as illustrated in Figure 2-4

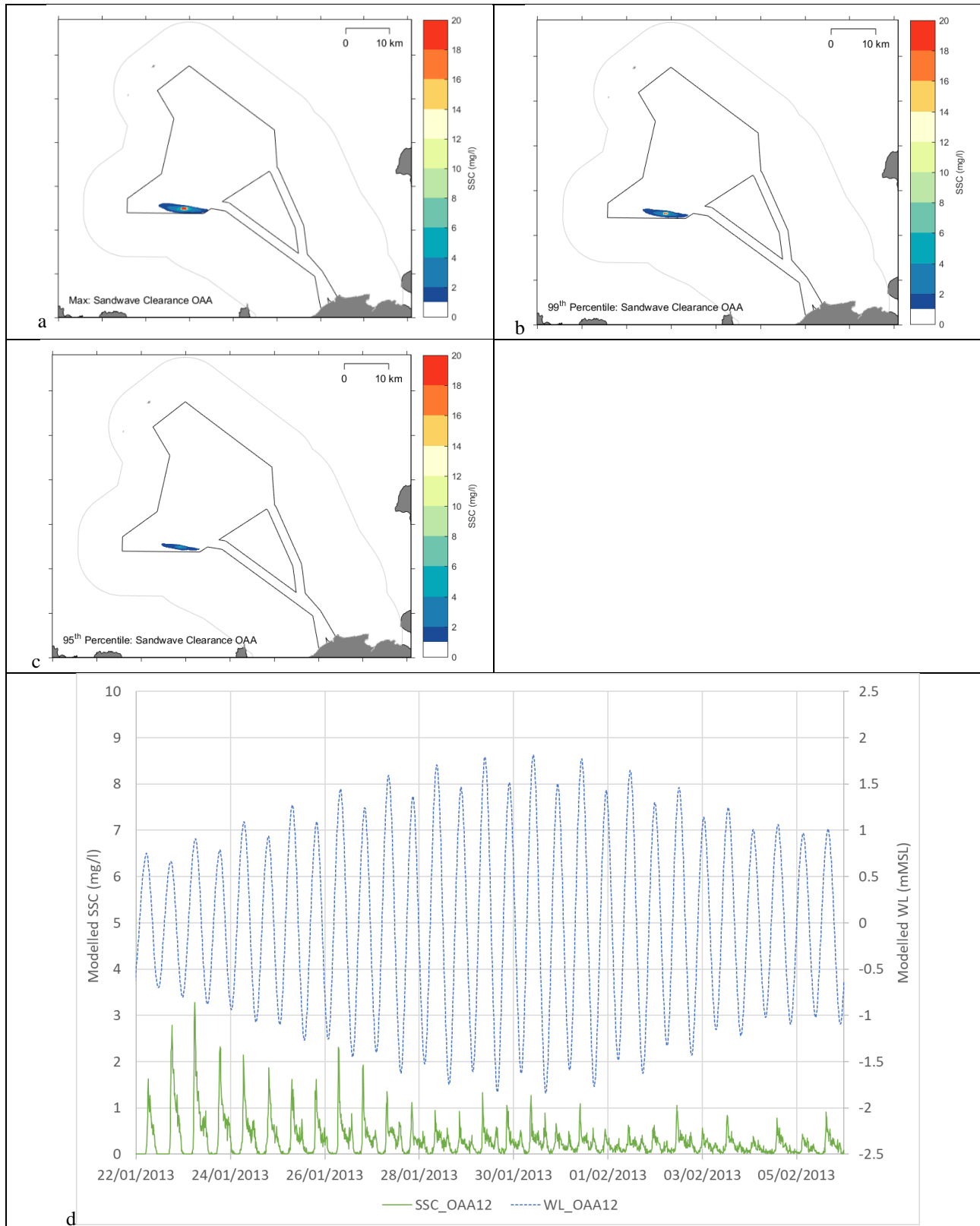


Figure 5-5 Model results for the CFE clearance within the OAA (a) maximum plume SSC and extent modelled across the 16-day model period; (b) 99<sup>th</sup> percentile SSC and extent; (c) 95<sup>th</sup> percentile SSC and extent; and (d) SSC timeseries from model observation location OAA12, as illustrated in Figure 2-4



#### 5.1.2.3.2 Offshore ECC

The modelled clearance track within the offshore ECC is illustrated in Figure 5-4. As the sediments along the offshore ECC have a marginally higher fines content section 3.3.2.2.1, this results in higher concentrations of SSC. Additionally, faster flows along the offshore ECC (section 3.7.2) means marginally larger plume extents. The model results of the maximum, 99<sup>th</sup> and 95<sup>th</sup> plume SSC and extents are presented in Figure 5-6. At the CFE disturbance site, instantaneous maximum SSC on the order of 1,200 mg/l is modelled to occur, which is much higher than is predicted for the same activity within the OAA. This is due to the increased fines content within offshore ECC sediments. Within the OAA, the applied percentage of fines within sediments was approximately 0.6%, compared with the percentage of fines within offshore ECC sediments at 2.6% (section 3.3.2.2.1). Based on the proportion of sediments which will become fully suspended, this results in a much larger SSC. The location of this maximum and the spatial distribution of the plume can be seen in Figure 5-6, with concentrations being highest just offshore of the landfall. Maximum plume extents within the offshore ECC are approximately 7 km to the east and 5 km to the west associated with the flood and ebb respectively. Again, the orientation of the plume is broadly parallel to the coast, but with the slow transit of the CFE during clearance, the plume has a broader north-south axis, with increased SSC reaching the coast. The slow clearance rate associated with CFE transit (i.e. at 25 m/hr) means concentrations may be elevated above background levels for longer periods, as sediment concentrations tend to build up. This is demonstrated by the 99<sup>th</sup> percentile where larger areas are at concentrations of 2 mg/l and above for over 3.6 hours (Figure 5-6). However, by the 95<sup>th</sup> percentile (i.e. approximately 18 hours) concentrations are generally less than 2 mg/l and at background levels characteristic to the offshore Project area (Figure 5-6).

To further evaluate for the potential duration and extent of maximum SSC concentrations, the timeseries of SSC from model extraction points ECC4, ECC9 and ECC10 were assessed as presented in Figure 5-6. ECC9 is located within a matter of metres to the west of the modelled CFE track and <1 km from the coastline at the Crosskirk landfall location (Figure 5-4). Consequently, this location sees an instantaneous spike in peak SSC of over 10 mg/l when the CFE occurs here on 29<sup>th</sup> January. However, even over the course of a tidal cycle, as the flood tide turns and begins to ebb, the SSC falls almost immediately to levels consistent with background concentrations. The modelled CFE clearance activity starts within the offshore ECC at the Greeny Geo location (Figure 5-4) and Figure 5-6 shows the consequences of this activity at ECC9 (approximately 2 km west of this clearance) in the lead up to 24<sup>th</sup> January, with a spike in SSC around the 22<sup>nd</sup> January. However, this spike is <4 mg/l and therefore is indiscernible from background SSC. The increases in SSC are only present on the flood tide which carries the plume east from Greeny Geo over ECC9.

ECC10 is located approximately 200 m from the coast at Greeny Geo (Figure 5-4). The point is also located approximately 300 m from the modelled CFE clearance track which begins to the north of the observation point (Figure 5-4). ECC10 is located almost equidistantly between the CFE track and the coastline. Consequently, peaks in SSC at ECC10 are picked up when the plume is being directed south towards the coast between the flood and ebb transition. At this distance, the SSC at ECC10 reaches peaks of approximately 5 mg/l before rapidly returning to 0 mg/l within a few tidal cycles. These peaks in SSC are never beyond the range of background concentrations. Some slight indiscernible variation in SSC is also seen at ECC10 in the days after 30<sup>th</sup> January (shown in Figure 5-6). This fluctuation is likely as a result of the plume associated with CFE activity commencing at this time approximately 2 km northeast of ECC10 within the Crosskirk offshore ECC.

ECC4 is located approximately 3 km northeast and northwest of the modelled start of clearance activity at the landfall locations of Greeny Geo and Crosskirk respectively, with clearance occurring in the offshore direction towards ECC4 (Figure 5-4). At the closest, ECC4 is approximately 800 m east of the Greeny Geo clearance track and 700 m west of



the Crosskirk clearance track (Figure 5-4). It is noted that CFE disturbance at the landfall (i.e. 3 km away) is not represented in the SSC at ECC4 (approximately occurring around 24<sup>th</sup> January); however, as the clearance progresses offshore within the 16-day modelled period, small increases are observed to occur at the model observation point (i.e. the increase in peaks in Figure 5-6).

When the ongoing clearance is at its closest to ECC4 (<1 km) (Figure 5-4), it is noted that SSC at the observation point reach a maximum of 8 mg/l on the flood flow. Changes in SSC occur in accordance with the tides dependent on the direction in which the plume is being carried. The peak instantaneous SSC that may occur at the disturbance site will largely be fairly localised to the head of the CFE, so that by a kilometre away SSC levels reduce substantially.

Overall, the SSC reduces to less than 10 mg/l within 1 km of the discharge. SSC returns to background levels of less than 5 mg/l at distances of 2 to 3 km, as evidenced by the changes in Figure 5-6 at ECC4, ECC9 and ECC10. The duration of such high SSC levels are again expected to be short lived as demonstrated by the timeseries of ECC4 and the 99<sup>th</sup> and 95<sup>th</sup> percentile results (Figure 5-6), where SSC reduces by several mg/l between successive flood tides. Therefore, on completion of the bedform clearance works, plume effects are not expected to last for more than a few tidal cycles and within the illustrated maximum extents across the whole offshore Project and study area.

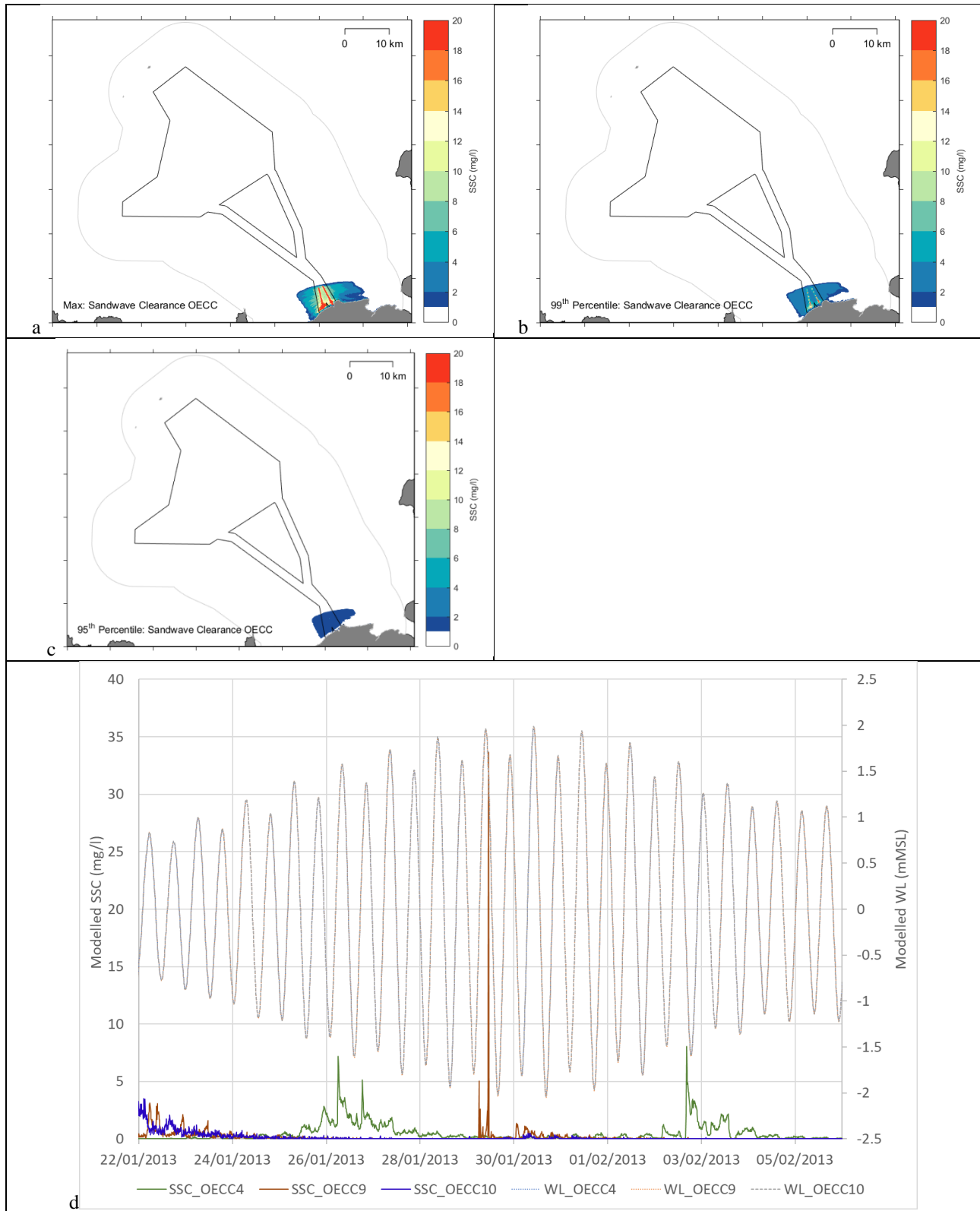


Figure 5-6 Model results for the CFE clearance within the offshore ECC, (a) maximum plume SSC and extent modelled across the 16-day model period; (b) 99<sup>th</sup> percentile SSC and extent; (c) 95<sup>th</sup> percentile SSC and extent; and (d) SSC timeseries from model observation locations ECC4, ECC9 and ECC10 as illustrated in Figure 2-4



### 5.1.3 WTG and OSP Foundation Installation

Drilling of the seabed for the installation of WTG monopiles has the potential to result in the complete breakup of the underlying bedrock and could result in the discharge of disaggregated sediment at the surface. Considering the friable nature of the bedrock underlying the offshore Project area, this is expected to occur. The relevance of the composition of the bedrock is described fully in sections 3.2.2 and 3.3.2. The project parameters that underpin the assessment are included in section 4.3, while the assumptions applied to the modelling are described in section 4.4.1.2.4 and section 4.4.1.2.5. The worst case disturbance impact was assessed to occur in relation to drilling of the largest monopile foundation (section 4.3). The drilling could either be undertaken at one WTG foundation at a time or two foundations at a time, so the completed modelling has assessed both options. Figure 5-7 illustrates the modelled drilling locations for single and concurrent drilled foundations along the eastern margin of the OAA. Also included in Figure 5-7 are the model extraction locations, where a timeseries of flows, suspended sediment concentrations were extracted to evaluate the potential disturbance effects associated with the construction activity. In section 5.1.3.1, the modelled output regarding the drilling of a single WTG at a time is considered, while section 5.1.3.2 covers the results for drilling two WTGs concurrently. As described in section 5.1.3.1, the applied modelling approach is continuous over the 16-day period, so with drilling one monopile taking approximately 135-hours, and an assumed 9-hour stand down as the drilling vessel relocates, results in approximately 2.5 WTGs being drilled within the model period, as reflected in the modelled results. As introduced in 5.1.1 and described for bedform clearance (sections 5.1.2.2 and 0), the same approach is applied in terms of only assessing for the SSC magnitude and extent associated with the sediment plume as a result of the passive deposition phase.

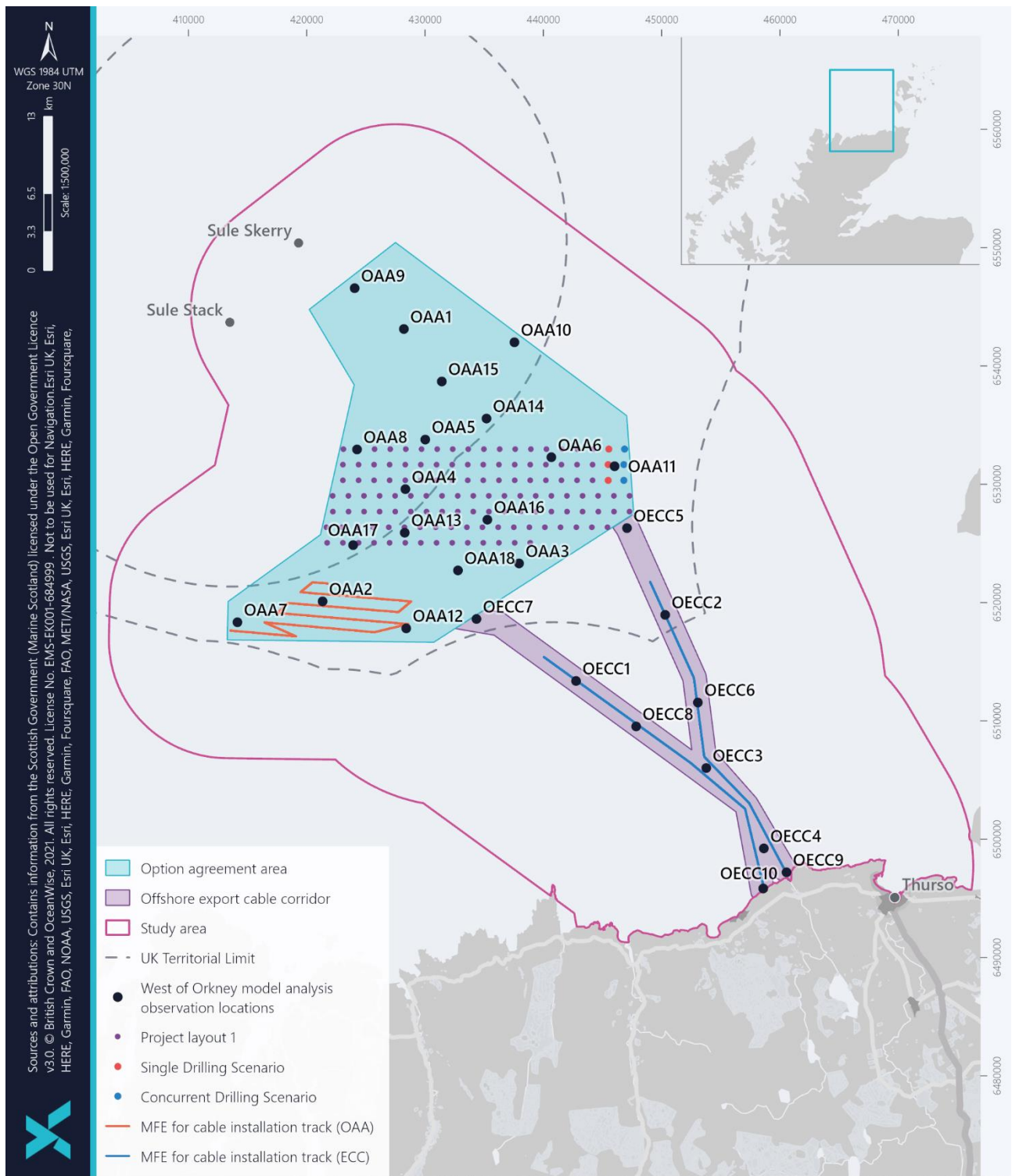


Figure 5-7 Modelled foundation drilling (single and concurrent) and indicative cable installation tracks (inter-array/interconnectors and export), in association with the model extraction locations, as illustrated in Figure 2-4



### 5.1.3.1 Drilling of one WTG

The modelled maximum spatial extent and magnitude of the sediment plume associated with drilling of a single WTG (and up to 2.5 WTGs drilled sequentially across the 16-day modelling period) is shown in Figure 5-8. The maximum plume extent accounts for both flood and ebb tides over the 16-day time period. The WTG locations were modelled along the eastern edge of the OAA (Figure 5-7), with results demonstrating a plume extending beyond the OAA but remaining well within the study area. The spatial extent of the plume reaches a maximum extent of approximately 5 km east and west, on the flood and ebb tide respectively. The SSC within much of the plume is  $\leq 6$  mg/l. This is relatively consistent with background conditions for the OAA (see section 3.9.2.2). The maximum SSC at the drilling location is 48 mg/l, with the SSC occurring in the immediate vicinity of the drill site, before quickly reducing.

With regards to timescales over which this return to background conditions occurs, Figure 5-8 shows the change in SSC with time over the 16-day period. The 99<sup>th</sup> percentile represents SSC conditions over a 3.6-hour period within the 16-day drilling activity window. The greatest plume extent will occur in the areas shown in Figure 5-8, for a maximum of 3.6 hours over the 16-day drilling period. As before, this is not necessarily suggestive of a continuous time period. However, as drilling is limited to a specific location, in this instance, the 3.6 hours is likely to be relatively continuous occurring mid-way through drilling. From the percentiles presented in Figure 5-8, it is inferred that between 3.6 (i.e. represented by the 99<sup>th</sup> percentile) and 18 hours (represented by the 95<sup>th</sup> percentile) post-drilling, the plume extent is already significantly reduced. 72 hours after the fact, the area has all but returned to background levels and beyond this point (Figure 5-8), and after 180 hours (7.5 days) the plume has completely dispersed. This rapid dispersion is evidenced by Figure 5-8. Modelled plume extents and magnitudes at particular tidal states are further illustrated in Appendix B.2.1.

Model data extraction point OAA11 lies approximately 800 m west of the modelled WTG drilling activity (Figure 5-7). SSC levels are extracted from this point show how the presence of the plume varies according to the tide and what levels of SSC are likely to occur at that location. With the drilling occurring approximately 800 m east of OAA11 (Figure 5-7), maximum SSC of 7 mg/l are observed on an ebb flow. This is as a result of the plume being carried in the ebb direction (i.e. west). Based on the timeseries of SSC at OAA11, when the tide changes to the flood, the plume is carried east of the WTG and away from OAA11, therefore we see a corresponding drop in SSC levels to approximately 1 mg/l (Figure 5-8). Over the course of a tidal cycle, SSC return to very low background levels at a location approximately 800 m from the sediment source. However, due to model resolution, for the simplicity of reference in this discussion, and in order to provide a conservative figure, it has been assumed that by 1 km away from the drilling location, SSC will return to background levels. Additionally, as OAA11 is located west of the modelled drilling location (Figure 5-7), the peaks in SSC occur on the ebb tide – the 1 km distance also allows for potential increased distances travelled by the sediment plume on the flood tide to the east.

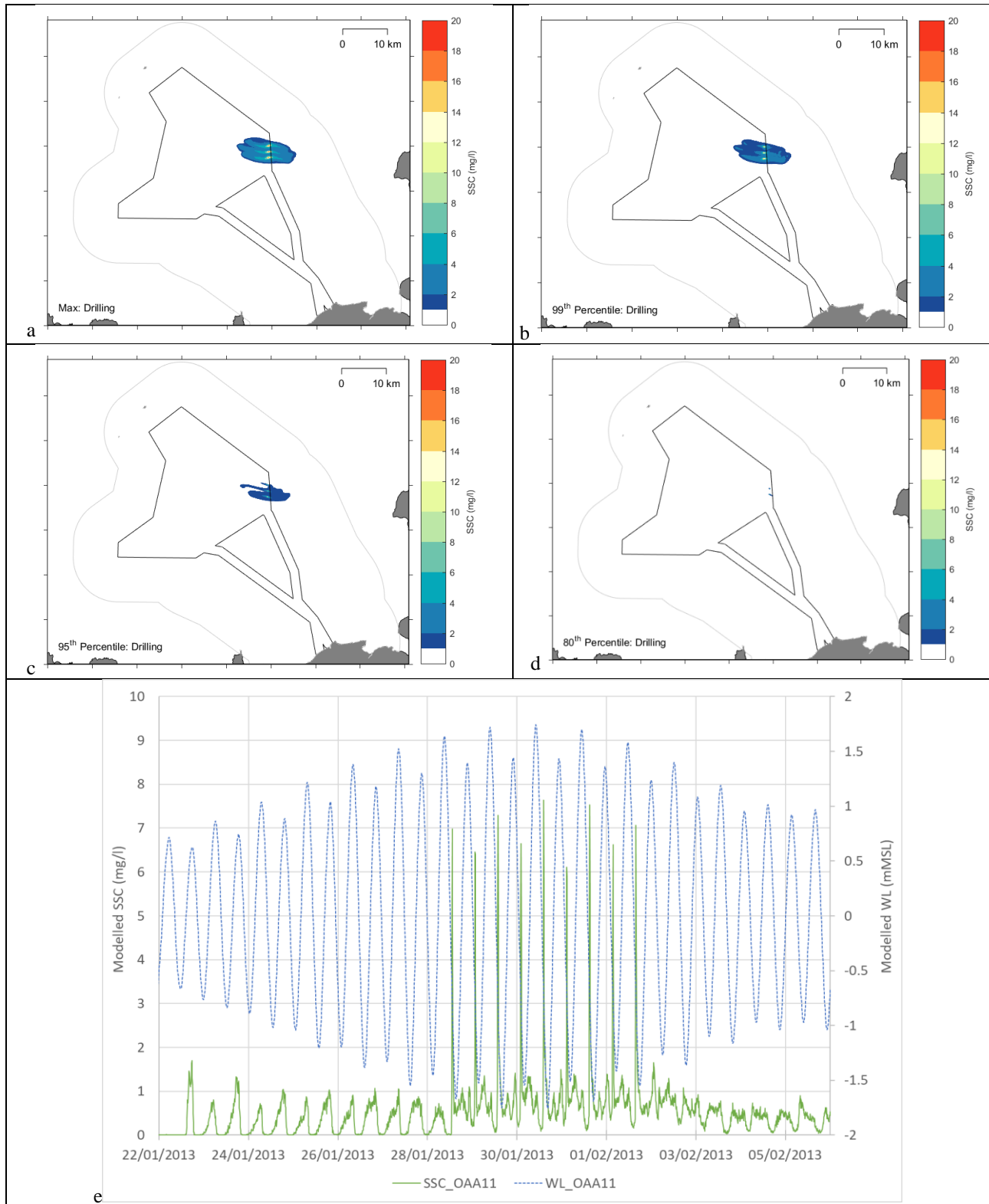


Figure 5-8 Model results for drilling of a single monopile WTG (a) maximum plume SSC and extent modelled across the 16-day model period; (b) 99<sup>th</sup> percentile SSC and extent; (c) 95<sup>th</sup> percentile SSC and extent; (d) 80<sup>th</sup> percentile SSC and extent; and (e) SSC timeseries from model observation location OAA11, as illustrated in Figure 2-4



### 5.1.3.2 Drilling of two WTGs concurrently

Over a 16-day model period, a total of four WTGs could be fully installed with another two part-way completed in this modelling scenario. The modelled drill location is illustrated in Figure 5-7, with the model results presented in Figure 5-9. When drilling two WTGs at a time, SSC is higher; the instantaneous maximum SSC is 76 mg/l, which is less than double what can be expected for one WTG alone. This maximum SSC is due to the plumes from each WTG coalescing and resulting in a combined increase.

Initially, the extent of the plume is relatively similar in Figure 5-9 when compared against Figure 5-8 above. However, the SSC within the plume is higher. Drilling two WTGs at once results in much of the plume having an SSC of 6 mg/l (Figure 5-9), which is marginally higher than under the single WTG scenario. Over time, the rate of decay of the plume is slower when two WTGs are drilled concurrently. The 95<sup>th</sup> percentile result in Figure 5-9 shows that after approximately 18 hours the plume, while smaller in extent, is still present. However, it is important to note that the SSC within the plume is <10 mg/l. Comparatively, under the single drilling scenario, after the same amount of time the plume was beginning to disperse before eventually having almost completely dissipated after 72 hours (the 80<sup>th</sup> percentile result). In Figure 5-9, after 72 hours the plume is still present, albeit at SSC levels consistent with the background conditions.

The timing of the peaks in SSC at OAA11 are consistent under both drilling scenarios, however when two WTGs are drilled the fall in SSC after the peaks is less immediate. SSC reaches approximately the same levels (9 mg/l) between the two drilling scenarios but return to baseline takes slightly longer. During the drilling activity, between 28<sup>th</sup> January to 2<sup>nd</sup> February, the peaks in SSC occur twice as often, on a flood and ebb tide. In comparison, when only one WTG is drilled the peaks at OAA11 only occur on the ebb tide (Figure 5-8). Additionally, during the slack period of the tidal cycle, the SSC at OAA11 remains marginally elevated at approximately 3 mg/l (Figure 5-9). Not until the drilling activity is complete does the SSC fall back to 0 mg/l. However, it is important to note that even this elevated SSC is still within the range expected for baseline conditions.

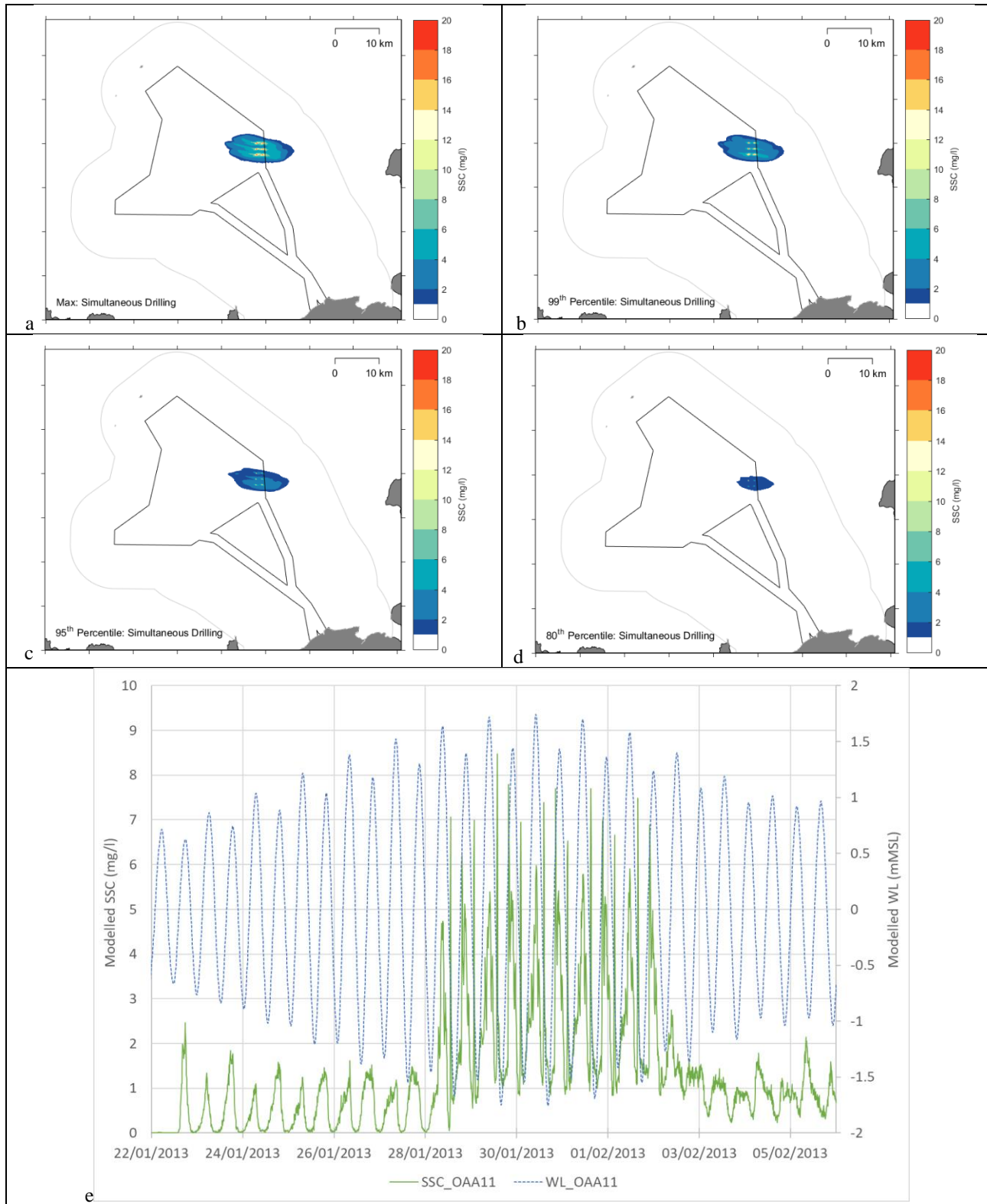


Figure 5-9 Model results for drilling two monopile WTGs concurrently (a) maximum plume SSC and extent modelled across the 16-day model period; (b) 99<sup>th</sup> percentile SSC and extent; (c) 95<sup>th</sup> percentile SSC and extent; (d) 80<sup>th</sup> percentile SSC and extent; and (e) SSC timeseries from model observation locations OAA11, as illustrated in Figure 2-4



## 5.1.4 Cable Installation

Cable installation could occur by a range of methods as described in section 4.3, with CFE considered to provide the worst case disturbance, and as such has been modelled and assessed. The project parameters that underpin the assessment are included in section 4.3, while the assumptions applied to the modelling are described in section 4.4.1.2.3, differentiating the seabed sediment that occurs across the OAA and offshore ECC, as detailed in section 3.3.2.2.1. Figure 5-7 illustrates the modelled cable installation locations within the OAA and along the offshore ECC, alongside the model extraction locations, where a timeseries of flows, suspended sediment concentrations were extracted to evaluate the potential disturbance effects associated with the construction activity. Model results for the installation within the OAA and offshore ECC are described in sections 5.1.4.1 and 0 respectively. As introduced in 5.1.1 and described for bedform clearance (sections 5.1.2.2 and 0), the same approach is applied in terms of only assessing for the SSC magnitude and extent associated with the sediment plume as a result of the passive deposition phase.

### 5.1.4.1 Cable Installation OAA (Inter-array and Interconnector)

Model results for cable installation by CFE within the OAA are illustrated in Figure 5-10. The plume generated by the CFE for cable installation is approximately 2 km in extent on a flood or ebb tide. The plume is at its longest at the turn of the tide when flow speeds are comparatively lower. The plume is also marginally longer on a spring tide. Most of the time there is no real visible plume extent, the area of increase SSC is highly localised to the immediate location of the CFE taking place. The speed of CFE for cable installation is faster than for bedform clearance (discussed in section 5.1.2.3.1), at around 125 m/hr. The faster speed of CFE during cable installation means that the plume diluted and dispersed quicker associated with the ebb and flood flow speeds, instead of building up as during bedform clearance.

The maximum SSC level associated with CFE for cable lay is 20 mg/l. The SSC associated with the CFE track is very distinct within the OAA. The track moves back and forth on itself at a spacing of approximately 1 km. However, as the track is easily visible in Figure 5-10, the plume extent does occlude this and therefore its extent does not reach beyond 1 km in a north-south axis. As the tides flow east-west, the plume as stated above, can be up to 2 km in these directions. Based on the results of the 99<sup>th</sup> percentile, the locations and extent of maximum SSC along the installation track are isolated to small pockets with SSC of above 2 mg/l, but still less than 4 mg/l (Figure 5-10). Therefore, the duration of effects from this construction activity are short-lived. This was explored further with the timeseries of SSC from OAA12, located approximately 300 m southeast of the CFE track. Changes in SSC associated with the activity at this distance are barely perceptible at this distance, even during flood flow (Figure 5-10).

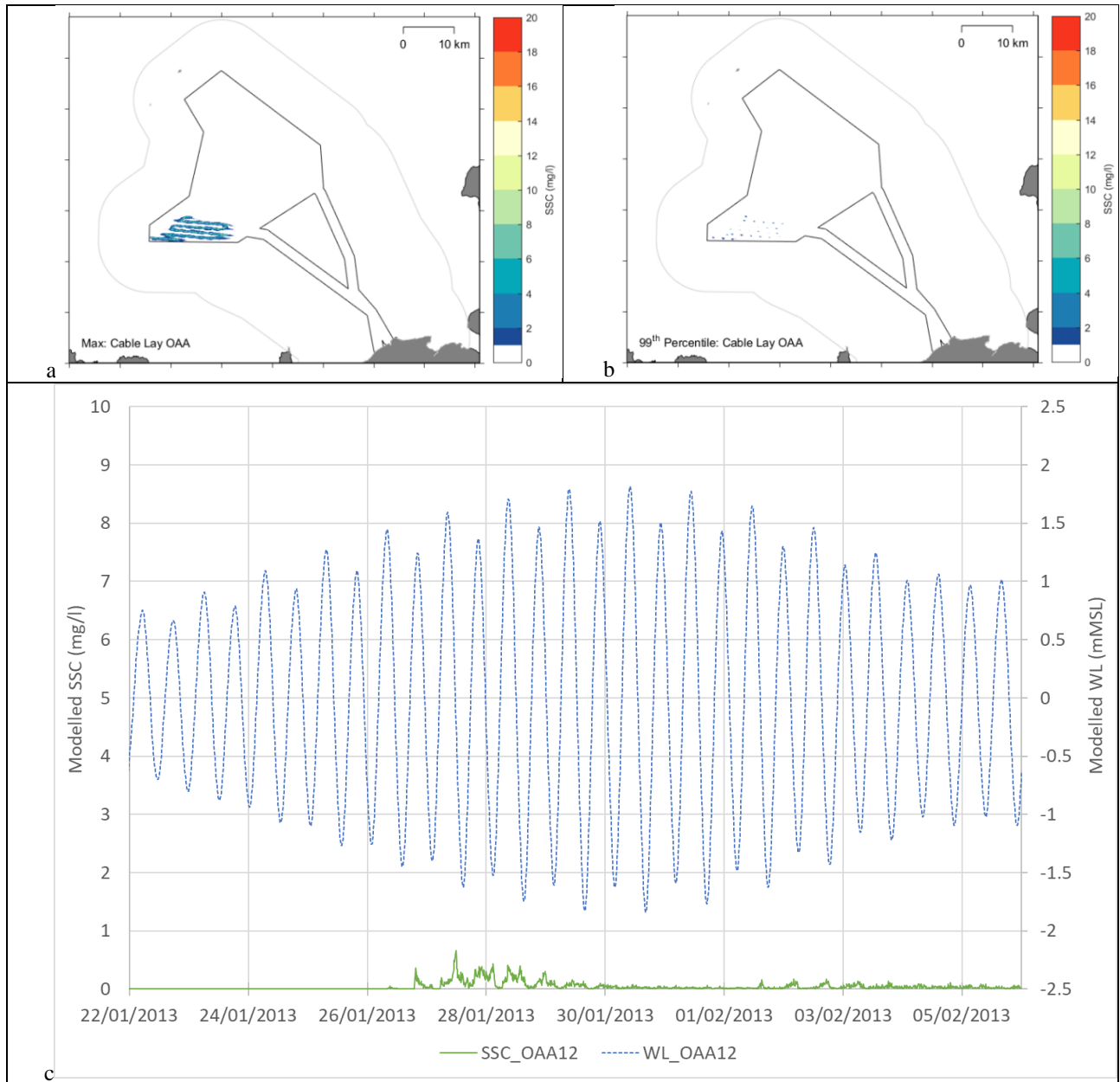


Figure 5-10 Model results for cable installation by CFE within the OAA (a) maximum plume SSC and extent modelled across the 16-day model period; (b) 99<sup>th</sup> percentile SSC and extent; (c) 95<sup>th</sup> percentile SSC and extent; and (d) SSC timeseries from model observation location OAA12, as illustrated in Figure 2-4



### 5.1.4.2 Cable Installation offshore ECC (Export)

Model results for cable installation by CFE within the offshore ECC are illustrated in Figure 5-11. The SSC generated by the use of CFE for cable installation within the offshore ECC reaches an instantaneous maximum of 550 mg/l. This is considerably higher than for CFE activity within the OAA (section 5.1.4.1). This difference is replicated in the results for bedform clearance by CFE (in section 5.1.2.3.2). As before, the reason for this is attributed mostly to the finer sediment component in the offshore ECC and the shallower depths that occur towards the coast. The on average finer sediment is more susceptible to being lifted into suspension. Consequently, the model predicts greater immediate maximum values of SSC within the offshore ECC compared to the OAA. The plume generated by cable installation CFE within the offshore ECC generates a plume approximately 4 km in extent on an ebb and flood tide (Figure 5-11). While there is little difference in plume extent under flow and ebb tide conditions, closer to the coast, the plume extends on a flood/ebb tide and remains a single plume formation from the source. Comparatively, further offshore within the offshore ECC, the plume disperses more quickly upon formation, so the plume seldom remains as one long column. The results of the 99<sup>th</sup> percentile demonstrate that the locations and extent of maximum SSC along the installation track are isolated to small pockets with SSC of above 2 mg/l, but still less than 4 mg/l (Figure 5-11).

There is no difference between the SSC at the coast versus further offshore. Model extraction point ECC1 and ECC9 are located within approximately 60 m and 30 m of the CFE track respectively. As shown in Figure 5-11, the level of SSC at this close distance is already back down to background levels. This suggests that, while the plume may reach up to 4 km from the location of CFE, the levels are so low that they are indiscernible against background SSC. Sediment disperses rapidly so the drop from the maximum instantaneous release of 550 mg/l to background levels occurs within tens of metres. The plume also appears to disperse completely within a single tidal cycle as the peaks in SSC are only visible once in Figure 5-11, corresponding to a single tidal cycle.

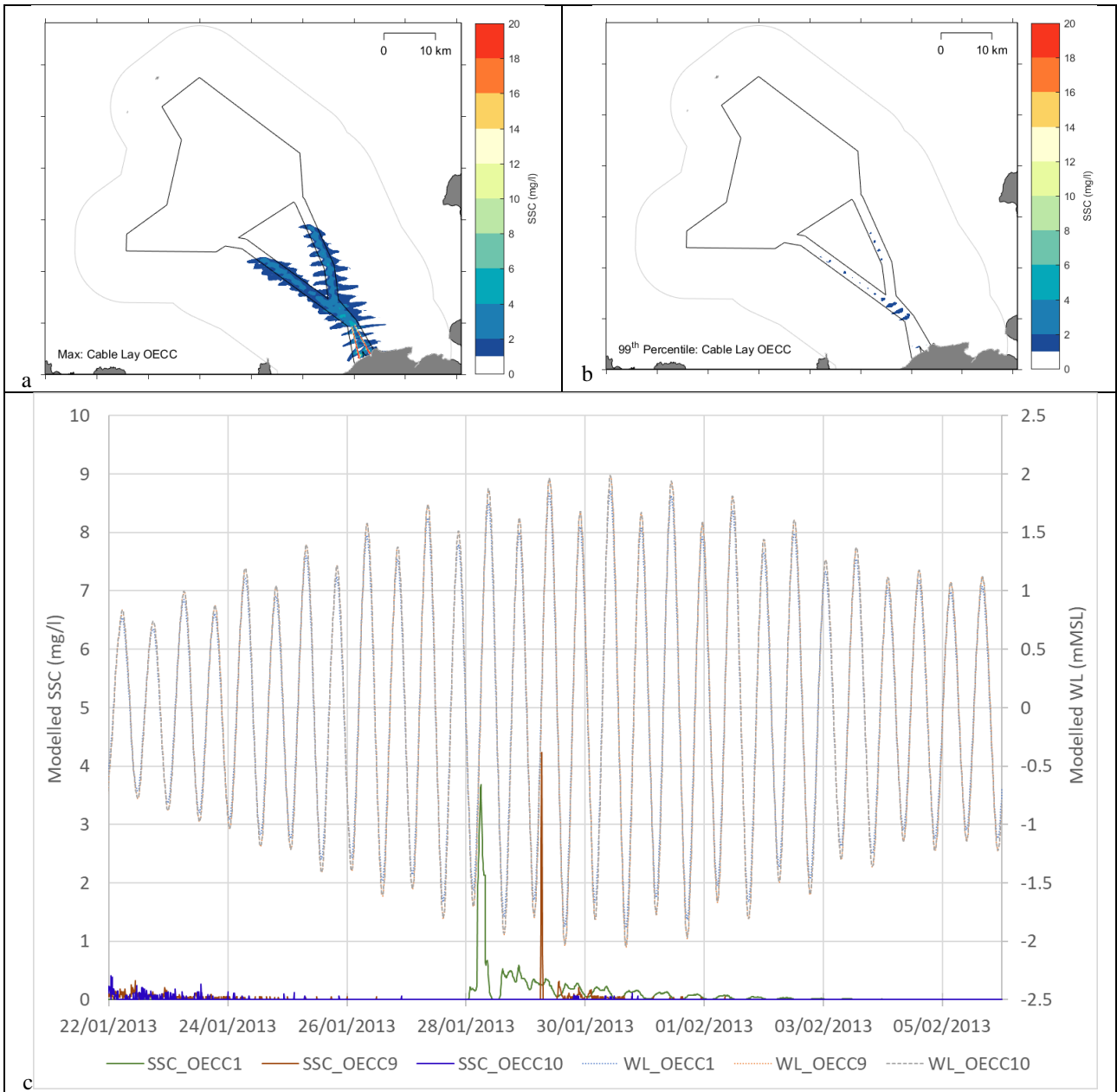


Figure 5-11 Model results for cable installation by CFE within the offshore ECC (a) maximum plume SSC and extent modelled across the 16-day model period; (b) 99<sup>th</sup> percentile SSC and extent; (c) 95<sup>th</sup> percentile SSC and extent; and (d) SSC timeseries from model observation location ECC1, ECC9 and ECC10, as illustrated in Figure 2-4



## 5.1.5 Project in-combination Construction Activities

There is a possibility that some of the construction activities considered will overlap in duration. The activities which have the greatest potential to result in an in-combination effect are those which occur within the OAA: WTG foundation drilling; bedform clearance by CFE; and cable burial by CFE. The basis for the model assumed that these activities would be, at a minimum, occurring at a spacing consistent with the proposed WTG spacing (1,320 m; minimum spacing associated with the largest WTGs); therefore, at the closest point, the activities will be 1,320 m apart. These three activities were modelled together based on the underlying assumptions of the activity in isolation and generated the following results.

With all three activities occurring concurrently, the maximum instantaneous SSC was approximately 58 mg/l. This is relatively consistent with the SSC generated by these activities alone (in sections 5.1.2.3.1, 5.1.3 and 5.1.4.1). The highest SSC generated by activities within the OAA is attributed to bedform clearance by CFE. This had a maximum instantaneous SSC of approximately 48 mg/l which will provide the largest contribution to the in-combination SSC. Per Figure 5-12, the maximum plume extent spatially covers the combined area for all three in-combination activities, with a maximum extent of up to approximately 7 km east and west (depending on the tide). This maximum represents the absolute worst case across the 16-day modelled period. During that time, the plume will vary according to the tide. The cumulative influence of the SSC is most apparent as the tide changes and the plume direction switches; this results in some overlap between the plumes generated by the different activities as the plume extent exceeds the spacing of the activities (1,320 m).

The most concentrated area of the plume is associated with concurrent CFE clearance and drilling activities. The plume extent associated with the cable installation is much more dispersive and after 3.6 hours has disappeared, leaving plume exclusively attributed to clearance and drilling. Despite the extent of the plume being greater under the in-combination scenario, the concentrations within the plume are relatively in-keeping with the concentrations expected during each activity alone. In relative terms, the decay associated with the absolute maximum SSC occurs over a similar time scale as each of the activities individually, and 72 hours after the fact, the plume is almost completely gone (Figure 5-12).

Observation points OAA6, OAA11 and OAA14 are located closest to the modelled in-combination scenario. OAA6 is located approximately 800 m from CFE activities associated with cable installation within the OAA, 1.5 km from the closest modelled CFE bedform clearance activity, and 2.5 km from the modelled WTG foundation drilling. OAA11 is 5 km, 6.5 km and 2 km from the cable installation, WTG foundation drilling and bedform clearance activity respectively. OAA14 is 5 km from the WTG drilling and cable installation activities and 2.5 km from the CFE clearance. The SSC at these three locations is shown in Figure 5-12 over the modelled time period. Ultimately, the change in SSC over the modelled time period shown in Figure 5-12 is in-keeping with the observations at points within the OAA for activities occurring in isolation. SSC is never above 3 mg/l, even at the closest distance of less than a kilometre, the SSC generally remains low during the activity time period across the modelled observation locations (Figure 5-12). Even at OAA6, which is closest to the CFE clearance activity (which, per the findings in section 5.1.2.3.1, alone generates the greatest increase in SSC), the observed levels of SSC are consistent with background SSC (<3 mg/l). Under the WTG foundation drilling modelled scenarios described in section 5.1.3, the activity was located much closer to OAA11, hence Figure 5-12 showing a comparatively reduced SSC at OAA11 (<3 mg/l). The plume extent only overlaps with OAA11 for a brief period of time during peak flood times when the plume extent is greatest.

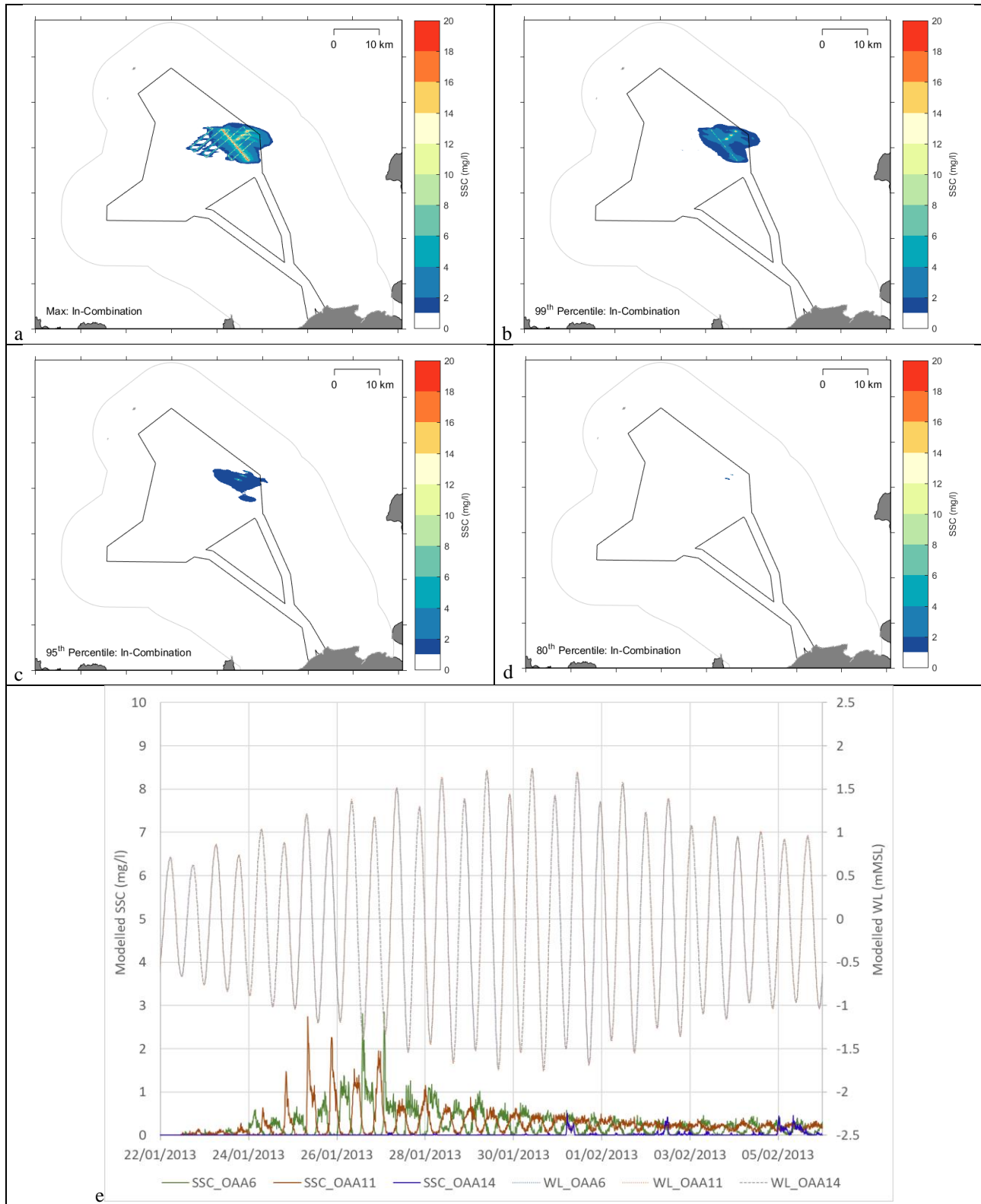


Figure 5-12 Model results for the in-combination assessment within the OAA (a) maximum plume SSC and extent modelled across the 16-day model period; (b) 99<sup>th</sup> percentile SSC and extent; (c) 95<sup>th</sup> percentile SSC and extent; (d) 80<sup>th</sup> percentile SSC and extent; and (e) SSC timeseries from model observation locations OAA6, OAA11 and OAA14, as illustrated in Figure 2-4



## 5.1.6 HDD Installation

HDD is the proposed landfall installation method as described in section 4.3. Some dredging of up to six exit pits (i.e. five plus one spare) measuring up to 10 m wide x 30 m long x up to 5 m deep per pit, may be required at the exit point of each HDD bore. The pits will be orientated offshore, with the 30 m length extending from the approximately HDD exit in the cross-shore direction. The excavated material would be disposed of or stored beside the exit pits as sediment berms to infill following natural processes. Based on the pit dimensions for the six exit pits, a total volume of up to 9,000 m<sup>3</sup> could be excavated, based on an estimated excavation volume of 1,500 m<sup>3</sup> per pit. The excavated material could be side cast creating temporary sediment berms adjacent to the pit. It is assumed that the height of the temporary side-cast sediment berm, would be the same or less than that applied to protection (i.e. a berm height of up to 3 m) and associated with this height is a minimum berm width of 17 m (assuming a trapezoidal shaped berm). The sediment berm could be left as is or backfilled after the operation, with the requirement determined post-consent following further detailed engineering investigation. Depending on ground conditions, it is possible that a single pit for all five cables may be considered, leading to a minimum of 60 m wide pit, extending 30 m offshore.

Although HDD installation activities at the landfall were not directly modelled, the completed modelling for other construction activities can be used to assess for potential effects from the HDD installation. In terms of immediate disturbance to the seabed, dredging using a backhoe or suction dredgers at a minimum depth of up to 10 mLAT would result in a similar level of modelled disturbance close to the coast in equivalent water depths. The backhoe dredgers or suction dredgers which may be used for excavation of the HDD pits would side-cast the dredged material and cause disturbance between that modelled for CFE disturbance at the seabed and overflow from TSHD from the surface. The modelled CFE results within the offshore ECC, as described in section 5.1.2.3.2, showed that, while the instantaneous SSC may be relatively high (550 mg/l), this disperses over a very short distance from the location of the activity (<100 m) before returning to background levels. ECC9 is located in <10 m water depth therefore the results shown in Figure 5-6 at this location can be considered equivalent to those anticipated at the HDD exit pits.

With respect to the discharge of PLONOR<sup>11</sup> drilling fluids at punch-out of the HDD exit, small volumes of drilling fluids could be discharged. However, this material will very quickly disperse in line with the flow processes resulting in levels less than that modelled for construction activities.

Further consideration of the temporary presence of the receiver pits on the physical properties of the coastline and landfall is provided in section 5.3, as part of potential landfall changes associated with construction activities.

## 5.2 Loss or Alteration of Seabed Type

All the previously considered, construction activities can result in the loss or alteration of seabed type, albeit at varying magnitudes (section 5.1), so results are presented and discussed as grouped previously. This section considers the introduction of subsea infrastructure including foundations, cables and remedial protection, the disturbance footprint associated with construction activities and the sedimentation (extent and deposition thickness) that would occur associated with the different construction activities. It is the case that on disturbance or release of sediment, the much larger proportion would fall directly to the seabed associated with the active phase of seabed deposition. This differs from the smaller proportion of sediment, which largely constitutes fines, that would develop into a plume as part of

---

<sup>11</sup> *Chemicals that Pose Little or No Risk (PLONOR) to the marine environment as classified by the OSPAR Commission.*



the passive phase, such as has been modelled and assessed in section 5.1. Therefore, with respect to sedimentation, this section focusses on the proportion of sediment which does not enter into suspension, but instead falls directly to the seabed during the active phase of sediment deposition.

Through scaling down of the fine sediment component across the offshore Project area (to account for the sediment modelled to form a plume), this assessment assumes up to 99.75% of all sediment to be cleared during seabed preparation across the offshore Project will fall directly to the seabed. The remaining percentage of sediment (0.25%) has been accounted for in the plume modelling in section 5.1. The determined total percentage for the offshore Project comprises 99.88% from the OAA and 99.48% from the offshore ECC. The difference in percentages is again with respect to the marginally larger percentage of fine sediment present within the offshore ECC, so the overall 99.75% for the whole offshore Project takes into account the specific sediment context within the two areas of the Project. It is these scaled percentage sediment volumes that are used to determine the sedimentation thickness and potential extent associated with the active deposition phase. It is also the case that the sedimentation extent and deposition thickness are inversely linked, so different sedimentation scenarios are considered and compared against the offshore Project footprints (i.e. for the indicative DMPA, OAA, offshore ECC and total offshore Project area). Sedimentation associated with the passive phase, i.e. from the sediment plumes considered in section 5.1, is also discussed, but it should be noted that this occurs on much smaller millimetric scales across a much wider area, and would largely be indiscernible from the surrounding seabed.

## 5.2.1 Seabed Preparation

### 5.2.1.1 Boulder clearance

Boulder clearance will entail relocation of boulders to areas adjacent to the clearance site or elsewhere within the offshore Project (section 4.3). The extent of sediment disturbance associated with this preparation activity has been also described in section 5.1.2.1. With regards to loss or alteration of the seabed in relation to this activity, section 3.3.2.2.1 notes the prevalence of boulders throughout the offshore Project area. Boulder fields are reported as being variably of high and medium density. Given the ubiquitous presence of boulders, any which would be removed during seabed preparations would likely be placed in environments with similar properties, i.e. also having a medium to high density boulders. As stated in section 4.3 and Table 4-2, a corridor of up to 30 m per cable could be cleared (15 m each side of the proposed cable route). Boulders will likely only be moved a relatively short distance to ensure technical and safety risks are eliminated. Consequently, it is not expected that any movement of boulders would change the composition of the seabed within the offshore Project area.

### 5.2.1.2 Bedform Clearance by Dredge and Disposal

As summarised for the Project design in section 4.3, up to 3.5 m of seabed sediment could be cleared where bedforms are present within the offshore Project area. This could occur over a total footprint of 26 km<sup>2</sup> across the offshore Project (Table 4-2). This footprint constitutes an area of potential loss or alteration of seabed type. With respect to the sediment deposition associated with this construction activity, based on the sediment proportions for direct seabed sedimentation, i.e. 99.75% of the sediment bulk as described in section 5.1.1, Table 5-1 outlines the sediment volumes used to inform the sedimentation properties, in comparison to the total amount of material cleared as



detailed in the Project Description in section 4.3 and where the remainder is considered to have dispersed associated with the plume.

Table 5-1 Volumes of sediment which will fall directly to the seabed associated with the active deposition phase

	OAA (M <sup>3</sup> )	OFFSHORE ECC (M <sup>3</sup> )	TOTAL PROJECT (M <sup>3</sup> )
<b>Total sediment disturbance volume</b>	1,014,720	495,000	1,509,720
<b>Sediment volume for direct deposition</b>	1,013,502	492,426	1,505,928

A total of 1,509,720 m<sup>3</sup> is to be cleared across the whole offshore Project area, with the TSHD vessel hopper capacity (i.e. volume) of 35,000 m<sup>3</sup>, which equates to a total of approximately 150 trips by the TSHD to deposit cleared sediment within the indicative DMPA. The 150 total trips comprise of approximately 101 in relation to the OAA and 49 from the offshore ECC. The number of trips is applied for modelling purposes only and is not a direct representation of the construction programme to be completed by the Project.

As sedimentation extent and deposition thickness are inversely linked, Table 5-2 shows the deposition thickness and sedimentation extent under different theoretical sediment deposition scenarios, based on the volumes in Table 5-1. The sedimentation extent is also presented as a proportion or percentage area for different components of the offshore Project, based on the range of clearance and disposal options. The depositional scenarios assume deposition as a cone, which would be based on the maximum angle of repose of the sediment and the total volume, of which there is a finite amount, or material is uniformly spread to a given thickness over the available area. The formation of a cone shaped deposit associated with all 150 disposal discharge events is unrealistic and assumes that all the sediment (i.e. every TSHD vessel load will be deposited in the same location while the vessel is stationary). Furthermore, deposition in the steepest cone formation assumes that the gradient of deposited material will remain at the angle of repose. This scenario will not occur and is therefore excluded from Table 5-2, but the steepest possible cone, is the starting basis to inform increasing radii, and by increasing the cone radius beyond that of the steepest cone, the thickness of sediment decreases. Another evaluated scenario is that the TSHD will be able to deposit the material at a constant thickness. Under a minimum possible theoretical thickness of sediment deposition 0.01 m, approximately 68% of the indicative DMPA would be covered (Table 5-2). In reality, the TSHD will be moving while the deposition occurs and, as the vessel capacity is limited, the 150 trips will ensure that deposition is spread throughout the DMPA. The realistic sedimentation extent and depositional thickness for the total offshore Project volume would be between the estimated extremes as represented by results in Table 5-2. As demonstrated in Table 5-2, the smaller extent of approximately 0.88 km<sup>2</sup> equated to deposition thickness of just over 5 m, whereas the largest deposition extent of 15.06 km<sup>2</sup> equated to a deposition thickness of only 0.1 m.

The deposit thickness in Table 5-2 is additionally split by clearance within the OAA and offshore ECC. The majority of material to be cleared will originate from within the OAA, with a total of 1,013,502 m<sup>3</sup> being cleared within the OAA. While the thinnest layer of deposition would cover approximately 46% of the indicative DMPA, in the context of the whole offshore Project area, only 1.3% of the offshore Project area would be covered. As the smallest volume of



material is being cleared from within the offshore ECC, the deposition thicknesses and the areas of coverage are smaller than for the OAA. In practice, it is also important to remember that the same sediment may be subsequently resuspended and resettled elsewhere as part of the ongoing natural sediment transport regime which is known to be dynamic with the combined influence of flows and waves (section 3.9.2). The clearance process will be occurring on top of the deposition of relatively mobile sediment, albeit at greater volumes. The deposition will not be acting in isolation and so the full implications of the activity may not be as stark as if it was occurring in a less dynamic area.

In addition to the potential sedimentation extent and thickness illustrated in Table 5-2, the completed numerical modelling assessed the potential sedimentation associated with approximately 0.25% sediment bulk within the plume, the results of which are illustrated in Figure 5-13. Generally, in the modelled scenarios for the dredged and disposal, maximum deposition of only 2 mm was modelled (remembering sedimentation is scaled across the 100 m by 100 m model grid cell) and this was only modelled within the DMPA. Elsewhere across the OAA and offshore ECC, associated with where drag-head disturbance and overflow occurred, sedimentation thickness was <0.1 mm. The modelled results indicate that sedimentation from any plume would be indiscernible from the surrounding seabed (Figure 5-13).

Table 5-2 Dredge and disposal estimated sedimentation extent and deposition thickness, associated with the total Project, OAA and offshore ECC clearance volumes

	DEPOSITION ASSUMPTION (m)	DEPOSITION THICKNESS (m)	SEDIMENTATION AREA (km <sup>2</sup> )	PERCENTAGE DISPOSAL AREA	PERCENTAGE OAA / OFFSHORE ECC	PERCENTAGE TOTAL OFFSHORE PROJECT AREA
<b>Total Project</b>						
<b>Cone<sup>12</sup></b>	4 x radius	5.16	0.88	3.98%	N/A	0.11%
	5 x radius	3.30	1.37	6.22%	N/A	0.18%
<b>Uniform</b>	2	2	0.75	3.42%	N/A	0.10%
	1.5	1.5	1.00	4.56%	N/A	0.13%
	1	1	1.51	6.85%	N/A	0.19%
	0.5	0.5	3.01	13.69%	N/A	0.39%
	0.1	0.10	15.06	68.45%	N/A	1.93%
<b>OAA only (WTGs, OSP and inter-array and interconnector cables)</b>						
<b>Cone<sup>13</sup></b>	4 x radius	4.52	0.67	3.06%	0.10%	0.09%
	5 x radius	2.89	1.05	4.78%	0.16%	0.13%
<b>Uniform</b>	2	2	0.51	2.30%	0.08%	0.06%
	1.5	1.5	0.68	3.07%	0.10%	0.09%
	1	1	1.01	4.61%	0.15%	0.13%

<sup>12</sup> The cone depositional scenario applied at four and five times the radius, can be considered to analogous to four or five deposition locations, without accounting for the dispersal by flows.



	DEPOSITION ASSUMPTION (m)	DEPOSITION THICKNESS (m)	SEDIMENTATION AREA (km <sup>2</sup> )	PERCENTAGE DISPOSAL AREA	PERCENTAGE OAA / OFFSHORE ECC	PERCENTAGE TOTAL OFFSHORE PROJECT AREA
	0.5	0.50	2.03	9.21%	0.31%	0.26%
	0.1	0.10	10.14	46.07%	1.54%	1.30%
<b>Offshore ECC (export cables)</b>						
<b>Cone<sup>13</sup></b>	4 x radius	3.55	0.42	1.89%	0.33%	0.05%
	5 x radius	2.27	0.65	2.95%	0.52%	0.08%
	2	2	0.25	1.12%	0.20%	0.03%
<b>Uniform</b>	1.5	1.5	0.33	1.49%	0.26%	0.04%
	1	1	0.49	2.24%	0.40%	0.06%
	0.5	0.50	0.98	4.48%	0.79%	0.13%
	0.1	0.10	4.92	22.38%	3.95%	0.63%

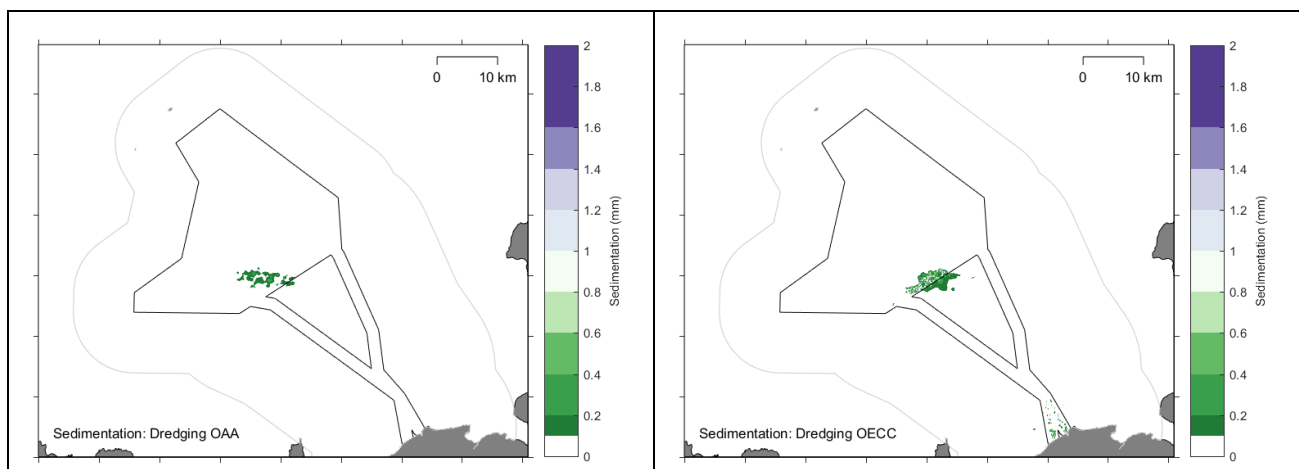


Figure 5-13 Modelled sedimentation associated with dredge and disposal clearance across the OAA and offshore ECC

### 5.2.1.3 Sandwave Clearance by Controlled Flow Excavator

As introduced in section 5.2.1.2, up to 3.5 m of seabed sediment could be cleared across a total footprint of 26 km<sup>2</sup> where bedforms are present (Table 4-2). The method for determining the deposition of sediment in the wake of seabed clearance by CFE accounts for the activity, as the disturbance occurs at the seabed and will be transient and continuous as the CFE moves. This differs from the disposal process evaluated in section 5.2.1.2 which involves disposal from the sea surface, with little to no transit. As CFE occurs at the seabed, local flows have been taken into account; a range from 0.25 m/s to 1 m/s is considered based on the environmental description provided in section



3.7.2. Additionally, a range of sediments (from fine sand to fine gravel) have been assessed due to the variation in sediment sizes within the offshore Project area (section 3.3.2.2). However, it should be noted that the applied analyses assumes the entire sediment bulk comprises the assessed sediment size when in reality, the sediment characterisation across the offshore Project, as described in section 3.3.2.2.1, demonstrates varying proportions of sediment fractions. A number of potential CFE heights above the seabed (5 m, 10 m and 15 m) have also been considered, which relates to the potential height of the CFE unit above the seabed and the height disturbed sediment could lift above the seabed during the activity. While some of these scenarios are not realistic, they provide a full range of sediment deposition thicknesses and sedimentation extent associated with the maximum and minimum PDE, with the reality most likely being within the defined envelope. The CFE clearance analyses assumes a uniform layer of disposal. A cone scenario, as described in section 5.2.1.2, is not applicable for this type of activity.

The results of these scenarios with regards to the deposition thickness and area of cover associated with the total offshore Project clearance volumes (i.e. inclusive of all clearance within the OAA and offshore ECC) are shown in Table 5-3. The areas of sediment deposition are also shown as a percentage of the OAA/offshore ECC and offshore Project as a whole. Though deposition will happen in the immediate surroundings of the activity, the percentages are provided to give some context and idea of scale to the activity. General trends show that, across all scenarios, faster flow speeds result in a greater dispersion of sediment therefore cover a larger area of the OAA/offshore ECC/offshore Project (Table 5-3). Inversely correlated to this is the thickness of the deposit. As the theoretical CFE height above the seabed increases, the thickness also decreases. This is because the CFE height directly affects the extent of dispersal – the higher the CFE the further the disturbed material will spread. The final variable accounted for in the analysis was sediment size; as the sediment size increases, its potential to be spread over greater areas decreases. Larger sediments fall to the seabed faster. Additionally, based on the principals outlined previously, larger sediments form thicker deposits. Calculated theoretical deposition thickness, which are unrealistic, e.g. where the deposition thickness is similar to or greater than the water depth across the offshore Project area, are excluded from Table 5-3 and the completed assessment. This applies to the deposition of fine gravel and coarse sand, at all flow speeds, based on an CFE height of 1 m, where sedimentation extents are very small, but the deposition thickness are at or greater than half the water depth.

Deposited fine gravel for varying thicknesses could cover an area of between 0.02 km<sup>2</sup> and 0.3 km<sup>2</sup> depending on the current speeds and CFE height (Table 5-3). Assuming an CFE height of 10 m (in the middle of the range analysed), approximately 0.05% of the total offshore Project area would be covered under flows of 0.25 m/s associated with a theoretical deposition thickness of 4.1 m. With flow speeds of 1 m/s, 0.2% of the total offshore Project would be covered by fine gravels with a theoretical deposition thickness of up to 1 m (Table 5-3). Using the same parameters, but instead describing the results for fine sands, the areas of cover are increased. Under flow speeds of 0.25 m/s, up to 0.8% of the total offshore Project area would be covered with a theoretical deposition thickness of up to 0.14 m. Faster flow speeds of 1 m/s increase this to 3.2% of the with a theoretical deposition thickness of up to 0.04 m. Ultimately, the area of deposition cover, while variable, is relatively small within the context of the whole offshore Project area (Table 5-3). For the assessed sediment sizes, with the exception of fine sand, the area of total offshore Project area affected by deposition is <1%, albeit to varying deposition thicknesses. As the larger volume of sediment disturbance is associated with clearance within the OAA (Table 4-2), the larger proportion of deposition will in turn be in relation to the clearance activities within the OAA.

In terms of the depositional thickness impacts, Table 5-3 demonstrates that the worst theoretical deposition thickness is associated with the dispersion of gravel, at the lower MFE height and slowest flow speeds. The proportion of varying



sediment grain sizes across the offshore Project indicates the seabed mainly comprises sand with the highest proportion (approximately 40% – 70%), which is present in all (i.e. 100%) samples across the OAA and offshore ECC (Table 3-2). Gravel also occurs, at lower percentage proportions (maximum up to 40%) and is present in between 10% and 70% of samples across the OAA and offshore ECC. Therefore, the theoretical deposition thickness for gravel can be scaled down, with the deposition thickness in relation to medium and coarse sand more likely to occur. Therefore, depending on the height of the CFE head, the flow speed and sediment grain sizes on the seabed during clearance, deposition thicknesses between 0.1 m and 3.9 m, based on medium and coarse sand. Similar deposition thickness could theoretically occur across the OAA and offshore ECC, however what would vary is the sedimentation area, based on the fact that there is a finite amount of sediment disturbance in relation to each construction activity. As it is the surface sediment being displaced, ultimately the clearance will not result in a change in seabed sediment type. Although, sediment may be deposited away from the clearance site, the sediment would form part of the wider sediment transport regime and not necessarily constitute a loss or change to the seabed and sediment type.

With respect to the modelled sedimentation from the plume, Figure 5-14 illustrates the modelled results for CFE clearance across the OAA and offshore ECC. Thickness of up to 0.6 mm could occur away from the immediate disturbance site, reducing to <0.2 mm towards the plume extent. Along the clearance track up to 10 mm of sediment would be directly displaced adjacent to the clearance track, accounting for the deposition thickness (Figure 5-14). Again, as described for dredge and disposal in section 5.2.1.2, sedimentation as a result of the plume would be largely indiscernible from the surrounding seabed.

Table 5-3 CFE clearance estimated sedimentation extent and deposition thickness, associated with the total offshore Project clearance volumes (inclusive of all clearance within the OAA and offshore ECC)

CURRENT SPEED (m/s)	CFE HEIGHT ABOVE SEABED (m)	FINE GRAVEL			COARSE SAND			MEDIUM SAND			FINE SAND		
		DEPOSITION THICKNESS (m)	AREA (km <sup>2</sup> )	PERCENTAGE OFFSHORE PROJECT AREA	DEPOSITION THICKNESS (m)	AREA (km <sup>2</sup> )	PERCENTAGE OFFSHORE PROJECT AREA	DEPOSITION THICKNESS (m)	AREA (km <sup>2</sup> )	PERCENTAGE OFFSHORE PROJECT AREA	DEPOSITION THICKNESS (m)	AREA (km <sup>2</sup> )	PERCENTAGE OFFSHORE PROJECT AREA
0.25	5	8.1	0.2	0.02%	3.9	0.4	0.05%	1.4	1.1	0.14%	0.28	3.5	0.45%
0.5	5	4.1	0.4	0.05%	2.0	0.8	0.10%	0.7	2.2	0.28%	0.14	7.0	0.90%
0.75	5	2.7	0.6	0.07%	1.3	1.2	0.15%	0.5	3.2	0.41%	0.09	10.5	1.34%
1	5	2.0	0.7	0.10%	1.0	1.5	0.20%	0.4	4.3	0.55%	0.07	14.0	1.79%
0.25	10	4.1	0.4	0.05%	2.0	0.8	0.10%	0.7	1.9	0.24%	0.14	6.2	0.80%
0.5	10	2.0	0.7	0.10%	1.0	1.5	0.20%	0.4	3.7	0.48%	0.07	12.5	1.59%
0.75	10	1.4	1.1	0.14%	0.7	2.3	0.30%	0.2	5.6	0.71%	0.05	18.7	2.39%
1	10	1.0	1.5	0.19%	0.5	3.1	0.39%	0.2	7.4	0.95%	0.04	24.9	3.19%
0.25	15	2.7	0.6	0.07%	1.3	1.2	0.15%	0.5	2.4	0.31%	0.09	9.0	1.15%
0.5	15	1.4	1.1	0.14%	0.7	2.3	0.30%	0.2	4.8	0.62%	0.05	17.9	2.29%
0.75	15	0.9	1.7	0.21%	0.4	3.5	0.44%	0.2	7.2	0.92%	0.03	26.9	3.44%
1	15	0.7	2.2	0.29%	0.3	4.6	0.59%	0.1	9.6	1.23%	0.02	35.8	4.59%

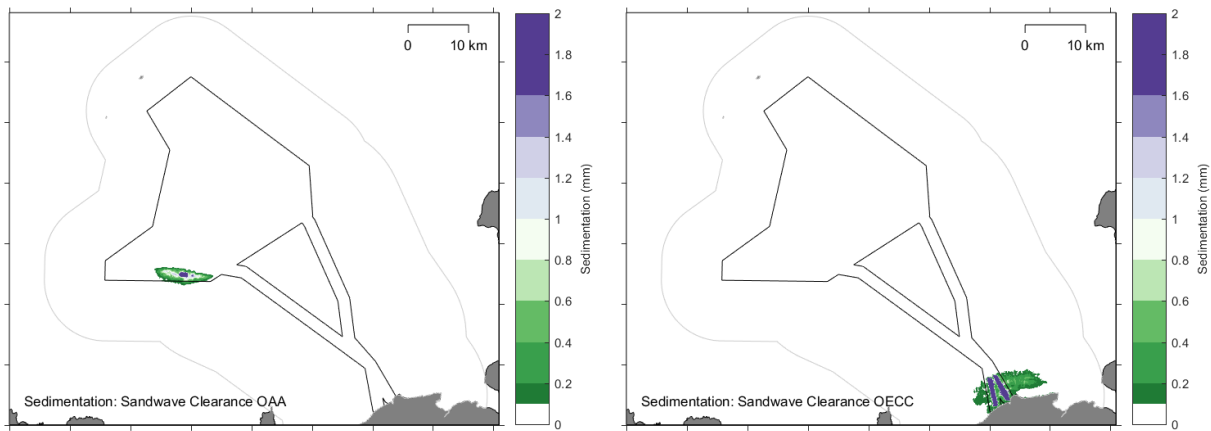


Figure 5-14 Modelled sedimentation associated with CFE clearance across the OAA and offshore ECC.

## 5.2.2 WTG and OSP Foundation Installation

Infrastructure footprints are as summarised in the Project design for WTGs and OSPs in Table 4-3 and Table 4-4 respectively. A total of up to 1.36 km<sup>2</sup> could be covered by foundations and scour protection, associated with the largest foundation footprints from the suction bucket jacket options, equating to approximately 0.2% of the OAA and offshore Project area.

In addition to the infrastructure footprint, there is the potential for sedimentation from construction activities contributing to the loss or alteration of seabed type. Analysis of the sedimentation extent and deposition thickness associated with WTG and OSP foundation installation applies the same approach as described for disposal within the indicative DMPA. Drilling is a static activity and, although the activity itself occurs at the seabed, as described in section 4.3 and applied in modelling in section 4.4.1.2.4, discharge of sediment may occur at the seabed or at the sea surface. As a worst case with regards to seabed disturbance, it has been assumed that discharge will occur at the sea surface as completed for the modelling (section 4.4.1.2.4). Using the volumes of sediment to be drilled as part of foundation installation (in Table 4-3 and Table 4-4,) and based on the different foundation types (described in section 4.3), the WTG monopile, the WTG piled jacket and piled OSP jacket are assessed here using the maximum parameters, to estimate the sedimentation extent and deposition thickness.

It is additionally important to note that the bedrock (as described in section 3.2.2) is sandstone. Although it differs from the superficial till within much of the offshore Project area, there are some outcrops of the bedrock. Ultimately, the act of drilling and bringing the bedrock to the surface is not considered to be a change in seabed type. The friable sandstone will likely break up into sandy components and have similar properties to the existing seabed sediment.

Overall, the area of deposition and its thickness varies depending on the foundation type. On an individual pile basis, the area of sedimentation associated with the OSP and WTG jacket foundations is the same – due to their dimensional parameters being the same. The monopile WTG has the largest sedimentation extent per WTG, as the volume to be drilled per monopile foundation is much larger, even compared with the total volume associated with the 16 drilled piles required for the OSP (i.e. based on eight jacket legs, with two drilled piles per leg). As before, the thickness of



the deposit is inversely correlated with the sedimentation area, so the deposition thickness is largest with the smallest sedimentation extent. On the basis that sediment will be discharged at the sea surface, the theoretical sediment extent increases with water depth as the sediment has further to fall. Sediment will be transported over a greater distance due to advection. As the sediment is more dispersed, the thickness is reduced.

Based on the theoretical deposition scenarios (as a cone or uniformly deposited) for a WTG monopile, the deposition thickness per WTG varies between 0.25 m and 4.00 m, with an associated sedimentation percentage cover of 0.84% and 0.16% of the OAA respectively, for all 125 WTGs (Table 5-4). For WTG jacket, smaller deposition thicknesses and sedimentation extents were determined, where deposition thicknesses ranged between 0.25 m and 1.53 m, with sedimentation coverage of 0.19% and 0.09% of the OAA respectively, for all 125 WTGs. Deposition thickness and sedimentation extents associated with OSPs were larger than those estimated for WTG jackets, but still less than estimated for WTG monopolies (Table 5-4). The sum of the sedimentation extents associated with the WTG monopiles and OSPs, still results in less than 1% of the OAA being covered with 0.25 m sediment.

As the drilling would be ongoing for a number of hours across multiple flood and ebb tidal cycles, the pattern of sedimentation and deposition would alter with the varying flow conditions. Therefore, the actual deposition thickness and sedimentation extent and coverage would likely be within the assessed ranges represented in Table 5-4. With the deposition of sediment, the material would in turn form part of the sediment transport regime across the region.

The modelling assessed the potential sedimentation associated with sediments which were taken up into the plume (approximately 0.25% of the sediment bulk). The results of this sedimentation within the OAA associated with installation of WTG foundations (one at a time or simultaneously) are shown in Figure 5-15. Thickness of up to 1.2 mm could occur close to the location of the drilling activity, reducing to <0.2 mm at the furthest extent of the plume. In terms of the difference in sedimentation between the single WTG and two WTGs being drilled concurrently, thicknesses of up to 1.2 mm occur in very small, localised patches when one WTG foundation is being drilled. When two are being drilled, the extent of sedimentation up to 1.2 mm thick is more widespread. Even in areas of the maximum sedimentation thickness, this is unlikely to be discernible from the existing surrounding seabed conditions.

Table 5-4 Deposition thickness and sedimentation area associated with WTG and OSP foundation installation

DEPOSITION ASSUMPTION (M)	DEPOSITION THICKNESS (m)	SEABED DEPOSITION AREA (m <sup>2</sup> )	SEABED DEPOSITION AREA (m <sup>2</sup> )	SEABED DEPOSITION AREA (km <sup>2</sup> )	PERCENTAGE OF COVERAGE WITHIN OAA	
		Per pile	Per WTG / OSP	125 WTG / 5 OSP		
<b>WTG monopile<sup>13</sup></b>						
<b>Cone<sup>14</sup></b>	2 x radius	4.00	8,246	8,246	1.03	0.16%

<sup>13</sup> Monopile foundations have only one pile, hence the deposition area and thickness are the same per pile as for per WTG under this foundation option.

<sup>14</sup> The cone depositional scenario applied for drilling tries to account for the potential dispersion associated with flows due to the continuous nature of the activity. Therefore, the settling velocity and sedimentation distance for gravel sized sediment across the range of depths that WTG foundations could be installed at within the OAA, is used to infer the potential minimum depositional radius. The sedimentation distance for gravels (based on an average flow speed of 0.5 m/s) is similar to the twice and three times the radius of the steepest depositional cone.



DEPOSITION ASSUMPTION (M)	DEPOSITION THICKNESS (m)	SEABED DEPOSITION AREA (m <sup>2</sup> )	SEABED DEPOSITION AREA (m <sup>2</sup> )	SEABED DEPOSITION AREA (km <sup>2</sup> )	PERCENTAGE OF COVERAGE WITHIN OAA	
	3 x radius	1.78	18,554	18,554	2.32	0.35%
<b>Uniform</b>	1	1	11,000	11,000	1.38	0.21%
	0.5	0.5	22,000	22,000	2.75	0.42%
	0.25	0.25	44,000	44,000	5.50	0.84%
	<b>WTG jacket (with four piles)</b>					
<b>Cone<sup>15</sup></b>	2 x radius	1.53	1,199	4,797	0.60	0.09%
	3 x radius	0.68	2,698	10,793	1.35	0.21%
<b>Uniform</b>	1	1	610	2,440	0.31	0.05%
	0.5	0.5	1,220	4,880	0.61	0.09%
	0.25	0.25	2,440	9,760	1.22	0.19%
	<b>OSP jacket (with 16 piles)</b>					
<b>Cone<sup>15</sup></b>	2 x radius	1.50	1,160	18,553	0.09	0.01%
	3 x radius	0.67	2,609	41,743	0.21	0.03%
<b>Uniform</b>	1	1	580	9,280	0.05	0.01%
	0.5	0.5	1,160	18,560	0.09	0.01%
	0.25	0.25	2,320	37,120	0.19	0.03%

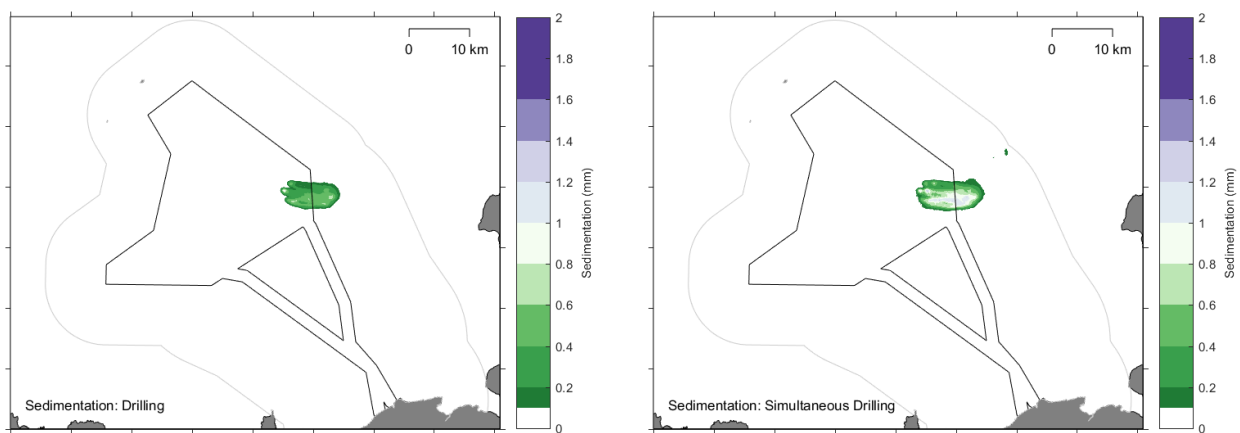


Figure 5-15 Modelled sedimentation associated with drilling one WTG monopile and two simultaneously



### 5.2.3 Cable Installation

While CFE can be used for bedform clearance (discussed above in section 5.2.1.3), it also provides the worst case for method of cable trenching during installation. Compared to clearance, which is a slower process involving flattening of seabed features, trenching will occur relatively quickly with a transit rate of 150 m/hr for export and interconnector cables, and 200 m/hr for inter-array cables. The intention is that the majority of the cables are buried, and so it is important that the sediment being displaced by CFE or during trenching, largely remains within the trench. In addition, because of the more targeted scope of trenching activities, the dimensions of the proposed trench activity are smaller than that of the CFE clearance parameters, as described in section 4.4.2.1. Table 4-5 summarises the trench properties, with a target depth of up to 3 m, maximum width of 5 m, over a total length of 835 km for the offshore Project (comprising the export cable, inter-array and interconnectors), within which sediment would be displaced. In addition to the direct displacement of seabed sediment with the cable trench, there is the potential for installation of cable and crossing protection also summarised in Table 4-5. Across the offshore Project, up to a total of footprint of 5.98 km<sup>2</sup> of cable protection is likely to be installed associated with cables and crossings equating to only 0.9% of the offshore Project area, resulting in a potential change of seabed type.

A further pathway for the loss or alteration of seabed type associated with this construction activity is through the displacement of trenched sediment, resulting in changes to seabed levels. The method to calculate for the deposition thickness and sedimentation extent is as described for clearance in section 5.2.1.3, but also accounts for the differing transit speed and trench dimensions, in determining the displaced volume per unit area and therefore the sedimentation properties. The analyses assumes sedimentation and deposition will occur downstream of the activity as it progresses and in line with flow. A downstream dispersion distance has also been provided to suggest the extent of sediment deposition in association with this thickness. It also important to note that, as CFE occurs while moving, the maximum thickness in the wake of the activity will only be temporary as the sediment in the immediate lee of the activity will continuously be disturbed as the CFE progresses.

Due to the more targeted nature of trenching, the CFE height above the seabed has been assumed to be either 1 m, 5 m or 10 m. The deposition analysis takes into account a range of flow speeds (0.25 m/s, 0.5 m/s, 0.75 m/s and 1 m/s), in addition to the range of sediments, as are known to occur in the offshore Project area. The results of the deposition analysis for CFE cable trenching are shown in Table 5-5. As explained above, deposition areas are not provided as for other activities before. As the trenching parameters are the same across the whole offshore Project area, the results in Table 5-5 are applicable to trenching activity both within the OAA and offshore ECC.

The downstream deposition distance is based on the settling velocity of different sediment sizes and the flow speeds. Finer sediments disperse further downstream of the trenching activity when compared to coarser sediments. The thickness of deposition also decreases with sediment size. With increasing CFE height, the dispersion distance increases. This is as expected, the greater the CFE height, the further sediment will be dispersed and, in the case of finer sediments these will be subject to water flows further afield. Under the CFE height of 10 m and flow speeds of 1 m/s, fine sand can travel up to 1 km from the location of the activity. At this distance, the thickness of deposition is very thin at 0.02 m. Generally, the thickness of fine sand deposits are always <1 m. For larger sediments, like fine gravel, the range in deposition thickness ranges from <1 m to 17.4 m (under the smallest CFE height). In reality, the CFE height and flow speeds will be somewhere between the extreme ends of the range presented in Table 5-5. Overall, deposition will occur within 1 km of the activity. Deposition will ultimately not be uniform and also will be temporary given the CFE process will continue and, in doing so, will re-disturb any deposits.



While the results in Table 5-5 apply to all cable installation occurring across the OAA and within the offshore ECC, the differing proportions of gravels, sands and fines within the sediment will result in different location-specific dispersion thicknesses. Within the offshore ECC sediments have a higher fines component (approximately 2.6%) versus within the OAA (approximately 0.6%). Consequently, the thickness of the deposits in the OAA is likely to be slightly greater albeit covering a smaller area. The inverse is true of the offshore ECC. However, the dispersion distance and deposition thickness will vary even within these areas according to the specific sediment conditions which the CFE will pass through.

The sedimentation associated with the within plume (discussed in section 5.1.4) generated by cable installation by CFE is shown in Figure 5-16; this is split according to the extent of cable lay within the OAA and offshore ECC which could theoretically be achieved within the modelled 16-day period. Within the OAA, the sedimentation thickness is very low at <0.6 mm within the track of activity. Furthermore, the sedimentation is highly localised within the area of immediate disturbance; sedimentation does not occur in areas beyond the direct CFE path. Comparatively, in the offshore ECC, sedimentation results in a marginally thicker layer. Thickness of up to 0.8 mm could occur close to the location of the drilling activity, reducing to <0.2 mm at the furthest extent of the plume. The plume extent associated with this activity within the offshore ECC is greater than within the OAA (section 5.1.4), therefore the extent of sedimentation is similarly greater. However, sedimentation occurs almost exclusively within the offshore Project area boundary. Areas beyond this are only subject to sedimentation up to 0.2 mm in thickness. Overall, the sedimentation which may result due to cable installation will be indiscernible from the existing surrounding seabed conditions.



Table 5-5 Deposition thickness associated with cable installation by CFE

CURRENT SPEED (m/s)	CFE HEIGHT (m)	DOWNSTREAM DISPERSION DISTANCE (m)	DEPOSITION THICKNESS (m)	DOWNSTREAM DISPERSION DISTANCE (m)	DEPOSITION THICKNESS (m)	DOWNSTREAM DISPERSION DISTANCE (m)	DEPOSITION THICKNESS (m)	DOWNSTREAM DISPERSION DISTANCE (m)	DEPOSITION THICKNESS (m)
		FINE GRAVEL		COARSE SAND		MEDIUM SAND		FINE SAND	
0.25	1	0.86	17.40	1.79	8.40	5.00	3.00	25.00	0.60
0.5	1	1.72	8.70	3.57	4.20	10.00	1.50	50.00	0.30
0.75	1	2.59	5.80	5.36	2.80	15.00	1.00	75.00	0.20
1	1	3.45	4.35	7.14	2.10	20.00	0.75	100.00	0.15
0.25	5	4.31	3.48	8.93	1.68	25.00	0.60	125.00	0.12
0.5	5	8.62	1.74	17.86	0.84	50.00	0.30	250.00	0.06
0.75	5	12.93	1.16	26.79	0.56	75.00	0.20	375.00	0.04
1	5	17.24	0.87	35.71	0.42	100.00	0.15	500.00	0.03
0.25	10	8.62	1.74	17.86	0.84	50.00	0.30	250.00	0.06
0.5	10	17.24	0.87	35.71	0.42	100.00	0.15	500.00	0.03
0.75	10	25.86	0.58	53.57	0.28	150.00	0.10	750.00	0.02
1	10	34.48	0.44	71.43	0.21	200.00	0.08	1000.00	0.02

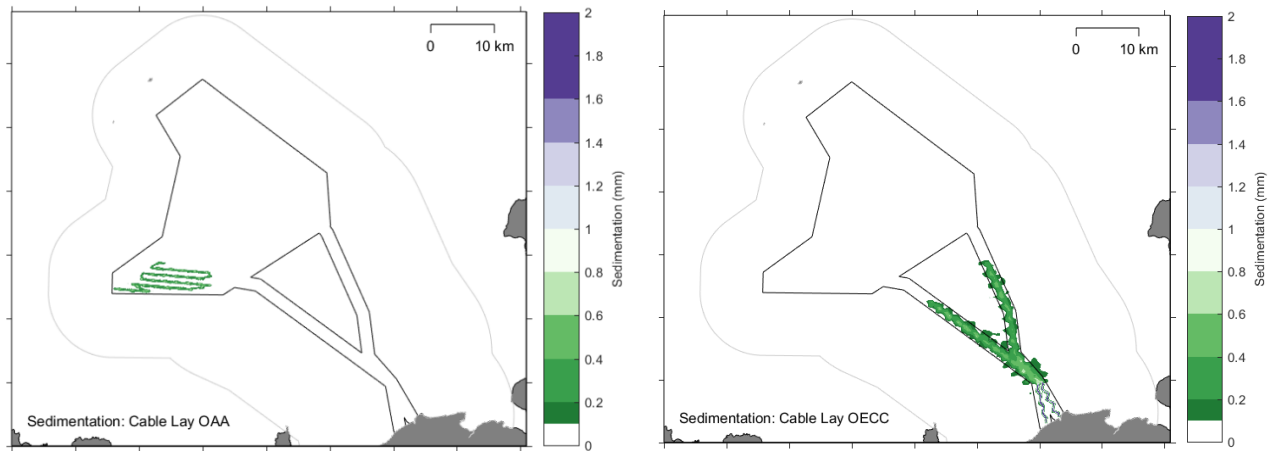


Figure 5-16 Modelled sedimentation associated with cable installation by CFE within the OAA and offshore ECC

### 5.3 Potential Landfall Changes

As described in section 3.11, the coastline at the offshore ECC landfall at Crosskirk and Greeny Geo area are characterised by hard and mixed substrates, which are erosion resistant. Site characterisation of bedrock and Quaternary geology based on site-specific surveys identifies the presence of Quaternary glacial till and outcropping bedrock in the few kilometres offshore from the coast (sections 3.2.2 and 3.3.2 and Figure 3-3). Completed analysis of the coastline from 2004 until 2021 also demonstrate little to no change occurring in the low water position, with only variations interpreted to be due to the varying tidal states at which the Google Earth imagery was acquired. This led to the conclusion that erosion is not a process which occurs in the area and the area is considered to be stable as represented in the Scottish coastal characterisation study and the EMODnet coast type (section 3.11).

In terms of the seabed in the nearshore area, approximately 1 km off the coast at the Crosskirk landfall location, a large bedform feature was identified (described in section 3.5.2.2) which is defined by deeper superficial sediments. It appears to be a bank which runs parallel with the coast. No repeat bathymetry was available to assess for seabed changes. However, the completed sediment transport potential for model observation locations close to the landfall (i.e. ECC9 and ECC10 for the Crosskirk and Greeny Geo landfalls respectively), based on the minimum HDD exit depth of 10 mLAT, indicated that waves are the dominant transport mechanism. This would still be the case under the more realistic HDD exit depth of 20 mLAT. Under the analysed period due to the coarse seabed (assumed to be 0.8 mm, representative of gravely sand from site-specific surveys) and water depths, waves could cause sediment up to very fine gravel (represented by a mean grain size of 3 mm) to be mobilised at both landfall locations (section 3.9.2.1, Table 3-13 and Table 3-14). Flows would be unable to move sediment in isolation based on the modelled flow speeds at these inshore locations and coarse seabed. Therefore, at these landfall, waves are considered to be the important marine process to govern changes during construction activities and the ongoing operation of the offshore Project.

As introduced in section 5.1.6 above for the HDD installation, some dredging of exit pits measuring up to 10 m wide x 30 m long x up to 5 m deep, may be required at the exit point, assessed at a minimum depth of 10 mLAT, although a more realistic exit depth is from 20 mLAT and deeper. Up to six pits may be excavated with an excavation volume 1,500 m<sup>3</sup> per pit and total of up to 9,000 m<sup>3</sup>. It is assumed the pits will be orientated offshore, with the 30 m length extending from the approximately HDD exit in the cross-shore direction. The excavated material could be disposed



of or temporarily stored beside the exit pits as side-cast sediment berms, which could be back-filled on completion of cable installation or left to infill following natural processes. It is assumed that the height of the temporary side-cast sediment berm, would be the same or less than that applied to protection (i.e. a berm height of up to 3 m) and an associated with this height is a minimum berm width of 17 m (assuming a trapezoidal shaped berm. Depending on ground conditions, it is possible that a single pit for all five cables may be considered, leading to a minimum 60 m wide pit, extending 30 m offshore. There is the potential for both temporary trenches and berms in the nearshore area; therefore, the worst case is assessed on the basis that the trenches (for each pit separately and grouped into one single pit) and sediment berms are left to infill naturally.

Due to the relatively long period waves that are characteristic of the offshore Project area (at around 9.5 seconds and calculated wavelength of approximately 61 m), depths of around 70 m are when the waves transition from deep water to transitional breaking waves that feel the bottom. For even longer period waves of around 11 seconds, characteristic of the mean omni-direction wave condition calculated for offshore wave hindcast 1 location (Table 3-8), the majority of the OAA and offshore ECC can be considered to be within a transitional breaking wave regime, as the water depths are less than half the wavelength (calculated as approximately 190 m) associated with the 11 seconds period waves. On approach to the coast and landfall at the worst case 10 mLAT depth, waves of 11 seconds and above would begin to shoal, including steepen and breaking, with the 9.5 second waves breaking at shallower water depths. For the shorter period waves of around 6 seconds recorded at the Dounreay WaveNet site, these would begin to shoal and break at even shallow depths still of around 3 m water depths. With the excavation of a 60 m wide but 30 m long pit, there is the potential for localised interference with the longer period waves, where the deeper water depth created by the pit would mean wave shoaling and breaking occurs closer inshore at a shallower water depth. Also the introduction of the pit could be similar to that of offshore orientated rip channels in the seabed. Waves propagating to the coast occur at a much larger, regional, mesoscale, so the effect from the presence of the single 60 m wide excavation pit would not ultimately disrupt the entire wave from progressing, but instead locally delay the shoaling process and likely introduce concentration of offshore flows through the pit. However, it is noted that complex bathymetry exists near the landfalls, particularly the Crosskirk landfall, with the morphology and rip channels naturally representing the effect the pit would have (Figure 5-17). In the instance the excavation pits are installed as individual 10 m wide pits, there is also the potential for interference, but the narrower profile of the pits with respect to the wave approach would mean the wave is less likely to feel the narrower deeper area within the pit.

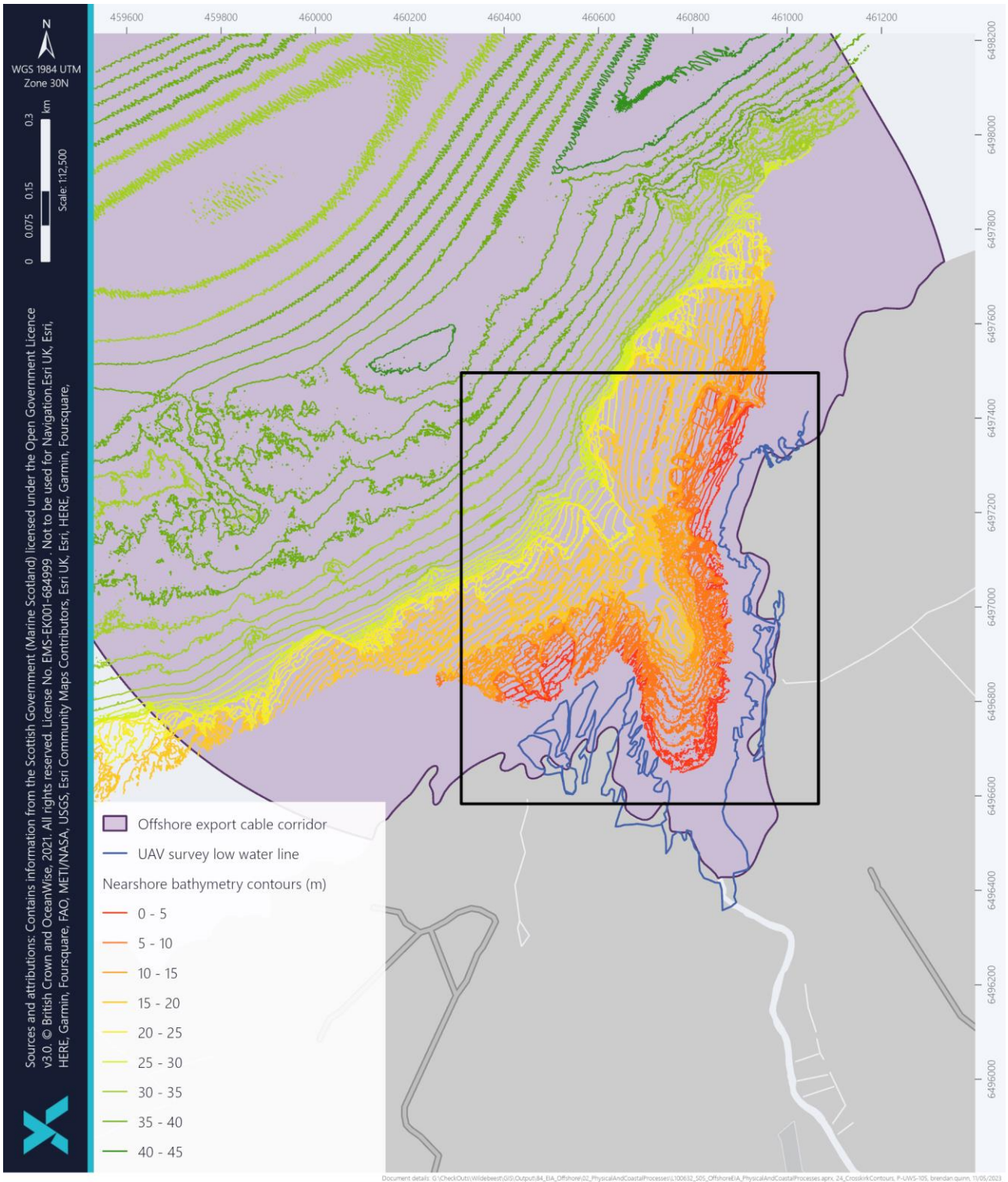


Figure 5-17 Seabed morphology and potential rip channel illustrated through seabed contours at Crosskirk landfall



With the side-casting of the excavated material creating a sediment berm of up to 3 m and 17 m wide based on each excavation pit, the presence of the berm could again theoretically interact with wave shoaling and breaking of the longer period waves. However, as it is assumed the berm would be orientated perpendicular to the coast, it would be parallel with the wave approach direction and therefore not disrupt but locally increase wave shoaling along the length of the berm. It could be that, with the presence of the single 60 m wide excavation pit and associated sediment berms, there could be a localised region of mixed sea state, with areas of delayed shoaling and breaking adjacent to locations of increased shoaling. This effect or area of mixed sea states would likely extend tens of metres from the locations of the exit pits and sediment berms towards the coast and in the offshore direction. The requirement for backfilling the exit pits will be determined post-consent following further engineering investigations. The potential for blockage to flows and sediment transport as a result of the sediment berm is the same as the operational impact of potential changes to sediment transport assessed in section 6.3. The completed analyses based on the CIRIA formula for a submerged dam (introduced in section 4.4.2.2 and applied in section 6.3.2.2), based on the potential for a rock berms at the worst case 10 mLAT depth, identified that there was no change to flows downstream. Therefore, there would expected to be no change at the more realistic HDD exit depth of 20 mLAT. As there was not considered to be any change to flows, there was not considered to be any onward changes to sediment transport associated to flows, but as has been demonstrated for the landfall locations, transport due to flows in isolation is limited at the landfalls, with the main transport occurring in relation to waves.

The PDE states that the excavation pit could be back filled mechanically or left to do so naturally. The requirement for backfilling the exit pits will be determined post-consent following further engineering investigations. In the instance that it was left to backfill naturally, the coarse nature of the seabed at the landfalls means it would primarily require wave activity to back fill. Based on the estimated sediment transport potential calculated at the landfall locations ECC9 and ECC10, waves with a significant wave height of 1.5 m and 9.5 second period could move the seabed material present, with little contribution from flows. Although these particular waves are only observed to occur around 7.5% of the time in the approximately 3.5-year wave observation record at the Dounreay site, waves of over 0.5 m significant height associated with a period of 9 seconds and over occurred over 60% of the time during the observation record (Table 3-9). Based on the frequency of the wave events, it is estimated that the pits could naturally backfill, but this would occur over a period of months to over a year or more, depending on the occurrence and frequency of the larger and longer period waves. Should finer sediment be present, it is likely that this could be winnowed away during intermittent periods of stronger current flows, leaving a coarser sediment fraction, which is not uncharacteristic to the seabed at the landfall.



## 6 ASSESSMENT OF OPERATION STAGE

### 6.1 Potential Changes to Tides

#### 6.1.1 Overview

The baseline tidal conditions comprising water levels and flow properties are described in Section 3.6.2 and 3.7.2 respectively, with key properties summarised here. For the majority of the OAA and the offshore ECC, modelled mean peak flow for a spring tide is recorded as being between 0.5 m/s and 1.0 m/s. Equivalent peak neap flows are typically expected to be around 50% less than those on springs. Tidal flows in the area are oriented with a flood to the east and ebb to the west. Although the wider region associated with the northwest Scottish continental shelf is considered to have a marginal flood dominance, a factor attributed to flow speeds, which results in an easterly-orientated flood residual with speeds of less than 0.1 m/s. Speeds within the parameters outlined above were used to define the baseline conditions of the model, summarised below.

The model set up used to investigate the potential changes to tides are introduced in section 4.4.1.3 and described in further detail in the modelling technical report in Appendix B. The conditions described above formed the basis of the pre-construction model conditions, against this background, the impacts of the installed WTGs during the operational stage of the windfarm were established. Assessment on the potential changes to flows across offshore locations associated with the OAA and offshore ECC are presented in section 6.1.2 below. The potential onward implications of changes to flows at the landfalls and to the coastal morphology is considered in section 6.6.

#### 6.1.2 Assessment

##### 6.1.2.1 Blockage Density

The blockage density effects were compared within the offshore Project area between the different monopile foundation sizes, based on the approach introduced in section 4.4.2.2.1. Blockage density for jackets was not quantitatively assessed as this is considered to be less than that for monopiles, due to the smaller piles and the opportunity for flow to continue through the legs and braces of a jacket foundation. In all cases, the number of WTGs is consistently assumed to be 125. The mean blockage density for the maximum monopile WTG foundation option is based on the assumed blockage width of each foundation being 15.25 m (based on a base and sea surface diameter of 18 m and 12.5 m respectively) and assumes the WTGs will be spaced 1,320 m apart (the minimum spacing associated with the largest foundation), at approximately 87 times the blockage width (Table 6-1). Smaller diameter monopiles of 13 m and 11 m, had a spacing of 1,000 m and 944 m respectively (as per dimensions set out in chapter 5: Project description of the Offshore EIA Report). Based on the blockage width determined for the smaller monopile foundation sizes, this provided a ratio of 105 and 99 times of the blockage width respectively (Table 6-1). Therefore, the largest monopile foundation was considered to provide the worst case potential for blockage and as a result directly informed the analyses results set out below and modelling results presented in sections 6.1.2.2 and 6.2.2.

The mean blockage density is based on the representative blockage width per foundation, relative to the available OAA, compared to the maximum blockage density which is based on the representative blockage width per foundation relative to the minimum WTG spacing. The mean blockage density assumes foundations are spread



equally throughout the entirety of the OAA, therefore in reality the blockage density is likely to be somewhere between the mean and maximum values. These statistics were calculated for the varying monopile foundation sizes, recognising that the potential blockage from jacket options would be less than that from monopiles, due to their smaller pile size and the continuation of flow through the jacket legs. Results of the calculated mean and maximum blockage density are summarised in Table 6-1.

As shown in Table 6-1, the maximum blockage density across all foundation types and sizes ranges from 8.8 to 10.7 m/km<sup>2</sup>, based on the OAA covering an area of 656.65 km<sup>2</sup>, which factors into the density calculation. The spacing between foundations is an important influence on the flows within the OAA and wider area. The presence of a foundation through the water column will cause a divergence in flow around the structure, with turbulence occurring in the wake of each individual foundation, the length of which would vary in relation to the flow properties and blockage width through the water column. Given the width of the foundations (the maximum diameter being that of a monopile at 18 m) and the minimum spacing associated with the largest foundations, the flow separation associated with each individual structure is expected to reconverge downstream of the WTG, with the turbulence immediately adjacent to the WTG structure quickly dissipating over a certain distance, expected to be in the region of several hundred metres. The minimum spacing of the foundation sizes means that the turbulence associated with each WTG would not coalesce with that from the next adjacent structure, illustrating the relative low blockage density calculated for the offshore Project (Table 6-1).

*Table 6-1 Blockage density for monopile foundation sizes, based on 125 WTGs and five OSPs (based on monopiles as a proxy)*

DIAMETER (m)	BLOCKAGE WIDTH (m)	MINIMUM WTG SPACING (m)	RATIO BLOCKAGE WIDTH TO SPACING	BLOCKAGE DENSITY (m/km <sup>2</sup> )	
				Mean	Maximum
18	15.25	1,320	87	3.0	8.8
11	9.5	1,000	105	1.9	9.5
11	9.5	944	99	1.9	10.7

### 6.1.2.2 Modelling Results

Overall, the model outputs demonstrate that there are no changes in water level within the offshore Project at any stage of the tide. Furthermore, although flow separation may occur locally with respect to each WTG, overall, that the divergence of flows around each WTG individually is not sufficient to generate an overall change to current speeds as described for Layout 11 and 2 below. Based on extracted baseline and post-construction flows at 28 model extraction locations, comparison of the absolute change in flow properties at the extraction locations, demonstrated changes of less than 0.01 m/s, with some model extraction locations demonstrating no change at all. Therefore, it is considered that the minimum spacing between WTGs (Table 6-1) allows for sufficient space for currents to recover in the wake of each structure prior to encountering the next WTG, per the understanding that wakes would dissipate



over a distance  $\leq 1,200$  m. Consequently, there is not considered to be any overall impact on currents post-construction and considered unlikely that any measurable changes will occur.

#### 6.1.2.2.1 Layout 1

With respect to Layout 1, the model outputs demonstrates that there is no discernible change in water levels at any tidal state across the offshore Project or study area, while changes in the residual flows are generally less than  $\pm 0.01$  m/s (Appendix B). The spacing between WTGs is sufficient to allow recovery of flows in the lee of the structure. This is evident in Figure 6-1 and in Appendix B.5.1.1, which shows that the spatial change in flows is isolated to the immediate wake of the WTGs. Overall, the residual flows show evidence of coalescing within the very centre of the OAA but it is notable that areas of change are limited to WTGs in isolation. Across most of the OAA and applied study area, there are no changes to peak and residual flows above 0.001 m/s. However, there are small, localised changes of both increases and decreases in current speed predominantly constrained within the OAA. The areas where increases and decreases in current speed occur change with tidal state, but the magnitude of change is typically less than 0.002 m/s.

The area of absolute change in spring flows is much smaller when compared to the absolute change in neap flows predicted by the model. The scale of difference is the same (i.e. very small), however the spatial extent of change is much greater on a neap tide. Common to both spring and neap tides is the general location of this change; change occurs predominantly in the west of the OAA. To the northwest of the WTGs, there is a predicted increase in flow speeds. Comparatively, to the southwest, along the edge of the WTGs, there is a decrease in current speeds (Appendix B.5.1.1).

The location of change varies on a tidal cycle with the flood and ebb. Generally, the model predicts that flow speeds would decrease amidst the WTGs. On an ebb tide, during which flows are travelling east to west, speeds are reduced in the east of the OAA with a slight increase in the west along the edge of the WTGs. The opposite is true for flood tides which travel west to east. However, while the absolute change in flow speeds suggests that the difference in flows is of a similar scale between tides, the extent of change varies spatially; the absolute change in flows is greater on an ebb tide. This is true for both spring and neap tides. Proportionately, the percentage change in flow speeds highlights how small this absolute change is. When looking at the percentage change, the difference in flows post-construction is reduced and more similar between flood and ebb tides.

Areas of change outside the OAA (around Orkney and the in the lochs and bays along the north coast of Scotland) picked up by the model (represented in the model results in Figure 6-1 and Figure 6-2) are not due to the presence of the WTGs, but instead relate to fluctuations in the model associated with the wetting and drying of model grid cells coast at the coast. The scale of change attributed to the WTGs is in-keeping with this expected model variation. Furthermore, such a small change in flow speeds will be hard to ascertain in reality as this is likely to be captured within the natural variation expected of the area. The model properties and the influence on the modelled outputs, including the aforementioned effects at the coast is described further in Appendix B.5.

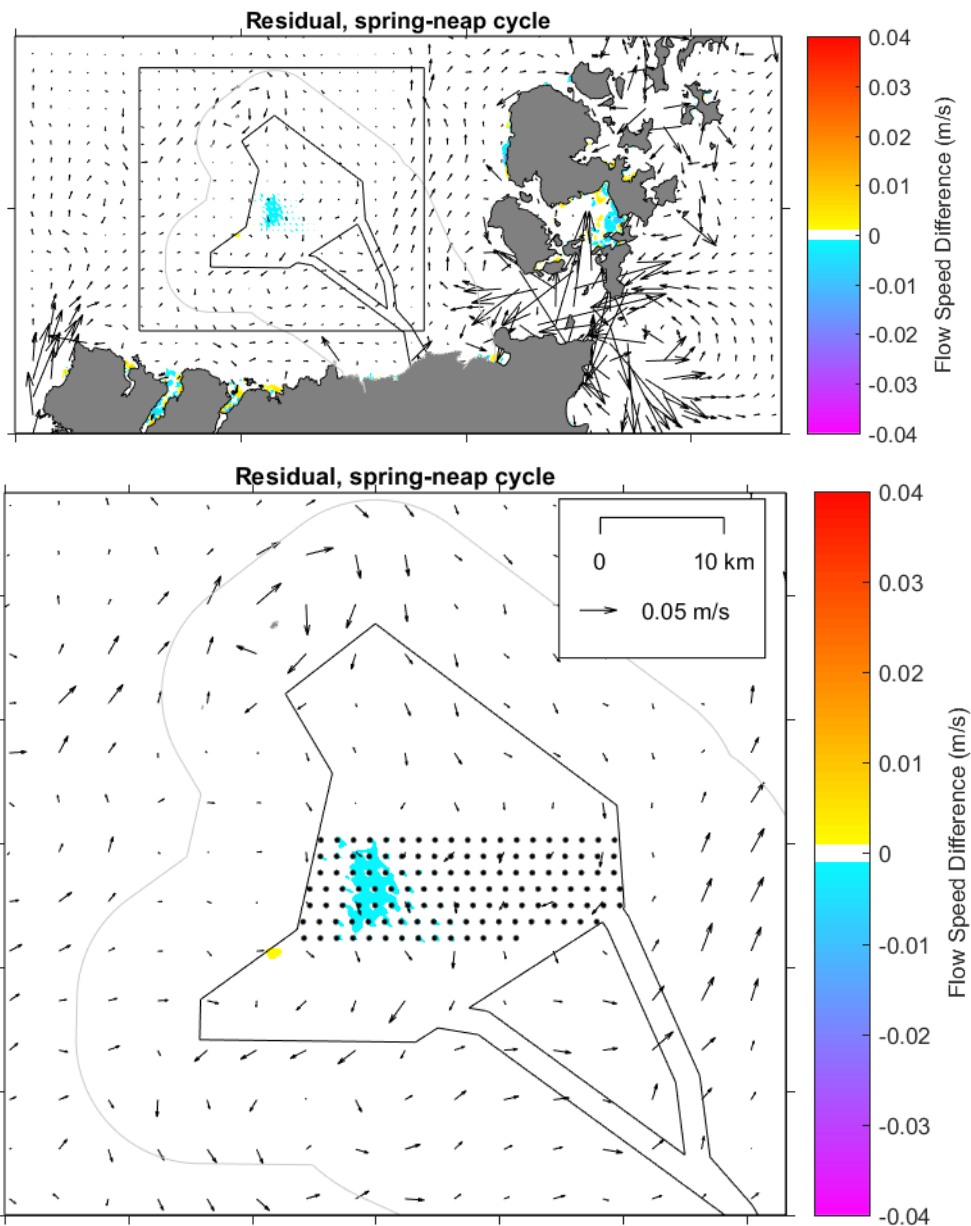


Figure 6-1 Modelled post-construction residual flows with respect to Layout 1, results are for the model domain (top) and offshore Project area zoom (bottom). Colours illustrate the post-construction flow speed difference, while the vectors illustrate the baseline residual flow speed and direction<sup>15</sup>

A comparison of tidal conditions was completed between the modelled baseline conditions, described in section 3.7.2, and the modelled operational conditions. The comparison analysed for changes to water levels and flows over a consistent 15-day period before and after installation of the WTGs. Water levels were compared at all observational model points (shown in Figure 2-4).

<sup>15</sup> Areas of change outside the OAA picked up by the model (as represented in the model results in Figure 6 1 and Figure 6 2) are not due to the presence of the WTGs, but instead relate to fluctuations in the model associated with the wetting and drying of model grid cells at the coast.



The water levels post-construction, following Layout 1, showed no perceptible difference when compared against baseline conditions. Water levels remained much the same during the operational stage of the Project. Any variation was extremely slight, no more than  $\pm 0.0002$  m. This marginal change occurred across all model observation points, including those within the offshore ECC, which are located further from the WTGs. Consequently, there is no clear discernible pattern to water level change post-construction. Given the scale of change discussed above, this is not surprising; these minor changes in water level are likely to be attributable to nominal variations in the model outputs.

The same is evident for flow speeds. The scale of change is  $\pm 0.0021$  m/s. The full scale of this variation is most apparent at OAA8, OAA17 and ECC5. These points are located in water depths of 71 mLAT, 57 mLAT, and 96 mLAT respectively. OAA8 and OAA17 are located along the westernmost boundary of the OAA and in the southwest of the OAA respectively. Both points are within the WTGs arranged as part of Layout 1. ECC5 is located at the start of the northernmost offshore ECC close to the OAA boundary. However, other observation points are also located within the OAA and do not show such variation in flows. Notably the degree of difference within the offshore ECC (with the exception of ECC5) is generally less. Within the offshore ECC, the scale of change ranges  $\pm 0.003$  m/s, with no changes observed at the landfall locations represented by ECC9 and ECC10. This indicates that with distance from the OAA there is a reduction in influence of the WTGs. However, within the OAA, there are no clear patterns in changes to flow speeds. Importantly however, given the discussion above and the model results shown in Figure 6-1, the scale of post-construction change is such that it is not discernible against natural variation throughout the offshore Project area as a whole.

#### 6.1.2.2.2 Layout 2

As with Layout 1, the model results for Layout 2 demonstrates that there is no discernible change in water levels at any tidal state across the offshore Project or study area (Appendix B). As the WTGs in Layout 2 are spread across two areas of the OAA, the change in flows is concentrated to these locations with the centre of the OAA being devoid of WTGs exhibiting no change in flows. The scale of change is the same as for Layout 1 – the absolute change in flow speeds is  $< \pm 0.01$  m/s equating to a change of less than 0.1% (Figure 6-2). The absolute and percentage change in flows according to neap, spring, ebb and flood tides is shown in full in Appendix B.5.1.2.

Mostly, as before, the extent of change in residual flows is spatially limited to the immediate WTG surroundings. Particularly in the south of the site, the modelled change in flows on a spring tide in the wake of the WTGs only appears to coalesce in a small area of the OAA (Figure 6-2). There is more evidence of a larger cumulative area of change under neap tide conditions where the spatial extent of change is larger. Overall, the extent of change is greater on a neap tide than a spring tide, and the presence of Layout 2 shows a more variable change across the OAA compared to Layout 1.

Between ebb and flood tides the location of change remains consistent; however, areas which show an increase in current speeds on a flood show a decrease on an ebb tide and visa versa depending on the direction of flow. However, as described for Layout 1 above, the degree of change is such that these changes in flows would be imperceptible in reality. The scale of change is well within the range of natural variation.

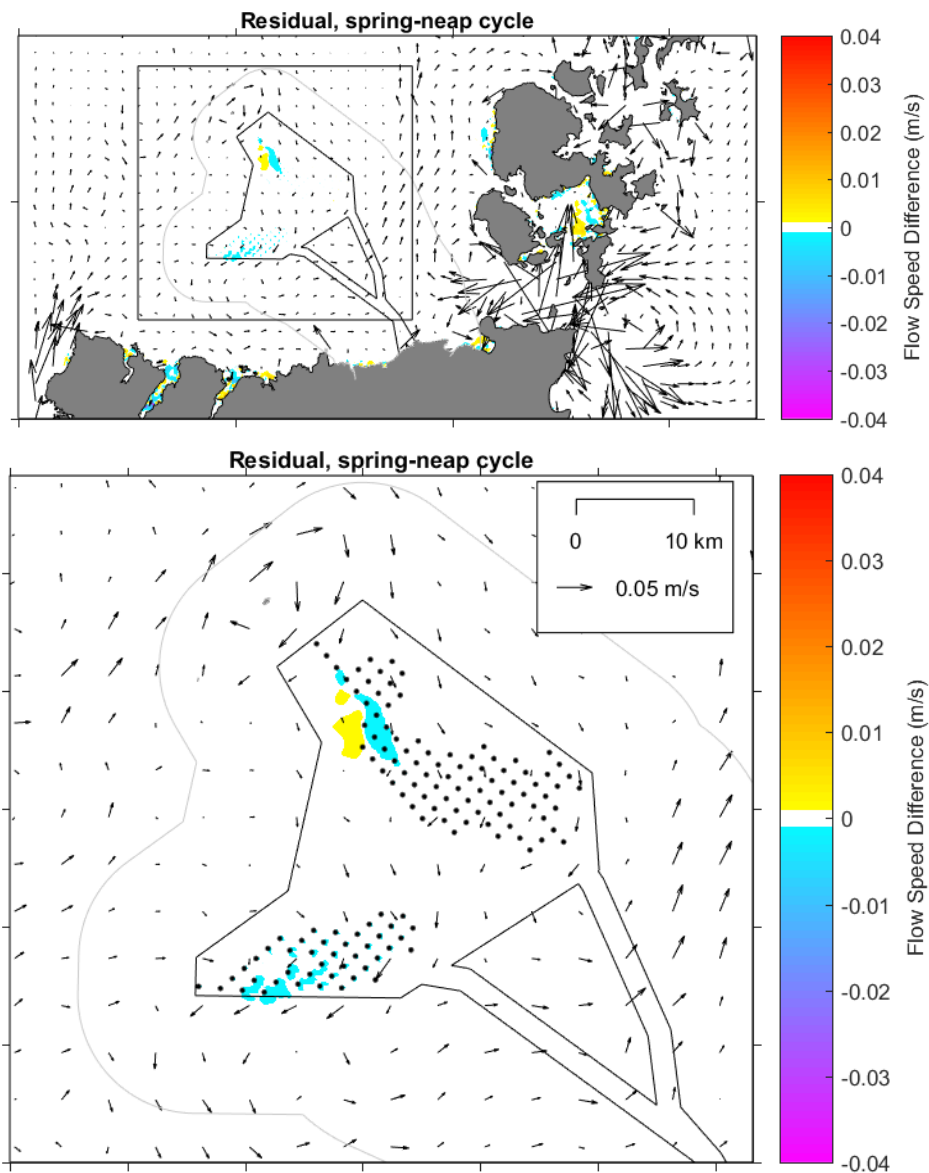


Figure 6-2 Modelled post-construction residual flows with respect to Layout 2, results are for the model domain (top) and offshore Project area zoom (bottom). Colours illustrate the post-construction flow speed difference, while the vectors illustrate the baseline residual flow speed and direction<sup>12</sup>

A comparison of tidal conditions was completed for Layout 2, as for Layout 1 before (in section 6.1.2.2.1). Water levels post-construction, again showed no perceptible difference when compared against baseline conditions, with extremely slight variation  $\pm 0.0003$  m. As for Layout 1, this very small change occurred across all model observation points, suggesting there is no relationship between water levels and the WTGs installed as part of Layout 2. Overall, regardless of layout there is almost no change to water levels as a result of the WTGs.

The difference in post-consent flow speeds varies from  $-0.0019$  m/s to  $0.0031$  m/s. This is mostly limited to model observation points within the OAA. As for Layout 1, points within the offshore ECC (particularly those close to the coast) show less change when compared against baseline conditions, which applies to the landfall locations



represented by ECC9 and ECC10. The greatest variation in flows is seen at OAA9, OAA15 and OAA18. Broadly speaking, these locations do correspond to the WTGs in Layout 2. However, as for Layout 1, other observation points within the OAA do not show variation like this. While it is possible to correlate these changes in flows to the presence of the WTGs, it is hard to definitively explain the changes spatially as there is no consistency to the patterns. It is important to reiterate that the scale of change described above and shown in Figure 6-2 is minimal therefore, possibly beyond the bounds of model sensitivity. Most importantly, the extent of change is not noticeable against natural variation in conditions.

## 6.2 Potential Changes to Waves

### 6.2.1 Overview

The baseline wave conditions are described in Section 3.8.2, with key properties summarised here. The wave regime within the offshore Project area is influenced by both local waves and swell waves which originate further afield. Waves with a significant height of 1-1.5 m and corresponding periods of 9-10 s are most frequent in the OAA, with similar waves also occurring at the landfall. Most waves originate from the west, northwest and north, with varying properties associated with different percentiles and return periods. Consequently, these directional waves form the focus of the following assessment. The model scenarios described in section 4.4.1.3 outline the basis for the analyses within the following sections. As described above, based on the prevailing wave directions, model analysis was undertaken for a range of wave conditions. The wave and wind parameters which formed the baseline conditions for the model are presented in Table 6-2. Once these baseline conditions were established, the model was run to determine any operational effects on the wave regime due to the presence of the offshore Project. This was completed for the two WTG layouts (Figure 4-1), with each WTG layout resulting in varying changes to the wave conditions, the results of which are presented in Section 6.2.2.1 and Section 6.2.2.2 for Layout 1 and 2 respectively.

*Table 6-2 Wave parameters (significant wave height, wave period, and wind direction) modelled for baseline characterisation and to investigate operational impacts*

Direction	West (270°)			Northwest (315°)			North (0° / 360°)		
	Hs (m)	Tp (s)	Wind speed (m/s)	Hs (m)	Tp (s)	Wind speed (m/s)	Hs (m)	Tp (s)	Wind speed (m/s)
<b>50<sup>th</sup> Percentile</b>	2.62	11.0	9.3	2.22	10.6	7.1	2.06	10.4	7.2
<b>90<sup>th</sup> Percentile</b>	5.06	13.0	16.0	4.34	12.5	13.3	3.88	12.1	12.8
<b>1 in 1 Return Period</b>	10.2	15.7	24.8	9.2	15.3	23.1	8.2	14.8	21.2
<b>1 in 5 Return Period</b>	12.0	16.4	27.5	10.8	15.9	25.8	9.6	15.4	23.8
<b>1 in 10 Return Period</b>	12.6	16.7	28.3	11.4	16.2	26.6	10.1	15.7	24.7
<b>1 in 50 Return Period</b>	13.6	17.0	29.4	12.3	16.5	27.8	10.9	16.0	25.9
<b>1 in 100 Return Period</b>	14.0	17.2	29.8	12.6	16.7	28.3	11.2	16.2	26.4



Assessment on the potential changes to waves across offshore locations associated with the OAA and offshore ECC are presented in section 6.2 below. The potential onward implications of changes to waves at the landfalls and to the coastal morphology is considered in section 6.6.

## 6.2.2 Assessment

As determined for potential changes to tides (section 6.1.2.2), overall, the modelling results demonstrate little to no changes to the wave regime. Where these occur with respect to OWF structures, the changes have typically been shown by plotting the changes down to a very small difference and based on the scale of the changes it is considered unlikely that any measurable changes will occur, within the offshore Project area and downstream at the coast, within the applied study area and beyond.

### 6.2.2.1 Layout 1

The model outputs indicated that, post-installation, the presence of the WTGs within the OAA may cause a change in the local wave regime. Figure 6-3, Figure 6-4 and Figure 6-5 illustrate the absolute change in significant wave height and period, and percentage change in significant wave height when compared against baseline wave conditions (presented in Table 6-2). Figure 6-6 shows the post-construction percentage change in significant wave height within the wider regional context. The model outputs shown in Figure 6-3, Figure 6-4 and Figure 6-5 can also be seen in Appendix B.9.2, which provides a wider view of the offshore Project area and shows the model outputs across the full range of wave conditions analysed (50<sup>th</sup> percentile, 90<sup>th</sup> percentile, 1 in 1, 1 in 5, 1 in 10, 1 in 50 and 1 in 100 return period waves). Waves originating from the three prevailing directions investigated are all influenced by the presence of the offshore Project beyond the extent of the study area (Figure 6-3, Figure 6-4 and Figure 6-5), however, this effect is minimal in absolute and relative terms as demonstrated below.

For all wave approach directions, there is a marginal increase in wave height upstream of the offshore Project OAA (with respect to the wave approach direction), with the reverse occurring downstream. The changes are observed for all wave approach directions and assessed percentiles or return periods, with the largest change being observed to occur for the smallest waves, i.e. the 50<sup>th</sup> percentile conditions. Although the extent of absolute change may appear to be far reaching and extend beyond the applied study area, the scale on which this change occurs is very small and equates to less than a 0.04 m change in significant wave height in absolute terms. For example, the 50<sup>th</sup> percentile waves (from all approach directions) experience a change in height of less than 0.04 m (Figure 6-3, Figure 6-4 and Figure 6-5). The 50<sup>th</sup> percentile waves are defined as those which 50% of waves will exceed in height and period. Conversely, the remaining 50% will be smaller than the 50<sup>th</sup> percentile wave. The absolute change is highest in line with the individual turbines. However, when looking at the extent of change at below  $\pm 0.04$  m, the region of change attributed to each WTG begins to coalesce. In terms of the relative percentage change in  $H_s$  associated with the smaller 50<sup>th</sup> percentile wave, relative changes of less than 2% significant wave height occur within the offshore Project and study area, beyond these extent, the relative change is less than 1%. There is little to no change to wave period anywhere within the offshore Project or study area, under all assessed wave conditions and directions (Figure 6-3, Figure 6-4 and Figure 6-5).

By way of comparison, the change to most extreme wave conditions (1 in 100 year return period events) are also shown in Figure 6-3, Figure 6-4 and Figure 6-5. In absolute terms, the degree of change and spatial extent of change



appear to be similar between the two wave conditions. However, in relative terms, the percentage change in wave height is less than 0.5% for the 1 in 100 year extreme waves.. Proportionately, an absolute change of 0.04 m in significant wave height is larger with respect to a smaller wave. This demonstrates that the larger waves that occur across the northwest Scottish continental shelf are less affected by the presence of the offshore Project. These waves are so large that they pass through the OAA largely unimpeded. The variation in percentage change can be seen across all modelled wave conditions in Appendix B.9.2.

A number of locations within the OAA and offshore ECC were selected to inform the baseline and post-construction characteristics across the offshore Project (see section 2.1.6) and enable assessment of the sediment transport potential. The wave properties at these metocean extraction locations (Figure 2-4) were extracted to contextualise the absolute change shown in Figure 6-3, Figure 6-4 and Figure 6-5. By way of example, the absolute change in Hs and Tp for the 50<sup>th</sup> percentile and 1 in 100-year waves, from all directions are shown in Table 6-3 for selected locations within the offshore Project area. The change represents the absolute difference in wave conditions before and after construction. The statistics within the table highlight the small degree of post-construction change in Hs, with little to no change occurring in Tp (Table 6-3), which supports the results shown in Figure 6-3, Figure 6-4 and Figure 6-5. Furthermore, there appears to be relatively little difference between the extent of change in the OAA versus the offshore ECC; overall, there is no consistent evidence to suggest that wave conditions within the OAA are more affected by the WTGs compared to the offshore ECC.

Table 6-3 Post-construction change in wave parameters at points within the offshore Project area (Layout 1) for the metocean extraction locations illustrated in Figure 2-4

ANALYSIS LOCATION	50 <sup>TH</sup> PERCENTILE WAVE		1 IN 100 YEAR WAVE	
	Hs (m)	Tp (s)	Hs (m)	Tp (s)
<b>North</b>				
OAA4	0	0.01	0	0
OAA10	-0.02	0	-0.02	0
ECC2	0	0	0.01	0
ECC4	0	0	0.01	0
ECC9 (Crosskirk)	0	0	0	0
ECC10 (Greeny Geo)	0	0	0	0
<b>Northwest</b>				
OAA4	-0.01	-0.01	-0.01	0
OAA10	-0.01	-0.02	-0.01	0
ECC2	0.02	-0.01	0.03	0
ECC4	0.01	-0.01	0.01	0
ECC9 (Crosskirk)	0.02	0	0	0



ANALYSIS LOCATION	50 <sup>TH</sup> PERCENTILE WAVE		1 IN 100 YEAR WAVE	
	Hs (m)	Tp (s)	Hs (m)	Tp (s)
ECC10 (Greeny Geo)	0	0	0	0
<b>West</b>				
OAA4	-0.02	0	-0.01	0
OAA10	0	0	0	0
ECC2	0.01	0	0.02	0
ECC4	0	0	0.01	0
ECC9 (Crosskirk)	0.01	0	0	0.01
ECC10 (Greeny Geo)	0	0	0	0.01

Spatially, the extent of change influenced by the windfarm is greatest for waves originating in the north and northwest. This is due to the orientation of these waves in relation to the foundations in Layout 1; north and northwest waves are perpendicular to the WTG layout. Waves from the west (Figure 6-5) are exposed to the narrower side of the WTG layout therefore the spatial increase in wave height due to the presence of the OWF is smaller. Figure 6-6 shows that the influence of the windfarm does generate a change in wave height that reaches the coastline of the Orkney Islands and Scottish mainland (depending on the direction of prevailing waves). However, as stated previously, the change in wave height is so small within the offshore Project, at less than 0.04 m, reducing even further beyond the study area to less than 0.02 m absolute change, meaning that it is imperceptible across the OAA, and even less so further afield. The same is considered to apply at the landfall locations at Crosskirk and Greeny Geo, represented by difference calculations for model observation locations ECC9 and ECC10 in Table 6-3, whereby the presence of the offshore WTG foundation structures within the OAA are not considered to change wave conditions at the coast. When considering the granularity and accuracy of the model at such low levels of change, in reality, the predicted change in absolute wave height of  $\leq 0.04$  m will not result in any difference to the wave regime overall. Consequently, there will be no impact on the coastline associated with this change in wave parameters. Overall, the change in significant wave height during the operational stage of the offshore Project, in absolute terms, is minimal and not be felt within the parameters of normal variation.



Waves originating from the north

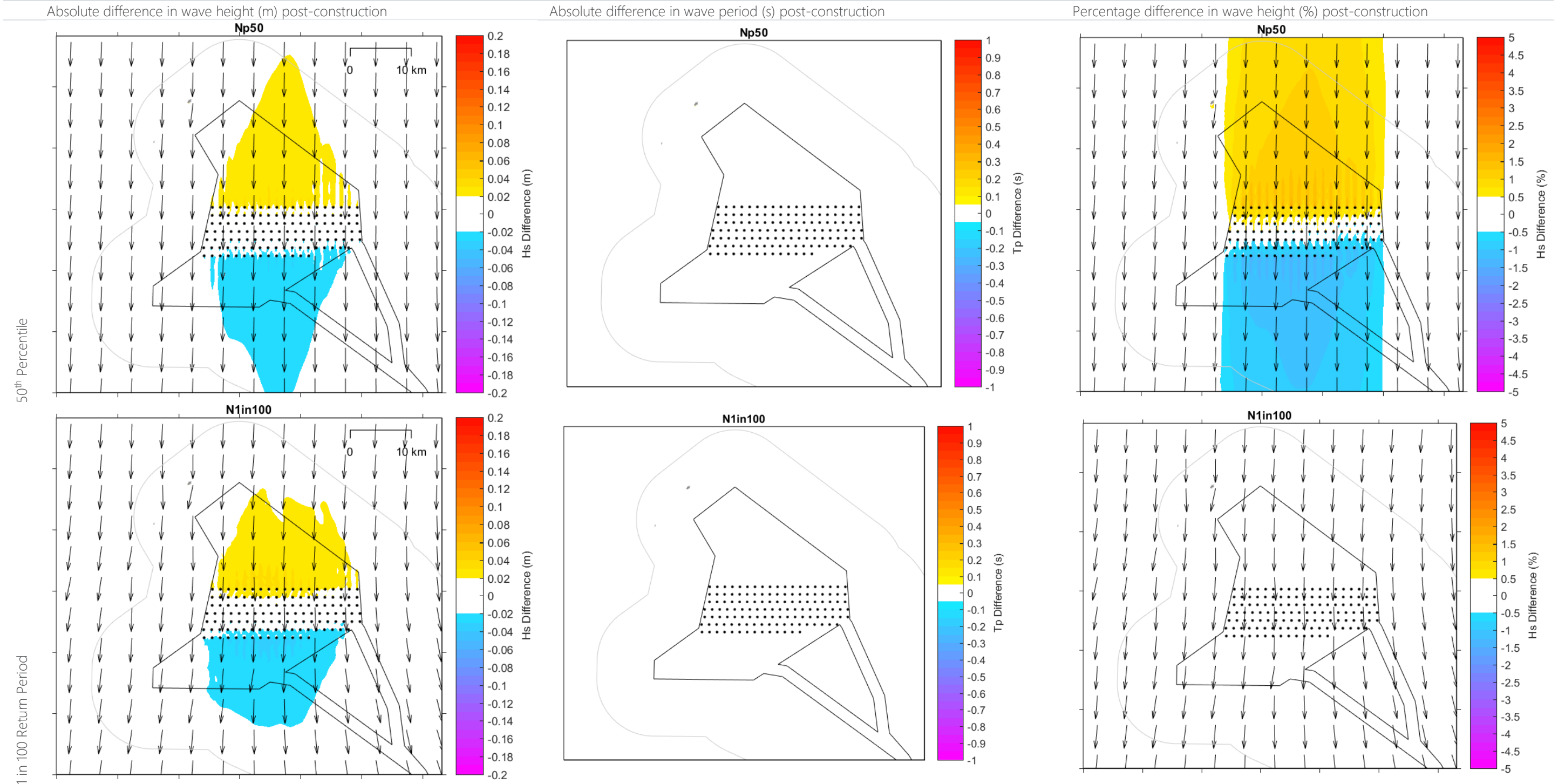


Figure 6-3 Potential change in waves originating from the north post-construction (Layout 1)



Waves originating from the northwest

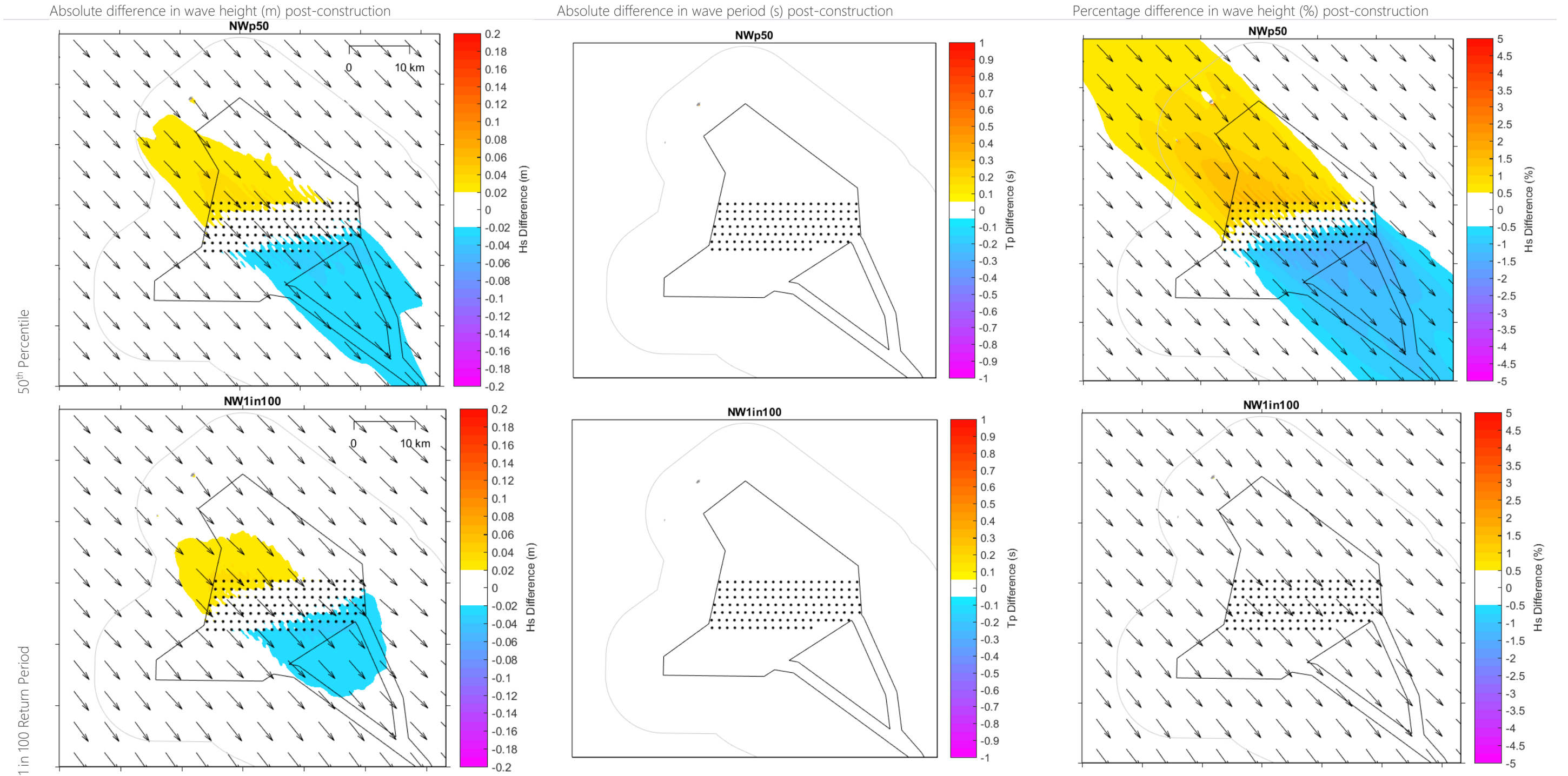


Figure 6-4 Potential change in waves originating from the northwest post-construction (Layout 1)



Waves originating from the west

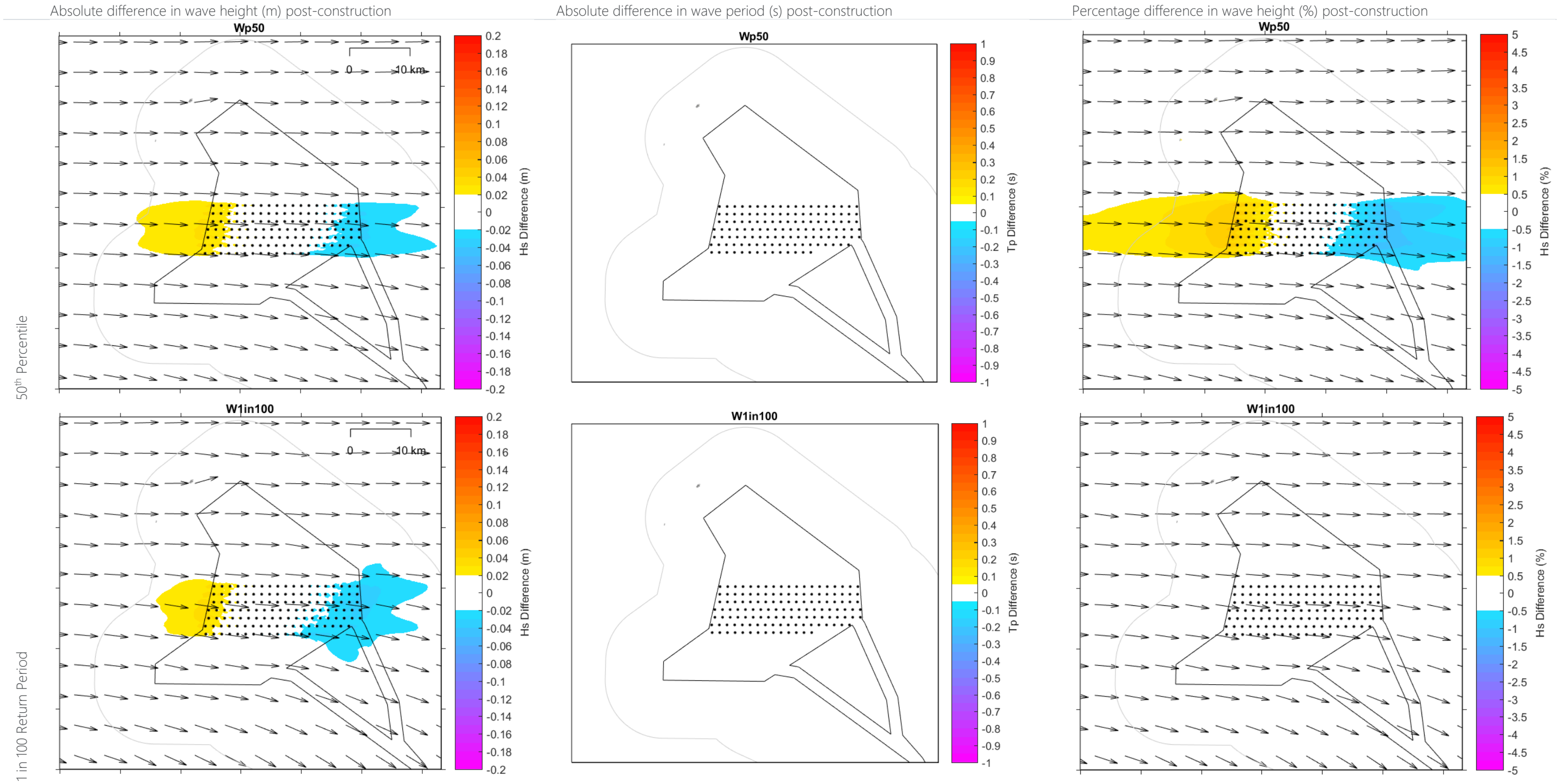
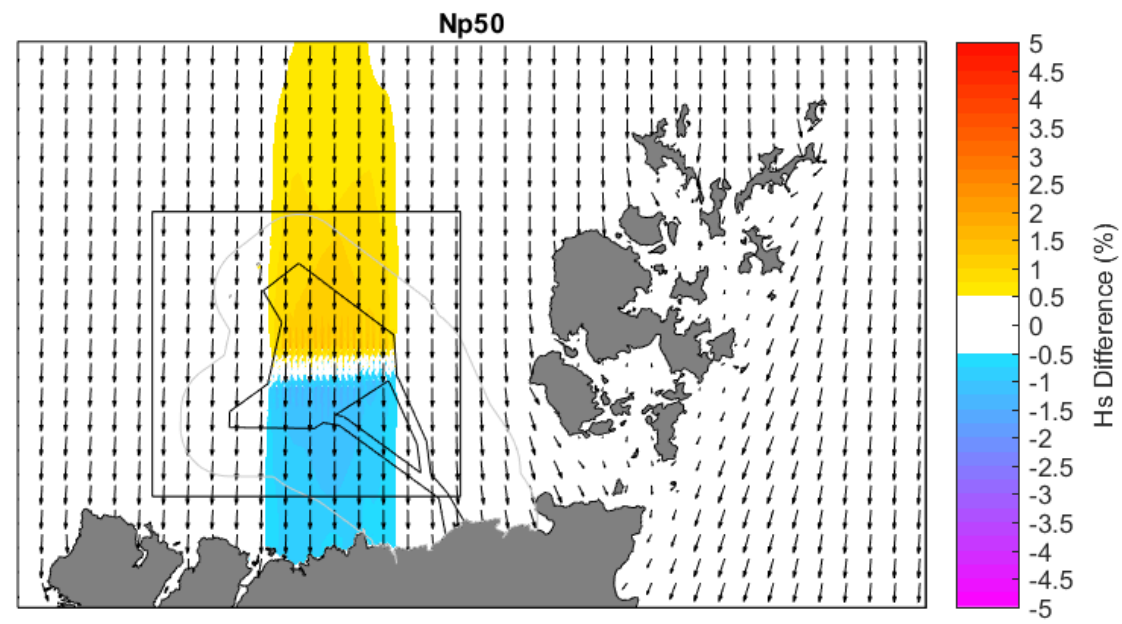


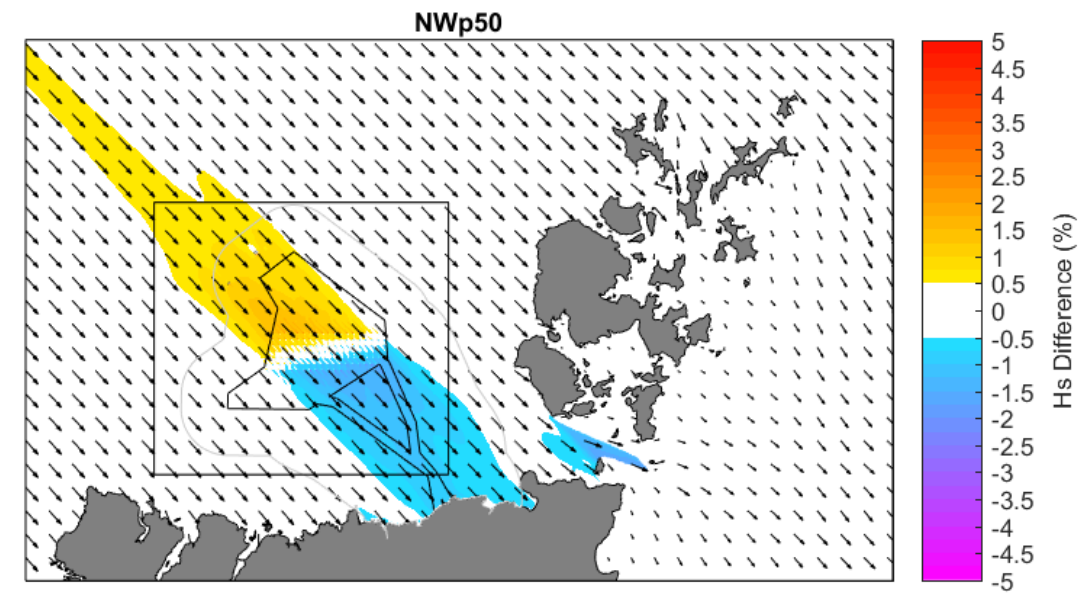
Figure 6-5 Potential change in waves originating from the west post-construction (Layout 1)



Waves originating from the north



Waves originating from the northwest



Waves originating from the west

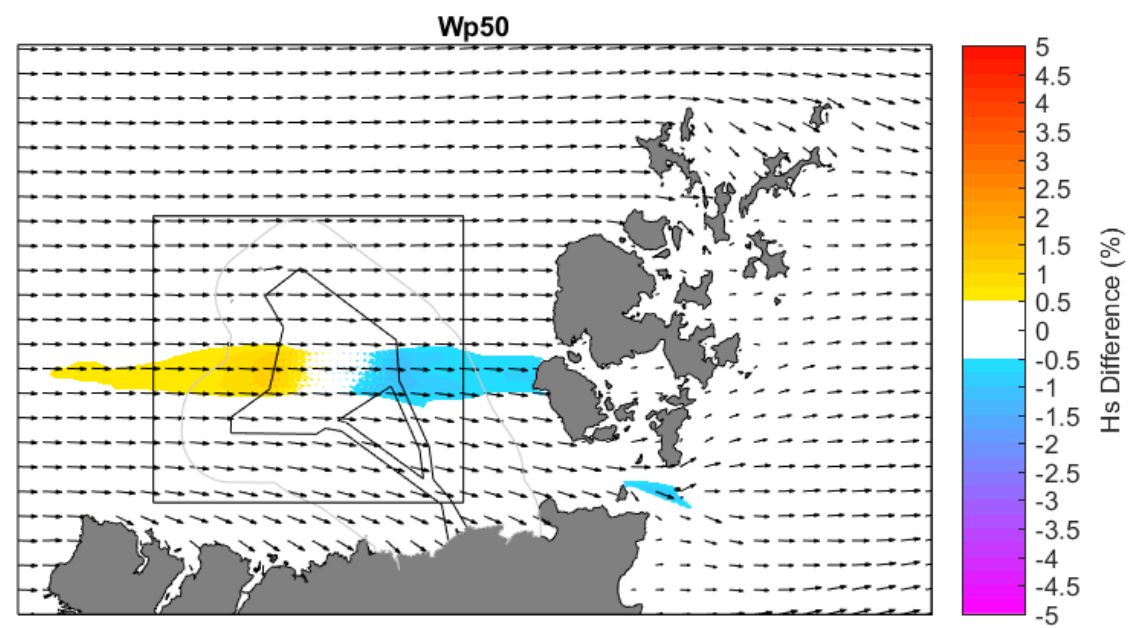


Figure 6-6 Post-construction percentage change in significant wave height of 50<sup>th</sup> percentile waves originating from the north, northwest, and west



## 6.2.2.2 Layout 2

The post-construction change in the wave climate differed spatially between the Layouts 1 and 2, although there is the marginal upstream increase and downstream decrease occurring as described for Layout 1. Figure 6-7, Figure 6-8 and Figure 6-9 illustrate the absolute change in significant wave height and period, and percentage change in significant wave height associated with Layout 2, when compared against baseline wave conditions (presented in Table 6-2). Figure 6-10 shows the post-construction percentage change in significant wave height within the wider regional context. Appendix B.9.3 shows the offshore Project area in the wider context and presents the full range of analysed wind conditions.

For all wave approach directions and conditions, the absolute change in significant wave height is again generally less than 0.06 m, with little to no change in the wave period (Figure 6-7, Figure 6-8 and Figure 6-9). Spatially, the extent of change associated with Layout 2 differs from Layout 1. With regards to waves originating from the north, the presence of the northern group of WTGs on the Stormy Bank appears to have a sheltering effect on waves to the south. There is very little absolute change in significant wave height (<0.04 m) to 50<sup>th</sup> percentile waves and 1 in 100 year waves. The marginally higher levels of change are focussed on the WTGs which protrude from the OAA in the northwest. When looking at the extent of change as a percentage, the change in significant wave height is again limited to less than 2% for 50<sup>th</sup> percentile waves and is even smaller for the extreme 1 in 100 year waves at less than 0.5% relative change.

For waves originating from the northwest and west, the degree of change is similar in scale; however, the spatial extent varies in line with the prevailing wave direction. Interestingly, for the 1 in 100 year waves coming from the northwest and west, the percentage change is <0.25% as it has not been visually captured in Figure 6-8 and Figure 6-9, thereby indicating a small absolute change. This further enforces that the scale of change identified by the model is so marginal that it will not be felt within the parameters of normal variation.

As with Layout 1, per Figure 6-10, changes to the wave parameters do appear to extend to shore. However, as before, the scale of change is such that there will be no change to the wave regime within the offshore Project area, nor along the coast.

The full suite of model outputs for Layout 2, as shown in Appendix B.9.3, picks up some change in wave period outside of the study area, although as described in section 6.1.2.2.1, modelled changes at the coast relate to the wetting and drying of the West of Orkney model grid cells at the coast, and is not attributable to the presence of the WTGs. Such fluctuations are expected within the modelling process in areas where flooding and drying might occur. As the scale of change is beyond the level of accuracy of the model, it is hard to discern any impacts as being due to the WTG structures considering that, in reality, changes at this scale would not be measurable in the marine environment.

The wave properties at a number of model observation locations were extracted to contextualise the absolute change shown in Figure 6-7 to Figure 6-10. By way of example, the absolute change in  $H_s$  and  $T_p$  for the 50<sup>th</sup> percentile and 1 in 100-year waves, from all directions are shown in Table 6-4 for selected locations within the offshore Project area. The change represents the absolute difference in wave conditions before and after construction. These statistics highlight how small the extent of change is in the post-construction wave parameters (Table 6-4). This reflects the model outputs visualised in Figure 6-7, Figure 6-8, Figure 6-9, and Figure 6-10. Additionally, the extent of change is



consistent between the OAA and offshore ECC. Therefore, the evidence suggests that the presence of WTGs will not result in perceptible changes to the local wave regime. As for Layout 1, little to no changes are considered to occur to waves at the landfall locations at Crosskirk and Greeny Geo based on the presence of the offshore WTG foundation structures, represented by difference calculations for model observation locations ECC9 and ECC10 in Table 6-4.

Table 6-4 Post-construction changes in wave parameters at points within the offshore Project area (Layout 2), for the metocean extraction locations illustrated in Figure 2-4

ANALYSIS LOCATION	50 <sup>TH</sup> PERCENTILE WAVE		1 IN 100 YEAR WAVE	
	Hs (m)	Tp (s)	Hs (m)	Tp (s)
<b>North</b>				
OAA4	0	0	0.01	0
OAA10	-0.02	0	-0.02	0
ECC2	0	0	0.01	0
ECC4	0	0	0	0
ECC9 (Crosskirk)	0	0	0	0
ECC10 (Greeny Geo)	0	0	0	0
<b>Northwest</b>				
OAA4	0	0	0	0
OAA10	-0.01	0	0	0
ECC2	0.02	0	0.02	0
ECC4	0	0	0.01	0
ECC9 (Crosskirk)	0	0	0	0
ECC10 (Greeny Geo)	0	0	0	0
<b>West</b>				
OAA4	-0.02	0	-0.01	0
OAA10	0.01	0	0.01	0
ECC2	0.02	0	0.02	0
ECC4	0	0	0.01	0
ECC9 (Crosskirk)	0	0	0	0.01
ECC10 (Greeny Geo)	0	0	0	0.01



Waves originating from the north

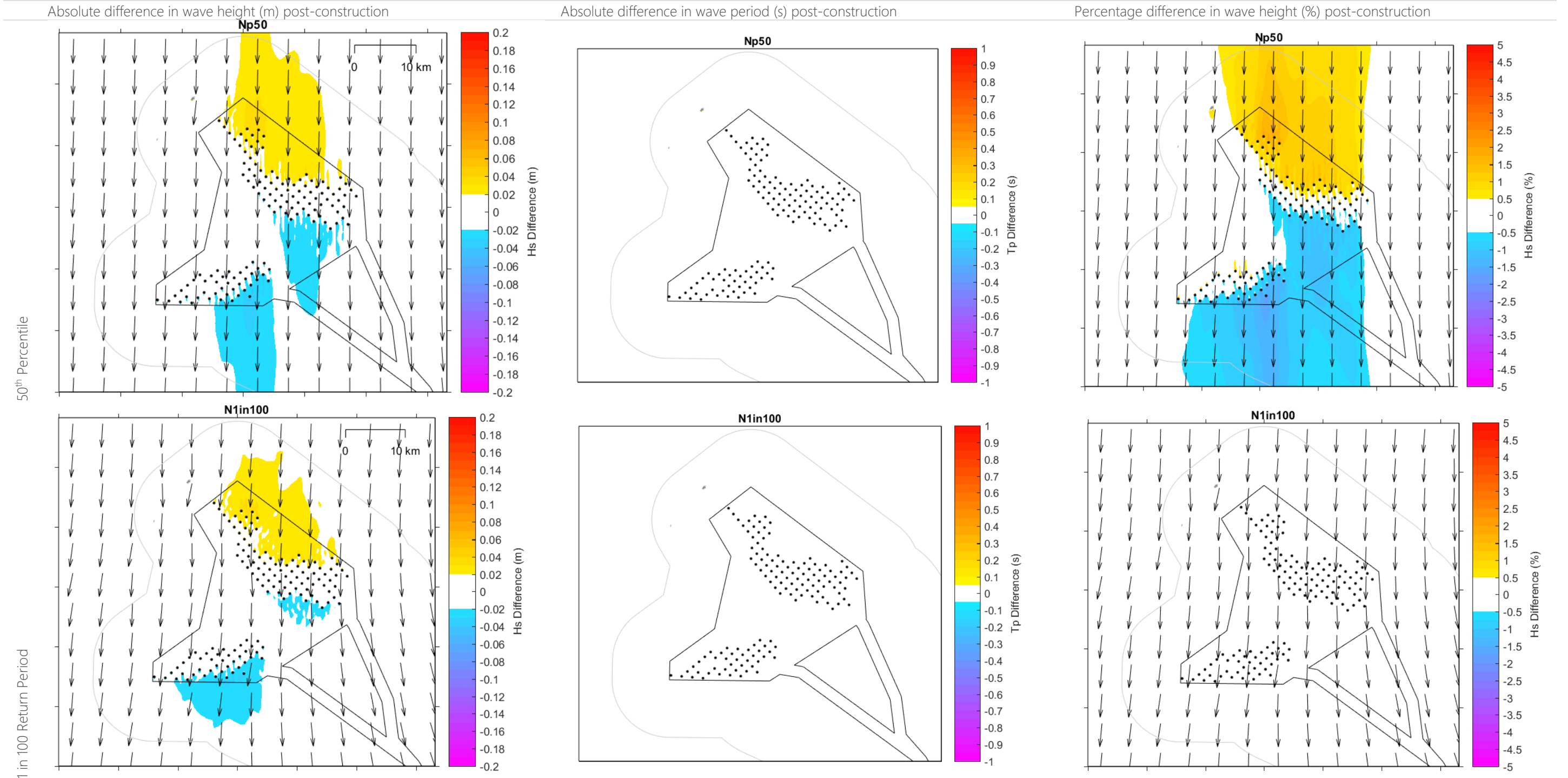


Figure 6-7 Potential change in waves originating from the north post-construction (Layout 2)



Waves originating from the northwest

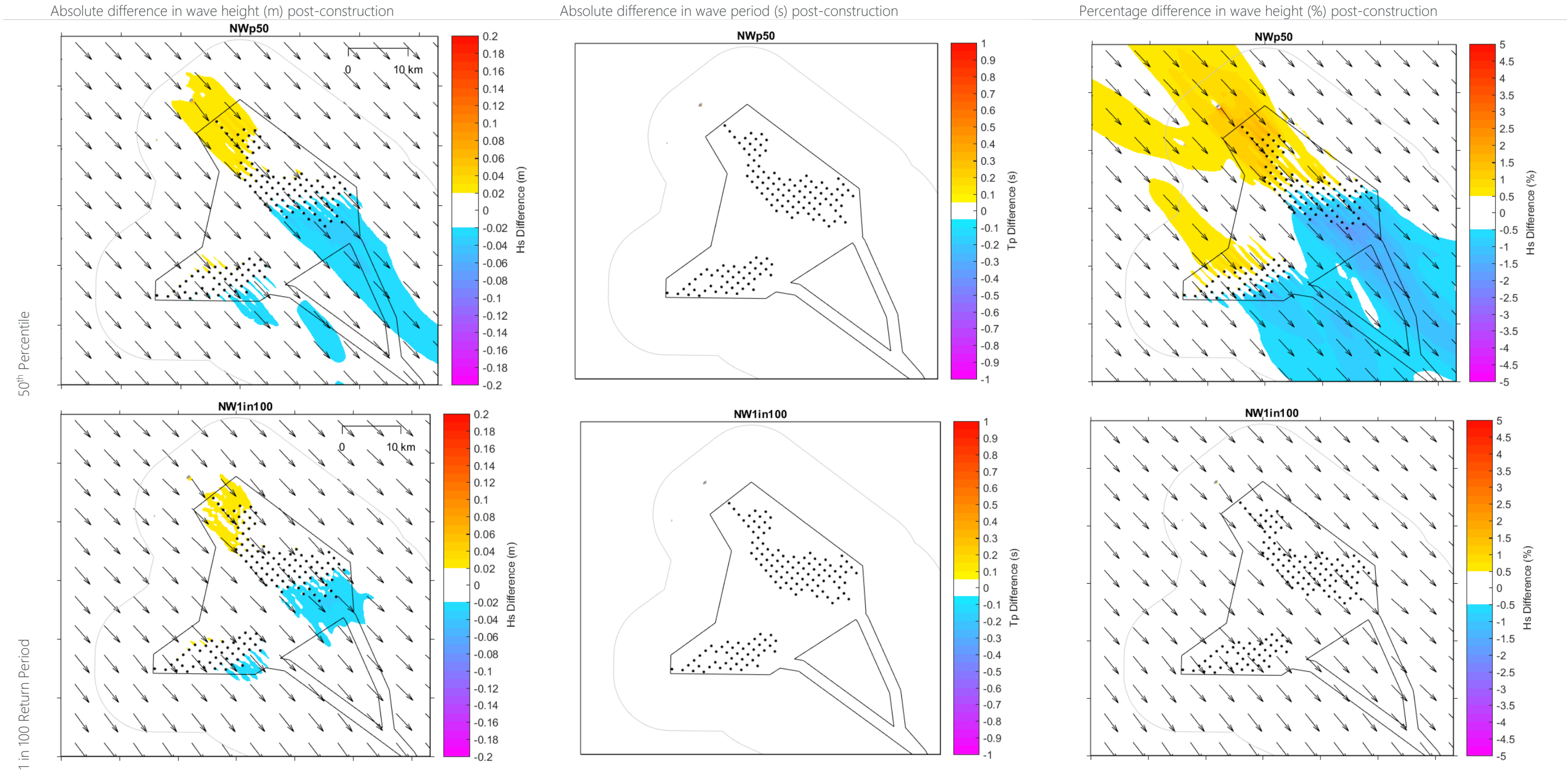


Figure 6-8 Potential change in waves originating from the northwest post-construction (Layout 2)



Waves originating from the west

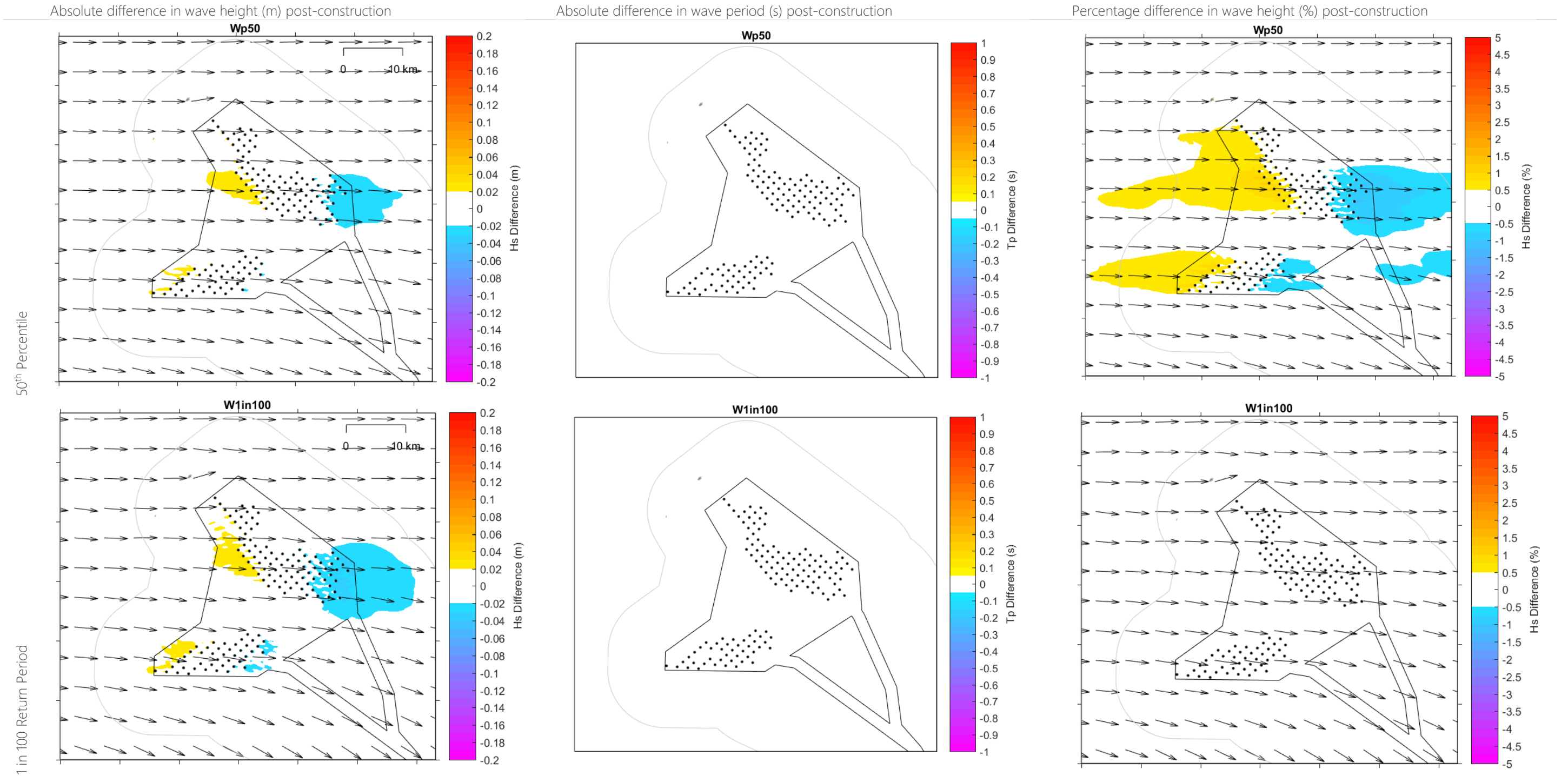
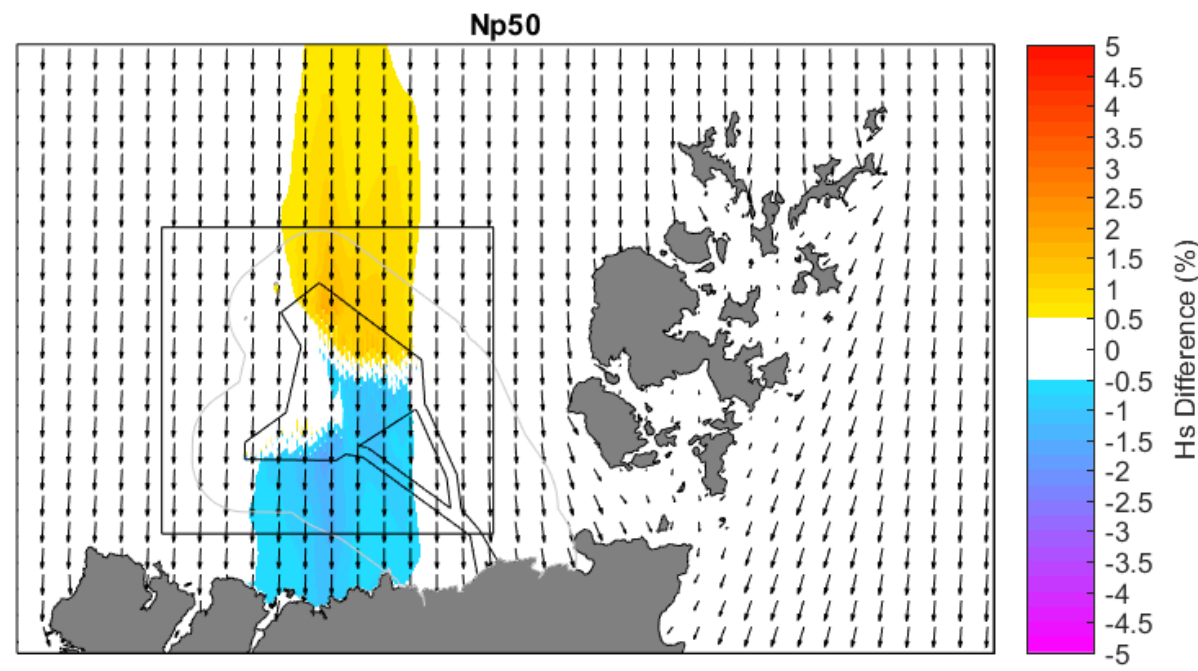


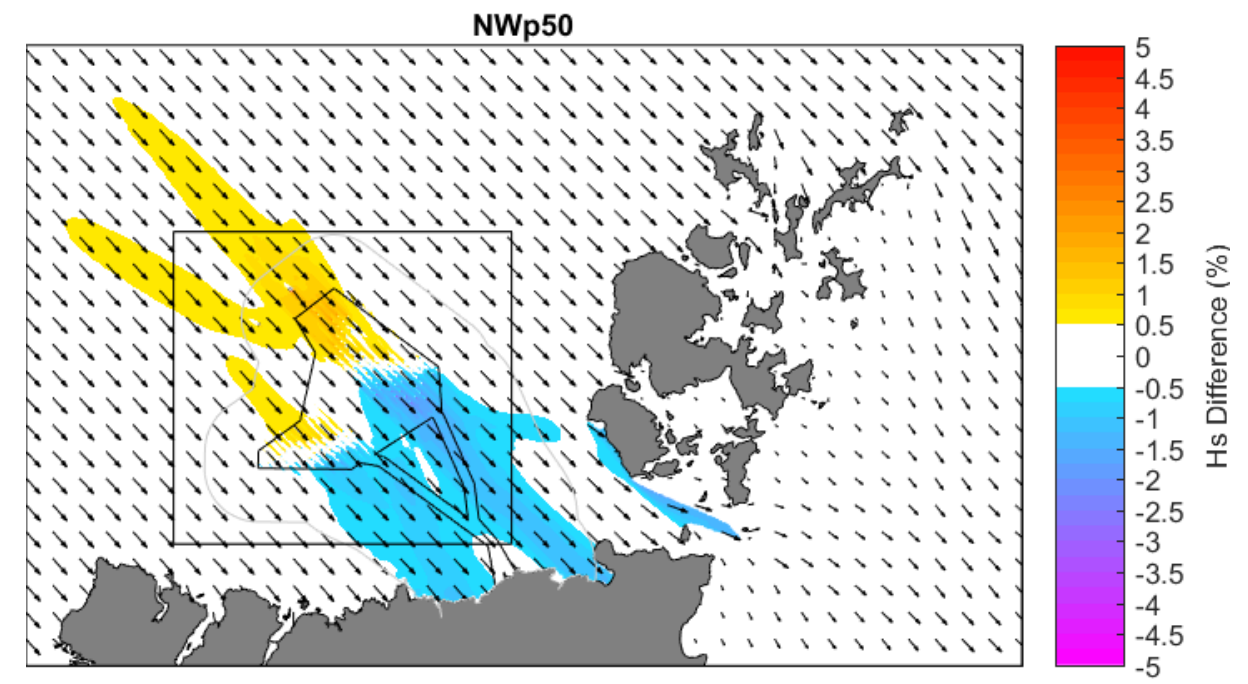
Figure 6-9 Potential change in waves originating from the west post-construction (Layout 2)



Waves originating from the north



Waves originating from the northwest



Waves originating from the west

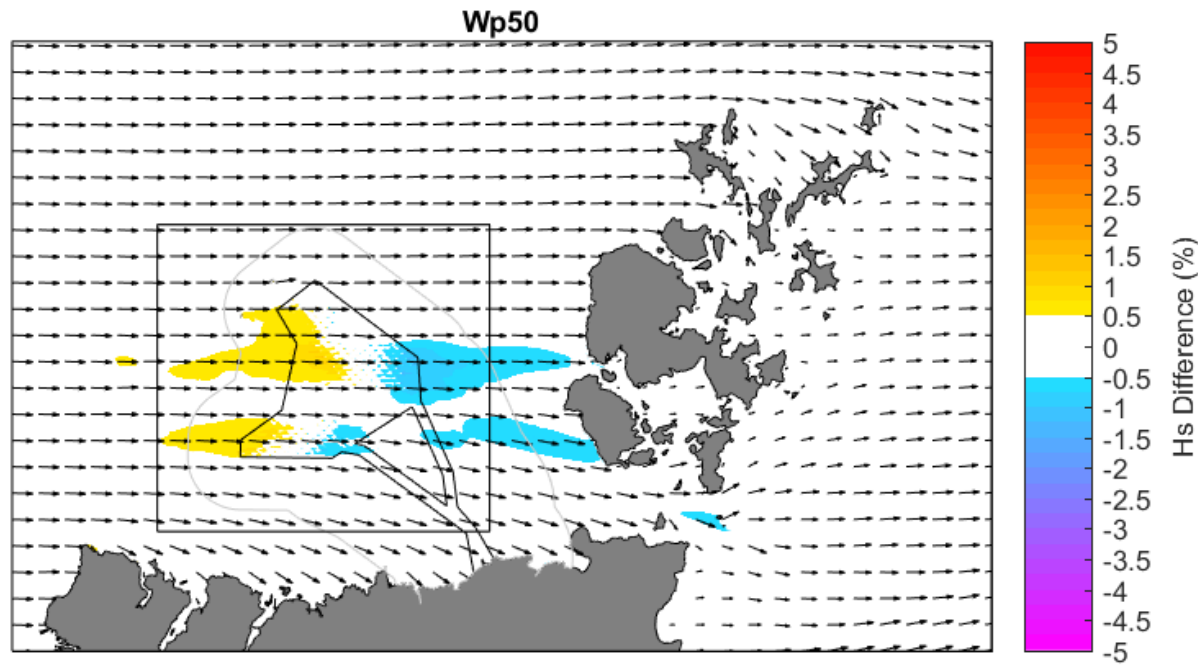


Figure 6-10 Post-construction percentage change in significant wave height of 50<sup>th</sup> percentile waves originating from the north, northwest, and west



## 6.3 Potential Changes to Sediment Transport

### 6.3.1 Overview

The metocean conditions characteristic of the offshore Project area are responsible for sediment transport processes, including as bed load or suspended load (sections 3.6.2, 3.7.2, 3.8.2, 3.9.2 and 3.9.2). Based on the wave and tidal properties across the offshore Project area, there is the potential for sediment mobility as reflected in the sediment transport baseline characterisation (section 3.9.2), with currents being the primary driver. In isolation, currents were able to generate sediment mobility of fine, medium and coarse sands across most locations within the OAA; this is consistent with morphological features identified within the offshore Project area as described in section 3.5.2. Sediment transport was most likely on spring tides than on peak neap tides. At some locations within the OAA and offshore ECC, wave conditions alone were also able to generate sediment mobility (due to larger waves being able to pick up sediments). Within the offshore ECC, sediment mobility is greater close to the coast. Finer sediments are mobile up to 61% of the time in some locations, with medium and coarse sands only just less mobile. Assessments of the potential changes to sediment transport across offshore locations associated with the OAA and offshore ECC are presented in section 6.3.2 below. The potential onward implications of changes to sediment transport at the landfalls and to the coastal morphology are considered in section 6.6.

### 6.3.2 Assessment

In section 3.9.2, the percentage mobility according to different sediment sizes at the different analysed locations within the offshore Project area were presented for selected model observation locations (Figure 2-4), flows and waves (Table 3-13 and Table 3-14). The following analysis generated a similar output allowing comparison between the baseline sediment transport conditions and the post-construction conditions.

The process to determine the sediment transport was the same as in section 3.9.2 for the baseline conditions. The baseline sediment transport was established using flows extracted from the model and set wave parameters. The baseline sediment transport was based on time-series flows obtained from the model, the most frequently occurring wave (1.5 m, 9.5 s) and the omni-directional mean wave properties (2.6 m, 11 s) informed by the decadal timeseries from wave hindcast 1. These wave parameters were thought to be universal in capturing the conditions across the whole offshore Project area. In order to ensure that pre- and post-construction conditions can be directly compared, these wave parameters were maintained for the post-construction sediment transport analysis. The omni-directional mean wave statistic includes some of the more extreme wave conditions. Therefore, it is likely that this will capture any changes in post-construction waves. Particularly given the minimal changes in waves predicted post-construction, as described in section 6.2.2. For the post-construction assessment, the model flows at the extracted locations within the offshore Project area were obtained for post-construction (i.e. operational) conditions.

Operational changes to tides and waves on the whole are considered in sections 6.1 and 6.2 respectively. Ultimately, the magnitude of change in flows and waves is so small locally that there is no perceptible change to metocean conditions overall at the offshore Project scale and regionally. Consequently, it is unlikely that there will be any change to sediment transport. The findings of the assessment are described in section 6.3.2.1 below.



### 6.3.2.1 Changes to Sediment Transport as a Result of Changes to Flows and Waves

The post-construction sediment transport mobility indicates that there is very little change across the board. Table 6-5 and Table 6-6 present the equivalent operational results to the baseline conditions in Table 3-13 and Table 3-14 respectively under Layout 1. The two tables show the differing results according to the two different wave conditions (the most frequently occurring wave and the omni-directional mean wave respectively). Table 6-7 and Table 6-8 present the equivalent data for Layout 2. The overall trends in sediment mobility remain the same between the pre- and post-construction conditions.

At only two locations there is a marginal change in mobility of fine sediments by a maximum of  $\pm 1\%$ . Changes are consistent across all sediment sizes meaning generally, an increase in sediment transport is exhibited equally across all sediments. Under baseline conditions gravels were never mobile (except at the landfalls in relation to waves), this remains true under operational conditions. Changes in sediment transport during the operational stage of the Project occur at OAA3 (under Layout 1) and OAA9 (under Layout 2). These changes are both seen under the most frequently occurring wave conditions. An increase of 1% is observed at OAA3 and a decrease of 1% is observed at OAA9. No change was identified within the offshore ECC.

The change at these two locations within the OAA is attributed to a very marginal difference in the mobility of fine sands. At OAA3, mobility occurred during 773 instances (out of 2,305) during the 16-day assessment period. This is an increase from 771 instances under baseline conditions. OAA3 is located close to the southern extent of the WTGs, but not within the OAA itself, under Layout 1. The observation point location also does not correspond to the areas in Figure 6-1 or Figure 6-2 that illustrate small reductions in post construction residual flows).

OAA9 is located to the northeast of the WTGs in Layout 2, and is not located in the midst of the WTGs. The change in sediment transport at OAA9 under the Layout 2 scenario is due to a decrease in instances of mobility of fine sands from 1,166 (under baseline conditions) to 1,162 (post-construction). These four instances represent 40 minutes within the 15-day assessment period during which sediment transport of fine sands was marginally below recorded baseline levels. As described in section 6.1.2.2, changes in tidal flows were observed to have a slight change in range at OAA9 when compared to baseline conditions, amongst other locations. This change in flows is clearly reflected in the change in sediment transport. Although it is important to emphasise the very small degree of change. Overall, there is no real change in sediment transport across the offshore Project area. At the two observation points where change is seen, it is very limited in scale. Furthermore, because only two points showed any change before versus after construction, it is not possible to draw any consistent relationship between these changes and the presence of the WTGs, in either layout.



Table 6-5 Post-construction sediment mobility potential (Layout 1) at analysed locations across the offshore Project area using model-extracted time series flows and a wave with a height of 1.5 m and a period of 9.5 s; mobility potential is given as a percentage of time for varying sediment

SEABED SEDIMENT	FINE SAND	MEDIUM SAND	COARSE SAND	VERY FINE GRAVEL	FINE GRAVEL	MEDIUM GRAVEL	
SEDIMENT SIZE (MM)	0.175	0.35	0.63	3	6	11	
OAA3 (69 mLAT)	Currents only	27%	19%	8%	0%	0%	0%
		Mobile spring and peak neap tides, not mobile at lowest neaps	Mobile spring tides only	Mobile spring tides only	Not mobile	Not mobile	Not mobile
	Waves only	0%	0%	0%	0%	0%	0%
		Not mobile	Not mobile	Not mobile	Not mobile	Not mobile	Not mobile
Currents and waves	34%	25%	12%	0%	0%	0%	
	Mobile spring and peak neap tides, not mobile at lowest neaps	Mobile spring and peak neap tides, not mobile at lowest neaps	Mobile spring tides only	Not mobile	Not mobile	Not mobile	
OAA4 (69 mLAT)	Currents only	31%	23%	12%	0%	0%	0%
		Mobile spring and peak neap tides, not mobile at lowest neaps	Mobile spring tides, not mobile at lowest neaps	Mobile peak spring tides	Not mobile	Not mobile	Not mobile
	Waves only	0%	0%	0%	0%	0%	0%
		Not mobile	Not mobile	Not mobile	Not mobile	Not mobile	Not mobile
Currents and waves	37%	28%	16%	0%	0%	0%	
	Mobile spring and peak neap tides, not mobile at lowest neaps	Mobile spring tides, not mobile at lowest neaps	Mobile peak spring tides	Not mobile	Not mobile	Not mobile	
OAA7 (54 mLAT)	Currents only	39%	32%	20%	0%	0%	0%
		Mobile spring and peak neap tides, not mobile at lowest neaps	Mobile spring and peak neap tides, not mobile at lowest neaps	Mobile spring tides, not mobile at lowest neaps	Not mobile	Not mobile	Not mobile
	Waves only	100%	100%	9%	0%	0%	0%
		Always mobile	Always mobile	Always mobile	Not mobile	Not mobile	Not mobile
Currents and waves	50%	41%	29%	0%	0%	0%	
	Mobile spring and peak neap tides, not mobile at lowest neaps	Mobile spring and peak neap tides, not mobile at lowest neaps	Mobile spring tides, not mobile at lowest neaps	Not mobile	Not mobile	Not mobile	
OAA9 (54 mLAT)	Currents only	36%	28%	16%	0%	0%	0%
		Mobile spring and peak neap tides, not mobile at lowest neaps	Mobile spring and peak neap tides, not mobile at lowest neaps	Mobile spring tides only	Not mobile	Not mobile	Not mobile
	Waves only	0%	0%	0%	0%	0%	0%
		Not mobile	Not mobile	Not mobile	Not mobile	Not mobile	Not mobile
Currents and waves	51%	40%	26%	0%	0%	0%	
	Mobile spring and peak neap tides, not mobile at lowest neaps	Mobile spring and peak neap tides, not mobile at lowest neaps	Mobile spring tides only	Not mobile	Not mobile	Not mobile	
OAA10 (69 mLAT)	Currents only	20%	11%	1%	0%	0%	0%
		Mobile only peak spring tides	Mobile only peak spring tides	Mobile only peak spring tides	Not mobile	Not mobile	Not mobile
	Waves only	0%	0%	0%	0%	0%	0%
		Not mobile	Not mobile	Not mobile	Not mobile	Not mobile	Not mobile
Currents and waves	27%	17%	4%	0%	0%	0%	
	Mobile spring and peak neap tides, not mobile at lowest neaps	Mobile only peak spring tides	Mobile only peak spring tides	Not mobile	Not mobile	Not mobile	
OAA11 (63 mLAT)	Currents only	20%	12%	0%	0%	0%	0%
		Mobile only peak spring tides	Mobile only peak spring tides	Not mobile	Not mobile	Not mobile	Not mobile
	Waves only	0%	0%	0%	0%	0%	0%
		Not mobile	Not mobile	Not mobile	Not mobile	Not mobile	Not mobile
Currents and waves	29%	19%	5%	0%	0%	0%	
	Mobile only peak spring tides	Mobile only peak spring tides	Mobile only peak spring tides	Not mobile	Not mobile	Not mobile	
ECC1 (83 mLAT)	Currents only	31%	24%	12%	0%	0%	0%
		Mobile spring and peak neap tides, not mobile at lowest neaps	Mobile spring and peak neap tides, not mobile at lowest neaps	Mobile peak spring tides only	Not mobile	Not mobile	Not mobile
	Waves only	0%	0%	0%	0%	0%	0%
		Not mobile	Not mobile	Not mobile	Not mobile	Not mobile	Not mobile
Currents and waves	34%	26%	14%	0%	0%	0%	
	Mobile spring and peak neap tides, not mobile at lowest neaps	Mobile spring and peak neap tides, not mobile at lowest neaps	Mobile peak spring tides only	Not mobile	Not mobile	Not mobile	
ECC2		19%	10%	0%	0%	0%	



SEABED SEDIMENT		FINE SAND	MEDIUM SAND	COARSE SAND	VERY FINE GRAVEL	FINE GRAVEL	MEDIUM GRAVEL
SEDIMENT SIZE (MM)		0.175	0.35	0.63	3	6	11
<b>(98 mLAT)</b>	Currents only	Mobile peak spring tides only	Mobile peak spring tides only	Not mobile	Not mobile	Not mobile	Not mobile
	Waves only	0%	0%	0%	0%	0%	0%
		Not mobile	Not mobile	Not mobile	Not mobile	Not mobile	Not mobile
Currents and waves	20%	11%	1%	0%	0%	0%	
	Mobile peak spring tides only	Mobile peak spring tides only	Mobile peak spring tides only	Mobile peak spring tides only	Not mobile	Not mobile	Not mobile
<b>ECC3 (95 mLAT)</b>	Currents only	37%	29%	17%	0%	0%	0%
		Mobile spring and peak neap tides, not mobile at lowest neaps	Mobile spring tide only	Mobile peak spring tides only	Not mobile	Not mobile	Not mobile
	Waves only	0%	0%	0%	0%	0%	0%
		Not mobile	Not mobile	Not mobile	Not mobile	Not mobile	Not mobile
Currents and waves	38%	30%	18%	0%	0%	0%	
	Mobile spring and peak neap tides, not mobile at lowest neaps	Mobile spring tide only	Mobile peak spring tides only	Not mobile	Not mobile	Not mobile	
<b>ECC4 (56 mLAT)</b>	Currents only	54%	46%	33%	0%	0%	0%
		Mobile spring and peak neap tides, not mobile at lowest neaps	Mobile spring and peak neap tides, not mobile at lowest neaps	Mobile spring and peak neap tides, not mobile at lowest neaps	Not mobile	Not mobile	Not mobile
	Waves only	0%	0%	0%	0%	0%	0%
		Not mobile	Not mobile	Not mobile	Not mobile	Not mobile	Not mobile
Currents and waves	63%	56%	42%	0%	0%	0%	
	Mobile spring and peak neap tides, not mobile at lowest neaps	Mobile spring and peak neap tides, not mobile at lowest neaps	Mobile spring and peak neap tides, not mobile at lowest neaps	Not mobile	Not mobile	Not mobile	
<b>ECC9 (10 mLAT)</b>	Currents only	0%	0%	0%	0%	0%	0%
		Not mobile	Not mobile	Not mobile	Not mobile	Not mobile	Not mobile
	Waves only	100%	100%	100%	34%	0%	0%
		Always mobile	Always mobile	Always mobile	Partially mobile	Not mobile	Not mobile
Currents and waves	62%	49%	19%	0%	0%	0%	
	Mobile during faster flows	Mobile only during periods of fastest tidal (spring and neap) flows	Mobile only during periods of fastest spring tidal flows	Not mobile	Not mobile	Not mobile	
<b>ECC10 (10 mLAT)</b>	Currents only	0%	0%	0%	0%	0%	0%
		Not mobile	Not mobile	Not mobile	Not mobile	Not mobile	Not mobile
	Waves only	100%	100%	100%	34%	0%	0%
		Always mobile	Always mobile	Always mobile	Partially mobile	Not mobile	Not mobile
Currents and waves	46%	29%	10%	0%	0%	0%	
	Mobile during faster flows	Mobile only during periods of fastest tidal (spring and neap) flows	Mobile only during periods of fastest spring tidal flows	Not mobile	Not mobile	Not mobile	

The current time series is for a 15-day period between 16/01/2013 and 31/01/2013, covering a spring neap tidal cycle post-construction. Data was extracted from a number of locations across the project area with only a few are presented to demonstrate the potential for any spatial variability, water depths associated with each assessed location was applied in calculating the sediment transport potential. For the analytical scenarios with currents and waves, the same current time series was applied with a single consistent wave with a  $H_s$  of 1.5 m and  $T_p$  of 9.5 seconds, consistent for the entire spring neap tidal cycle.



Table 6-6 Post-construction sediment mobility potential (Layout 1) at analysed locations across the offshore Project area using model-extracted time series flows and a wave with a height of 2.6 m and a period of 11 s; mobility potential is given as a percentage

SEABED SEDIMENT		FINE SAND	MEDIUM SAND	COARSE SAND	VERY FINE GRAVEL	FINE GRAVEL	MEDIUM GRAVEL
SEDIMENT SIZE (MM)		0.175	0.35	0.63	3	6	11
OAA3 (69 mLAT)	Currents only	27%	19%	8%	0%	0%	0%
		Mobile spring and peak neap tides, not mobile at lowest neaps	Mobile spring tides only	Mobile spring tides only	Not mobile	Not mobile	Not mobile
	Waves only	100%	22%	0%	0%	0%	0%
		Always mobile	Mobile spring tides only	Not mobile	Not mobile	Not mobile	Not mobile
	Currents and waves	46%	35%	22%	0%	0%	0%
		Mobile spring and peak neap tides, not mobile at lowest neaps	Mobile spring and peak neap tides, not mobile at lowest neaps	Mobile spring tides only	Not mobile	Not mobile	Not mobile
OAA4 (69 mLAT)	Currents only	31%	23%	12%	0%	0%	0%
		Mobile spring and peak neap tides, not mobile at lowest neaps	Mobile spring tides only	Mobile spring tides only	Not mobile	Not mobile	Not mobile
	Waves only	100%	21%	0%	0%	0%	0%
		Always mobile	Mobile spring tides only	Not mobile	Not mobile	Not mobile	Not mobile
	Currents and waves	50%	40%	26%	0%	0%	0%
		Mobile spring and peak neap tides, not mobile at lowest neaps	Mobile spring and peak neap tides, not mobile at lowest neaps	Mobile spring tides only	Not mobile	Not mobile	Not mobile
OAA7 (54 mLAT)	Currents only	39%	32%	20%	0%	0%	0%
		Mobile spring and peak neap tides, not mobile at lowest neaps	Mobile spring and peak neap tides, not mobile at lowest neaps	Mobile spring tides only	Not mobile	Not mobile	Not mobile
	Waves only	100%	100%	100%	0%	0%	0%
		Always mobile	Always mobile	Always mobile	Not mobile	Not mobile	Not mobile
	Currents and waves	62%	54%	40%	0%	0%	0%
		Mobile spring and peak neap tides, not mobile at lowest neaps	Mobile spring and peak neap tides, not mobile at lowest neaps	Mobile spring and peak neap tides, not mobile at lowest neaps	Not mobile	Not mobile	Not mobile
OAA9 (54 mLAT)	Currents only	36%	28%	16%	0%	0%	0%
		Mobile spring and peak neap tides, not mobile at lowest neaps	Mobile spring and peak neap tides, not mobile at lowest neaps	Mobile spring tides only	Not mobile	Not mobile	Not mobile
	Waves only	100%	100%	100%	0%	0%	0%
		Always mobile	Always mobile	Always mobile	Not mobile	Not mobile	Not mobile
	Currents and waves	65%	56%	39%	0%	0%	0%
		Mobile spring and peak neap tides, not mobile at lowest neaps	Mobile spring and peak neap tides, not mobile at lowest neaps	Mobile spring and peak neap tides, not mobile at lowest neaps	Not mobile	Not mobile	Not mobile
OAA10 (69 mLAT)	Currents only	20%	11%	1%	0%	0%	0%
		Mobile spring tides only	Mobile spring tides only	Mobile peak spring tides only	Not mobile	Not mobile	Not mobile
	Waves only	0%	0%	0%	0%	0%	0%
		Not mobile	Not mobile	Not mobile	Not mobile	Not mobile	Not mobile
	Currents and waves	39%	29%	14%	0%	0%	0%
		Mobile spring and peak neap tides, not mobile at lowest neaps	Mobile spring and peak neap tides, not mobile at lowest neaps	Mobile spring tides only	Not mobile	Not mobile	Not mobile
OAA11 (63 mLAT)	Currents only	20%	12%	0%	0%	0%	0%
		Mobile on spring tides only	Mobile on spring tides only	Not mobile	Not mobile	Not mobile	Not mobile
	Waves only	94%	0%	0%	0%	0%	0%
		Mobile spring and peak neap tides, not mobile at lowest neaps	Not mobile	Not mobile	Not mobile	Not mobile	Not mobile
	Currents and waves	42%	32%	16%	0%	0%	0%
		Mobile spring and peak neap tides, not mobile at lowest neaps	Mobile spring and peak neap tides, not mobile at lowest neaps	Mobile on spring tides only	Not mobile	Not mobile	Not mobile
ECC1 (83 mLAT)	Currents only	31%	24%	12%	0%	0%	0%
		Mobile spring and peak neap tides, not mobile at lowest neaps	Mobile spring tides only	Mobile spring tides only	Not mobile	Not mobile	Not mobile
	Waves only	0%	0%	0%	0%	0%	0%
		Not mobile	Not mobile	Not mobile	Not mobile	Not mobile	Not mobile
	Currents and waves	43%	34%	21%	0%	0%	0%
		Mobile spring and peak neap tides, not mobile at lowest neaps	Mobile spring tides only	Mobile spring tides only	Not mobile	Not mobile	Not mobile



SEABED SEDIMENT	FINE SAND	MEDIUM SAND	COARSE SAND	VERY FINE GRAVEL	FINE GRAVEL	MEDIUM GRAVEL
SEDIMENT SIZE (MM)	0.175	0.35	0.63	3	6	11
Currents and waves	Mobile spring and peak neap tides, not mobile at lowest neaps	Mobile spring and peak neap tides, not mobile at lowest neaps	Mobile spring tides only	Not mobile	Not mobile	Not mobile
ECC2 (98 mLAT)	Currents only	19%	10%	0%	0%	0%
		Mobile spring tides only	Mobile peak spring tides only	Not mobile	Not mobile	Not mobile
	Waves only	0%	0%	0%	0%	0%
		Not mobile	Not mobile	Not mobile	Not mobile	Not mobile
Currents and waves	27%	18%	4%	0%	0%	0%
		Mobile spring tides only	Mobile peak spring tides only	Mobile peak spring tides only	Not mobile	Not mobile
ECC3 (95 mLAT)	Currents only	37%	29%	17%	0%	0%
		Mobile spring and peak neap tides, not mobile at lowest neaps	Mobile spring and peak neap tides, not mobile at lowest neaps	Mobile spring tides only	Not mobile	Not mobile
	Waves only	0%	0%	0%	0%	0%
		Not mobile	Not mobile	Not mobile	Not mobile	Not mobile
Currents and waves	45%	36%	24%	0%	0%	0%
		Mobile spring and peak neap tides, not mobile at lowest neaps	Mobile spring and peak neap tides, not mobile at lowest neaps	Mobile spring tides only	Not mobile	Not mobile
ECC4 (56 mLAT)	Currents only	54%	46%	33%	0%	0%
		Mobile spring and peak neap tides, not mobile at lowest neaps	Mobile spring and peak neap tides, not mobile at lowest neaps	Mobile spring and peak neap tides, not mobile at lowest neaps	Not mobile	Not mobile
	Waves only	100%	100%	100%	0%	0%
		Always mobile	Always mobile	Always mobile	Not mobile	Not mobile
Currents and waves	71%	66%	55%	0%	0%	0%
		Mobile spring and peak neap tides, not mobile at lowest neaps	Mobile spring and peak neap tides, not mobile at lowest neaps	Mobile spring and peak neap tides, not mobile at lowest neaps	Not mobile	Not mobile
ECC9 (10 mLAT)	Currents only	0%	0%	0%	0%	0%
		Not mobile	Not mobile	Not mobile	Not mobile	Not mobile
	Waves only	100%	100%	100%	100%	8%
		Always mobile	Always mobile	Always mobile	Always mobile	Mobile peak spring tides only
Currents and waves	79%	72%	58%	0%	0%	0%
		Mobile under most tidal conditions, except for a duration either side of high water	Mobile under most tidal conditions, except for a duration either side of low water	Mobile only during periods of fastest tidal flows	Not mobile	Not mobile
ECC10 (10 mLAT)	Currents only	0%	0%	0%	0%	0%
		Not mobile	Not mobile	Not mobile	Not mobile	Not mobile
	Waves only	100%	100%	100%	100%	8%
		Always mobile	Always mobile	Always mobile	Always mobile	Mobile peak spring tides only
Currents and waves	80%	69%	40%	0%	0%	0%
		Mobile under most tidal conditions, except for a duration either side of high water	Mobile under most tidal conditions, except for a duration either side of low water	Mobile only during periods of fastest tidal flows	Not mobile	Not mobile

The current time series is for a 15-day period between 16/01/2013 and 31/01/2013, covering a spring neap tidal cycle post-construction. Data was extracted from a number of locations across the project area with only a few are presented to demonstrate the potential for any spatial variability, water depths associated with each assessed location was applied in calculating the sediment transport potential. For the analytical scenarios with currents and waves, the same current time series was applied with a single consistent wave with a Hs of 2.6 m and Tp of 11 seconds, consistent for the entire spring neap tidal cycle.



Table 6-7 Post-construction sediment mobility potential (Layout 2) at analysed locations across the offshore Project area using model-extracted time series flows and a wave with a height of 1.5 m and a period of 9.5 s; mobility potential is given as a percentage

SEABED SEDIMENT		FINE SAND	MEDIUM SAND	COARSE SAND	VERY FINE GRAVEL	FINE GRAVEL	MEDIUM GRAVEL
SEDIMENT SIZE (MM)		0.175	0.35	0.63	3	6	11
OAA3 (69 mLAT)	Currents only	27%	19%	8%	0%	0%	0%
		Mobile spring and peak neap tides, not mobile at lowest neaps	Mobile spring tides only	Mobile spring tides only	Not mobile	Not mobile	Not mobile
	Waves only	0%	0%	0%	0%	0%	0%
		Not mobile	Not mobile	Not mobile	Not mobile	Not mobile	Not mobile
Currents and waves	33%	25%	12%	0%	0%	0%	
	Mobile spring and peak neap tides, not mobile at lowest neaps	Mobile spring and peak neap tides, not mobile at lowest neaps	Mobile spring tides only	Not mobile	Not mobile	Not mobile	
OAA4 (69 mLAT)	Currents only	31%	23%	12%	0%	0%	0%
		Mobile spring and peak neap tides, not mobile at lowest neaps	Mobile spring tides, not mobile at lowest neaps	Mobile peak spring tides	Not mobile	Not mobile	Not mobile
	Waves only	0%	0%	0%	0%	0%	0%
		Not mobile	Not mobile	Not mobile	Not mobile	Not mobile	Not mobile
Currents and waves	37%	29%	16%	0%	0%	0%	
	Mobile spring and peak neap tides, not mobile at lowest neaps	Mobile spring tides, not mobile at lowest neaps	Mobile peak spring tides	Not mobile	Not mobile	Not mobile	
OAA7 (54 mLAT)	Currents only	39%	32%	20%	0%	0%	0%
		Mobile spring and peak neap tides, not mobile at lowest neaps	Mobile spring and peak neap tides, not mobile at lowest neaps	Mobile spring tides, not mobile at lowest neaps	Not mobile	Not mobile	Not mobile
	Waves only	100%	100%	9%	0%	0%	0%
		Always mobile	Always mobile	Mobile peak spring tides	Not mobile	Not mobile	Not mobile
Currents and waves	50%	41%	29%	0%	0%	0%	
	Mobile spring and peak neap tides, not mobile at lowest neaps	Mobile spring and peak neap tides, not mobile at lowest neaps	Mobile spring tides, not mobile at lowest neaps	Not mobile	Not mobile	Not mobile	
OAA9 (54 mLAT)	Currents only	36%	28%	16%	0%	0%	0%
		Mobile spring and peak neap tides, not mobile at lowest neaps	Mobile spring and peak neap tides, not mobile at lowest neaps	Mobile spring tides only	Not mobile	Not mobile	Not mobile
	Waves only	0%	0%	0%	0%	0%	0%
		Not mobile	Not mobile	Not mobile	Not mobile	Not mobile	Not mobile
Currents and waves	50%	40%	26%	0%	0%	0%	
	Mobile spring and peak neap tides, not mobile at lowest neaps	Mobile spring and peak neap tides, not mobile at lowest neaps	Mobile spring tides only	Not mobile	Not mobile	Not mobile	
OAA10 (69 mLAT)	Currents only	20%	11%	1%	0%	0%	0%
		Mobile only peak spring tides	Mobile only peak spring tides	Mobile only peak spring tides	Not mobile	Not mobile	Not mobile
	Waves only	0%	0%	0%	0%	0%	0%
		Not mobile	Not mobile	Not mobile	Not mobile	Not mobile	Not mobile
Currents and waves	27%	17%	4%	0%	0%	0%	
	Mobile spring and peak neap tides, not mobile at lowest neaps	Mobile only peak spring tides	Mobile only peak spring tides	Not mobile	Not mobile	Not mobile	
OAA11 (63 mLAT)	Currents only	20%	12%	0%	0%	0%	0%
		Mobile only peak spring tides	Mobile only peak spring tides	Not mobile	Not mobile	Not mobile	Not mobile
	Waves only	0%	0%	0%	0%	0%	0%
		Not mobile	Not mobile	Not mobile	Not mobile	Not mobile	Not mobile
Currents and waves	29%	19%	5%	0%	0%	0%	
	Mobile only peak spring tides	Mobile only peak spring tides	Mobile only peak spring tides	Not mobile	Not mobile	Not mobile	
ECC1 (83 mLAT)	Currents only	31%	24%	12%	0%	0%	0%
		Mobile spring and peak neap tides, not mobile at lowest neaps	Mobile spring and peak neap tides, not mobile at lowest neaps	Mobile peak spring tides only	Not mobile	Not mobile	Not mobile
	Waves only	0%	0%	0%	0%	0%	0%
		Not mobile	Not mobile	Not mobile	Not mobile	Not mobile	Not mobile
Currents and waves	34%	26%	14%	0%	0%	0%	
	Mobile spring and peak neap tides, not mobile at lowest neaps	Mobile spring and peak neap tides, not mobile at lowest neaps	Mobile peak spring tides only	Not mobile	Not mobile	Not mobile	
ECC2		19%	10%	0%	0%	0%	



SEABED SEDIMENT		FINE SAND	MEDIUM SAND	COARSE SAND	VERY FINE GRAVEL	FINE GRAVEL	MEDIUM GRAVEL
SEDIMENT SIZE (MM)		0.175	0.35	0.63	3	6	11
<b>(98 mLAT)</b>	Currents only	Mobile peak spring tides only	Mobile peak spring tides only	Not mobile	Not mobile	Not mobile	Not mobile
	Waves only	0%	0%	0%	0%	0%	0%
		Not mobile	Not mobile	Not mobile	Not mobile	Not mobile	Not mobile
Currents and waves	20%	11%	1%	0%	0%	0%	
	Mobile peak spring tides only	Mobile peak spring tides only	Not mobile	Not mobile	Not mobile	Not mobile	
<b>ECC3 (95 mLAT)</b>	Currents only	37%	29%	17%	0%	0%	0%
		Mobile spring and peak neap tides, not mobile at lowest neaps	Mobile spring tide only	Mobile peak spring tides only	Not mobile	Not mobile	Not mobile
	Waves only	0%	0%	0%	0%	0%	0%
		Not mobile	Not mobile	Not mobile	Not mobile	Not mobile	Not mobile
	Currents and waves	38%	30%	18%	0%	0%	0%
		Mobile spring and peak neap tides, not mobile at lowest neaps	Mobile spring tide only	Mobile peak spring tides only	Not mobile	Not mobile	Not mobile
<b>ECC4 (56 mLAT)</b>	Currents only	54%	46%	33%	0%	0%	0%
		Mobile spring and peak neap tides, not mobile at lowest neaps	Mobile spring and peak neap tides, not mobile at lowest neaps	Mobile spring and peak neap tides, not mobile at lowest neaps	Not mobile	Not mobile	Not mobile
	Waves only	0%	0%	0%	0%	0%	0%
		Not mobile	Not mobile	Not mobile	Not mobile	Not mobile	Not mobile
	Currents and waves	63%	56%	42%	0%	0%	0%
		Mobile spring and peak neap tides, not mobile at lowest neaps	Mobile spring and peak neap tides, not mobile at lowest neaps	Mobile spring and peak neap tides, not mobile at lowest neaps	Not mobile	Not mobile	Not mobile
<b>ECC9 (10 mLAT)</b>	Currents only	0%	0%	0%	0%	0%	0%
		Not mobile	Not mobile	Not mobile	Not mobile	Not mobile	Not mobile
	Waves only	100%	100%	100%	34%	0%	0%
		Always mobile	Always mobile	Always mobile	Partially mobile	Not mobile	Not mobile
	Currents and waves	62%	49%	19%	0%	0%	0%
		Mobile during faster flows	Mobile only during periods of fastest tidal (spring and neap) flows	Mobile only during periods of fastest spring tidal flows	Not mobile	Not mobile	Not mobile
<b>ECC10 (10 mLAT)</b>	Currents only	0%	0%	0%	0%	0%	0%
		Not mobile	Not mobile	Not mobile	Not mobile	Not mobile	Not mobile
	Waves only	100%	100%	100%	34%	0%	0%
		Always mobile	Always mobile	Always mobile	Partially mobile	Not mobile	Not mobile
	Currents and waves	46%	29%	10%	0%	0%	0%
		Mobile during faster flows	Mobile only during periods of fastest tidal (spring and neap) flows	Mobile only during periods of fastest spring tidal flows	Not mobile	Not mobile	Not mobile

The current time series is for a 15-day period between 16/01/2013 and 31/01/2013, covering a spring neap tidal cycle post-construction. Data was extracted from a number of locations across the project area with only a few are presented to demonstrate the potential for any spatial variability, water depths associated with each assessed location was applied in calculating the sediment transport potential. For the analytical scenarios with currents and waves, the same current time series was applied with a single consistent wave with a Hs of 1.5 m and Tp of 9.5 seconds, consistent for the entire spring neap tidal cycle.



Table 6-8 Post-construction sediment mobility potential (Layout 2) at analysed locations across the offshore Project area using model-extracted time series flows and a wave with a height of 2.6 m and a period of 11 s; mobility potential is given as a percentage

SEABED SEDIMENT		FINE SAND	MEDIUM SAND	COARSE SAND	VERY FINE GRAVEL	FINE GRAVEL	MEDIUM GRAVEL
SEDIMENT SIZE (MM)		0.175	0.35	0.63	3	6	11
OAA3 (69 mLAT)	Currents only	27%	19%	8%	0%	0%	0%
		Mobile spring and peak neap tides, not mobile at lowest neaps	Mobile spring tides only	Mobile spring tides only	Not mobile	Not mobile	Not mobile
	Waves only	100%	22%	0%	0%	0%	0%
OAA4 (69 mLAT)	Currents only	46%	35%	22%	0%	0%	0%
		Mobile spring and peak neap tides, not mobile at lowest neaps	Mobile spring and peak neap tides, not mobile at lowest neaps	Mobile spring tides only	Not mobile	Not mobile	Not mobile
	Waves only	100%	21%	0%	0%	0%	0%
OAA7 (54 mLAT)	Currents only	50%	40%	26%	0%	0%	0%
		Mobile spring and peak neap tides, not mobile at lowest neaps	Mobile spring and peak neap tides, not mobile at lowest neaps	Mobile spring tides only	Not mobile	Not mobile	Not mobile
	Waves only	100%	100%	100%	0%	0%	0%
OAA9 (54 mLAT)	Currents only	39%	32%	20%	0%	0%	0%
		Mobile spring and peak neap tides, not mobile at lowest neaps	Mobile spring and peak neap tides, not mobile at lowest neaps	Mobile spring tides only	Not mobile	Not mobile	Not mobile
	Waves only	100%	100%	100%	0%	0%	0%
OAA10 (69 mLAT)	Currents only	62%	54%	40%	0%	0%	0%
		Mobile spring and peak neap tides, not mobile at lowest neaps	Mobile spring and peak neap tides, not mobile at lowest neaps	Mobile spring and peak neap tides, not mobile at lowest neaps	Not mobile	Not mobile	Not mobile
	Waves only	100%	100%	100%	0%	0%	0%
OAA11 (63 mLAT)	Currents only	36%	28%	16%	0%	0%	0%
		Mobile spring and peak neap tides, not mobile at lowest neaps	Mobile spring and peak neap tides, not mobile at lowest neaps	Mobile spring tides only	Not mobile	Not mobile	Not mobile
	Waves only	100%	100%	100%	0%	0%	0%
ECC1 (83 mLAT)	Currents only	20%	11%	1%	0%	0%	0%
		Mobile spring tides only	Mobile spring tides only	Mobile peak spring tides only	Not mobile	Not mobile	Not mobile
	Waves only	0%	0%	0%	0%	0%	0%
ECC1 (83 mLAT)	Currents only	39%	29%	14%	0%	0%	0%
		Mobile spring and peak neap tides, not mobile at lowest neaps	Mobile spring and peak neap tides, not mobile at lowest neaps	Mobile spring tides only	Not mobile	Not mobile	Not mobile
	Waves only	94%	0%	0%	0%	0%	0%
ECC1 (83 mLAT)	Currents only	20%	12%	0%	0%	0%	0%
		Mobile on spring tides only	Mobile on spring tides only	Not mobile	Not mobile	Not mobile	Not mobile
	Waves only	0%	0%	0%	0%	0%	0%
ECC1 (83 mLAT)	Currents only	42%	32%	17%	0%	0%	0%
		Mobile spring and peak neap tides, not mobile at lowest neaps	Mobile spring and peak neap tides, not mobile at lowest neaps	Mobile on spring tides only	Not mobile	Not mobile	Not mobile
	Waves only	0%	0%	0%	0%	0%	0%
ECC1 (83 mLAT)	Currents only	31%	24%	12%	0%	0%	0%
		Mobile spring and peak neap tides, not mobile at lowest neaps	Mobile spring tides only	Mobile spring tides only	Not mobile	Not mobile	Not mobile
	Waves only	0%	0%	0%	0%	0%	0%
ECC1 (83 mLAT)	Currents only	43%	34%	21%	0%	0%	0%
		Mobile spring and peak neap tides, not mobile at lowest neaps	Mobile spring tides only	Mobile spring tides only	Not mobile	Not mobile	Not mobile
	Waves only	0%	0%	0%	0%	0%	0%



SEABED SEDIMENT		FINE SAND	MEDIUM SAND	COARSE SAND	VERY FINE GRAVEL	FINE GRAVEL	MEDIUM GRAVEL
SEDIMENT SIZE (MM)		0.175	0.35	0.63	3	6	11
	Currents and waves	Mobile spring and peak neap tides, not mobile at lowest neaps	Mobile spring and peak neap tides, not mobile at lowest neaps	Mobile spring tides only	Not mobile	Not mobile	Not mobile
ECC2 (98 mLAT)	Currents only	19%	10%	0%	0%	0%	0%
		Mobile spring tides only	Mobile peak spring tides only	Not mobile	Not mobile	Not mobile	Not mobile
	Waves only	0%	0%	0%	0%	0%	0%
		Not mobile	Not mobile	Not mobile	Not mobile	Not mobile	Not mobile
Currents and waves	27%	18%	4%	0%	0%	0%	
	Mobile spring tides only	Mobile peak spring tides only	Mobile peak spring tides only	Not mobile	Not mobile	Not mobile	
ECC3 (95 mLAT)	Currents only	37%	29%	17%	0%	0%	0%
		Mobile spring and peak neap tides, not mobile at lowest neaps	Mobile spring and peak neap tides, not mobile at lowest neaps	Mobile spring tides only	Not mobile	Not mobile	Not mobile
	Waves only	0%	0%	0%	0%	0%	0%
		Not mobile	Not mobile	Not mobile	Not mobile	Not mobile	Not mobile
Currents and waves	45%	36%	24%	0%	0%	0%	
	Mobile spring and peak neap tides, not mobile at lowest neaps	Mobile spring and peak neap tides, not mobile at lowest neaps	Mobile spring tides only	Not mobile	Not mobile	Not mobile	
ECC4 (56 mLAT)	Currents only	54%	46%	33%	0%	0%	0%
		Mobile spring and peak neap tides, not mobile at lowest neaps	Mobile spring and peak neap tides, not mobile at lowest neaps	Mobile spring and peak neap tides, not mobile at lowest neaps	Not mobile	Not mobile	Not mobile
	Waves only	100%	100%	100%	0%	0%	0%
		Always mobile	Always mobile	Always mobile	Not mobile	Not mobile	Not mobile
Currents and waves	71%	66%	55%	0%	0%	0%	
	Mobile spring and peak neap tides, not mobile at lowest neaps	Mobile spring and peak neap tides, not mobile at lowest neaps	Mobile spring and peak neap tides, not mobile at lowest neaps	Not mobile	Not mobile	Not mobile	
ECC9 (10 mLAT)	Currents only	0%	0%	0%	0%	0%	0%
		Not mobile	Not mobile	Not mobile	Not mobile	Not mobile	Not mobile
	Waves only	100%	100%	100%	34%	0%	0%
		Always mobile	Always mobile	Always mobile	Partially mobile	Not mobile	Not mobile
Currents and waves	62%	49%	19%	0%	0%	0%	
	Mobile during faster flows	Mobile only during periods of fastest tidal (spring and neap) flows	Mobile only during periods of fastest spring tidal flows	Not mobile	Not mobile	Not mobile	
ECC10 (10 mLAT)	Currents only	0%	0%	0%	0%	0%	0%
		Not mobile	Not mobile	Not mobile	Not mobile	Not mobile	Not mobile
	Waves only	100%	100%	100%	34%	0%	0%
		Always mobile	Always mobile	Always mobile	Partially mobile	Not mobile	Not mobile
Currents and waves	46%	29%	10%	0%	0%	0%	
	Mobile during faster flows	Mobile only during periods of fastest tidal (spring and neap) flows	Mobile only during periods of fastest spring tidal flows	Not mobile	Not mobile	Not mobile	

The current time series is for a 15-day period between 16/01/2013 and 31/01/2013, covering a spring neap tidal cycle post-construction. Data was extracted from a number of locations across the project area with only a few are presented to demonstrate the potential for any spatial variability, water depths associated with each assessed location was applied in calculating the sediment transport potential. For the analytical scenarios with currents and waves, the same current time series was applied with a single consistent wave with a Hs of 2.6 m and Tp of 11 seconds, consistent for the entire spring neap tidal cycle.



### 6.3.2.2 Near-Bed Blockage of Sediment Transport

In addition to blockage within the water column, the presence of rock berms and structures on the seabed has implications on near-bed flows and consequences on bedload transport. Rock placement within the offshore Project area could be installed as cable protection or as a scour mitigation measure around installed structures. This is of greatest impact along the offshore ECC, particularly in shallower waters where the presence of rock protection proportionately takes up more space within the water column. Using the method outlined in section 4.4.2.2.3, the impact on flows because of the presence of rock berms along the offshore ECC was analysed.

Table 6-9 shows the predicted change in spring and neap currents at the shallowest point in the OAA and offshore ECC. The shallowest depth along the offshore ECC at which a rock berm can be placed is 10 mLAT, based on the worst case HDD exit depth, although a more realistic exit depth is from 20 mLAT. This would involve rock placement at the absolute shallowest depth at which the HDD exit pit could be located. Based on baseline conditions within the offshore ECC and the dimensions of the rock berm (described in section 4.4.2.2.3), at the shallowest point along the offshore ECC the flow speed may change by up to 0.04% on a neap tide. When comparing the absolute change in flow speeds pre- and post-installation, the difference is so small that it is not notable at two decimal places. On a spring tide no change is observed.

The shallowest point within the OAA is 41 mLAT. At this depth, the presence of the rock berm will not generate a change in flows. As there is no change at the shallowest points, Table 6-9 does not include the deeper locations.

Table 6-9 Blockage due to rock placement

LOCATION	ANALYSED WATER DEPTHS (MLAT)	FLOW SPEED		SPRING <sup>2</sup>		NEAP <sup>2</sup>	
		Spring (M/S) <sup>1</sup>	Neap	Downstream flow speed	Percentage change	Downstream flow speed	Percentage change
offshore ECC	10	0.72	0.26	0.72	No Change	0.26	0.040%
OAA	41	0.74	0.56	0.74	No Change	0.56	No Change

<sup>1</sup>: Flow speed across the offshore Project informed by the baseline characterisation (section 3.7.2); and

<sup>2</sup>: Assessed changes to flow speeds as a result of the 3 m high rock protection.

The consequences of changes on sediment transport are addressed in full in section 6.3.2. However, to summarise the above findings, with respect to the potential for near-bed blockage of flow and sediment transport, the presence of protection on the seabed will not result in any demonstrable change to flows. Therefore, changes to sediment transport are unlikely.



## 6.4 Potential Changes to Water Column Stratification

### 6.4.1 Overview

Stratification in the water column with regards to both salinity and temperature, is dependent on metocean conditions, with the season also exerting influence, with warmer and less dense water occurring over the summer months. Metocean conditions with respect to flows and waves together determine the extent of mixing in the water column which varies within the offshore Project area seasonally and over the course of the tidal cycle, as evidence of stratification is more apparent on a neap tide (as described in Section 3.10.2.2). Based on the site-specific surveys of water column properties across the offshore Project area (Section 2.1.3.2), temperature variance through the water column ranged between 13.3 °C and 14.5 °C, while salinity varied between 34.55 psu and 35.00 psu (section 3.10.2.2). Typically, the stratification in terms of the warmer and less saline water was observed within the upper 30 m of water and not apparent from nearshore locations (section 3.10.2.2). Based on the information collected during the site-specific surveys and modelled outputs from the PFOW climatology (O'Hara and Campbell, 2021), the presence of the stratification across the northwest Scottish continental shelf is temporary (during the summer months) and considered unlikely to constitute a front (Section 3.10.2) and is more representative of seasonal stratification. From the West of Orkney model calibration and validation (Appendix A), freshwater inputs are not demonstrated to influence flows across the OAA. Therefore, by proxy, freshwater inputs are also not considered to influence mixing and stratification across the OAA, although Sharples *et al.* (2022) indicate freshwater input can influence the timing and development of stratification in coastal areas. The apparent absence of stratification in the nearshore locations could be due to the proximity to the coast and the survey period (section 3.10.2.2).

The understanding of post-construction changes to metocean conditions in the offshore Project area have determined that the change in flows and wave properties remain largely unchanged by the presence of the WTGs within the OAA (Section 6.1 and Section 6.2 respectively). Overall, the spatial extent of change is largely limited to the immediate WTG surroundings. Most importantly, the scale of absolute change in both flow speeds and wave height and period is so small. In relative terms, this equates to a very small percentage change and, in reality, the scale of change would be imperceptible against natural variation expected in the offshore region. The following sections describe the conclusions drawn above with regards to currents and waves in the context of impacts on water column stratification.

### 6.4.2 Assessment

A number of other studies have investigated for the potential for impacts of offshore wind farms developments on regional fronts and stratifications either in isolation or cumulatively. These have been based on both site observations following construction (Schultze *et al.*, 2020 and Floeter *et al.*, 2017) and modelling results (Carpenter *et al.*, 2016; Cazenave *et al.*, 2016). In addition, theoretical assessments have been completed on the basis of oceanographic processes and boundary layer physics (Dorrel *et al.*, 2022).

Schultze *et al.* (2020) investigated the possible impact of a monopile on the mixing of a stratified water column and presented observations on monitoring of the thermal water structure in the lee wake of a foundation (6 m diameter monopile in a water depth of 24 m) of the DanTsyk offshore wind farm off the west coast of Denmark (in the German Bight of the North Sea). Monitoring on 25 May 2015 was considered to exhibit a relatively weak level of thermal



stratification in the wider environment, with the temperature variance between the sea surface layer (circa 10 m deep) and bottom water being around 0.5 °C (Figure 6-11). During the towed survey, when the CTD (deployed on an 8 m vertical string) moved past the monopile downstream (i.e., blue areas in Figure 6-11, with the first at around 300 m and the second at around 450 m downstream) increased mixing appears to narrow down the spread of temperatures from around 0.5 to around 0.2 to 0.3 °C.

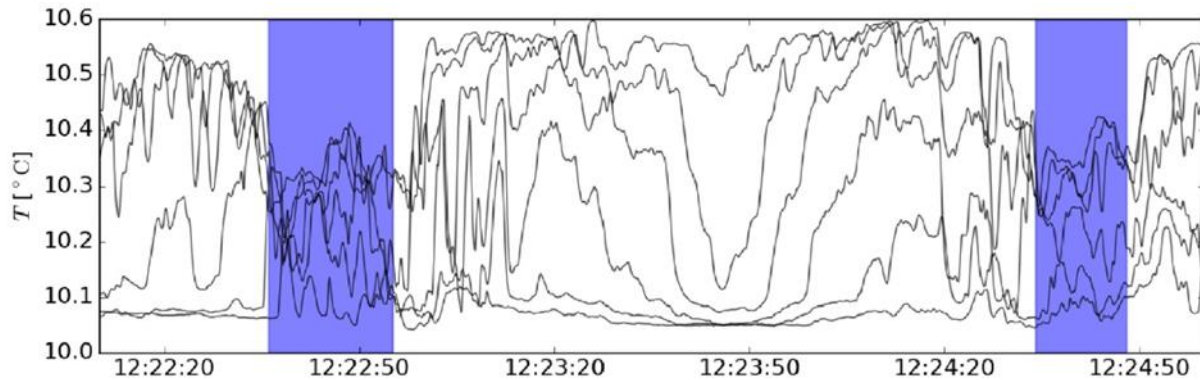


Figure 6-11 Time series of vertical temperature measurements towed past a monopile (from Shultze *et al.* (2020))

A second period of monitoring took place on 19 July 2017 on a different part of the wind farm. The stratification on this date was considered to be stronger than the conditions from 2015 with a temperature difference of around 2.1°C between the surface layer and lower bottom water. Despite the apparent stronger water column stratification at this time no clear influence of increased mixing due to the monopile foundation was observed, even at the closest transects at 200 and 400 m downstream of the monopile foundation. It was noted in Schultze *et al.*, (2020) that no observations were obtained at closer than 200 m downstream, in the instance the stratification was disrupted, it would have been in really close proximity to the foundation, at distances less than 200 m. An interpretation for the lack of influence on the thermal stratification at distances at and greater than 200 m, is that stronger buoyancy in the more developed stratified water remained the dominant effect over increased mixing from the foundation (which dissipates exponentially in magnitude away from the foundation) (Schultze *et al.*, 2020). Schultze *et al.*, (2020) concluded that although a single WTG foundation could increase turbulence and mixing, these occur locally and can generally be considered to be low. However, large scale OWFs were considered to be able to affect the vertical structure of weak stratification, where the OWF was built over a large area and the stratification was influenced or built up over a regional scale. Where there was evidence of strong stratification, the presence of the OWF was less likely to affect it, as the processes defining the stratification were more dominant regionally. Although, salinity was not considered within the Schultze *et al.*, (2020) study, it is inferred that similar very-near field mixing and recovery with increasing distance (tens to hundreds of metres) is also likely to occur to salinity. This is due to the observed association between the thermal and salinity stratification represented within the site-specific surveys across the offshore Project as described in section 3.10.2.2.

Carpenter *et al.*, (2016) investigated the potential for large scale changes in stratification in tidal shelf seas (i.e. the German Bight region of the North Sea) attributed to the cumulative presence of offshore windfarms. The study concluded that stratification is broken down very gradually by interaction with a windfarm, with the process potentially occurring over a timescale in the order of 100 to 500 days. However, these timescales suggested are likely to be highly conservative. Therefore, the overall conclusion was that no large-scale changes to stratification within the



North Sea are expected based on proposed levels of development (current at time of publication). Although, it was suggested that in future large-scale development scenarios, there could be a significant decrease in stratification in the North Sea should a considerable portion of the shelf sea be filled with OWFs. Though the level of offshore windfarm development has increased substantially since the conclusions of Carpenter *et al.*, (2016) were established, at present, the proposed West of Orkney Windfarm, is located outside of the North Sea and in deeper waters.

Carpenter *et al.* (2016) also hypothesised that drag forces from scour protection around foundations may further exacerbate turbulent mixing beyond the influence of foundations alone. However, as described in section 3.10.2, stratification mainly occurs in the upper 30 m of the water column. In relation to the depth at which scour protection will be installed (i.e. the water depths within the OAA), the influence of rock on the seabed is unlikely to contribute significantly to increased mixing. Therefore, the primary influence on stratification in this context will be the presence of the WTGs and OSP foundations.

Cazenave *et al.*, (2016) used a regional scale 3D hydrodynamic model with a representation of WTG foundation structure to investigate the influence of the WTG structures within an OWF on shelf sea vertical mixing, focussing on the Irish Sea. The modelled results indicated that the introduction of OWF structures influenced mixing within the model domain. Horizontally, foundation structures were modelled to reduce flow velocities at several times the foundation diameter, in some cases up to 250 times the foundation diameter, and even larger when considering the full array of OWF foundations (Cazenave *et al.*, 2016). Vertically, the foundations increased mixing of the water column due to flow up and down each monopile. In areas where stratification occurs, the increased vertical mixing resulted in a decrease in stratification between 5 and 15%, the horizontal extent of which was larger than the sum of the monopile footprints. However, the limitations of the model were discussed, which suggested the applied model scale and parameterisation was not entirely appropriate to fully distinguish the mixing processes at the OAA and wider regional scales. Therefore, although it is recognised that WTG foundation structures within an OWF may have some influence on stratification locally, it does in turn suggest that naturally occurring stratification would be completely mixed by the presence of foundation structures (Cazenave *et al.*, 2016).

Dorrell *et al.*, (2022) discussed the potential for increased water column mixing as a results of anthropogenic infrastructure in the marine environment, particularly in relation to new offshore wind developments. On the basis of previous analytical, modelling and observation studies on the potential influence of OWF infrastructure on vertical mixing of shelf seas, and consideration of analogous processes of water column mixing in varying marine environments associated with oceanographic and sub mesoscale<sup>16</sup> processes, the potential for mixing was recognised. However, the length scales of the mixing and consequence on stratification were less clearly defined, with local and natural topographical characteristics further influencing the development of stratification.

Available information would all confirm the likely influence on vertical water column and potential stratification mixing in the immediate vicinity of the monopile foundations within the offshore Project OAA. However, the spatial length scales of this influence are considered to be in line with the information suggested in the PFOW climatology (O'Hara and Campbell, 2021). The Project-specific environmental, water column survey (SS5: Benthic environmental baseline report), as introduced in section 2.1.3.2, and described for the offshore Project area in section 3.10.2.2, confirmed the

---

<sup>16</sup> Dorell *et al.*, (2022) define ocean submesoscale process as those that occur on spatial scales on the order of 1 to tens of kilometres, but less than 100 km. Submesoscale processes are considered to be more energetic and support mixing in shelf seas and are generated as result of tidal flow and topographic interactions.



presence of stratification within the months of July and August (section 3.10.2.2), with the PFOW climatology indicating seasonal stratification between the months of May and August (section 3.10.2.1), equating to approximately four months of the year. The outputs from the PFOW climatology would indicate strong stratification with the maximum temperature and salinity variance observed during site-specific surveys supporting this assertion (section 3.10.2). When stratification is present, it is possible that foundations may cause some minor decrease in the strength of water column stratification across the OAA, in the immediate vicinity and wake of the foundations, due to increased mixing. The mixing length scales are considered to be in the order of hundreds of metres and several times the foundation diameter. However, the mixing length scale is still considered to be less than the applied separation, which at a minimum is approximately 73 times the foundation diameter (monopiles in this case). Field observations from Schultze *et al.*, (2020) would support this understanding as during periods of strong stratification, mixing length scales were less than 10 times the foundation diameter. It is therefore also considered unlikely that water, which is stratified entering the OAA, will become fully mixed on moving through the offshore Project, particularly the OAA. The measured stratification of the north coast of Scotland is interpreted to be strong, based on the temperature and salinity range with depth, the consistent presence for up to four-months of the year and the presence during all tidal states, albeit stronger under neap conditions (section 3.10.2). Therefore, regional scale patterns of stratification interpreted to exist in this part of the northwest Scottish continental shelf will be unaffected and will continue to be subject to natural processes and variability in line with the mesoscale processes. Consequently, the presence of the Project alone will not affect local water column stratification.

Several authors evaluating the potential impact of offshore anthropogenic infrastructure on mesoscale processes, including stratification, stress the importance of cumulative effects from multiple large offshore wind developments, covering hundreds of kilometres cumulatively (Carpenter *et al.*, 2016; Floeter *et al.*, 2017; Schultze *et al.*, 2020; Dorrell *et al.*, 2022). In the context of the offshore Project, the West of Orkney offshore windfarm off the northwest coast of Scotland on the northwest Scottish continental shelf is the only development at present. The proposed PFOWF, closer to the coast, is considerably smaller at a maximum of up to 10 WTGs, so is not considered to be at sufficient scale to contribute to the cumulative effects described by the above authors. Therefore, at present, there is not considered to be the potential for the cumulative disruption to stratification that is described for other areas across the North Sea.

## 6.5 Potential Seabed Scour

### 6.5.1 Overview

This section introduces the concept of scour, explains the circumstances surrounding its formation (section 6.5.2) and applies this to the proposed installation of WTG and OSPs in the OAA (section 6.5.3.4). The Project assumption is that the majority of cables (interconnectors and export) will be trenched and buried, or cable protection measures will be in place. It is not considered that scour would occur around the cable protection measures. Therefore, scour formation in association with cables is not considered further. As introduced in Section 4.4.4, presents the estimated scour potential associated with the offshore infrastructure. Furthermore, as part of an embedded mitigation measure scour protection is to be installed during construction should detailed design investigations demonstrate the requirement. Therefore, the assessment completed in this section is to set out the scour properties that have informed the offshore Project's design to date.



## 6.5.2 Scour formation

With the installation of a foundation through the water column, the presence of the structure will locally disturb the ambient flow and affect bed shear stress, thereby resulting in an associated increase in localised sediment transport and erosion (Whitehouse, 1998). The presence of a vertical installation in the water column generates a pressure gradient in the water flow upstream of the installation. The flow is then directed down towards the seabed when it comes into contact with the installation. When the downflow interacts with the seabed an eddy is formed and is shed in the wake of the installation generating vortices downstream. This acts to increase bed shear stress and generates erosion (Whitehouse, 1998). This process is termed 'scour'. The process of scour makes sediments available for assimilation into the sediment transport regime. Scour reaches an equilibrium depth when material is transported into the scour hole at the same rate at which it is transported out.

The extent and depth of scouring is mainly related to the scale and shape of the structure and the soil properties (e.g. angle of repose, which dictates the steepest angle relative to the horizontal plane before material on the slope face begins to slide). Generally, for uniform structures, when the ratio of the structure diameter to the water depth is less than 0.5, the scour depth is a function of the pile diameter. This is referred to as 'local scour'.

Detailed information on the site conditions which govern scour potential (tidal range, water depth, wave-tide climate, geological properties of the surface and sub-surface seabed sediments) is provided in section 3.3.2.

### 6.5.2.1 Local sediment transport regime and backfill rates

When sediment transport is active and the seabed is highly mobile, this can be described as a 'live-bed regime'. Under such regimes, the scour rate can be relatively fast. Conversely, in circumstances where conditions are calmer and sediment transport is not a predominant feature, this instead constitutes a 'clear water regime'. This distinction is particularly important with regards to determining backfilling of scour holes so it is important to define the conditions appropriate to the offshore Project area.

As described in section 3.3.2.2, the offshore Project area consists mainly of medium sand and all sizes of gravel. Across the offshore Project area, sediment transport for finer sediments (as far as coarse sand) occurs variably over the course of a tidal cycle. Fine sands are mostly mobile 30% of the time, typically on spring tides (section 3.9.2.1). Larger sediments are mobile less frequently. Given the sediment transport mobility characteristic of the offshore Project area, and the defining characteristics of the two regimes described above, the offshore Project area can be considered to have a clear-water regime. Consequently, mobility of sediment and subsequent scouring will occur mostly on spring tides (i.e. during times of increased sediment transport), therefore rates of backfilling will be relatively low, and largely associated with periods of fastest flow speeds, which occur for a smaller proportion of time.

### 6.5.2.2 Scour pit alignment and symmetry

Generally, for uniform slender cylindrical monopiles a near-circular formation of scour occurs. Although this is also dependant on the influence of tidal flows. In the case of non-cylindrical foundations which have a more complex shape, the separation of water flow around the structure is not uniform. This results in formation of scour which is spread differently around the base of the structure. Irrespective of the shape of the installation, asymmetry in the



local currents can influence asymmetry of the scour that forms. The offshore Project area is flood dominant with more energetic currents travelling from west to east, however, the residual has been demonstrated to be small / weak, as less than 0.05 m/s (Section 3.7.2). The implication of this being that there will be a degree of asymmetry around the foundation, although it is not expected to be pronounced.

### 6.5.2.3 Group and global scour

Typically, scour is limited to the immediate surroundings of the individual structures and is limited to scaled of tens of metres, with scour holes of a few thousand cubic metres per foundation. When piles are closely spaced (for example as part of multi-legged jacket structures) then the extents of local scouring around each pile can overlap and cumulatively create a wider area of 'group scour'. This aspect does not apply to monopile structures. At a larger scale, 'global scour' describes the formation of shallow, wide depressions under and around individual installations. This scour is independent of general changes in seabed level, which are governed by large scale erosion, deposition and bedform movement.

## 6.5.3 OAA Scour Assessment

### 6.5.3.1 WTG foundation dimensions and layout

As introduced in section 4.3, there are three proposed foundation types for the (125) WTGs: monopile, piled jacket and suction bucket jacket, for which there are numerous sub-options. The information shown throughout this section represents the worst case per each of the three foundation types (Table 4-3). The infrastructure parameters, which relate mostly to scour generation (i.e. dimensions of the foundations) include:

- The worst case monopile option involves a pile with an 18 m diameter per WTG;
- The worst case piled jacket involves four piles per WTG jacket, each of which is spaced 41 m away from one another at the seabed. Each of the piles is 4 m in diameter; and
- The suction bucket option does not require piles, however each of the four suction buckets at the foot of the foundation are, in the worst case, 4 m in diameter. The suction buckets are also spaced 41 m apart from one another.

The potential for group scour only relates to the jacket options, where the legs act locally and cumulatively in the generation of scour. The two assessed worst case layouts (Layout 1 and 2) (i.e. with respect to marine physical and coastal processes) for the WTGs in the OAA are shown in Figure 4-1. While the WTG spacing remains consistent between these layouts, it varies between foundation type (Table 4-3). However, based on the ratio between individual foundation diameter and the associated spacing (Table 4-3), scour is not expected to coalesce between foundations, and is therefore not considered further. For the purposes of the technical report, the area of scour which may be generated by each of these methods is described. Scour formation associated with these WTG options is discussed in Section 6.5.3.4, along with scour protection measures.



### 6.5.3.2 OSP foundation dimensions and layout

There are two proposed foundation types for the (5) OSPs: piled jacket and suction bucket. The options are fully described in Table 4-4 (section 4.3), however a summary is provided below of the worst case, which relates to the larger structures:

- The piled jacket foundation OSPs have eight legs each, spaced 58 m apart at the seabed. Each of the legs has two piles, 4 m in diameter;
- The suction bucket jackets have 8 legs, each with a diameter of 4 m spaced 58 m at the seabed. The diameter of a single suction bucket is 8 m;
- The larger piled jacket has eight legs each, with each legs having two piles of 4 m in diameter. The eight legs are spaced 63 m apart from each other on the seabed; and
- The larger suction bucket has eight legs, each with a diameter of 4 m spaced 63 m apart at the seabed. The diameter of a single suction bucket is 8 m.

Each of these options is considered with regards to scour formation in the subsequent sections. The provision of scour protection is also considered in section 6.5.3.4 and Table 4-3 and Table 4-4.

### 6.5.3.3 Approach to quantification of scour

Although the 50-year extreme wave, current and combined wave and current conditions were considered under the marine physical and coastal processes assessment, the Project design parameters used to define the worst case scour properties were based on current alone extremes, which assumed a depth averaged current of 2.35 m/s. Scour properties were calculated prior to the availability site-specific sediment data, so a worst case grain size of 0.063 mm was used, representative of coarse silt/fine sand. In actuality, as per section 3.3.2.2, the sediment sizes across the offshore Project area are variable and typically larger. The offshore Project area typically comprises medium sand which was found in 100% of sediment samples and constituted a maximum of 69% within any one sample, therefore the applied sediment size for the scour analyses is considered to apply more conservatism. The water depth within the OAA, which corresponds to the proposed location of the WTGs, ranges from 50 to 70 m. A water depth of 70 m was used to determine the scour extent. Based on the assumed sediment properties, a worst case critical angle of repose of 27° has been assumed.

Time limitations on scour development were not included, therefore it is assumed that the full equilibrium depth is reached based on the extreme current conditions. However, it is noted that the potential for scour could occur with the flow (section 3.7) and wave conditions (section 3.8) characteristic to the site, although the associated equilibrium scour would be less than that for extreme conditions, due to the lower forcing processes.

To estimate scour depth, approaches described in Hydraulic Engineering Circular No. 18 (HEC-18) (US Department of Transportation Federal Highway Administration, 2012) for currents only, Sumer & Fredsoe (2001; 2002), for waves and currents and Petersen, which also accounts for waves and currents were applied. Bed shear stress was calculated using formulae from Soulsby (1997).



The geometry of the foundations also influences the generation of scour. For the purposes of the calculations done here, the following assumptions were followed:

- No tapering of foundation;
- The jacket legs were not angled;
- The scour is calculated based on the dimensions of each of the three foundation options alone, without the presence of secondary items for example pile caps; and
- The volume of material eroded from the scour hole is approximated to the dimensions of the scour hole.

With regards to assumptions specific to the three foundation options, the truncation of the suction bucket jacket followed Harris, *et al.*, (2021) and pin pile jacket followed the Harris and Whitehouse (2021). To account for global scour, which is a feature relevant to two of the proposed WTG and both OSP foundation options, a factor of 1.1 was used for the pin pile jacket as the spacing between the legs of the jacket is large in comparison to the diameter of the individual legs. A factor of 1.4 was used to account for the closer spacing of the suction buckets on the legs of the jacket under this option.

It is important to note that these parameters are largely based on reported literature and therefore there is some inherent uncertainty in the results. Another compounding factor which has not been considered in the calculation of scour is the presence and migration of bedforms in the area; in the offshore Project area sandwaves may pass through the scour hole and exacerbate scour depths but this has not been accounted for here. These assumptions are consistent for the scour estimates pertaining to both the WTG foundations and the OSP foundations.

#### 6.5.3.4 Potential Scour at WTGs and OSPs

The scour dimensions described in Table 6-10 and represent the maximum scour extent derived from the worst case PDE parameters and under extreme metocean conditions for WTGs and OSPs respectively. Scour depth, extent and volume are shown according to each of the three possible WTG and two OSP foundation options.

For WTGs, Table 6-10 demonstrates that the WTG monopile foundation will incur the greatest scour depth and extent. The scour depth generated when using the monopile foundation type will generate an area of scour approximately 41 m in extent and approximately 21 m deep. This scour hole is roughly twice the size of those generated using the piled jacket and suction bucket jacket foundation options. For OSPs, the worst scour is estimated for the suction bucket jacket (Table 6-10), with the scour properties, still being less than that estimated for the monopile foundation (Table 6-10).

The rate of natural backfilling within the OAA is likely to be low due to the nature of the local sediment transport regime (section 3.9.2.1). Therefore, once these scour holes are generated, they will remain largely unchanged. Possibly, the influence of storms will assist in the infilling of the scour holes or enlarging it further with respect to the storm. However, these events are relatively rare and also short in duration. As the offshore Project area is flood dominant, with those flows coming from the west, the scour generated could be asymmetrical (as mentioned in



section 6.5.2.2). However, given the low flow residual (section 3.7.2.3), the asymmetry in any scour is unlikely to be pronounced.

Furthermore, although the extent of scour would be minimal in relation to the presence of the WTG and OSP foundations, measures will be taken to mitigate against its formation outright. Particularly as the backfill of scour once formed is unlikely to return the seabed to its initial condition. Table 6-10 describes the potential scour associated with the offshore Project foundation structures, while the scour protection estimates integrated into the Project design are presented in Table 4-3 and Table 4-4 for WTG and OSP foundations respectively. The quantities of scour protection material which are proposed in association with the WTG and OSP foundation options respectively. Rock armour is the worst case assumption for protection. Rock/gravel with a median grain size of up to a maximum of ~0.4-0.6 m. Potentially an additional filter layer of finer material of the order 0.01-0.1 m median grain size will be required beneath the rock armour layer. While rock is assumed as the base case for the scour protection, other potential alternative materials which may be used are mattresses, mats or sheets that can be made of various materials including concrete and rubber; frond mats made of plastics or other materials held down by weights or anchors; geotextile or filter bags with infill material usually sand or rock but could be other materials; and prefabricated concrete blocks. Other innovative methods may also come to market the Project might want to consider. The scour protection is expected to be placed in a circular form surrounding the entirety of the foundation at the seabed.

Table 6-10 Predicted scour associated with the three WTG and OSP foundation options

		MONOPILE	PILED JACKET	SUCTION BUCKET JACKET	OSP JACKET	OSP SUCTION BUCKET
<b>Maximum estimated scour depth (m)</b>		~21	~10	~10	~11	~13
<b>Maximum estimated scour extent from edge of pile, including global scour (m)</b>		~41	~20	~20	~22	~26

Scour protection already incorporated into the Project design are provide in Table 4-3 and Table 4-4 for WTG and OSP foundations respectively.

## 6.6 Potential Changes to Landfall

### 6.6.1 Overview

The coastline at the offshore ECC landfall at Crosskirk and Greeny Geo has been demonstrated to be stable and erosion resistant, characterised by hard and mixed substrates of glacial till and outcropping bedrock in the nearshore area, described in detail section 3.11 and summarised in section 5.3.



The assessment of potential changes to landfall associated with the operation of the offshore Project mainly relates to the presence of the HDD, export cables and the requirement for additional rock protection should it be required. It was raised by Regulators and consultees during the consultation process regarding the potential for re-exposure of buried cables at landfall and changes to coastal processes and landfall morphology from remedial protection measures. It is on this basis the assessment is completed, drawing together understanding of the coastal morphology, completed modelling and quantitative analyses of potential changes to flows, waves and sediment transport as considered in sections 6.1, 6.2 and 6.3 respectively.

## 6.6.2 Assessment

Section 5.3 assesses the potential impacts of construction of the HDD landfall, including the excavation of exit pits (potentially up to 60 m wide, 30 m long and 5 m deep) at the HDD exit point. It was discussed that there is the potential for interference with the shoaling and breaking of long period waves, along with the concentration and channelling of offshore orientated flows, likely resulting in a localised area of mixed sea state, which would be the case until the pits backfilled naturally and the sediment berms winnowed down.

Other potential sources of change to the landfall associated with installed infrastructure, include the installation of a rock berm associated with the export cable and HDD exit pit, and potential changes to hydrodynamics, waves and sediment transport. The minimum depth at which a rock berm could be installed would be 10 mLAT (although based on a more realistic HDD exit of 20 mLAT, would result in a deeper minimum depth) and the potential influence of a berm at this depth is assessed fully in section 6.3.2 with regards to near-bed blockage effects to flows and sediment transport. Overall, it was concluded in section 6.3.2 that the berm would not affect flows downstream, at minimum depth of 10 mLAT, therefore there is no expected change to the landfall based on changes to tidal properties. With respect to the potential waves, these would be the same as that described for construction impacts in section 5.3 until which point the seabed returns to pre-construction seabed levels and beyond which there would not be considered to be any further localised interference with breaking waves.

With respect to the potential for re-exposure of buried cables at landfall, analyses of the sediment transport potential has demonstrated the capability of waves to mobilise sediment at the landfalls. Therefore, theoretically with the occurrence of storm or extreme events, there is the potential for erosion across the landfall area, but this would not necessarily be localised to the installed cable and HDD exit pit but occur more broadly at tens to hundreds of meters or even larger sections along the coastline. With such storm or extreme events, eroded material could temporarily be moved offshore to then be transported back into the nearshore area under natural coastal processes. Should the described nearshore erosion occur, the cable or HDD exit pit could be exposed for a period of time until natural coastal processes transport material back onshore. It is not possible to precisely say the duration of exposure and natural re-burial, as this would be dependent on the degree of erosion and resulting exposure. Should it be necessary that remedial protection is required in the form of additional rock protection, this is more likely to be required at depths of 10 mLAT or deeper associated with the installed cable. It is also likely that the remedial protection would be orientated perpendicular to the coast, parallel to the wave approach to the coastline, in line with wave diffraction processes. The potential for blockages to flows and sediment transport of any new additional remedial protection at these depths, will be in line with that already assessed for the operational presence of rock protection and depths of 10 mLAT and deeper (section 6.3.2). The presence of rock protection of up to 3 m and base width of 20 m did not result in downstream changes to water levels, flows and by association sediment transport. With respect to waves, the long period waves may theoretically feel the presence of the rock protection at slightly deeper depths (associated



with marginally further offshore locations) than the waves normally would do, leading to a loss in wave energy due to increased friction. However, the low profile of the rock protection, the berm design allowing for the ongoing transmission of the wave (i.e. the wave would move through the berm, rather than reflect from a solid wall) and the larger regional scale of the wave processes, would mean any interference to the wave would be constrained to over the berm, leading to only a marginal and localised loss in wave energy. The regional scale wave diffraction and shoaling would mean that the potential localised energy loss as the wave progresses over the rock protection, will not translate to an overall change in the wave energy at the coast. Therefore, with no changes to the flows or waves, even with the additional introduction of remedial protection if required, there is not anticipated to be any change to the coastal morphology under the operation of the offshore Project.



## 7 REFERENCES

ABPmer, (2008). Atlas of UK Marine Renewable Energy Resources. Interactive Map, Available online at: <https://www.renewables-atlas.info/explore-the-atlas/>. [Accessed 19/09/2022].

ABPmer, (2018). SEASTATES Metocean Data and Statistics Interactive Map. Available online at <https://www.seastates.net/explore-data/>. [Accessed 19/09/2022]

Arthur, R.S., (1951). The Effects of Islands on Surface Waves

Barne, J.H., Robson, C.F., Kaznowska, S.S., Doody, J.P., & Davidson, N.C., eds., (1996). Coasts and seas of the United Kingdom. Region 3 North-east Scotland: Cape Wrath to St. Cyrus. Peterborough, Joint Nature Conservation Committee. (Coastal Directories Series.)

BGS, (1981). Caithness Solid Geology Sheet (58N-04W). Institute of Geological Sciences. Available online at: <https://largeimages.bgs.ac.uk/iip/mapsportal.html?id=1003744>

BGS, (1989). Sutherland Solid Geology Sheet (58N-04W). Institute of Geological Sciences. Available online at: <https://largeimages.bgs.ac.uk/iip/mapsportal.html?id=1003879> [Accessed 19/09/2022].

BGS, (2015) Geology of Britain viewer Available online at: <http://mapapps.bgs.ac.uk/geologyofbritain/home.html> [Accessed 19/09/2022].

BGS, (2020b) Free downloads – Browsing, Available online at: <https://www2.bgs.ac.uk/downloads/browse.cfm>. [Accessed 19/09/2022].

BGS, (2022) BGS Offshore GeoIndex. Available online at: [https://mapapps2.bgs.ac.uk/geoindex\\_offshore/home.html? ga=2.53031727.641647902.1655812172.2025367756.1627475166](https://mapapps2.bgs.ac.uk/geoindex_offshore/home.html? ga=2.53031727.641647902.1655812172.2025367756.1627475166). [Accessed 19/09/2022].

British Oceanographic Data centre, (2022). UK Tide Gauge Network Data Search. [https://www.bodc.ac.uk/data/hosted\\_data\\_systems/sea\\_level/uk\\_tide\\_gauge\\_network/#ull](https://www.bodc.ac.uk/data/hosted_data_systems/sea_level/uk_tide_gauge_network/#ull) [Accessed 19/09/2022].

Carpenter, J.R., Merkelbach, L., Callies, U., Clark, S., Gaslikova, L., Baschek, B., (2016). Potential Impacts of Offshore Wind Farms on North Sea Stratification. PLoS ONE 11(8): e0160830. doi:10.1371/journal.pone.0160830

Cazenave, P. W., Torres, R., and Allen, I. J., (2016). Unstructured grid modelling of offshore wind farm impacts on seasonally stratified shelf seas. Progress in Oceanography 145 (2016) 25–41. <http://dx.doi.org/10.1016/j.pocean.2016.04.004>

Cefas, (2022). WaveNet. Available online at <https://wavenet.cefas.co.uk/map> [Accessed 19/09/2022]



Cefas, (2016). Suspended Sediment Climatologies around the UK. Report for the UK Department for Business, Energy & Industrial Strategy offshore energy Strategic Environmental Assessment programme.

Christiansen, N., Daewel, U., Djath, B., and Schrum, C., (2022). Emergence of Large-Scale Hydrodynamic Structures Due to Atmospheric Offshore Wind Farm Wakes. *Front. Mar. Sci.* 9:818501. doi: 10.3389/fmars.2022.818501

Dawson, S., Powell, V.A., Duck, R.W., and McGlashan, D.J., (2013). Discussion of Rennie, A.F. and Hansom, J.D. (2011) Sea level trend reversal: Land uplift outpaced by sea level rise on Scotland's coast. *Geomorphology*, 125 (1), 193-202

Dawson, M., Howard, T., Tinjer, J., Lowe J., Bricheno, L., Calvert, D., Edwards, T., Gregory, J., Harris, G., Krijnen, J., Pickering, M., Roberts, C. and Wolf, J., (2018). UKCP18 Marine Report.

DECC, (2016a). UK Offshore Energy Strategic Environmental Assessment 3 (OESEA3): Geology, Substrates & Coastal Processes. Available online at: [https://assets.publishing.service.gov.uk/government/uploads/system/uploads/attachment\\_data/file/504536/OESEA3\\_A1b\\_geology\\_substrates.pdf](https://assets.publishing.service.gov.uk/government/uploads/system/uploads/attachment_data/file/504536/OESEA3_A1b_geology_substrates.pdf) [Accessed 19/09/2022].

DECC, (2016b). UK Offshore Energy Strategic Environmental Assessment 3 (OESEA3). Appendix 1D - Water Environment (Regional Sea 6 &7). Available online at: [https://assets.publishing.service.gov.uk/government/uploads/system/uploads/attachment\\_data/file/504541/OESEA3\\_A1d\\_Water\\_environment.pdf](https://assets.publishing.service.gov.uk/government/uploads/system/uploads/attachment_data/file/504541/OESEA3_A1d_Water_environment.pdf). [Accessed 19/09/2022]

Dorrell, R.M., Lloyd, C.J., Lincoln, B.J., Rippeth, T.P., Taylor, J.R., Caulfield, C.C.P., Sharples, J., Polton, J.A., Scannell, B.D., Greaves, D.M., Hall, R.A. and Simpson, J.H., (2022), Anthropogenic Mixing in Seasonally Stratified Shelf Seas by Offshore Wind Farm Infrastructure. *Front. Mar. Sci.* 9:830927. doi: 10.3389/fmars.2022.830927

Dynamic Coast, (2022). Dynamic Coast 2. Available online at: <https://www.dynamiccoast.com/>

EMEC. (2020). Metocean Site Characterisation of Billia Croo test site

EMEC, (2020). Data West of Orkney Data Review

EMODnet Bathymetry Consortium, (2020). EMODnet Digital Bathymetry (DTM).

EMODnet, (2021). EMODnet Geology Mapper. Available online at: <https://www.emodnet-geology.eu/map-viewer/> [Accessed 19/09/2022].

Fairley, I., Masters, I. and Karunaratna, H., (2015). The cumulative impact of tidal stream turbine arrays on sediment transport in the Pentland Firth, *Renewable Energy*, 80, pp. 755–769. Available online at: <https://doi.org/10.1016/j.renene.2015.03.004>. [Accessed 19/09/2022].

Fitton, J.M., Hansom, J.D., and Rennie, A.F., (2017) Dynamic Coast - National Coastal Change Assessment: Cell 4 - Duncansby Head to Cape Wrath, CRW2014/2. Available online at:



<https://www.dynamiccoast.com/files/reports/NCCA%20-%20Cell%204%20-%20Duncansby%20Head%20to%20Cape%20Wrath.pdf> [Accessed 19/09/2022].

Floeter, J., van Beusekom, J.E.E., Auch, D., Callies, U., Carpenter, J., Dudeck, T., (2017). Pelagic effects of offshore wind farm foundations in the stratified North Sea. *Prog. Oceanogr.* 156, 154–173. doi: 10.1016/j.pocean.2017.07.003

Harris, J.M., Draper, S., Yao, W. and An, H., (2021). Scour Development Around Monopile and Jacket Foundations in Silty Sands. In Rice, J., Liu, X., Sasanakul, I., Mcllroy, M. and Xiao, M., (Eds), 2021. 10<sup>th</sup> International Conference on Scour and Erosion. Arlington, Virginia, USA.

Harris, J.M. and Whitehouse, J.S., (2021). Scour Development Around Truncated Cylinders: A Modified Approach. In Rice, J., Liu, X., Sasanakul, I., Mcllroy, M. and Xiao, M. (Eds), 2021. 10<sup>th</sup> International Conference on Scour and Erosion. Arlington, Virginia, USA.

Hashemi, R.M., Neill, S.P., and Davies, A.G., (2014). A coupled tide-wave model for the NW European shelf seas. *Geophysical and Astrophysical Fluid Dynamics*. Available online at: <https://doi.org/10.1080/03091929.2014.944909> [Accessed 19/09/2022].

Highwind Ltd, (2022). Pentland Offshore Floating Windfarm Offshore Environmental Impact Assessment Report.

Horsburgh, K., Rennie, A. and Palmer, M., (2020). Impacts of climate change on sea-level rise relevant to the coastal and marine environment around the UK. *MCCIP Science Review 2020*, 116–131. Hurst, M.D., Muir, F.M.E., Rennie, A.F. and Hansom, J.D., (2021). *Dynamic Coast: Future Coastal Erosion*, (2021) CRW2017\_08. Scotland's Centre of Expertise for Waters (CREW). Available online at [crew.ac.uk/publications](http://crew.ac.uk/publications) [Accessed 19/09/2022]

Institute of Geological Sciences (1972a). BH72/28 Borehole Record. Available online at: [http://marinedata.bgs.ac.uk/Samples/WEB/58N005W/58N005W\\_4.pdf](http://marinedata.bgs.ac.uk/Samples/WEB/58N005W/58N005W_4.pdf) [Accessed 19/09/2022].

Institute of Geological Sciences (1972b). BH73/31 Borehole Record. Available online at: [http://marinedata.bgs.ac.uk/Samples/WEB/58N005W/58N005W\\_7.pdf](http://marinedata.bgs.ac.uk/Samples/WEB/58N005W/58N005W_7.pdf) [Accessed 19/09/2022].

Institute of Geological Sciences (1972c). BH72/26 Borehole Record. Available online at: [http://marinedata.bgs.ac.uk/Samples/WEB/58N005W/58N005W\\_3.pdf](http://marinedata.bgs.ac.uk/Samples/WEB/58N005W/58N005W_3.pdf) [Accessed 19/09/2022].

Institute of Geological Sciences (1972d). BH72/27 Borehole Record. Available online at: [http://marinedata.bgs.ac.uk/Samples/WEB/58N004W/58N004W\\_38.pdf](http://marinedata.bgs.ac.uk/Samples/WEB/58N004W/58N004W_38.pdf) [Accessed 19/09/2022].

JNCC, (2019). Geological Conservation Review (GCR) csv extract of the GCR database (part) - Geological Conservation Review (GCR) database extract. Available online at: <https://data.jncc.gov.uk/data/b0f53582-f93d-4e70-8ff9-0f16b660e4ad/GCR-Extracted-TopCat-20190807.csv>. [Accessed 19/09/2022].

Marine Scotland, (2020). Scotland's Marine Assessment 2020. Available online at: <https://marine.gov.scot/sma/> [Accessed 19/09/2022].

Marine Scotland, (2016). The Scottish Shelf Model. Part 2: Pentland Firth and Orkney Waters Sub-Domain. *Scottish Marine and Freshwater Science*, 7(4), 248. <https://doi.org/10.7489/1693-1>. [Accessed 19/09/2022].



Marine Scotland (2022). Scoping Opinion for West of Orkney Windfarm. Available from: <https://marinefrom:https://marine.gov.scot/ml/west-orkney-wind-farm> [Accessed 02/02/2023].

Miller, P.I. and Christodoulou, S., (2014). Frequent locations of oceanic fronts as an indicator of pelagic diversity: Application to marine protected areas and renewables. Available online at: <https://www.sciencedirect.com/science/article/abs/pii/S0308597X13002066?via%3Dihub> [Accessed 19/09/2022].

National Oceanography Centre, (2021). Tidal Current Vertical Profiles. Available online at: <https://noc.ac.uk/files/documents/business/current-vertical-profiles.pdf> [Accessed 19/09/2022].

NatureScot, (2022). Protected sites information. Available online at [https://gateway.snh.gov.uk/natural-spaces/inspire\\_download\\_atom.xml](https://gateway.snh.gov.uk/natural-spaces/inspire_download_atom.xml) [Accessed 19/09/2022]

NatureScot, (2008a). Pennylands Site of Special Scientific Interest Citation, Highland (Caithness). Available online at: <https://sitelink.nature.scot/site/1278>. [Accessed 19/09/2022].

NatureScot (2008b). Pennylands Site of Special Scientific Interest Site Management Statement. Available online at: <https://sitelink.nature.scot/site/1278>. [Accessed 19/09/2022].

NatureScot (2008c). Ushat Head Site of Special Scientific Interest Site Management Statement. Available online at: <https://sitelink.nature.scot/site/1585> [Accessed 19/09/2022].

NatureScot (2008d). Sandside Bay Site of Special Scientific Interest Site Management Statement. Available online at: <https://sitelink.nature.scot/site/1405>. [Accessed 19/09/2022].

NatureScot (2008e). Sandside Bay Site of Special Scientific Interest Operations Requiring Consent from Scottish Natural Heritage. Available online at: <https://sitelink.nature.scot/site/1405> [Accessed 19/09/2022].

NatureScot (2009a). Red Point Coast Site of Special Scientific Interest Site Management Statement. Available online at: <https://sitelink.nature.scot/site/1338>. [Accessed 19/09/2022].

NatureScot (2009b). Red Point Coast Site of Special Scientific Interest Site Citation, Highland (Caithness/Sutherland). Available online at: <https://sitelink.nature.scot/site/1338>. [Accessed 19/09/2022].

NatureScot (2009c). Red Point Coast Site of Special Scientific Interest Operations Requiring Consent from Scottish Natural Heritage. Available online at: <https://sitelink.nature.scot/site/1338>. [Accessed 19/09/2022].

NatureScot (2009d). Holborn Head Site of Special Scientific Interest Site Management Statement. Available online at: <https://sitelink.nature.scot/site/789>. [Accessed 19/09/2022].

NatureScot (2010a). Strathy Coast Site of Special Scientific Interest Site Management Statement. Available online at: <https://sitelink.nature.scot/site/1689>. [Accessed 19/09/2022].



NatureScot (2010b). Dunnet Head Site of Special Scientific Interest Site Management Statement. Available online at: <https://sitelink.nature.scot/site/571> [Accessed 19/09/2022].

NatureScot (2010c). Dunnet Head Site of Special Scientific Interest Operations Requiring Consent from Scottish Natural Heritage. Available online at: <https://sitelink.nature.scot/site/571> [Accessed 19/09/2022].

NatureScot (2010d). Strathy Coast Site of Special Scientific Interest Operations Requiring Consent from Scottish Natural Heritage. Available online at: <https://sitelink.nature.scot/site/1689> [Accessed 19/09/2022].

NatureScot (2019). Strathy Point Special Area of Conservation, Conservation Advice Package. Available online at: <https://sitelink.nature.scot/site/8386> [Accessed 19/09/2022].

Neill, S.P., Vogler, A., Goward-Brown, A.J., Baston, S., Lewis, M.J., Gillibrand, P.A., Waldman, S., and Woolf, D.K., (2017). The Wave and Tidal Resource of Scotland. Renewable Energy Volume 114. Part A, pages 3-17.

Neil, S.P., Lewis, M.J., Hashemi, M.R., Slater, E., Lawrence, J., and Spall, S.A., (2014). Inter-annual and inter-seasonal variability of the Orkney wave power resource.

Neil, S.P. and Hashemi, M.R., (2013). Wave power variability over the northwest European shelf seas. Appl Energy, 106 (2013), pp. 31-46

NTSLF, (2022). National Tidal and Sea Level Facility: Tidal Predictions. Available online at: <https://ntslf.org/> [Accessed 19/09/2022].

Ocean Infinity (2023a). Offshore Geophysical Site Investigation: West of Orkney Windfarm. Volume 1 OAA Results Report, West Of Orkney Windfarm, United Kingdom. Q2-Q3 2022. Document No. GB-GEN-00-MMT-000007. March 2023.

Ocean Infinity (2023b). Offshore Geophysical Site Investigation: West of Orkney Windfarm. Volume 2a ECC Results Report (Whiten Head Bank to Crosskirk), West Of Orkney Windfarm, United Kingdom. Q2-Q3 2022. Document No. GB-GEN-00-MMT-000007. March 2023.

Ocean Infinity (2023c). Offshore Geophysical Site Investigation: West of Orkney Windfarm. Volume 2b ECC Results Report (Stormy Bank to Crosskirk), West Of Orkney Windfarm, United Kingdom. Q2-Q3 2022. Document No. GB-GEN-00-MMT-000007. March 2023.

Ocean Infinity (2023d). Offshore Geotechnical Site Investigation: West of Orkney Windfarm. Volume I – Shallow Geotechnical Report, West Of Orkney Windfarm, United Kingdom. Q2-Q3 2022. Document No. GB-GEN-00-MMT-000036. March 2023.

O'Hara Murray, R. and Campbell, L., (2021). Pentland Firth and Orkney Waters Climatology 1.02. doi: 10.7489/12041-1



O'Hara Murray, R.B., and Gallego, A., (2017). A modelling study of the tidal stream resource of the Pentland Firth, Scotland. *Renewable Energy*, 102(B), 326–340. Available online at <https://doi.org/10.1016/j.renene.2016.10.053> [Accessed 14/09/2022]

OpenHydro and SSE, (2015). *Brimms Tidal Array: Baseline Physical Processes Environment*

Orkney Islands Council, (2020). *Orkney Islands Marine Region: State of the Environment Assessment*

OWC, 2022. *West of Orkney Offshore Wind Farm. Crosskirk Landfall Additional Export Cable Routes Assessment. Document No.: 100-WOW-OFC-A-DN-0001-01.OWPL (2022a). West of Orkney Wind Farm Scoping Report.*

OWPL (2022a). *West of Orkney Wind Farm Scoping Report.*

OWPL, (2022b). *Marine Physical and Coastal Processes, Benthic Ecology and Fish Ecology Consultation meeting minutes. Meeting held June 2022.*

OWPL, (2023). *EIA Metocean Design Basis. Doc No. WO1-WOW-MET-AM-BD-0001*

Partrac, (2013). *SSE Renewables – Costa Head Metocean, ADCP Data Report, Phase V – Costa Head. May 2013.*

Price, D., Stuver, C., Johnson, H., Gallego, A., & O'Hara Murray, R. (2016). The Scottish Shelf Model. Part 2: Pentland Firth and Orkney Waters Sub-Domain. *Scottish Marine and Freshwater Science*, 7(4), 248. <https://doi.org/10.7489/1693-1> [Accessed 19/09/2022].

Ramsay, D.L. and Brampton, A.H., (2000). *Coastal Cells in Scotland: Cell – 4 – Duncansby Head to Cape Wrath. Scottish Natural Heritage Research, Survey and Monitoring Report No 146.*

Schultze, L., Merkelbach, L., Horstmann, J., Raasch, S., and Carpenter, J., (2020). Increased mixing and turbulence in the wake of offshore wind farm foundations. *J. Geophys. Res. Oceans* 125, e2019JC015858. doi: 10.1029/2019JC015858

Scottish Government, (2016). *Pilot Pentland Firth and Orkney Waters Spatial Plan. Available online at <https://www.gov.scot/binaries/content/documents/govscot/publications/factsheet/2016/03/pilot-pentland-firth-orkney-waters-marine-spatial-plan/documents/00497299-pdf/00497299-pdf/govscot%3Adocument/00497299.pdf>* [Accessed 07/09/2022]

Scottish Natural Heritage (SNH), (2014). *Seasonal shelf-sea front mapping using satellite ocean colour to support development of the Scottish MPA network. Scottish Natural Heritage. Commissioned Report No. 538.*

Soulsby, R.L., (1997) *Dynamics of marine sands. A manual for practical applications. Thomas Telford Publications, London, 249 p.*

Sharples, J., Holt, J., Wakelin, S. and Palmer, M.R., 2022. *Climate change impacts on stratification relevant to the UK and Ireland. MCCIP Science Review 2022, 11 pp.*



Spectrum, (2023). West of Orkney Windfarm Nearshore Geophysical Survey. Results and Charts Report – Volume 1 Rev 1 (02.22.16.PROC)

UKHO, (1954). Chart 1954 Cape Wrath to Pentland Firth including Orkney (1 to 200k)

UKHO, (2022). Admiralty Total Tide software.

Wolf, J., Woolf, D. and Bricheno, L., (2020). Impacts of climate change on storms and waves relevant to the coastal and marine environment around the UK. MCCIP Science Review 2020, 132–157.



## 8 ABBREVIATIONS

TERM	DEFINITION
3D	Three Dimensional
ADCP	Acoustic Current Doppler Profile
ATT	Admiralty TotalTide Software
BEIS	Department for Business, Energy and Industrial Strategy
BGS	British Geological Survey
BODC	British Oceanographic Data Centre
CD	Chart Datum
CFSR	Climate Forecast System Reanalysis
CIRIA	Construction Industry Research and Information Association
CPT	Cone Penetration Test
CTD	Conductivity, temperature and depth
DD	Domain Decomposition
DECC	Department of Energy and Climate Change
DHI	Danish Hydraulics Institute
DMPA	Dredge Material Placement Area
DTM	Digital Terrain Model
DVV	Dual Van Veen
ECC	Export Cable Corridor
EIA	Environment Impact Assessment
EIAR	Environment Impact Assessment Report
EMODnet	European Marine Observation and Data Network
EMEC	European Marine Energy Centre
FLiDAR	Floating light detection and radar
FM	Flexible Mesh
HAT	Highest Astronomical Tide
HD	Hydrodynamic
HDD	Horizontal Direction Drilling
HEC	Hydraulic Engineering Circular
HF	High Frequency
Hs	Significant Wave Height
HG	Hamon Grab



TERM	DEFINITION
HW	High Water
HYCOM	Hybrid Coordinate Ocean Model
IEMA	Institute of Environmental Management and Assessment
Km	Kilometres
KP	Kilometre Point
LAT	Lowest Astronomical Tide
LF	Low Frequency
LW	Low Water
m	Metres
m/day	Metres per day
Max	Maximum
MBES	Multibeam Echosounder
Met	Meteorological
CFE	Mass Flow Excavator
mg/l	Milligram Per Litre
MHW	Mean High Water
MHWN	Mean High Water Neap
MHWS	Mean High Water Springs
Min	Minimum
MLW	Mean Low Water
MLWN	Mean Low Water Neap
MLWS	Mean Low Water Springs
mm	Millimetre
MoW	MetOceanWorks
MPA	Marine Protected Area
m/s	Metres per second
MSL	Mean Sea Level
MT	Mud Transport
N	North
NCMPA	Nature Conservation Marine Protected Area
NTSLF	National Tidal and Sea Level Facility
NTU	Nephelometric Turbidity Units
OAA	Option Agreement Area



TERM	DEFINITION
OEL	Ocean Ecology Limited
OI	Ocean Infinity
OSP	Offshore Substation Platforms
OSPAR	Oslo/Paris Convention
OWF	Offshore Wind Farm
OWPL	Offshore Wind Power Limited
P	percentile
PCS	Port and Coastal Solutions
PE	Peak Ebb
PF	Peak Flood
PFOW	Pentland Firth and Orkney Waters
PFOWF	Pentland Firth Offshore Wind Farm
PLGR	Pre-Lay Grapnel Run
PLONOR	Poses Little or No Risk to the Environment
Ppt	Parts per thousand
PSA	Particle Size Analysis
psu	Practical Salinity Unit
PT	Particle Tracking
RCP	Representative Concentration Pathway
RMSE	Root Mean Square Error
RP	Return Period
s	Second
SAC	Special Area Of Conservation
SBP	Sub-Bottom Profiler
SI	Scatter Index
SPA	Special Protection Area
SPM	Suspended Particulate Matter
SSC	Suspended Sediment Concentration
SSS	Side-Scan Sonar
SSSI	Site Of Special Scientific Interest
SW	Spectral Wave
SWAN	Simulating Waves Nearshore
Tp	Wave Period



TERM	DEFINITION
TSHD	Trailing Suction Hopper Dredger
TSS	Total Suspended Sediment
UAV	Unmanned Aerial Vehicles
UHRS	Ultra-High Resolution Seismic
UK	United Kingdom
UKHO	United Kingdom Hydrographic Office
UKCP	UK Climate Projections
VC	Vibrocore
WODC	World Ocean Data Centre
WTGs	Wind Turbine Generators



## 9 GLOSSARY

TERM	DEFINITION
<b>Bathymetry</b>	A measurement of the depth at various locations within the offshore environment indicating the bedform features present such as shallow banks and steep slopes.
<b>Bedload parting zone</b>	Bedload parting zone in the marine environment defines a location in which there is a divergence in bedload sediment transport pathways, with transport occurring in opposing directions on either side of the bedload parting
<b>Clasts</b>	Fragments of smaller grains of mineral or rock (e.g., siltstone, sandstone, mudstone), or a fragment of boulders and cobbles.
<b>Climate Change</b>	A global change in the climate resulting in long-term changes to sea level with increasing sea level.
<b>Coast</b>	Where the ocean waves meet the land.
<b>Coastal Processes</b>	Natural processes that occur as waves intersect with the coastline, e.g., sediment transportation and deposition, and erosion. These processes can be altered due to offshore Project activities, such as with increased suspended sediment concentration, or modified flows and wave energy affecting mixing.
<b>Controlled Flow Excavator</b>	A controlled flow excavator is a tool that is capable of dredging the seabed to clear material and will be used for bedform clearance within the OAA and offshore Export Cable Corridor to prepare the seabed prior to installation of infrastructure.
<b>Diamict</b>	A term used to describe unsorted to poorly sorted sediment which can contain particles covering a range of sizes.
<b>Extreme Waves</b>	Waves that are of a significant height. The largest waves that can be expected to be formed in a region based on extreme conditions (i.e., storm conditions).
<b>Friable</b>	Term used to describe rock that has a tendency to be broken up easily.
<b>Foundation</b>	The foundation on which the wind turbine generators or offshore substation platforms are installed.
<b>Geology – Bedrock</b>	The composition of the bedrock as it was formed over time (e.g., rock, sandstone) which can be dated to geological eras (e.g., Palaeozoic) and geological periods (e.g., Permian, Triassic)
<b>Geology – Quaternary</b>	A geological period within the Cenozoic era spanning to present day in which the seabed sediment and deposits can be dated back to.
<b>Glacial Till</b>	Sediment that has been transported and deposited from glaciers.
<b>Highest Astronomical Tide</b>	The highest tidal levels which can be predicted to occur under average meteorological conditions and under any combination of astronomical conditions. The highest astronomical tide does not necessarily represent the highest levels which may occur as it represents average meteorological conditions, and storm surges may result in higher tidal levels.
<b>Hydrodynamic</b>	Hydrodynamics is concerned with the forces acting on or exerted by fluids.
<b>Interbedding</b>	Geological term used to describe when particular layers of rock lie between or alternate between layers comprised of different types of rock.



TERM	DEFINITION
<b>Landfall</b>	The location where the export cables will be brought ashore. The interface between the offshore and onshore environment.
<b>Lowest Astronomical Tide</b>	The lowest tidal levels which can be predicted to occur under average meteorological conditions and under any combination of astronomical conditions. The lowest astronomical tide does not necessarily represent the lowest levels which may occur as it represents average meteorological conditions, and storm surges may result in lower tidal levels.
<b>Mean High Water Spring</b>	The average throughout the year of the heights of two successive high waters during a 24-hour period in each month, when the tidal range is greatest (spring tides).
<b>Mean Low Water Spring</b>	The average throughout the year of the heights of two successive low waters during a 24-hour period in each month during spring tides.
<b>Mean Sea Level</b>	The average height of the sea surface for all tidal stages.
<b>Metocean</b>	Metocean conditions refer to the combined wind, wave and climate (etc.) conditions as found on a certain location.
<b>Morphology – Bedforms</b>	A bedform is a geological feature that develops as a result of bed material being moved by flows, for example sandwaves.
<b>Nearshore</b>	The location of the survey sampling referring to the region located closest to the coast towards landfall within the offshore Export Cable Corridor.
<b>Numerical Modelling</b>	Use of software to model the complex physics of hydrodynamic, wave and sediment transport processes.
<b>Offshore Export Cables</b>	A high voltage alternating current subsea power cable system, consisting of a three-core armoured submarine power cable with one (or more) fibre optic units embedded in the interstice, running from the offshore substation platforms to the transition joint bay (up to the point of mean high water springs). The offshore export cables transmit the electricity generated from the offshore wind farm to the onshore export cables for transmission onwards to the onshore substation.
<b>Offshore Export Cable Corridor</b>	The area within which the offshore export cables will be installed.
<b>Offshore Project</b>	The entire offshore Project, which defines the Red Line Boundary for the Section 36 Consent and the Marine Licence applications, including all offshore components seaward of mean high water springs (wind turbine generators, cables, foundations, offshore substation platforms and all other associated infrastructure), and all Project stages from pre-construction to decommissioning, including temporary works.
<b>Offshore Project Area</b>	The region which encompasses the option agreement area and the offshore Export Cable Corridor representing the extent of the offshore Project activities.
<b>Offshore Study Area</b>	Receptor specific area used to characterise the baseline. Each topic specific chapter will define what is considered to be the offshore study area and refer to this throughout as e.g., the physical and coastal processes offshore study area.
<b>Offshore Substation Platform</b>	Offshore platforms consisting of high voltage alternating current power cable substations



TERM	DEFINITION
<b>Option Agreement Area</b>	The OAA covers the array area in which the generation infrastructure including wind turbine generators, offshore substation platforms and offshore substation platform interconnector cables will be located.
<b>Outcropping</b>	Refers to bedrock geology being exposed at the surface.
<b>Return Period</b>	Statistical representation of the number of years when an event on average is expected to be exceeded.
<b>Salinity</b>	The quality or degree of being saline i.e., the quantity of salt within a sample.
<b>Scour</b>	A type of mark (e.g., a depression or pattern) observed within the sediment that can be associated with currents, or the movement of glaciers and boulders across the seabed.
<b>Seabed Sediment</b>	The composition of the sediment that is present on the seabed which can be categorised based on the fraction of the sediment that is coarse (gravel) or fine (sand).
<b>Sediment Transport</b>	The movement of sediment by the forces of currents and waves. Sediment transport potential refers to the amount of sediment that could be expected to move under a given combination of waves and currents and is not supply limited.
<b>Sediment Transport Pathway</b>	A sediment transport pathway indicates that there is a local direction or trend with regards to sediment transport .
<b>Stratification</b>	The separation of water in layers.
<b>Surge</b>	Difference in water level (positive or negative) as result of meteorological forcing from what is recorded or modelled to occur.
<b>Suspended sediment</b>	Sediment transported by a fluid that it is fine enough for turbulent eddies to outweigh settling of the particles.
<b>Suspended Sediment Concentration</b>	Mass of sediment in suspension per unit volume of water.
<b>Tessellated pavement</b>	A relatively flat rock surface which has been divided into rough rectangular blocks or polygon shapes by fractures or joints within the rock.
<b>Tidal asymmetry</b>	This is caused by differences in the duration and magnitude of flood and ebb tides.
<b>Tidal excursion</b>	The extent to which suspended sediment, resulting from seabed disturbance from the offshore Project activities, may be carried through physical processes (e.g., spring tides).
<b>Tide – Ebb Tide</b>	The receding tide, occurring between the time when the tide is highest to lowest.
<b>Tide – Flood Tide</b>	The incoming or rising tide, occurring between the time when the tide is lowest to highest.
<b>Tide – Neap Tide</b>	A tide just after the first or third quarters of the moon when there is least difference between high and low water:
<b>Tide – Spring Tide</b>	A tide just after a new or full moon, when there is the greatest difference between high and low water.
<b>Tidal regime</b>	The tidal regime in an area is based on the daily movement of the tide locally.



TERM	DEFINITION
<b>Tidal residual</b>	The difference between the total current and the linearly predicted tidal current for a given tidal state (i.e. flood / ebb or spring / neap).
<b>Total Suspended Solids</b>	A way of measuring suspended sediment concentrations through water sampling.
<b>Trailer Suction Hopper Dredger</b>	Trailer Suction Hopper Dredger (TSHD) is a proposed method for dredging. TSHD operates by pumping water at a high pressure into the seabed and then suctioning sediment up into a hopper onboard the vessel.
<b>Turbidity</b>	Water turbidity is a physical measure within water and is in respect of how clear or cloudy water is.
<b>Wave – Significant Wave Height</b>	The average height of the top third highest waves.
<b>Wave – Wave Period</b>	The period of a wave is the duration of time (in seconds) between wave peaks. Longer periods are typically associated with swell waves.
<b>Wave – Swell Wave</b>	Are waves are generated in a different region and tend to travel a considerable distance before breaking. Swell waves typically have longer periods and wavelengths and carry more energy.
<b>Wave – Wind Wave</b>	Locally generated waves, which remain within the same fetch
<b>Wave – Deep Water Wave</b>	Where the wavelength is less than twice the water depth. Typically referring to waves occurring in oceans and seas, where water depths are greater than twice the wave wavelength.
<b>Wave – Transitional Wave</b>	This is where waves a transforming from deep water wave to a breaking / shoaling wave, so the wave properties (height, period and wavelength) are such that the wave is beginning to feel the bottom, although not enough to increase friction and steepening as occurs during breaking.
<b>Wave – Transformation</b>	The change in the wave properties as it moves between different states as it typically begins to progress into shallower water with respect to the wavelength, height and period.
<b>Wave – Shoaling and Breaking</b>	Where the wave feels the seabed, leading to steepening. A number of conditions lead to shoaling / breaking, which mainly relate to the ratio between the wave height, wavelength and water depth. Typically for breaking waves, the wave height is greater than three quarters of the water depth.
<b>West of Orkney Windfarm / 'the Project'</b>	The entire offshore and onshore Projects, including all offshore components and onshore components and all Project stages from pre-construction to decommissioning. For the avoidance of doubt this does not include the offshore or onshore infrastructure associated with the connection to the Flotta Hydrogen Hub.
<b>Wind Turbine Generator</b>	The wind turbines that generate electricity consisting of tubular towers and blades attached to a nacelle housing mechanical and electrical generating equipment.



## APPENDIX A MARINE PHYSICAL PROCESSES MODELLING CALIBRATION AND VALIDATION REPORT

### A.1 Introduction

Xodus Group Limited (Xodus) is supporting Offshore Wind Power Limited (OWPL) in the development of the Environmental Impact Assessment (EIA) Report for the West of Orkney Windfarm (the Project) as part of the EIA process. Xodus are undertaking a marine physical and coastal processes technical study to inform the EIA. Xodus commissioned Port and Coastal Solutions Ltd (PCS) to develop and apply a suite of numerical modelling tools to assess construction and operational impacts of the proposed Project, with the following primary requirements in relation to the offshore components of the offshore Project.

- Develop hydrodynamic and spectral wave models covering both the proposed marine physical and coastal process study area and the Orkney Islands;
- Characterise the existing baseline conditions at the offshore Project based on the numerical modelling results and other available information;
- Apply the developed models to assess the effects of installation (for structures and cables) on marine physical processes; and
- Apply the developed models to assess the potential operational effects of two windfarm layouts comprising 125 WTGs (and offshore substation platforms) on marine physical processes.

This report (Appendix A) provides details on the setup and calibration of the numerical modelling tools which will be applied for the baseline and scheme assessments. The completed modelling, including underlying assumptions and results based on the developed West of Orkney model is presented in Appendix B.

#### A.1.1 Project Overview

The offshore Project is located off the north coast of Scotland, to the west of the Orkney Islands, within the N1 Plan Option area. The study area for the marine physical and coastal processes has been defined by using a 10 km buffer around the Option Agreement Area (OAA) and a 15 km buffer around the offshore Export Cable Corridor (ECC). An overview of the proposed offshore Project and associated study area is shown in Figure 1-1.

The key offshore Project elements which are relevant to the modelling study are as detailed within section 1.2 of the marine physical and coastal processes technical report.



## A.1.2 Report structure

This calibration and validation report herein is set out as follows:

- An overview of the Project is provided in Section 1;
- Details on modelling approach, including the software, model mesh, bathymetry and forcing conditions are provided in Section 2;
- The performance of the models is assessed against available calibration data using literature based guideline standards in Section 3; and
- A summary is provided Section 4.

Unless otherwise stated, levels are reported relative to Mean Sea Level (MSL), which is 2.86 m above Chart Datum (CD) at Scrabster (the closest standard port to the Project). Wind and wave directions are reported as the direction the wind and waves are coming from in degrees clockwise from True North. Current direction is reported as the direction the current is going to in degree clockwise from True North.

## A.2 Modelling approach

### A.2.1 Software

Numerical models of the North Sea off the north Scottish coast have been configured in the MIKE software, which is developed by the Danish Hydraulics Institute (DHI). The MIKE suite is internationally recognised state of the art software which has previously been adopted in the UK and internationally for similar projects, including Marine Scotland's (MS) Pentland Firth and Orkney Water's (PFOW) climatology (O'Hara and Campbell, 2021) and a number of other UK Offshore Wind Farm (OWF) developments. The MIKE suite includes hydrodynamic (HD), spectral wave (SW) and Particle Tracking (PT) modules which allows all necessary processes relevant to the coastal processes assessment to be simulated. In particular the modules include the following:

- The MIKE HD model simulates water level variations and flows in response to a variety of forcing functions in coastal regions and estuaries.
- The MIKE SW model allows for the growth, decay and transformation of wind-generated and swell waves in both offshore and coastal environments.
- The MIKE PT model simulates the transport of mud (cohesive sediment) and sand driven by flows and waves and the interaction of sediment with the bed, including settling, deposition and erosion. The model can be run in 3 dimensional (3D) mode which is critical for the assessment of construction impacts required for the study.

For this study the PT model is not setup to simulate baseline sediment transport but will only be applied to assess dispersion and deposition of sediment disturbed during construction. The PT model is therefore not subject to calibration and is not discussed further in this report.



The applied modules adopt a flexible mesh (FM) which allows the spatial resolution of the model mesh to be varied across the model domain. This enables suitable model resolutions to be adopted throughout, ensuring the model accuracy and efficiency can be balanced. For example, areas of interest and areas with complex topographic and bathymetric features (such as the Orkney Islands) can have a higher mesh resolution while a lower mesh resolution can be adopted away from these areas to ensure efficient model run times.

## A.2.2 Model Setup

Details of the mesh, bathymetry, boundary conditions and bed roughness applied in the MIKE HD and SW models are provided in the following sections. The model domain is as illustrated in Figure 1-2 and is applied to both the MIKE HD and SW models.

### A.2.2.1 Model Mesh

The HD and SW model meshes cover the same domain, but with different resolutions to reflect the different requirements of each model; the HD model has higher resolution across the Orkney Islands to ensure that the flows through them are accurately simulated, this is not required for the SW model with waves from the west to north sectors dominating. The SW model resolution can therefore be somewhat reduced away from the OAA so long as the key features which can affect wave growth and breaking are suitably resolved.

Both models extend across an area of approximately 85 km east-west and 30 km north-south centred on the OAA and Orkney Islands. The south boundary is placed to include the National Tide and Sea Level Facility (NTSLF) tide gauge sites at Kinlochbervie (close to the southwest boundary) and Wick (close to the southeast boundary) within the model domain so that the model's ability to replicate water levels against high quality observational data can be assessed.

The HD mesh resolution varies across the domain with highest resolution (100 m) at the cable landfall and across the OAA and with lowest resolution of 2 km at the offshore boundaries (Figure A-1). High resolution is also adopted across the Orkney Islands, with 100 m resolution along the coast, 250 m resolution across the Pentland Firth and 500 m elsewhere to ensure the islands and channels are accurately replicated.

A more regular mesh resolution was applied across the model domain for the SW model calibration setup, with a resolution of approximately 1 km throughout. This resolution was considered appropriate for model calibration, enabling the key bathymetric features to be resolved, but without including the influence of small-scale localised features that would not have been resolved in the MetoceanWorks (MoW) model (which has a resolution of approximately 5.5 km by 11 km) that was used to define the wave conditions in the OAA. For the baseline assessment and for the scheme impact assessment the waves will be rerun on the same mesh as the hydrodynamics to provide a more detailed description of wave conditions across the domain and to allow individual WTG structures to be placed in separate grid cells.

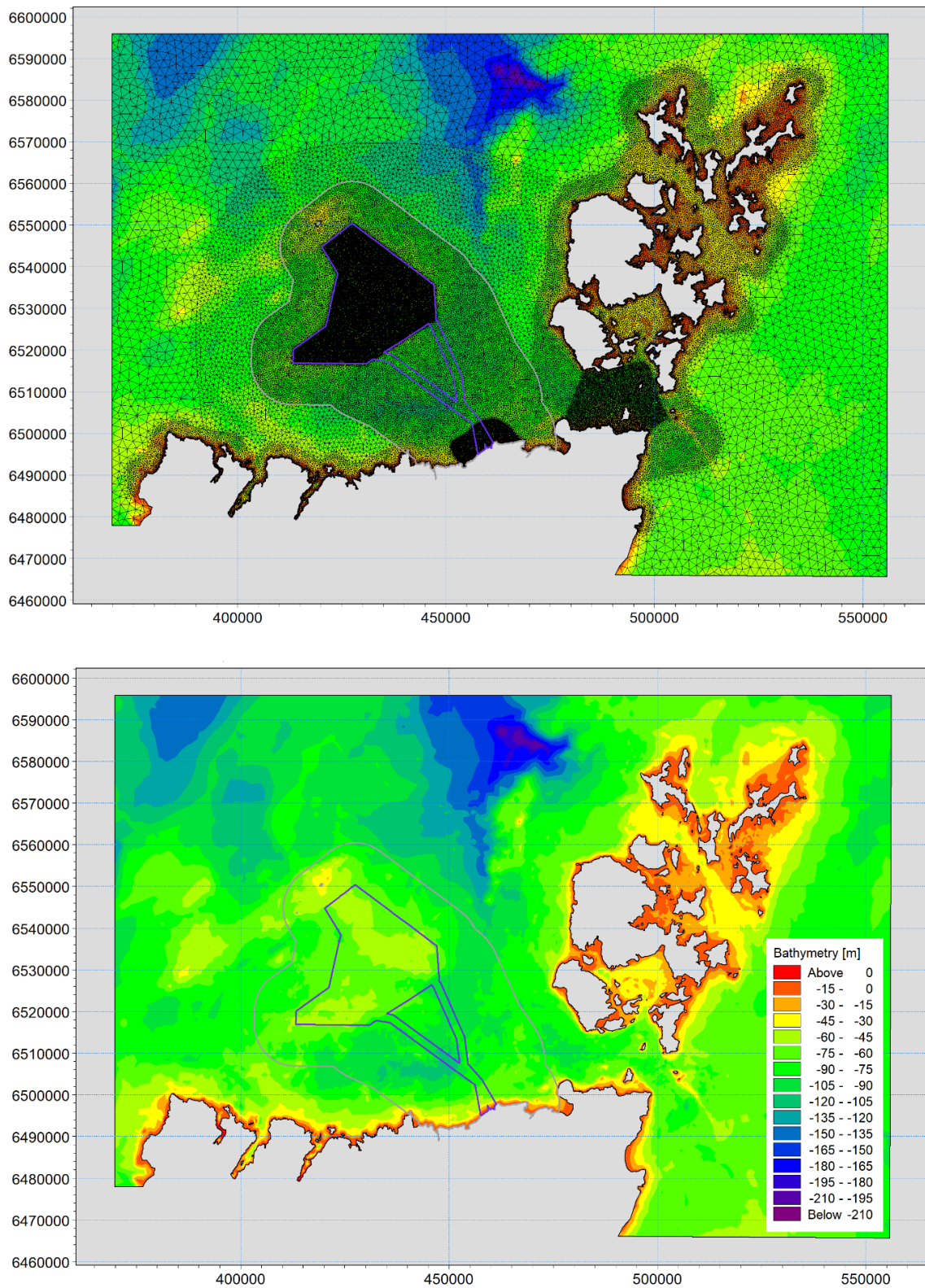


Figure A-1 West of Orkney model HD model flexible mesh (top) and the resulting interpolated bathymetry used in the modelling (bottom)



### A.2.2.2 Bathymetry

The bathymetry used in the HD and SW models is comprised of three key datasets;

- Survey data from Marine Scotland including the following surveys; Farr Point (2014), West Orkney (2013), North Orkney (2013) and Pentland Firth (2009);
- Survey data from United Kingdom Hydrographic Office (UKHO) Admiralty Inspire portal including the following surveys;

<ul style="list-style-type: none"> <li>– 2021 HI1709 Duncansby Head 2 m SDTP</li> <li>– 2021 HI1710 Sinclairs Bay to Smiths Bank 2 m SDT</li> <li>– 2020 2021-086803 Orkney Stromness</li> <li>– 2020 2021-086803 Orkney Scapa Pier</li> <li>– 2020 2021-086803 Orkney Lyness RoRo</li> <li>– 2020 2021-086803 Orkney Houton Bay</li> <li>– 2020 2021-086803 Orkney Graemsay Island Pier</li> <li>– 2021-086803 Orkney Graemsay Island Pier</li> <li>– 2020 2021-086803 Orkney Flotta West Weddel Sound</li> <li>– 2020 2021-086803 Orkney Deepdale Bay Gatnip</li> <li>– 2019 2020-037017 Orkney Stromness Marina</li> <li>– 2019 2020-037017 Orkney Glimps Holm and Lamb Holm Barriers</li> <li>– 2019 2020-037017 Orkney Burra Sound</li> <li>– 2019 2020-037017 Orkney Stronsay Harbour and Approach</li> <li>– 2019 2020-037017 Orkney Rapness Pier</li> <li>– 2019 2020-037017 Orkney Faray SE</li> <li>– 2019 2020-037017 Orkney Egilsay</li> <li>– 2013 2015-037434 Stromness Harbour</li> <li>– 2009 2010-027833 Scapa Flow Main Burra 4 m SB</li> <li>– 2009 2010-027833 Scapa Flow Main Burra 2 m SB</li> <li>– 2009 2010-027833 Scapa Flow Area 2a 2 m SB</li> <li>– 2009 2010-027833 Longhope 2 m SB</li> <li>– 2009 2010-027833 Kirkwall Bay Orkneys SB</li> <li>– 2008 2008-096155 Orkney Islands South Ronaldsay St Margarets Hope</li> <li>– 2008 HI1218 Approaches to the Orkney Islands Blk4</li> </ul>	<ul style="list-style-type: none"> <li>– 2007 2007-005274 Orkney Islands Approaches to Lyness</li> <li>– 2007 HI1202 Westray Firth to Stronsay Firth 2 m SB</li> <li>– 2007 HI1218 Approaches to the Orkney Islands Blk2</li> <li>– 2007 HI1218 Approaches to the Orkney Islands Blk3</li> <li>– 2006 2008-066958 Scapa Flow Blk2</li> <li>– 2006 2008-066958 Scapa Flow Blk1</li> <li>– 2005 M4424 Orkney Islands Stromness Cairston Roads Anchorage</li> <li>– 2005 2008-027254 Orkney Islands Scapa Flow Flotta Terminal Approaches</li> <li>– 2005 2008-027164 Orkney Islands Hoy Sound Houton Jetty Approach</li> <li>– 2005 HI1122 Sanday Sound to Westray Firth Blk1</li> <li>– 2005 HI1122 Sanday Sound to Westray Firth Blk2</li> <li>– 2005 HI1122 Sanday Sound to Westray Firth Blk3</li> <li>– 2003 2006-361500 Orkney Islands Golta Peninsula Flotta</li> <li>– 2000 2006-358807 Orkney Islands Stromness Harbour</li> <li>– 2000 2006-358806 Orkney Islands Scapa Bay</li> <li>– 2000 2006-358805 Orkney Islands Scapa Bay</li> <li>– 2000 2006-358804 Orkney Islands Graemsay Clestrain Sound</li> </ul>
--	---

- Bathymetry from the European (EMODnet) Digital Terrain Model (DTM), 2020 which has a 1/15<sup>th</sup> arc minute resolution (approximately 60 m by 115 m).



Data from the three sources was merged with preference given to the data in the order above. Prior to merging all data were corrected to MSL and reprojected to WGS 1984 UTM30N. The coverage of the various datasets is shown in Figure A-2.

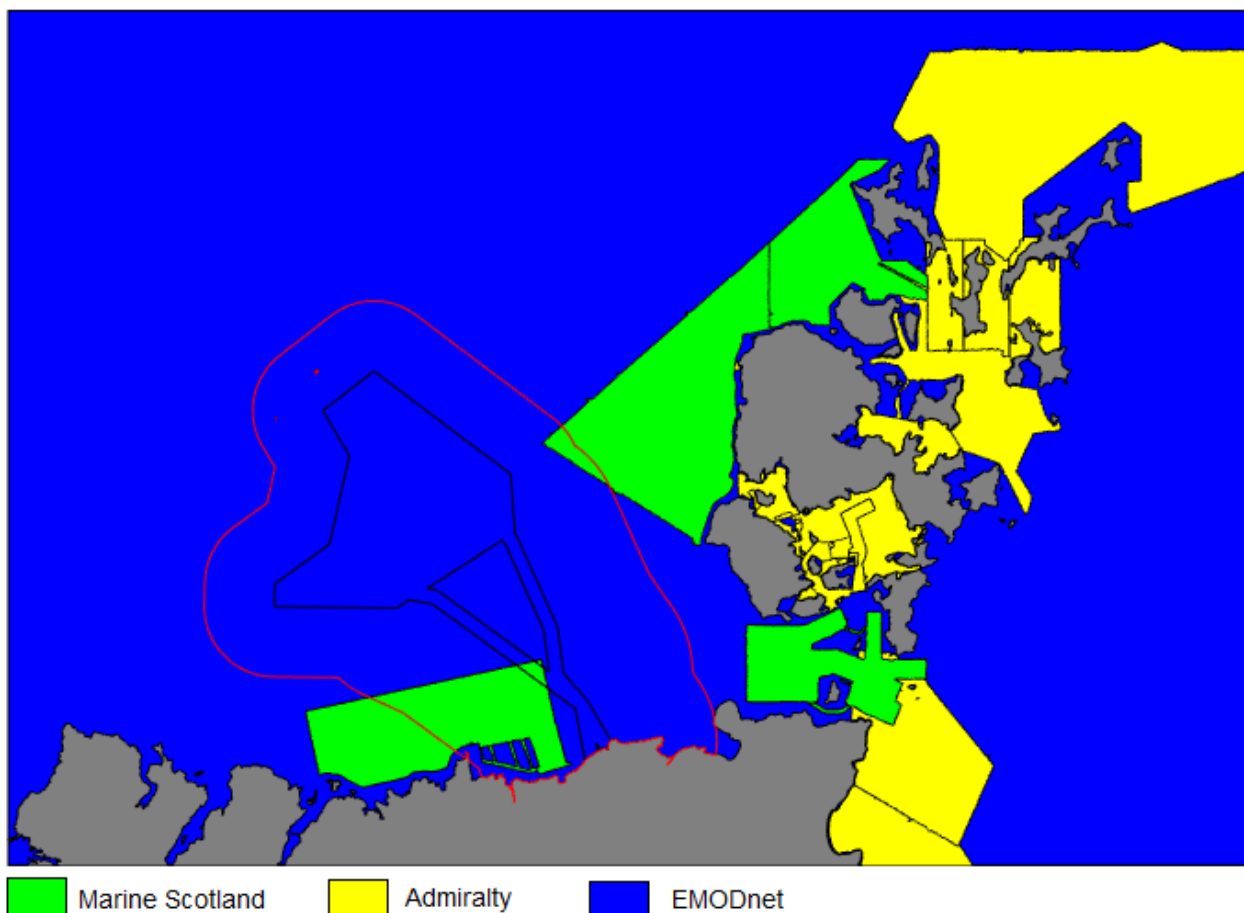


Figure A-2 Extent of bathymetric data coverage

### A.2.2.3 Model Boundaries

#### A.2.2.3.1 Tidal Boundaries

Water level boundaries from a number of sources were considered during the initial model setup to determine which data source most accurately replicated water levels at Kinlochberrie and Wick. This included the following global tidal models:

- DTU10 (Cheng and Andersen, 2011);
- TPXO 8.0 (Egbert *et al.*, 1994); and
- KMS (Andersen, 1995).



Of the three, DTU10 was found to most accurately replicate levels close to the southern boundary where high quality gauge data were available for tidal analysis based on water levels from Kinlochbervie and Wick. DTU10 constituents were therefore used to derive water level timeseries which were applied across all offshore boundaries.

### A.2.2.3.2 Freshwater Flows

To ensure that freshwater inputs do not influence flows in the OAA (and the offshore ECC, particularly close to the landfall site), sensitivity testing of the inclusion of river flow data from the UK National River Flow Archive (NRFA) (<https://nrfa.ceh.ac.uk/data>) was undertaken by including Q5 gauged flow (discharges that are only exceeded for 5% of the record duration) for the rivers in the model domain (Table A-1 ) throughout the model simulation. This assessment did not include all freshwater inputs from the Orkney Islands since the only data on the NRFA for the Orkney Islands was for the Durkadale.

The modelled flows and water levels across the OAA and offshore ECC were found to be insensitive to these freshwater flows, with Root Mean Square (RMS) differences for runs with and without the Q5 flow of less than 0.02 m/s and 0.02 m for flow and water levels, respectively.

Table A-1 River flow data (<https://nrfa.ceh.ac.uk/data>)

RIVER (STATION ID)	FLOW (m <sup>3</sup> /s)		
	Q5	Q50	MEAN
Wick (1001)	10.07	1.63	2.98
Halladale (96001)	19.06	2.33	4.98
Naver (96002)	50.20	9.80	15.78
Strathy (96003)	9.51	1.37	2.63
Strathmore (96004)	26.77	3.46	7.25
Dionard (96005)	17.72	2.90	5.25
Borgie (96006)	10.38	3.17	4.12
Thurso (97002)	29.73	5.23	8.98
Durkadale (107001)	1.66	0.29	0.49

## A.3 Model Calibration

Model calibration is the process of specifying model parameters so that the model reproduces observed data to a suitable level of accuracy. The forcing conditions and bed roughness are key calibration parameters and a number of sensitivity tests were undertaken as part of the calibration process. Calibration is an essential stage in the development of robust numerical modelling tools. However, there is currently no universal agreement on criteria for assessing coastal and estuarine numerical model calibration, partly because the procedure is both model/location and context dependent (Pye *et al.*, 2017). A number of studies have proposed calibration criteria including FWR (1993);



Bartlett (1998); ABPmer (2013); and Williams and Esteves (2017), while guidance provided in Pye *et al.*, (2017) referred to criteria presented in ABPmer (2013). The criteria do not significantly vary between sources and all authors acknowledge that their prescribed standards provide a good basis for assessing model performance, but experience has shown that sometimes they can be too prescriptive. Further they all agree on the need for visual checks to also be undertaken and note that under certain conditions, models can meet statistical calibration standards but appear to perform poorly. Conversely, seemingly accurate models (based on a visual assessment) can fall short of the guidelines. Consequently, a combination of both statistical calibration standards and visual checks should be used to ensure that the model can suitably replicate the local hydrodynamic and wave regime.

The model calibration and validation process for the hydrodynamic model entailed two consecutive spring-neap cycles, so the availability of observation and modelled hydrodynamic data (i.e. water levels and flows) from the Pentland Firth region,, influenced the applied calibration and validation period. The applied calibration period spanned between 15<sup>th</sup> January and 31<sup>st</sup> January 2013 (section A.3.3), while the validation period spanned between 31<sup>st</sup> January and 15<sup>th</sup> February 2013 (section A.3.4). Based on the calibrated and validated model period (i.e. between 15<sup>th</sup> January and 15<sup>th</sup> February 2013), the baseline conditions described in section B.3 and construction impacts described in section B.4, were also investigated for a spring-neap cycle within the applied calibration and validation period.

### A.3.1 Calibration and Validation Metrics

For the present study metrics and standards from Williams and Esteves (2017) relating to water levels, flows and waves have been adopted for assessing the model performance as these are considered to provide a comprehensive summary capturing standards for all variables. The metrics and standards are detailed in the following subsections.

#### A.3.1.1 Water Levels

In terms of the water levels, the following metrics have been considered:

- Modelled water levels (WL) should be within  $\pm 0.1$  m in absolute terms of the observed water levels, or 10% of the spring range and 15% of the neap range in relative terms. Level differences are calculated at the time of high water and low water to ensure that the model captures the tidal range. The calibration guideline standard will be considered to be met if it falls within either the absolute or relative standard;
- RMS surface elevation difference to be  $< 0.2$  m; and
- Mean phase difference to be within 15 minutes. Phase differences are calculated at HW, LW and throughout the time series.

#### A.3.1.2 Flows

In terms of the flow speeds, the following metrics have been considered:

- Differences should be less than 0.10 m/s in absolute terms (or 10 to 20% in relative terms), these are calculated at the time of peak flood (PF) and peak ebb (PE). This ensures that models capture the correct residual flow (since if flood and ebb are not separated a model could consistently over predict the flood and underpredict the ebb or vice-versa so that the differences cancel each other out). The calibration guideline standard will be considered to be met if it falls within either the absolute or relative standard;



- Directions at the time of PF and PE are within 10 degrees;
- RMS error of peak flow speed difference is  $< 0.2$  m/s; and
- The Scatter Index (SI), which is the RMS error normalised by the mean observed flow speed is  $< 0.5$ .

### A.3.1.3 Waves

With respect to waves, the following metrics are considered:

- Mean significant wave height ( $H_s$ ) should be within  $\pm 10\%$  of observed  $H_s$ ; and
- Peak wave period ( $T_p$ ) should be within 20% and wave direction should be within  $30^\circ$ .

### A.3.1.4 Calibration Approach

For the hydrodynamic model, the statistics defined above have been calculated and assessed against the quoted guideline standards. Iterative changes were applied to the model setup to improve the model calibration. It is noted here that the majority of the data available for model calibration and validation is subject to its own limitations (i.e. being predictions or derived from models) and these were taken into consideration during the calibration and validation process.

The hydrodynamic model calibration period spans a 15 day spring-neap cycle (16<sup>th</sup> to 31<sup>st</sup> January 2013), while the validation period spans a separate 15 day spring-neap cycle (31<sup>st</sup> January to 15<sup>th</sup> February 2013). These periods were selected as they coincided with the availability of measured Acoustic Current Doppler Profile (ADCP) data at Costa Head which is located to the northwest of the Orkney Islands. The data are described further in Section A.3.2 below.

The wave calibration focussed on replicating a range of statistical wave conditions rather than a time series of wave conditions. This was in view of the lack of site specific wave data within the OAA against which model calibration could be performed. Further details on the wave model calibration dataset are provided in Section A.3.2.

## A.3.2 Calibration and Validation data

The locations of all calibration data are shown in Figure A-3. The following data has been used for calibrating the hydrodynamic model;

- Predicted water levels at two class 'A' NTSLF gauge sites (Kinlochbervie and Wick);
- Predicted water levels from Admiralty Total Tide (ATT) for three standard port locations (Scrabster on the Scottish mainland and St Mary's Scapa Flow and Kirkwall on Mainland, Orkney);
- Predicted water levels From ATT for a secondary gauge site close to the OAA at Sule Skerry;
- Measured water levels from two ADCP deployments at Costa Head (ST03 and ST04), based on survey deployments between 16<sup>th</sup> January 2012 and 18<sup>th</sup> February 2013;



- Measured flows at two ADCP deployments at Costa Head (ST03 and ST04), based on the same survey period as water levels;
- Predicted flows from the PFOW climatology at three locations (PFOW1 to PFOW3) where calibration of the PFOW climatology against measured mooring data was undertaken. The calibration of the West of Orkney model at these sites took account of the known limitations in the PFOW climatology. The PFOW flows are simulated for 1993. To enable a comparison with the West of Orkney model the flows were harmonically analysed and the derived constituents were used to provide flow predictions for periods coinciding with the West of Orkney model run period; and
- ATT flows at three locations near the offshore Project area covering the OAA and landfall (SN028M, SN028F and SN028E).

The same data were used for validation as for calibration (but with validation considering a different spring-neap cycle).

For the calibration of the wave model, wave conditions were extracted from the MetOceanWorks (MoW) European Spectral Wave Nearshore (SWAN) model, which simulates waves for the 39-year period from 1979 to 2018, and is the wave hindcast location in Figure 2-3. The MoW model is driven by Climate Forecast System Reanalysis (CFSR) winds (<http://rda.ucar.edu/datasets/ds093.1/> and <http://rda.ucar.edu/datasets/sd094.1/>) and is run on a 0.1 degree grid, equivalent to a resolution of approximately 5.5 km x 11 km within the OAA. The waves were extracted from a site in the OAA (see Figure A-3) and analysed as part of a separate study to derive percentile (p) and return period (RP) waves (OWPL, 2022). Winds from CFSR were also analysed to provide similar results for the wind climate (OWPL, 2022). The results from the analysis are provided in section A.3.5.

Wave data were also available at the Dounreay Cefas WaveNet site for two six week periods, from the 26<sup>th</sup> October 1997 to the 7<sup>th</sup> December 1997 and from the 7<sup>th</sup> April 2001 to the 25<sup>th</sup> May 2001.

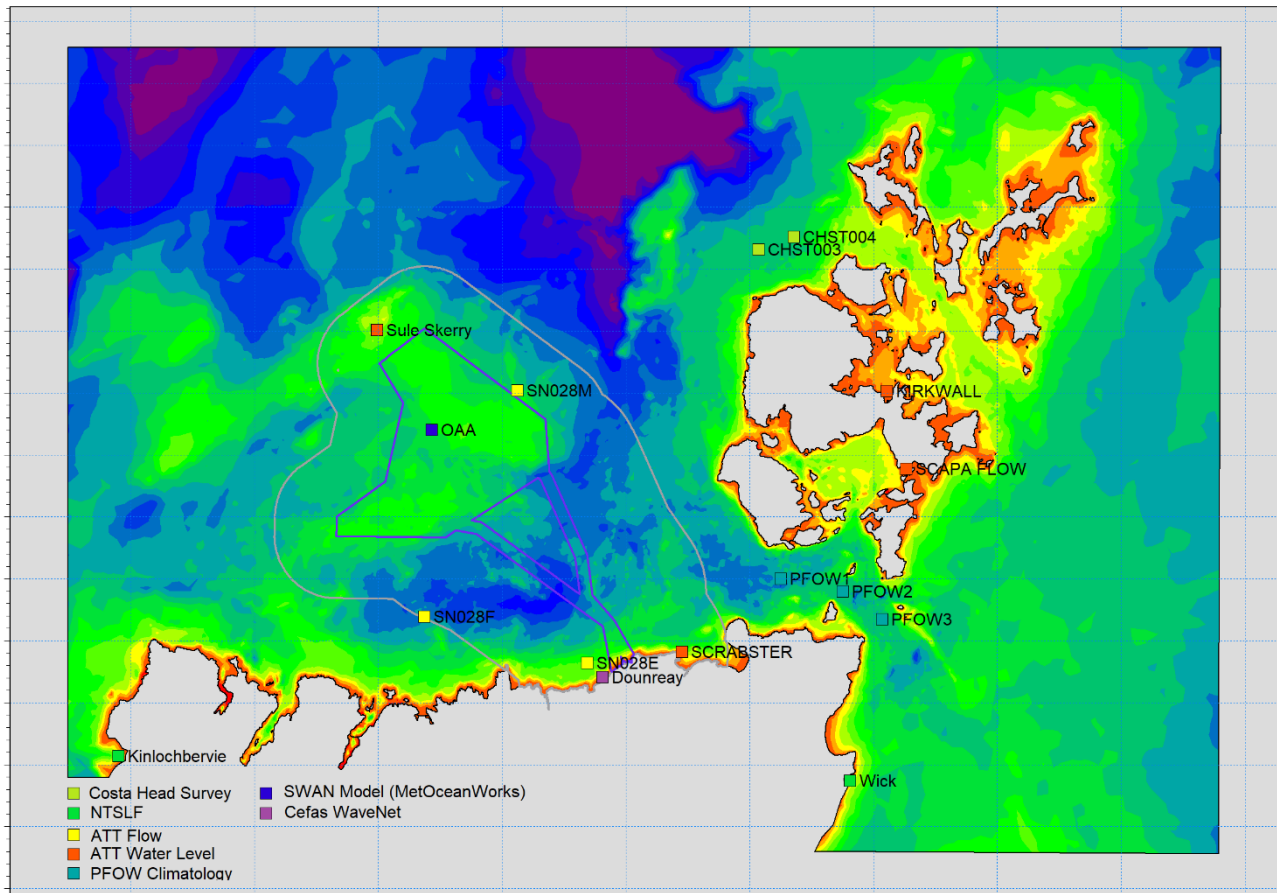


Figure A-3 Model Calibration Data Locations



Table A-2 Extreme wave and wind conditions as presented in OWPL (2023)

Dir (°N)	Return Periods															Percentiles					
	1			5			10			50			100			50%			90%		
	Hs (m)	Tp (s)	Wind speed (m/s)	Hs (m)	Tp (s)	Wind speed (m/s)	Hs (m)	Tp (s)	Wind speed (m/s)	Hs (m)	Tp (s)	Wind speed (m/s)	Hs (m)	Tp (s)	Wind speed (m/s)	Hs (m)	Tp (s)	Wind speed (m/s)	Hs (m)	Tp (s)	Wind speed (m/s)
0	8.2	14.8	21.2	9.6	15.4	23.8	10.1	15.7	24.7	10.9	16.0	25.9	11.2	16.2	26.4	2.06	10.4	7.2	3.88	12.1	12.8
45	6.1	13.7	16.7	7.2	14.2	19.1	7.5	14.5	19.9	8.1	14.7	21.1	8.3	14.9	21.5	1.76	10.0	9.4	3.15	11.5	14.4
90	5.5	13.4	15.4	6.5	13.9	17.7	6.8	14.1	18.4	7.4	14.4	19.6	7.6	14.5	20.0	1.77	10.0	11	3.10	11.5	15.9
135	5.5	13.3	15.2	6.4	13.9	17.5	6.7	14.1	18.2	7.3	14.3	19.3	7.5	14.5	19.8	2.00	10.3	12.2	3.29	11.7	17.4
180	5.9	13.6	16.3	7.0	14.1	18.7	7.3	14.4	19.4	7.9	14.6	20.6	8.1	14.8	21.1	2.24	10.6	12	3.45	11.8	16.5
225	7.3	14.4	19.5	8.6	15.0	22.1	9.0	15.2	22.9	9.8	15.5	24.1	10.1	15.7	24.6	2.35	10.7	11.2	3.89	12.1	16.2
270	10.2	15.7	24.8	12.0	16.4	27.5	12.6	16.7	28.3	13.6	17.0	29.4	14.0	17.2	29.8	2.62	11.0	9.3	5.06	13.0	16
315	9.2	15.3	23.1	10.8	15.9	25.8	11.4	16.2	26.6	12.3	16.5	27.8	12.6	16.7	28.3	2.22	10.6	7.1	4.34	12.5	13.3
OMN	10.2	15.7	24.8	12.0	16.4	27.5	12.6	16.7	28.3	13.6	17.0	29.4	14.0	17.2	29.8	2.31	10.7	8.6	4.51	12.6	15.1



### A.3.3 Hydrodynamic Model Calibration

To enable the West of Orkney model calibration and validation, a range of available metocean observations, hindcast data and outputs from existing models were applied as described in the following sections.

#### A.3.3.1 Calibration Data Constraints

During the model calibration process the bed roughness was iteratively modified to provide the best agreement between modelled and measured/predicted water levels and flows in the model domain.

##### A.3.3.1.1 Costa Head measured data between 16<sup>th</sup> January – 18<sup>th</sup> February 2013

Prior to comparing flows and water levels from the West of Orkney model against observed flows and water levels at the Costa Head deployments it is useful to understand the metocean conditions during the survey period (i.e. 16<sup>th</sup> January – 18<sup>th</sup> February 2013). The measured water levels at Kinlochbervie and Wick are shown along with the tidal surge in Figure A-4, while the wave and wind conditions from the OAA (from the MetoceanWorks (MoW model) and from CFSR, respectively) are shown in Figure A-5. The figures show the strong influence of meteorological forcing at times during the calibration (and validation) period. In particular, there is a notable positive surge in water levels towards the end of the calibration period (between the 26<sup>th</sup> and 31<sup>st</sup> January 2013) and large westerly waves of more than 6 m occurring at times (greater than 90<sup>th</sup> percentile waves). A harmonic analysis of the measured flows was undertaken but due to the large contribution from non-tidal influence during the survey period, coupled with the relatively weak tidal influence at Costa Head it was not possible to fully remove all of the non-tidal flow contributions.

##### A.3.3.1.2 Pentland Firth Orkney Waters (PFOW) climatology (O'Hara and Campbell, 2021)

A number of differences between water levels and flows from the PFOW climatology and the measured flows and water level were reported by O'Hara and Campbell (2021). The following are important to consider before making comparisons of flows and water levels from the West of Orkney model against those from the PFOW climatology:

- At PFOW1 the faster (westward, i.e. ebb) peak was over predicted by the PFOW model, while the slower (eastward, i.e. flood) peak was accurately reproduced;
- At PFOW2 the measured data showed no obvious asymmetry, however some asymmetry was apparent in the PFOW model;
- At PFOW3 the faster (eastward, i.e. flood) flow was overpredicted by the PFOW model, while the slower (westward, i.e. ebb) peak was underpredicted;
- The PFOW modelled water levels were approximately 0.5 hours earlier than measured water levels, although no phase difference was apparent in the PFOW modelled flows; and
- No comparisons were made of modelled and measured flow directions at PFOW1 to PFOW3. However, comparisons of modelled PFOW flows along transects indicated a good agreement between modelled and observed flow directions within the Pentland Firth.

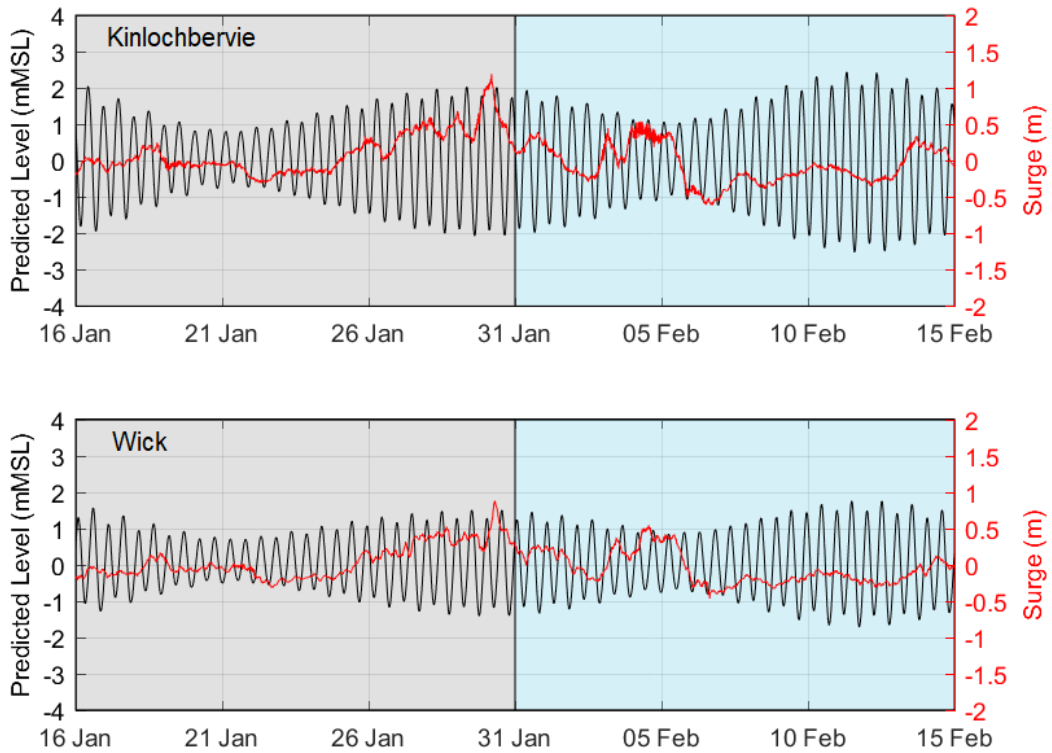


Figure A-4 Measured water levels at NTSLF sites during the model calibration and validation periods

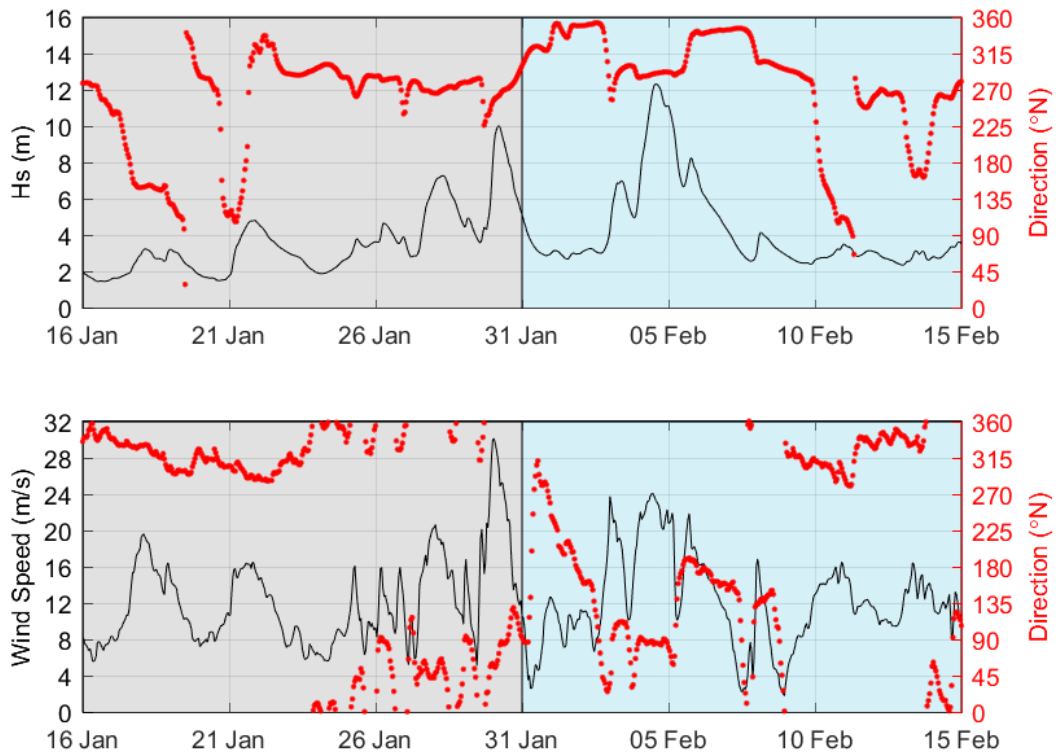


Figure A-5 Waves and wind conditions in the OAA during the model calibration and validation periods.



### A.3.3.1.3 ATT predicted data

There are constraints with the ATT water level and flow predictions which need to be considered ahead of comparing flows and water levels from the West of Orkney model against the ATT water levels and flows. The provenance of data used for ATT flow predictions is not known but can be subject to a number of shortcomings such as:

- Being historical in nature from a time when instrument accuracy may have been limited. This is likely to be particularly problematic in high flow environments such as in the Pentland Firth, with instruments even from fixed moorings (and even more so from boat surveys) being unlikely to remain on station, inducing artificial flows;
- Being representative of surface flows, rather than depth averaged flows. Surface flows can be strongly influenced by non tidal forcing and the rotation of surface flows at slack water periods is often opposed to the rotation of the depth average flow; and
- Being collected over a short duration and then scaled to represent flows for other tidal periods without detailed harmonic analysis to account for either the full influence of the tide and/or the removal of meteorological influences.

Comparisons of ATT flow predictions within the Pentland Firth against survey data reported in O'Hara and Campbell (2021) showed poor agreement with the ATT flows, with ATT predictions providing a poor representation of peak flows and the relative dominance of flood and ebb flows. For this reason, no comparisons are made against the West of Orkney model and ATT flows in the Pentland Firth. ATT flows are only considered for model calibration in close proximity to the OAA, although the accuracy of ATT in these areas remains uncertain.

### A.3.3.2 Water Levels

The timing and magnitude of peak water levels vary across the model domain with High Water (HW) at the south western boundary (at Kinlochbervie) occurring approximately four hours before HW at the south eastern boundary (at Wick). There is a reduction in tidal range in an offshore direction from approximately 4 m along the coast to approximately 3 m offshore during spring tides.

Plots of modelled water levels against water levels from the various datasets (see section A.3.2) are shown in Figure A-6 to Figure A-13. The tidal signal is symmetrical with a slight semi-diurnal variation (with one higher HW/LW and one slightly lower HW/LW each day). The plots show that the model replicates the shape, diurnal variability, phasing and amplitude of the tidal wave across the model domain with a good agreement in the timing and magnitude of peak levels at all sites.

The observed water levels at Costa Head (CHST003 and CHST004 Figure A-12 and Figure A-13) show the influence of the positive tidal surge towards the end of the calibration period between the 26<sup>th</sup> and 31<sup>st</sup> January 2013 (Section A.3.3.1.1), with measured levels above those in the model (which do not include the influence of meteorological forcing).

A statistical comparison between the modelled and measured water level data are provided in Table A-3. The plots and statistics show that the model meets all the calibration guidelines for water levels presented in Section A.3.1.

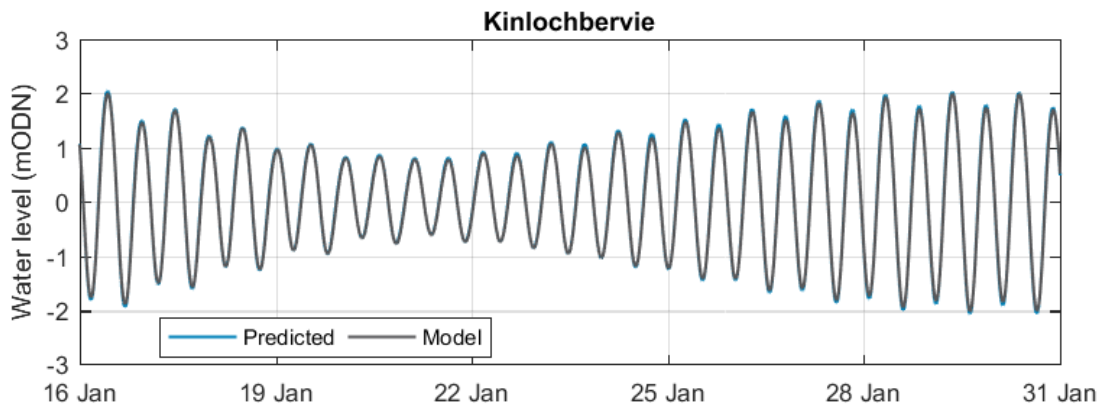


Figure A-6 Modelled and predicted water levels at Kinlochbervie during the model calibration period

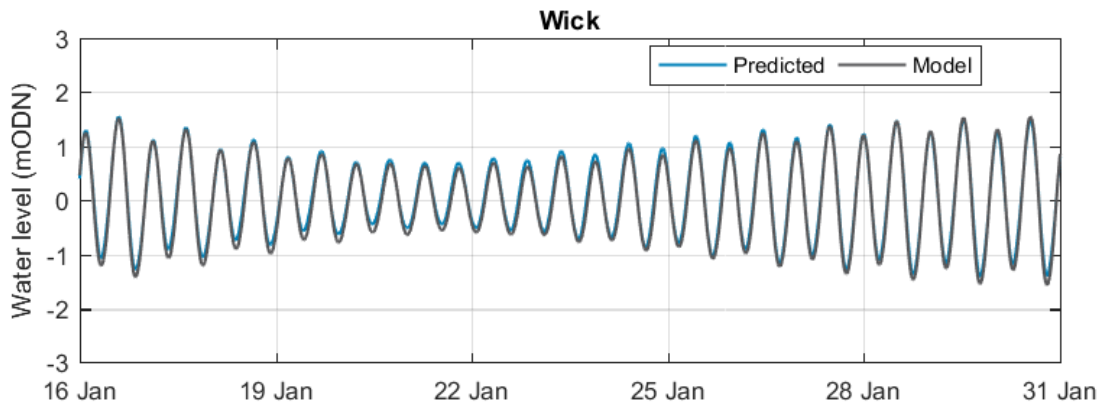


Figure A-7 Modelled and predicted water levels at Wick during the model calibration period

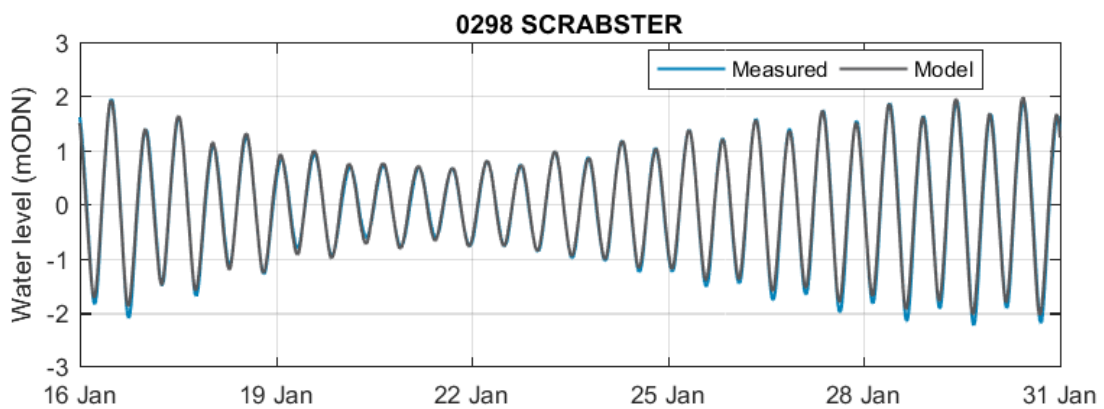


Figure A-8 Modelled and predicted water levels at Scrabster during the model calibration period

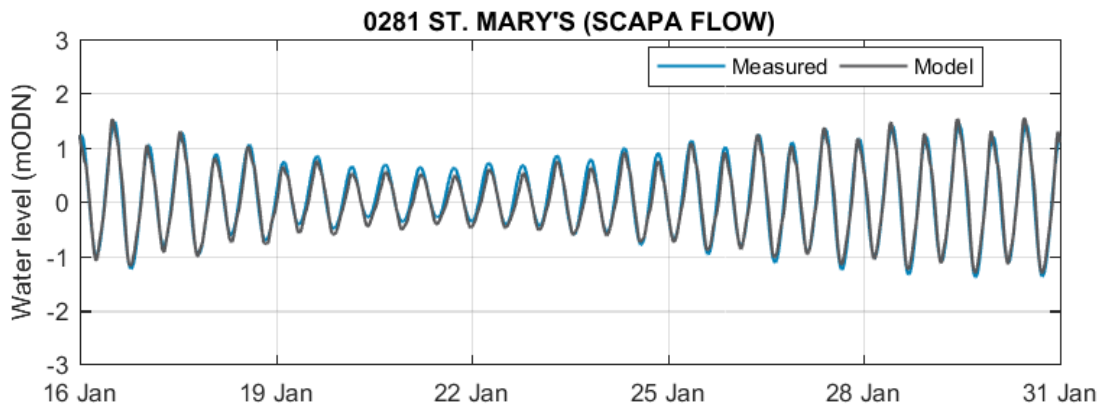


Figure A-9 Modelled and predicted water levels at St Mary's during the model calibration period

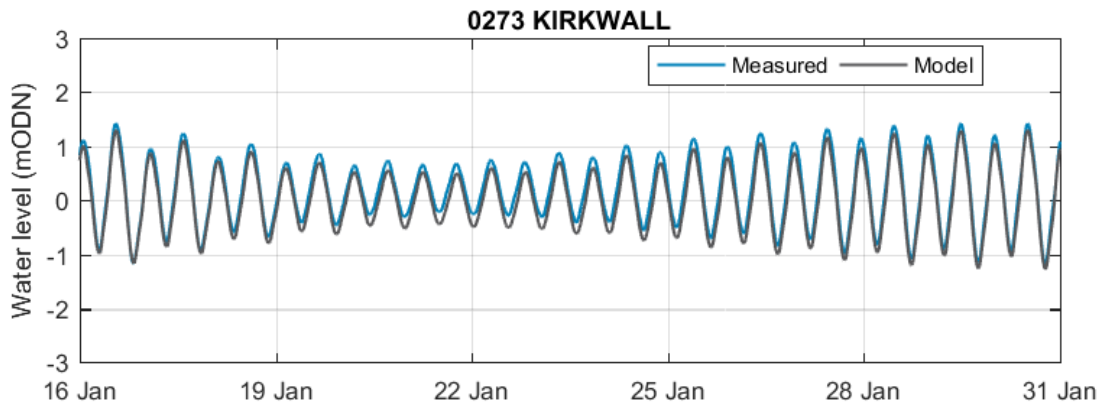


Figure A-10 Modelled and predicted water levels at Kirkwall during the model calibration period

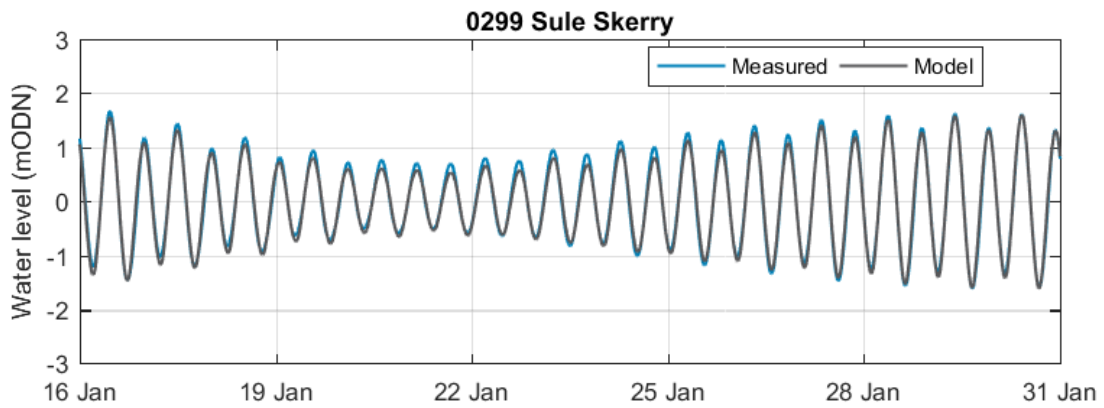


Figure A-11 Modelled and predicted water levels at Sule Skerry during the model calibration period

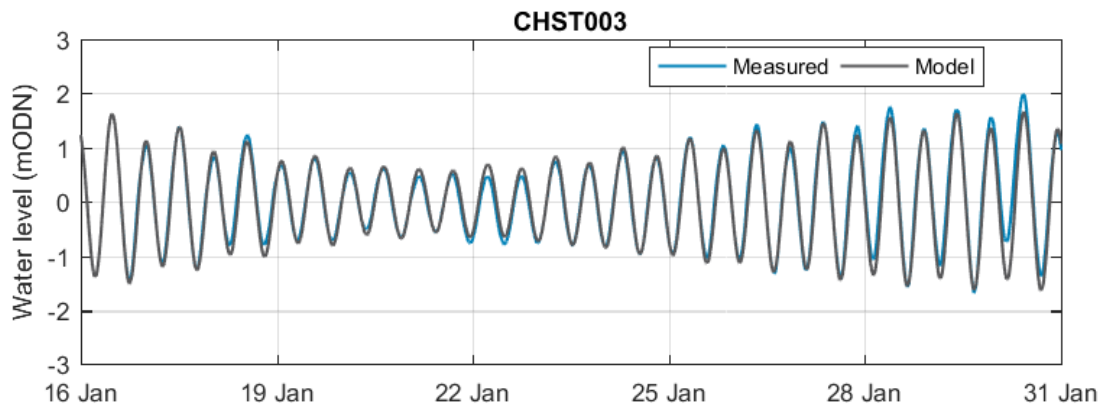


Figure A-12 Modelled and measured water levels at CHST003 during the model calibration period

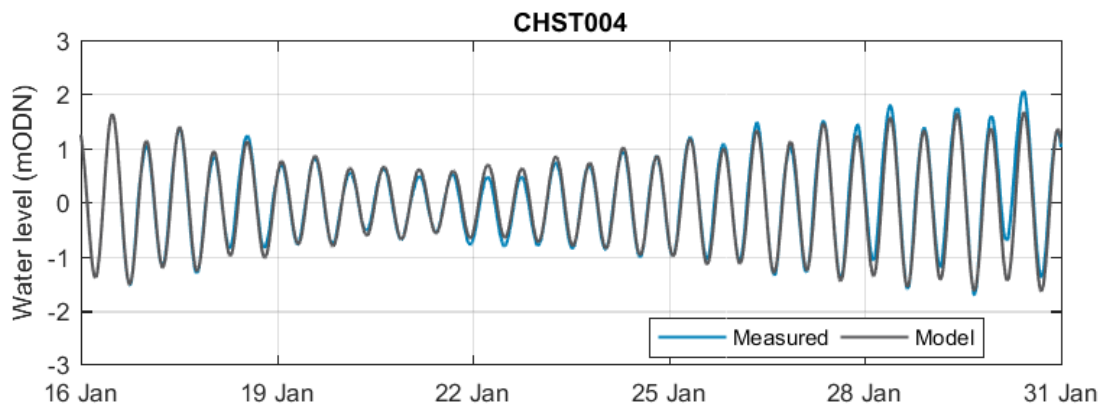


Figure A-13 Modelled and measured water levels at CHST004 during the model calibration period

Table A-3 Calibration Water Level Statistics

	WL DIFF (M)		WL DIFF (%)		RMSE (M)	PHASING DIFFERENCE (MINS)		
	HW	LW	HW	LW		HW	LW	ALL
Kinlochbervie	-0.04	0.02	-1	1	0.03	5	3	3
Wick	-0.05	-0.10	-3	-5	0.09	1	6	3
Scrabster	0.01	0.06	0	2	0.08	-5	-10	-8
St Mary's (Scapa Flow)	-0.07	-0.02	-4	-4	0.11	-5	0	13
Kirkwall	-0.16	-0.15	-10	-9	0.17	9	8	2



	WL DIFF (M)		WL DIFF (%)		RMSE (M)	PHASING DIFFERENCE (MINS)		
	HW	LW	HW	LW		HW	LW	ALL
Sule Skerry	-0.12	-0.03	-6	-1	0.08	4	8	0
CHST003	0	-0.07	0	-3	0.15	1	6	8
CHST004	-0.02	-0.05	-1	-2	0.16	1	5	8

### A.3.3.3 Flows

Within the model domain, the timing of peak flows occurs close to the times of high and low water. Within the OAA the peak flood flow typically occurs shortly before HW with flows in an easterly direction and the peak ebb flow occurs shortly before LW with flows in a westerly direction.

Before comparing time series of flows at discrete locations, a spatial map of maximum flow speed on a spring tide is shown in Figure A-14. These are compared to maximum flow speeds from the PFOV model (Figure A-15) and from modelled flows from ABPmer (2017) for the same model region as the PFOV model (Figure A-16). The maximum spring tide flows from the West of Orkney model show a very good agreement against the maximum flows from the PFOV climatology (section A.3.3.1.2) and ABPmer (2017) model with very fast flows (of more than 3.5 m/s) through the Pentland Firth and much slower flows (of less than 1 m/s) across the OAA.

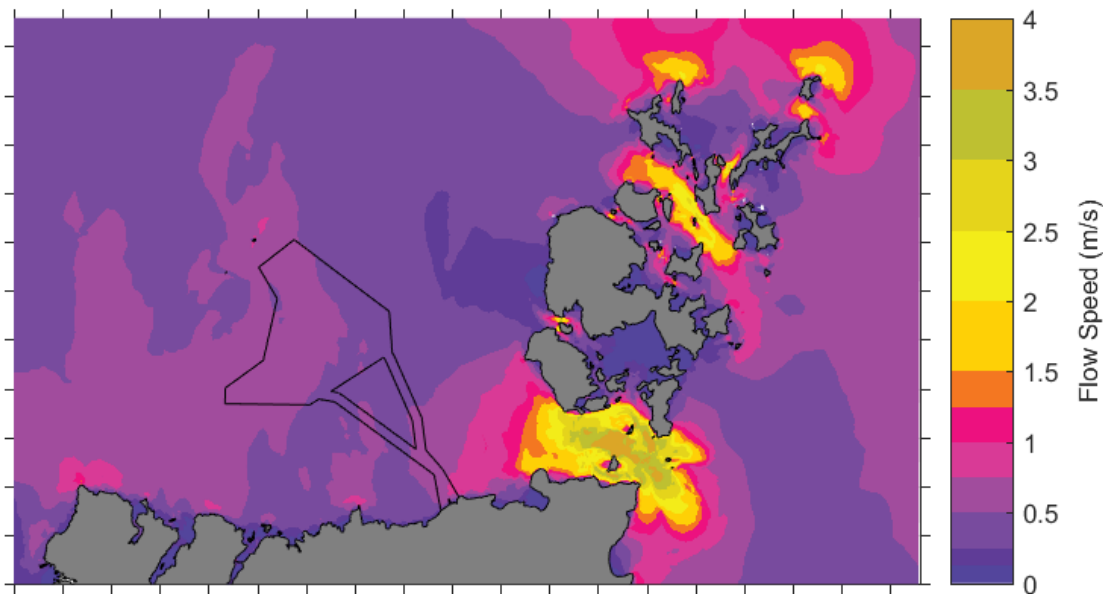


Figure A-14 Maximum spring tide flow speed from the West of Orkney model

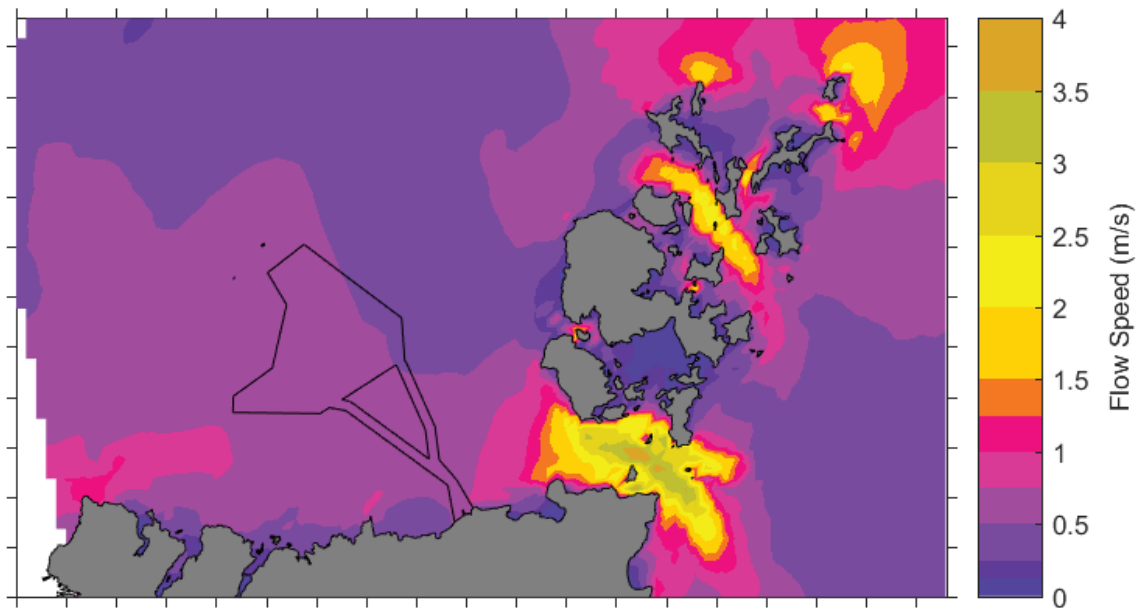


Figure A-15 Maximum spring tide flow speed from PFOW model

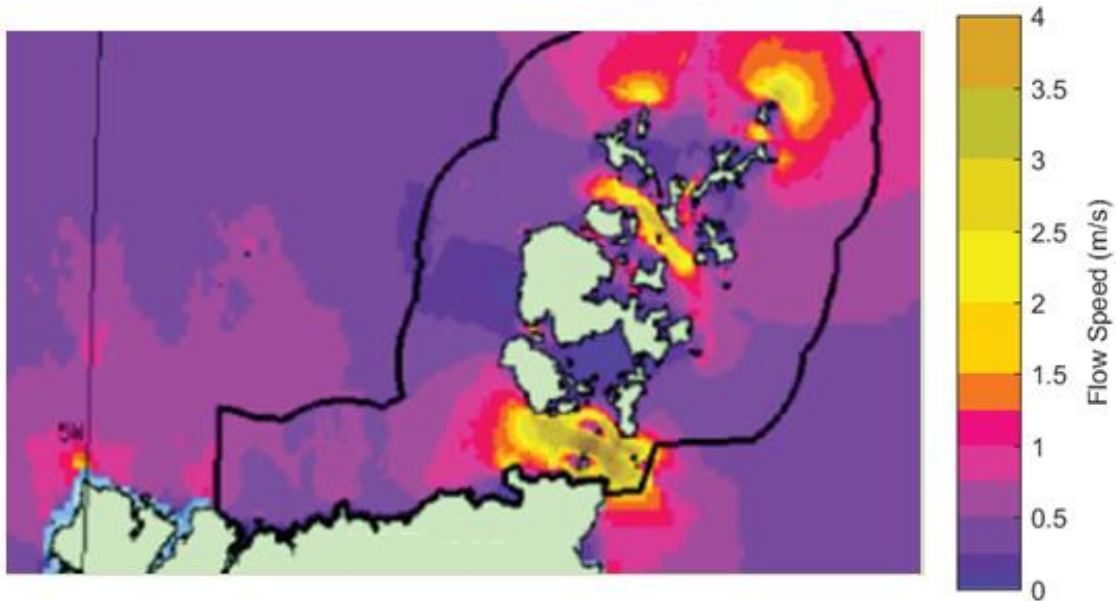


Figure A-16 Maximum spring tide flow speed from ABPmer model (ABPmer, 2017)

Plots of modelled flows are shown against measured flows at the Costa Head ADCP locations (CHST003 and CHST004) in Figure A-17 and Figure A-18. The model does not do a good job of replicating the observed flows in the later period of the measured data, particularly at the more offshore site of CHST003 where the meteorological influence is greatest. The improved agreement at CHST004, particularly during periods of lower wave heights and smaller tidal residuals (for example on the 21<sup>st</sup> January 2013) suggests that the model is capturing the tidal components of the flows at these sites but that the contribution from non-tidal forcing is dominant. The West of Orkney model



agreement is in line with the constraints of the measured data discussed in Section A.3.3.1.1. A sensitivity test was undertaken which included the influence of pressure and winds from CFSR. The West of Orkney model responds well to meteorological forcing and the inclusion of wind and pressure forcing was found to result in a notable improvement in modelled and measured flows at Costa Head (Figure A-19 to Figure A-20). The inclusion of meteorological forcing resulted in the model achieving the calibration guideline standards (Table A-4).

Comparisons of the modelled flows from the West of Orkney model developed in this study against modelled flows from the PFOW climatology (section A.3.3.1.2) are plotted in Figure A-21 to Figure A-23. The plots show a good agreement in flow speeds and directions across all three assessed sites (i.e. PFOW1, PFOW2 and PFOW3) within the Pentland Firth (Figure A-3). Furthermore, when the constraints of the PFOW model are taken into account, it is clear that the West of Orkney model is accurately replicating the strong tidal flows through the Pentland Firth.

Plots of the West of Orkney modelled flows are shown against ATT predictions at three tidal diamonds around the OAA and close to the cable landfall site (i.e. SN028M, SN028F and SN028E in Figure A-3) in Figure A-24 to Figure A-26. Taking account of the constraints in the ATT predictions it is considered that the West of Orkney model is doing a reasonable job of replicating the tidal flows across the Project and associated marine physical and coastal processes study area. The West of Orkney model predicts faster flows at SN028E on both the flood and the ebb and slower flows at SN028F on the ebb than the ATT predicted flows. Some sensitivity tests were undertaken in an attempt to improve the agreement at these locations, however any improvements gained at these sites resulted in a poorer calibration in flows through the Pentland Firth which is indirectly based on actual observational data.

Statistical measures of the modelled flows against the available calibration data during the calibration period are provided in Table A-4. Values in red show where the model did not achieve the guideline standards. However, in view of the constraints in the data described above it is considered that the model provides a good representation of the flows across the model domain and in particular in the study area. The RMS difference for flows through the Pentland Firth is close to the guideline standard, however the SI lies well below. This indicates that the RMS standard is likely to be over prescriptive in such a high flow environment.

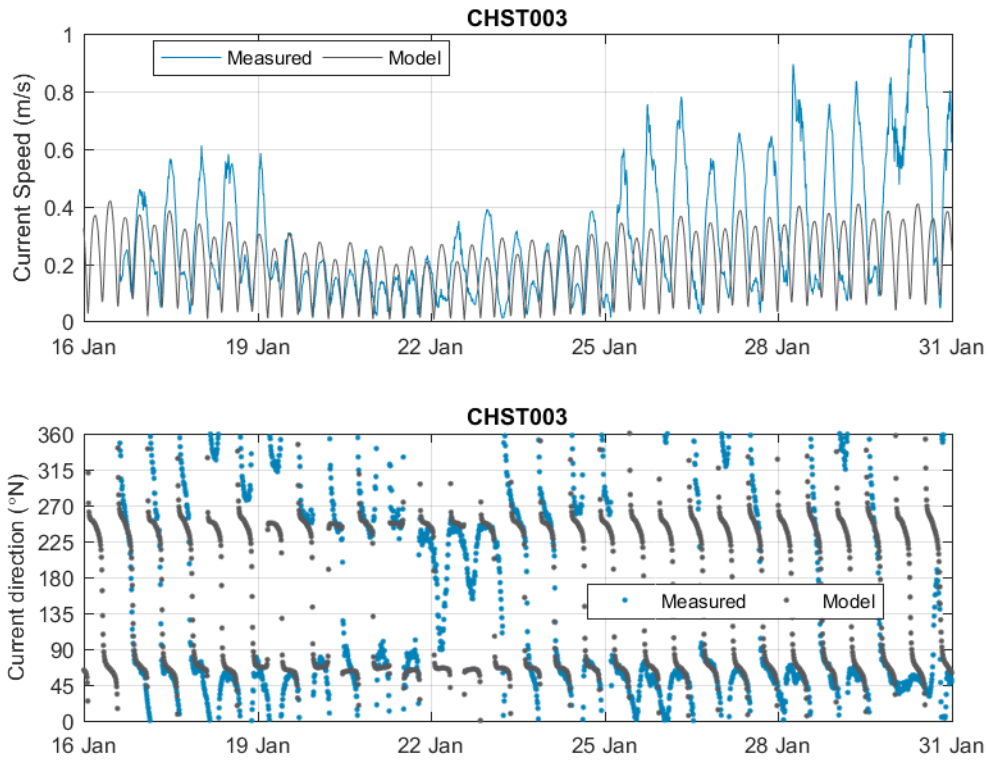


Figure A-17 Modelled and measured flows at CHST003 during the model calibration period

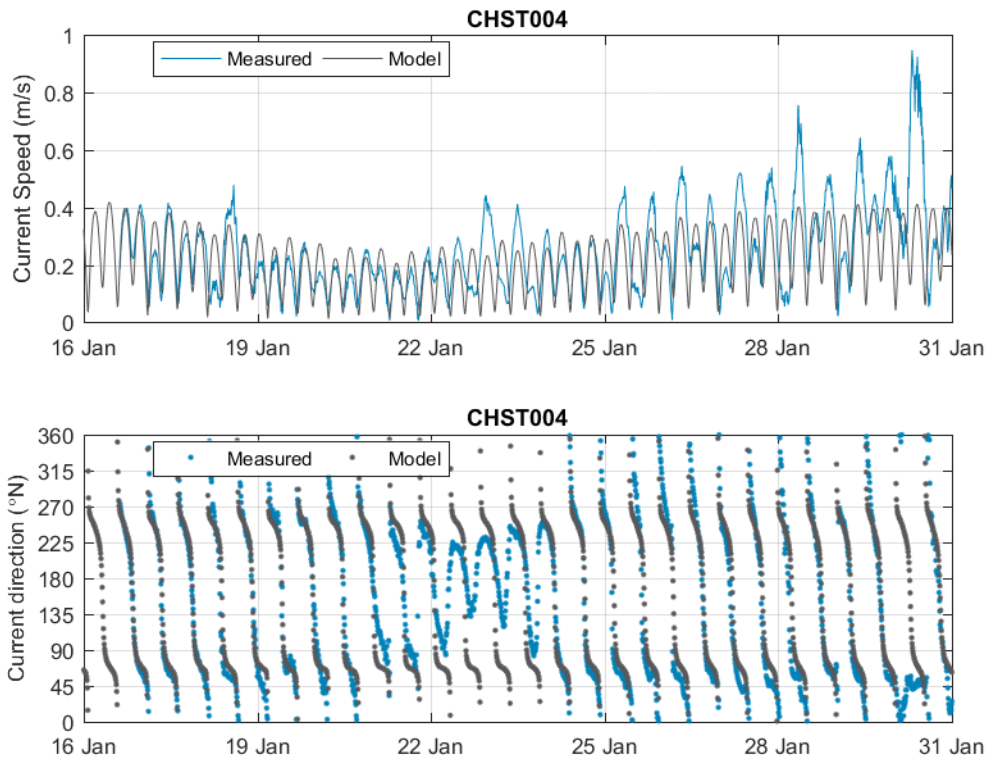


Figure A-18 Modelled and measured flows at CHST004 during the model calibration period

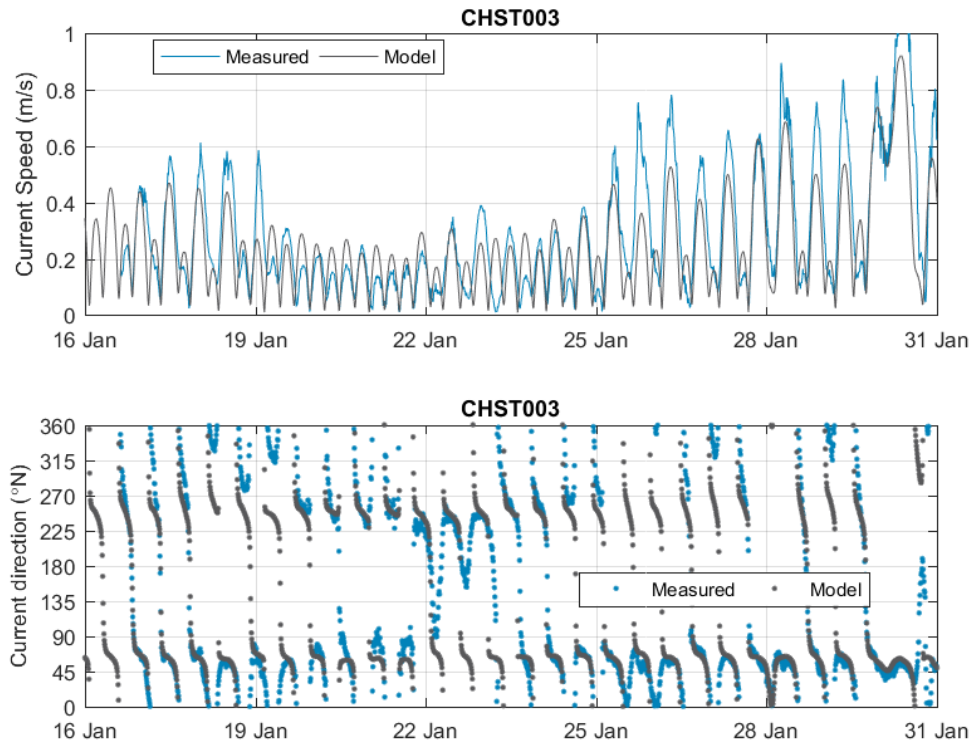


Figure A-19 Modelled and measured flows at CHST003 during the model calibration period, with meteorological forcing applied in the model

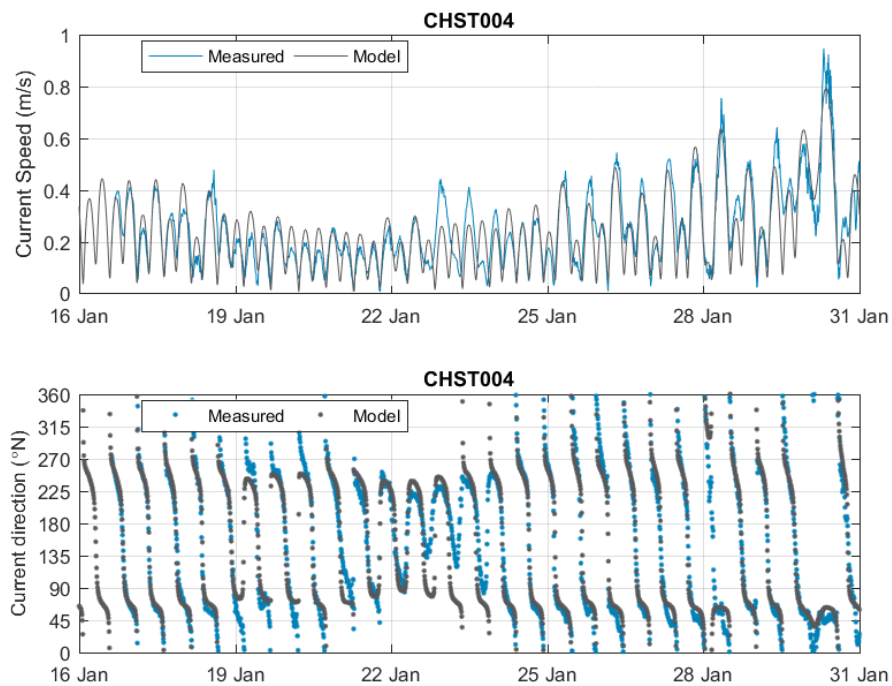


Figure A-20 Modelled and measured flows at CHST004 during the model calibration period, with meteorological forcing applied in the model

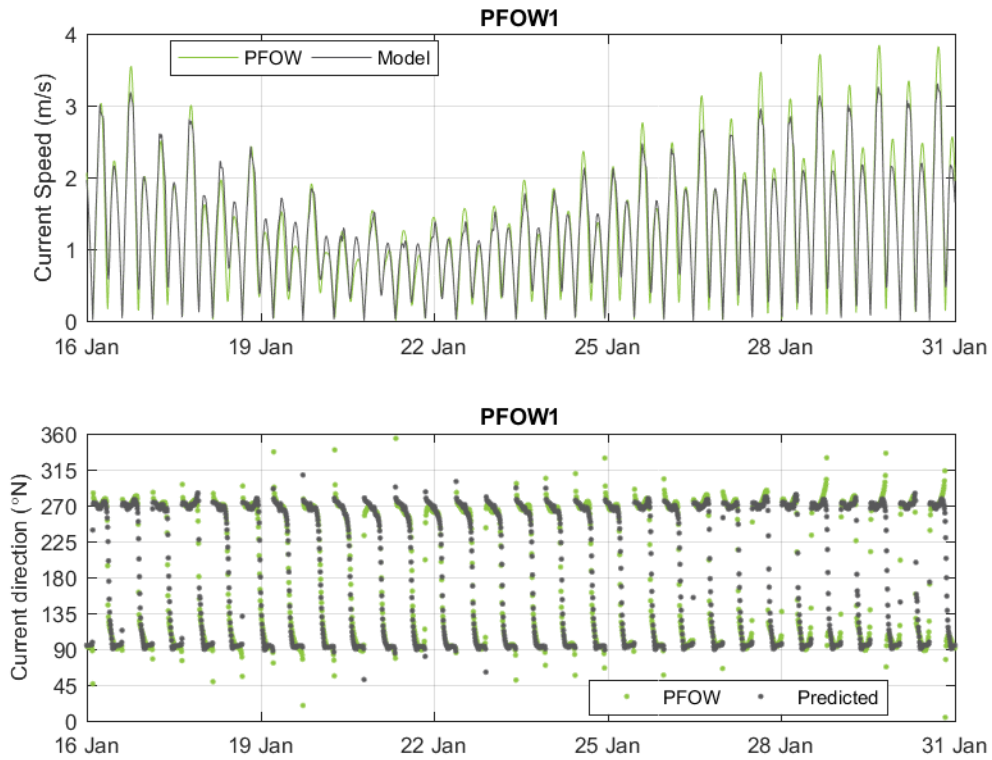


Figure A-21 Modelled flows at PFW1 during the model calibration period

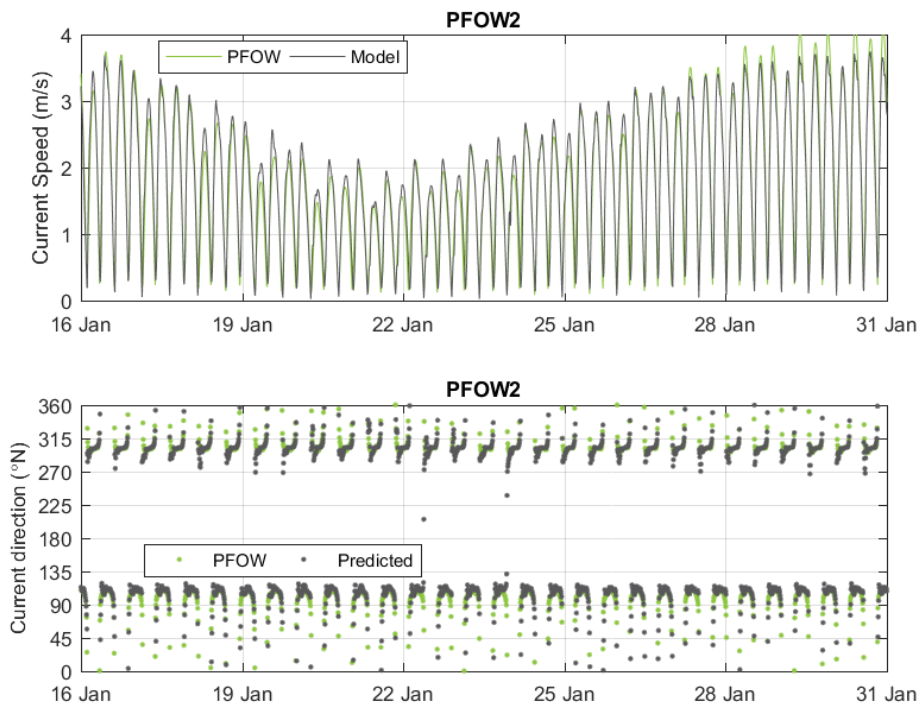


Figure A-22 Modelled flows at PFW2 during the model calibration period

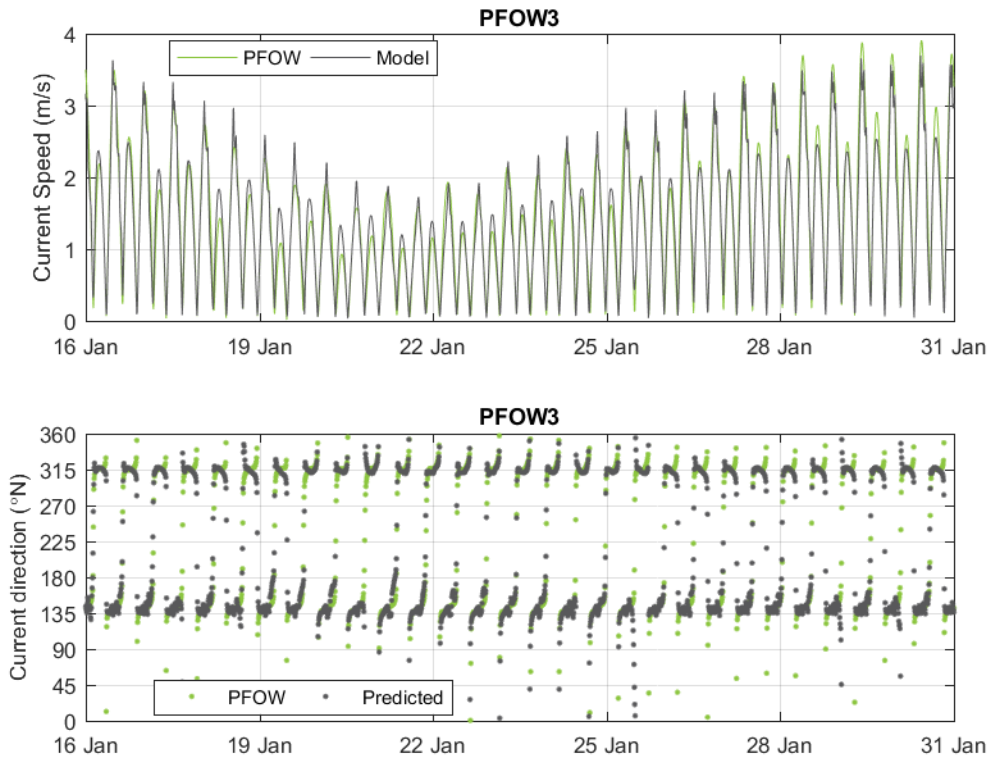


Figure A-23 Modelled flows at PFW03 during the model calibration period

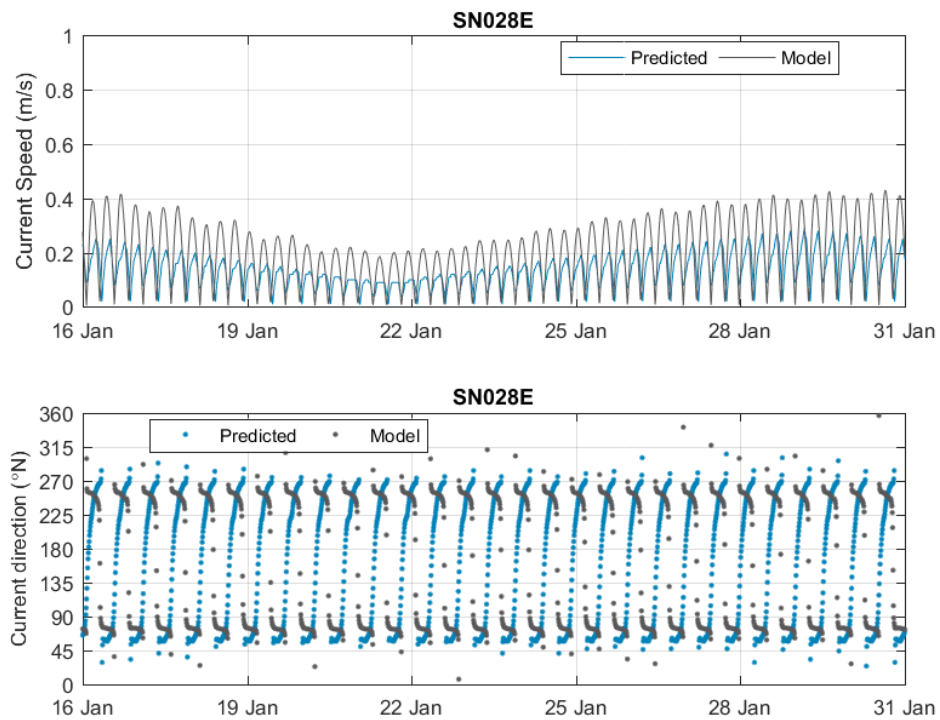


Figure A-24 Modelled and predicted flows at SN028E during the model calibration period

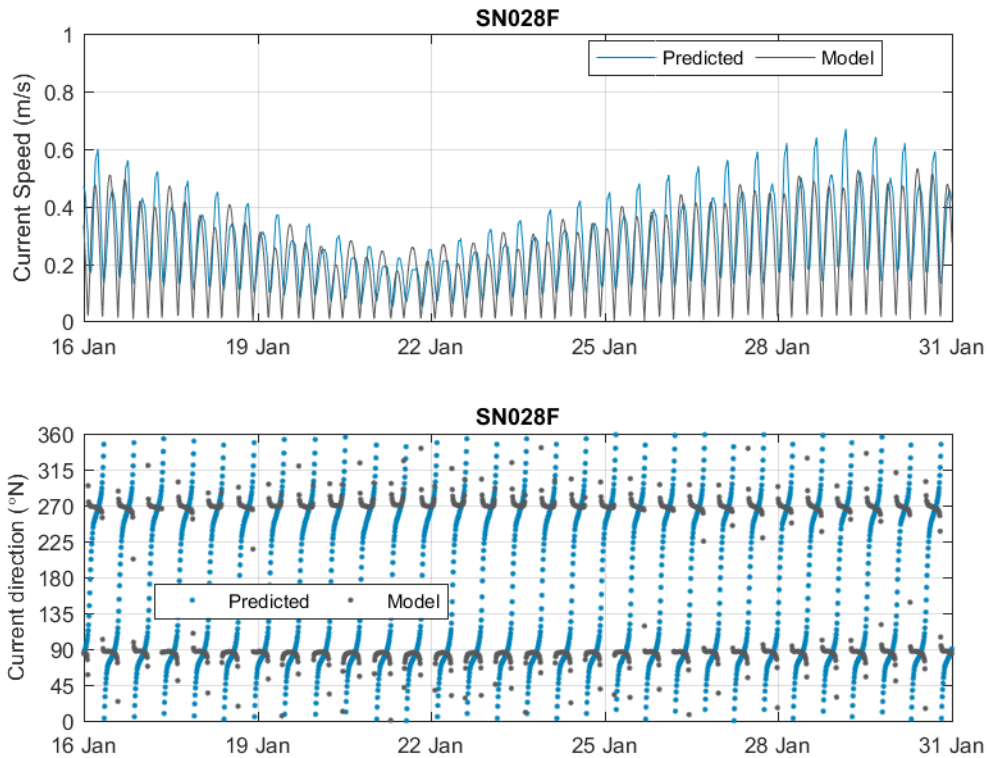


Figure A-25 Modelled and predicted flows at SN028F during the model calibration period

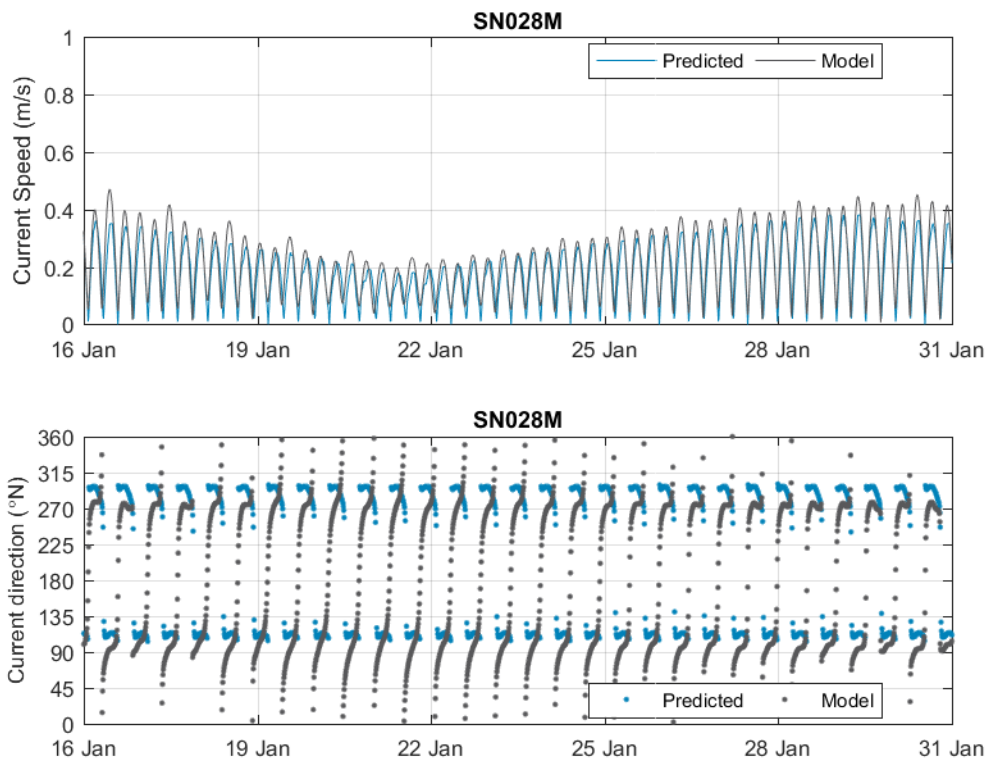


Figure A-26 Modelled and predicted flows at SN028M during the model calibration period



Table A-4 Calibration Flow Statistics

SITE NAME	FLOW SPEED DIFF (M/S)		FLOW SPEED DIFF (%)		RMSE (M/S)	SCATTER INDEX	DIRECTION DIFF (°)		PHASE DIFFERENCE (MINS)
	PF	PE	PF	PE			PF	PE	
CHST003	-0.16	0.06	-	9	0.22	0.76	-7	9	3
			13						
CHST004	-0.05	0.03	-5	7	0.22	0.52	-2	10	-10
CHST003m*	-0.08	0.03	-7	8	0.13	0.45	-9	-4	-17
CHST004m*	0.01	0	1	0	0.08	0.32	-2	3	-12
PFOW1	0.01	-	0	-4	0.19	0.07	-3	-1	5
		0.16							
PFOW2	0.04	0.12	-1	3	0.23	0.13	-2	1	2
PFOW3	0.16	0.11	4	4	0.22	0.15	-2	0	1
SN028E	0.13	0.13	48	50	0.09	0.66	14	4	-43
SN028F	0.02	-0.11	4	-	0.07	0.25	7	7	-43
			17						
SN028M	0.04	0.03	11	8	0.04	0.20	-17	-23	-17

m\* denotes model run which includes meteorological forcing. Values in red show where the model did not achieve the guideline standards.

### A.3.4 Hydrodynamic Model Validation

The model was setup to simulate hydrodynamics for the validation period, with no changes made to the model setup (other than the dates) as applied in the model calibration. The modelled water levels and flows from the validation period are compared against the same data as considered during the model calibration and the same constraints in the data as detailed in Section A.3.3 are therefore also applicable here.

#### A.3.4.1 Water Levels

West of Orkney modelled water levels are compared against the various data in Figure A-27 to Figure A-34 and the validation statistics are provided in Table A-5. The model shows a similar level of agreement against the data as during the calibration period, with all statistics remaining within the guideline standards.

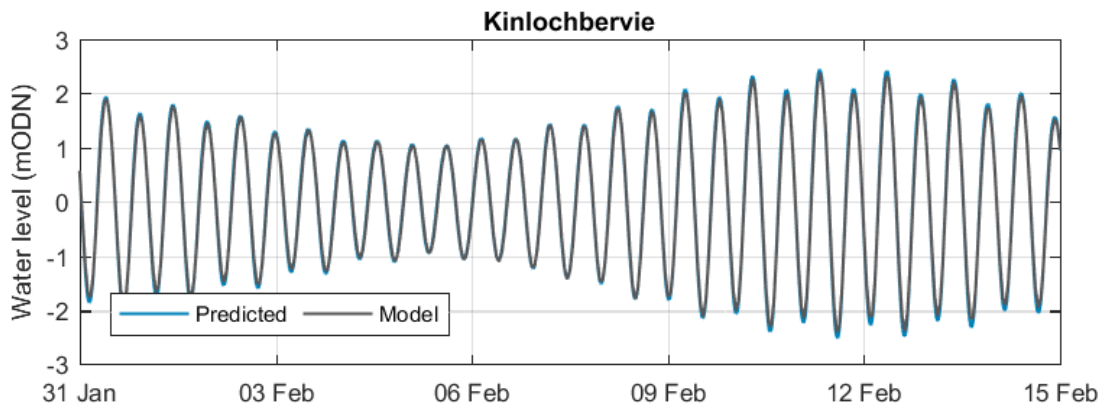


Figure A-27 Modelled and predicted water levels at Kinlochbervie during the model validation period

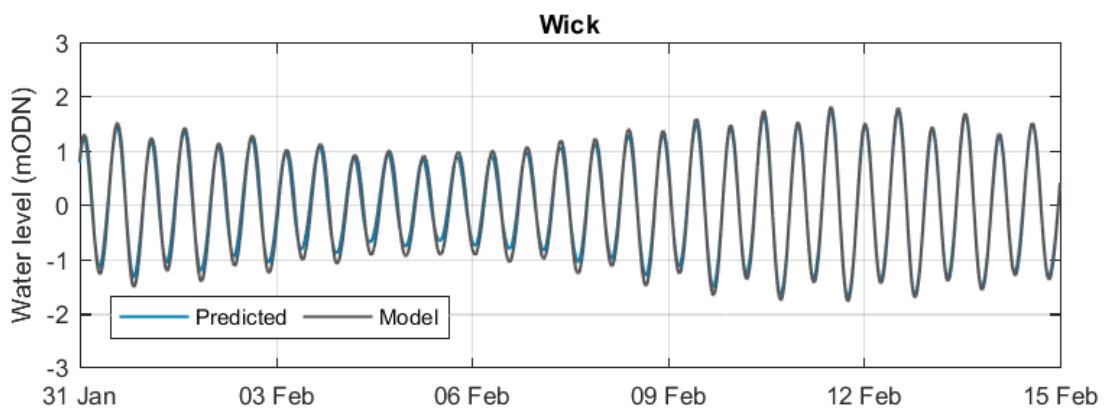


Figure A-28 Modelled and predicted water levels at Wick during the model validation period

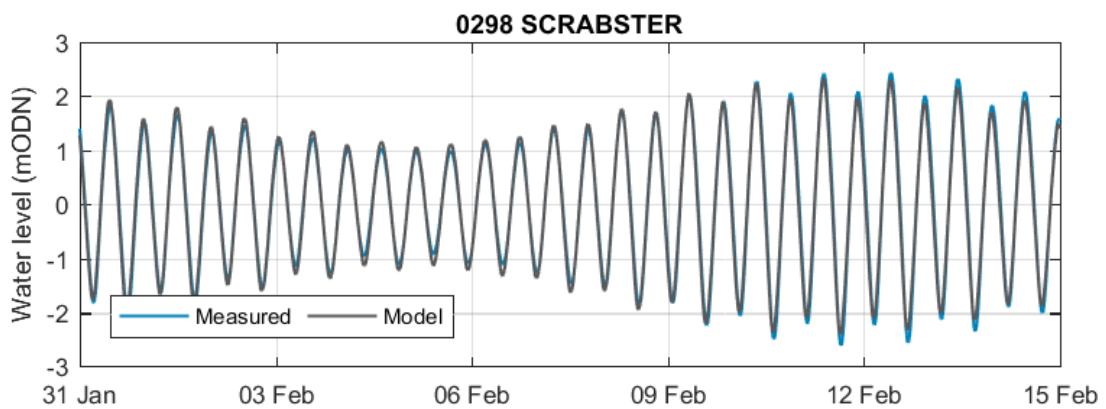


Figure A-29 Modelled and predicted water levels at Scrabster during the model validation period

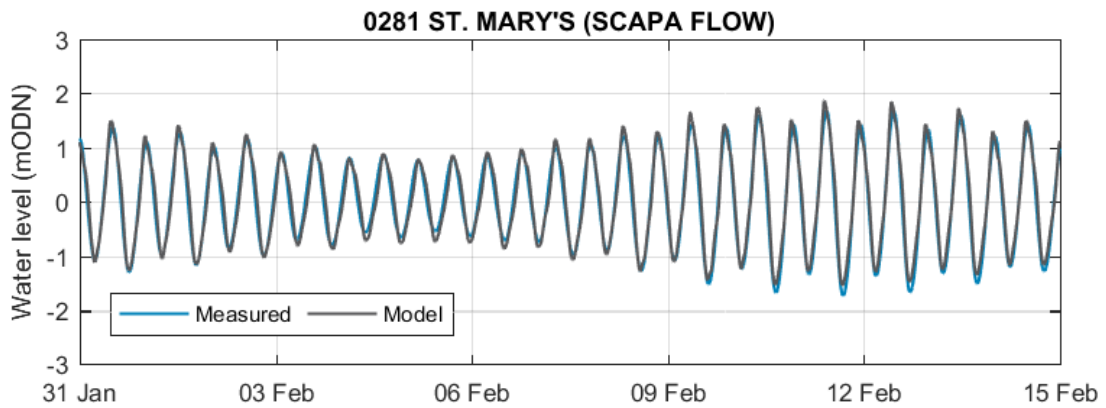


Figure A-30 Modelled and predicted water levels at St Mary's during the model validation period

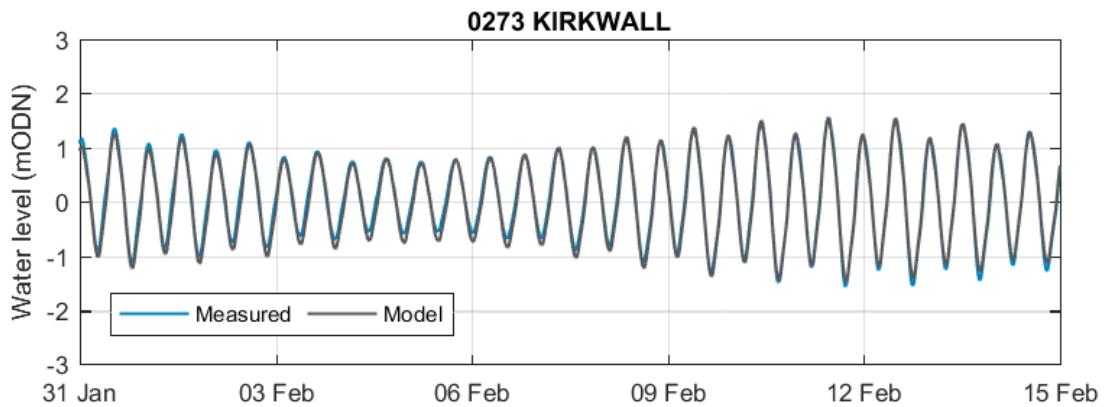


Figure A-31 Modelled and predicted water levels at Kirkwall during the model validation period

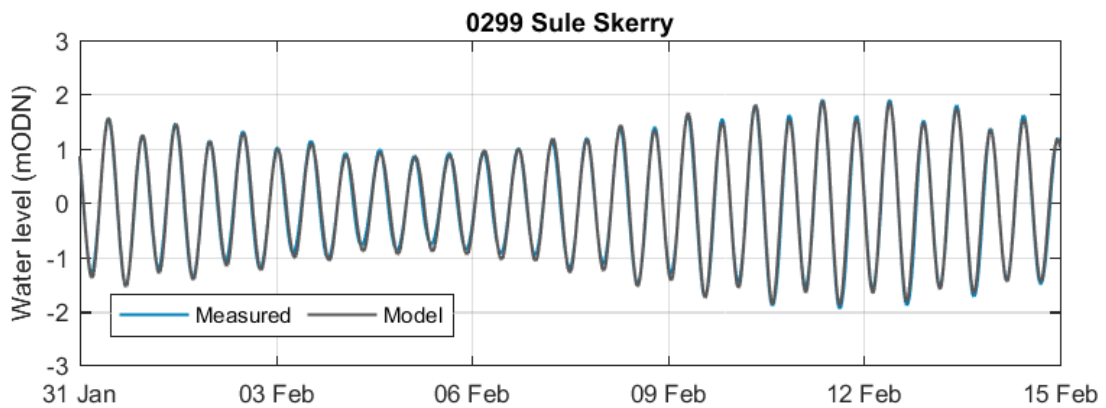


Figure A-32 Modelled and predicted water levels at Sule Skerry during the model validation period

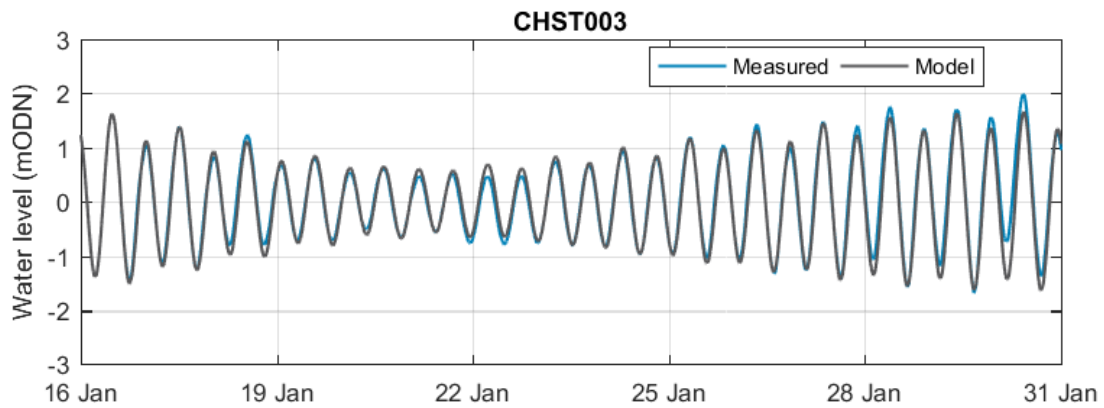


Figure A-33 Modelled and measured water levels at CHST003 during the model validation period

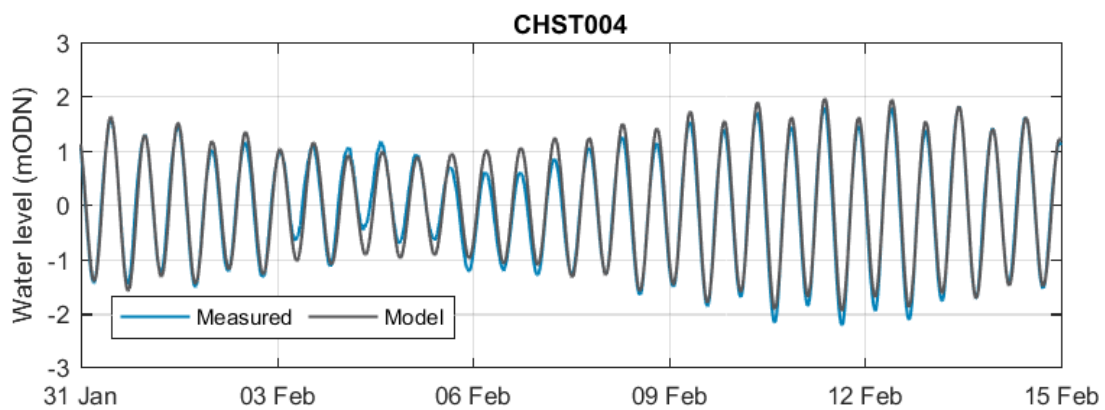


Figure A-34 Modelled and measured water levels at CHST004 during the model validation period

Table A-5 Validation Water Level Statistics

SITE NAME	WL DIFF (M)		WL DIFF (%)		RMSE (M)	PHASING DIFFERENCE (MINS)		
	HW	LW	HW	LW		HW	LW	ALL
Kinlochbervie	-0.03	0.04	-1	1	0.04	6	6	5
Wick	0.06	-0.14	2	-6	0.11	8	10	6
Scrabster	0.02	-0.01	1	0	0.09	-10	-13	-7
St Mary's (Scapa Flow)	0.06	0.01	3	0	0.13	-14	3	13
Kirkwall	0	-0.06	-1	-2	0.09	8	11	2



SITE NAME	WL DIFF (M)		WL DIFF (%)		RMSE (M)	PHASING DIFFERENCE (MINS)		
	HW	LW	HW	LW		HW	LW	ALL
Sule Skerry	-0.03	-0.06	-1	-2	0.09	8	11	2
CHST003	0.15	0	6	0	0.17	10	7	12
CHST004	0.14	0.02	5	1	0.17	10	7	12

### A.3.4.2 Flows

West of Orkney modelled flows are compared against the various data in Figure A-35 and Figure A-44 and the validation statistics are provided in Table A-6. The model shows a similar level of agreement against the data as during the calibration period, with a particularly good agreement with the PFOV flow through the Pentland Firth. As during the calibration period, the observed flows at Costa Head continue to show a notable influence from meteorological forcing, although there are longer periods of calmer conditions when the modelled flows agree well with those that were measured.

The statistics show that the model performance during the validation period is similar to those during the calibration period.

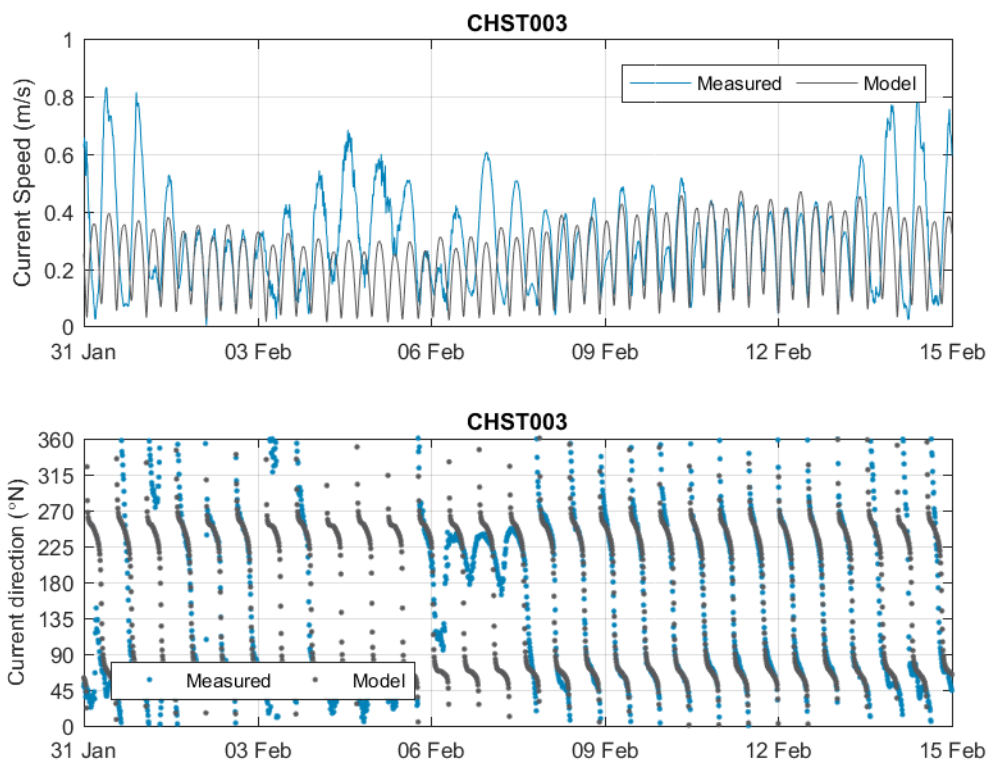


Figure A-35 Modelled and measured flows at CHST003 during the model validation period

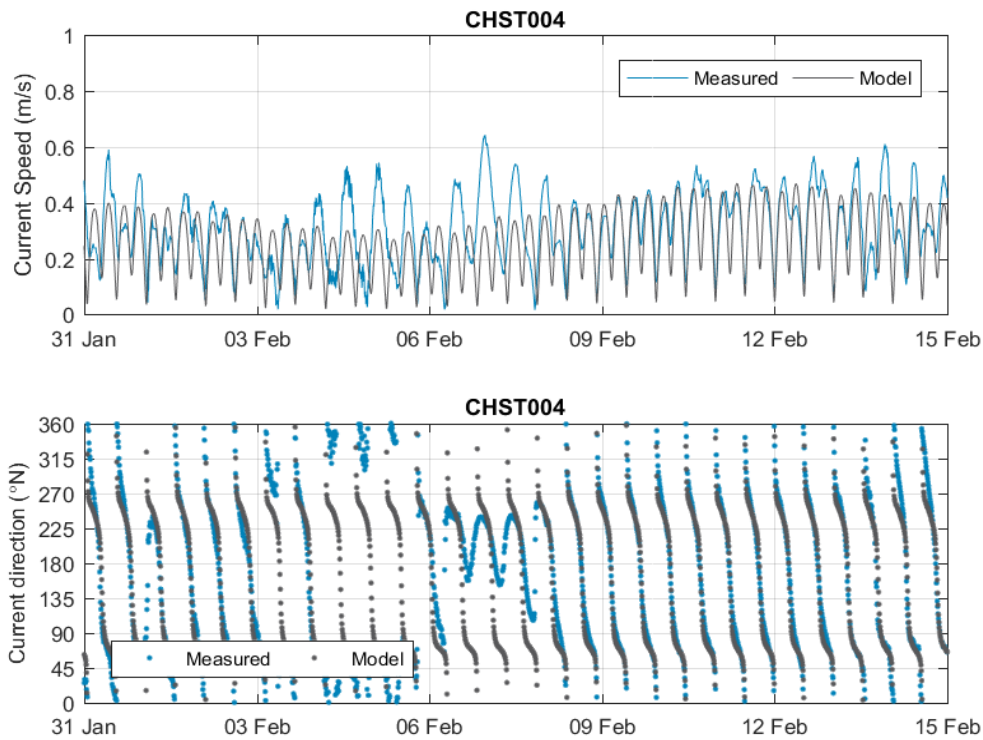


Figure A-36 Modelled and measured flows at CHST004 during the model validation period

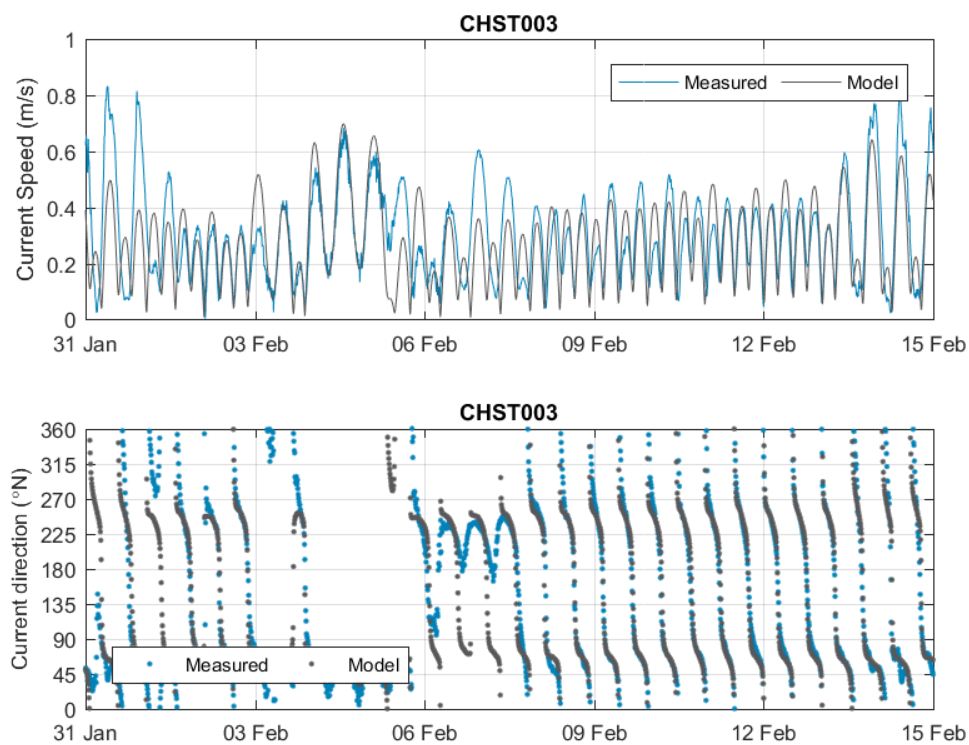


Figure A-37 Modelled and measured flows at CHST003 during the model validation period, with meteorological forcing applied in the model

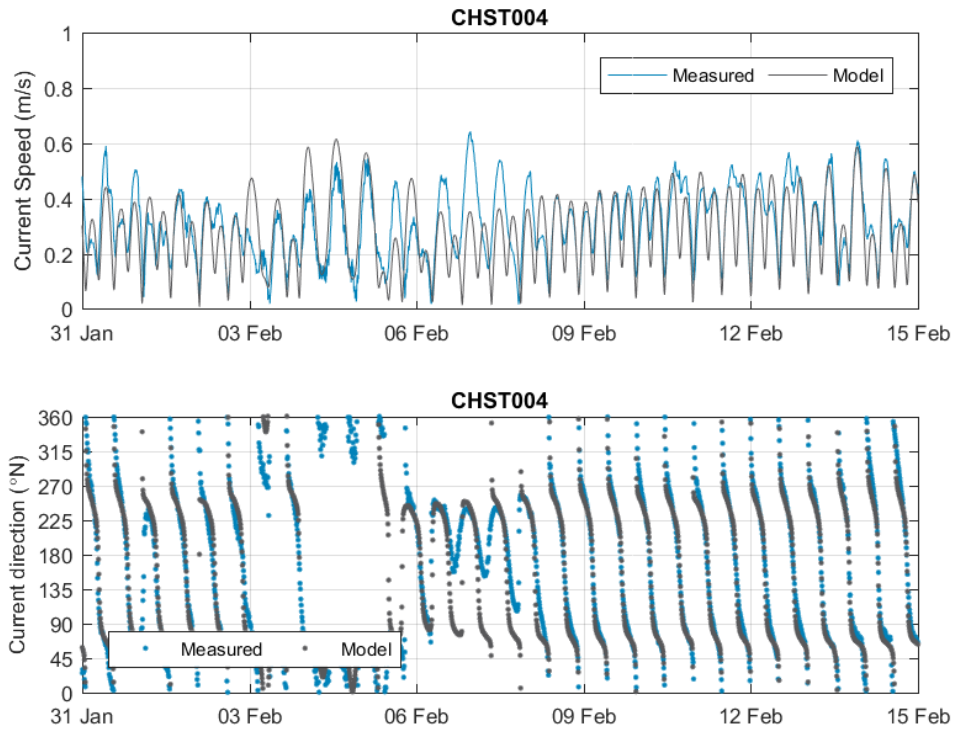


Figure A-38 Modelled and measured flows at CHST004 during the model validation period, with meteorological forcing applied in the model

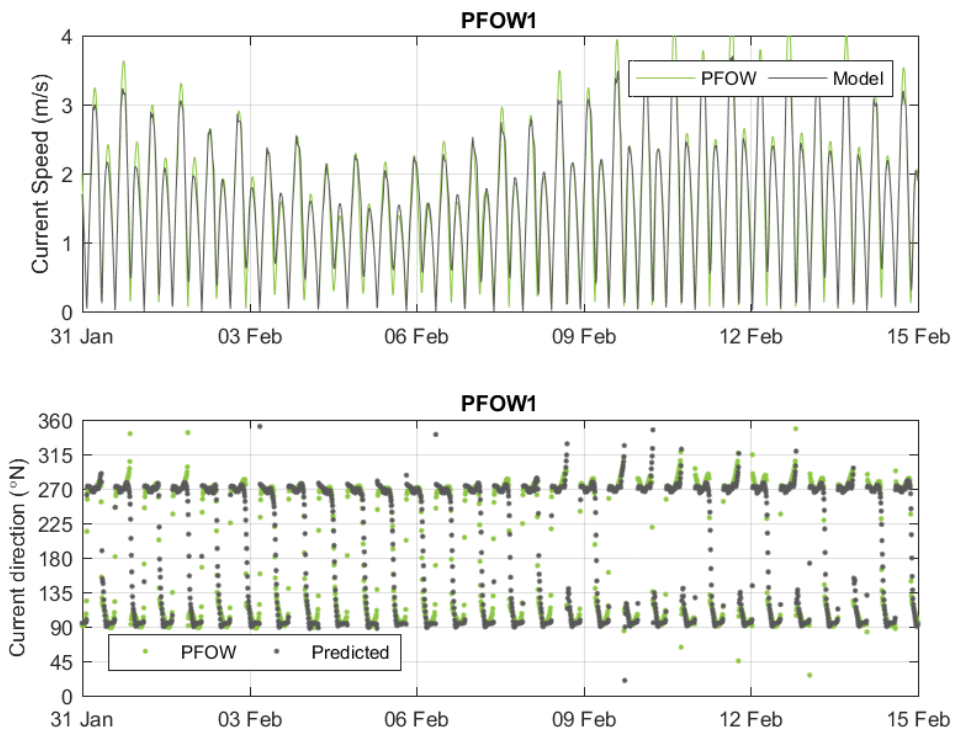


Figure A-39 Modelled flows at PFW01 during the model validation period

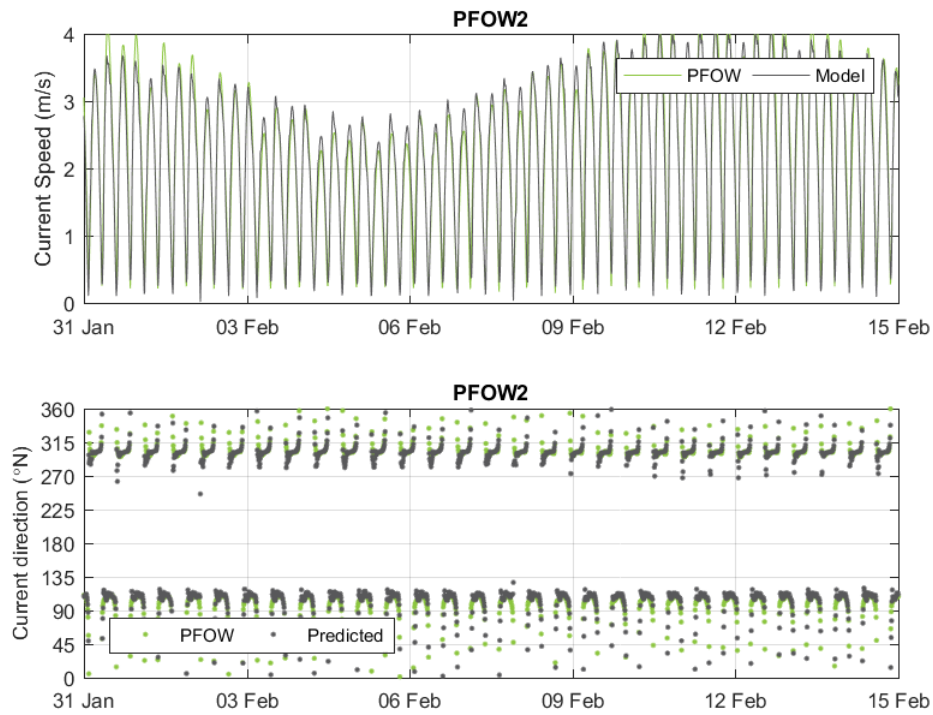


Figure A-40 Modelled flows at PFW2 during the model validation period

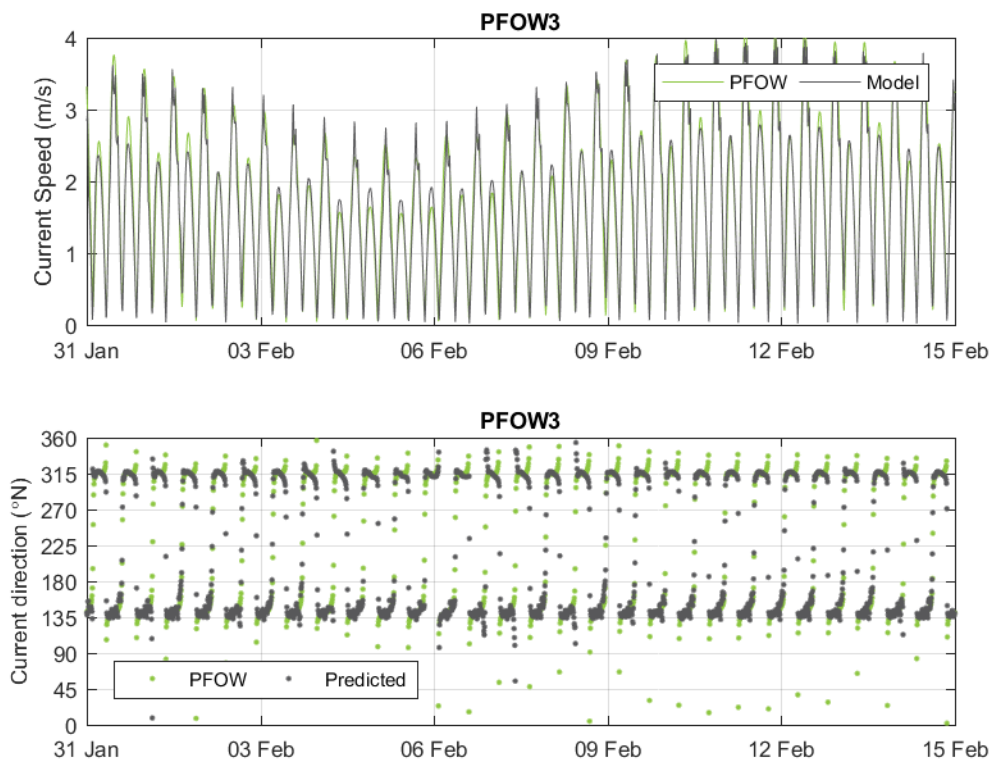


Figure A-41 Modelled flows at PFW3 during the model validation period

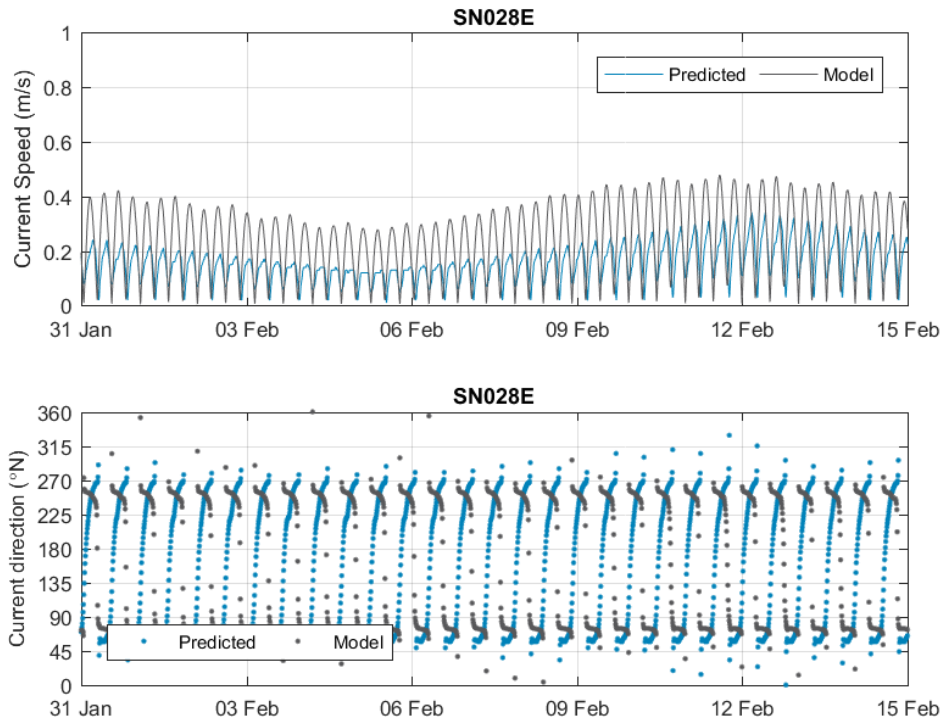


Figure A-42 Modelled and predicted flows at SN028E during the model validation period

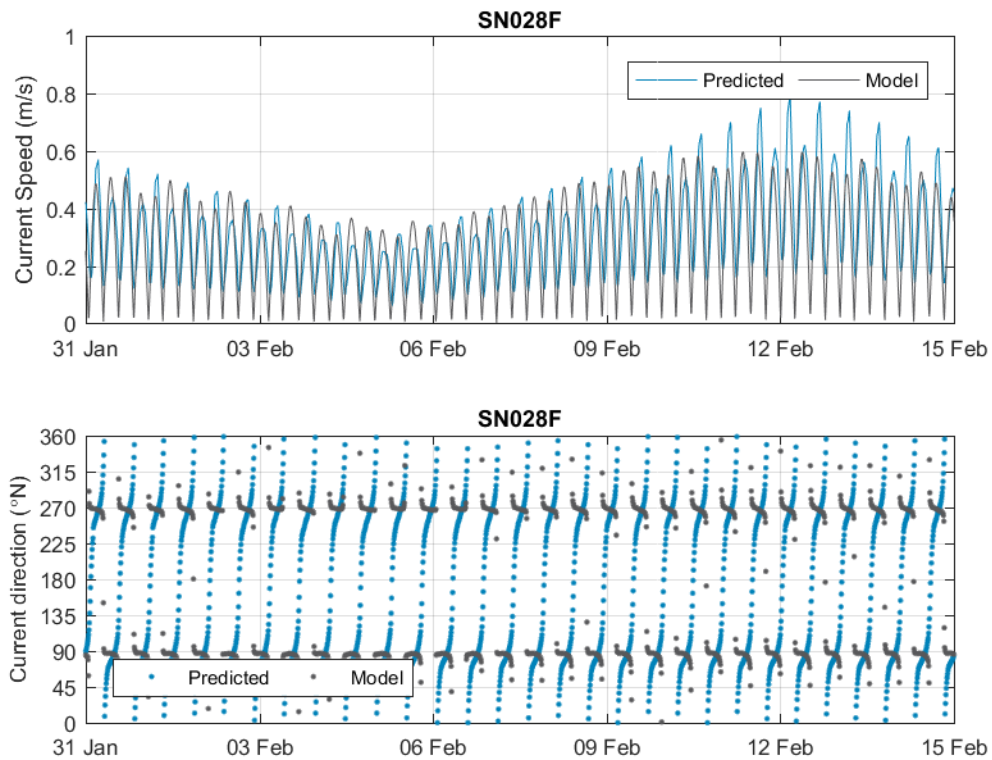


Figure A-43 Modelled and predicted flows at SN028F during the model validation period

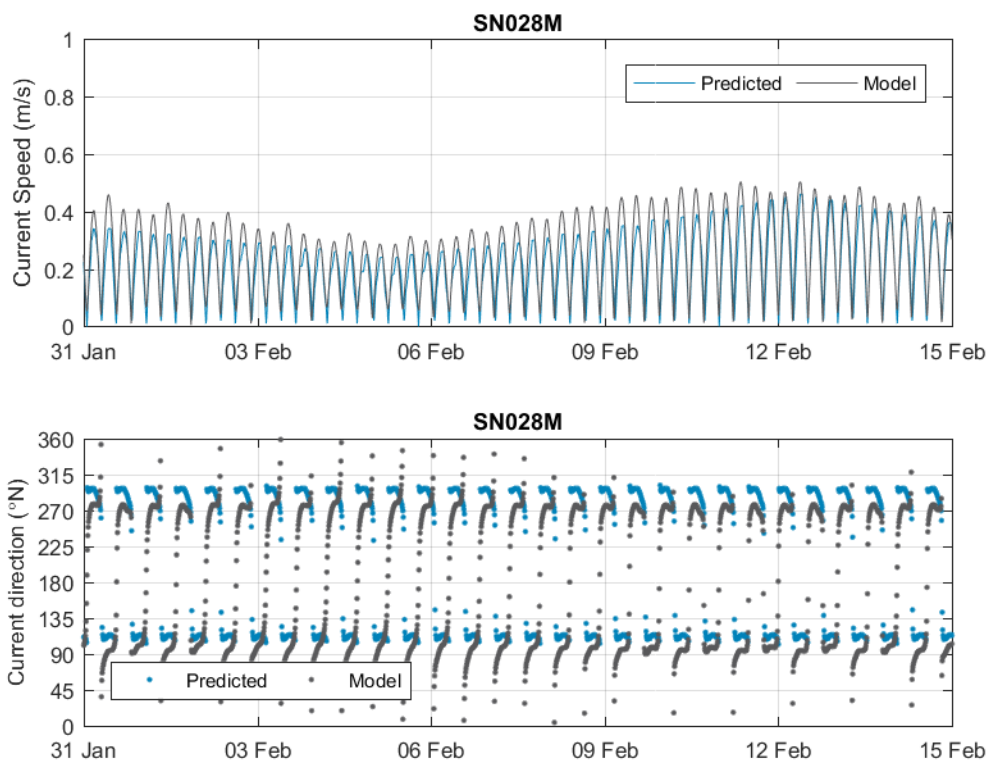


Figure A-44 Modelled and predicted flows at SN028M during the model validation period

Table A-6 Validation Flow Statistics

SITE NAME	FLOW SPEED DIFF (M/S)		FLOW SPEED DIFF (%)		RMSE (M/S)	SCATTER INDEX	DIRECTION DIFF (°)		PHASE DIFFERENCE (MINS)
	PF	PE	PF	PE			PF	PE	
CHST003	-0.08	0.02	-10	3	0.18	0.59	-7	34	-5
CHST004	0.02	-0.02	-3	-3	0.12	0.39	-16	-7	2
CHST003m*	0.03	0.02	-4	3	0.13	0.42	-8	10	-11
CHST004m*	0.01	-0.03	2	-5	0.11	0.35	-15	2	-6
PFOW1	0.05	-0.23	-2	-5	0.21	0.13	-4	-2	6
PFOW2	0.04	0.16	-1	4	0.23	0.10	0	0	1
PFOW3	0.10	0.01	2	0	0.20	0.11	-3	2	-1



SITE NAME	FLOW SPEED DIFF (M/S)		FLOW SPEED DIFF (%)		RMSE (M/S)	SCATTER INDEX	DIRECTION DIFF (°)		PHASE DIFFERENCE (MINS)
	PF	PE	PF	PE			PF	PE	
SN028E	0.17	0.18	55	60	0.12	0.76	14	3	-46
SN028F	0.05	-0.07	8	-9	0.07	0.22	7	6	-42
SN028M	0.07	0.06	15	13	0.05	0.22	-16	-20	-16

m\* denotes model run which includes meteorological forcing. Values in red again show where the model did not achieve the guideline standards for validation.

### A.3.5 Wave Model Calibration

Waves from the West to North sectors dominate at the OAA, occurring for more than 80% of the time (section 3.8.2). Further, due to the long fetch distance, waves from these directions are also notably larger than those from other, less exposed sectors. The wave model was therefore setup to replicate the extreme and percentile wave conditions from the West to North sectors (see section 3.8.2).

The main calibration parameters within the wave model (other than the driving conditions) are the bed roughness and wave breaking parameters. The bed roughness was set using a spatially constant friction coefficient of 0.002 m/s. For conservatism this is lower than the default value of 0.0077 m/s and from experience has provided a good model calibration in regions where wave data were available for model calibration. The wave breaking parameters were set to default values, which tend to be applicable in swell dominant environments, but can be too low where wind waves dominate. Although swell waves clearly dominate the local conditions within the West of Orkney model domain, a sensitivity test with reduced wave breaking (by increasing the wave steepness) was undertaken but was considered to be likely to result in an over prediction of wave heights (based on a comparison of modelled and measured wave heights at Dounreay for periods when wave conditions were similar to the events modelled).

The wind conditions applied were as per those given in OWPL (2023). Although these wind conditions may not necessarily occur in conjunction with the equivalent wave conditions, in lieu of any other data this was considered a suitable approach. The model boundaries were iteratively adjusted until the wave heights and wave periods within the site matched the prescribed conditions. The wave boundary conditions applied for the west, north west and north wave events are provided in Table A-7 to Table A-9 respectively.



Table A-7 Model boundary conditions for westerly wave events

EVENT	BOUNDARY CONDITION		OAA SITE (MODEL)		OAA (HINDCAST)	
	Hs (m)	T <sub>p</sub> (s)	Hs (m)	T <sub>p</sub> (s)	Hs (m)	T <sub>p</sub> (s)
50 <sup>th</sup> percentile	2.6	11.1	2.6	11	2.6	11
90 <sup>th</sup> percentile	5.2	12.8	5.1	13	5.1	13
1 in 1 year RP	10.8	15.25	10.2	15.7	10.2	15.7
1 in 5 year RP	12.9	15.9	12	16.4	12	16.4
1 in 10 year RP	13.65	16.2	12.6	16.7	12.6	16.7
1 in 50 year RP	15.2	16.4	13.6	17	13.6	17
1 in 100 year RP	15.8	16.6	14	17.2	14	17.2

Table A-8 Model boundary conditions for north westerly wave events

EVENT	BOUNDARY CONDITION		OAA SITE (MODEL)		OAA (HINDCAST)	
	Hs (m)	T <sub>p</sub> (s)	Hs (m)	T <sub>p</sub> (s)	Hs (m)	T <sub>p</sub> (s)
50 <sup>th</sup> percentile	2.25	10.6	2.2	10.6	2.2	10.6
90 <sup>th</sup> percentile	4.25	12.2	4.3	12.5	4.3	12.5
1 in 1 year RP	9.3	14.7	9.2	15.3	9.2	15.3
1 in 5 year RP	10.9	15.3	10.8	15.9	10.8	15.9
1 in 10 year RP	11.5	15.6	11.4	16.2	11.4	16.2
1 in 50 year RP	12.5	15.8	12.3	16.5	12.3	16.5
1 in 100 year RP	12.7	16.1	12.6	16.7	12.6	16.7



Table A-9 Model boundary conditions for northerly wave events

EVENT	BOUNDARY CONDITION		OAA SITE (MODEL)		OAA (HINDCAST)	
	Hs (m)	T <sub>p</sub> (s)	Hs (m)	T <sub>p</sub> (s)	Hs (m)	T <sub>p</sub> (s)
50 <sup>th</sup> percentile	2.1	10.5	2.1	10.4	2.1	10.4
90 <sup>th</sup> percentile	3.65	11.9	3.9	12.1	3.9	12.1
1 in 1 year RP	7.6	14.5	8.2	14.8	8.2	14.8
1 in 5 year RP	8.8	15.1	9.6	15.4	9.6	15.4
1 in 10 year RP	9.2	15.4	10.1	15.7	10.1	15.7
1 in 50 year RP	9.9	15.7	10.9	16	10.9	16
1 in 100 year RP	10.1	15.9	11.2	16.2	11.2	16.2

Given that the calibration only considers waves at a single point in the model domain, it is difficult to assess with any certainty the model's ability to replicate the transformation of waves across the model domain. To provide a high level assessment of this, times when waves close to the OAA analysis site (from WaveWatchIII (WWIII<sup>17</sup>)) were similar to the events modelled (direction within 10 degrees, Hs within 0.2 m and Tp within 1 sec) were identified. Wave conditions were then extracted from the West of Orkney model at the location of the Dounreay buoy (see Figure A-3 for location) for these events and were compared against measured wave heights, results are shown in Table A-10. The comparison was constrained to the period of data availability at the Dounreay buoy, which was a relatively short period of approximately three months. Of the events modelled, only p50 wave conditions occurred during the period of data availability.

Table A-10 Comparison of West of Orkney modelled and measured waves at Dounreay

EVENT	MODELLED H <sub>s</sub> AT DOUNREAY	MEASURED H <sub>s</sub> AT DOUNREAY
1. West p50 16 <sup>th</sup> Nov 1997	1.0	1.6
2. West p50 8 <sup>th</sup> April 2001	2.2	1.6
3. West p50 28 <sup>th</sup> April 2001	1.6	1.6
4. North p50 17 <sup>th</sup> April 2001	1.7	1.2
5. North West p50 3 <sup>rd</sup> Nov 1997	2.2	1.3

<sup>17</sup> WWIII hindcast timeseries data was used to investigate the wave transformation in order to calibrate the wave model (for the West of Orkney model).



The comparison demonstrates that the West of Orkney model predominantly tends to over-estimate the wave heights at Dounreay and can therefore be considered to be likely to provide a conservative assessment of the wave climate in the nearshore area, although it is noted that this assessment is constrained to relatively short period waves ( $T_p$  of 10 to 12 seconds) which will be less sensitive to bed roughness than the longer period waves ( $T_p$  up to 16 seconds) associated with more extreme storm conditions.

## A.4 Summary

A hydrodynamic and wave model of the North Sea off the north coast of Scotland has been configured in the MIKE FM software suite. The developed hydrodynamic model was calibrated to replicate tidal flows in the wider model region, while the wave model was calibrated to represent a set of typical and extreme wave conditions defined at a point within the OAA.

The hydrodynamic model accurately simulates water levels throughout the model domain and the flows through the Pentland Firth where high quality measured data for calibration exists. Plots of maximum flows from the West of Orkney model also agree well with maximum flows from other third party models. Additionally, when setup to include meteorological forcing the model also replicated observed non-tidal influences on flows at Costa Head. However, some differences between modelled and ATT flow predictions were found to result in the model not achieving the guideline standards for calibration. Given the low confidence in the ATT flows and the model's ability to accurately simulate flows from high quality measured data it was not considered appropriate to tune the model to better reproduce these flows.

The wave model is setup to simulate wave events within the OAA using a conservative bed roughness (i.e. lower than the default) and default wave breaking parameters which from experience is applicable in swell dominated wave environments. There is limited wave data to provide certainty in the model's ability to transform waves across the model domain but it is considered likely that the model provides a conservative assessment of wave conditions in the nearshore area.

Site specific hydrodynamic and wave data would greatly improve confidence in the model's ability to accurately simulate the conditions across the project area.



## A.5 References

- ABPmer, (2017). UK Renewables Atlas. Available online at <https://www.renewables-atlas.info/explore-the-atlas/> [Accessed 28/10/2022].
- ABPmer, (2013). Numerical Model Calibration and Validation Guidance. ABP Marine Environmental Research Ltd., File Note R/1400/112. ABPmer, Southampton.
- Andersen, (1995). Global ocean tides from ERS 1 and TOPEX/POSEIDON altimetry. *Journal of Geophysical Research* 100, C12. P25249-25260.
- Bartlett, J.M., (1998). Quality Control Manual for Computational Estuarine Modelling. Environment Agency R& 1 Technical Report W168, The Environment Agency, Bristol.
- Cheng, Y. and Andersen, O. B., (2011). Multimission empirical ocean tide modelling for shallow waters and polar seas. *Journal of Geophysical Research, Oceans*, Volume 116, Issue C11.
- Egbert, G.D., A.F. Bennett and M.G. Foreman (1994). TOPEX/POSEIDON tides estimated using a global inverse model. *Journal of Geophysical Research* Vol. 99, No. C12, 21,821-24,852.
- EMODnet Bathymetry Consortium, (2020). EMODnet Digital Bathymetry (DTM). <https://doi.org/10.12770/bb6a87dd-e579-4036-abe1-e649cea9881a>
- FWR, (1993). Framework for marine and estuarine model specification in the UK; The Foundation for Water Research (FWR).
- OWPL, (2023). West of Orkney Windfarm EIA Metocean Design Basis. Document number: WO1-WOW-MET-AM-BD-0001. May 2023.
- Pye, K., Blott, S.J. and Brown, J. (2017). Advice to inform development and guidance on marine, coastal and estuarine physical processes numerical modelling assessments. NRW Evidence Report 208, July 2017.
- NRA (2022). Flow data from multiple stations from the National River Archive (2022). Available online at: <https://nrfa.ceh.ac.uk/data> [Accessed 28/10/2022].
- O'Hara Murray, R., Campbell, L., (2021). Pentland Firth and Orkney Waters Climatology 1.02. doi: 10.7489/12041-1
- Williams, J.J. and Esteves, L.S., (2017). Guidance on setup, calibration and validation of hydrodynamic, wave and sediment models for shelf seas and estuaries. *Advances in civil engineering* (Volume 2017), 5251902, 25 pages.



## A.6 Abbreviations

TERM	DEFINITION
2D	2 Dimensional
3D	3 Dimensional
ADCP	Acoustic Doppler Current Profiler
ATT	Admiralty Total Tide
CD	Chart Datum
CFSR	Climate Forecast System Reanalysis
DD	Domain Decomposition
DHI	Danish Hydraulic Institute
DTM	Digital Terrain Model
DTU	Technical University of Denmark
E	East
EIA	Environmental Impact Assessment
EMODnet	European Marine Observation and Data Network
FM	Flexible Mesh
HD	Hydrodynamic
Hs	Significant Wave Height
HW	High Water
LW	Low Water
MoW	MetoceanWorks
MS	Marine Scotland
MSL	Mean Sea Level
MT	Mud Transport
N	North
NE	North East
NRFA	National River Flow Archive
NTSLF	National Tide and Sea Level Facility
NW	North West
OAA	Option Agreement Area
OSP	Offshore Substation Platform
OWF	Offshore Wind Farm
P	percentile



TERM	DEFINITION
PCS	Port and Coastal Solutions
PE	Peak Ebb
PF	Peak Flood
PFOW	Pentland Firth and Orkney Waters
Q5	5 <sup>th</sup> Quantile
RMS	Root Mean Square
RP	Return Period
S	South
SE	South East
SI	Scatter Index
SW	South West
SW	Spectral Wave
SWAN	Spectral Wave Nearshore
Tp	Peak Period
UKHO	UK Hydrographic Office
UTM	Universal Transverse Mercator
W	West
WL	Water Level
WOW	West of Orkneys Windfarm
WTG	Wind Turbine Generator
WWIII	WaveWatch III



## APPENDIX B MARINE PHYSICAL PROCESSES MODELLING RESULTS REPORT

### B.1 Introduction

Xodus are undertaking a marine physical and coastal processes technical study to inform the West of Orkney offshore EIA. Xodus commissioned Port and Coastal Solutions Ltd (PCS) to conduct marine physical and coastal processes modelling work. This report provides a summary of the results from the modelling work undertaken for the offshore Project. The development of the modelling tools was reported separately in the model calibration report (Appendix A), where the offshore Project and study area was also introduced. This modelling results report is structured as follows:

- An introduction is provided in Section B.1;
- Details on the proposed offshore Project and how these are implemented within the modelling is provided in Section B.2;
- The baseline characterisation as informed by the West of Orkney model is summarised in Section B.3;
- The construction impacts as informed by the West of Orkney model are detailed in Section B.4;
- The operational impacts as informed by the West of Orkney model are presented in Section B.5; and
- A summary of the key findings from the modelling study are discussed in Section B.6.

### B.2 The offshore Project

Full details on the proposed offshore Project are provided in chapter 5: Project description of the EIAR, while key project elements relating to the marine physical and coastal processes supporting study and this modelling study are presented in section 4.3. Only the relevant information for the marine physical processes modelling assessment and the applied assumptions are highlighted in this report.

#### B.2.1 Construction

At present there are a wide range of construction methods being considered for site preparation and cable and WTG foundation installation. A worst case was developed from the Project design and modelling scenarios were developed to assess the construction related impacts associated with the worst case.

The following construction activities and potential approaches have been modelled:

- Seabed preparation: one option for seabed preparation is to use a trailing suction hopper dredger (TSHD) to clear sandwaves ahead of installing the cables and foundations. Bedform clearance by Controlled Flow Excavator



(CFE) is the other method under consideration for seabed preparation. Due to the differences in the plume generation both methods were modelled;

- Cable burial: several methods are being considered for cable installation, but CFE is considered to provide the worst case disturbance to the seabed. The transport speed and sediment disturbance volume differs between cable burial and bedform clearance by CFE and as result the plume for cable burial has also been modelled; and
- Monopile drilling: drilling of the seabed for the installation of the monopiles has the potential to result in the complete breakup of the underlying bedrock and could result in the discharge of disaggregated sediment at the surface. The drilling could either be undertaken at one WTG foundation at a time or two foundations at a time. The modelling has therefore assessed both options.

All model simulations span a 16 day period, with construction activities commencing 0.5 days after the model start time to allow for model spin up. The modelled 16 day period used to investigate construction impacts repeat the same.

The following sections provide details of sediment disturbance rates from the three relevant potential construction activities.

### **B.2.1.1 Seabed Preparation By Dredger**

The inter-array and interconnector cables within the OAA and the export cables connecting the windfarm to the mainland within the offshore ECC will require burying in areas where sandwaves are present. Prior to installation these areas will require bedform clearance.

The in-situ volume of sediment estimated to require removal is 382,360 m<sup>3</sup> from the inter-array cables, 382,360 m<sup>3</sup> from the interconnector cables and 495,000 m<sup>3</sup> from the ECC. An additional in-situ volume of 250,000 m<sup>3</sup> will also need removal from the WTG locations as part of the seabed preparation.

#### ***B.2.1.1.1 Dredging Approach***

One option for seabed preparation is to dredge the areas where sandwaves are present and to place the dredged sediment within the offshore Project area.

The following dredge volumes are applicable:

- 1,014,720 m<sup>3</sup> from the OAA; and
- 495,000 m<sup>3</sup> from the offshore ECC.

This equates to a total volume of 1,509,720 m<sup>3</sup>. Assuming an in-situ density of 1,900 kg/m<sup>3</sup> and a water density of 1025 kg/m<sup>3</sup> the equivalent dry sediment mass to be dredged is 2,264,580 tonnes (based on a dry density of 1,500 kg/m<sup>3</sup>).

The water depths in the areas where bedform removal may be required could be up to 110 m. These water depths, combined with the spatial extent over which removal is required and the relative exposure to waves at the site mean that the options for dredger type are limited. It is expected that a large Trailer Suction Hopper Dredger (TSHD) will be required to dredge the deeper areas (> 80 m). Although it is possible that a medium to large TSHD could dredge



the shallower regions, for this assessment it was assumed that a large TSHD which can dredge to depths of at least 110 m will be adopted for all of the dredging. The higher production rates of a large TSHD compared to a medium TSHD will result in higher concentration plumes being generated and the assumption of a larger TSHD therefore represents a conservative approach in terms of suspended sediment concentration (SSC) impacts.

The large TSHD adopted for this assessment was assumed to have a hopper capacity of 35,000 m<sup>3</sup> and a fully loaded sailing speed of 16 knots. Although it is difficult to estimate the exact dredge production rate and associated time to fill the hopper (since it will vary with dredger and sediment type and water depth), for this assessment it was assumed that the hopper would on average take two hours to fill and that overflow would occur after the initial 30 minutes of dredging. In addition, the placement of dredge sediment through the hydraulic hopper doors was assumed to occur over a 10 minute duration.

Each hopper load was assumed to hold 15,050 tonnes of dry sediment (equivalent to approximately 10,033 m<sup>3</sup> in situ), therefore based on the dredge volumes quoted above it will take 101 dredger loads to prepare the seabed in the OAA and 49 dredger loads to prepare the seabed in the offshore ECC.

The areas requiring bedform clearance are not known and it was therefore assumed that clearance could occur across the full areas of the OAA and along the full length of the offshore ECC. In reality, the dredger will return to the same dredge track multiple times, since on each pass it is only likely to remove sediment across a width of around 20 m and to a depth of around 0.5 m and dredging will be focussed on a small area of the site. However, any plume from previous dredge cycles will have dispersed or settled on the bed and the adopted approach therefore provides a conservative assessment of the area which could be affected by sediment plumes.

Based on the volumes to be dredged and the assumed production rates, for seabed preparation in the OAA, dredging will occur for 202 hours. For seabed preparation in the offshore ECC, the dredging will occur for 98 hours. A vessel speed of 4 knots when dredging has been applied.

The dredged sediment will be placed within the offshore Project area boundaries. The exact placement location is not yet known but will be agreed with the Regulators during the approval process post-consent. For the purposes of modelling an indicative Dredge Material Placement Area (DMPA) within the Offshore Project area was assumed (see Figure B-1) This area was selected for both its central location (to aid reworking of sediment across the site following construction), its deeper water depths and also to maximise the available disposal area to inform seabed deposition analyses. Each of the 150 dredger loads was placed in a different cell within the DMPA, with the cells spread across the full extent of the area.

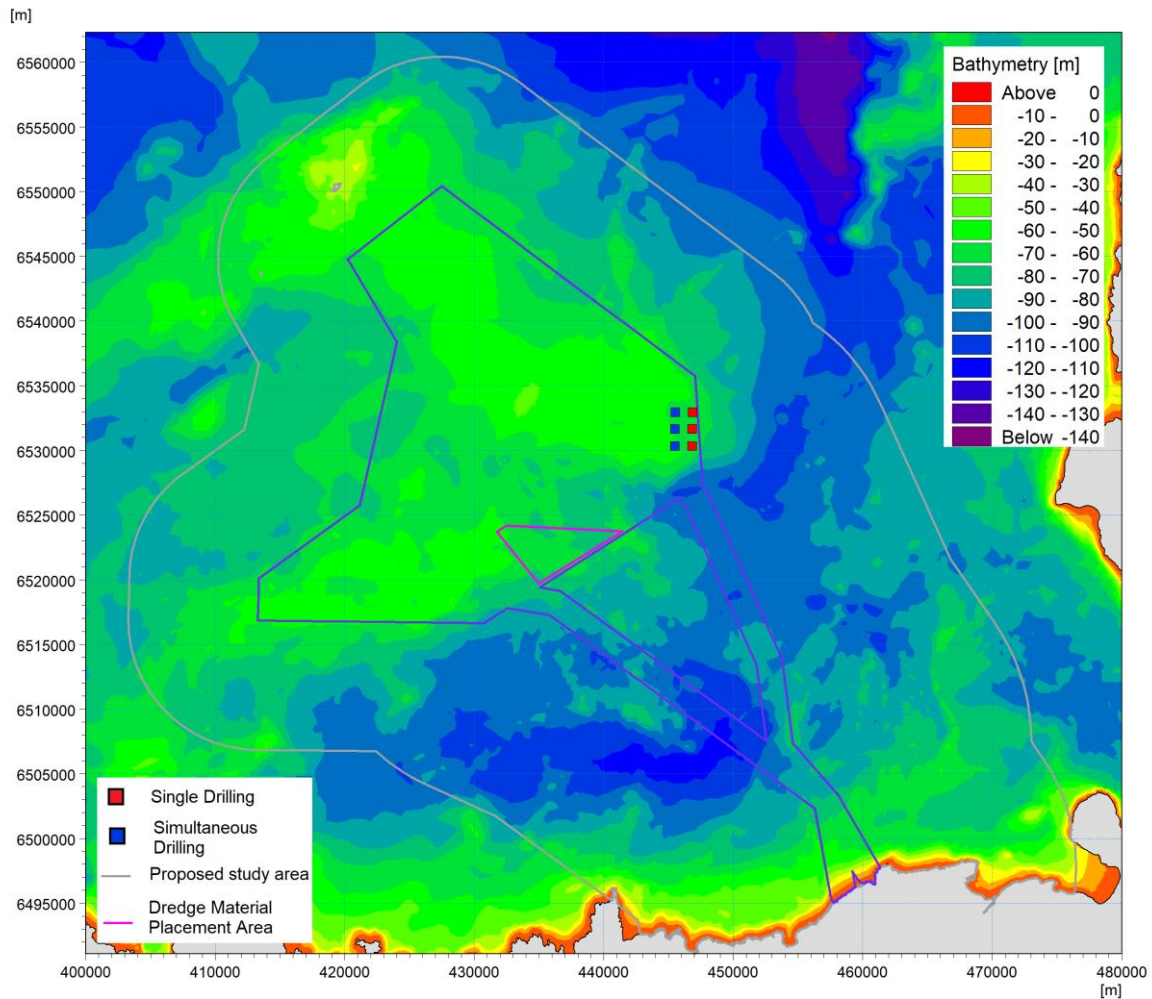


Figure B-1 Overview of the proposed development showing the indicative location of the placement site and WTG locations considered in the modelling assessment

Assuming a vessel speed of 16 knots during transit to/from the placement site, transit times are expected to be in the range of 10 to 50 minutes depending on the area being dredged. An average transit time of 30 minutes to and from the placement site has been applied throughout, yielding a total dredge cycle time of three hours and ten minutes.

If dredging were continuous the dredge would take 19.8 days to complete (with 13.3 days of dredging in the OAA and 6.5 days of dredging in the offshore ECC). In reality, there will be some downtime due to weather, vessel repositioning and vessel maintenance/crew change. Further, the assumed production rates are likely to be higher than can be achieved when dredging in deeper water and as such the time taken to dredge the site is likely to be longer than this. However, these assumptions provide a worst case assessment, resulting in a higher intensity of sediment disturbance. To ensure that the effects of the dredging are simulated across the full range of tidal conditions, the dredging in the offshore ECC and the OAA were considered as two separate model simulations.



### B.2.1.1.2 Dredging Source Terms

An overview of the likely amount of sediment suspended by different dredge types, also known as the source term, has been summarised by Becker et al. (2015). They suggest that the following percentages of the fine-grained silt and clay could be suspended during dredging by a TSHD:

- Draghead: 0 to 3% of the fine-grained silt and clay present in the sediment;
- Overflow: 0 to 20% of the fine-grained silt and clay present in the sediment; and
- Placement through hydraulic hopper doors: 0 to 10% of the fine-grained silt and clay present in the sediment.

The coarser sediment fractions (including fine sands) are expected to rapidly resettle to the bed within the area where the sediment disturbance occurs, while the fine-grained sediment (silt and clay) has the potential to be suspended by dredging. Due to the relatively low settling velocities of the fine-grained sediment they have the potential to remain in suspension and be transported away from the dredged area by currents. Therefore, only the dispersion of the finer sediment fractions (coarse silts to clays) are simulated in the model.

To characterise the local sediment properties, 67 surface sediment samples were collected within the footprint of the offshore Project area, with 34 samples collected in the OAA and 33 samples collected in the offshore ECC, as described within the marine physical and coastal processes technical report. The sediment samples were analysed to determine the particle size distribution (PSD) of the surface sediment throughout the offshore Project area. Based on the Folk (1954) classification the sediment was predominantly sandy gravel, with some slightly gravelly sand and some sand also present. The percentage of fine-grained silt and clay present in the sediment ranged from 0 to 8%, with lower percentages of fines present within the OAA compared to the offshore ECC (Table B-1). To better understand the variability in the sediment composition between the OAA and the offshore ECC the average percentage of fine grained silt and clay in each region has been calculated (Table B-1). The results show that on average 0.6% of the samples from the OAA are made up of fine-grained silt and clay, compared to an average fine-grained silt and clay composition of 2.6% for samples from the offshore ECC.

Table B-1 Average percentage of fine-grained sediment present in the OAA and offshore ECC informed by site-specific environmental sampling (section 2.1.3.1) reported in the marine physical and coastal processes technical study (section 3.3.2.2.1)

Region	Coarse/Medium (16-63µm)	Silt	Fine Silt (4-16µm)	Clay (<4µm)	All Silt and Clay (<63µm)
OAA	0.2%		0.2%	0.2%	0.6%
Offshore ECC	1.0%		0.9%	0.7%	2.6%
<i>Average</i>	0.6%		0.5%	0.4%	1.6%

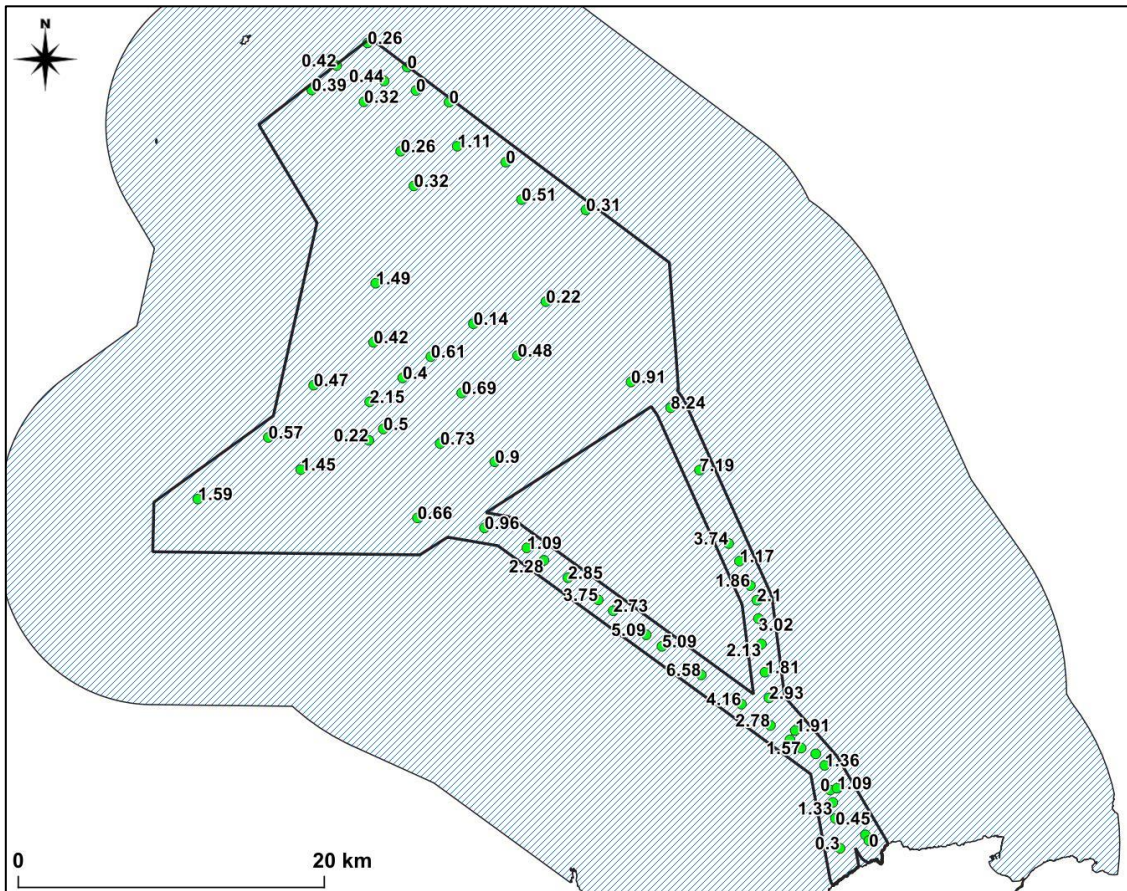


Figure B-2 Location of sediment samples within the OAA and offshore ECC along with the measured percentage of silt and clay sized particles in the samples used to inform this modelling study

Based on the differences in fine grained silt and clay composition, different source terms were applied for construction activities in the OAA and the offshore ECC. To provide a conservative approach, the upper limits of the suggested source term percentages were adopted, the resultant source terms are detailed in Table B-2.

Table B-2. Source terms for the bedform dredging in the two different regions

DREDGE PERIOD	OAA SOURCE TERMS	offshore ECC SOURCE TERMS
Draghead (0 to 30 mins)	0.4 kg/s	1.6 kg/s
Overflow + Draghead (30 to 120 mins)	2.9 kg/s	12.5 kg/s
Placement (10 min duration)	15.1 kg/s	65.2 kg/s

The source terms for the draghead and overflow were applied as moving source terms to replicate the movement of the dredger. For dredging of the OAA it was assumed that the dredge would start at the northern edge of the OAA, with the first track simulating a westward movement of the dredger and the subsequent track simulating an



eastward movement of the dredger to the south of the first track. This pattern of alternating westward and eastward tracks was continued to cover the whole OAA. Sediment dredged from the OAA was placed in the northern part of the placement area.

For dredging the offshore ECC it was assumed that the dredger would start at the nearshore end of the western cable route and transit offshore along the length of the offshore ECC before turning and repeating the same track in the opposite direction. The western cable route was dredged for the first half of the dredge simulation and the eastern cable route was dredged for the second half of the dredge simulation. Sediment dredged from the offshore ECC was placed in the southern part of the placement area.

## **B.2.1.2 Seabed Preparation By CFE**

### ***B.2.1.2.1 CFE Approach***

Bedform clearance by CFE will result in different sediment source terms than the dredging with a TSHD, with all of the sediment disturbance occurring close to the bed and at the location where clearance is required.

The expected rate of bedform clearance using an CFE is 25 m/hr. As provided in the Project design assumptions, the following assumptions are applied:

- An CFE footprint of 50 m, therefore requiring 20 passes to clear across 1 km width;
- Average sandwave height of 3.5 m;
- Unknown sandwave wavelength, but an assumed base width of 35 m;
- Sandwaves expected to need clearing from 19.2 km length of the cable route (across 1 km width); and
- The bedforms within the CFE footprint would be cleared to its base in one pass (i.e. 3.5 m height cleared within the 50 m footprint in one pass).

Assuming the CFE footprint and clearance properties summarised above results in a CFE clearance cross section of 175 m<sup>3</sup>/m, which based on a dry bed density of 1,500 kg/m<sup>3</sup> gives a sediment disturbance mass of 262,500 kg/m. Based on the bedform clearance rate of 25 m/hr, CFE footprint of 50 m, 19.2 km to be cleared at 1 km wide, it will take 15,360 hours (640 days) to clear bedforms along the export cable route. Assuming the full volume of sediment is suspended, the indicative rate of sediment disturbance is 1,823 kg/s.

The sediment disturbance rate would be the same for the clearance of bedforms anywhere across the offshore Project, although the varying fine sediment fraction would give rise to varying source terms as described in section B.2.1. In reality there will be some downtime due to weather, equipment and vessel maintenance and repositioning. However, the continual operation provides a worst case assessment and so was assumed for the modelling.

### ***B.2.1.2.2 CFE Source Terms***

The high concentration of sediment suspended will result in the formation of a dynamic plume which will descend rapidly back to the bed. The sediment release concentration is the same order of magnitude as that in the TSHD overflow and as such it is reasonable to assume that less than 20% of the sediment disturbed will disperse as individual



particles. Adopting a conservative value of 20% for dispersion and considering only the fine sediment, the indicative release rates are presented in Table B-3.

The source terms for the CFE were applied as moving source terms to replicate the actual transit speed. Due to the slower CFE transit time relative to that of the TSHD, the simulated CFE tracks were shorter than those for the dredging and only covered small parts of the OAA and offshore ECC.

Table B-3 Source terms for bedform clearance by CFE in the two different regions

ACTIVITY	OAA SOURCE TERMS	OFFSHORE ECC SOURCE TERMS
Bedform clearance by CFE	2.2 kg/s	9.5 kg/s

### B.2.1.3 Cable Burial

#### B.2.1.3.1 Cable Burial Approach

CFE is modelled as it considered to provide the worst case disturbance during cable installation for both the export cable and the inter array/ inter connector cables, based on the worst case Project design. The expected rate of cable burial using an CFE is 150 m/hr.

Assuming a trench width of 5 m and a depth of 3 m the in-situ volume of sediment disturbed by CFE along the entire 320 km export cable route (five cables, each 64 km long) is 4,800,000 m<sup>3</sup>. This is equivalent to a dry sediment mass of 7,200,000 tonnes, assuming a dry bed density of 1,500 kg/m<sup>3</sup>. Based on the cable burial rate it will take 2,133 hours (89 days) to install the export cables. Assuming the full volume of sediment is suspended the rate of sediment disturbance is 938 kg/s.

The sediment disturbance rate would again be the same for the cable installation across the offshore Project, with variations in source terms (section B.2.1.2) being a result of the fine sediment fraction between the OAA and offshore ECC. In reality there will be some downtime due to weather, equipment and vessel maintenance and repositioning. However, the continual operation provides a worst case assessment and so has been assumed for the modelling.

#### B.2.1.3.2 Cable Burial Source Terms

The high concentration of sediment suspended will result in the formation of a dynamic plume which will descend rapidly back to the bed. The sediment release concentration is the same order of magnitude as that in the TSHD overflow and as such it is reasonable to assume that less than 20% of the sediment disturbed will disperse as individual particles. Adopting a conservative value of 20% for dispersion and considering only the fine sediment, the release rates given in Table B-4 are considered applicable.

The source terms for the CFE were applied as moving source terms to replicate the actual transit speed. Due to the relatively slow CFE speed during cable installation, the modelled tracks only covered a relatively small area of the OAA. Most of the extent of the offshore ECC was covered, but only by a single pass (whereas five passes will be required to install all of the export cables).



Table B-4 Source terms for cable burial by CFE in the two different regions

ACTIVITY	OAA SOURCE TERMS	OFFSHORE ECC SOURCE TERMS
Cable burial by CFE	1.1 kg/s	4.9 kg/s

## B.2.1.4 Pile Drilling

### B.2.1.4.1 Drilling Approach

A range of different WTG foundations are currently being considered. The highest drilling rate and sediment disturbance rate is expected for the installation of the largest monopile which has an 18 m diameter on the bed<sup>18</sup>. The foundations will be drilled to a depth of 40 m below the seabed at a rate of 0.3 m per hour

Approximately 11,000 m<sup>3</sup> of sediment will be drilled for each monopile WTG foundation, with the drilling expected to take approximately 135 hours per foundation. It was assumed that up to two foundations will be installed concurrently. Two sediment dispersion scenarios were therefore undertaken, one considering drilling at one structure at a time and the second considering drilling at two structures at a time, with indicative drilling locations illustrated in Figure B-1. It is unknown whether the spoil from the drilling would be discharged at the seabed or at the surface of the water column. Based on this, the worst case assumption of the drill spoil being discharged at the surface of the water column was adopted.

### B.2.1.4.2 Drilling Source Terms

Based on the available geological information for the OAA, which is based on regional scale data from BGS, the following sediment/rock is applied in the modelling:

- 0 to 50 m depth: Holocene surface sediment of predominantly sandy gravel. The sediment composition is expected to be similar to the surface sediment samples detailed in Table B-1; and
- >5 m depth: bedrock made up of sandstone which can easily be broken down.

The depth of the surface sediment layer varies significantly across the site. To provide a conservative assessment with respect to sediment dispersion during construction a depth of 5 m for surface sediment was assumed across the OAA (since higher release rates are associated with the drilling through bedrock).

The exact composition of the sediment which makes up the sandstone is unknown and is expected to vary spatially. However, for the sediment to be classified as sandstone the majority of the particles it is made up of must be sand, meaning that it would be expected to have at least 70-80% sand particles. For this assessment it was assumed that 30% of the sediment making up the sandstone is silt and clay and that the drilling will fully breakdown all of the sediment in the sandstone to its individual particles. This is considered to represent a conservative assumption with

<sup>18</sup> This value has subsequently been revised to a 14 m diameter monopile since the modelling was completed.



the actual percentage of silt and clay present expected to be lower as well as some of the sandstone expected to remain as larger rock fragments (rather than completely disaggregating).

Based on the information on the drilling approach detailed above, and assuming a density of 2,600 kg/m<sup>3</sup> for sandstone, the sediment release rate during drilling is approximately 60 kg/s. Similar to sediment released during overflow, the high sediment concentration will affect the way the particles disperse in the water column with a dynamic plume likely to form which will descend to the bed at a much faster rate than the individual particles would settle, reducing the potential for fine-grained sediment to remain in suspension. To account for this, it was assumed that 20% of the fine-grained sediment present in the drilled material will remain in suspension, with the associated source term rates specified in Table B-5.

Table B-5. Source terms for the pile drilling

DREDGE PERIOD	SOURCE TERMS
Holocene Layer (0 – 5 m)	0.04 kg/s
Sandstone (>5 m)	3.5 kg/s

For the purposes of modelling it was assumed that drilling will be continuous during the installation of each WTG foundation and that there will be a nine hour gap between drilling subsequent foundations. Therefore over the 15.5 day period over which construction impacts were modelled, the drilling of two (four) complete foundations and half of the drilling of one (two) additional foundation (s) was simulated depending on whether one or two foundations are drilled at any one time. Six indicative WTG locations in the east of the OAA were selected for consideration in the modelling (see Figure B-1 – the red squares show structures drilled for the single drilling and blue squares show additional structures drilled for the simultaneous drilling).

### B.2.1.5 Project in-combination construction activities

There is a possibility that some of the construction activities will overlap. The activities which have the greatest potential to result in an in-combination effect are those which occur within the OAA: pile drilling; bedform clearance by CFE; and cable burial by CFE. These activities have been modelled in-combination, in line with the parameters described for each activity independently. The construction activities are modelled to occur approximately one-WTG spacing, based on the 18 m monopile foundation spacing.

## B.2.2 Operation

Following the design envelope approach, multiple designs for the offshore Project are under consideration, with differing structure types, dimensions and layouts. Two options have been identified as potentially providing the greatest blockage effect on marine physical processes and therefore the largest impact on flows and waves. These are layouts 1 and 2, both of which include 125 WTGs and 5 OSPs as introduced section 4.3 and illustrated in Figure 4-1. The foundation type with the largest blockage are conical monopiles with an 18 m diameter at the seabed reducing to a 12.5 m diameter 60 m above the seabed (Figure B-3). For simplicity the same structure dimensions



were assumed for both the WTGs and OSPs. This provides a worst case as only jackets (which provide a smaller blockage) are being considered for OSP's.

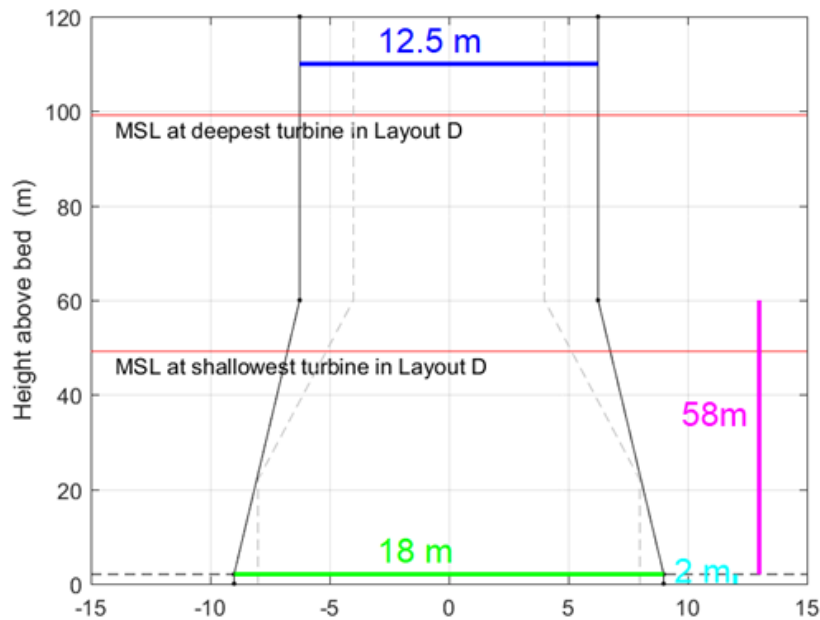


Figure B-3 Assumed dimensions of the monopile and OSP foundations within the water column for the modelling

### B.2.2.1 Hydrodynamic Model

The WTG and substations were represented in the MIKE HD model (within the West of Orkney model) using a subgrid scale structures technique. They were included as circular piers with a varying diameter through the water column as shown in Figure B-3. The locations of the WTG and substations were included in the model as shown in Figure B-1. The model mesh has a resolution of 100 m across the OAA to ensure that only one structure is in each grid cell and with a spacing of several grid cells between neighbouring structures.

To consider the impact for a full range of tidal conditions, the model was run with and without structures for a 15-day spring-neap cycle.

### B.2.2.2 Spectral Wave Model

The WTGs and substations were also represented in the MIKE SW model (within the of the West of Orkney model) using a subgrid scale structures technique. The structures which can be included in the SW model are different to those in the HD model, with circular piers in the SW model only having a single diameter through the water column. Sensitivity testing was undertaken for a range of WTG diameters between 18 m and 12.5 m and the results showed that the impacts to the waves were predicted to be relatively small regardless. Based on this, the maximum diameter for any sections of the WTGs and substations of 18 m has been adopted in the SW model. The same model mesh as used for HD was used for SW.



## B.3 Baseline Characterisation

This section provides an overview of the existing hydrodynamic and wave conditions in the study area to provide a baseline characterisation of these key metocean conditions.

### B.3.1 Hydrodynamic Conditions

Plots of the modelled water level across the offshore Project area, study area and the surrounding regions are shown at the time of peak flood (PF), high water (HW), peak ebb (PE) and low water (LW), for mean neap and spring tides in Figure B-4 and Figure B-5, respectively. The times of PF, HW, PE and LW vary across the model domain and the selected model timesteps are based on the timing of the tide within the OAA as follows:

- PF: the time at which eastward flows are at a maximum on the selected tide;
- HW: the time at which water level is at a maximum on the selected tide;
- PE: the time at which westward flows are at a maximum on the selected tide; and
- LW: the time at which water level is at a minimum on the selected tide.

Plots of the minimum and maximum water levels over the mean spring tide are also shown in Figure B-6 to demonstrate the tidal range in the region as the timing of the tide changes away from the OAA. The plots show the following:

- The similarities in water levels at the time of PF and HW and at the time of PE and LW indicate that the PF stage of the tide occurs close to HW while the PE stage of the tide occurs close to LW;
- Comparing the plots at HW and LW during a mean spring tide to the plots of the minimum and maximum water level over the spring tide shows that there is a phase difference between the timing of HW and LW to the west and east of the Orkney Islands. In addition, the tidal range is larger on the west side of the Orkney Islands (where the study area is located) compared to the east side, with the mean spring tidal range being approximately double;
- The largest tidal range (i.e. lowest low water and highest high water) occurs along the shoreline adjacent to the north coast of Scotland which includes part of the offshore ECC; and
- The tidal range reduces in a northerly direction across the study area, with a mean spring tidal range of 4 m at the offshore ECC adjacent to the shoreline reducing to 3.2 m at the northern end of the study area. The mean neap tidal range is predicted to be 2 m at the offshore ECC adjacent to the shoreline and 1.6 m at the northern end of the study area.

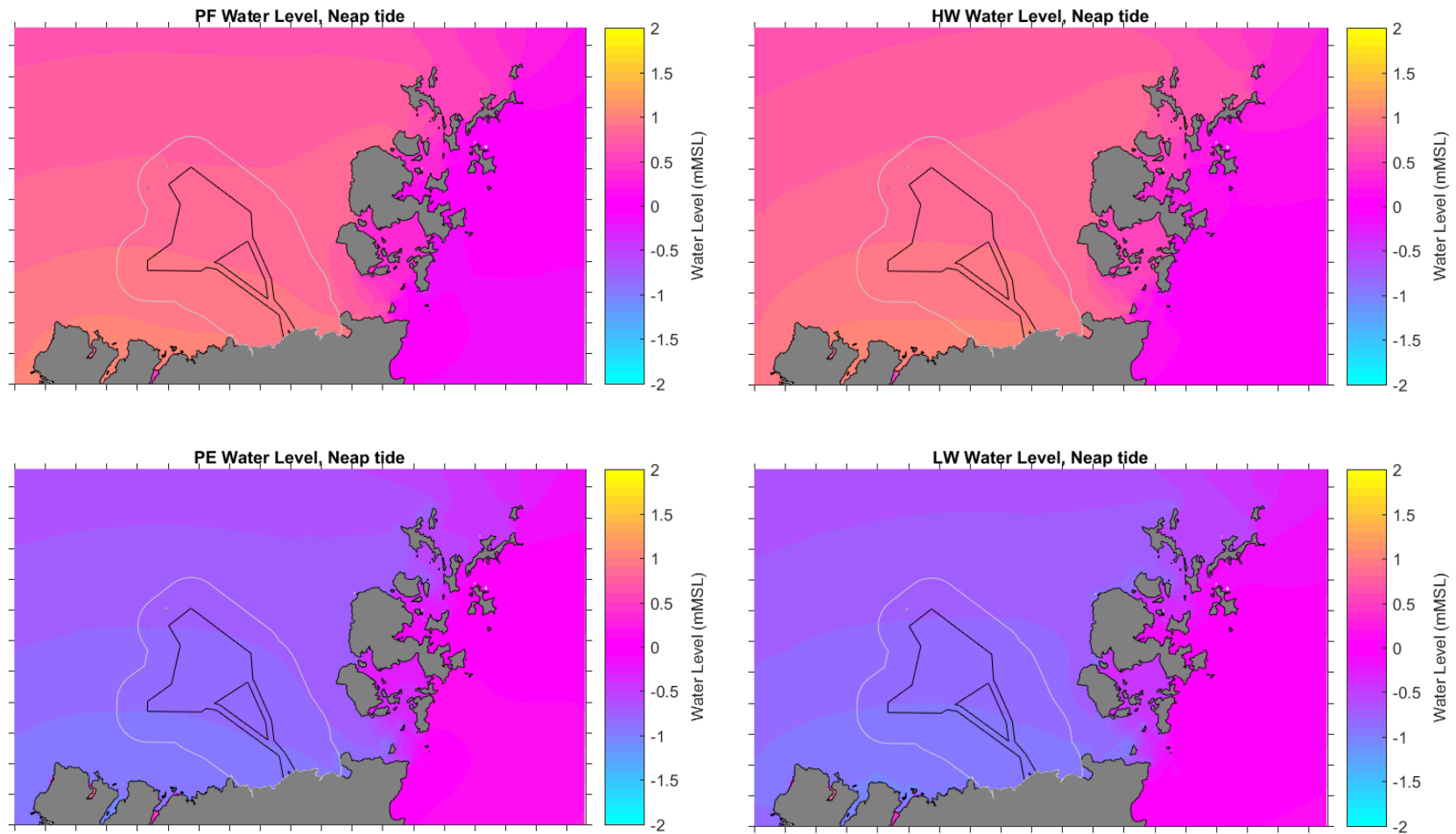


Figure B-4 Modelled water levels at varying tidal stages across the offshore Project area during a mean neap tide

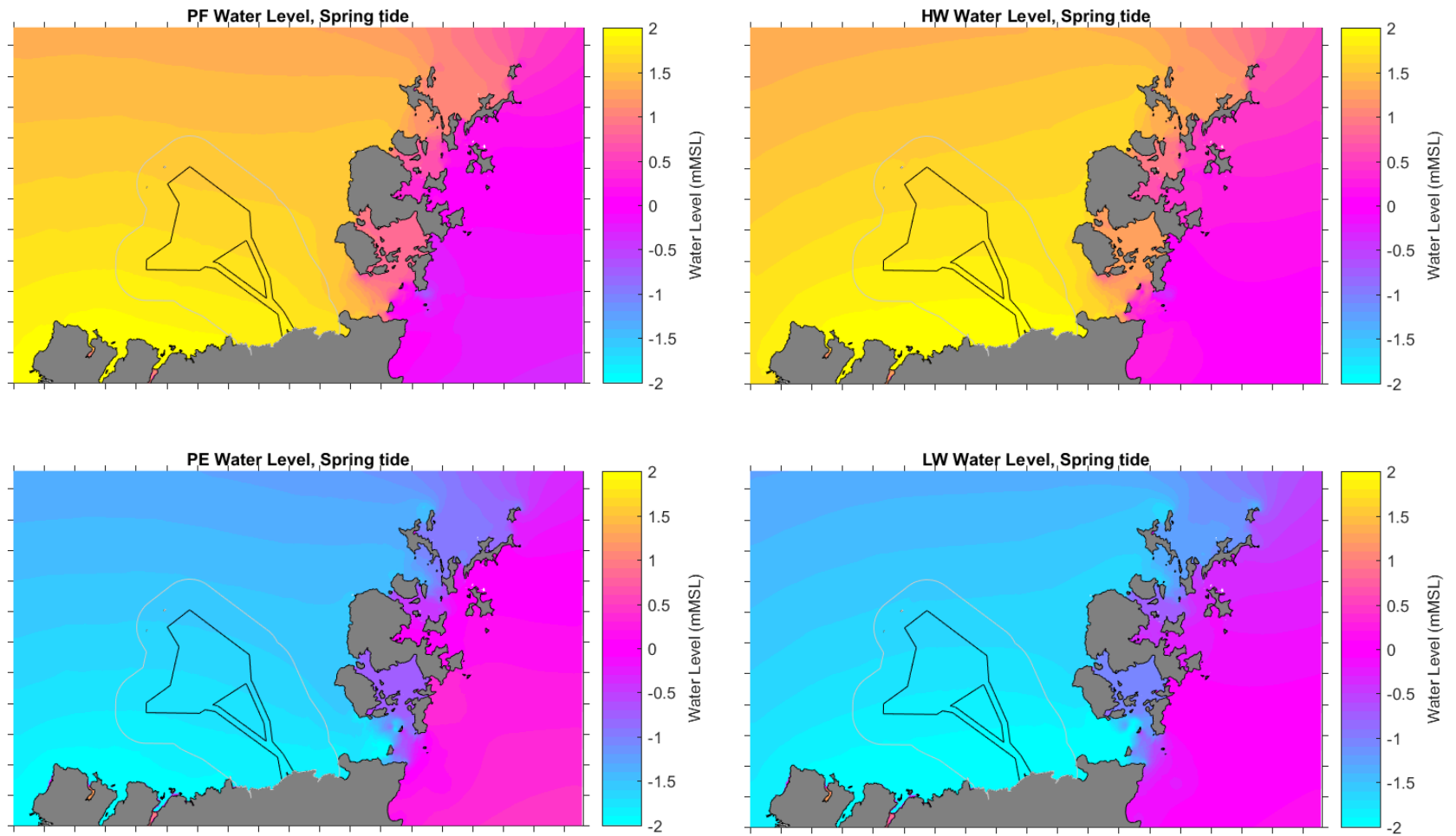


Figure B-5 Modelled water levels at varying tidal stages across the offshore Project area during a mean spring tide

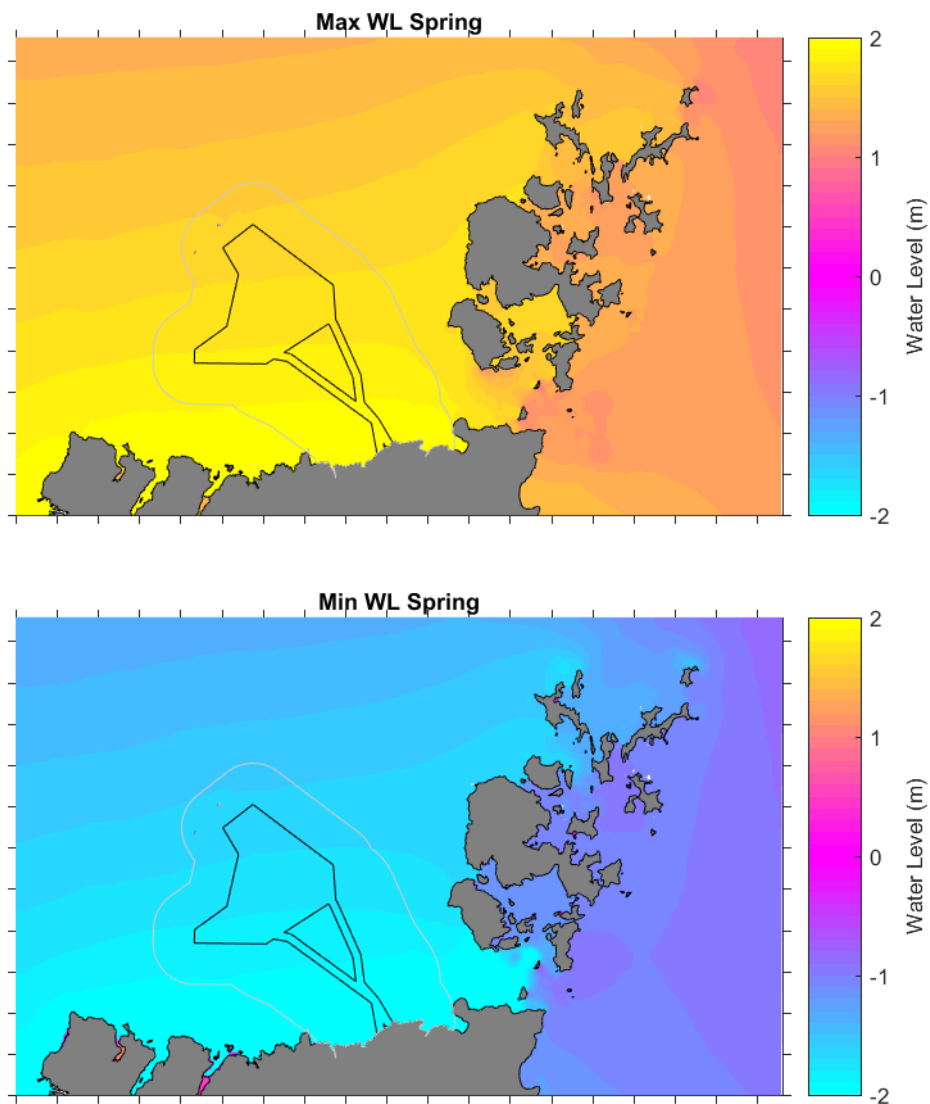


Figure B-6 Modelled maximum and minimum water levels during a mean spring tide

Map plots of the current speed across the offshore Project area, study area and the surrounding region are shown at the time of PF and PE during mean neap and spring tides are shown in Figure B-7. More detailed flow plots of mean spring PE and PF conditions are shown for just the study area in Figure B-8. Due to the significantly lower flows in the study area compared to those from the wider model domain, the flows in Figure B-8 are plotted to a different colour scale to those in Figure B-7. Plots of the current speed at HW and LW are not shown as the water level plots indicated that the timing of these is close to PF and PE and so the currents will be similar (albeit slightly lower) to those at PF and PE. Plots of the residual tidal flows across the study area are shown for mean neap and spring tides in Figure B-9 and over a 14.5 day spring neap tidal cycle in Figure B-10. The plots show the following:

- The highest current speeds in the region occur in the Pentland Firth, with speeds of more than 3 m/s occurring during spring tides and between 2 and 2.5 m/s during neap tides. High current speeds of more than 2 m/s also



occur around and between some of the Orkney Islands, while current speeds to the west and east of the Orkney Islands are lower and typically remain below 1 m/s;

- Within the study area the flood currents are to the east and the ebb currents are to the west;
- Current speeds within the offshore Project area offshore ECC are less than 0.8 m/s during both spring and neap tides. The highest currents (0.7 to 0.8 m/s) occur in the offshore ECC within 12 km of the shoreline;
- Higher current speeds occur in the areas adjacent to the OAA and offshore ECC. The highest current speeds close to the study area are more than 1 m/s to the east of the offshore ECC (associated with flows through the Pentland Firth); and
- The residual currents are generally low during both mean spring and neap tides and over a 14.5 day spring neap tidal cycle. The residual currents are below 0.05 m/s throughout the OAA, while areas of the offshore ECC have residual currents of up to 0.1 m/s in a north-easterly direction during neap tides. The area of the offshore ECC adjacent to the shoreline has a residual current of around 0.2 m/s in an easterly direction during spring tides.

To inform further assessments completed as part of the marine physical and coastal processes technical study, time series results have been extracted from the HD model to show how the water level, current speed and current direction vary over the spring neap tidal cycle at different locations within the OAA and offshore ECC. Results have been plotted at 28 model extraction locations throughout the OAA and offshore ECC areas as introduced in section 2.1.6 and illustrated in Figure 2-4. To illustrate the hydrodynamic conditions across the offshore Project area, plots from four locations which range between 56 km offshore (OAA1) to 3 km from the shore (ECC4) are shown in Figure B-11 and Figure B-12. The plots show the following:

- The magnitudes and temporal variability in water levels and flows is similar at all of the sites;
- The current speeds are higher during spring tides and lower during neap tides. Current speeds at the three furthest offshore sites were similar (peaks in speed ranging from 0.2 to 0.6 m/s), with the lowest speeds at OAA3, which was located approximately 35 km from the shoreline. Higher current speeds occurred at the site closest to the shoreline (ECC4, located 3 km from the shoreline), with the peaks in speed ranging from 0.3 to 0.7 m/s;
- Current directions at the time of peak speeds were comparable at the three furthest offshore sites, with peak flood currents to the east and peak ebb currents to the west. At the site closest to the shoreline the directions were rotated by around 20° due to the orientation of the coastline, so peak flood currents were to the east north-east and peak ebb currents were to the west south-west; and
- There is a gradual increase in the tidal range in a landward direction, with the furthest offshore site having a tidal range during the largest spring tide of 3.3 m, while the closest site to the shoreline had a tidal range of 4 m during the same spring tide.

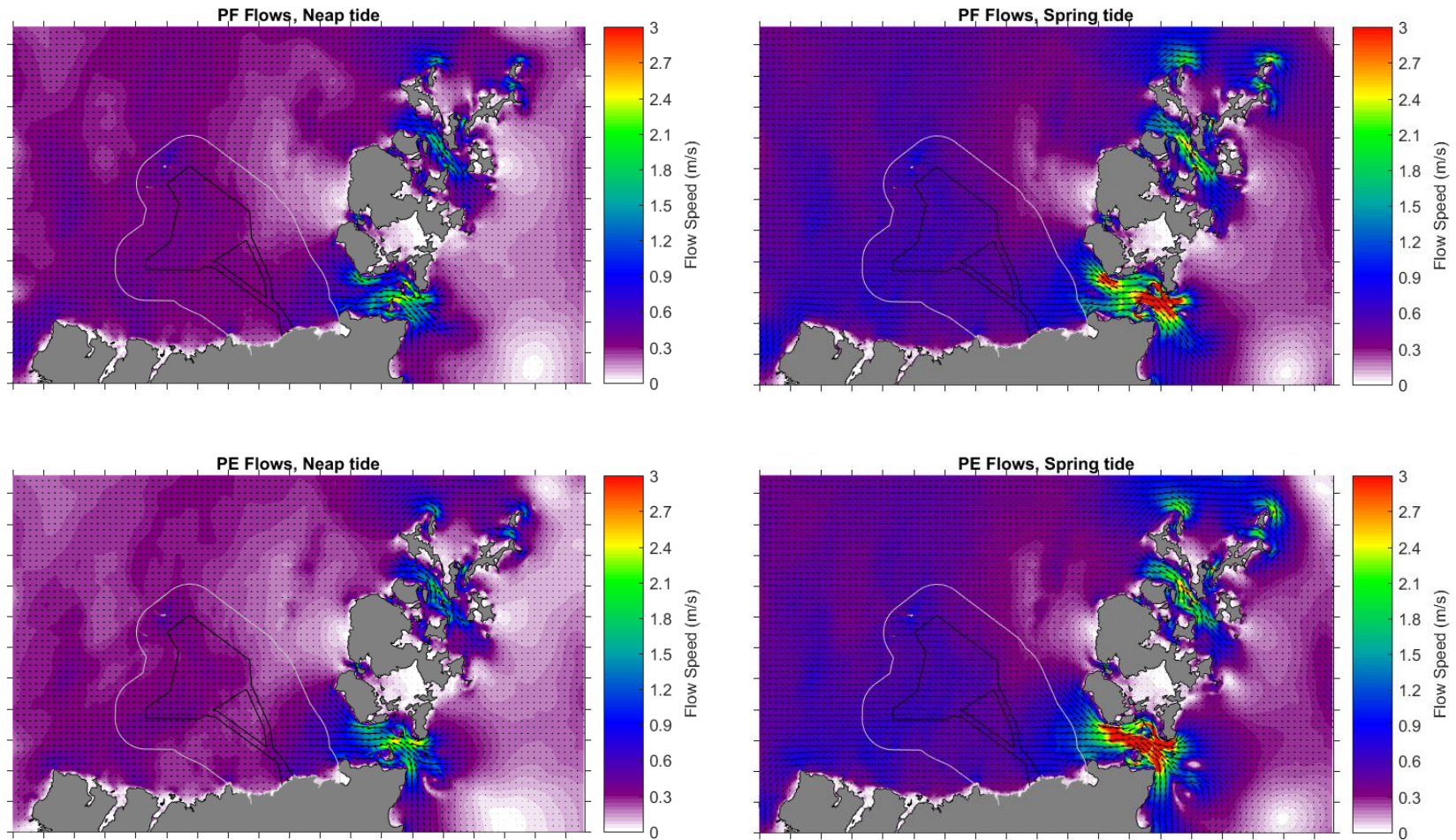


Figure B-7 Modelled peak flood (PF) and peak ebb (PE) tidal flows during mean neap (left) and spring tides (right)

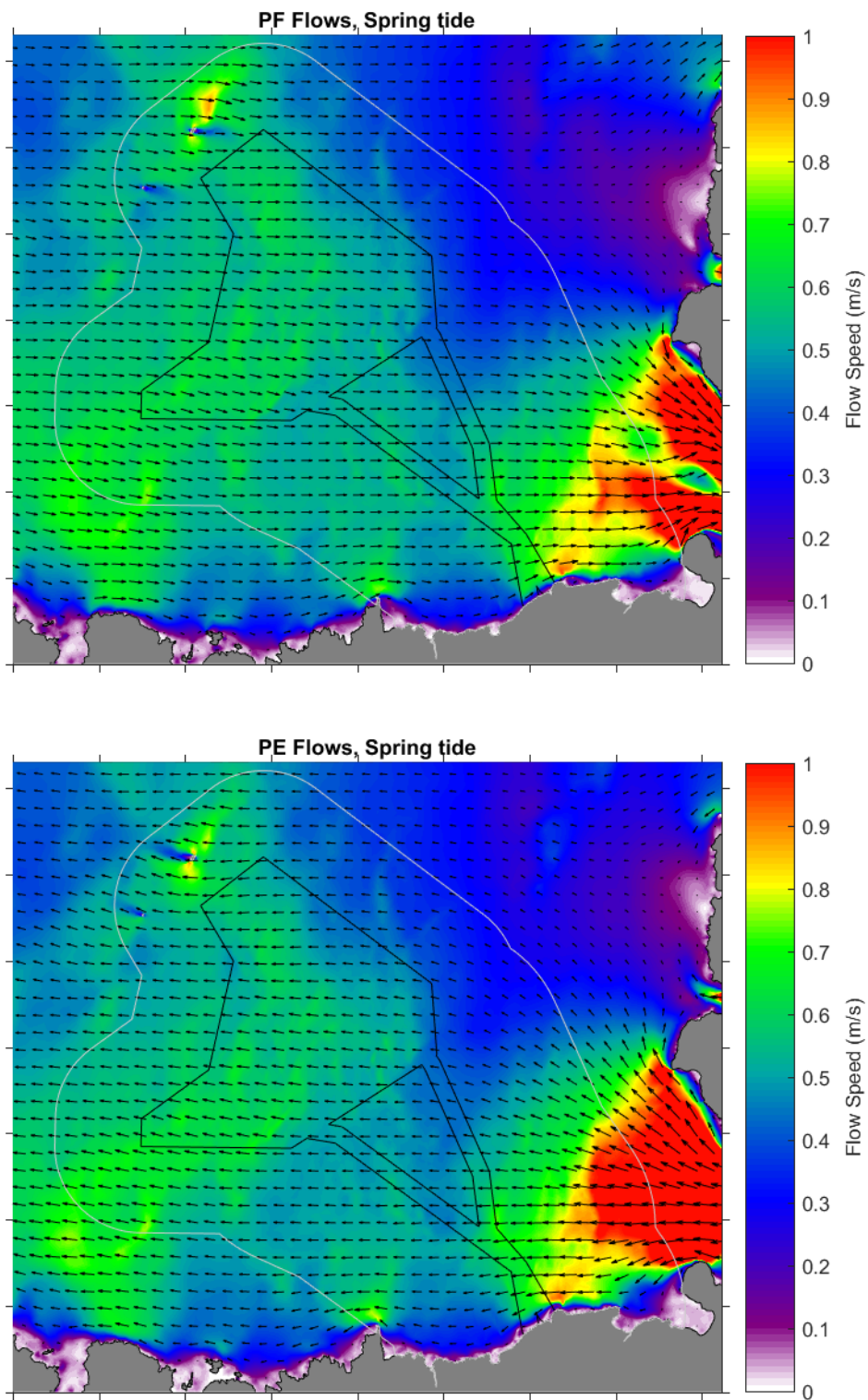


Figure B-8 Zoomed in plot of the study area showing the modelled peak flood (PF) and peak ebb (PE) tidal flows during a mean spring tide

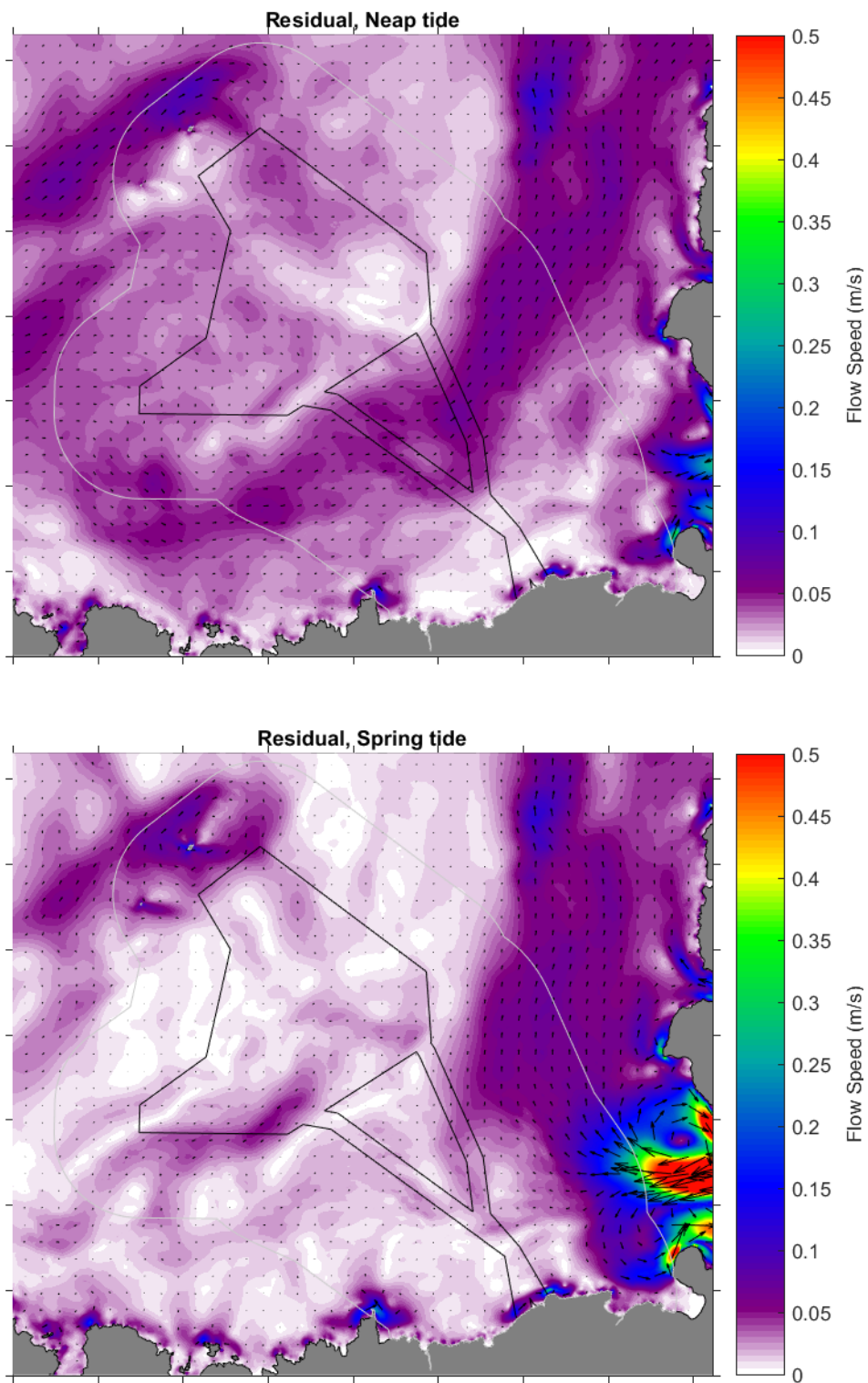


Figure B-9 Zoomed in plot of the study area showing the residual tidal flow during mean neap and spring tides

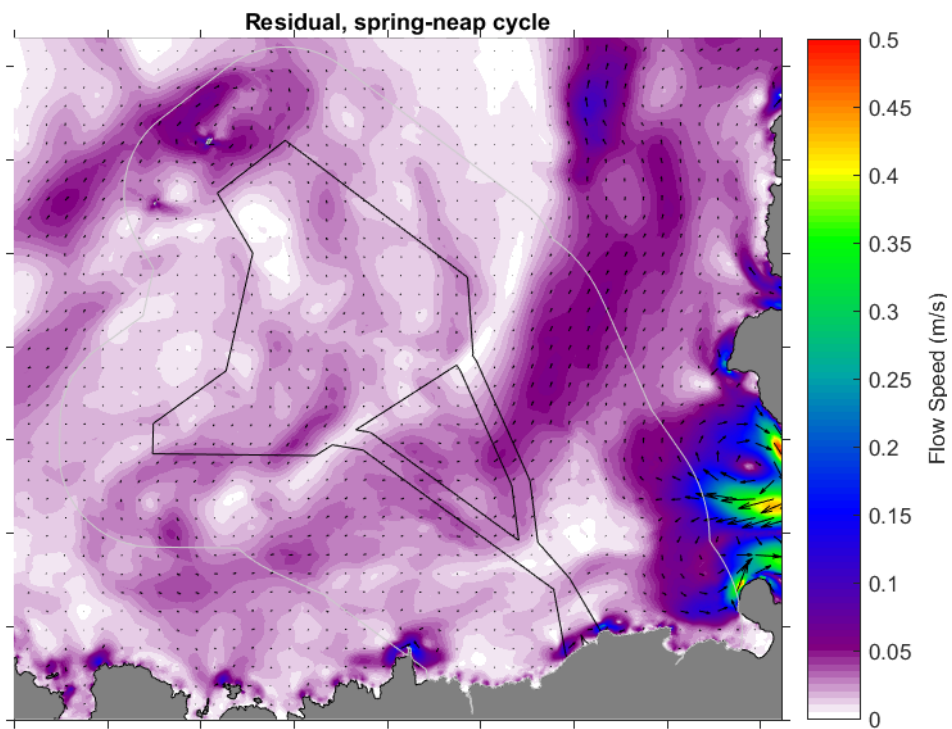


Figure B-10 Zoomed in plot of the study area showing the residual tidal flow over a 15 day spring neap tidal cycle.

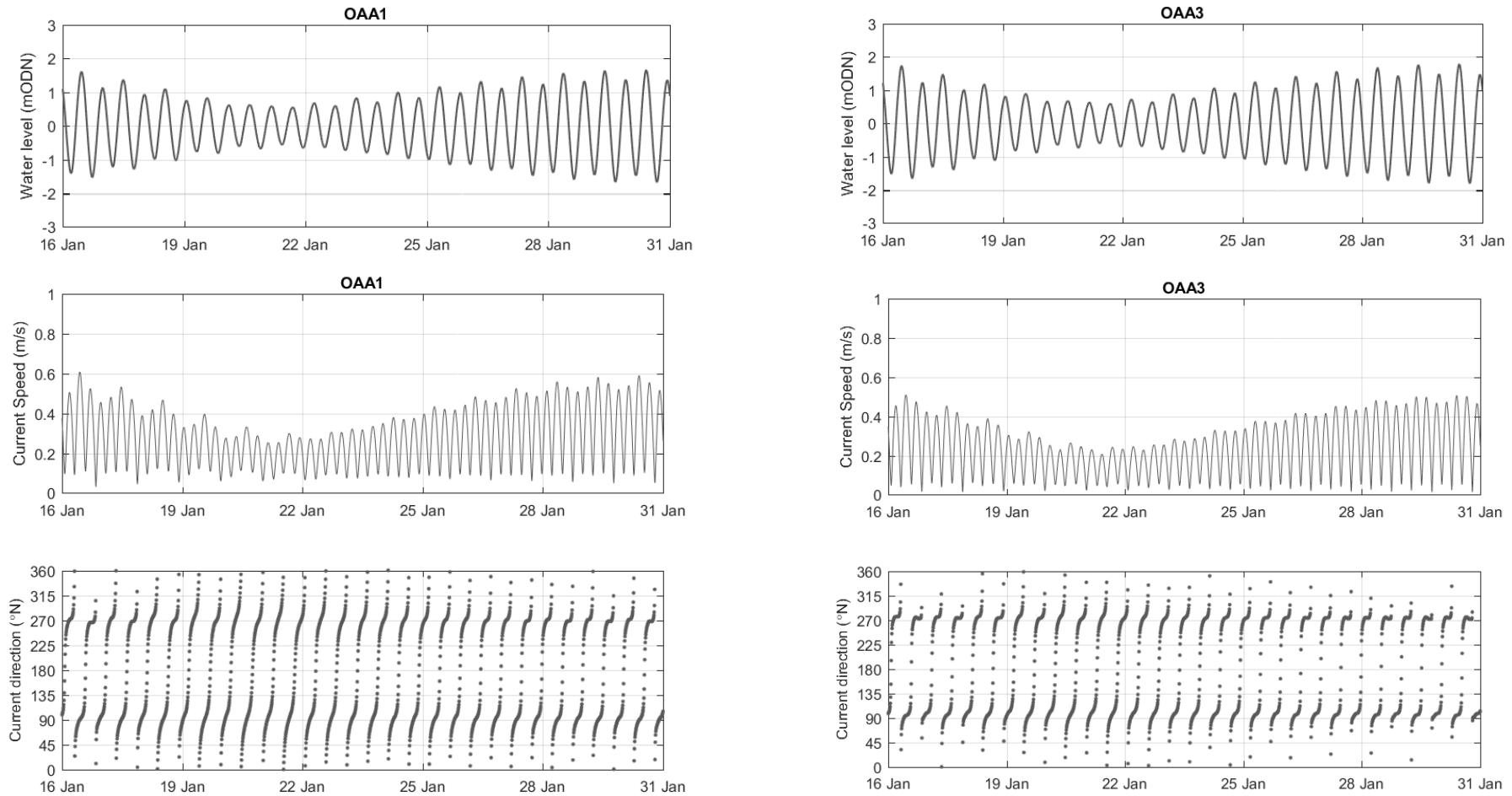


Figure B-11 Time series plot showing the water level, current speed and current direction at model extraction point OAA1 (left hand panels) and OAA3 (right hand panels) over the 16 day model simulation period. Model extraction locations are illustrated in Figure 2-4

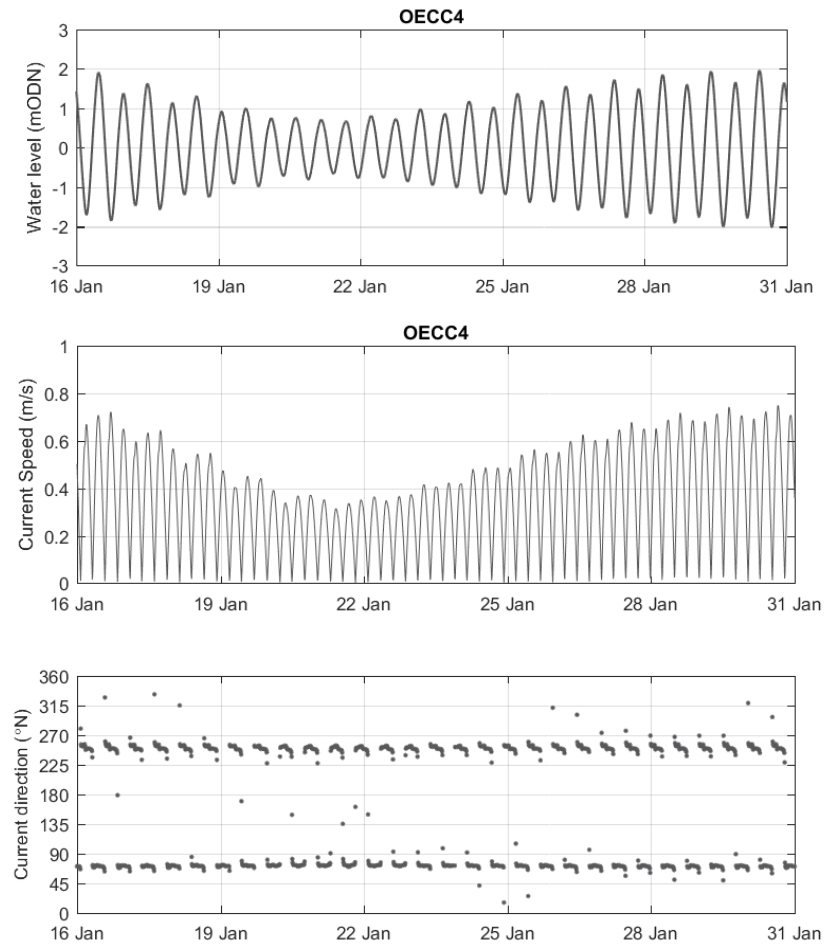
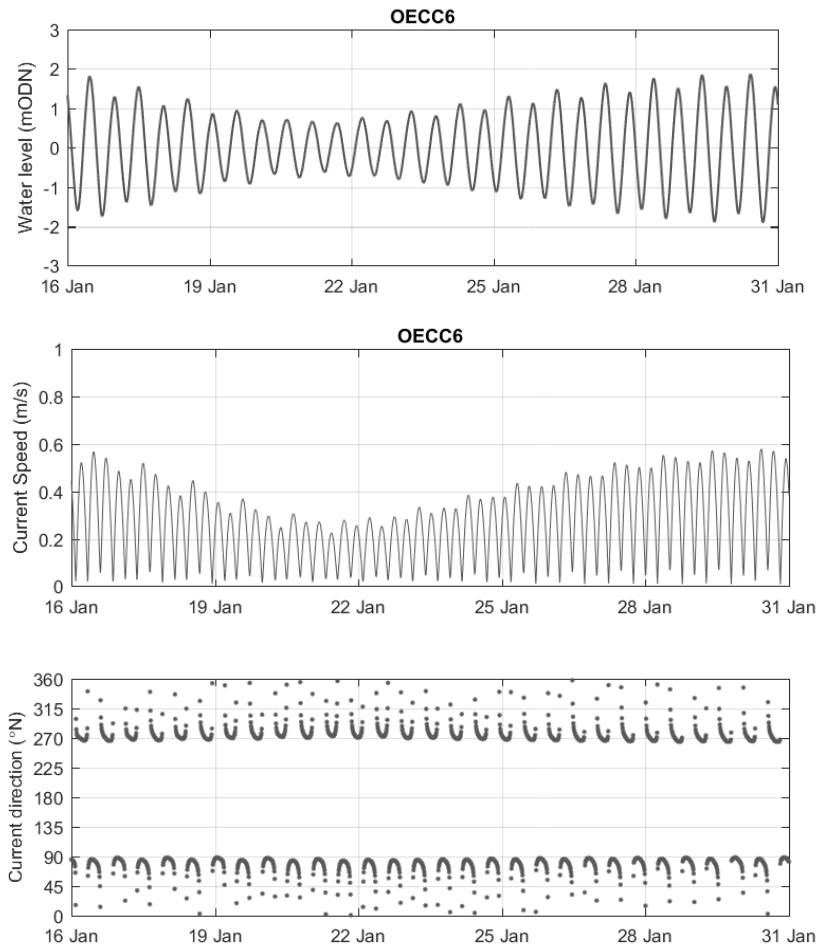


Figure B-12 Time series plot showing the water level, current speed and current direction at model extraction locations ECC6 (left hand panels) and ECC4 (right hand panels) over the 16 day model simulation period. Model extraction locations are illustrated in Figure 2-4



## B.3.2 Wave Conditions

The SW model was setup to simulate the waves during conditions which occur relatively frequently (50<sup>th</sup> and 90<sup>th</sup> percentile waves) and during extreme wave events (from 1 in 1 year annual recurrence interval (ARI) to a 1 in 100 year ARI). The dominant approach directions were informed by site-specific hindcast data and baseline characterisation presented in the marine physical and coastal processes technical study. These wave conditions were simulated from the west, north-west and north as these directions cover the range of possible approach directions of the most frequent and largest waves. Map results showing the significant wave height ( $H_s$ ) and wave direction are shown for all wave conditions in Appendix B.9.1, while selected results are presented here. The 90<sup>th</sup> percentile, 1 in 1 year ARI and 1 in 100 year ARI map results are shown for all three wave directions in Figure B-13. The plots show the following:

- There is a significant reduction in wave heights in the lee of the Orkney Islands due to the sheltering they provide;
- The 90<sup>th</sup> percentile  $H_s$  is relatively uniform through the study area, while there is more variability in wave height through the study area for the 1 in 1 and 1 in 100 year ARIs. For these more extreme wave events there is a reduction in the wave height closer to the shore. This is most defined when the waves are from the west as Cape Wrath provides some additional shelter along the northern coastline of Scotland; and
- The largest waves are from a westerly direction and the smallest waves are from a northerly direction.

As informed by the baseline characterisation, the dominant wave approach is from the west. Therefore, to better understand how the wave conditions within the study area vary, zoomed in plots of all the modelled wave events from a westerly direction are shown in Figure B-14 (plots of the other directions are included in Appendix B.9.1). In addition, wave conditions have been extracted from the wave model at the 28 model extraction locations around the OAA and offshore ECC (Figure 2-4) for all the modelled wave conditions. Results presented in Table B-6 and Table B-7 show the wave conditions at two output locations within the OAA and two within the offshore ECC. The output locations presented vary from 56 km offshore (i.e. towards the northern edge of the OAA) to 3 km offshore (i.e. close to where the offshore ECC reaches the coastline) and therefore they can be interpreted to show how the wave conditions vary through the study area. The results show the following:

- The wave height and wave direction are typically similar throughout the OAA, with some localised areas of slightly larger wave height predicted due to variations in the bathymetry;
- Within the offshore ECC there is a reduction in wave height from north to south, with the lowest wave heights adjacent to the northern coastline of Scotland. In addition, the wave direction gradually varies along the offshore ECC due to refraction, with the direction changing from westerly at the northern end of the corridor to north-westerly adjacent to the coastline;
- The tabulated wave conditions show that for a 1 in 100 year ARI wave event from the west the  $H_s$  would be around 14.5 m throughout the OAA, while it would reduce to 11.8 m mid way along the offshore ECC (16 km from the coastline) and down to 9.5 m at a distance of 3 km from the coastline. In addition, wave direction would change from 279° at the southern end of the OAA (35 km from the coastline) to 311° at a distance of 3 km from the coastline; and



- Peak wave periods within the OAA are typically around 10 seconds for waves from the north, with slightly longer period waves (around 12 seconds) for waves from the west. Storm waves have longer peak periods being 16-17 seconds for 1 in 100 year ARI wave events. Variations in peak period are relatively small across the OAA and offshore ECC, slightly reducing inshore for shorter period waves and slightly increasing inshore for longer period waves.

Table B-6 Wave model results at model extraction points OAA1 and OAA3 as per locations illustrated in Figure 2-4

WAVE CONDITION	OAA1 (56KM OFFSHORE)			OAA3 (35KM OFFSHORE)		
	H <sub>s</sub> (m)	T <sub>p</sub> (s)	Dir (°)	H <sub>s</sub> (m)	T <sub>p</sub> (s)	Dir (°)
North 50 <sup>th</sup> percentile	2.1	10.5	359	2.1	10.4	359
North 90 <sup>th</sup> percentile	3.8	12.1	359	4.0	12.2	0
North 1 in 1-yr ARI	8.1	14.8	359	8.2	14.9	0
North 1 in 5-yr ARI	9.5	15.4	359	9.5	15.5	0
North 1 in 10-yr ARI	10.0	15.7	359	9.9	15.8	0
North 1 in 50-yr ARI	10.8	16.0	359	10.7	16.1	0
North 1 in 100-yr ARI	11.1	16.2	359	10.9	16.3	0
North-west 50 <sup>th</sup> percentile	2.1	10.6	315	2.2	10.5	316
North-west 90 <sup>th</sup> percentile	4.2	12.5	314	4.4	12.6	316
North-west 1 in 1-yr ARI	9.4	15.2	315	9.3	15.3	317
North-west 1 in 5-yr ARI	11.0	15.9	315	10.9	15.9	317
North-west 1 in 10-yr ARI	11.6	16.2	316	11.5	16.2	318
North-west 1 in 50-yr ARI	12.5	16.5	316	12.4	16.5	318
North-west 1 in 100-yr ARI	12.8	16.7	316	12.7	16.7	318
West 50 <sup>th</sup> percentile	2.6	11.0	271	2.7	10.9	274
West 90 <sup>th</sup> percentile	5.2	13.1	272	5.4	13.1	275
West 1 in 1-yr ARI	10.9	16.0	275	10.9	16.0	280
West 1 in 5-yr ARI	12.5	16.4	272	12.6	16.5	278



WAVE CONDITION	OAA1 (56KM OFFSHORE)			OAA3 (35KM OFFSHORE)		
	H <sub>s</sub> (m)	T <sub>p</sub> (s)	Dir (°)	H <sub>s</sub> (m)	T <sub>p</sub> (s)	Dir (°)
West 1 in 10-yr ARI	13.1	16.7	272	13.2	16.8	278
West 1 in 50-yr ARI	14.1	17.1	272	14.2	17.1	278
West 1 in 100-yr ARI	14.4	17.3	272	14.5	17.3	279

Table B-7 Wave model results at model extraction points ECC6 and ECC4, as per locations illustrated in Figure 2-4

WAVE CONDITION	ECC6 (16KM OFFSHORE)			ECC4 (3KM OFFSHORE)		
	H <sub>s</sub> (m)	T <sub>p</sub> (s)	Dir (°)	H <sub>s</sub> (m)	T <sub>p</sub> (s)	Dir (°)
North 50 <sup>th</sup> percentile	2.1	10.4	357	1.9	10.2	354
North 90 <sup>th</sup> percentile	4.1	12.2	355	3.6	12.2	351
North 1 in 1-yr ARI	7.9	15.0	350	6.7	14.9	346
North 1 in 5-yr ARI	9.0	15.6	348	7.7	15.6	345
North 1 in 10-yr ARI	9.3	15.9	348	8.0	15.8	344
North 1 in 50-yr ARI	9.9	16.2	347	8.5	16.1	344
North 1 in 100-yr ARI	10.1	16.4	347	8.6	16.3	344
North-west 50 <sup>th</sup> percentile	2.2	10.6	316	2.2	10.6	316
North-west 90 <sup>th</sup> percentile	4.4	12.6	314	4.3	12.7	317
North-west 1 in 1-yr ARI	9.2	15.4	314	8.4	15.4	322
North-west 1 in 5-yr ARI	10.8	16.0	315	9.7	16.1	323
North-west 1 in 10-yr ARI	11.3	16.3	315	10.2	16.4	323
North-west 1 in 50-yr ARI	12.2	16.6	315	10.9	16.6	324
North-west 1 in 100-yr ARI	12.4	16.8	315	11.1	16.8	324
West 50 <sup>th</sup> percentile	2.5	10.7	280	1.8	10.5	291



WAVE CONDITION	ECC6 (16KM OFFSHORE)			ECC4 (3KM OFFSHORE)		
	H <sub>s</sub> (m)	T <sub>p</sub> (s)	Dir (°)	H <sub>s</sub> (m)	T <sub>p</sub> (s)	Dir (°)
West 90 <sup>th</sup> percentile	4.8	12.9	284	3.6	12.6	299
West 1 in 1-yr ARI	9.1	16.2	293	7.3	16.2	311
West 1 in 5-yr ARI	10.3	16.5	290	8.2	16.4	310
West 1 in 10-yr ARI	10.8	16.8	291	8.6	16.8	310
West 1 in 50-yr ARI	11.5	17.1	291	9.2	17.1	311
West 1 in 100-yr ARI	11.8	17.4	291	9.5	17.3	311

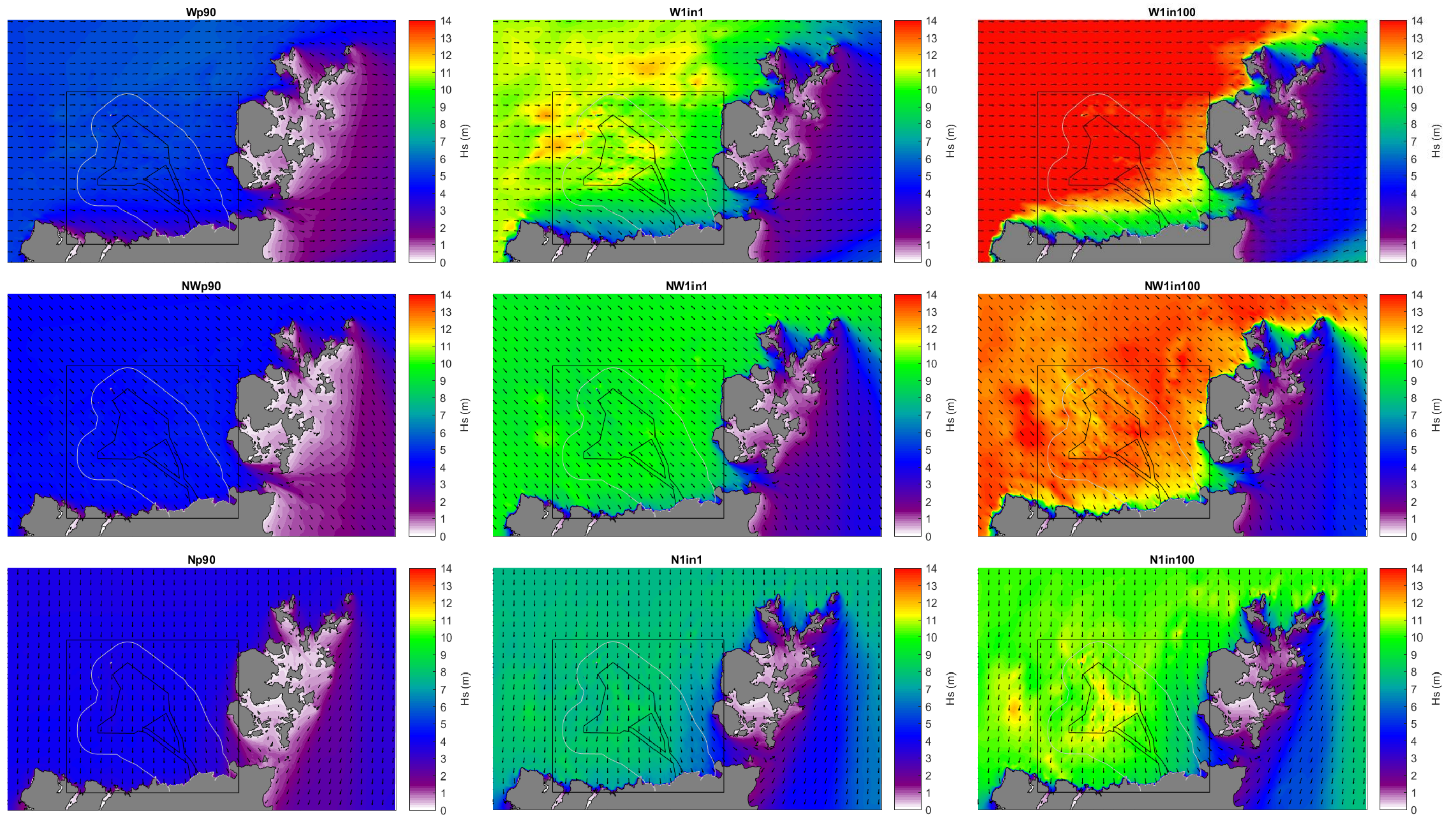


Figure B-13 Modelled wave height and wave direction for the 90<sup>th</sup> percentile wave condition (left hand panels), the 1 in 1 year ARI (middle panels) and the 1 in 100 year ARI (lower panels) for waves from the west (top panels), north-west (middle panels) and north (bottom panels)

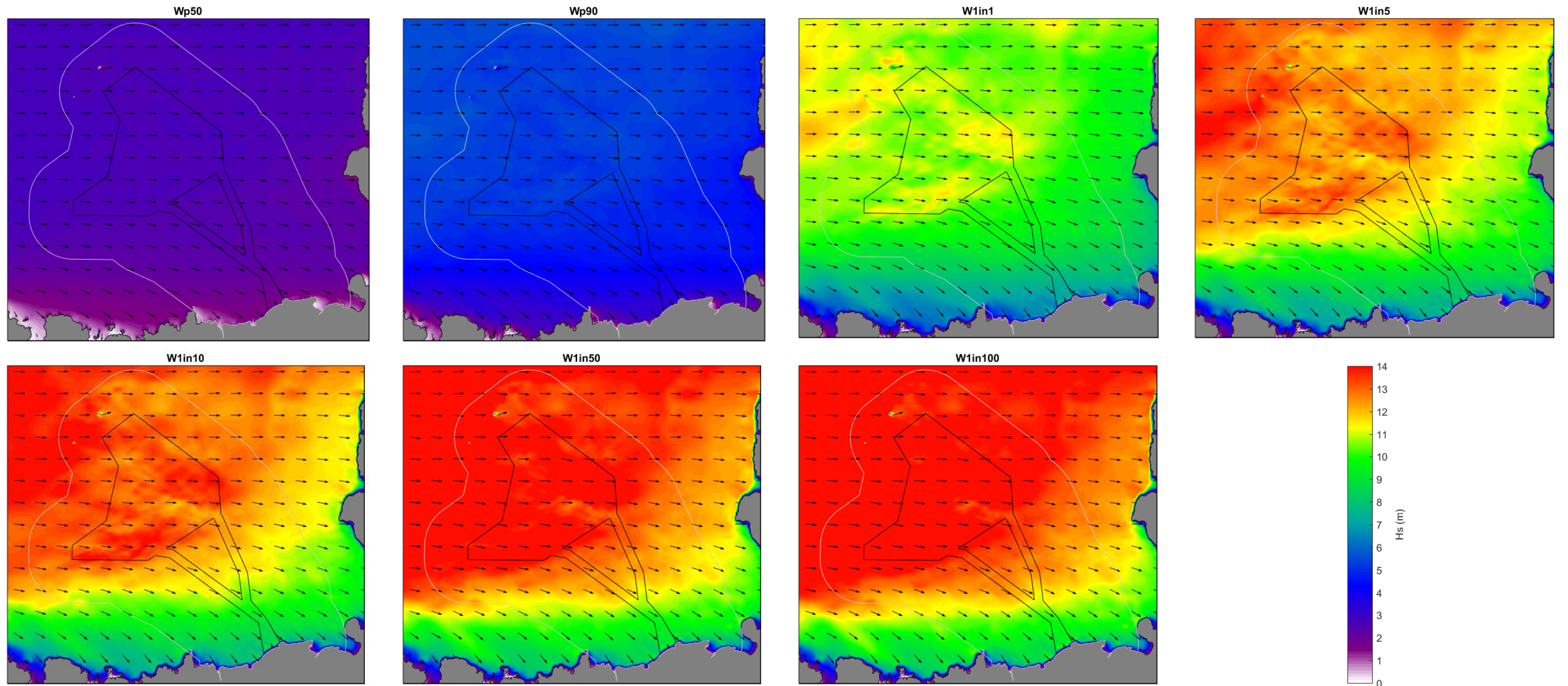


Figure B-14 Zoomed in plot of the study area showing the modelled wave height and direction for waves from the west for (upper panels left to right) the 50<sup>th</sup> percentile, 90<sup>th</sup> percentile, 1 in 1 year ARI, 1 in 5 year ARI, (lower panels left to right), 1 in 10 year ARI, 1 in 50 year ARI and 1 in 100 year ARI



## B.4 Construction Impacts

This section provides details of the potential construction impacts resulting from the installation of the infrastructure associated with the proposed development. As detailed in Section B.2.1, the construction process will involve the seabed preparation, cable burial and monopile drilling which will all disturb the seabed and have the potential to release suspended sediment into the water column. The MIKE 21 PT model was setup to represent a realistic representation of the sediment disturbance as a result of these activities over a 15.5-day spring/neap tidal cycle to capture the full range of potential impacts. Based on the dominant westerly wave approach direction, the model included the 50<sup>th</sup> percentile wave conditions from the west throughout the simulation to provide a representation of typical wave conditions and the potential influence of this on the sediment dispersion associated with construction activities. As many of the construction works will occur for a much longer duration than 15.5 days, the model results only provide a snapshot of the likely impacts for one location, but similar impacts will occur elsewhere within the OAA and offshore ECC. Results showing the predicted impacts to SSC and sedimentation from the PT model simulations are presented in the following sections.

The results for the seabed preparation, cable burial and pile drilling are presented in different sections for clarity. The results from each of the PT model simulations are presented in the form of:

- Spatial maps of statistical representations of the predicted increase in SSC due to the sediment released / disturbed / discharged by the construction activities, including the maximum SSC in each model grid cell and percentile plots of the SSC calculated for the period over which construction activities were simulated;
- Spatial maps of the sedimentation depth at the end of the model simulation due to the sediment released / disturbed / discharged by the construction activities; and
- Time series plots of the predicted SSC and sedimentation depth due to the sediment released / disturbed / discharged by the construction activities.

The plots shown vary depending on the results from the model simulation, with the plots aimed at providing an understanding of the key results from each simulation/construction activity.

It is important to note that the spatial maps of the maximum SSC and percentiles do not show an actual representation of the SSC at any point in time, rather they are duration-based plots which show statistical summaries of the SSC over the entire model simulation. The maximum SSC demonstrates the maximum concentrations that can be expected to occur at the given grid cell across the simulation period. The percentile plots show the value which the SSC is below for a given percentage of time over the period which construction activities were simulated for. For example, the 99<sup>th</sup> percentile plot shows the value that the SSC is below for 99% of the time over the 15.5 day period (i.e. this SSC is only exceeded for 1% of the time (3.72 hours)). Due to the shorter duration of bedform clearance by TSHD, the percentile plots for dredging are calculated only for the period of the dredge (13.3 days of dredging in the OAA and 6.5 days of dredging in the offshore ECC so that the 1% exceedance is 3.2 and 1.6 hours, respectively).



## B.4.1 Seabed Preparation

Results for the seabed preparation are provided in the following section for the impacts resulting from bedform clearance using a TSHD and a CFE.

### B.4.1.1 TSHD Bedform Clearance

There is no area with an SSC increase of above 1 mg/l visible on the 95<sup>th</sup> and lower percentile plots for either the dredging in the OAA or the offshore ECC. The 99<sup>th</sup> percentile and maximum SSC over the period when dredging was being undertaken (13.3 days for the OAA and 6.5 days for the offshore ECC) are shown for the seabed preparation using a TSHD in the OAA in Figure B-15 and in the offshore ECC in Figure B-16. Comparing the extent and magnitude of the SSC shown by the 99<sup>th</sup> percentile and maximum plots shows whether the SSC is often elevated close to the maximum values (the two plots will be similar) or if the SSC only remains elevated for a very short duration of time (less than 1% of the time, the maximum SSC will show a much larger extent and higher SSC than the 99<sup>th</sup> percentile). In addition, plots showing the sedimentation at the end of the model simulation are shown for both the OAA and offshore ECC in Figure B-17. The plots show the following:

- The SSC remained below 1 mg/l throughout the majority of the study area for the majority of the time (>99%) for dredging of both the OAA and offshore ECC;
- For the dredging of both the OAA and the offshore ECC the only location where the 99<sup>th</sup> percentile was above 1 mg/l was the placement site within the indicative DMPA, which is located in the south-eastern part of the OAA. This shows that the SSC was more regularly elevated in this area due to ongoing placement over the duration of the simulation. Within the placement site a 99<sup>th</sup> percentile increase in SSC of up to 4 mg/l occurred;
- The maximum SSC plots show that increases in SSC due to the bedform removal within the OAA were very localised to where the dredging activity was occurring and the SSC remained low (< 4 mg/l). The smallest plumes occur in the southern part of the OAA, this reflects the difference in tidal conditions during the time the dredger was operating in this region (small neap tides when slow flows reduced plume dispersion). While similar tidal conditions also occurred during dredging of the northern section of the OAA, the assumed dredger track was such that plumes from subsequent tracks resulted in some additive plume effects due to the short east-west extent in this region;
- Comparison between the maximum SSC for dredging in the OAA and offshore ECC regions shows that the offshore ECC is predicted to result in a higher increase in SSC. There was more fine-grained sediment present in this area resulting in higher sediment release rates and the sediment remaining in suspension longer;
- The maximum SSC plots of the dredging in the offshore ECC shows an SSC of up to 4 mg/l throughout the majority of the cable corridor except for the landward 6 km where the maximum SSC increases are more than 20 mg/l. The higher SSC in this area of the offshore ECC is due to the shallower water depths compared to the remainder of the offshore ECC (depths of -65 to -2 m CD compared to depths of -80 to -115 m CD in the remainder of the offshore ECC) combined with the model mesh being higher resolution in the area (100 m, compared to 500 m), meaning that the initial dilution of the suspended sediment is less compared to the remainder of the cable corridor;



- The placement of the dredged sediment from both the OAA and the offshore ECC is predicted to result in localised plumes where the sediment is placed with a maximum SSC of more than 20 mg/l. The SSC quickly reduces away from where the sediment was placed, with the majority of the placement area experiencing increases in SSC of less than 6 mg/l. The increased SSC resulting from the placement of sediment is predicted to be higher for sediment from the offshore ECC compared to the OAA due to the higher percentage of fine-grained silt and clay present; and
- Sedimentation resulting from the sediment suspended by the dredging and placement activities (i.e., not including the sediment which settles straight to the bed following placement) is predicted to be below 0.1 mm throughout the majority of the OAA and offshore ECC. The only location where it is predicted to be above 0.1 mm for the dredging of the OAA is within the placement area. For the dredging of the offshore ECC sedimentation of above 0.1 mm is also predicted in the placement area. In addition, sedimentation of more than 0.1 mm is also predicted in small patches along the landward 6 km of the cable corridor.

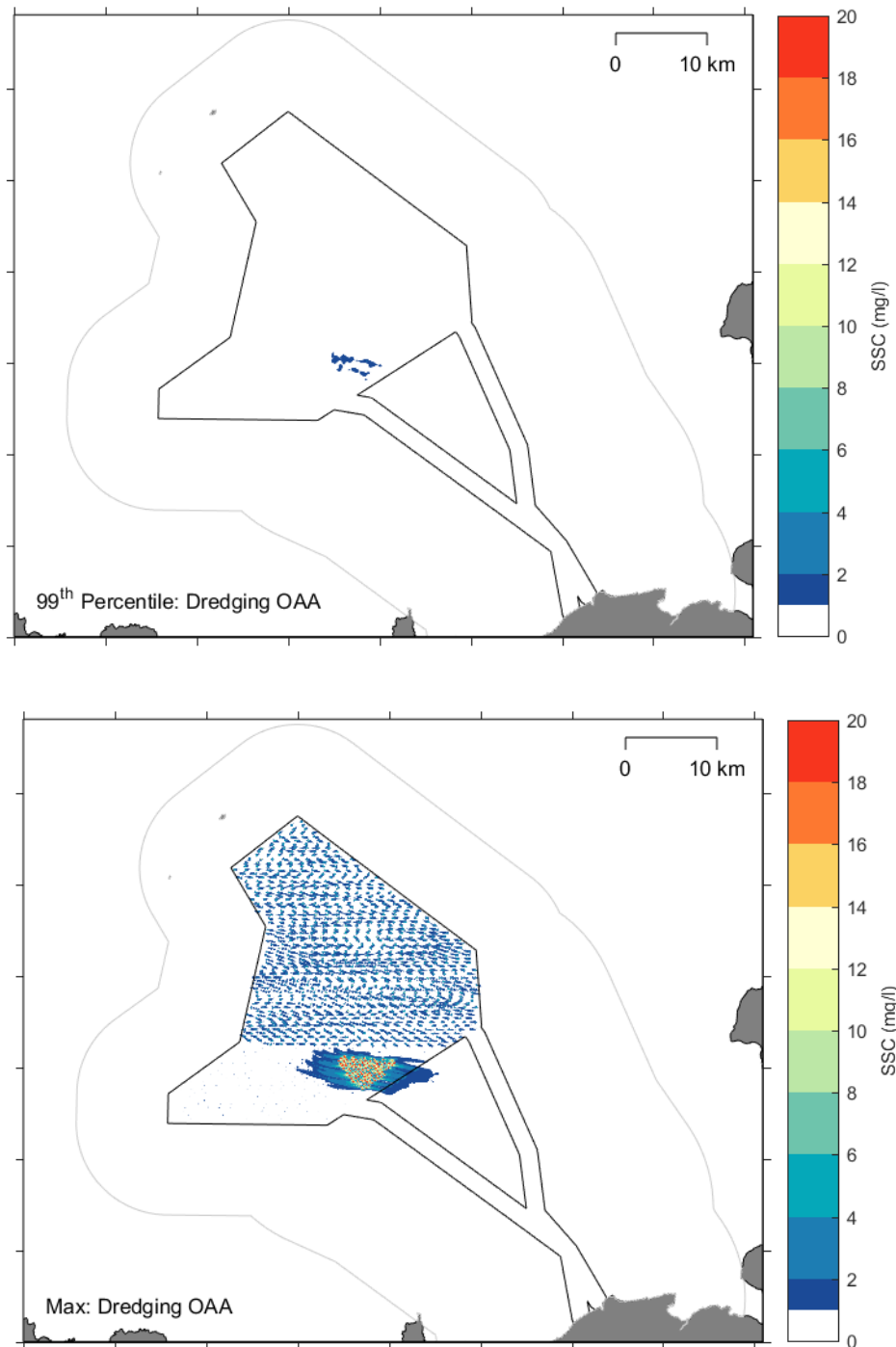


Figure B-15 Modelled 99<sup>th</sup> percentile (top) and maximum (bottom) SSC from the PT model simulation for seabed preparation in the OAA using a TSHD

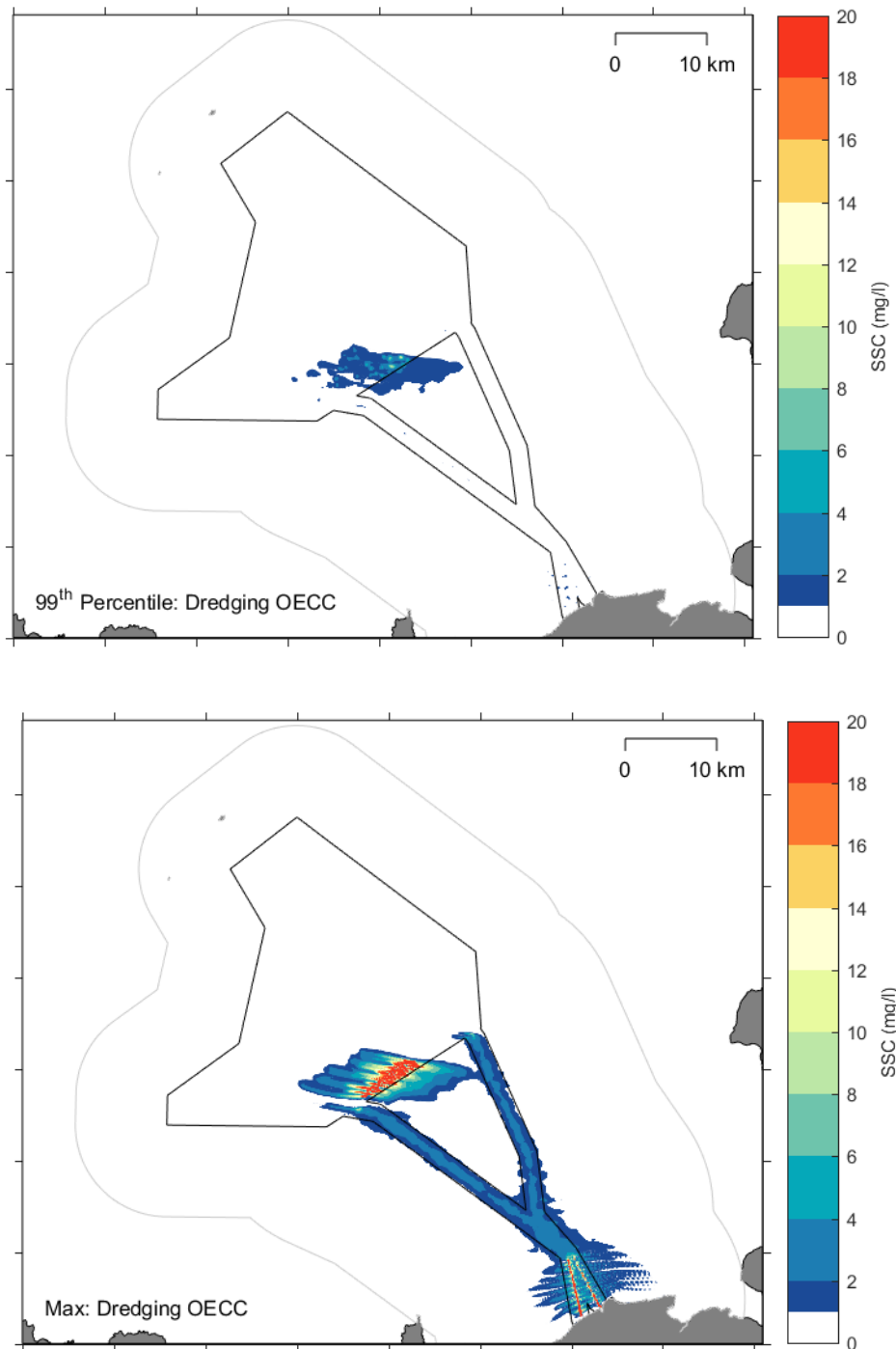


Figure B-16 Modelled 99<sup>th</sup> percentile (top) and maximum (bottom) SSC from the PT model simulation for seabed preparation in the offshore ECC using a TSHD

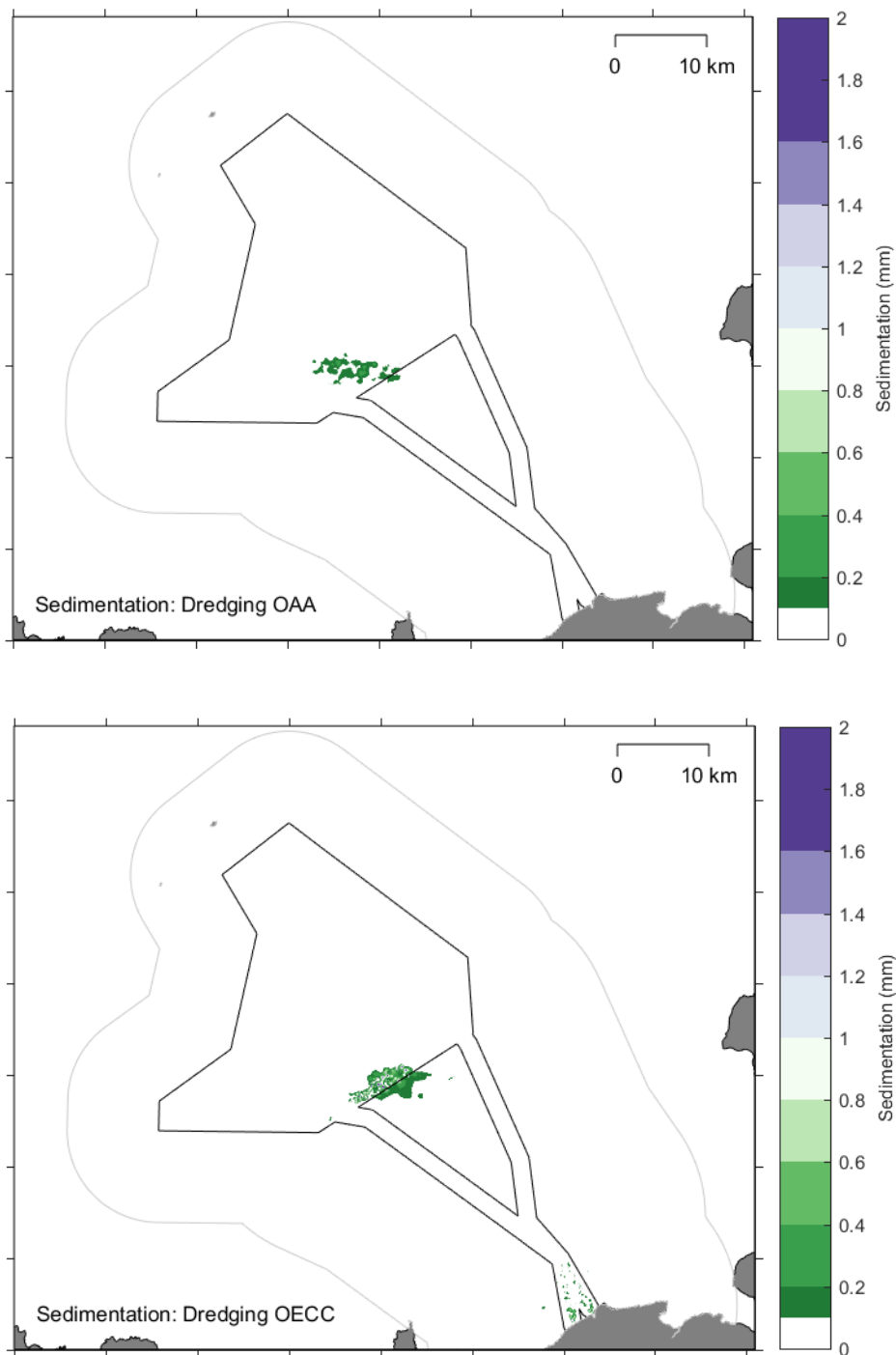


Figure B-17 Modelled sedimentation from the PT model simulation for seabed preparation in the OAA (top) and offshore ECC (bottom) using a TSHD

Time series plots of the SSC and sedimentation at selected model extraction locations (Figure 2-4) over the model simulation have been created. The plots show very little or no SSC or sedimentation at the majority of the sites and so only the sites with the largest predicted impacts are presented. Time series plots for dredging in the OAA are shown for a site in the dredge area (OAA8) and at the placement site (OAA3) in Figure B-18 and Figure B-19, while



plots for dredging in the offshore ECC are shown for a site in the dredge area (ECC4) and at the placement site (OAA3) in Figure B-20 and Figure B-21 respectively. The plots show the following:

- The peaks in SSC at all sites are short duration peaks of relatively low concentration. The peaks only occur a few times over the simulation period at the sites closest to the dredging activity, with a peak in SSC of less than 2 mg/l within the OAA and just under 5 mg/l in the offshore ECC. Within the indicative DMPA placement area the peaks in SSC occur more frequently, with peaks higher for the placement of sediment from the OAA (peaks of just over 10 mg/l) compared to the offshore ECC (peaks of around 5 mg/l); and
- The sedimentation at most sites shows a small and gradual increase over the simulation period. The final sedimentation depth at the end of model simulation is still less than 0.1 mm at the dredge activity sites for both the OAA and offshore ECC dredging, while at the indicative DMPA placement site the sedimentation was only below 0.1 mm for dredging in the OAA. The placement from dredging in the offshore ECC resulted in sedimentation of almost 0.4 mm at OAA3 due to placements occurring in close proximity to the site near the start of the dredge. For subsequent dredge cycles with placements at greater distances from the extraction location the increase in sedimentation was more gradual so that sedimentation at the end of the run remained below 0.5 mm.

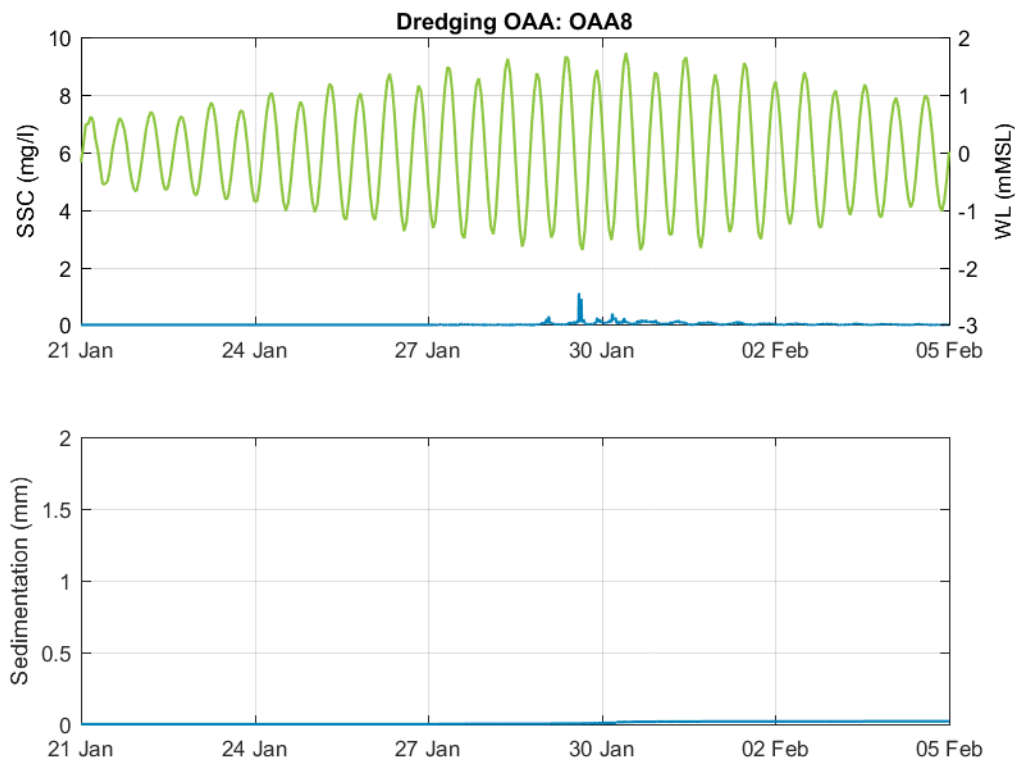


Figure B-18 Modelled SSC and sedimentation at OAA8 for seabed preparation in the OAA using a TSHD

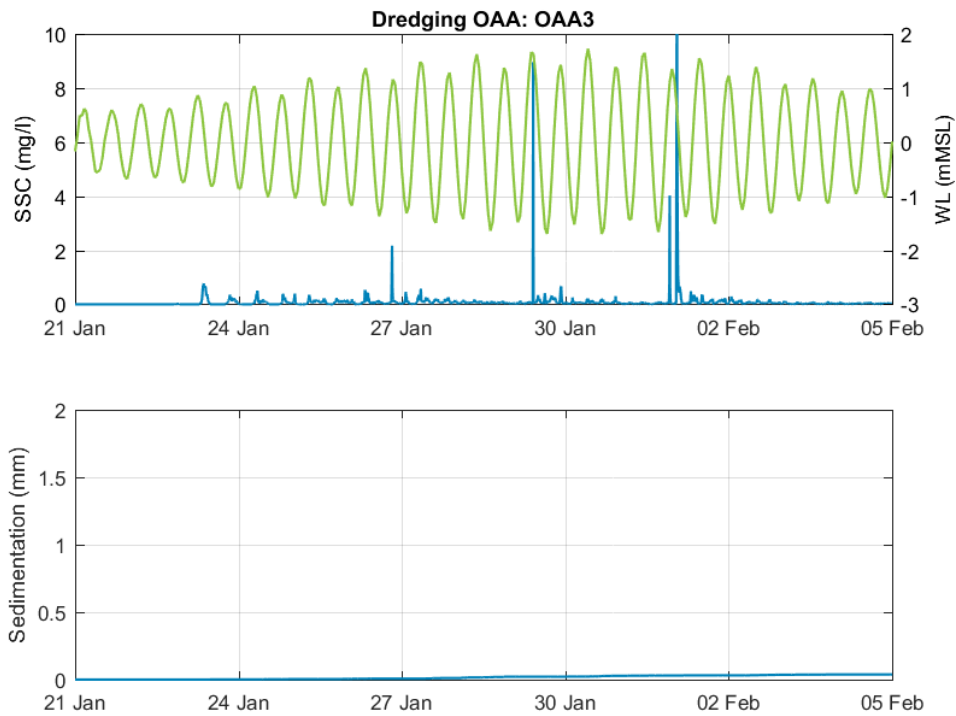


Figure B-19 Modelled SSC and sedimentation at OAA3 as a result of placement within the indicative DMPA during seabed preparation in the OAA using a TSHD

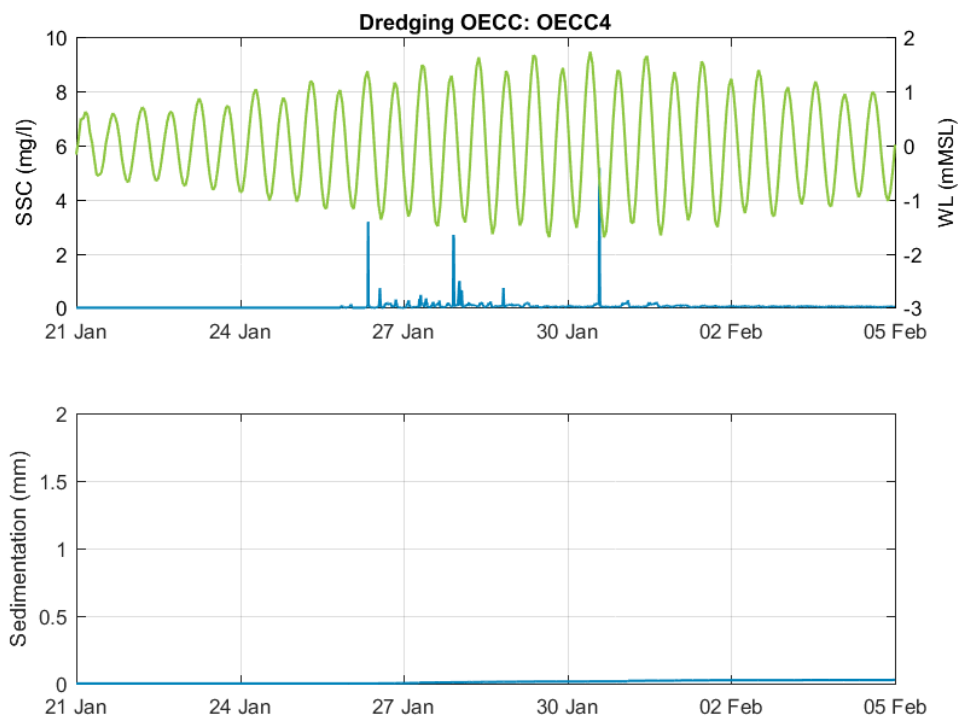


Figure B-20 Modelled SSC and sedimentation at ECC4 for seabed preparation in the offshore ECC using a TSHD

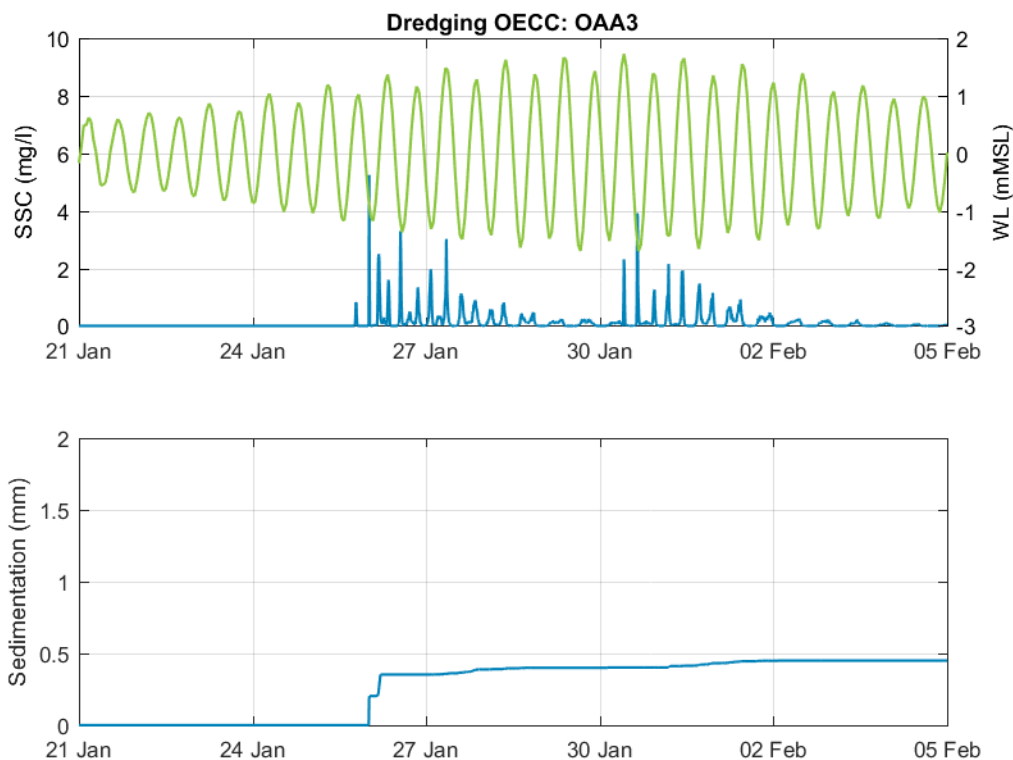


Figure B-21 Modelled SSC and sedimentation at OAA3 as a result of placement within the indicative DMPA during for seabed preparation in the offshore ECC using a TSHD

To investigate the decay of placement plumes in more detail, the reduction in maximum SSC following placement from sediment dredged from the OAA and offshore ECC, is shown for the three hours after placement in Figure B-22, which shows:

- Generally, the placement plume is advected away from the placement site by the tidal currents;
- Plume concentrations are higher for the placement of dredged material from the offshore ECC due to the higher percentage of fines; and
- The high concentrations in the placement plume (up to just under 70 mg/l for sediment placed from the OAA and almost 400 mg/l for sediment placed from the offshore ECC) rapidly reduce to less than 6 mg/l within one hour of placement.

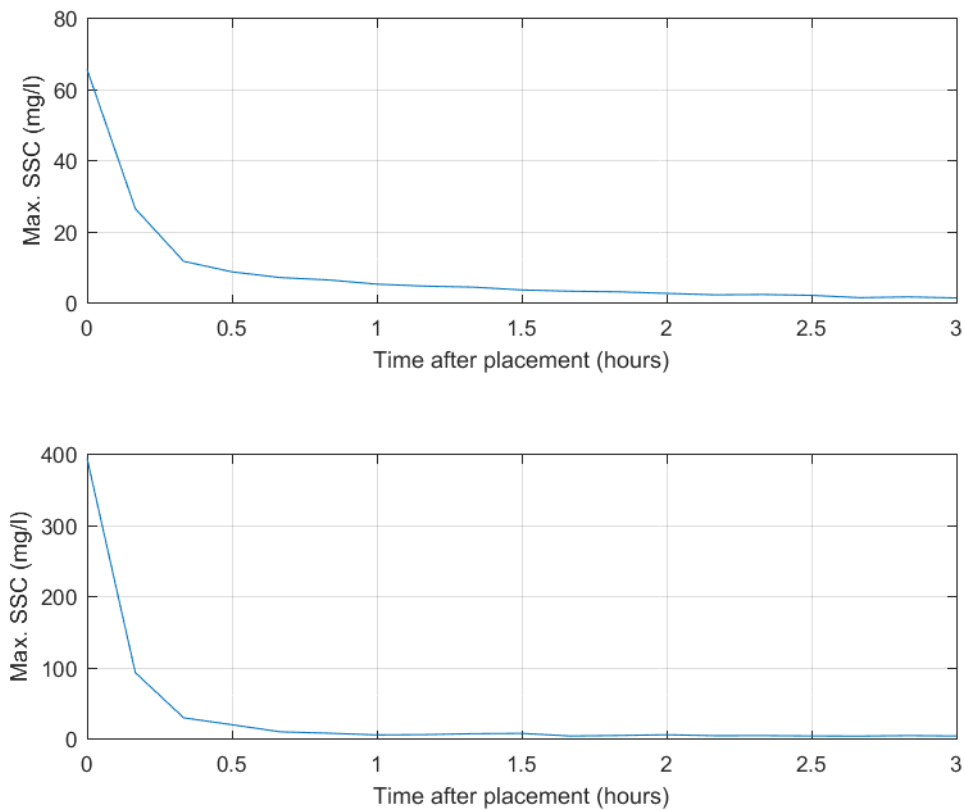


Figure B-22 Decay in SSC placement plume concentration associated with seabed preparation in the OAA (upper) and seabed preparation in the offshore ECC (lower)

### B.4.1.2 Clearance by CFE

There is a very small area with an SSC of more than 1 mg/l visible on the 80<sup>th</sup> percentile SSC for the bedform clearance in the OAA, while for the clearance in the offshore ECC there is an area of between 1 and 2 mg/l visible on the 95<sup>th</sup> percentile SSC, but with no SSC of more than 1 mg/l visible for the lower percentiles. The 99<sup>th</sup> percentile and maximum SSC over the 15.5 day period over which construction activities were simulated are shown for the seabed preparation using a CFE in the OAA in Figure B-23 and in the offshore ECC in Figure B-24. In addition, plots showing the sedimentation at the end of the model simulation are shown for both the OAA and offshore ECC in Figure B-25. When assessing the plots and comparing results to the plots when the clearance is undertaken by the TSHD it is important to note that the clearance by the CFE is much slower than by the TSHD, with the total clearance of the OAA and offshore ECC is calculated to take 640 days compared to 20 days for the TSHD, based on clearance volumes provided within the Project design. Therefore, the calculated clearance timeframe does not account for the construction programme. As the plots for the clearance by the CFE only represent two 15.5 day periods (one for the OAA and one for the offshore ECC) they represent less than 5% of the total activity required, while the plots for the TSHD represent all of the removal activity. The plots show the following:



- The model simulates sediment disturbance from bedform clearance in the southern part of the OAA and along the landward 6 km of the offshore ECC along two tracks centred on the western and eastern cable corridors. The southern part of the OAA was adopted as an area of potentially higher spreading due to the slightly faster flow residuals, while the landward 6 km of the offshore ECC was adopted as it was found to be where the higher SSC plume resulted for the TSHD;
- The 99<sup>th</sup> percentile increase in SSC for the bedform clearance by the CFE in the OAA was up to 28.6 mg/l (Figure B-23). The elevated SSC was in a localised area and the concentrations in the plume quickly reduce to less than 4 mg/l within a couple of kilometres. The plume extends in an east/west direction due to both the track orientation along which the bedform clearance was simulated in the model and the dominant tidal flow directions in the area (Figure B-23). The similarity between the 99<sup>th</sup> percentile and maximum SSC indicates that the SSC is regularly elevated in this area throughout the simulation period as a result of the slow forward movement of the CFE;
- The 99<sup>th</sup> percentile increase in SSC for the bedform clearance by the CFE in the offshore ECC was predominantly less than 4 mg/l outside of the offshore ECC and typically less than 10 mg/l within the offshore ECC with some isolated areas of more than 20 mg/l also present (Figure B-24). The maximum SSC was above 20 mg/l within the area where the clearance activity was being undertaken, but rapidly reduces to less than 4 mg/l at distances of more than 7 km from the simulated clearance track (Figure B-24). As with the clearance in the OAA, the similarity between the 99<sup>th</sup> percentile and maximum SSC indicates that the SSC is regularly elevated in this area throughout the simulation period;
- The sedimentation shows that the clearance activity in both areas is predicted to result in more than 2 mm of sedimentation where the clearance is undertaken and less than 1 mm away from these areas (Figure B-25). Sedimentation of more than 0.1 mm is predicted to extend approximately 6 km to the east of the offshore ECC boundary as a result of the offshore ECC bedform clearance. Depending on the exact location of clearance required in the OAA, sedimentation of more than 0.1 mm could also extend 6 km beyond the OAA boundary; and
- Although the SSC and sedimentation predictions show very localised and small increases, the relative increases compared to using the TSHD are much higher and will also occur for a much longer duration (32 times longer), albeit in different parts of the OAA and offshore ECC local to the bedform clearance activity.

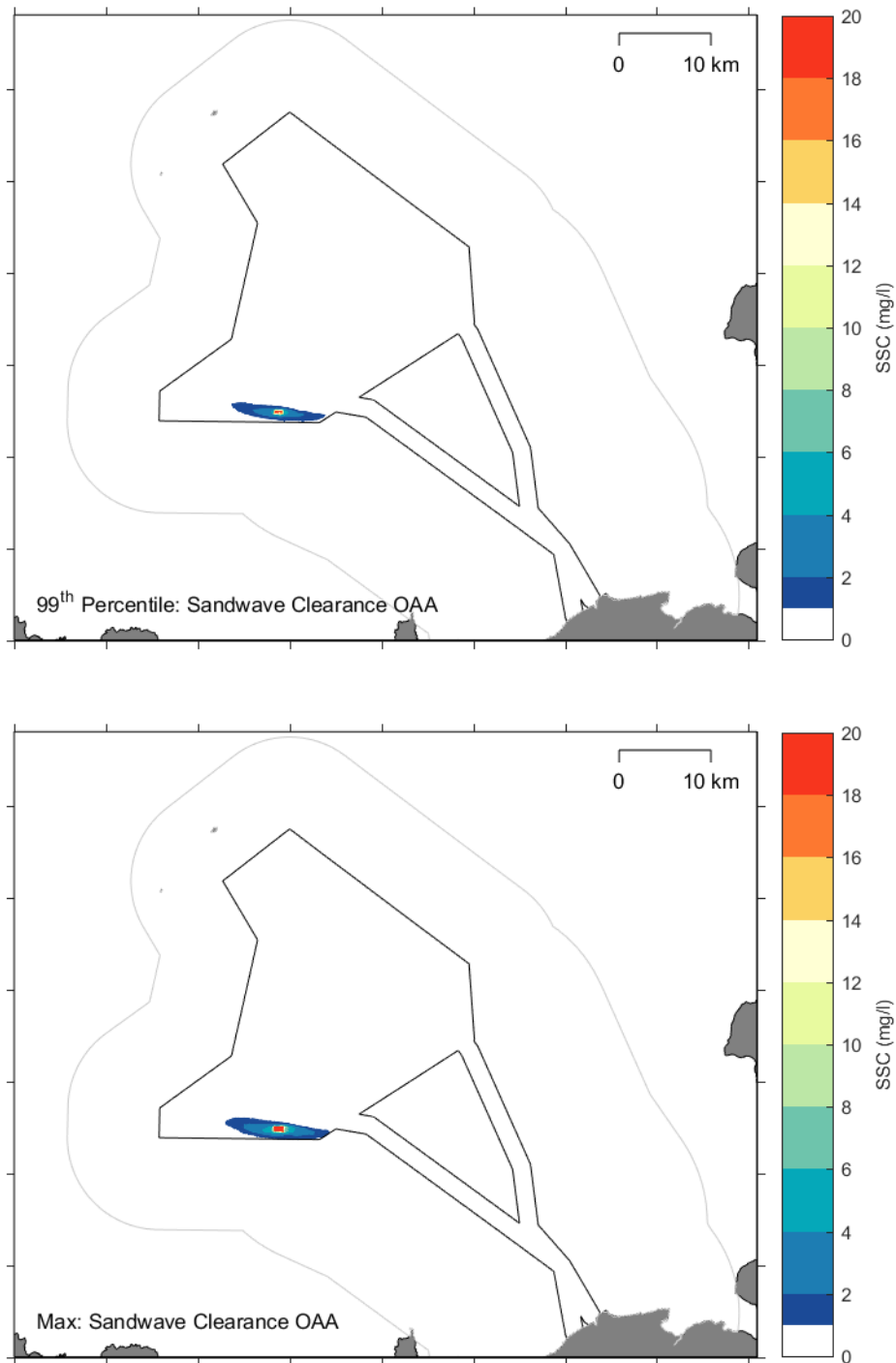


Figure B-23 Modelled 99<sup>th</sup> percentile (top) and maximum (bottom) SSC from the PT model simulation for seabed preparation in the OAA using the CFE

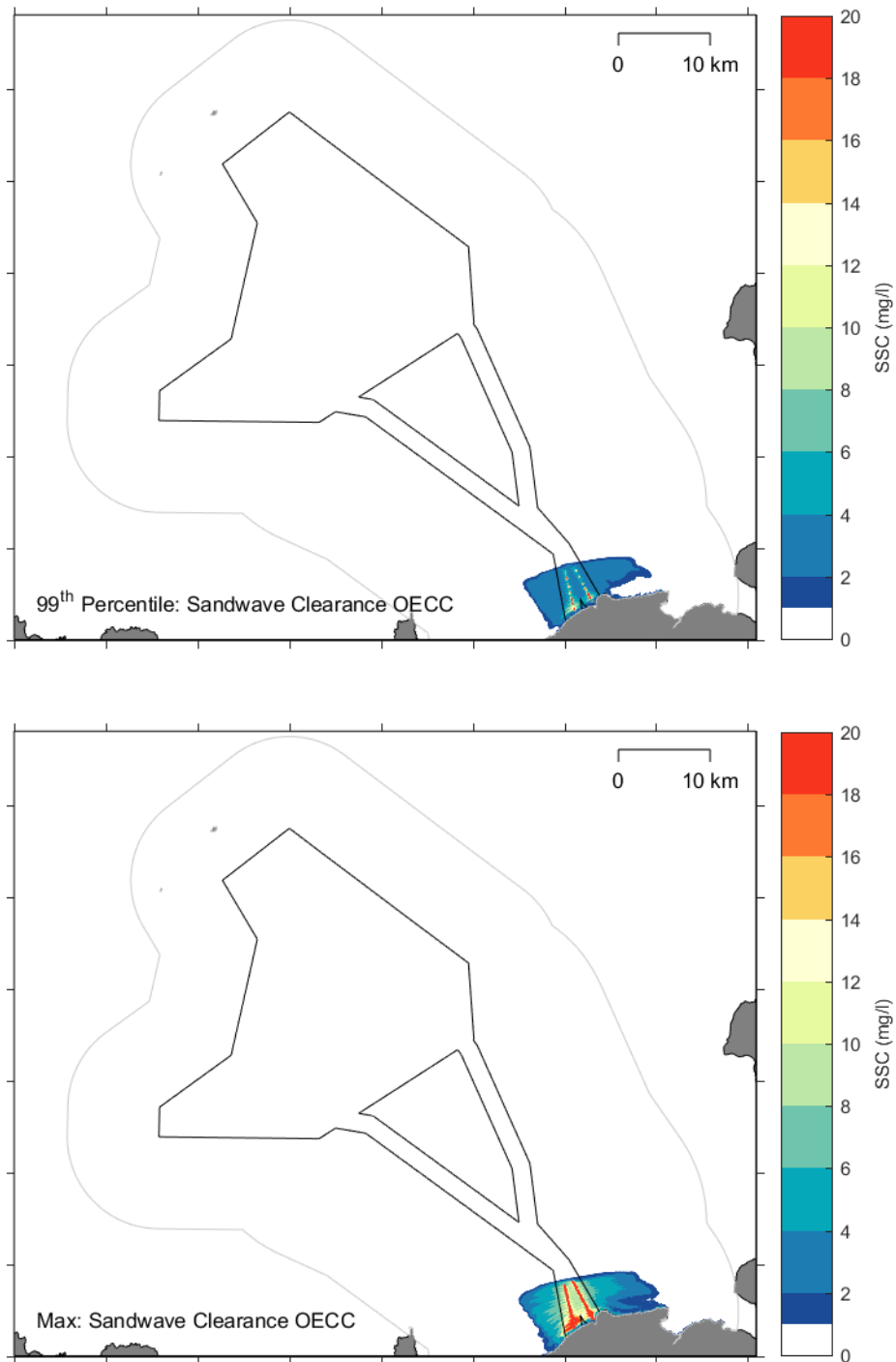


Figure B-24 Modelled 99<sup>th</sup> percentile (top) and maximum (bottom) SSC from the PT model simulation for seabed preparation in the offshore ECC using the CFE

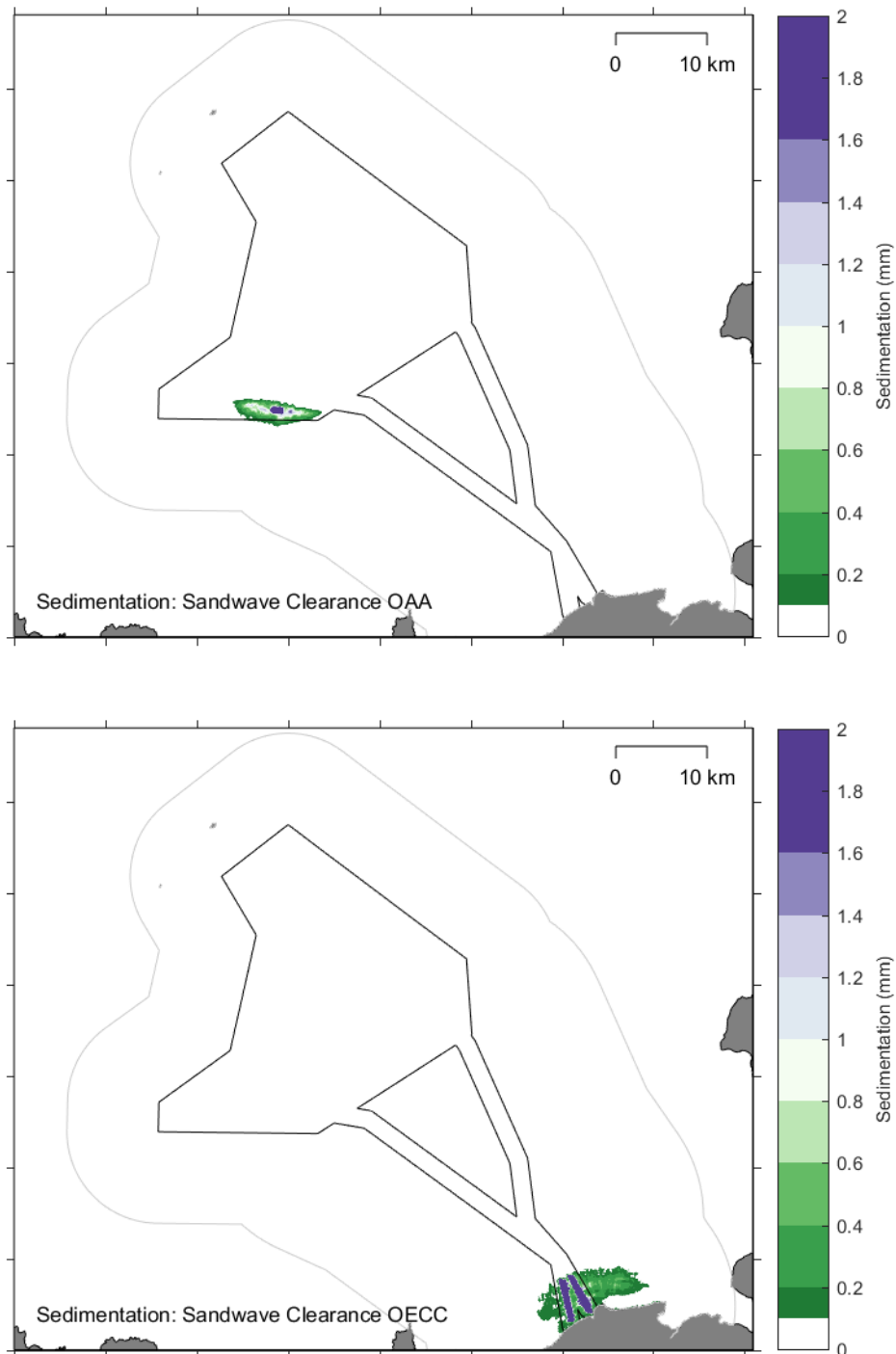


Figure B-25 Modelled sedimentation from the PT model simulation for bedform clearance using the CFE in the OAA (top) and offshore ECC (bottom).

Time series plots of the SSC and sedimentation over the model simulation have been created for selected model extraction locations (Figure 2-4). The plots show very little or no SSC or sedimentation at the majority of the sites and so only the sites with the largest predicted impacts are presented. Time series plots for bedform clearance are shown



for the site closest to the modelled clearance track in the OAA (OAA12) in Figure B-26, and for two sites close to the modelled clearance track in the offshore ECC (ECC4 and ECC9) in Figure B-27 and Figure B-28. The plots show the following:

- Peaks in SSC for clearance in the OAA peak around the time of high water (when flows advect the plume towards the extraction location) and are typically less than 3 mg/l (Figure B-26);
- Peaks in SSC for clearance in the offshore ECC are up to 8 mg/l at ECC4 occurring when the CFE passes downstream of the extraction location and with much lower SSC (around 1 mg/l) at other times (Figure B-27). Comparatively peaks at ECC9, which is in shallower water along the coast, reach 30 mg/l when the modelled CFE track transits very close by but with more typical peaks of 1 to 2 mg/l (Figure B-28); and
- The sedimentation at the sites close to the clearance activity show a consistent increase over the simulation period. The final sedimentation depth at the end of the simulation remains below 0.5 mm at OAA12 (Figure B-26) and ECC4 (Figure B-27) but is much higher at ECC9 (almost 11 mm, Figure B-28). This higher sedimentation is likely to be caused by a number of factors including the close proximity of the sediment disturbance in the model to the extraction location (within 40 m) and the reduced energy from tidal flows and wave processes in the nearshore area resulting in reduced dispersion and more rapid settling to the bed.

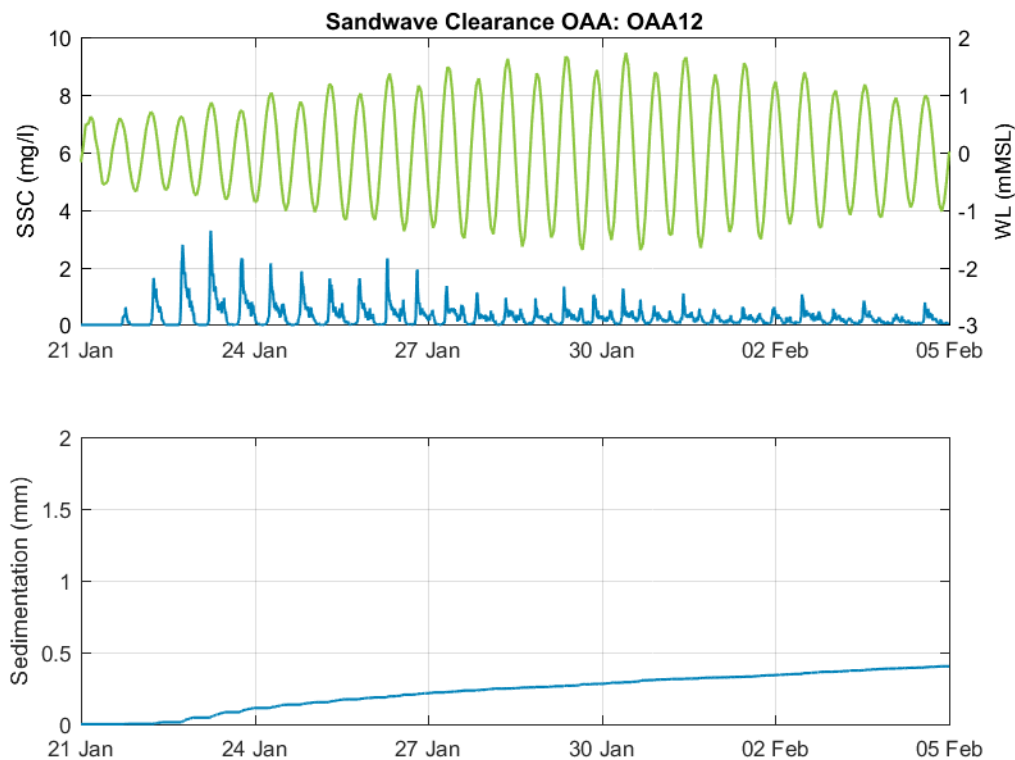


Figure B-26 Modelled SSC and sedimentation at OAA12 for seabed preparation in the OAA using the CFE

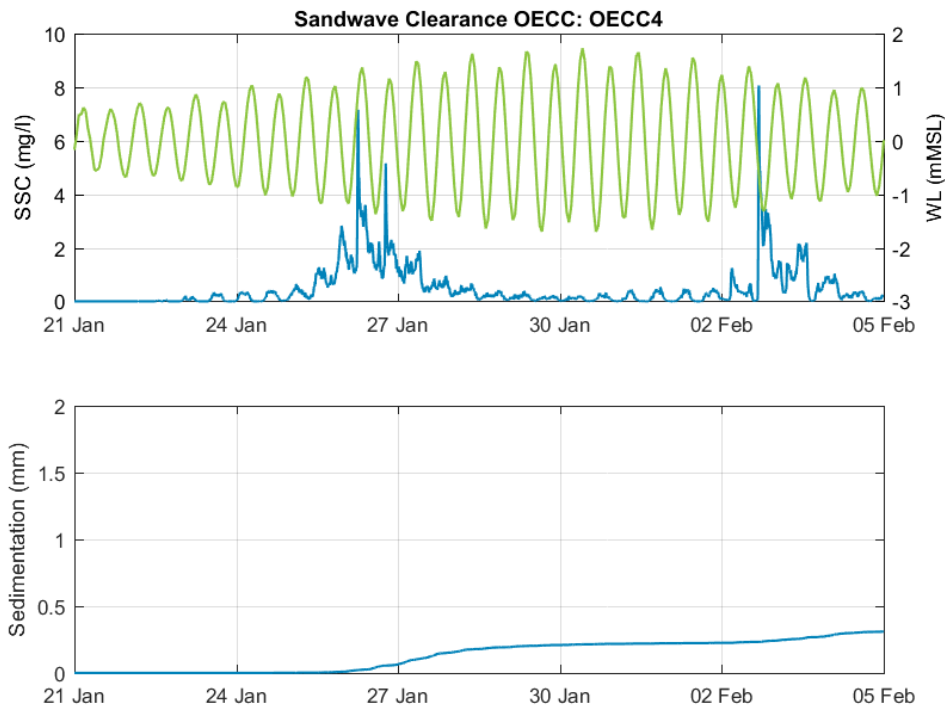


Figure B-27 Modelled SSC and sedimentation at ECC4 for seabed preparation in the offshore ECC using the CFE

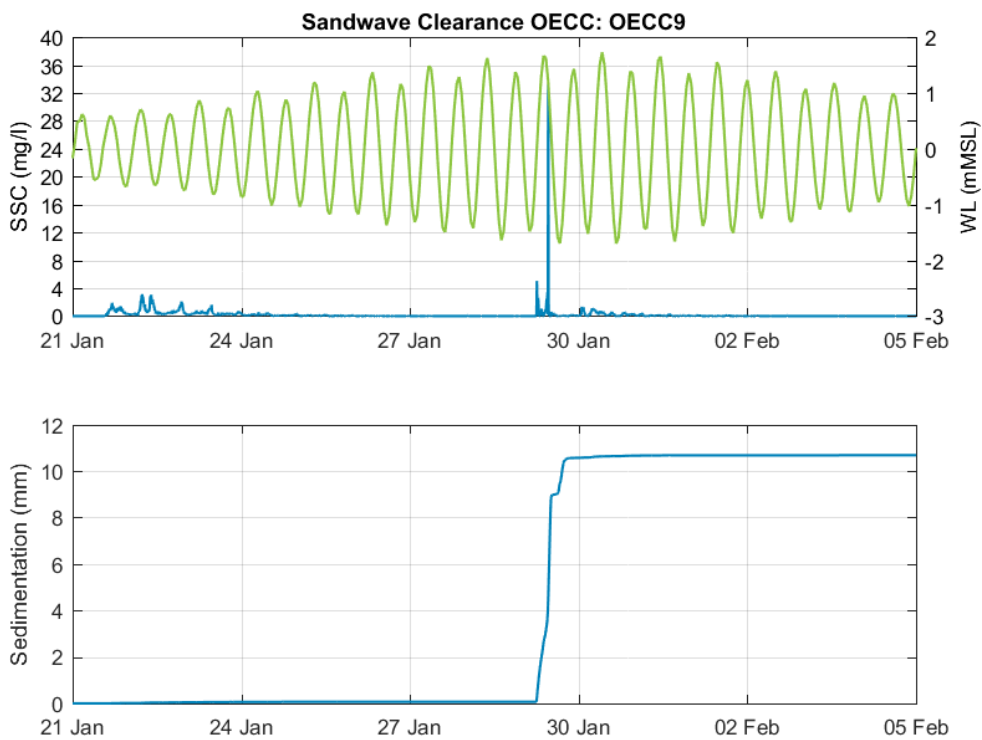


Figure B-28 Modelled SSC and sedimentation at ECC9 for seabed preparation in the offshore ECC using the CFE



## B.4.2 Cable Burial

There is no area with an increase in SSC of above 1 mg/l visible on the 95<sup>th</sup> (or lower) percentile plots for the cable burial in the OAA or the offshore ECC. The 99<sup>th</sup> percentile and maximum SSC over the 15.5 day period over which construction activities were simulated are shown for the cable burial in the OAA in Figure B-29 and in the offshore ECC in Figure B-30. In addition, plots of the sedimentation at the end of the model simulation are shown for cable burial in both the OAA and offshore ECC in Figure B-31. When interpreting the plots, it is important to note that the cable burial is predicted to take 89 days to complete which means that as the plots for the clearance by the CFE only represent two 15.5-day periods (one for the OAA and one for the offshore ECC) they represent a third of the total activity required. The plots show the following:

- The 99<sup>th</sup> percentile increase in SSC from the cable burial activity in the OAA is predicted to generally be less than 1 mg/l, although there are some small, isolated patches with an SSC of 1 to 2 mg/l (Figure B-29). The maximum SSC shows that the peak SSC is up to 8 mg/l, but that the area with elevated SSC remains very localised to where the activity is being undertaken with very limited transport of the suspended sediment predicted (Figure B-29). This is likely to be a result of relatively low tidal currents combined with the suspended sediment being disturbed close to the seabed. The difference between the 99<sup>th</sup> percentile and maximum SSC shows that the SSC due to the cable lay only remained elevated for a short duration of time (less than 1%);
- The 99<sup>th</sup> percentile increase in SSC from the cable burial activity in the offshore ECC is also predicted to generally be less than 1 mg/l, although there are some small, isolated patches with an SSC of 1 to 2 mg/l (Figure B-30). The maximum SSC shows that peaks in SSC of more than 20 mg/l can occur along the cable route within 6 km of the shoreline, but that this rapidly reduces to less than 4 mg/l away from the cable route. A maximum SSC of up to 2 mg/l can extend up to 5 km beyond the offshore ECC boundaries (Figure B-30). The difference between the 99<sup>th</sup> percentile and maximum SSC shows that the SSC due to the cable lay only remained elevated for a short duration of time (less than 1%); and
- Sedimentation of up to 1 mm is predicted where the burial activity is being undertaken for both the OAA and offshore ECC activities. Sedimentation of more than 0.1 mm is predicted to remain constrained within the OAA and offshore ECC boundaries (Figure B-31).

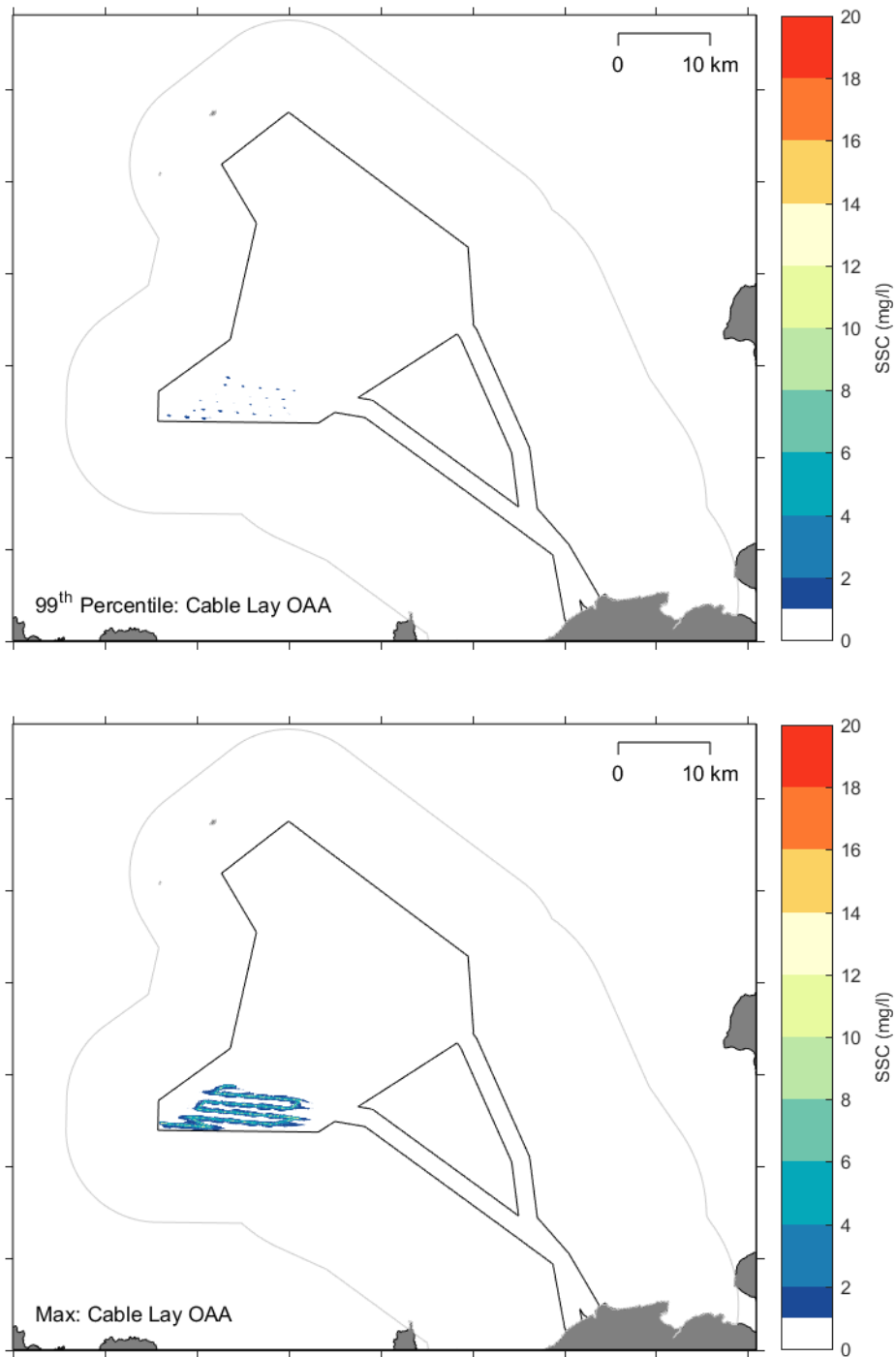


Figure B-29 Modelled 99<sup>th</sup> percentile (top) and maximum (bottom) SSC from the PT model simulation for cable burial in the OOA using the CFE.

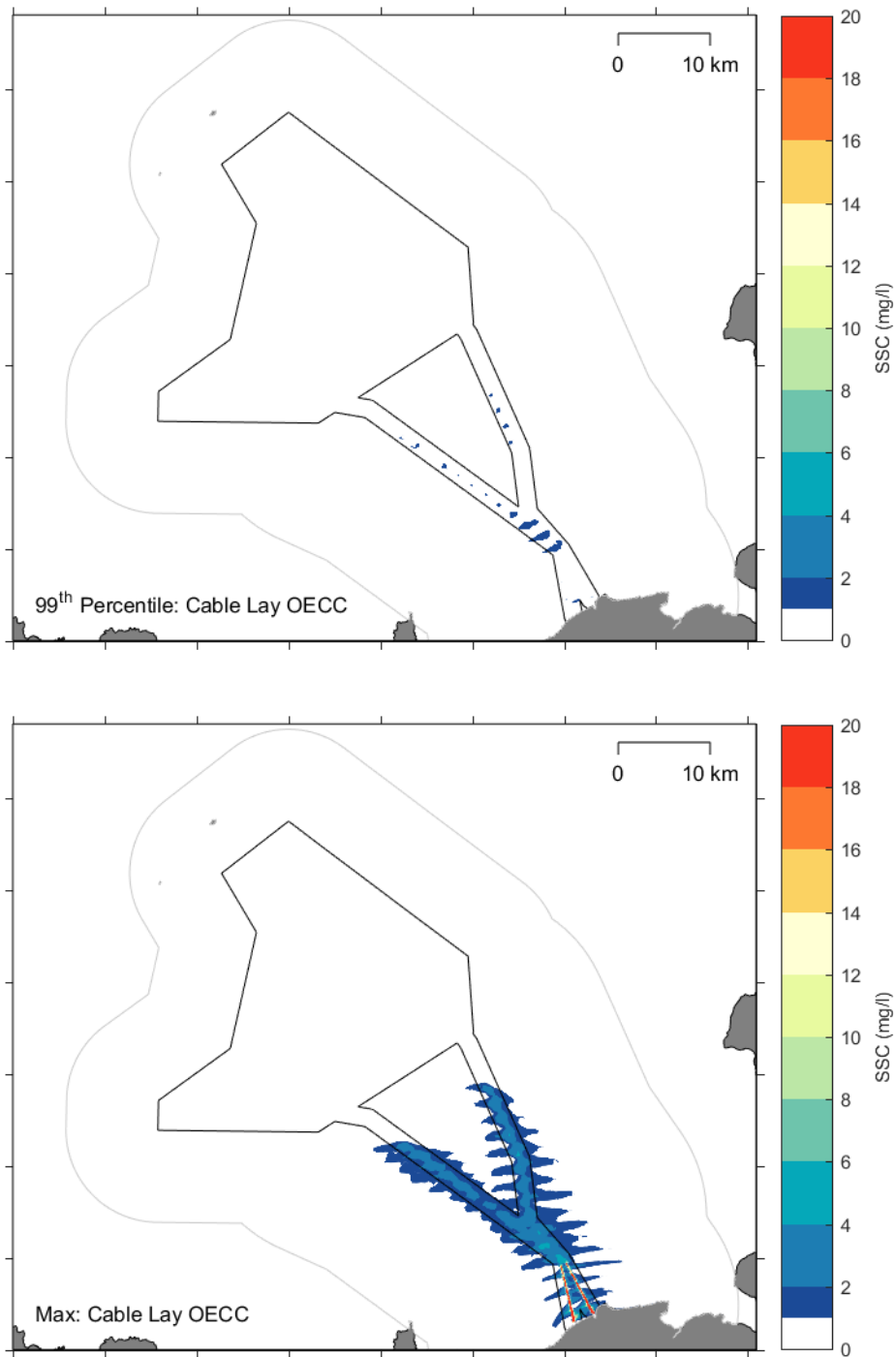


Figure B-30 Modelled 99<sup>th</sup> percentile (top) and maximum (bottom) SSC from the PT model simulation for cable burial in the offshore ECC using the CFE.

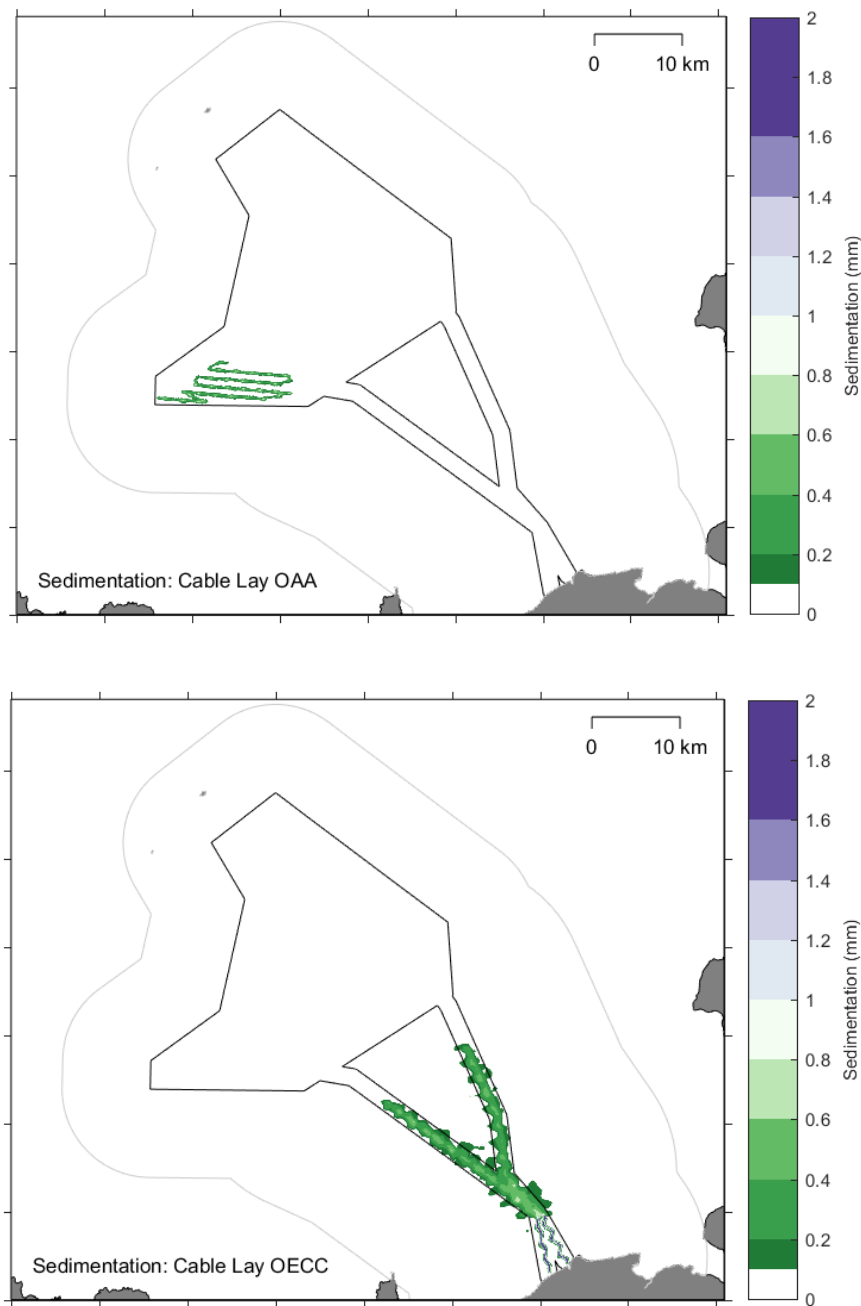


Figure B-31 Modelled sedimentation from the PT model simulation for cable burial using the CFE in the OAA (top) and offshore ECC (bottom).

Time series plots of the SSC and sedimentation at selected model extraction locations (Figure 2-4) over the 16-day model simulation have been created. The plots show very little or no SSC or sedimentation at the majority of the sites and so only the sites with the largest predicted impacts are presented. Time series plots for cable burial using the CFE in the OAA and the offshore ECC are shown for OAA2 in Figure B-32 and ECC3 in Figure B-33, these extraction locations are the closest points to the cable burial track simulated in the model (350 m from the OAA track and 500 m from the offshore ECC track). The plots show the following:



- Peaks in SSC for the burial activity in the OAA (Figure B-32) and offshore ECC (Figure B-33) are less than 1 mg/l and 2 mg/l, respectively.
- The sedimentation at the sites close to the burial activity show a consistent increase over the 15-day simulation. The final sedimentation depth at the end of the model simulation was less than 0.1 mm within the OAA and approximately 0.4 mm within the offshore ECC.

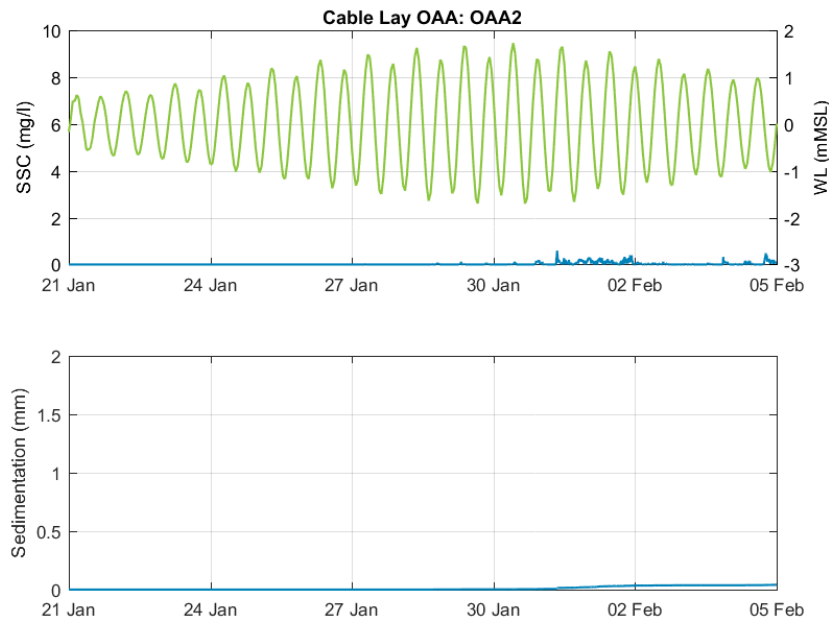


Figure B-32 Modelled SSC and sedimentation at OAA2 for cable burial in the OAA using the CFE.

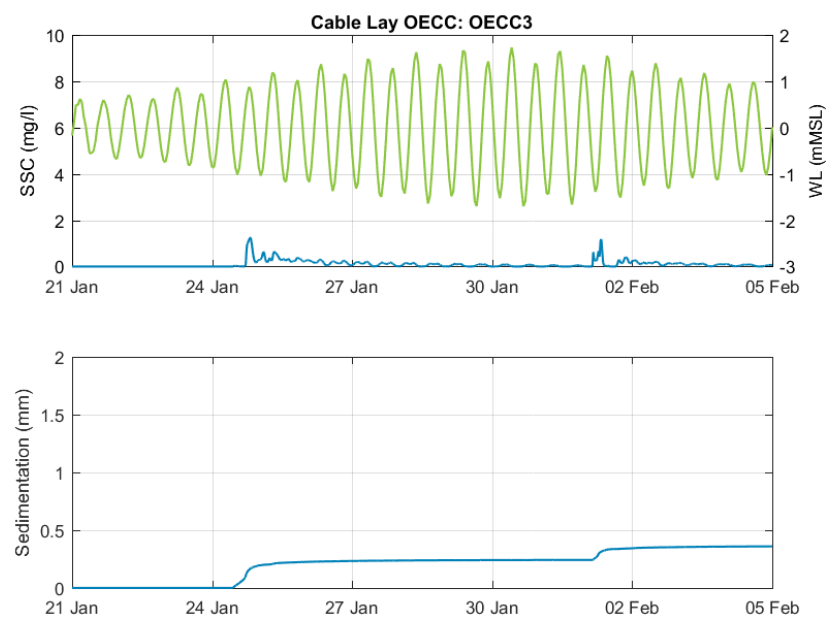


Figure B-33 Modelled SSC and sedimentation at ECC3 for cable burial in the offshore ECC using the CFE.



### B.4.3 Pile Drilling

There is a very small area with an SSC of more than 1 mg/l visible on the 80<sup>th</sup> percentile SSC for the pile drilling of a single structure at a time, while for drilling of two structures at once the area with elevated SSC is larger but remains predominantly below 2 mg/l. The 99<sup>th</sup> percentile and maximum SSC over the 15.5 day period over which construction activities were simulated are shown for the monopile drilling at one structure at a time in Figure B-34 and for drilling at two locations at a time in Figure B-35. In addition, plots showing the sedimentation at the end of the simulations are shown for drilling both one structure and two structures at a time in Figure B-36. When assessing the plots, it is important to note that the monopile drilling is predicted to take 135 hours per WTG and so over the model simulation approximately 2.5 WTG piles will have been drilled for the single structure drilling and 4 complete WTG piles and two half drilled piles for the dual structure drilling. The plots show the following:

- The 99<sup>th</sup> percentile SSC when drilling one structure at a time shows peaks in SSC of up to 42.1 mg/l where the piles are located (i.e., where the drilling is being undertaken), this rapidly reduces to less than 4 mg/l away from the piles (Figure B-34). A plume of more than 1 mg/l extends approximately 5 km to the west and east of the piles, and as the piles are along the eastern boundary of the OAA this extends beyond the OAA boundary. The maximum SSC when drilling one structure at a time shows a similar extent to the 99<sup>th</sup> percentile and a similar peak in SSC at the pile, but with a larger extent where the SSC is between 2 and 6 mg/l. The similarity between the 99<sup>th</sup> percentile and maximum SSC (Figure B-34) indicates that the SSC is regularly elevated in this area throughout the simulation period (due to the drilling being continuous);
- The 99<sup>th</sup> percentile and maximum SSC results show a similar but slightly larger plume extent for drilling two structures at once compared to just one structure at a time (Figure B-35). In addition, the SSC is also predicted to be slightly higher when drilling two structures at once;
- The extent of the areas with sedimentation of more than 0.1 mm are predicted to be very similar to the extent of the 99<sup>th</sup> percentile and maximum SSC of more than 1 mg/l. For the simulation drilling one structure at a time the majority of the sedimentation is predicted to be less than 0.6 mm (Figure B-36), while when drilling two structures at a time the sedimentation was between 0.8 and 1.2 mm for approximately half of the area experiencing sedimentation (Figure B-36); and
- Given the WTG spacing (down to 1,320 m) and the extent of the area experiencing elevated SSC and sedimentation, as additional structures are drilled the period of exposure to elevated SSC and the depth of sedimentation will increase.

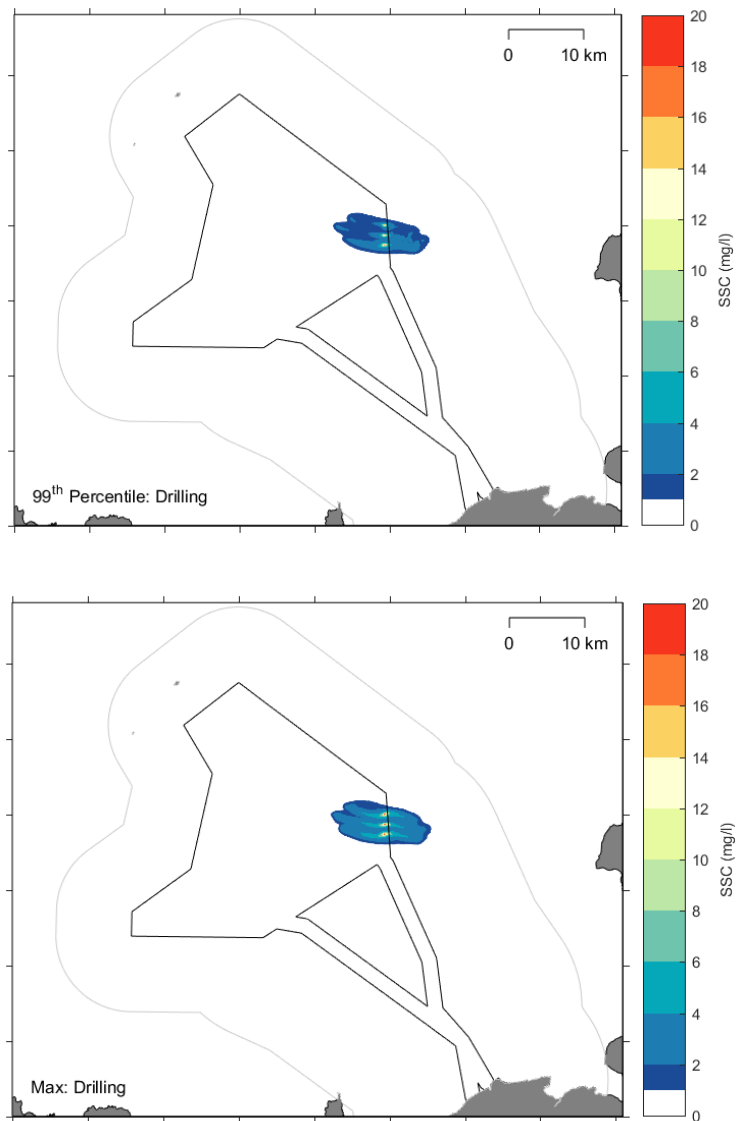


Figure B-34 Modelled 99<sup>th</sup> percentile (top) and maximum (bottom) SSC from the PT model simulation for monopile drilling at one structure at a time.

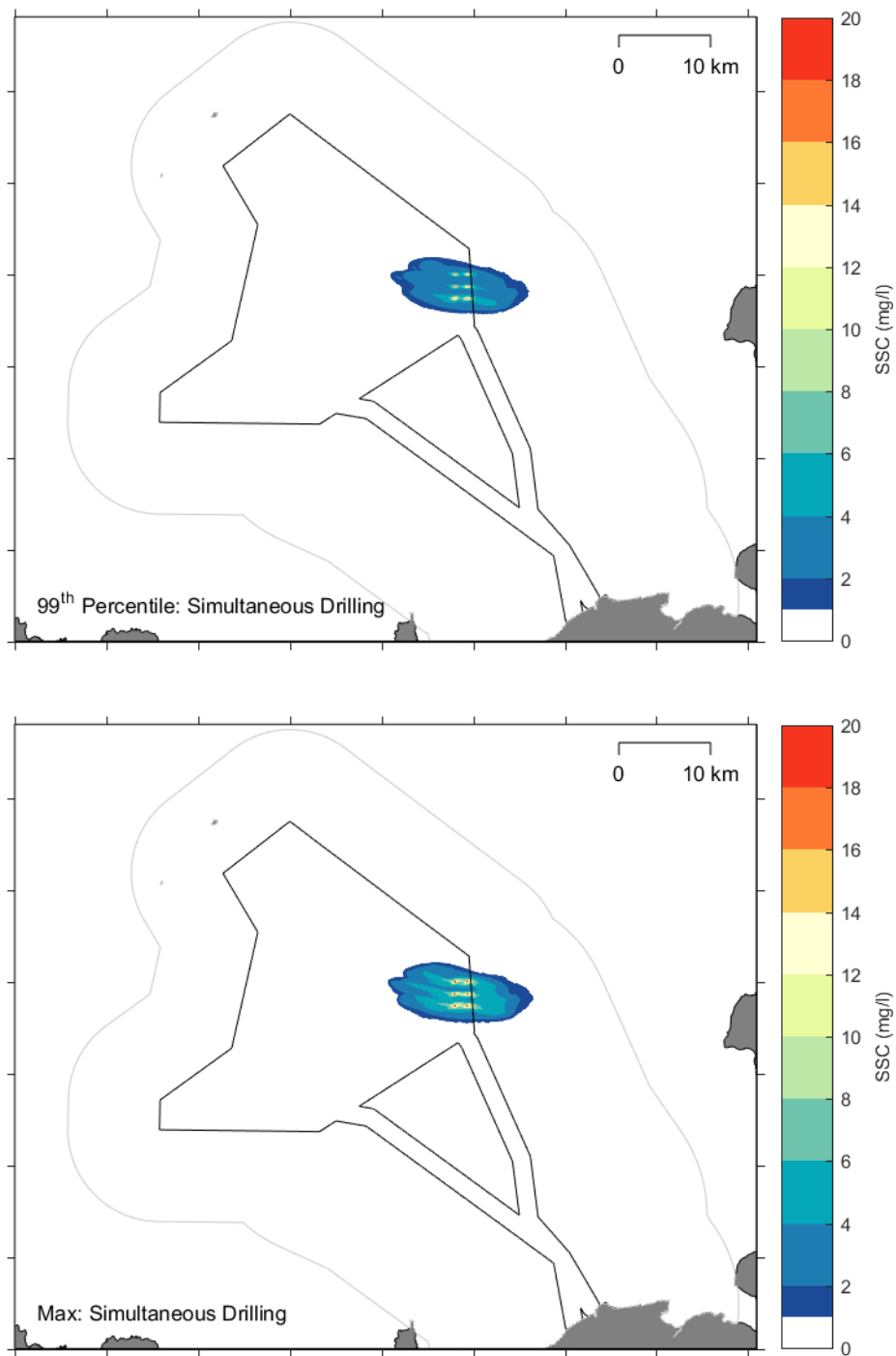


Figure B-35 Modelled 99th percentile (top) and maximum (bottom) SSC from the PT model simulation for monopile drilling at two structures at a time.

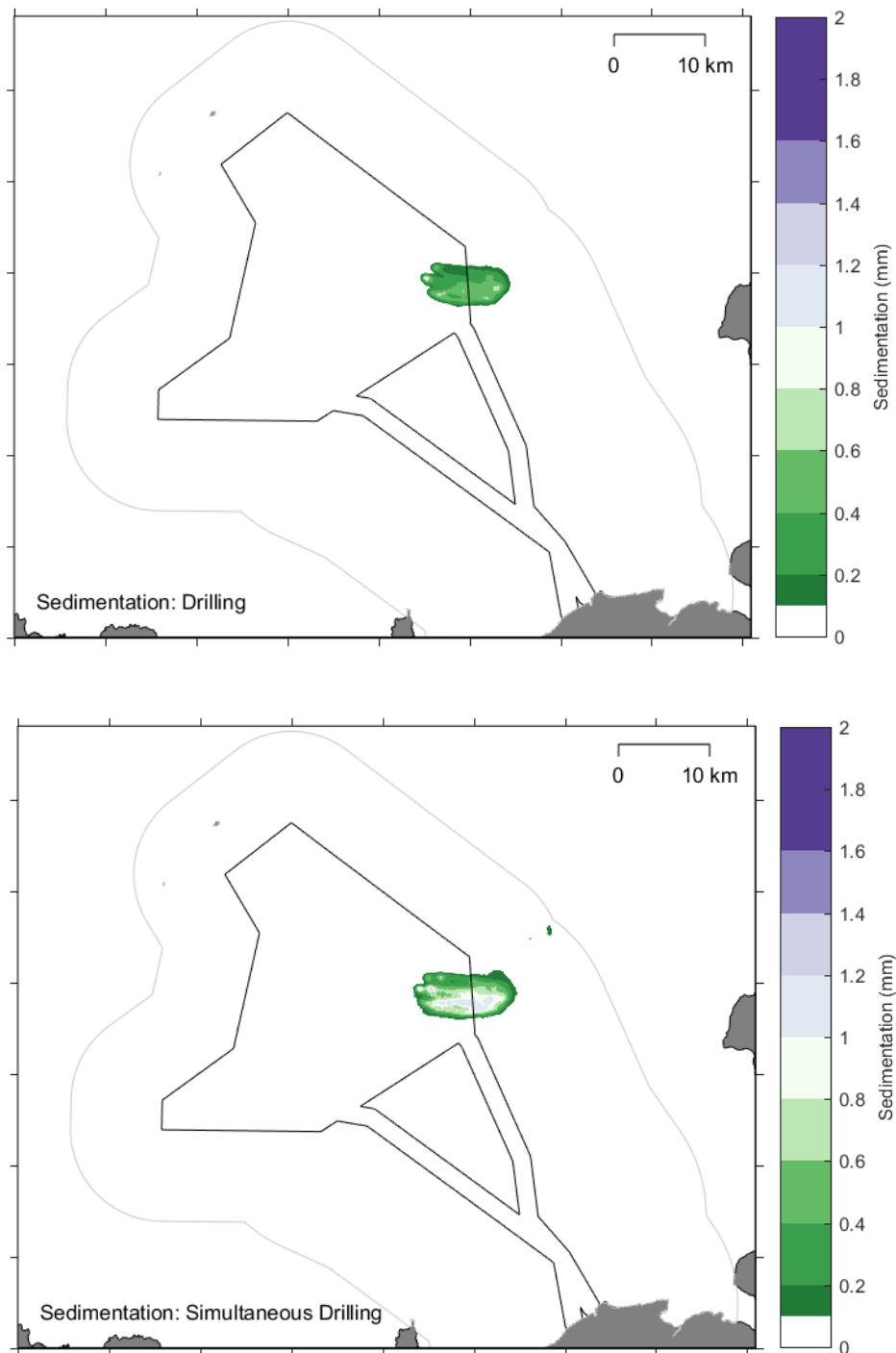


Figure B-36 Modelled sedimentation from the PT model simulation for monopile drilling at one structure at a time (top) and two structures at once (bottom).



Time series plots of the SSC and sedimentation over the model simulation have been created for selected model extraction locations (Figure 2-4). The plots show very little or no SSC or sedimentation at the majority of the sites and only the sites with predicted impacts are presented. Time series plots are shown for monopile drilling at one structure at a time at OAA11 and OAA6 in Figure B-37 and Figure B-38 and for drilling two structures at a time at the two same sites in Figure B-39 and Figure B-40. The plots show the following:

- There are frequent increases in SSC which occur for a longer duration than for the seabed preparation and cable burial activities. Short duration peaks in SSC at OAA11 are up to 8 mg/l, but with more prolonged increases of around 1 mg/l when 1 monopile is being drilled at a time (Figure B-37). In comparison the SSC is elevated by 2 to 4 mg/l (and with peaks of more than 8 mg/l) when two monopiles are being drilled at once (Figure B-39). The duration of the elevated SSC at the site due to the drilling will be controlled by the tidal currents, with the elevated SSC only occurring for the duration when the tidal current is flowing from the pile drilling location to the model extraction site and when the current is strong enough to transport the suspended sediment that distance;
- OAA11 lies approximately 800 m west of the second structure drilled in the simulation when one monopile is drilled at a time and 600 m east of the second structure drilled when two monopiles are drilled at the same time. The periods of higher SSC and greatest rate of sedimentation coincide with the drilling of this structure (from midday on the 27<sup>th</sup> January to 2 am on the 2<sup>nd</sup> February);
- The sedimentation at OAA11 shows a consistent increase over the 5-to-6-day period of the simulation when drilling was at the monopile closest to the extraction point and a more gradual rate of sedimentation when drilling was occurring at other structures. The final sedimentation depth at OAA11 at the end of the model simulation is approximately 0.4 mm when 1 monopile is being drilled at a time (Figure B-37) compared to approximately 0.7 mm when two monopiles are being drilled at once (Figure B-39); and
- No sedimentation occurs at OAA6 when one monopile is drilled (Figure B-38), while sedimentation of less than 0.1 mm occurs when two monopiles are drilled at once (Figure B-40). This is because the simultaneous drilling scenario considers drilling at a structure which is 5 km to the east of OAA6, while the closest structure drilled for one structure at a time is more than 6 km away.

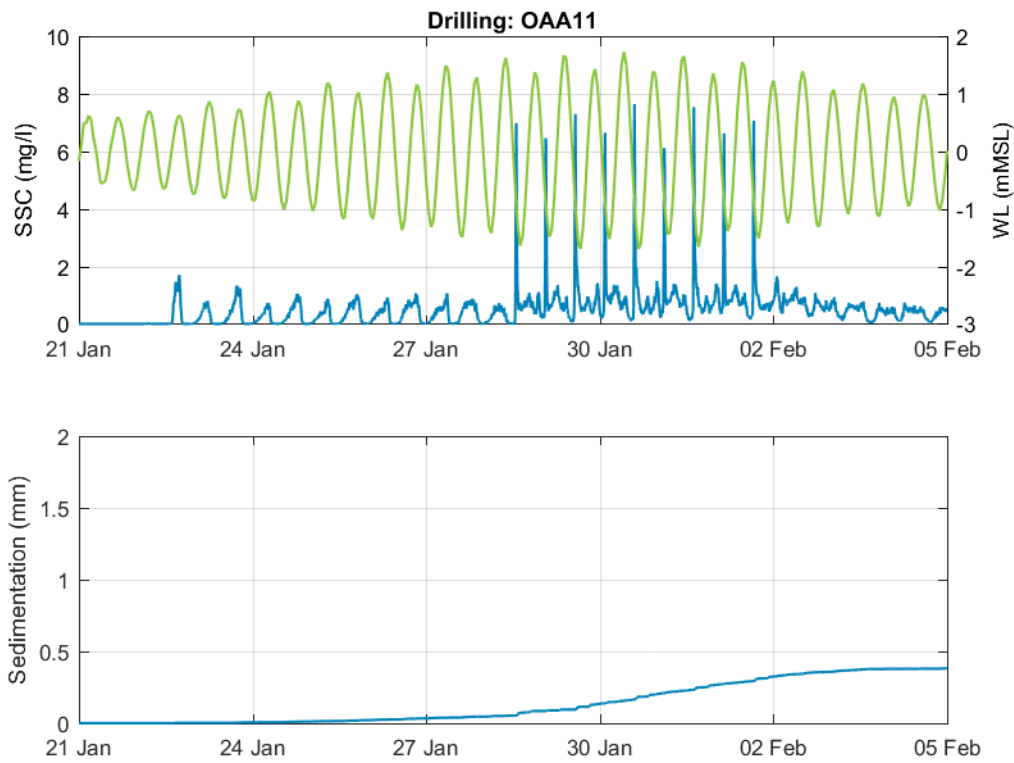


Figure B-37 Modelled SSC and sedimentation at OAA11 for monopile drilling at one structure at a time.

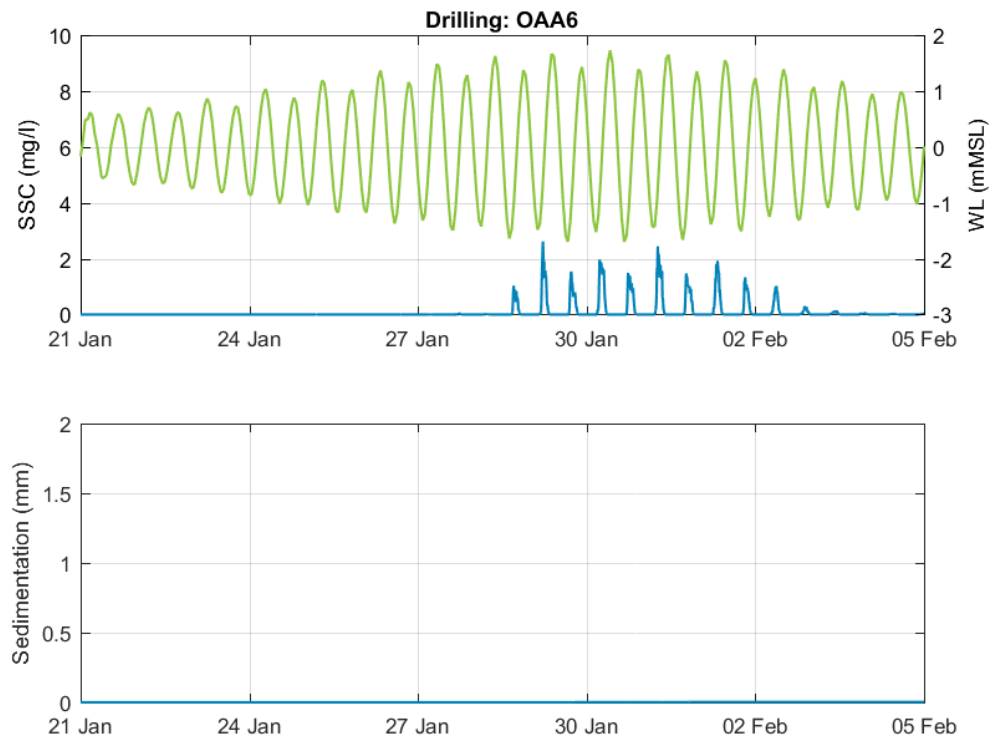


Figure B-38 Modelled SSC and sedimentation at OAA6 for monopile drilling at one structure at a time.

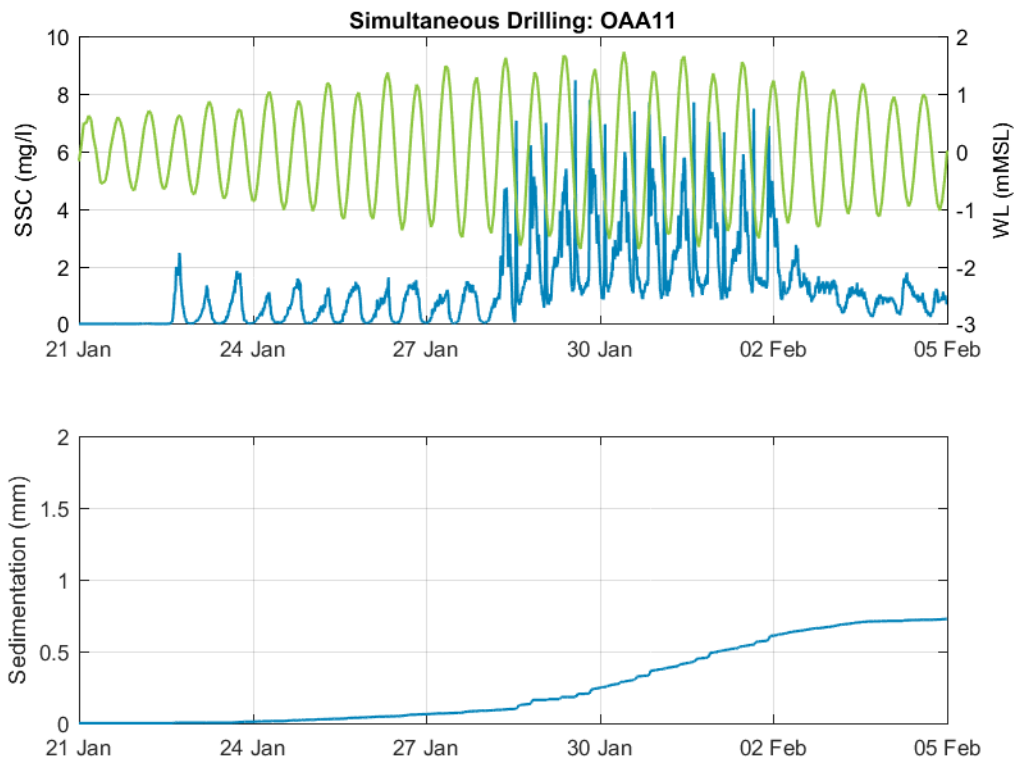


Figure B-39 Modelled SSC and sedimentation at OAA11 for monopile drilling at two structures at a time.

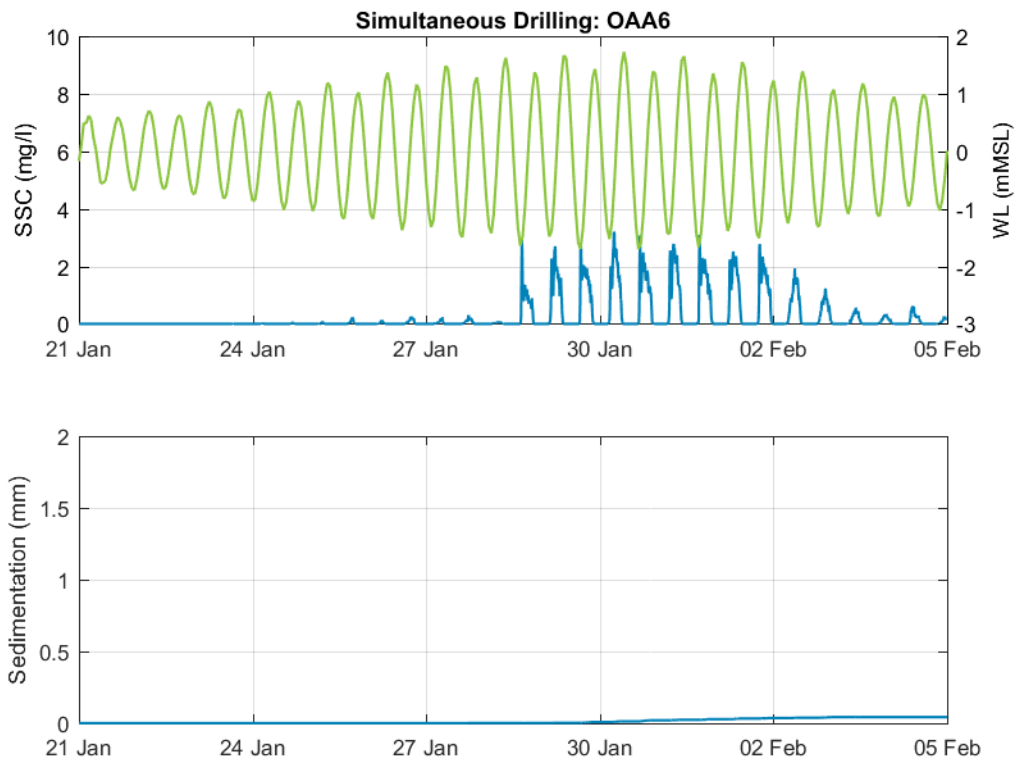


Figure B-40 Modelled SSC and sedimentation at OAA6 for monopile drilling at two structures at a time.



To show the decay of the plumes from drilling in more detail, map plots of SSC at individual timesteps after drilling the first structure are shown in Figure B-41 to Figure B-44 and after the drilling of the second structure in Figure B-45 to Figure B-48. In addition, the reduction in max SSC in the plume following cessation of drilling is shown in Figure B-49. Be

The plots show:

- The sediment in suspension is dispersed with the tidal flows, with the elongate plume shape resulting from the sustained period of sediment discharge;
- SSC concentrations reduce with both distance from the drill site and with time after the drilling ceases; and
- Within one hour after the cessation of drilling, peak plume concentrations are around 5 mg/l or less.

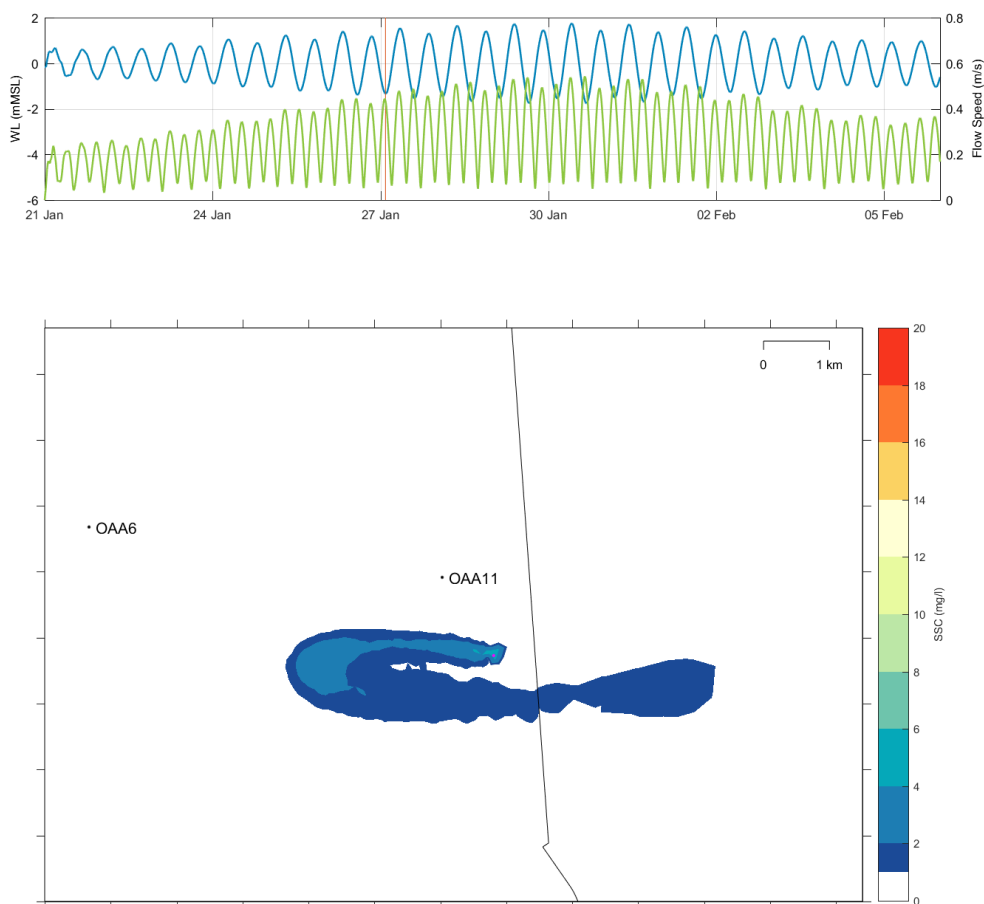


Figure B-41 Modelled SSC from pile drilling, example plume at the end of drilling the first structure

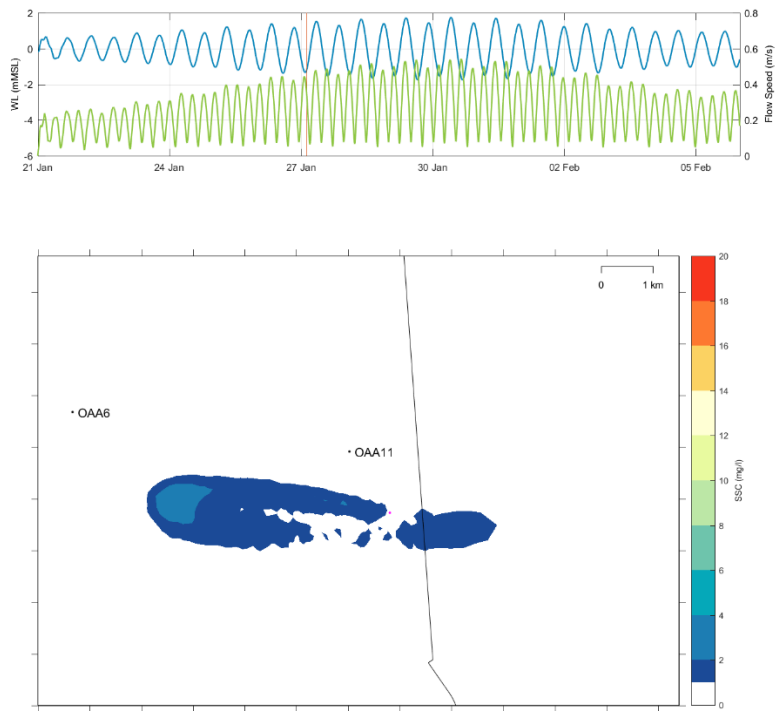


Figure B-42 Modelled SSC from pile drilling, example plume 1 hour after drilling the first structure

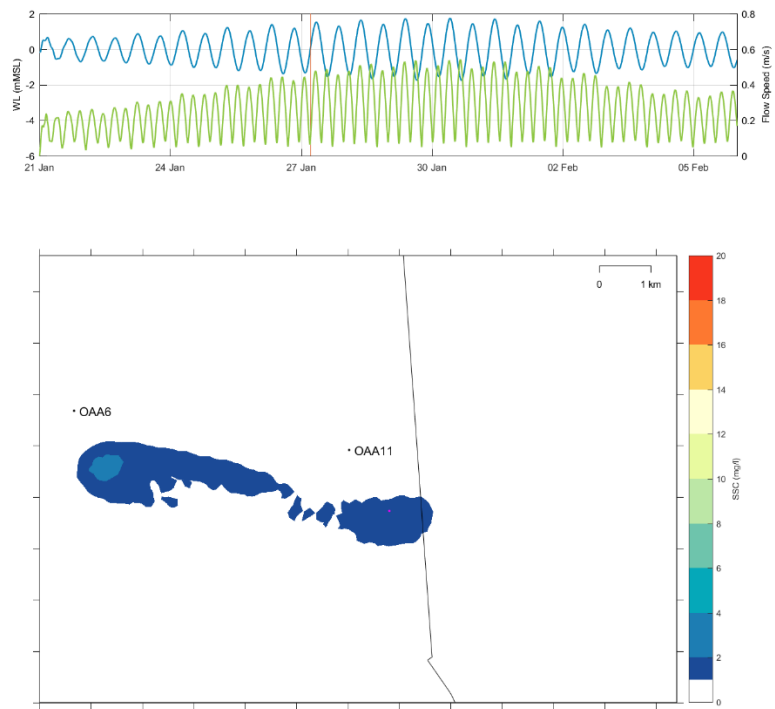


Figure B-43 Modelled SSC from pile drilling, example plume 3 hours after drilling the first structure

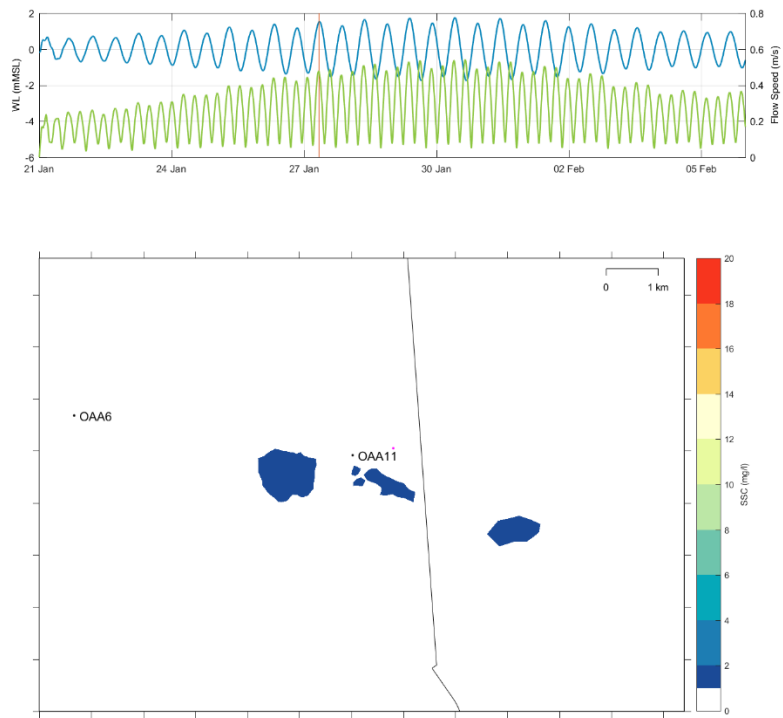


Figure B-44 Modelled SSC from pile drilling, example plume 6 hours after drilling the first structure

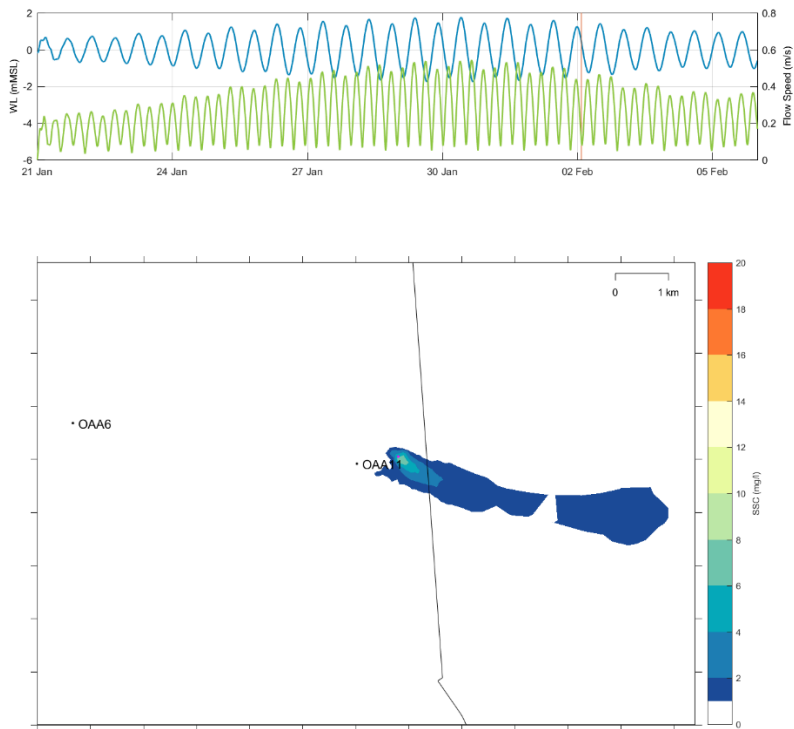


Figure B-45 Modelled SSC from pile drilling, example plume at the end of drilling the second structure

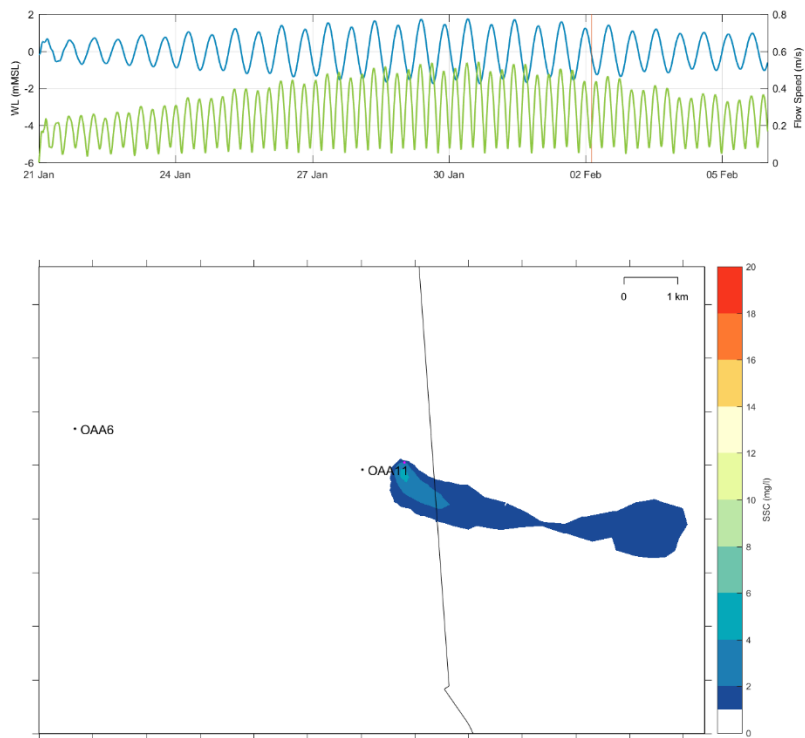


Figure B-46 Modelled SSC from pile drilling, example plume 1 hour after drilling the second structure

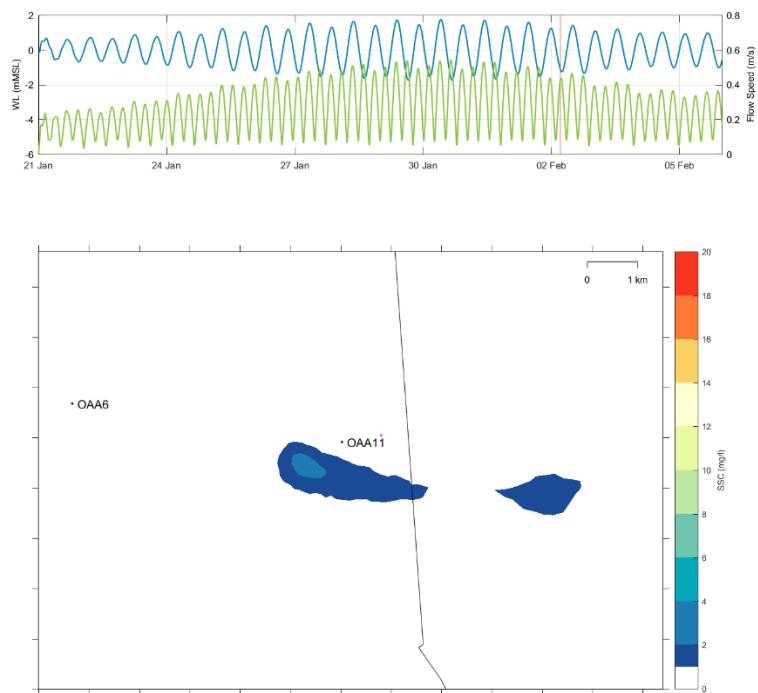


Figure B-47 Modelled SSC from pile drilling, example plume 3 hours after drilling the second structure

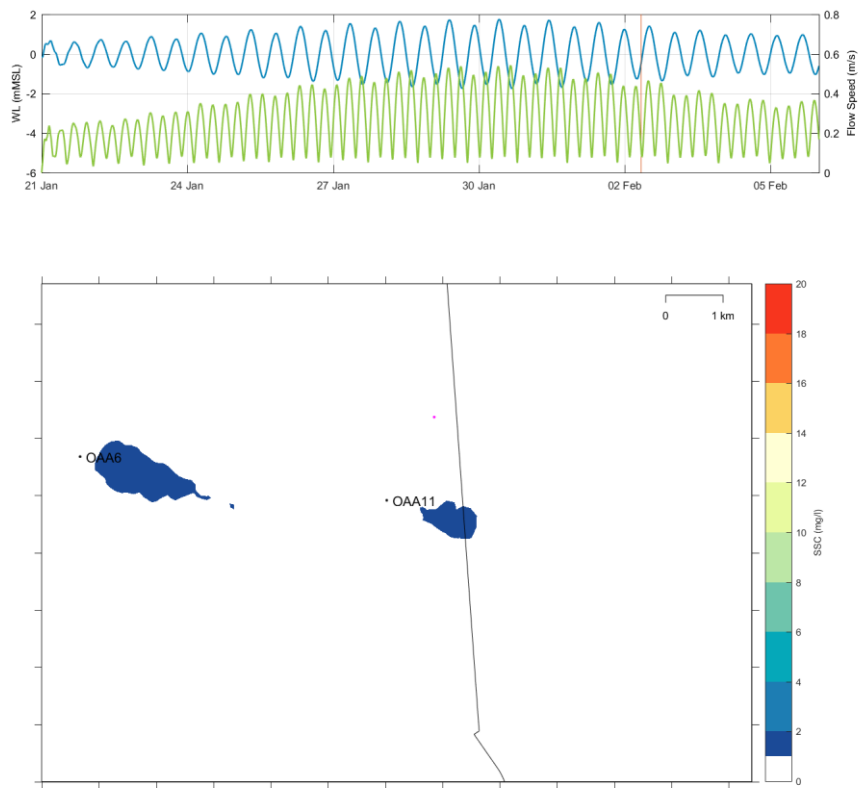


Figure B-48 Modelled SSC from pile drilling, example plume 6 hours after drilling the second structure

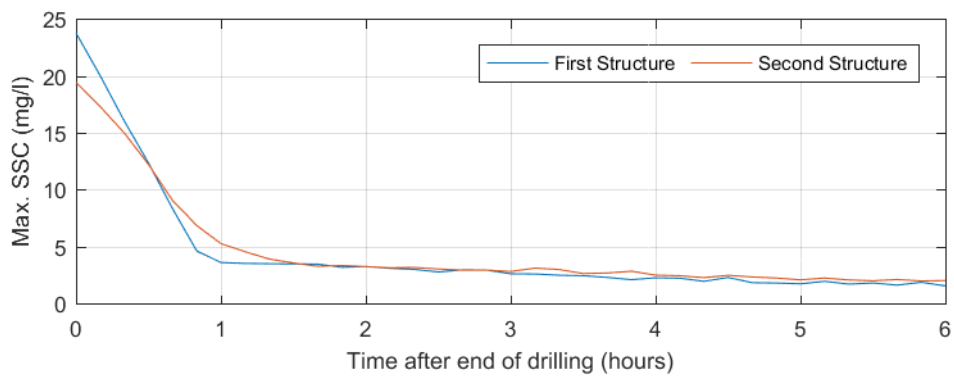


Figure B-49 Decay in SSC plume concentration associated with pile drilling



## B.4.4 In-combination

As for pile drilling and bedform clearance in the OAA, there is a very small area with an increase in SSC of more than 1 mg/l visible on the 80<sup>th</sup> percentile SSC for the in-combination construction scenario. The 99<sup>th</sup> percentile and maximum SSC over the 15.5-day period over which construction activities were simulated are shown for the in-combination construction scenario in Figure B-50. In addition, a plot of sedimentation at the end of the simulation is shown in Figure B-51. As noted from the assessments for individual construction activities, when considering the plots, it is important to note that over the model simulation only a small proportion of the required activities is completed. The plots show the following:

- The 99<sup>th</sup> percentile SSC shows peaks in SSC of more than 20 mg/l where the piles are located (i.e., where the drilling is being undertaken) and peaks of around 10 mg/l along the track where bedform clearance by CFE was simulated in the model (Figure B-50). No clear increase in SSC along the track where cable burial was simulated is evident in the 99<sup>th</sup> percentile SSC;
- Increases in peak SSC rapidly reduce to less than 4 mg/l away from the piles and the CFE bedform clearance track (Figure B-50). The 99<sup>th</sup> percentile increases in SSC of more than 2 mg/l extend over an area approximately 12 km to east-west and approximately 10 km north-south (Figure B-50);
- The maximum SSC shows a similar extent to the 99<sup>th</sup> percentile, but with the track where cable burial was simulated also visible (Figure B-50). This indicates that the plume from the cable burial is relatively short-lived while the plumes from the drilling and bedform clearance are more sustained; and
- The extent of the areas with sedimentation of more than 0.1 mm are predicted to be very similar to the extent of the maximum SSC of more than 1 mg/l. The highest sedimentation (>2 mm) lies directly along the bedform clearance track. Elsewhere, sedimentation remains below 1 mm (Figure B-51).

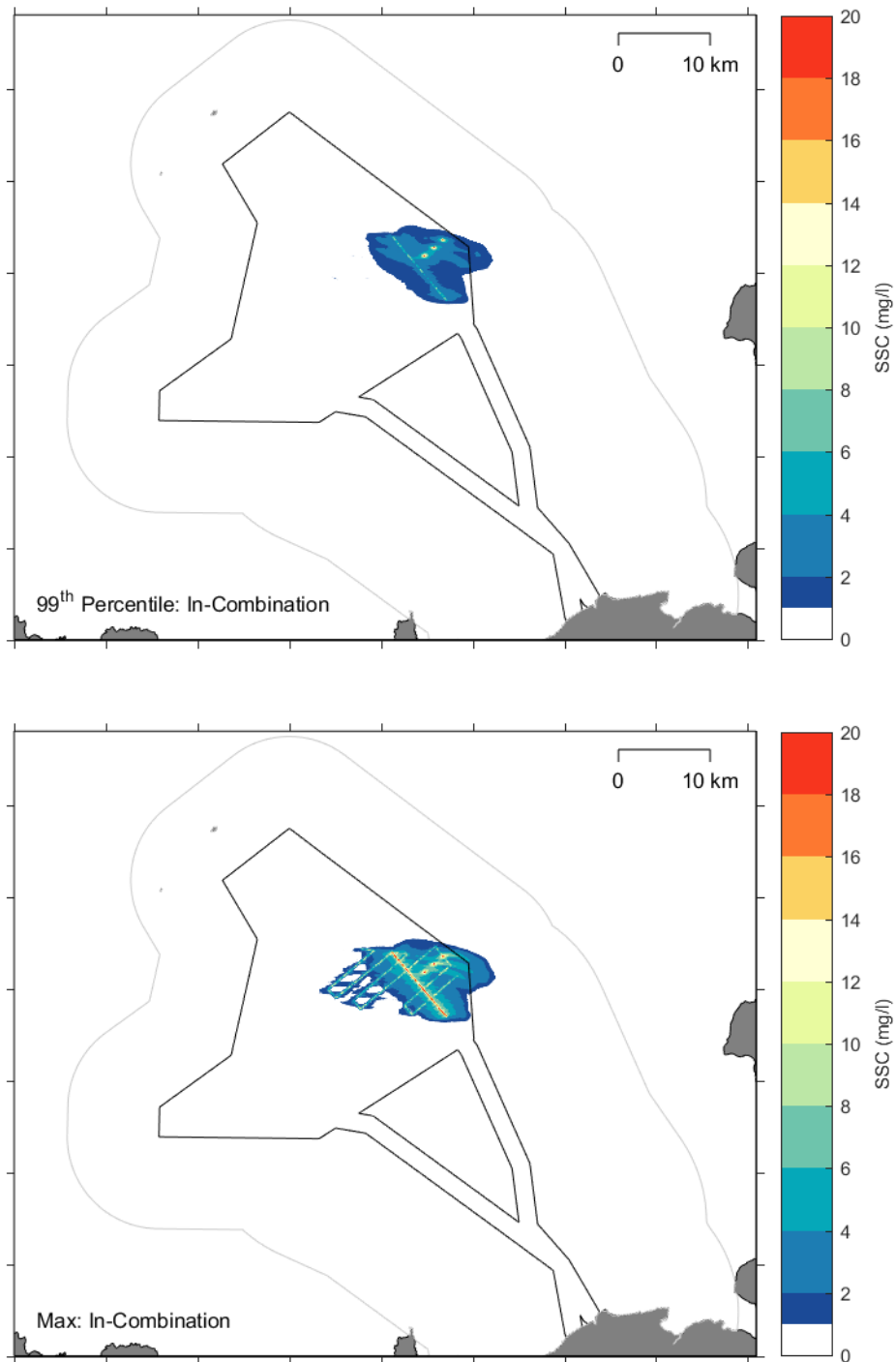


Figure B-50 Modelled 99<sup>th</sup> percentile (top) and maximum (bottom) SSC from the in-combination construction scenario

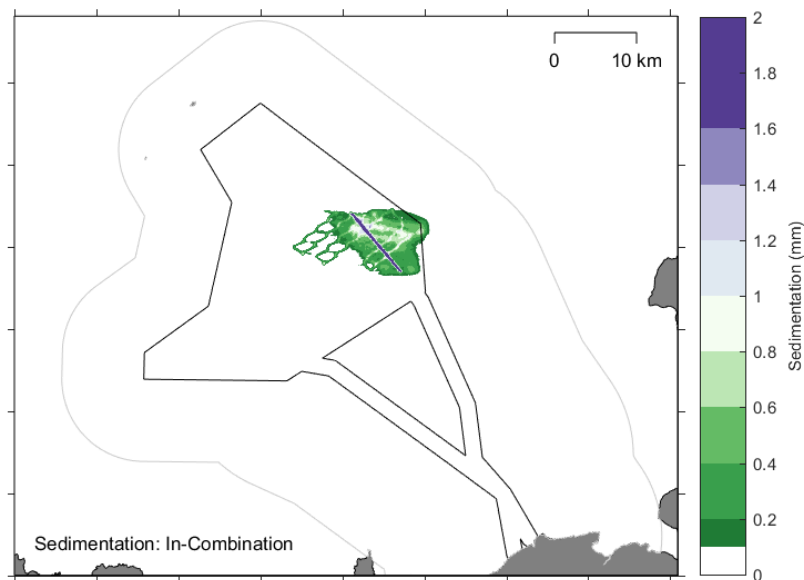


Figure B-51 Modelled sedimentation from the in-combination construction scenario

Time series plots of the SSC and sedimentation at selected model extraction locations (Figure 2-4) over the 16-day model simulation have been created. The plots show very little or no SSC or sedimentation at the majority of the sites and only the sites with largest predicted impacts are presented. Time series plots are shown for OAA6 and OAA11 in Figure B-52 and Figure B-53, respectively. For context, OAA6 lies within 420 m of the cable burial track, within 1.5 km of the bedform clearance track and within 3 km of the closest (first) structure drilled in the model simulation and OAA11 lies within 2.2 km of the cable burial track, 2 km of the bedform clearance track and within 5 km of the closest structure drilled. The plots show the following:

- There are frequent increases in SSC which occur for similar durations as seen for pile drilling. Increases in SSC are typically around 1 mg/l at OAA6 and OAA11, with some shorter duration peaks of more than 2 mg/l occurring when the first (closest) structure was being drilled. The duration of the elevated SSC at the site due to the drilling will be controlled by the tidal currents, with the elevated SSC only occurring for the duration when the tidal current is flowing from the pile drilling location to the site and when the current is strong enough to transport the suspended sediment that distance;
- The increases in SSC at OAA6 and OAA11 are less than for just the pile drilling since different structures (in closer proximity to the extraction points) were considered for that scenario. The periods of higher SSC and the highest rate of sedimentation coincide with the drilling of the closest structure (from midday on the 21<sup>st</sup> January to 2 am on the 27<sup>th</sup> January); and
- The sedimentation at OAA6 and OAA11 shows a consistent increase over the 5-to-6-day period of the simulation when drilling was at the monopile closest to the extraction point and a more gradual rate of sedimentation when drilling was occurring at other structures. The final sedimentation depth at OAA11 at the end of the model simulation is approximately 0.3 mm.

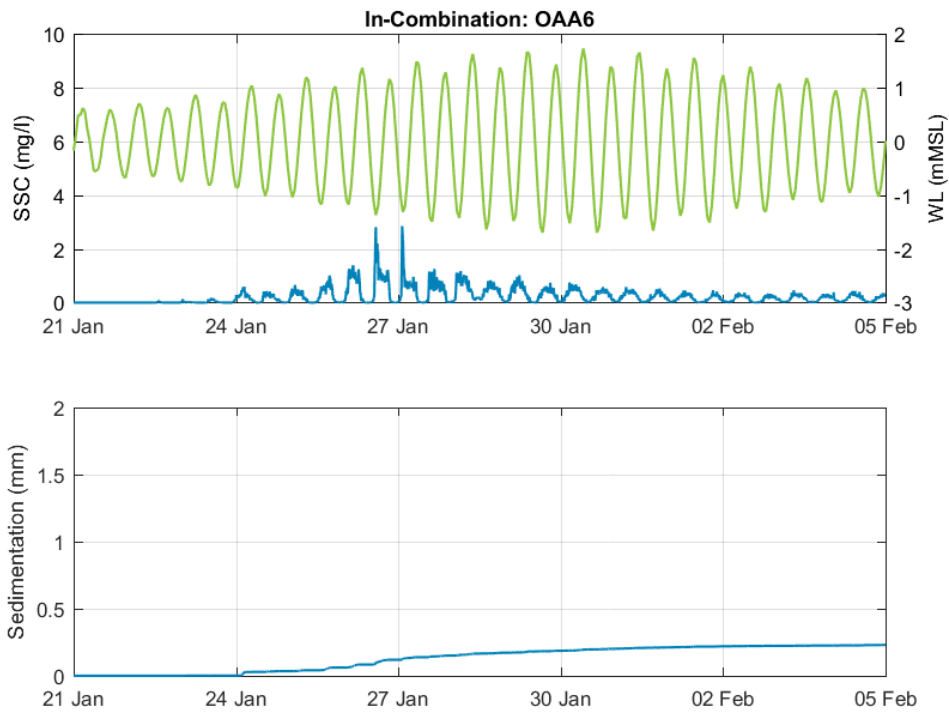


Figure B-52 Modelled SSC and sedimentation at OAA6 the in-combination construction scenario

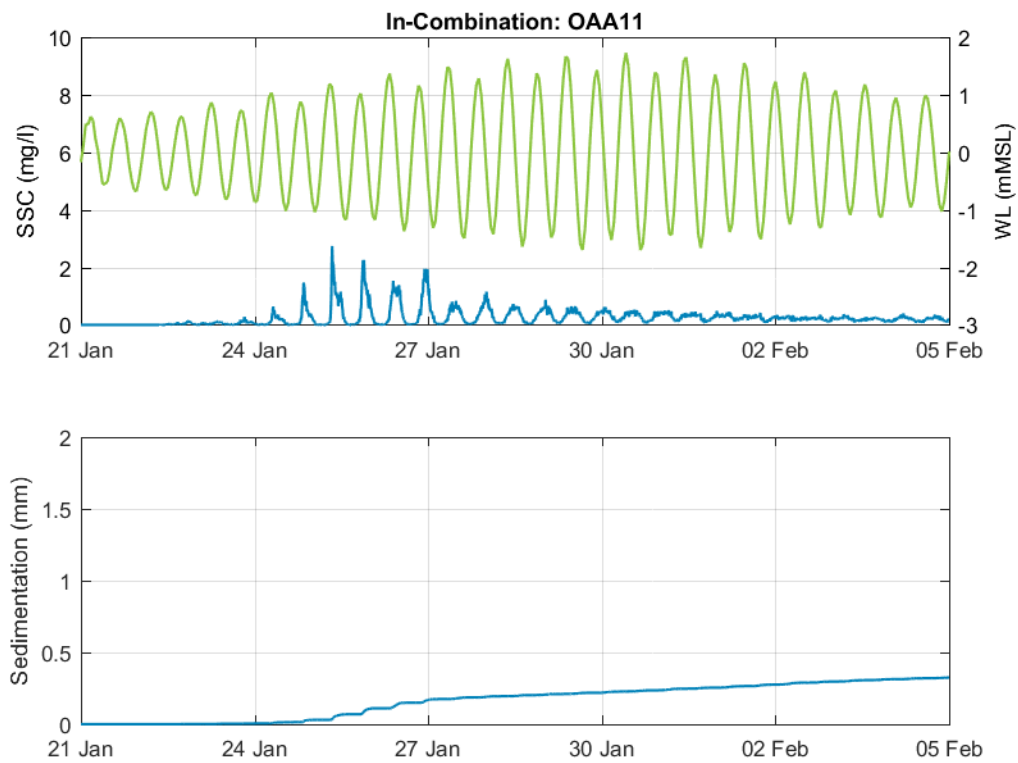


Figure B-53 Modelled SSC and sedimentation at OAA11 the in-combination construction scenario



## B.5 Operational Impacts

This section provides details of the potential operational impacts resulting from the WTG and OSP foundations. Results showing the predicted impacts of the structures on water levels and current from the HD model simulations and on waves from the SW model simulations are presented in the following sections.

### B.5.1 Hydrodynamic Impacts

The HD model was setup to simulate a 15 day spring-neap period for the baseline and the two offshore Project scheme configurations (layouts 1 and 2). Comparisons between the results from the scheme and baseline model setups have been made to determine the potential impacts of the development on water levels and currents in and around the OAA. The change in the maximum water level in each model element over the model simulation due to the two layouts was calculated but the results showed no changes of more than  $\pm 0.001$  m, which would be indiscernible from natural variation. This means that there are not predicted to be any changes in water levels within the study area at any stage of the tide under spring and neap conditions for either Layout 1 or Layout 2. Some areas of localised areas with changes of less than  $\pm 0.005$  m are predicted in some of the small bays and tidal lochs along the mainland and Orkney Islands. These changes vary depending on the tidal state, suggesting that the changes are due to a small change in phase of the tidal signal resulting in localised instantaneous changes to water level as opposed to actual reductions or increases in absolute water levels. Due to the location of these changes it is expected that they result from the flooding and drying of cells in shallow water and are not representative of impacts from the offshore Project area.

The change in current speed due to the two layouts over the region are shown for mean spring and mean neap tides in Figure B-54 and Figure B-56 (for Layout 1 spring and neap tides respectively) and Figure B-57 and Figure B-59 (for Layout 2 spring and neap tides respectively). Zoomed in plots of the OAA region for spring tides are shown in Figure B-55 and Figure B-58 for Layout 1 and Layout 2 respectively. Zoomed in plots of the change in the maximum current speed in each model element over the model simulation due to the two layouts are shown in Figure B-60. Plots of the change in the current speed residual over a 15 day spring neap tidal cycle as a result of the two layouts are shown in Figure B-61 and Figure B-62 for Layout 1 and Layout 2 respectively. A summary of the results in relation to both layouts 1 and 2 are presented below, except where reference is explicitly made to a particular layout:

- Across most of the OAA and surrounding area, there are no changes to peak and residual flows above 0.001 m/s (Figure B-60, Figure B-61 and Figure B-62);
- There are small, localised changes of both increases and decreases in current speed predominantly constrained within the OAA. The areas where increases and decreases in current speed occur change with tidal state. The magnitude of change is typically less than 0.002 m/s (Figure B-54 and Figure B-56 (for Layout 1 spring and neap tides respectively) and Figure B-57 and Figure B-59 (for Layout 2 spring and neap tides respectively));
- There are some localised areas where increases and decreases in current speed are predicted away from the OAA. These are located adjacent to the mainland and Orkney Islands shorelines and within the Pentland Firth (Figure B-54 and Figure B-56 (for Layout 1 spring and neap tides respectively) and Figure B-57 and Figure B-59 (for Layout 2 spring and neap tides respectively)). As the changes show increases and decreases directly adjacent



to each other (i.e. no area with zero change between) the changes are likely to be a numerical artefact resulting from flooding and drying and plotting the changes down to a very small difference (0.001 m/s) rather than an actual change;

- The increases and decreases in current speed within the OAA cover a slightly larger area for layout 2 compared to layout 1 as the WTGs are spread over more of the OAA. The zoomed in plots showing the WTG locations help to highlight this (Figure B-55 and Figure B-58 for Layout 1 and Layout 2 respectively );
- The changes in current speed are predicted to be similar during spring and neap tides;
- In areas of change, the residual current is predicted to predominantly experience a reduction in current speed around the WTGs of less than 0.002 m/s (Figure B-61 and Figure B-62), although a slight increase is also predicted around the edges of the WTG region (Figure B-62); and
- Positive and negative changes are predicted in the residual current in most of the bays and lochs along the north coast of the mainland as well as a couple of locations around the Orkney Islands (Figure B-61 and Figure B-62). However, as with the changes in current speed where there was no area with zero change between the positive and negative changes, the changes are likely to be a numerical artefact resulting from plotting the changes down to a relatively small difference rather than an actual change.

Time series showing the changes in hydrodynamics due to the two WTG layouts (1 and 2) have been extracted and analysed at the model extraction locations (Figure 2-4). The change in water level plots consistently showed negligible changes at all sites for both layouts, with maximum differences of less than 0.0005 m. The changes to current speed and direction are small but vary spatially and between the two layouts and so plots of the changes at selected sites within each layout and away from both layouts are shown in Figure B-63. Time series are shown at OAA1 and OAA2 which lie within layout 2 (but not within layout 1), at OAA4 and OAA16 which lie within layout 1 (but not within layout 2) and at ECC1 which is outside of both layouts. The time series plots show the following:

- The changes in current speed and direction are consistently small throughout the simulation period and the OAA, with changes of up to  $\pm 0.0025$  mm/s and  $\pm 1.5^\circ$ ;
- There is significant spatial variability in the changes. At OAA1 the flows are changed for layout 2 but not for layout 1, while at OAA2 the changes in flow are more similar for both layouts (even though both extraction points are within layout 2 and not within layout 1);
- The changes in both current speed and direction switch between being positive or negative depending on the state of the tide, showing that the overall net change is even smaller than the maximum changes noted above; and
- Changes at the extraction point outside of both WTG layouts are very similar for both layouts. The changes in current speed are less than 0.0005 m/s with similar positive and negative changes occurring. There is typically no change in current direction, but there are occasional short duration spikes which coincide with periods of slower flows when the tide is changing.



### B.5.1.1 Layout 1 Modelled Flow Speed Difference

#### B.5.1.1.1 Spring

Absolute difference in flow speed post-construction (m/s)

Percentage difference in flow speed post-construction (%)

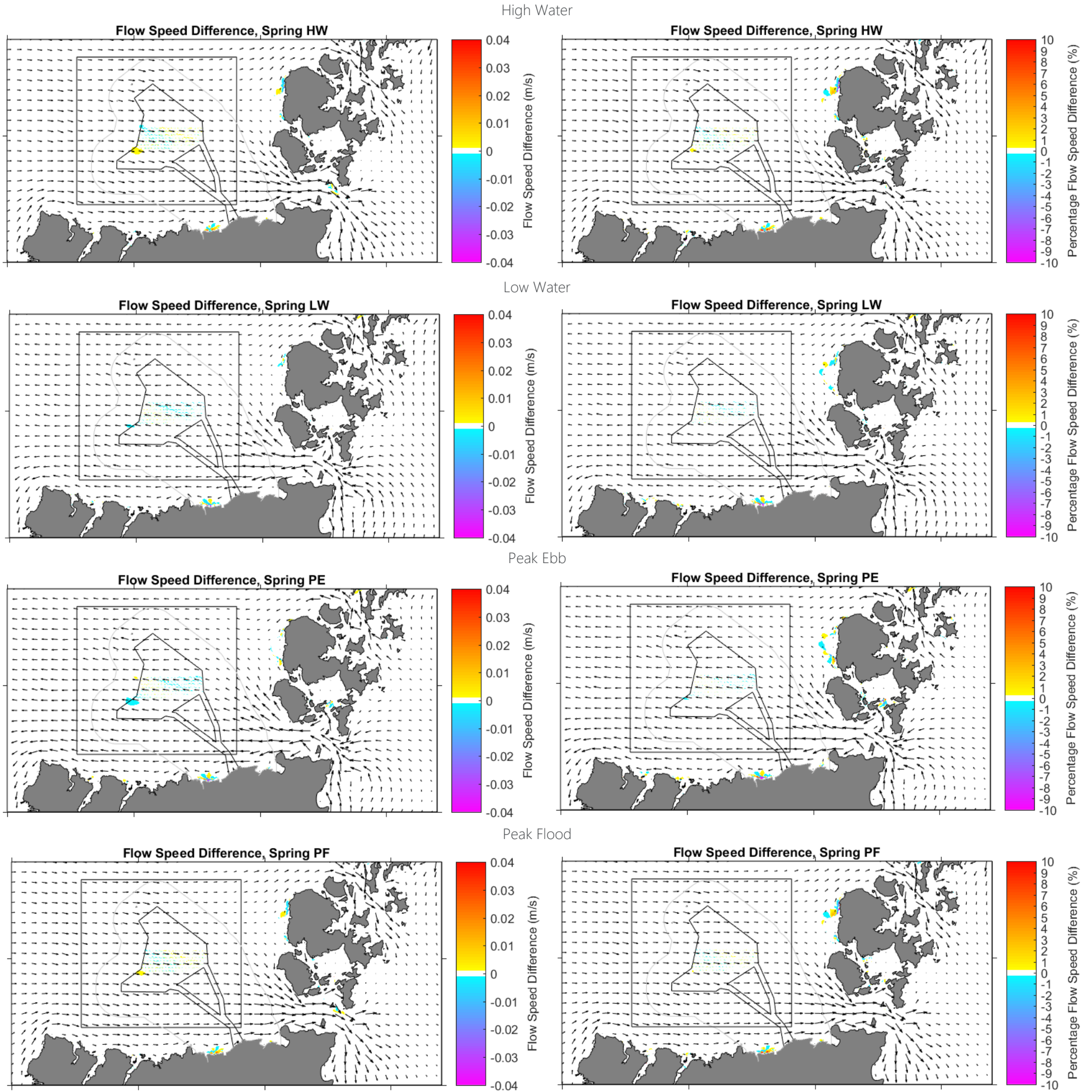


Figure B-54 Modelled absolute and percentage change at varying tidal stages in the OAA during a mean spring tide for layout 1<sup>19</sup>

<sup>19</sup> Areas of change outside the OAA picked up by the model are not due to the presence of the WTGs, but instead relate to fluctuations in the model associated with the wetting and drying of model grid cells at the coast.

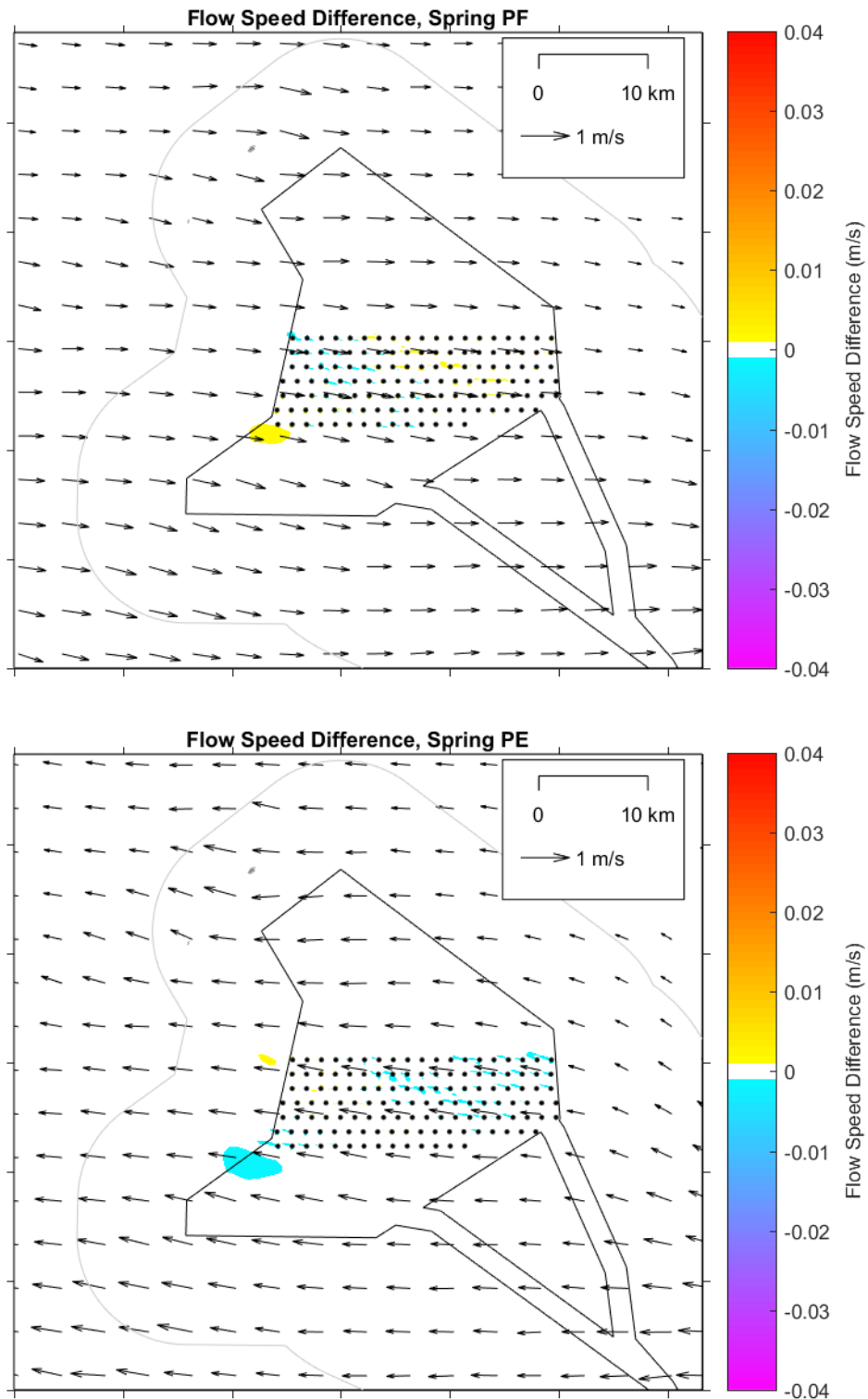


Figure B-55 Modelled change in current speed at peak flood and peak ebb in the OAA during a mean spring tide for layout 1, zoomed across the OAA



B.5.1.1.2 Neap

Absolute difference in flow speed post-construction (m/s)

Percentage difference in flow speed post-construction (%)

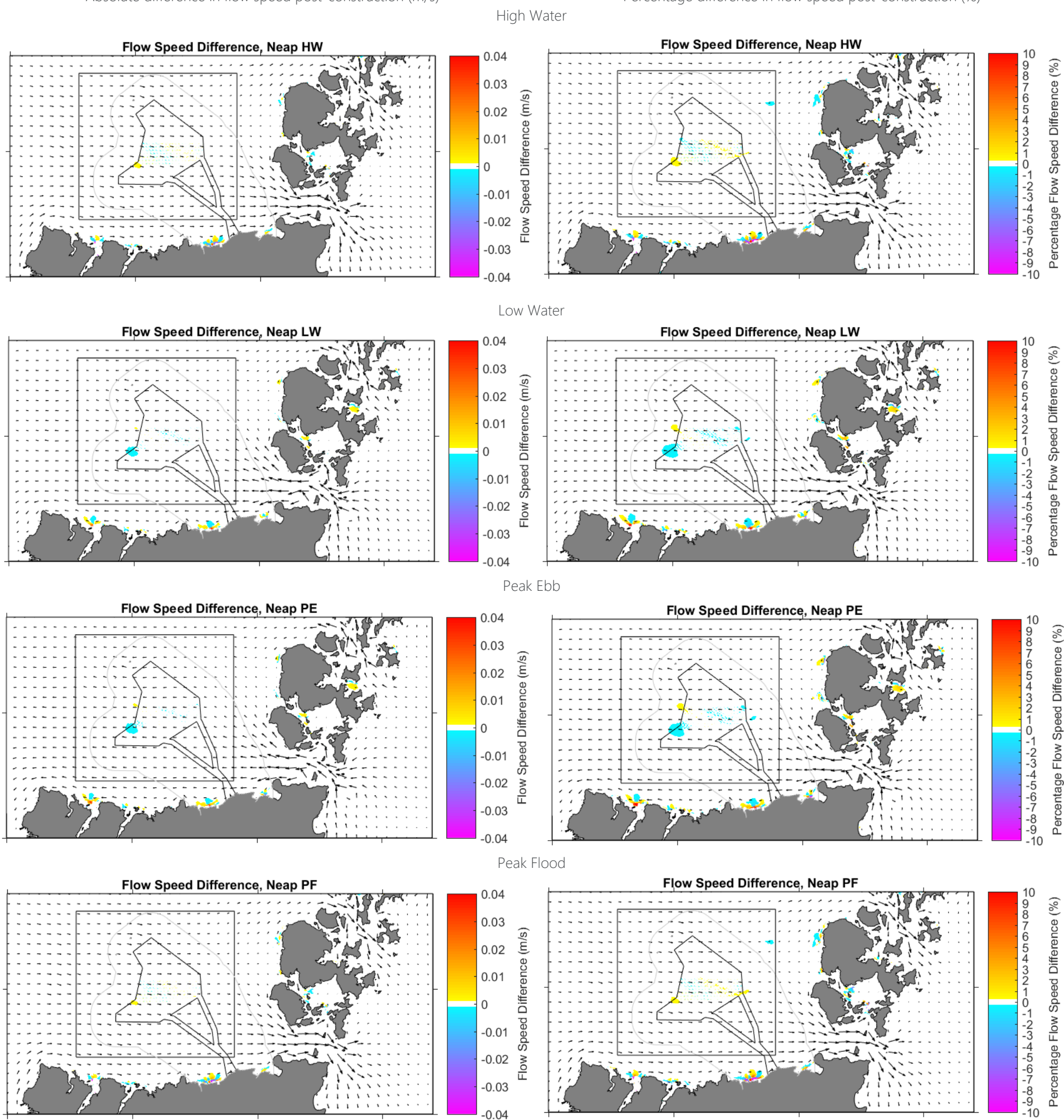


Figure B-56 Modelled absolute and percentage change at varying tidal stages in the OAA during a mean neap tide for layout 1



### B.5.1.2 Layout 2 Modelled Flow Speed Difference

#### B.5.1.2.1 Spring

Absolute difference in flow speed post-construction (m/s)

Percentage difference in flow speed post-construction (%)

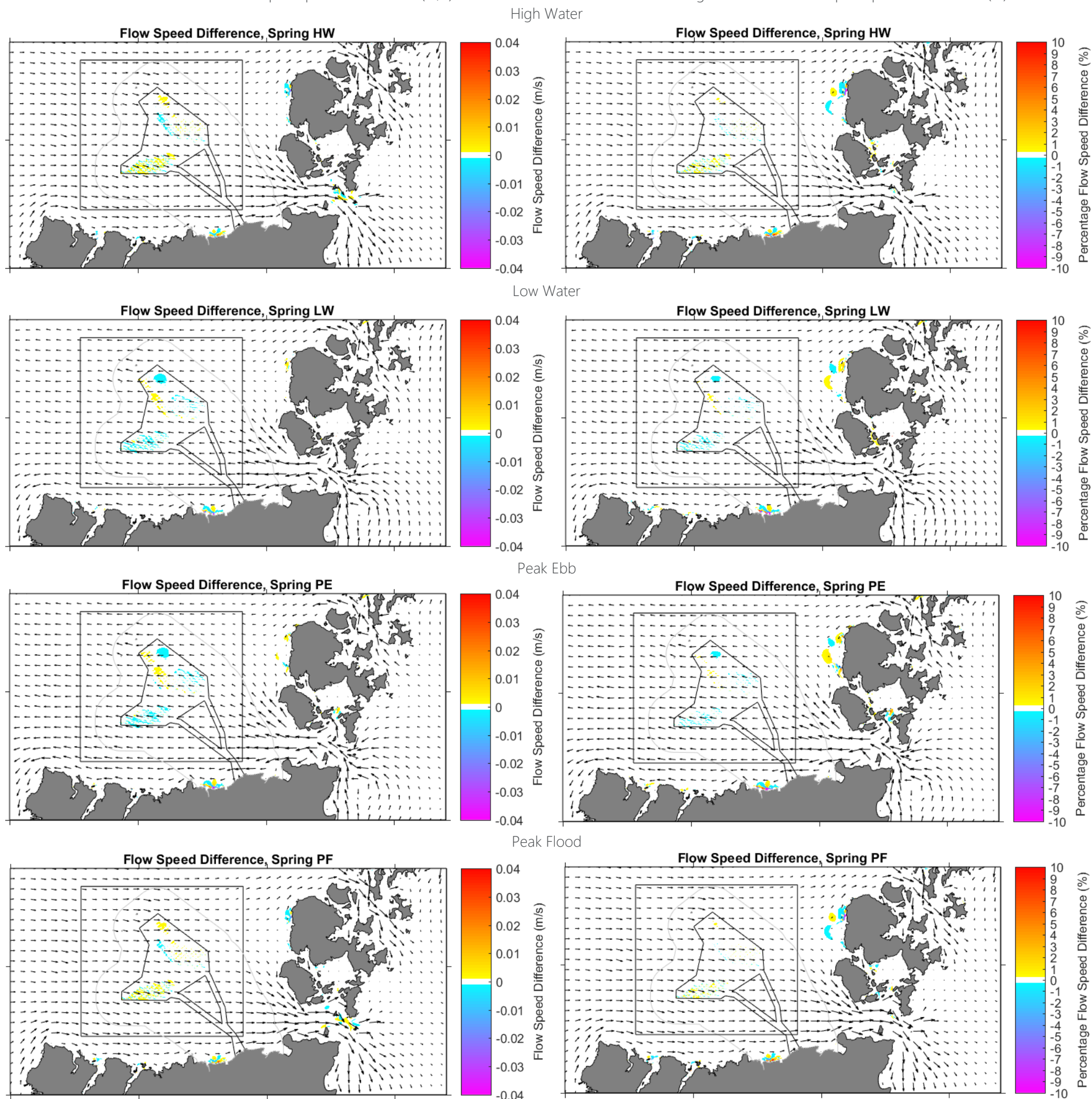


Figure B-57 Modelled absolute and percentage change at varying tidal stages in the OAA during a mean spring tide for layout 2

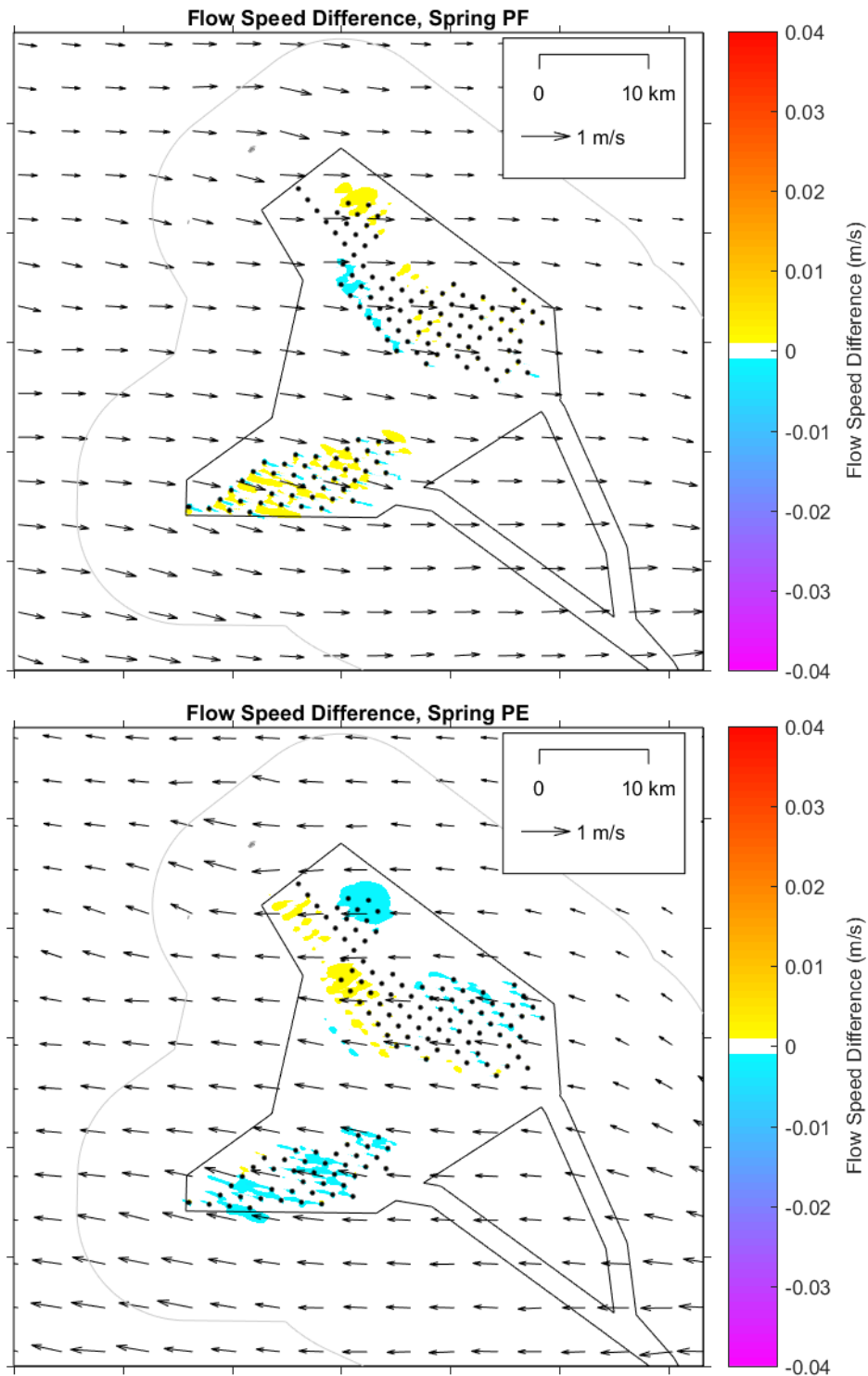


Figure B-58 Modelled change in current speed at peak flood and peak ebb in the OAA during a mean spring tide for layout 2, zoomed across the OAA



B.5.1.2.2 Neap

Absolute difference in flow speed post-construction (m/s)

Percentage difference in flow speed post-construction (%)

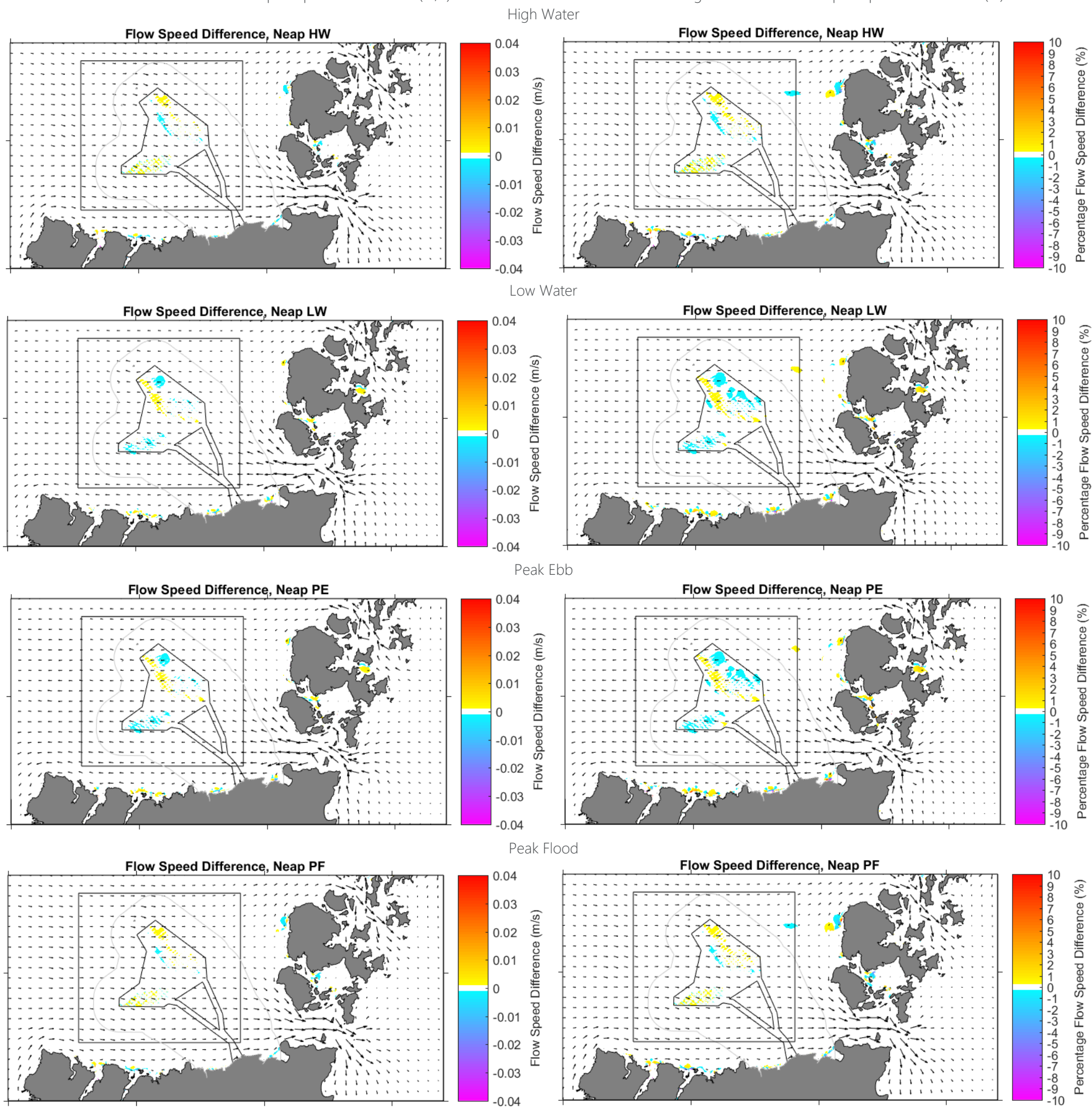


Figure B-59 Modelled absolute and percentage change in current speed at varying tidal stages in the OAA during a mean neap tide for layout 2



### B.5.1.3 Modelled Maximum and Residual Flow Speed Difference

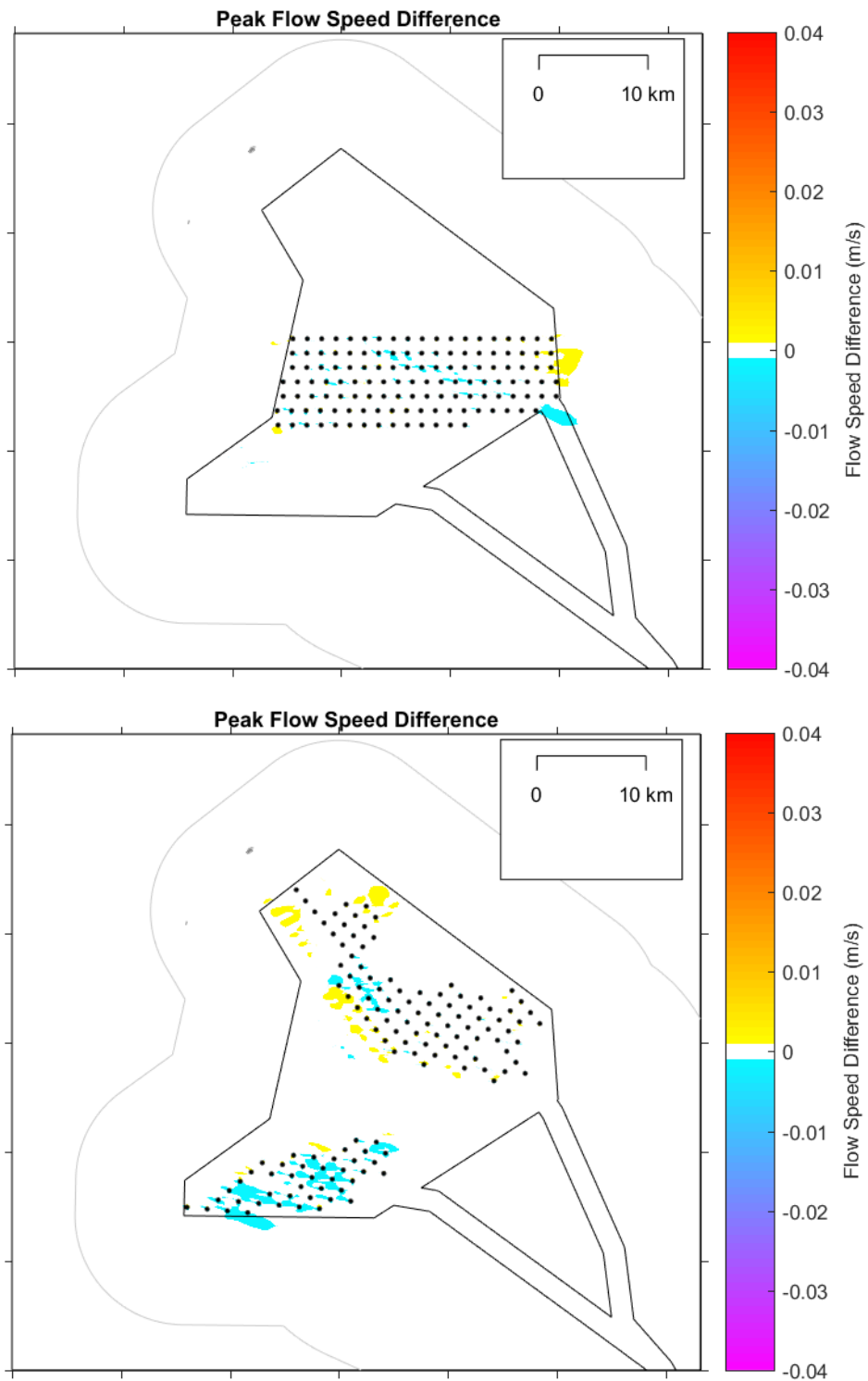


Figure B-60 Modelled change in maximum current speed over the 15 day simulation in the OAA for layout 1 (top) and layout 2 (bottom).

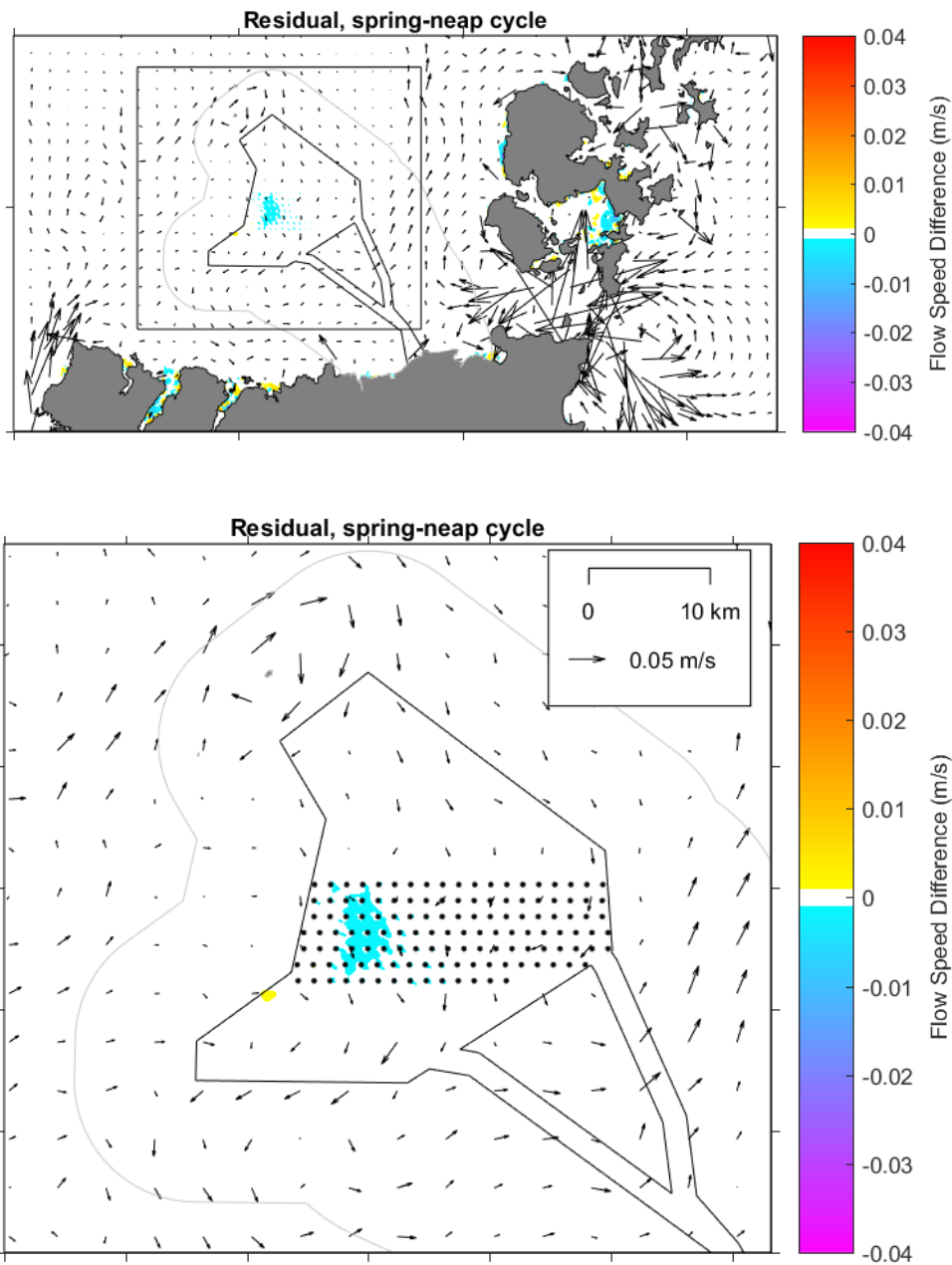


Figure B-61 Modelled change in residual current speed over a spring neap tidal cycle for layout. Colours illustrate the post-construction flow speed difference, while the vectors illustrate the baseline residual flow speed and direction<sup>20</sup>

<sup>20</sup> Areas of change outside the OAA picked up by the model (as represented in the model results in Figure 6 1 and Figure 6 2) are not due to the presence of the WTGs, but instead relate to fluctuations in the model associated with the wetting and drying of model grid cells at the coast.

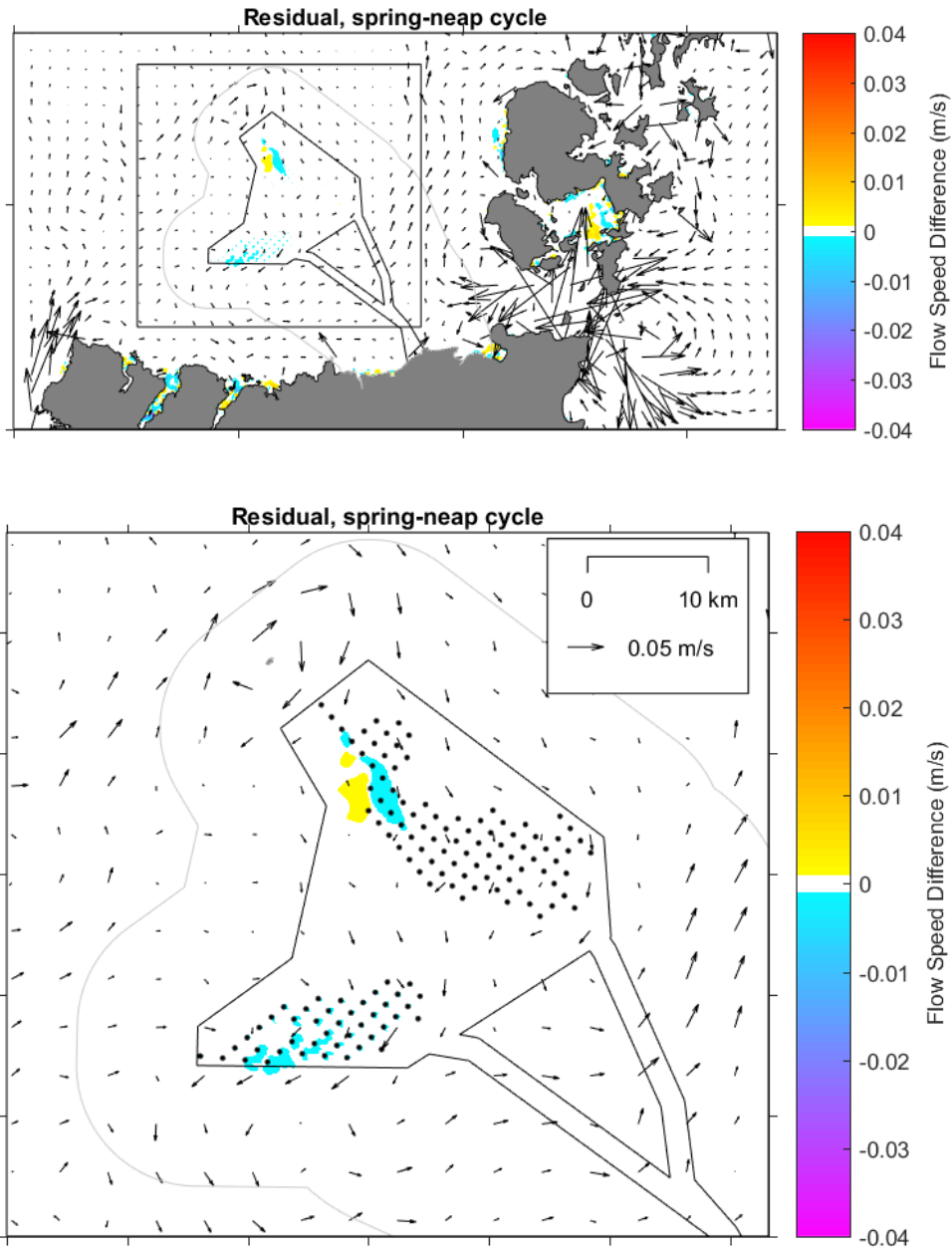


Figure B-62 Modelled change in residual current speed over a spring neap tidal cycle for layout 2. Colours illustrate the post-construction flow speed difference, while the vectors illustrate the baseline residual flow speed and direction <sup>18</sup>



### B.5.1.4 Layout 2 Modelled Flow Speed Difference

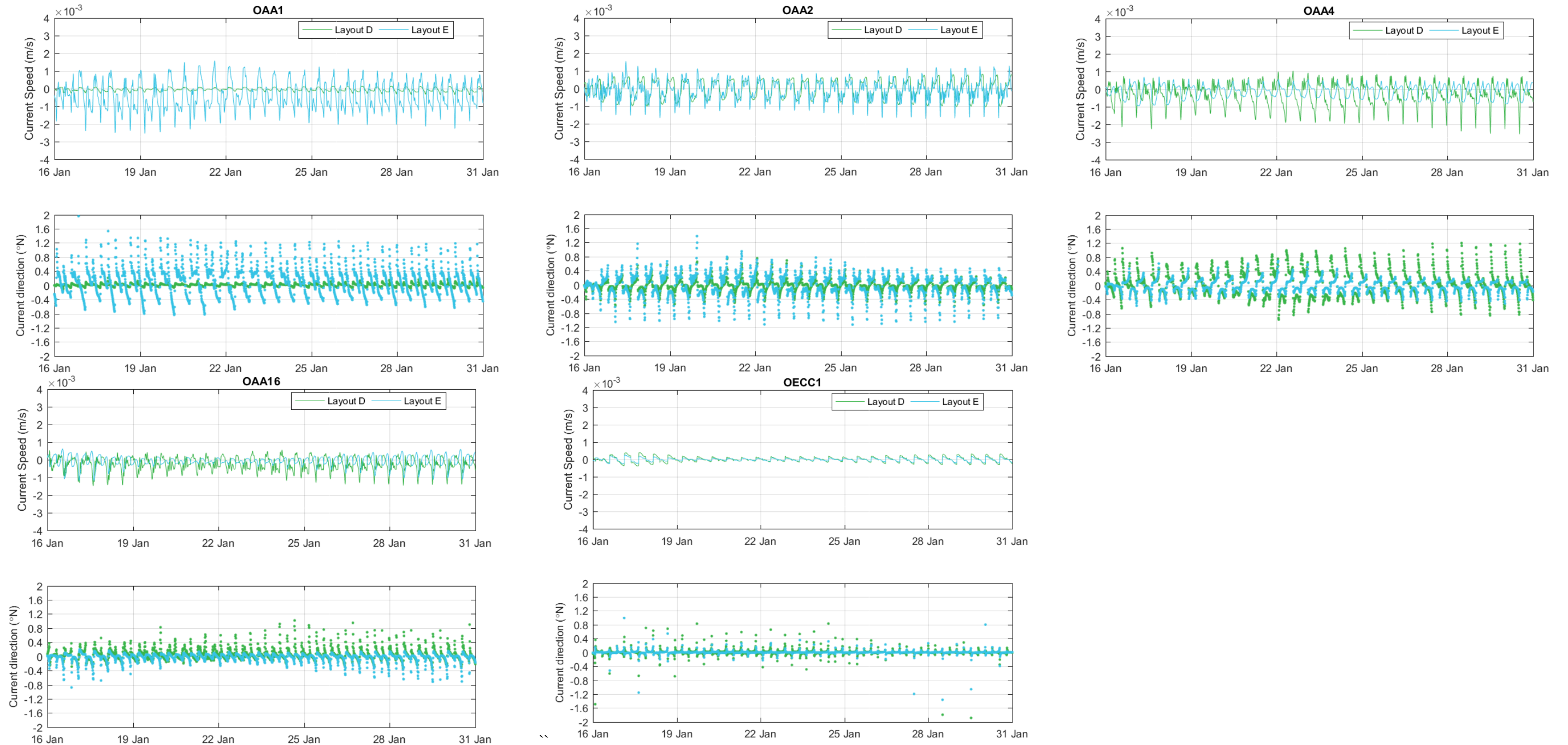


Figure B-63 Modelled change in current speed and direction at (upper panels left to right) OAA1 (within Layout 2), OAA2 (within Layout 2), OAA4 (within layout 1) (lower panels left to right) OAA16 (within Layout 1) and ECC1 due to layouts 1 and 2.



## B.5.2 Wave Impacts

The SW model was setup to simulate wave conditions ranging from the 50<sup>th</sup> percentile to the 1 in 100 year ARI for the baseline and the two offshore Project scheme configurations (layouts 1 and 2) for wave directions from the west, north-west and north. Comparison between the results from the scheme and baseline model setups have been made to determine the potential impacts of the development on wave conditions in and around the study area. Changes in  $H_s$  for the 90<sup>th</sup> percentile wave conditions and the 1 in 100 year ARI wave conditions due to the two layouts are shown in Figure B-64 and Figure B-65. These plots provide an overview of the wave modelling results, showing results for typical waves (90<sup>th</sup> percentile) and extreme waves (100 year ARI). The plots show that waves from the north result in the largest changes in  $H_s$  and so zoomed in plots of the OAA showing the associated percentage change in  $H_s$  relative to baseline conditions are shown for the two layouts for the 90<sup>th</sup> percentile and 100 year ARI waves from the north in Figure B-66. The model results show the following:

- Changes in  $H_s$  due to the two layouts are predicted to be relatively small, with changes less than  $\pm 0.05$  m for both typical and extreme waves;
- The blockage caused by the WTG structures are predicted to result in a small increase in  $H_s$  on the side of the WTGs exposed to the oncoming wave direction due to reflections off the circular WTGs and a small reduction in  $H_s$  on the opposite side of the WTGs in the lee of the oncoming wave direction due to the WTGs providing some sheltering;
- Layout 1 is predicted to result in a larger area of increases and decreases in  $H_s$  compared to Layout 2. This is due to all the WTGs being located in one region resulting in a slightly larger impact to the waves; and
- Relative to the baseline wave conditions, the spatial maps show that changes in  $H_s$  are less than 1.5% outside of the OAA for the 90<sup>th</sup> percentile wave conditions and less than 0.5% throughout for the 100 year ARI.

Wave conditions have been extracted from the wave model at 28 locations around the OAA and offshore ECC for all modelled wave conditions for the baseline and two layouts. A comparison between the baseline and post-construction layouts show that  $T_p$  is not predicted to change at any of the locations, while the maximum change in wave direction was  $\pm 0.3^\circ$ . Changes in  $H_s$  of up to  $\pm 1.3\%$  are predicted within the OAA, while changes of up to  $\pm 0.5\%$  are predicted within the offshore ECC for the 90<sup>th</sup> percentile wave conditions. For the larger 100 year ARI wave event, the changes were less than 0.5% at all locations. Results of the modelled absolute significant wave height difference, absolute peak wave period difference and percentage significant wave height difference are shown for the varying wave approach directions and ARI events in section B.9.2 for Layout 1 and Section B.9.3 for Layout 2. Additional zoomed results of the percentage significant wave height difference covering the OAA for all ARI waves are also provided in Section B.9.2.4 for Layout 1 and Section B.9.3.4 for Layout 2.

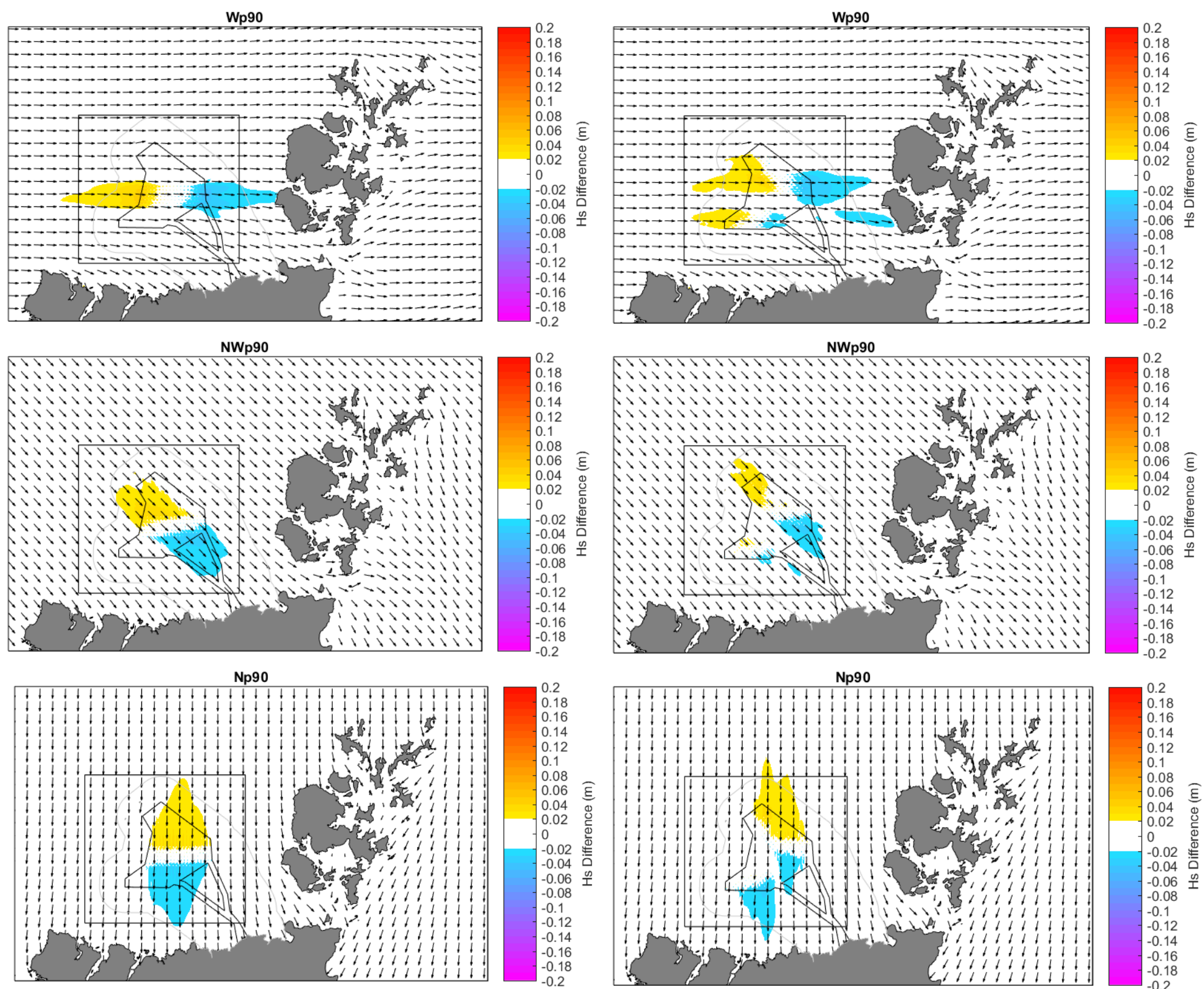


Figure B-64 Modelled change in wave height due to layout 1 (left hand panels) and layout 2 (right hand panels) for the 90<sup>th</sup> percentile wave condition from the west (upper panels), north-west (middle panels) and north (lower panels).

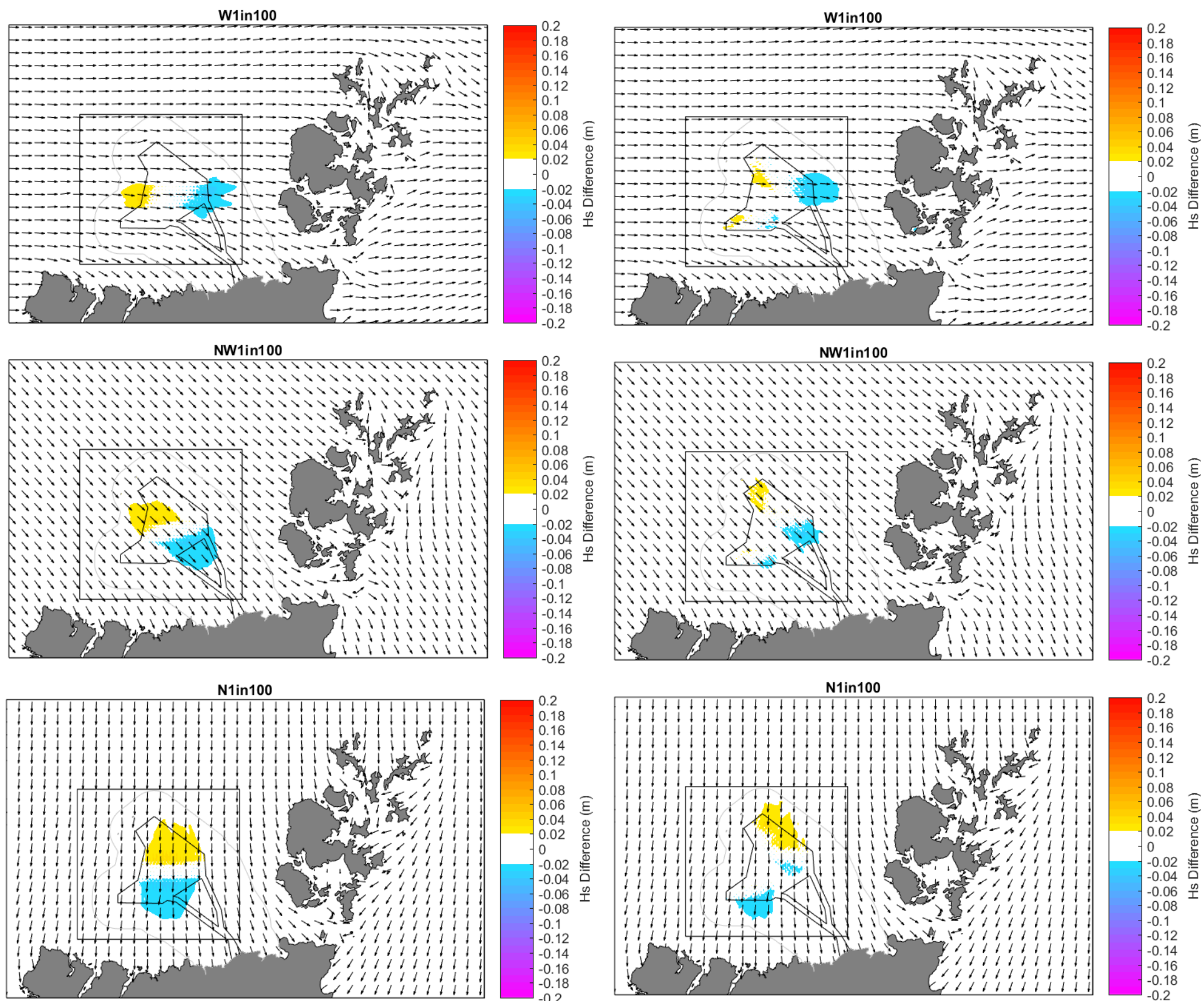


Figure B-65 Modelled change in wave height due to layout 1 (left hand panels) and layout 2 (right hand panels) for the 1 in 100 year ARI wave condition from the west (upper panels), north-west (middle panels) and north (lower panels).

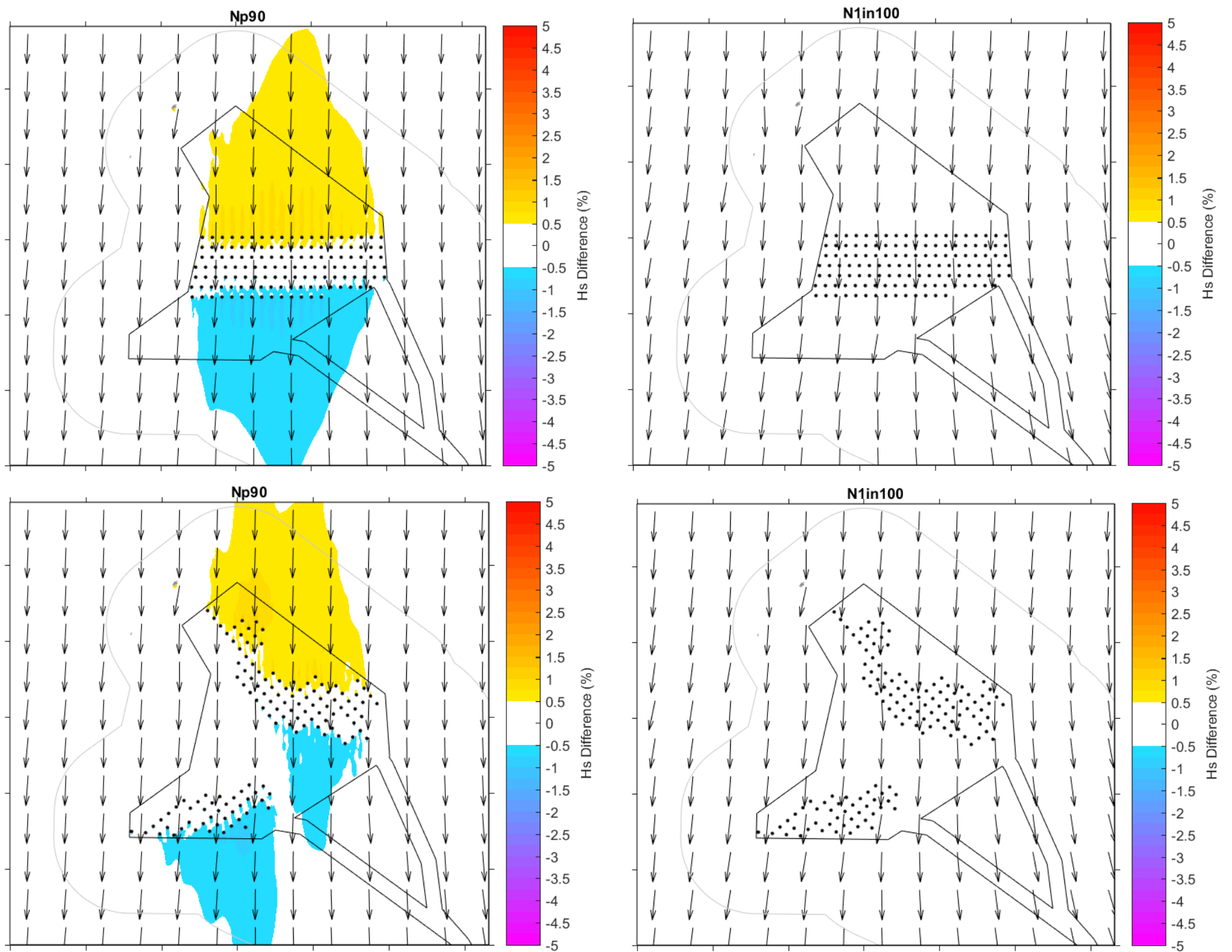


Figure B-66 Modelled percentage change in wave height relative to the baseline conditions due to layouts 1 (top) and 2 (bottom) for the 90<sup>th</sup> percentile wave condition from the north (left hand panels) and for the 1 in 100 year ARI wave conditions from the north (right hand panels).



## B.6 Summary

This technical report has presented results from a suite of numerical models to inform a marine physical processes assessment of the offshore Project. Results from numerical models which simulate tidal flow, waves and sediment dispersion have been presented to characterise the existing baseline conditions and to assess the construction and operational impacts on marine coastal processes.

Results from the characterisation of the existing baseline metocean conditions in the area have shown that:

- The largest tidal range (i.e. lowest low water and highest high water) occurs along the shoreline adjacent to the north coast of Scotland which includes part of the offshore ECC. The tidal range reduces in a northerly direction across the study area, with a mean spring tidal range of 4 m at the offshore ECC adjacent to the shoreline reducing to 3.2 m at the northern end of the study area. The mean neap tidal range is predicted to be 2 m at the offshore ECC adjacent to the shoreline and 1.6 m at the northern end of the study area;
- Within the OAA and offshore ECC the PF stage of the tide occurs close to HW while the PE stage of the tide occurs close to LW;
- Within the study area the flood currents are to the east and the ebb currents are to the west;
- The highest current speeds in the region occur in the Pentland Firth, with speeds of more than 3 m/s occurring during spring tides and between 2 and 2.5 m/s during neap tides. Current speeds within the OAA and offshore ECC are less than 0.8 m/s during both spring and neap tides. The highest currents (peaks of 0.7 to 0.8 m/s) occur in the offshore ECC within 12 km of the shoreline;
- Residual flows in the OAA and offshore ECC are low, typically less than 0.05 m/s, except along the inshore section of the offshore ECC where residual flows are around 0.10 m/s.
- The largest waves are from a westerly direction and the smallest waves are from a northerly direction; and
- Wave height and wave direction are typically similar throughout the OAA, while within the offshore ECC there is a reduction in wave height from north to south. The wave direction in the offshore ECC has more potential to vary due to refraction occurring in the shallower water close to the shoreline.

Potential construction related impacts arising from the disturbance and dispersion of sediment in the marine environment were assessed for bedform clearance, cable burial and pile drilling. Two potential methods were considered for bedform clearance, dredging by TSHD and bed disturbance by CFE. Results from the modelling of the construction related impacts have shown that:

- Impacts for all construction activities (both in terms of SSC and sedimentation) were limited to an area within one tidal excursion (which is 7 km on a spring tide and approximately half this on a neap tide), although across most of the area changes in SSC and sedimentation were very low (< 4 mg/l and <1 mm);



- Bedform clearance by TSHD resulted in small localised and short lived increases in SSC, mainly as a result of the placement of the sediment within the OAA;
- Bedform clearance by CFE results in more extensive plumes which persist for longer durations due to the slow rate of clearance by this method compared to clearance by a TSHD;
- Bedform clearance by CFE along the offshore ECC is likely to result in deposition of up to around 1 mm at distances of approximately 6 km to the east of the cable corridor;
- Impacts from cable burial by CFE are of a lower magnitude (both in terms of SSC and sedimentation) than those from bedform clearance by CFE. This is a result of lower sediment disturbance rates, quicker transit times and a disturbance closer to the seabed; and
- Areas of increased SSC and sedimentation from pile drilling extend over an area which is greater than the distance between WTGs. The drilling of all structures in the OAA is therefore expected to result in sedimentation at greater depths than shown for the limited number of piles drilled in the modelling simulations.

Operational impacts for two different layouts for conical monopile structures which were deemed to provide the largest blockage to flows and waves and therefore have the potential to result in the largest impacts were also assessed. Results from the modelling of the blockage effect during operation showed that:

- Neither layout assessed resulted in any notable changes in water levels;
- Both layouts resulted in small, localised areas of increased and reduced flows, the magnitude of these changes were less than 0.002 m/s;
- changes in residual flows were constrained to a small area and represented a small change of less than 0.002 m/s;
- The area of impacted flow was slightly larger for layout 2 than for layout 1 due to the larger spread of the WTGs;
- Both layouts resulted in small changes to significant wave heights, these changes were predicted to be less than  $\pm 0.05$  m for both typical and extreme waves;
- The area with impacts to wave heights was larger for layout 1 than for layout 2. This was due to all the WTGs being located in one region resulting in a slightly larger impact to the waves; and
- Relative to the baseline wave conditions, the spatial maps show that changes in  $H_s$  were less than 1.5% outside of the OAA for the 90<sup>th</sup> percentile wave conditions and less than 0.5% throughout for the 100 year ARI.

Overall, the modelling results have predicted that the construction and operational impacts can be considered to be relatively small and are predominantly constrained within the OAA and offshore ECC areas. The construction works were predicted to have the potential to result in increases in SSC of more than 20 mg/l, but these were typically shown to be very localised to where the construction activity was being undertaken (i.e. within the OAA or offshore ECC areas). The persistence of elevated concentrations will depend on the duration of the activity. Although plots of



predicted changes in tidal flows and waves due to the proposed structures have been presented, these changes have typically been shown by plotting the changes down to a very small difference and based on the scale of the changes it is considered unlikely that any measurable changes will occur.

## B.7 References

ABPmer, (2008). Atlas of UK Marine Renewable Energy Resources, (2008). Available online at: ABPmer.. <http://www.renewables-atlas.info/> [Accessed 02/09/2022]

Becker, J., van Eekelen, Z., van Wichen, J., de Lange, W., Damsma, T., Smolders, T., and van Koningsveld, M., (2015). Estimating source terms for far field dredge plume modelling. *Journal of Environmental Management*, 149, 282-293.

Folk, R.L., (1954). The Distinction between Grain Size and Mineral Composition in Sedimentary-Rock Nomenclature. *The Journal of Geology*, 62, 344-359.

O'Hara Murray, R., Campbell, L., (2021). Pentland Firth and Orkney Waters Climatology 1.02. doi: 10.7489/12041-1

PCS, (2022). – Numerical modelling calibration report for West of Orkney Windfarm offshore EIA Report. Appendix A of this marine physical and coastal processes technical report,

## B.8 Acronyms

TERM	DEFINITION
ARI	Annual Recurrence Intervals
CD	Chart Datum
DHI	Danish Hydraulics Institute
DMPA	Dredge Material Placement Area
ECC	Export Cable Corridor
EIA	Environmental Impact Assessment
HD	Hydrodynamics
Hs	Significant Wave Height
HW	High Water
LW	Low Water
CFE	Controlled Flow Excavator
MS	Marine Scotland



TERM	DEFINITION
OAA	Option Agreement Area
OSP	Offshore Substation Platform
OWF	Offshore Wind Farm
OWPL	Offshore Wind Power Limited
PCS	Port and Coastal Solution
PE	Peak Ebb
PF	Peak Flood
PFOW	Pentland Firth and Orkney Waters
PSD	Particle Size Distribution
PT	Particle Tracking
SSC	Suspended Sediment Concentration
SW	Spectral Wave
TSHD	Trailer Suction Hopper Dredger
Tp	Peak Period
WOW	West of Orkney Windfarm
WTG	Wind Turbine Generator



## B.9 Additional Figures

### B.9.1 Baseline $H_s$ Map Plots

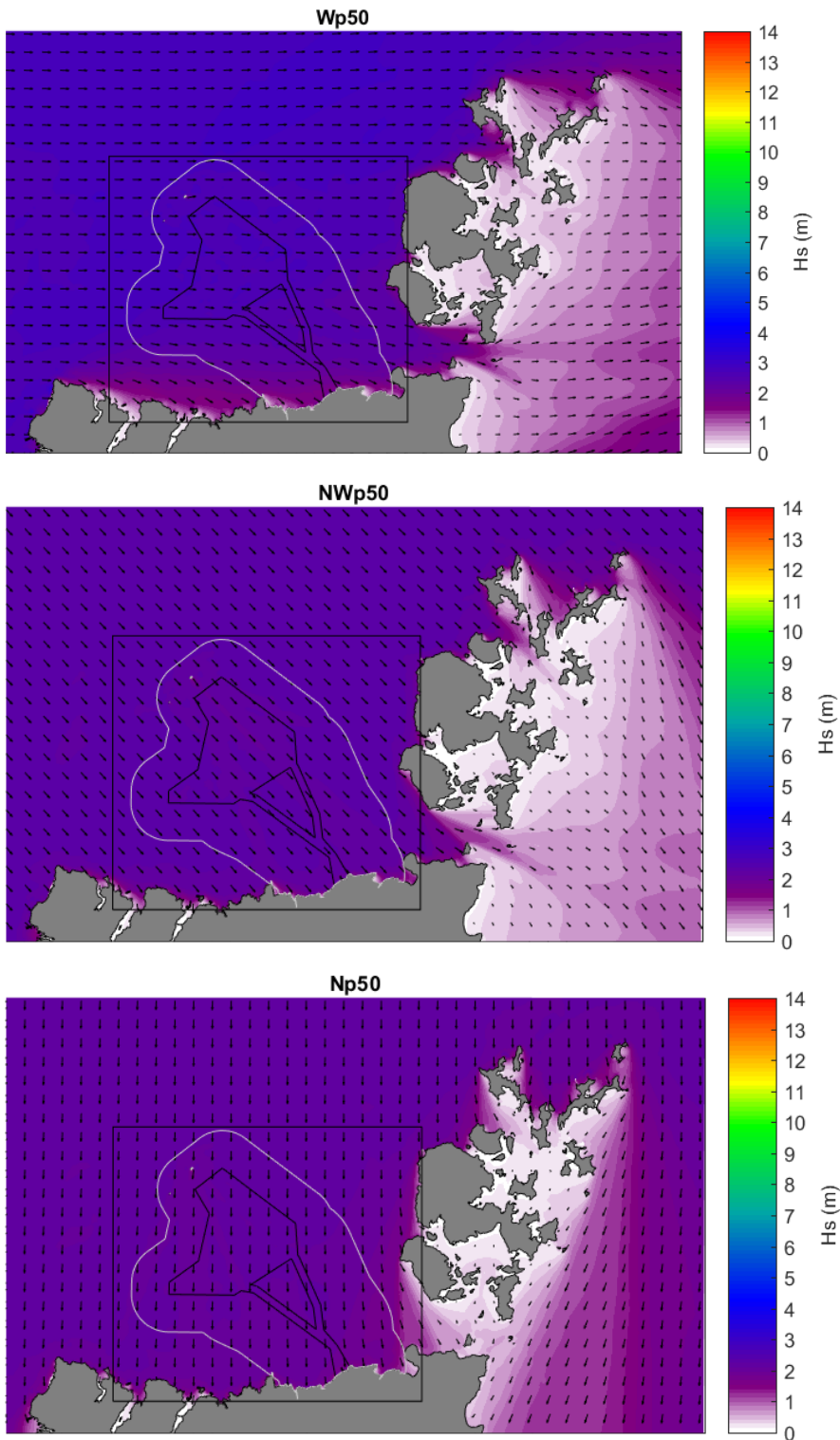


Figure B-67 Modelled wave height and wave direction for the 50<sup>th</sup> percentile wave condition from the west (top), north-west (middle) and north (bottom).

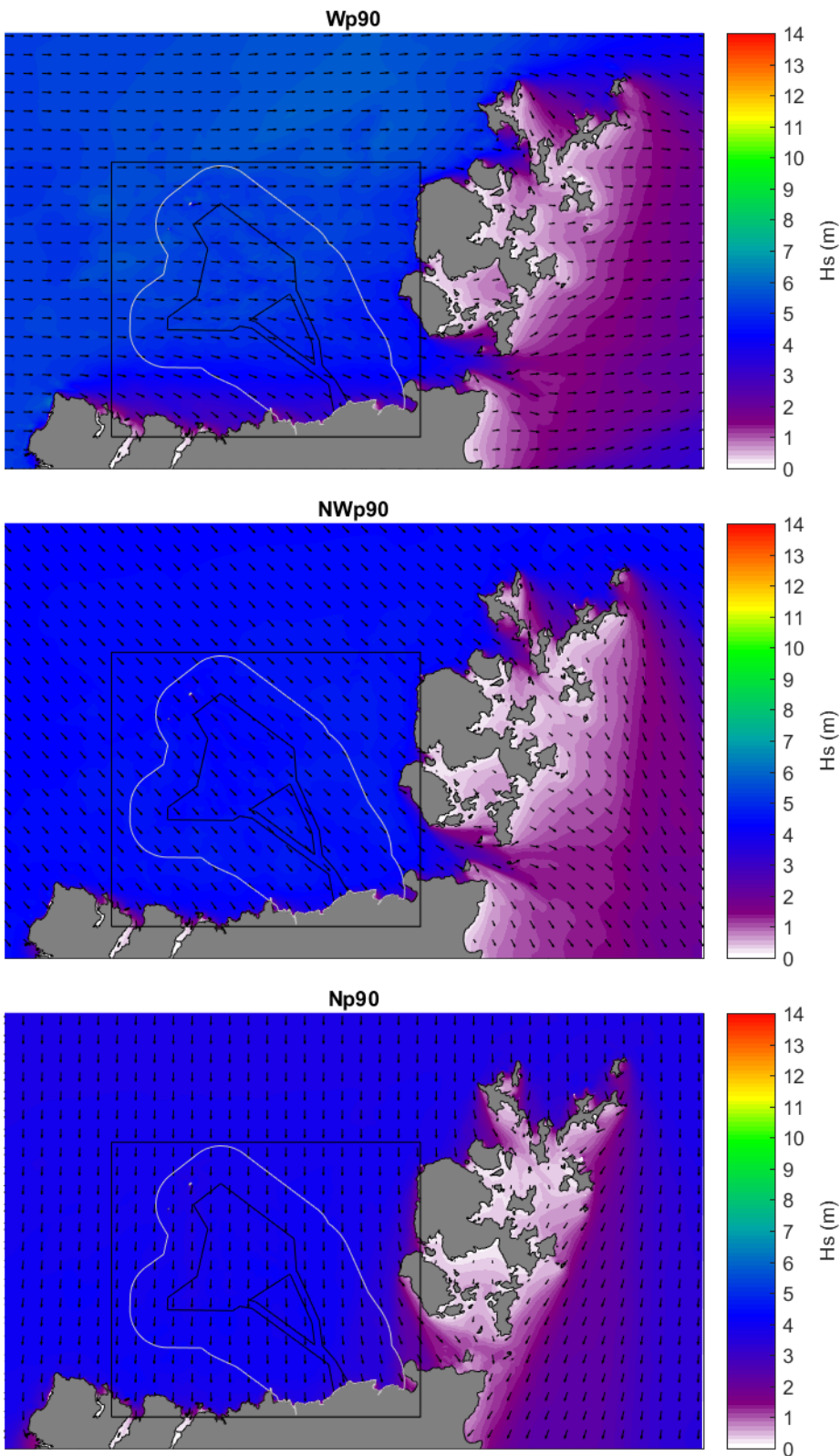


Figure B-68 Modelled wave height and wave direction for the 90<sup>th</sup> percentile wave condition from the west (top), north-west (middle) and north (bottom).

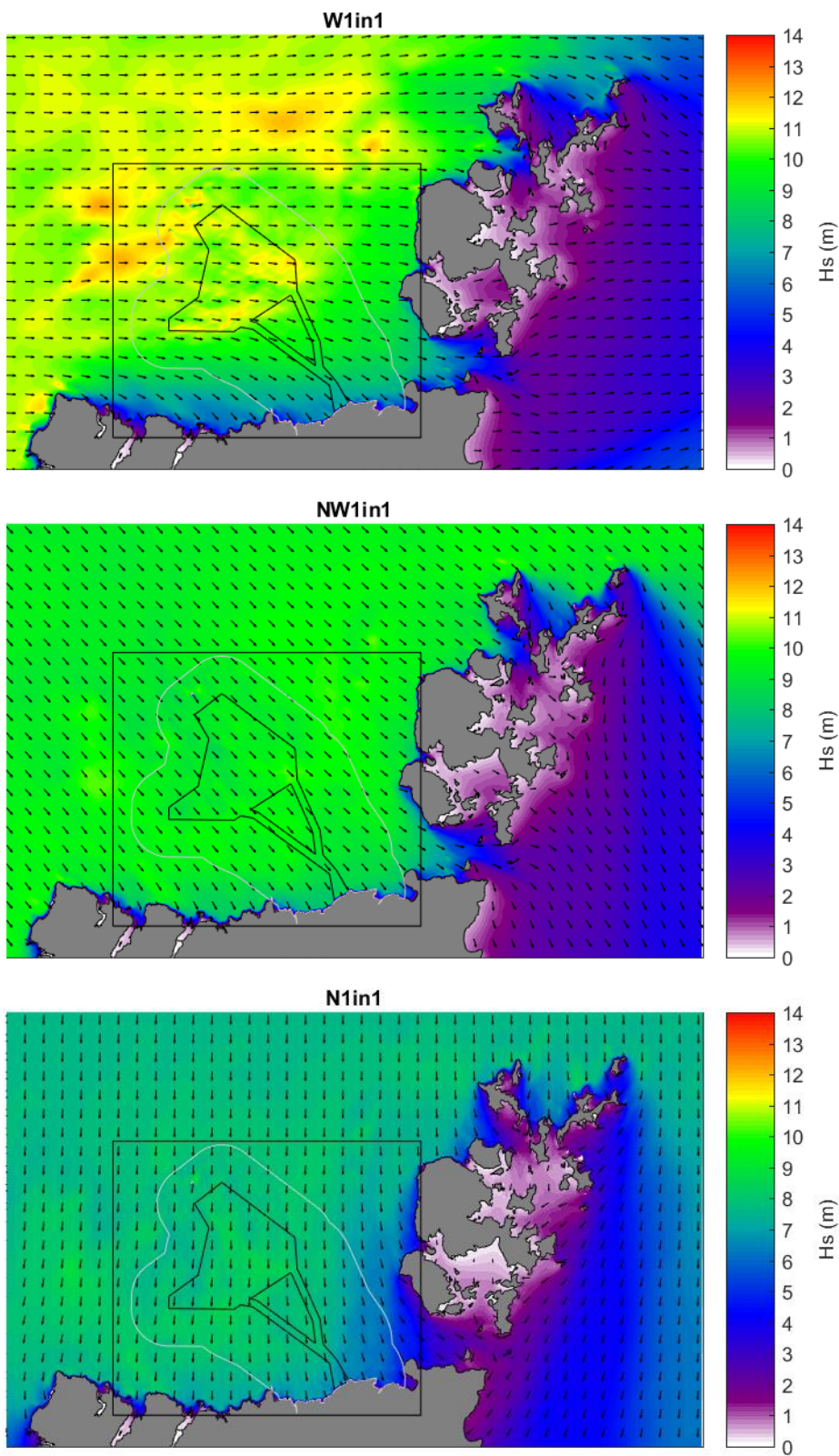


Figure B-69 Modelled wave height and wave direction for the 1 in 1 year ARI from the west (top), north-west (middle) and north (bottom).

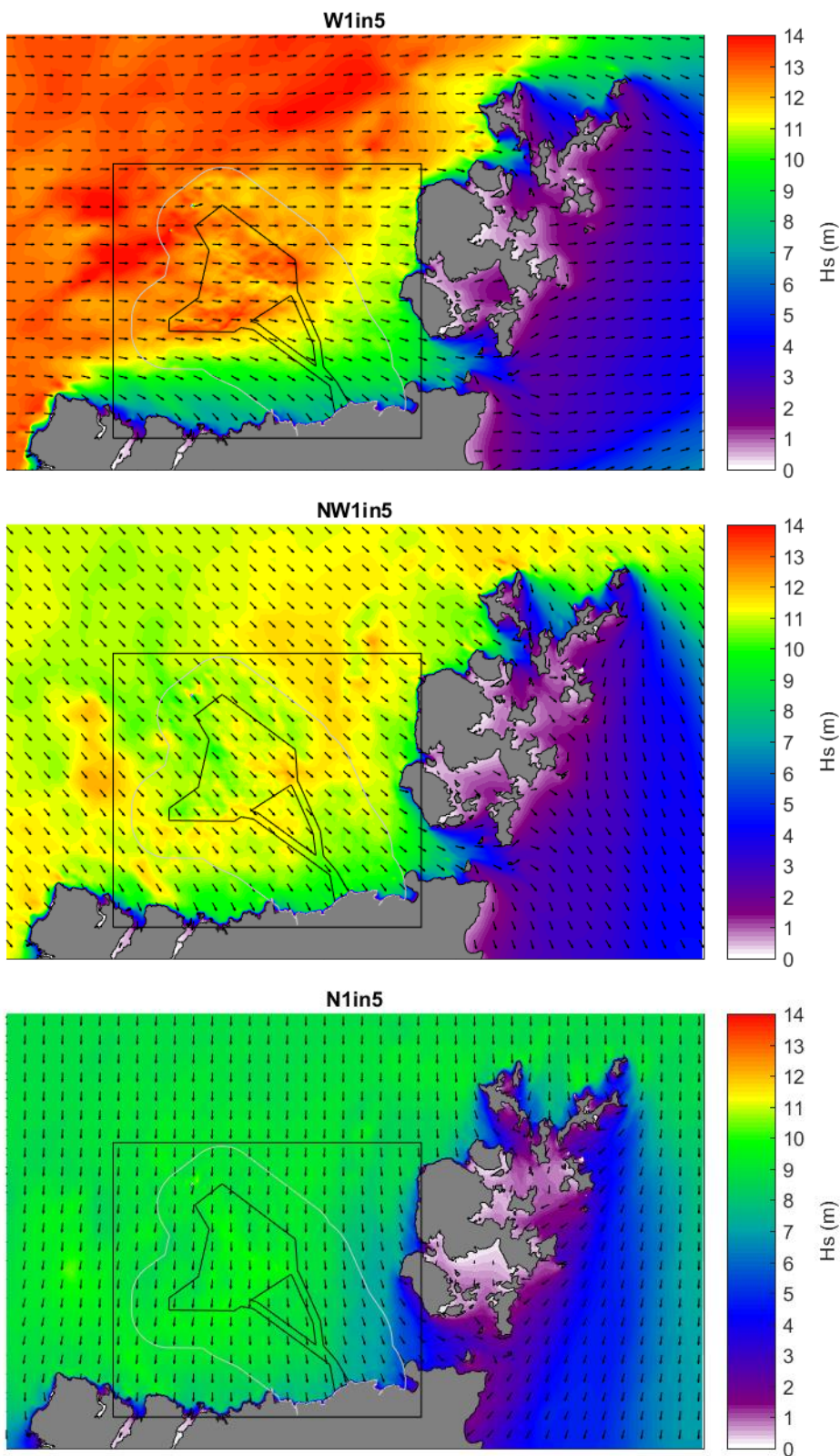


Figure B-70 Modelled wave height and wave direction for the 1 in 5 year ARI from the west (top), north-west (middle) and north (bottom).

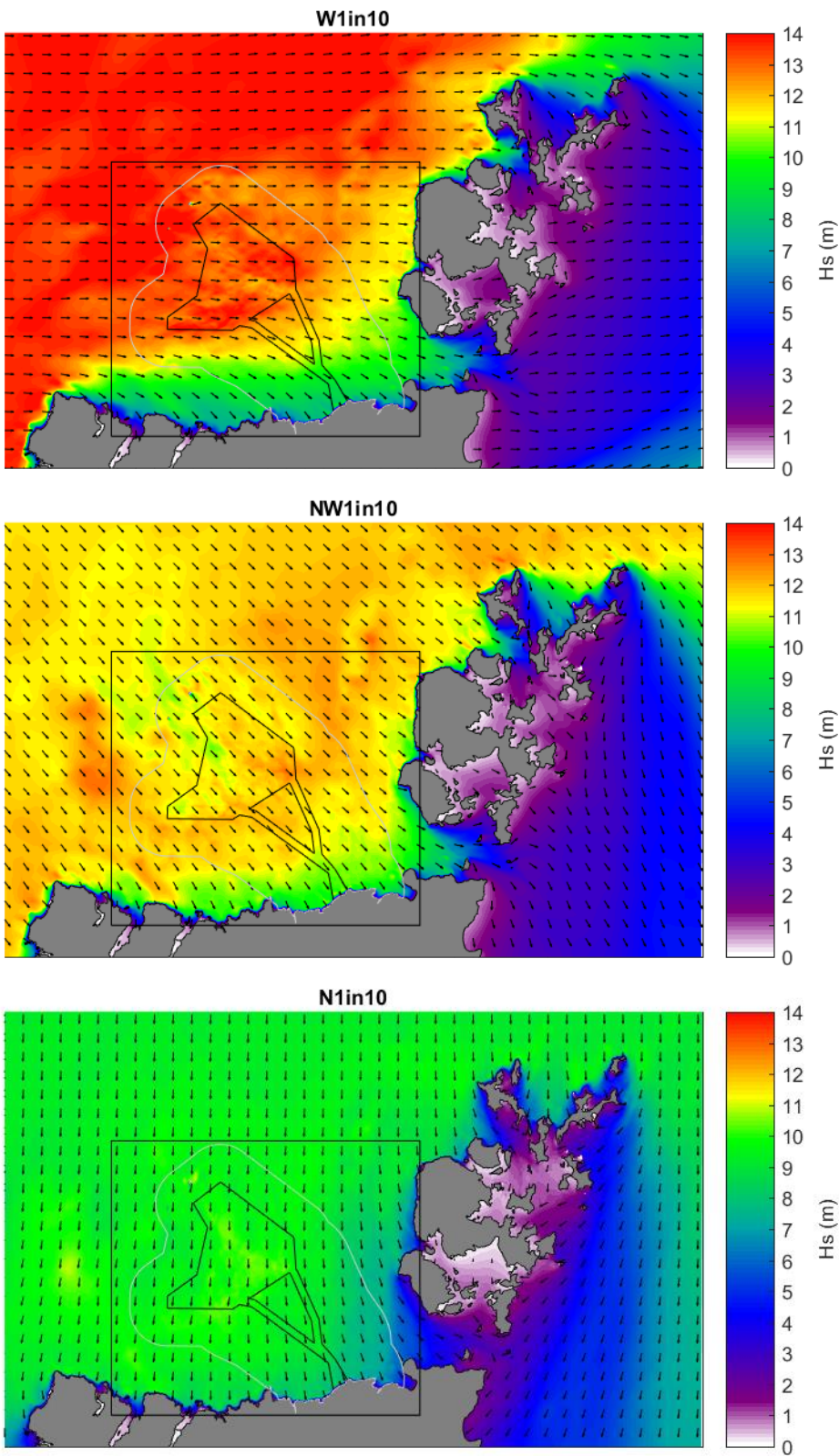


Figure B-71 Modelled wave height and wave direction for the 1 in 10 year ARI from the west (top), north-west (middle) and north (bottom).

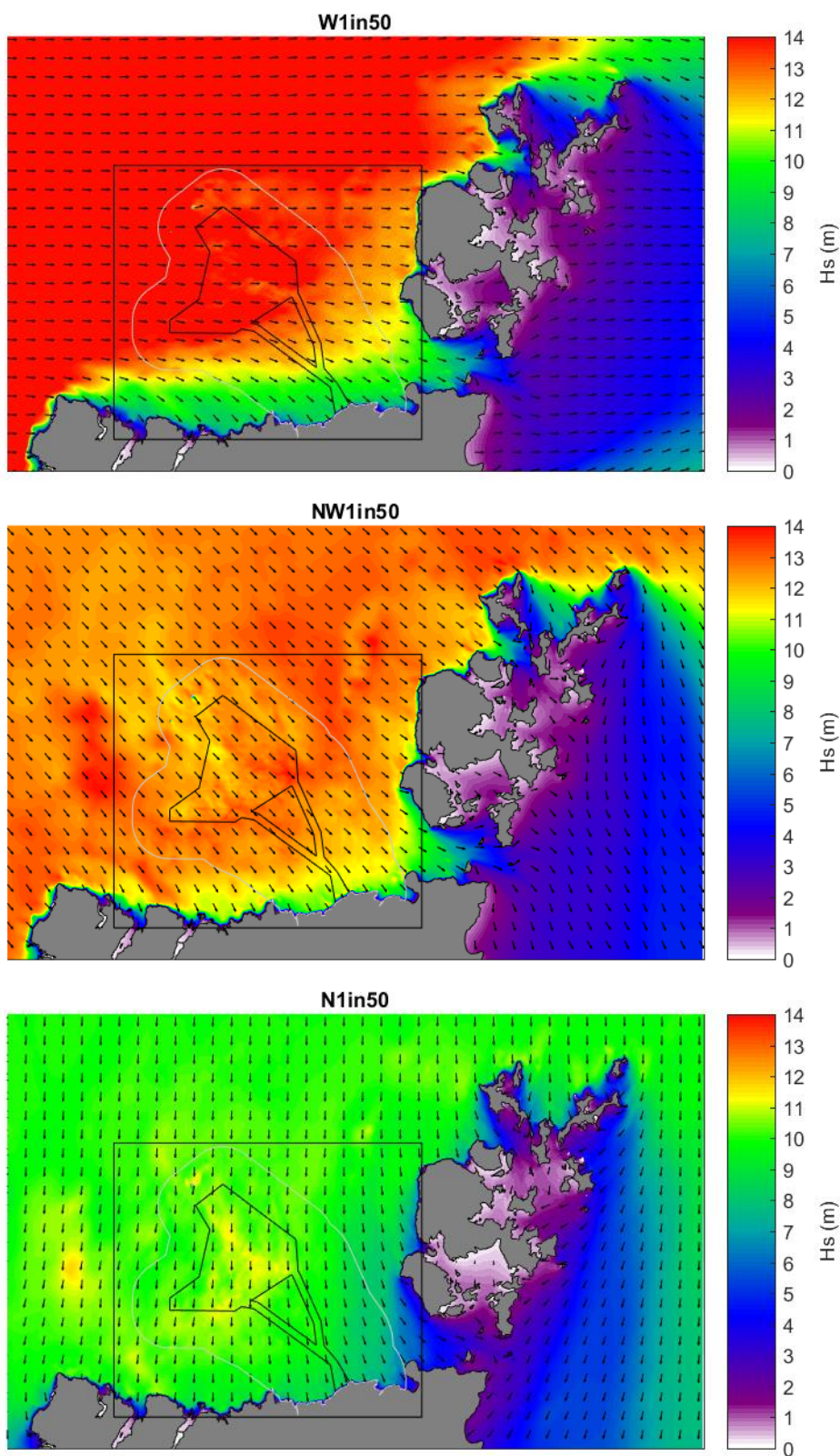


Figure B-72 Modelled wave height and wave direction for the 1 in 50 year ARI from the west (top), north-west (middle) and north (bottom).

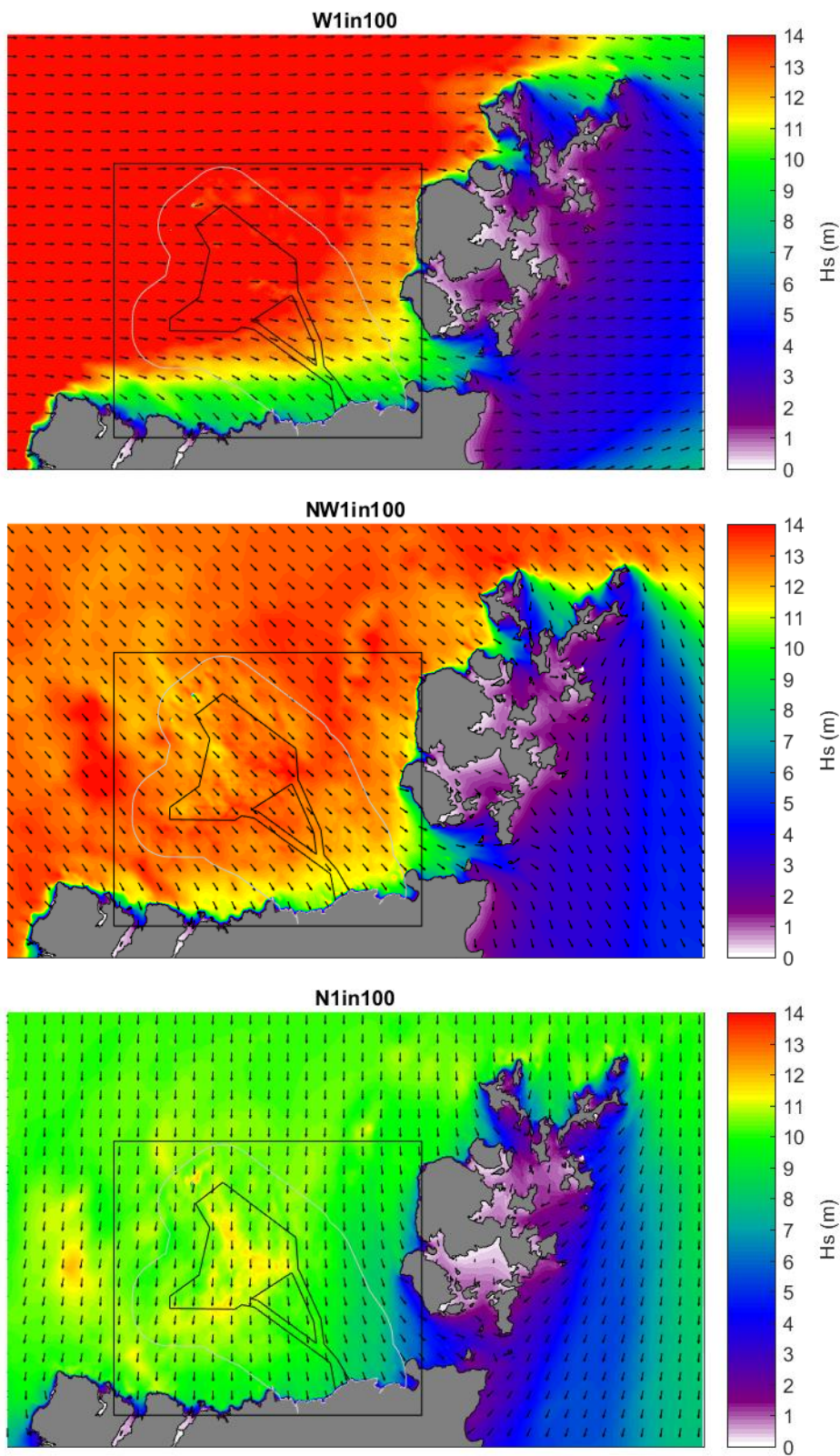


Figure B-73 Modelled wave height and wave direction for the 1 in 100 year ARI from the west (top), north-west (middle) and north (bottom).



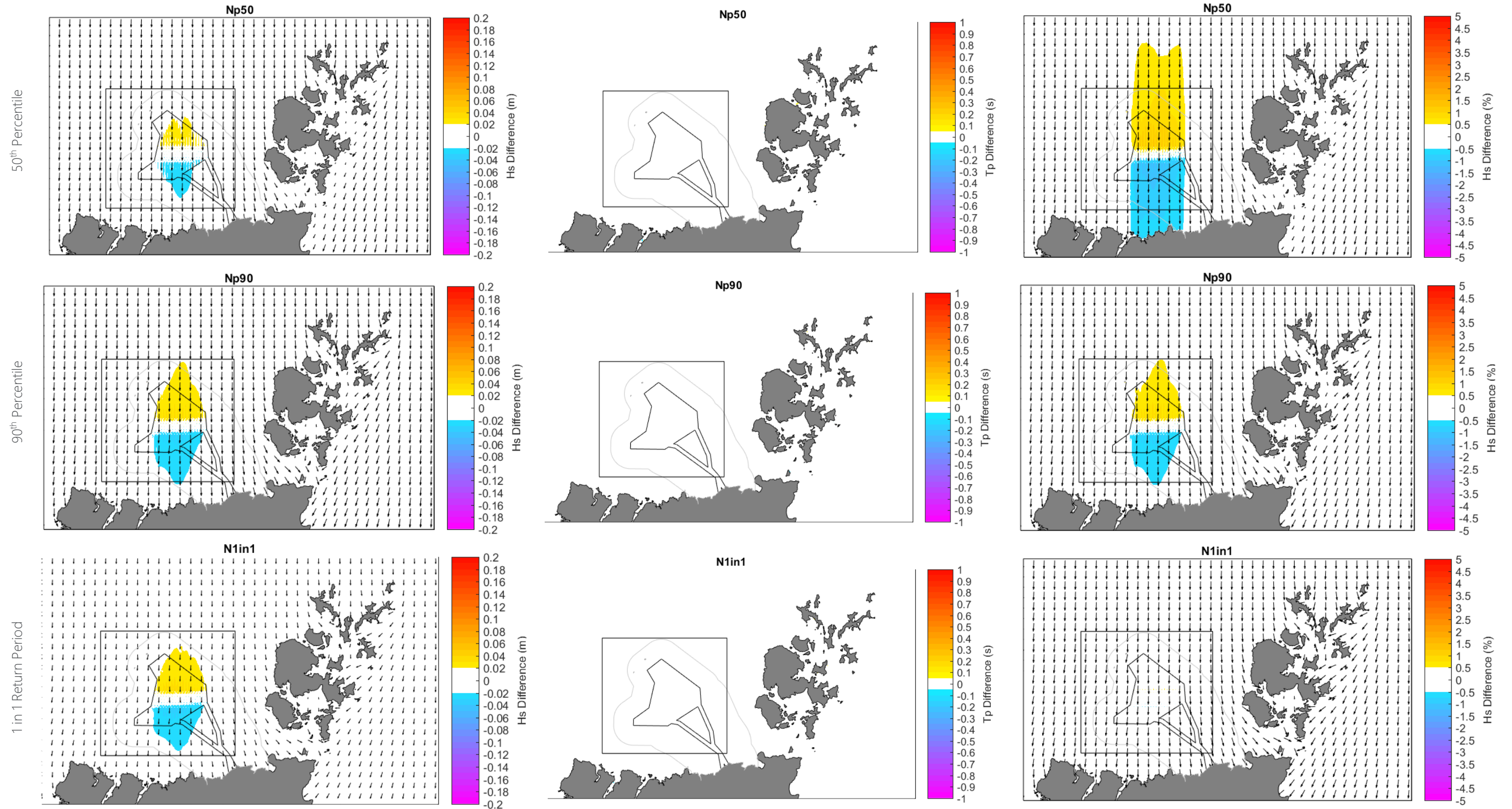
## B.9.2 Layout 1 Post-Construction Scheme Impacts on Waves

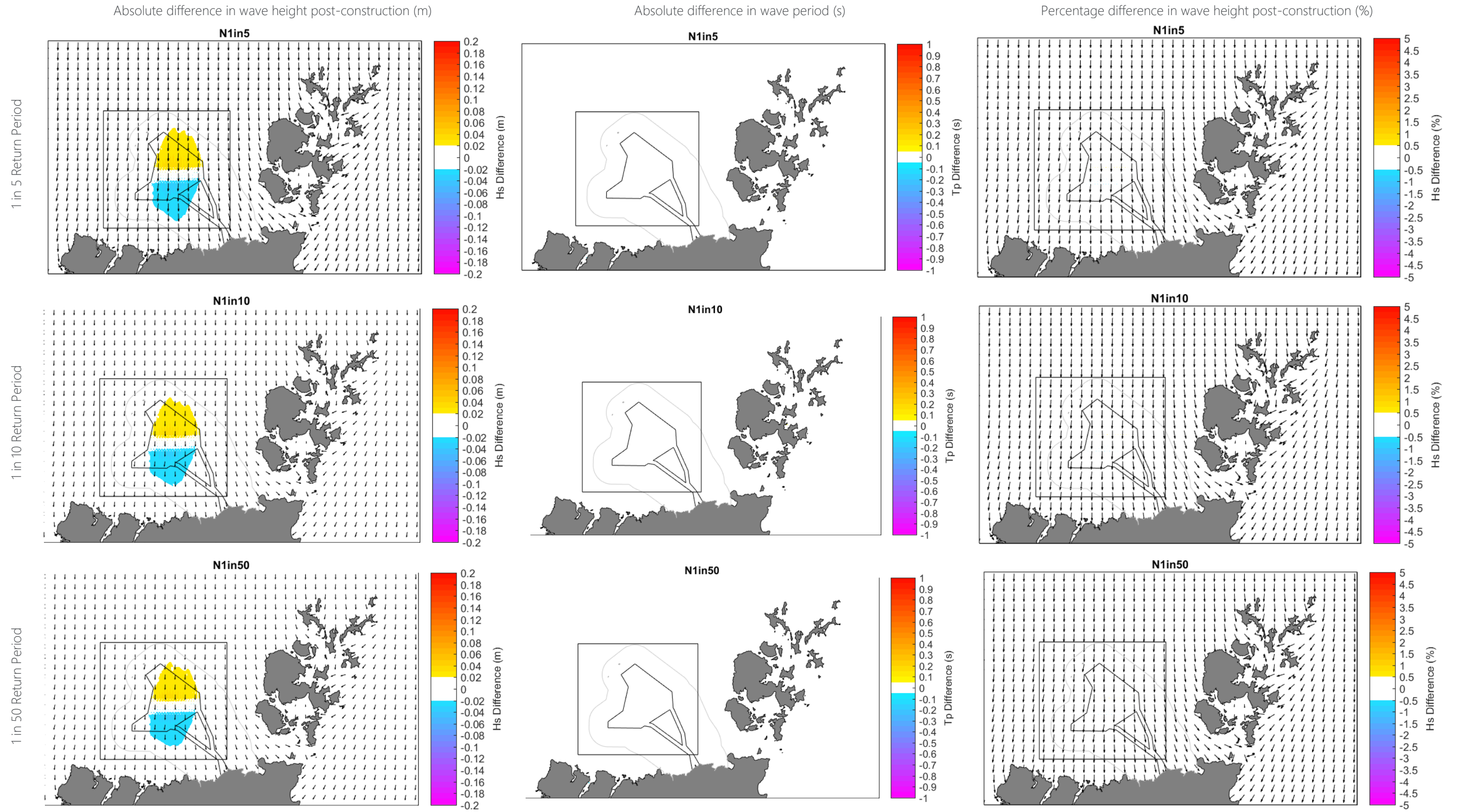
### B.9.2.1 Waves Originating from the North

Absolute difference in wave height post-construction (m)

Absolute difference in wave period (s)

Percentage difference in wave height post-construction (%)





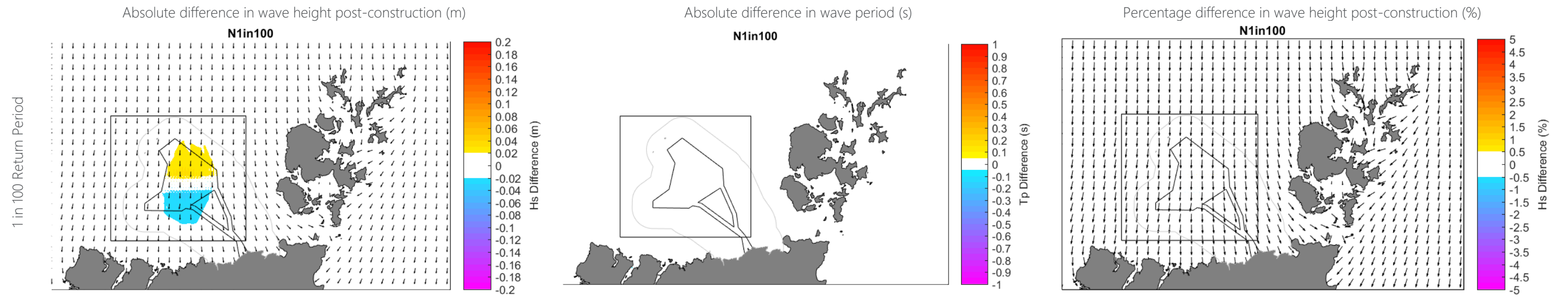


Figure B-74 Modelled change in absolute significant wave height difference (left) absolute peak period (centre) and percentage significant wave height difference (right) for layout 1 for waves approaching from the north for varying return period conditions

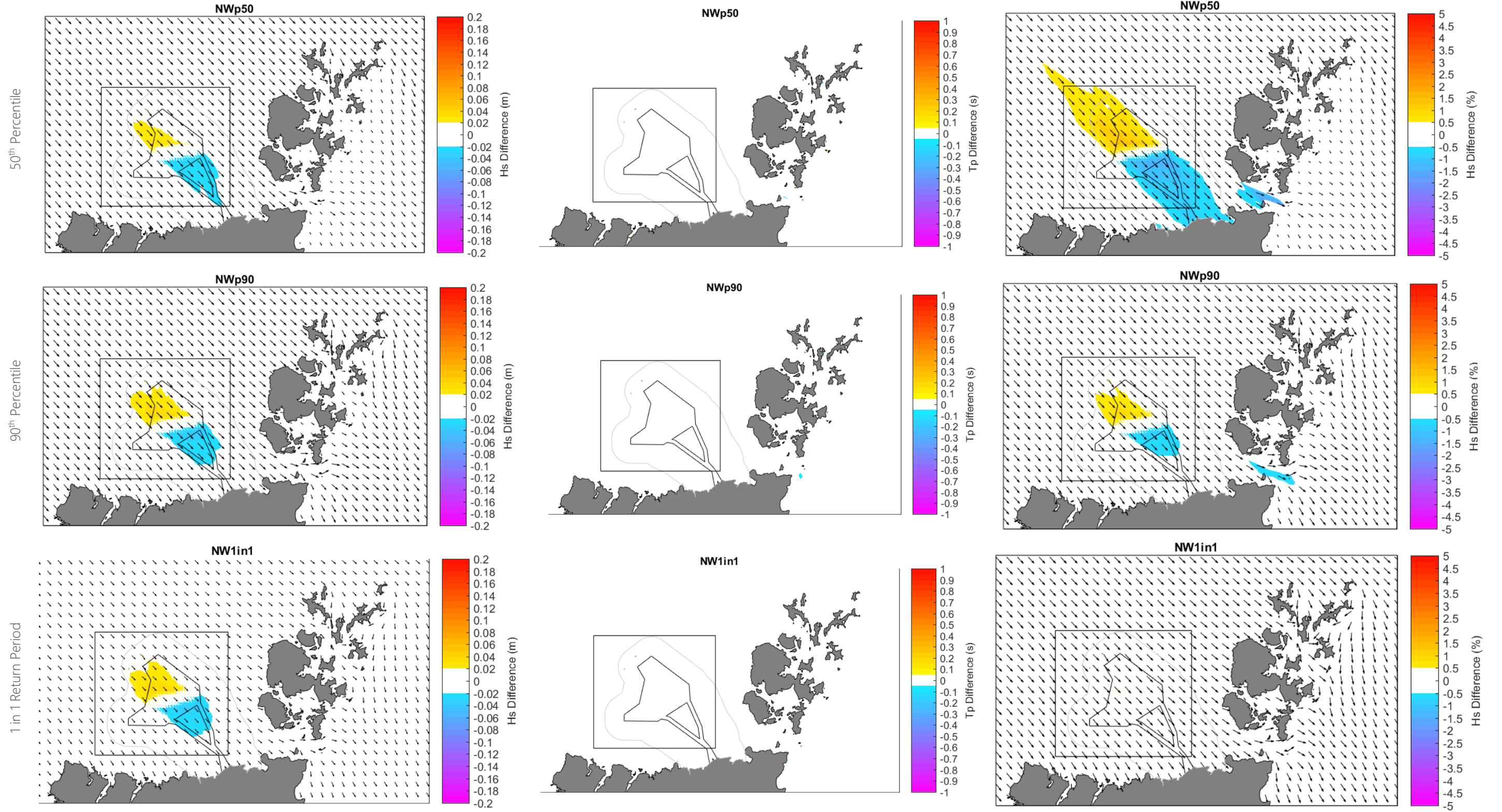


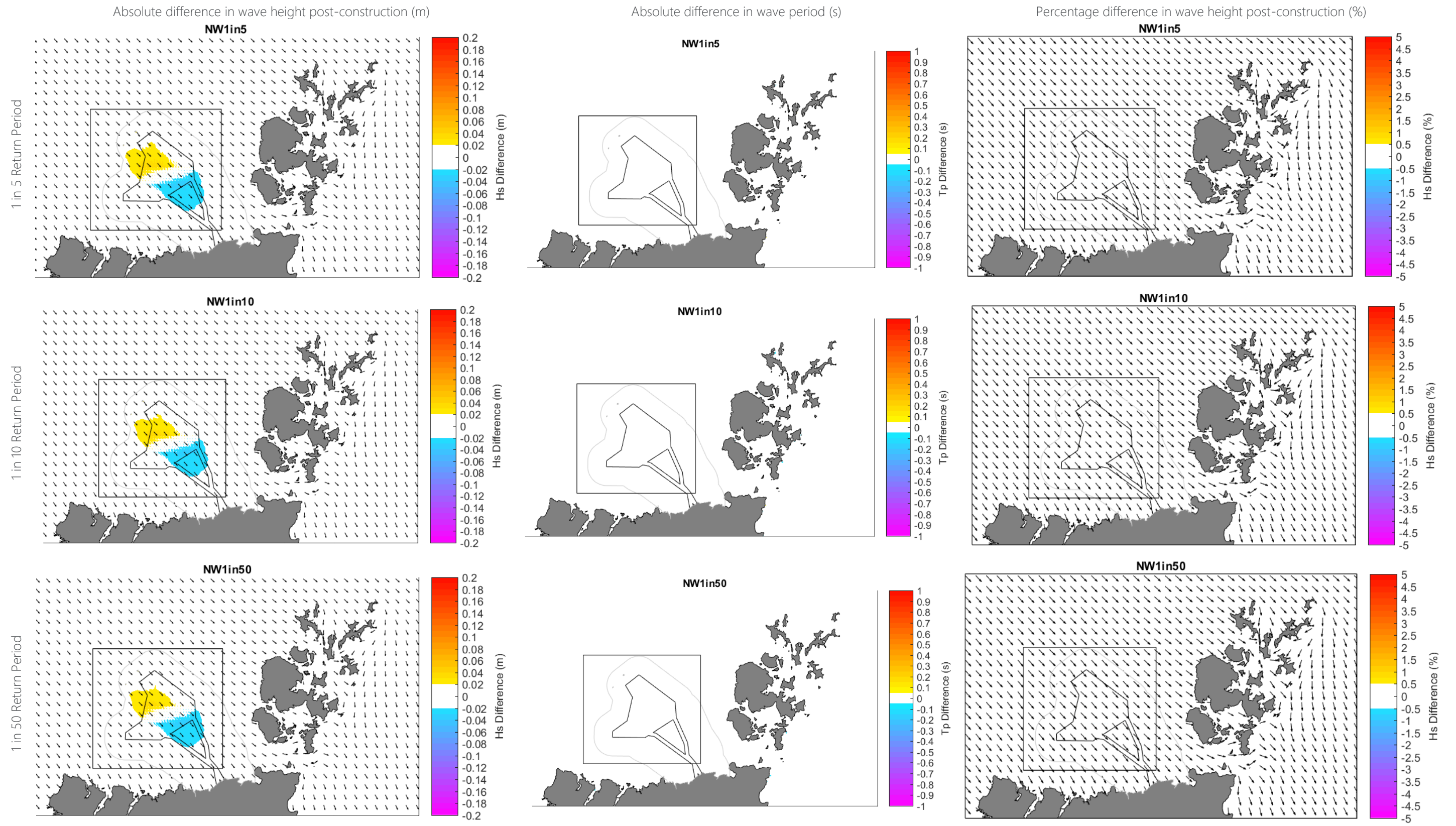
### B.9.2.2 Waves Originating from the Northwest

Absolute difference in wave height post-construction (m)

Absolute difference in wave period (s)

Percentage difference in wave height post-construction (%)





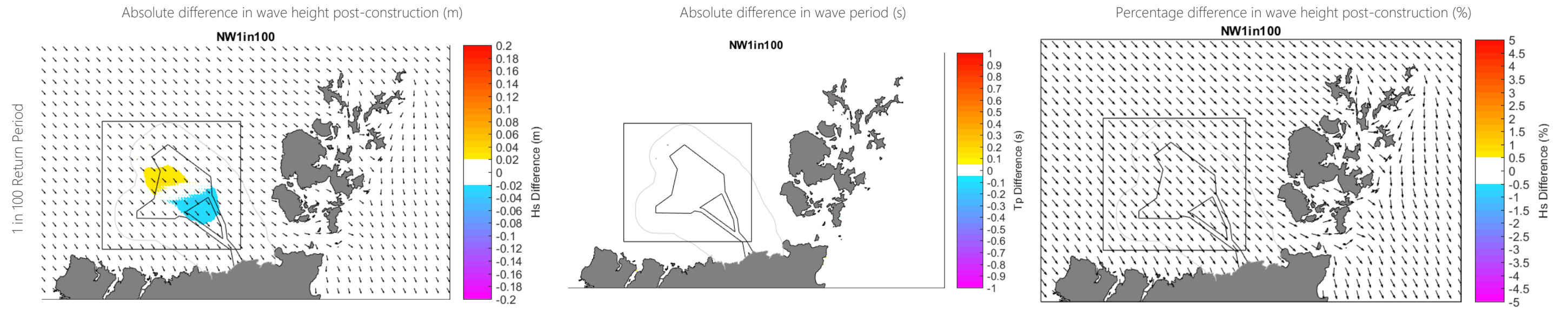


Figure B-75 Modelled change in absolute significant wave height difference (left) absolute peak period (centre) and percentage significant wave height difference (right) for layout 1 for waves approaching from the northwest for varying return period conditions

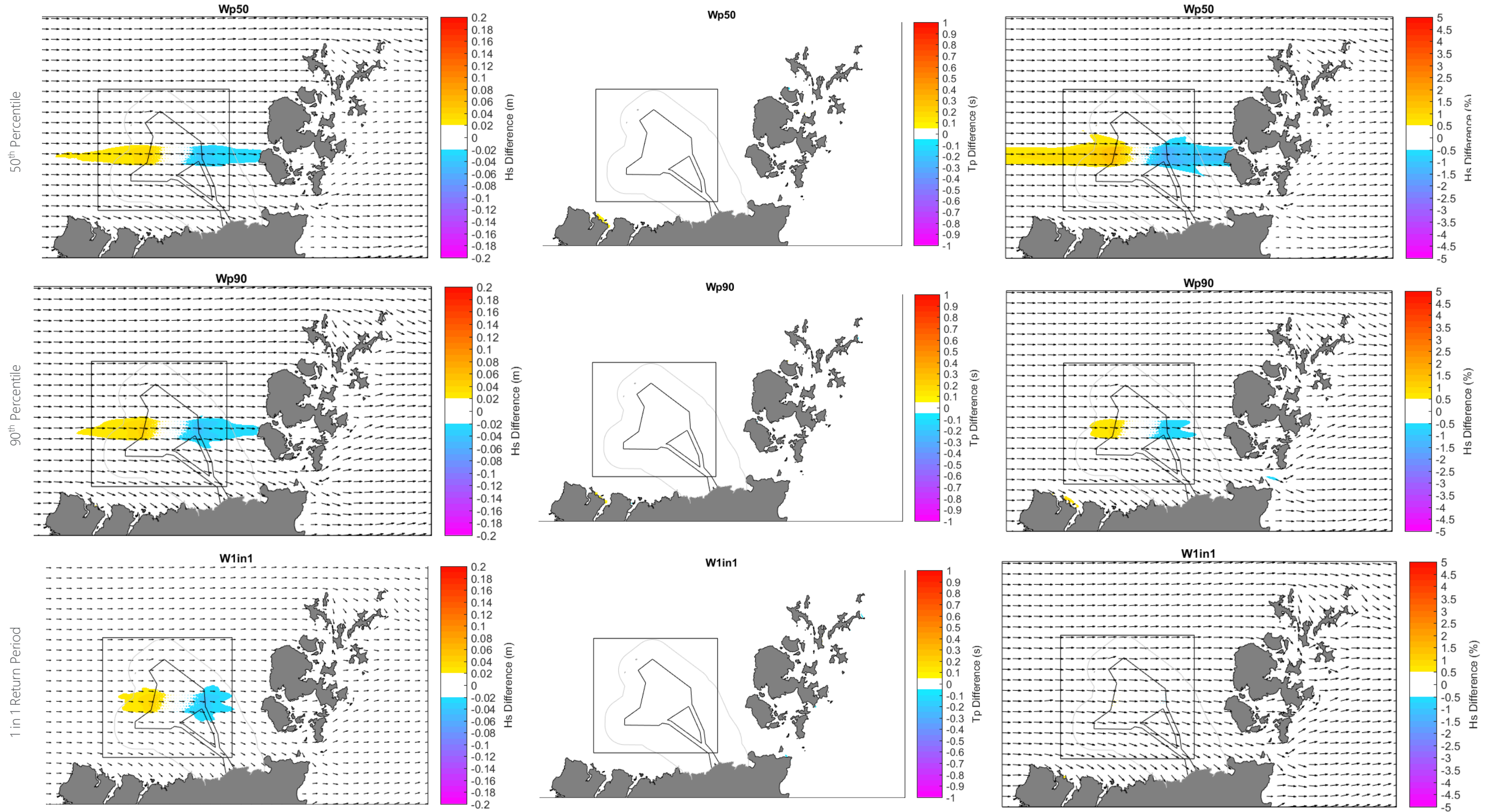


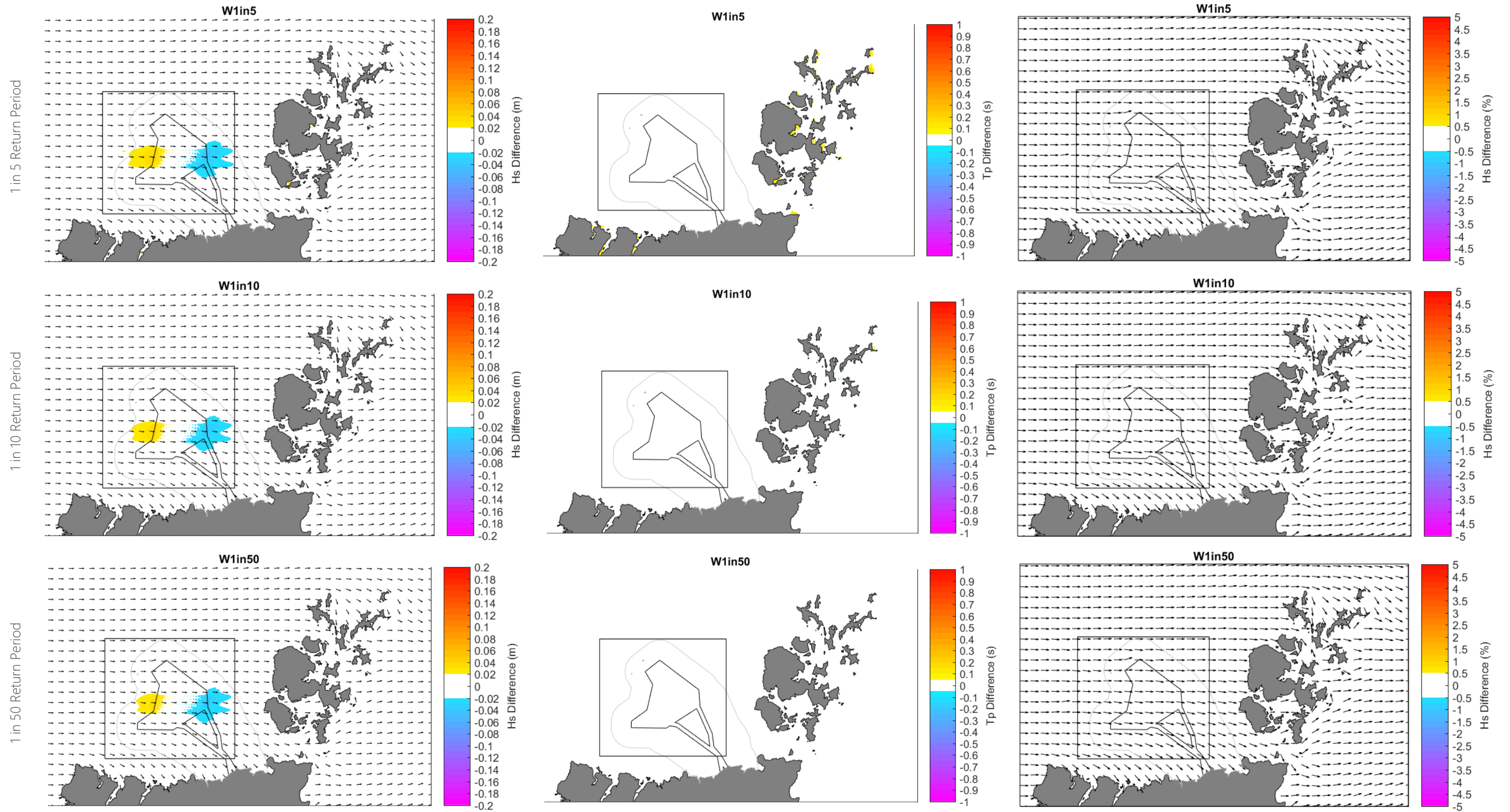
### B.9.2.3 Waves Originating from the West

Absolute difference in wave height post-construction (m)

Absolute difference in wave period (s)

Percentage difference in wave height post-construction (%)





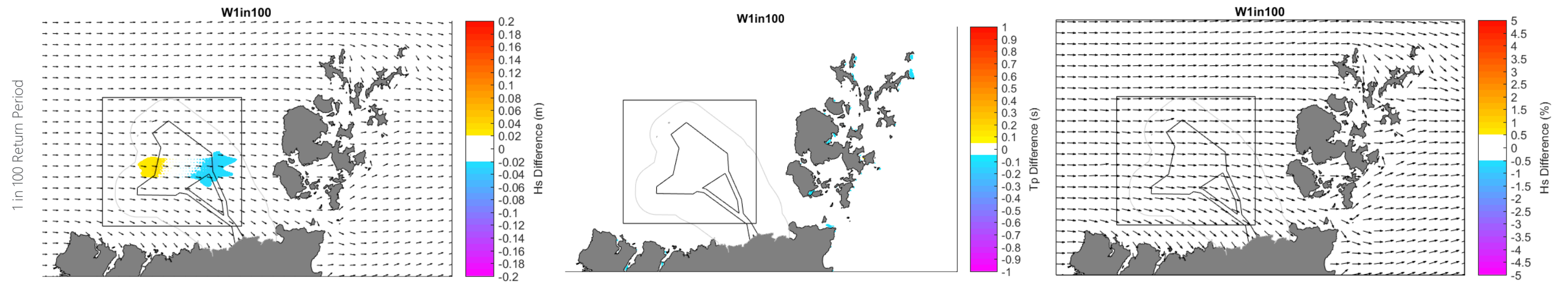


Figure B-76 Modelled change in absolute significant wave height difference (left) absolute peak period (centre) and percentage significant wave height difference (right) for layout 1 for waves approaching from the west for varying return period conditions



### B.9.2.4 Modelled Percentage Significant Wave Height Difference Zoomed Across the OAA

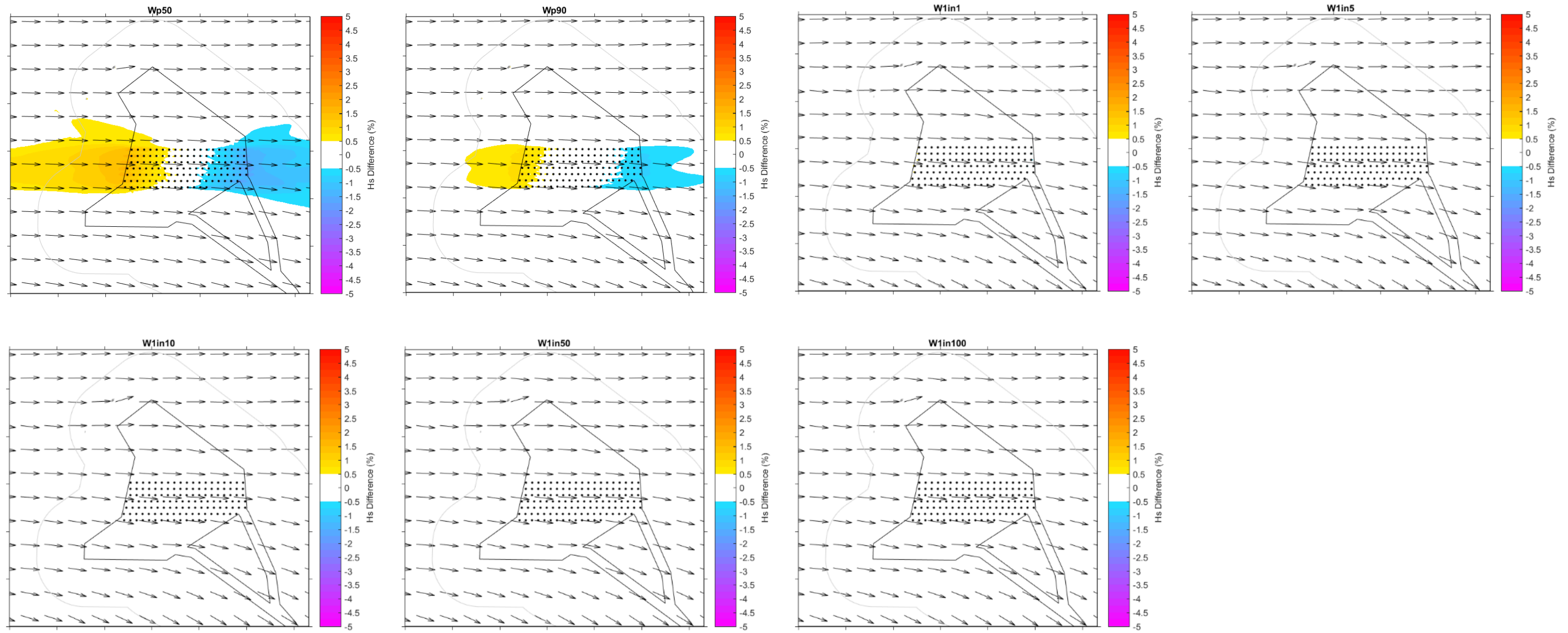


Figure B-77 Modelled percentage change in wave height relative to the baseline conditions due to layout 1 for waves from the West

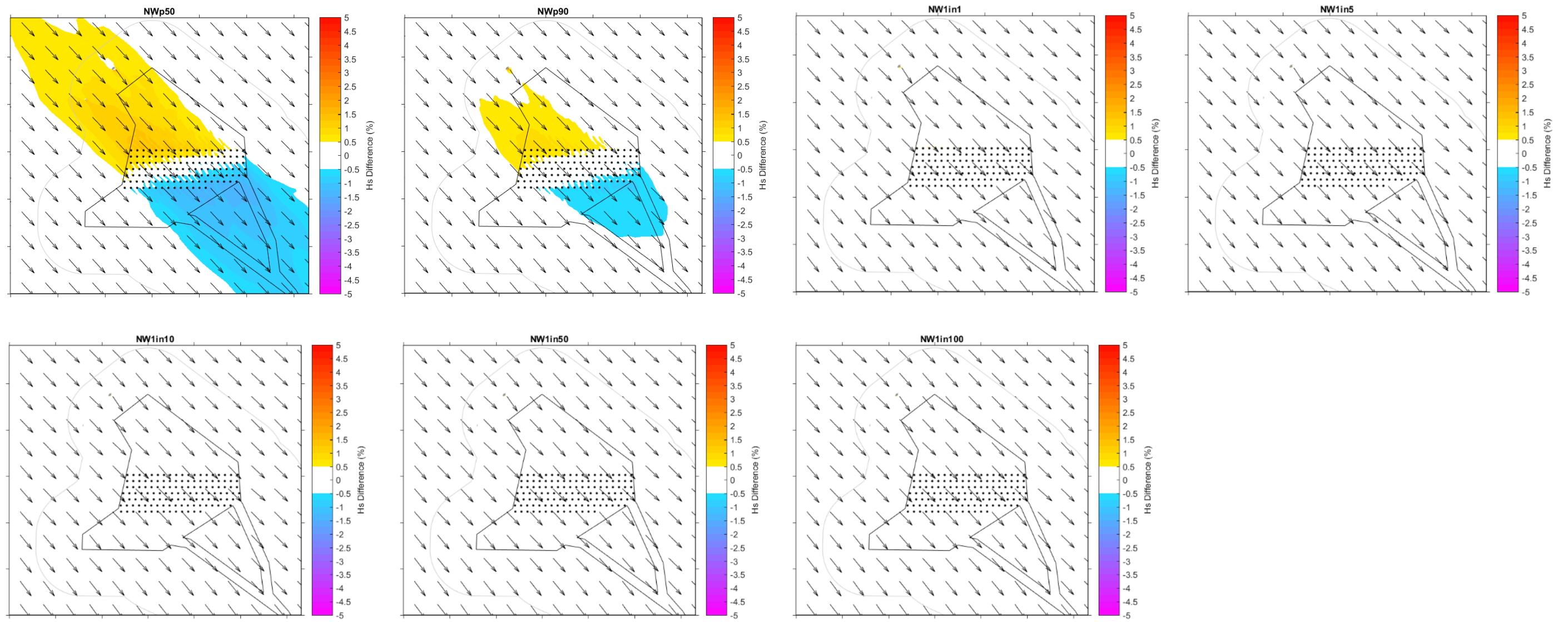


Figure B-78 Modelled percentage change in wave height relative to the baseline conditions due to layout 1 for waves from the North West

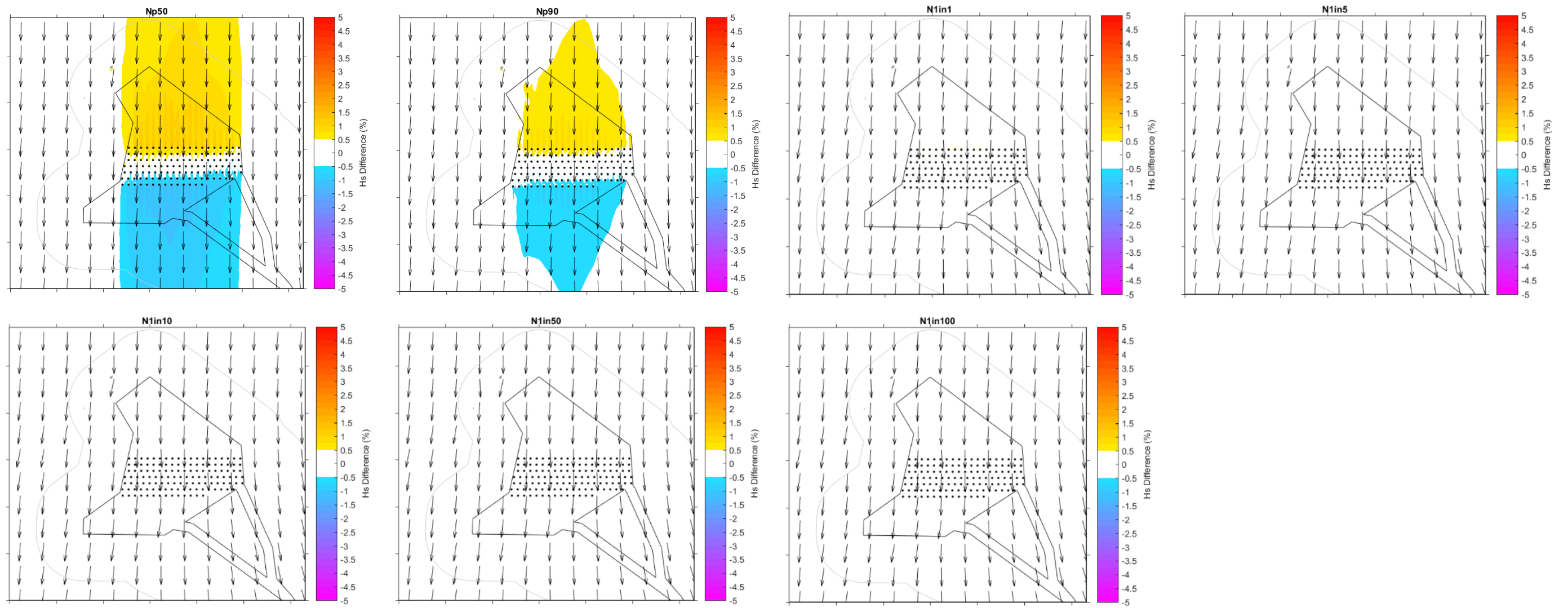
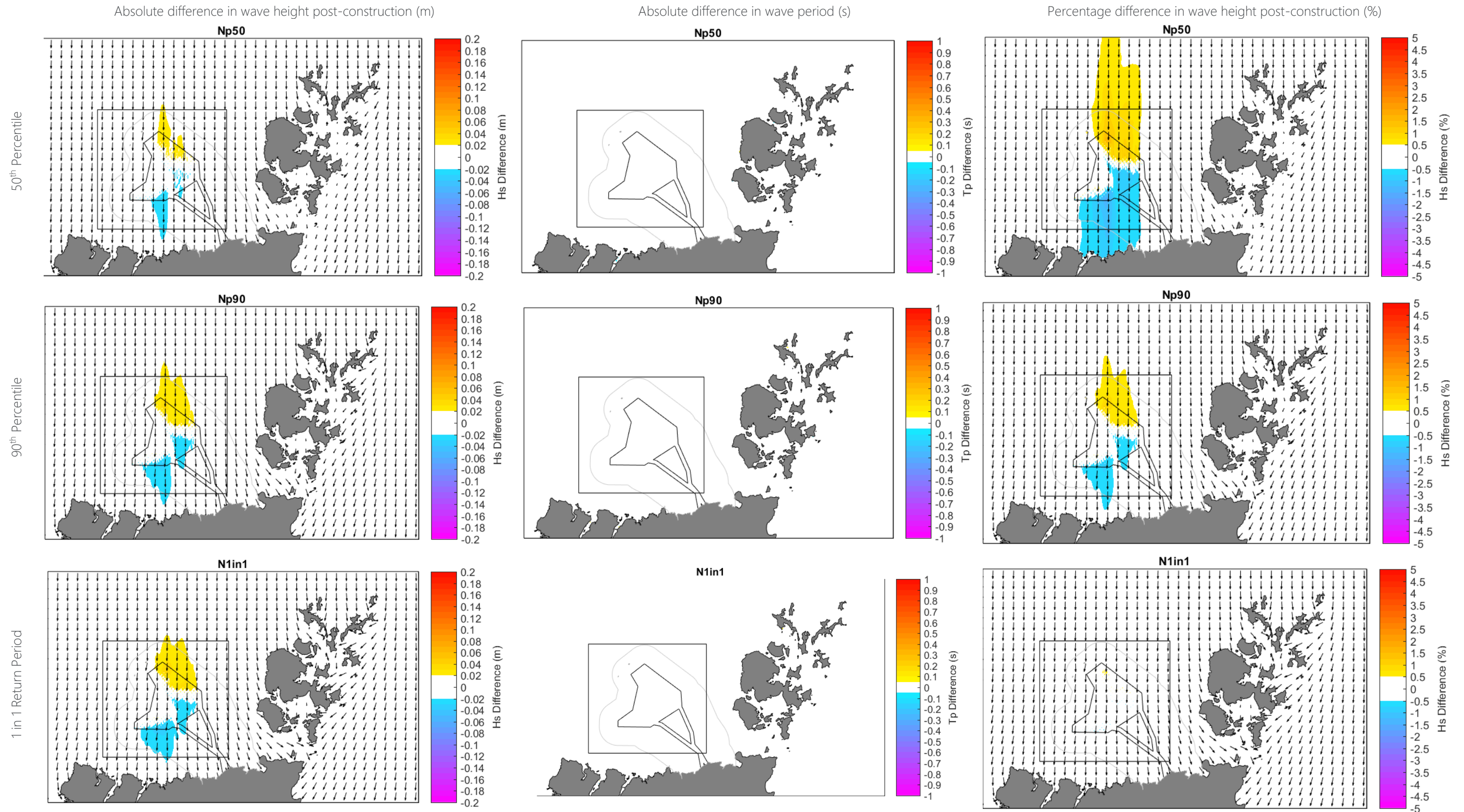


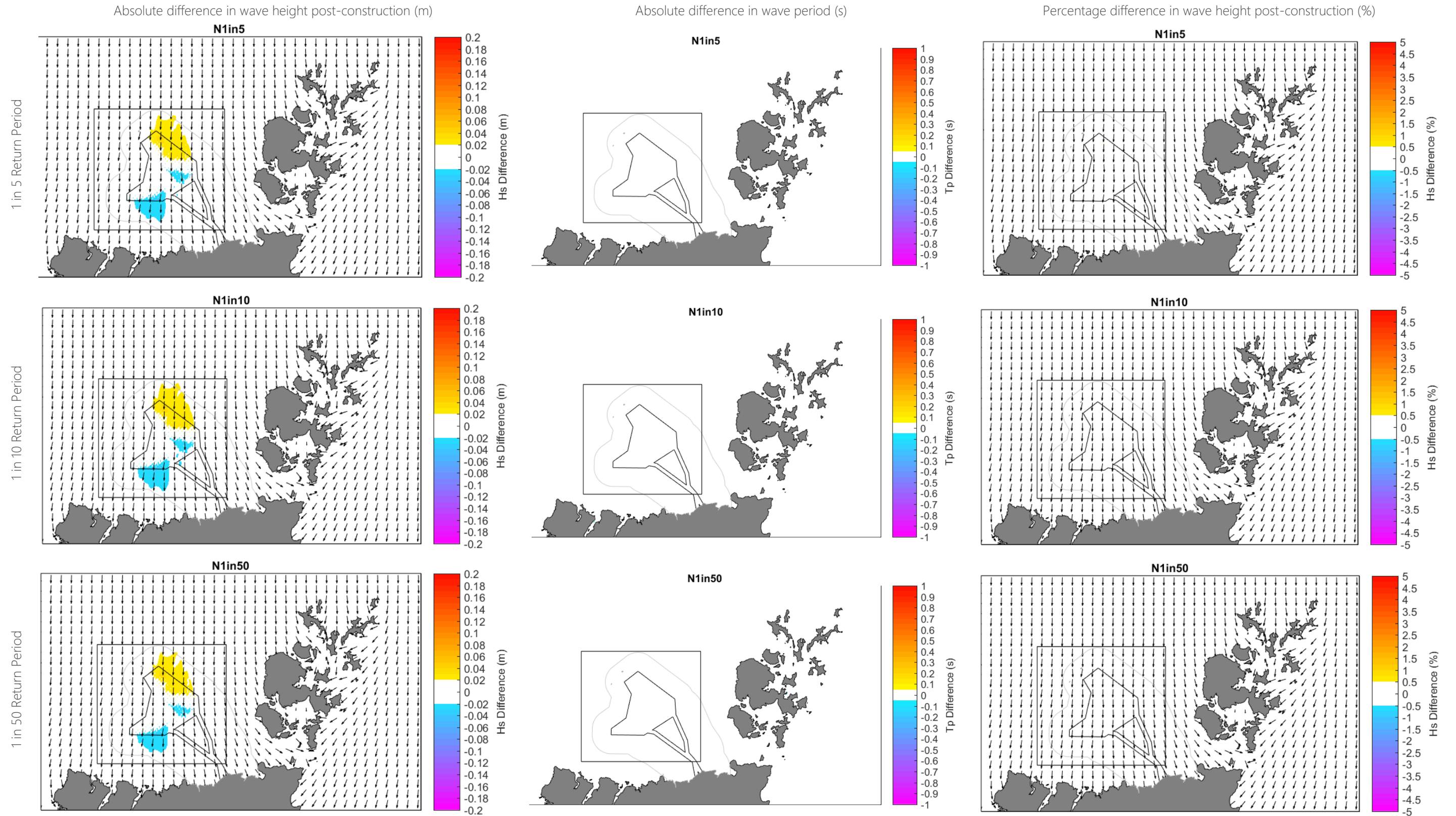
Figure B-79 Modelled percentage change in wave height relative to the baseline conditions due to layouts 1 for waves from the North



### B.9.3 Layout 2 Post-Construction Scheme Impacts on Waves

#### B.9.3.1 Waves Originating from the North





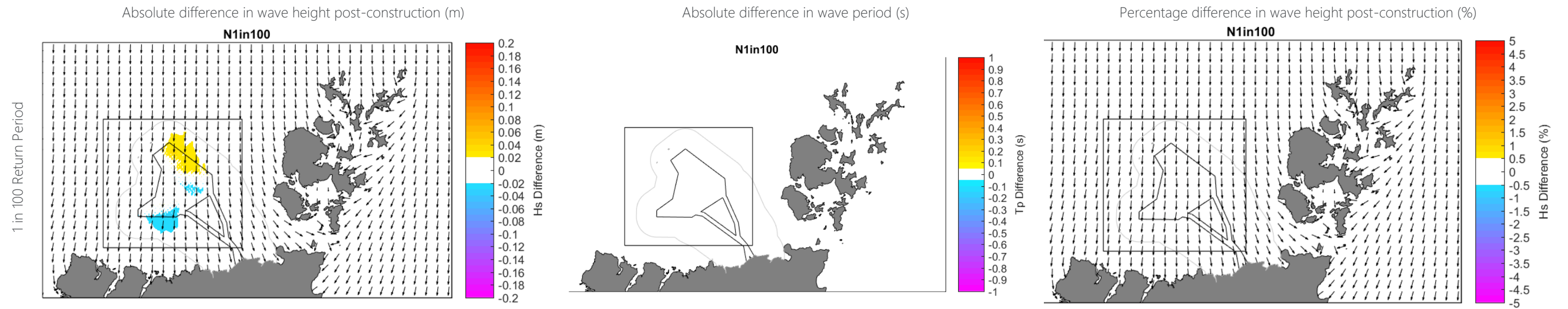


Figure B-80 Modelled change in absolute significant wave height difference (left) absolute peak period (centre) and percentage significant wave height difference (right) for layout 2 for waves approaching from the north for varying return period conditions

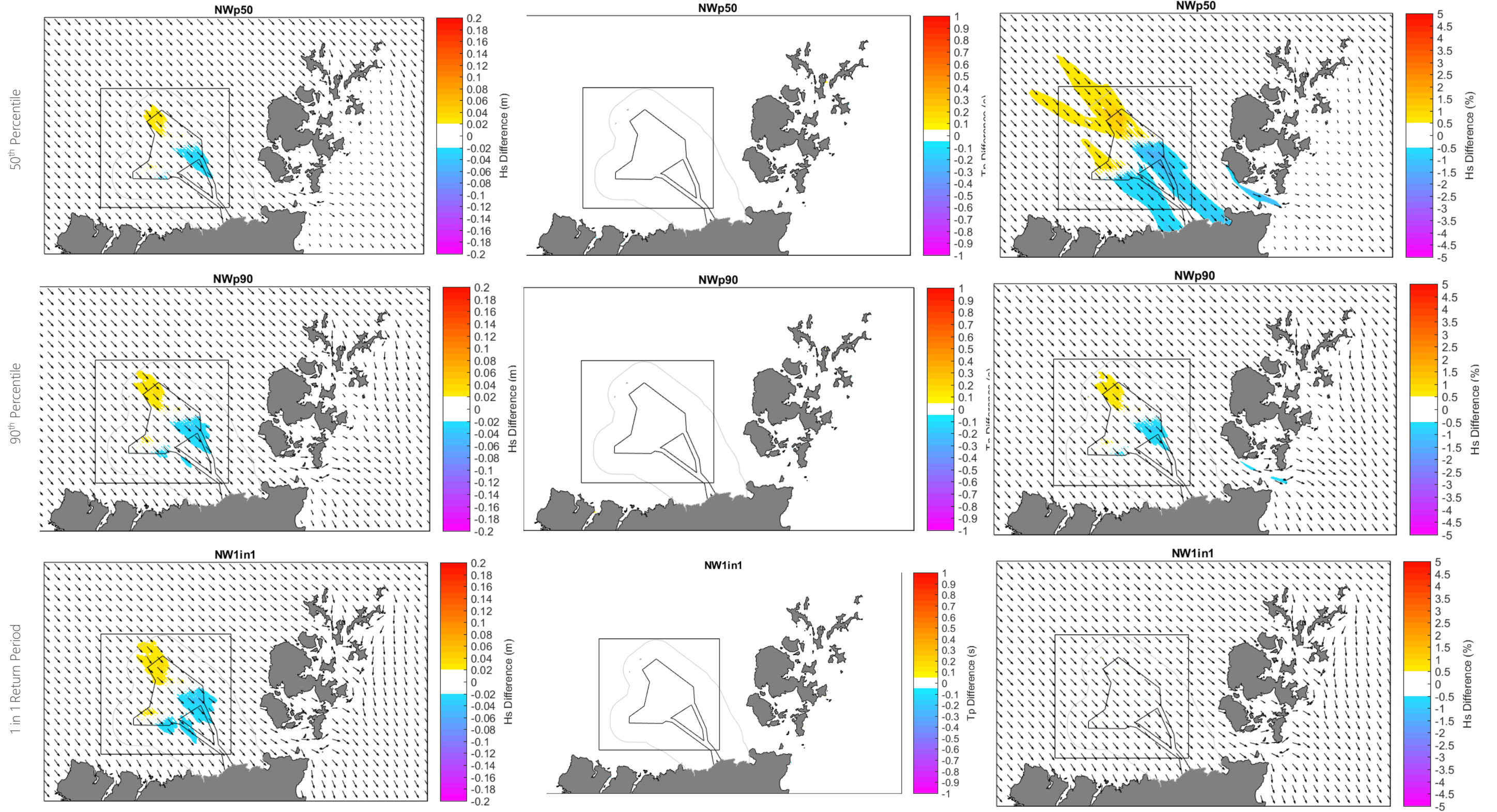


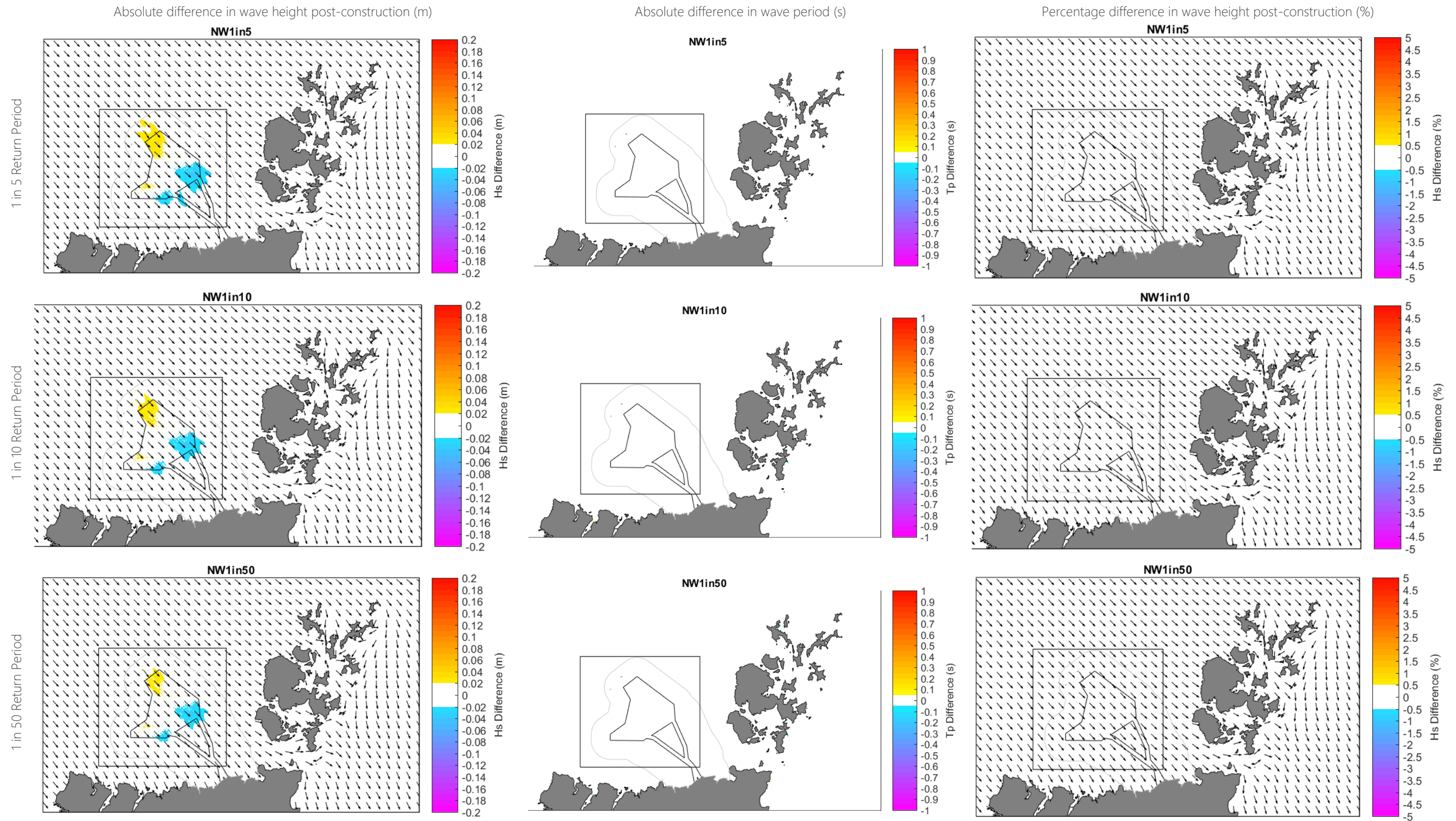
### B.9.3.2 Waves Originating from the Northwest

Absolute difference in wave height post-construction (m)

Absolute difference in wave period (s)

Percentage difference in wave height post-construction (%)





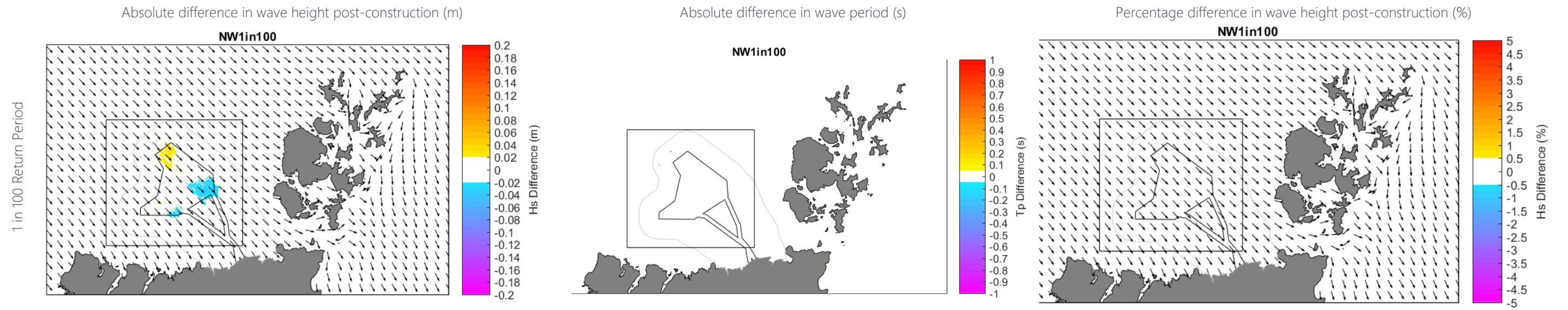


Figure B-81 Modelled change in absolute significant wave height difference (left) absolute peak period (centre) and percentage significant wave height difference (right) for layout 2 for waves approaching from the northwest for varying return period conditions

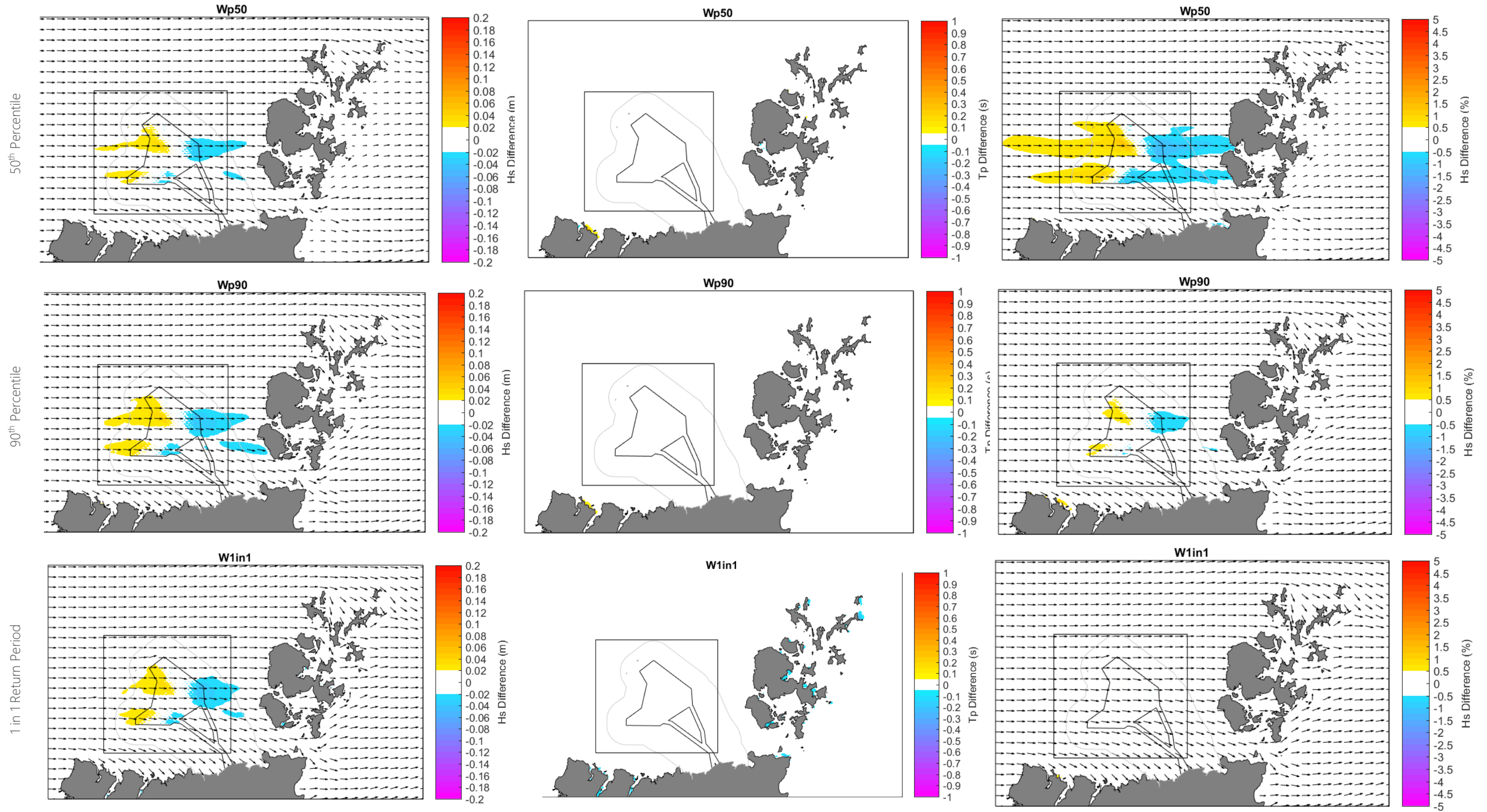


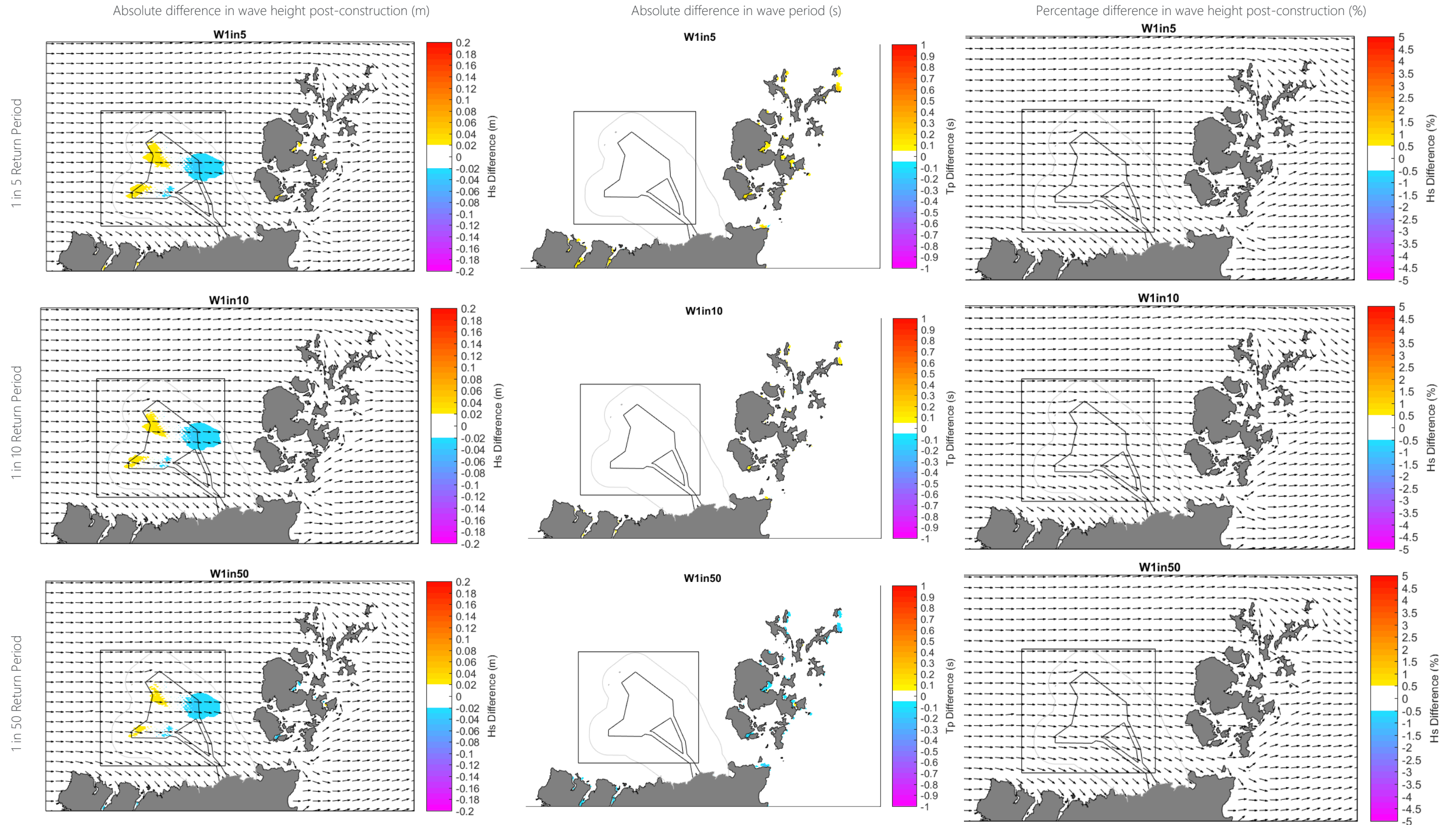
### B.9.3.3 Waves Originating from the West

Absolute difference in wave height post-construction (m)

Absolute difference in wave period (s)

Percentage difference in wave height post-construction (%)





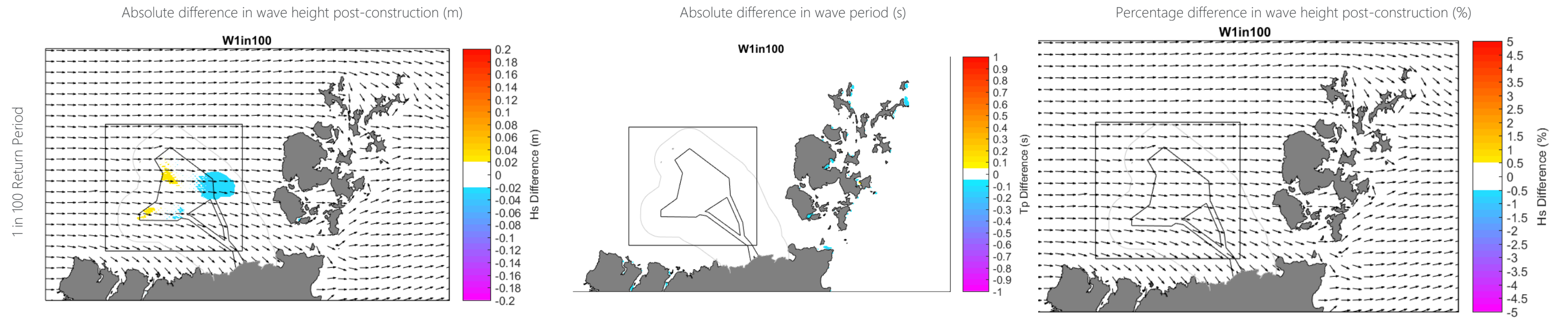


Figure B-82 Modelled change in absolute significant wave height difference (left) absolute peak period (centre) and percentage significant wave height difference (right) for layout 2 for waves approaching from the west for varying return period conditions



### B.9.3.4 Modelled Percentage Significant Wave Height Difference Zoomed Across the OAA

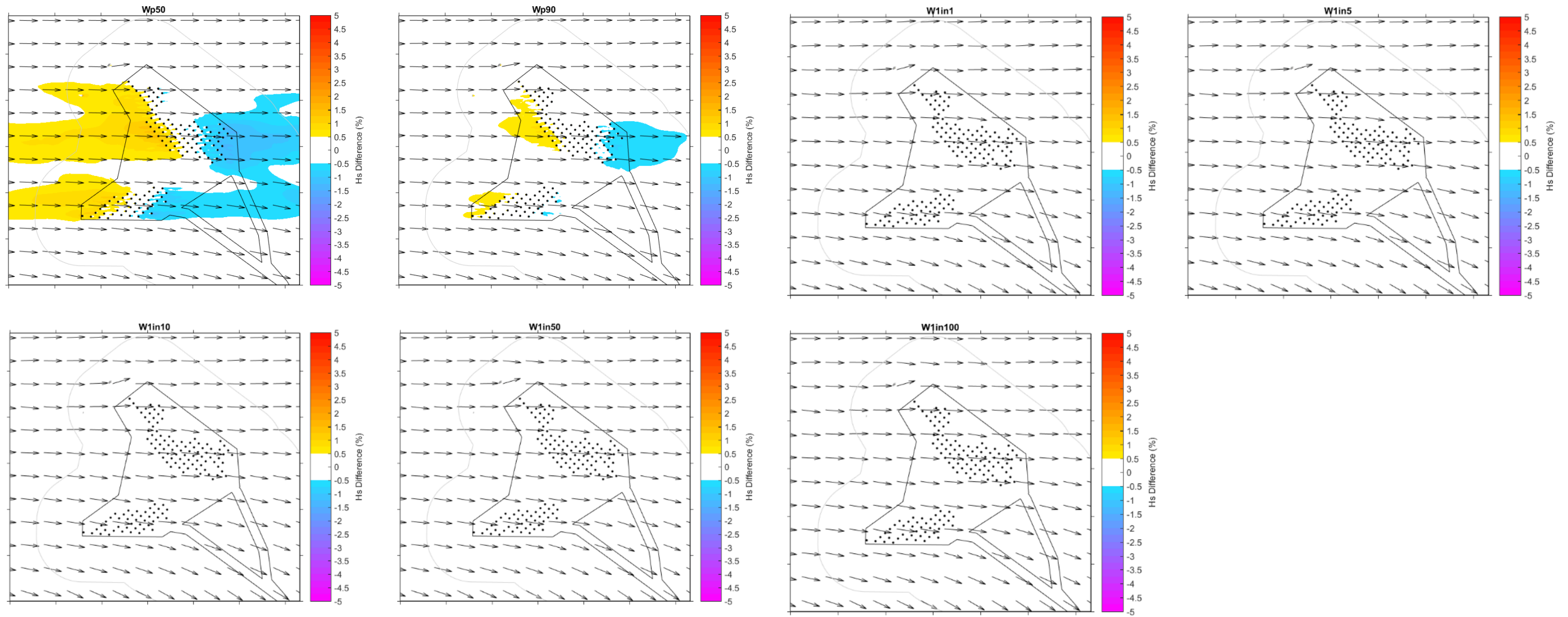


Figure B-83 Modelled percentage change in wave height relative to the baseline conditions due to layout 2 for waves from the West

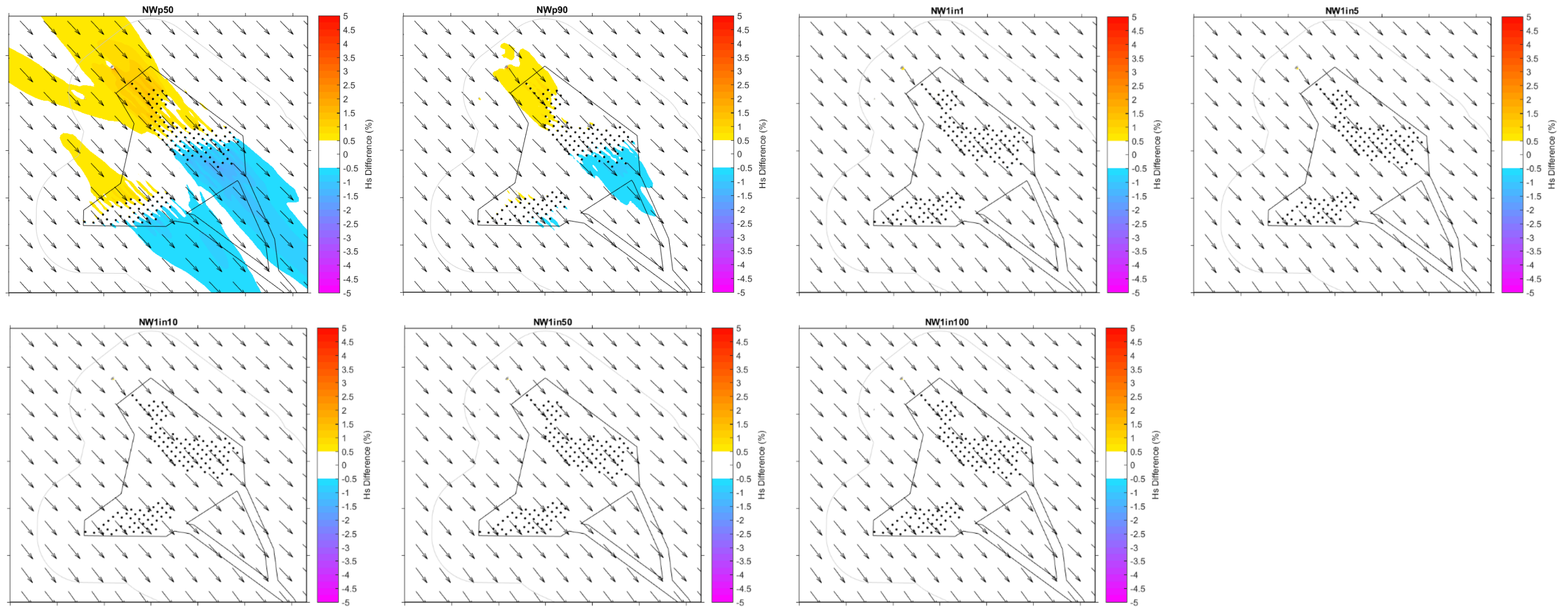


Figure B-84 Modelled percentage change in wave height relative to the baseline conditions due to layout 2 for waves from the North West

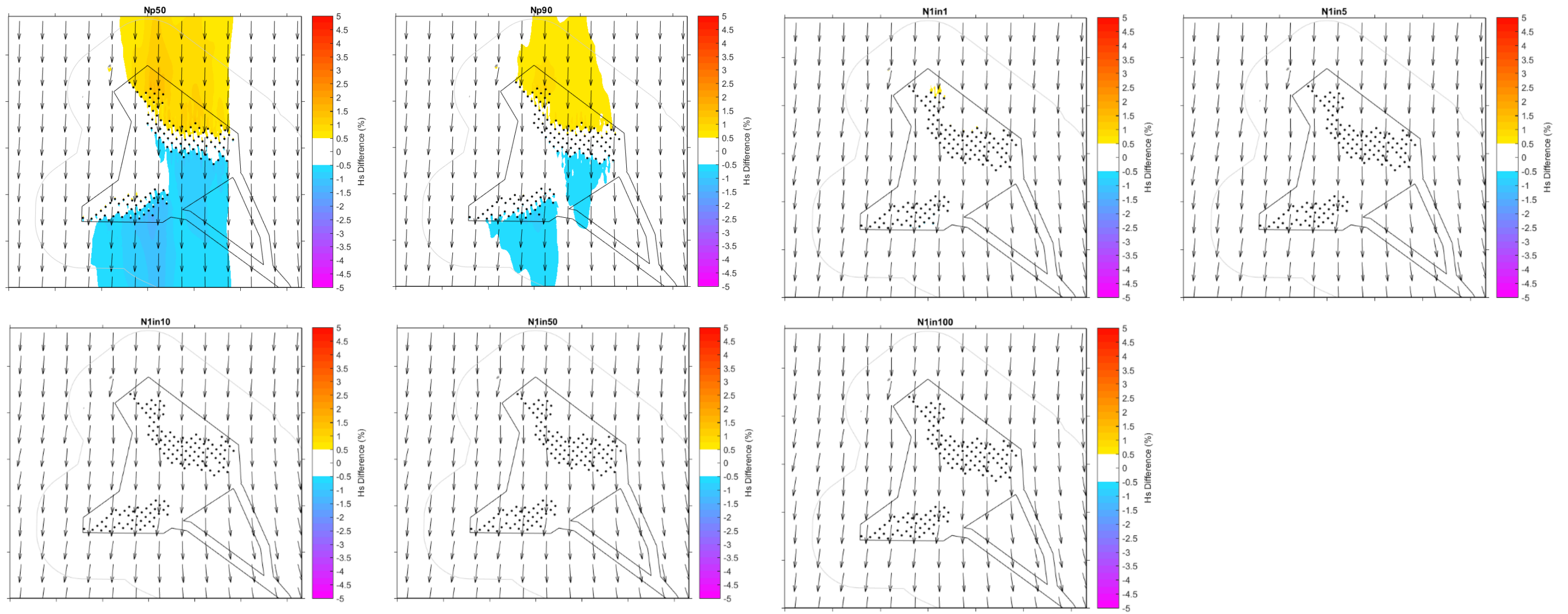


Figure B-85 Modelled percentage change in wave height relative to the baseline conditions due to layout 2 for waves from the North